University of Kentucky
UKnowledge

Theses and Dissertations--Civil Engineering | Civil Engineering

2014

CONTROL OF THE SURFICIAL FINE-GRAINED LAMINAE UPON STREAM CARBON AND NITROGEN CYCLES

William I. Ford III
University of Kentucky, wiford2@g.uky.edu

Click here to let us know how access to this document benefits you.

Recommended Citation
Ford, William I. III, "CONTROL OF THE SURFICIAL FINE-GRAINED LAMINAE UPON STREAM CARBON AND NITROGEN CYCLES" (2014). *Theses and Dissertations--Civil Engineering*. 21.
https://uknowledge.uky.edu/ce_etds/21

This Doctoral Dissertation is brought to you for free and open access by the Civil Engineering at UKnowledge. It has been accepted for inclusion in Theses and Dissertations--Civil Engineering by an authorized administrator of UKnowledge. For more information, please contact UKnowledge@lsv.uky.edu.

STUDENT AGREEMENT:

I represent that my thesis or dissertation and abstract are my original work. Proper attribution has been given to all outside sources. I understand that I am solely responsible for obtaining any needed copyright permissions. I have obtained needed written permission statement(s) from the owner(s) of each third-party copyrighted matter to be included in my work, allowing electronic distribution (if such use is not permitted by the fair use doctrine) which will be submitted to UKnowledge as Additional File.

I hereby grant to The University of Kentucky and its agents the irrevocable, non-exclusive, and royalty-free license to archive and make accessible my work in whole or in part in all forms of media, now or hereafter known. I agree that the document mentioned above may be made available immediately for worldwide access unless an embargo applies.

I retain all other ownership rights to the copyright of my work. I also retain the right to use in future works (such as articles or books) all or part of my work. I understand that I am free to register the copyright to my work.

REVIEW, APPROVAL AND ACCEPTANCE

The document mentioned above has been reviewed and accepted by the student's advisor, on behalf of the advisory committee, and by the Director of Graduate Studies (DGS), on behalf of the program; we verify that this is the final, approved version of the student's thesis including all changes required by the advisory committee. The undersigned agree to abide by the statements above.

William I. Ford III, Student

Dr. James F. Fox, Major Professor

Dr. Yi-Tin Wang, Director of Graduate Studies

CONTROL OF THE SURFICIAL FINE-GRAINED LAMINAE UPON STREAM CARBON AND NITROGEN CYCLE

DISSERTATION

A dissertation submitted in partial fulfillment of the
requirements for the degree of Doctor of Philosophy in the College of Engineering
at the University of Kentucky

By

William Isaac Ford III

Lexington, Kentucky

Director: Dr. James F. Fox, Professor of Civil Engineering

Lexington, Kentucky

2014

Copyright © William Isaac Ford III 2014

ABSTRACT OF DISSERTATION

CONTROL OF THE SURFICIAL FINE-GRAINED LAMINAE UPON STREAM CARBON AND NITROGEN CYCLE

This dissertation investigated the impact of the Surficial Fine-Grained Laminae (SFGL) upon stream biogeochemical cycles to constrain stream C and N budgets. Collection and analysis of 8 years of transported sediment elemental and isotopic signatures, weekly, from a SFGL dominated stream, a novel dissolved C and N dataset, statistical and time-series analysis of sediment and dissolved data, and development of a comprehensive modeling framework that couples hydrodynamics, sediment, C and N biogeochemistry, and stable isotope sub-models to simulate fluvial C and N budgets was used. SFGL C modeling suggests benthic particulate C stocks and transport vary seasonally and annually but are in a state of long-term equilibrium which is governed by negative feedback mechanisms whereby high POC export due to extreme hydrologic events and high frequency hydrologic events reduces benthic particulate C stocks and inhibits benthic particulate C growth. Model distribution fitting suggests transported particulate C in SFGL streams is Gamma distributed; in which statistical moments are governed by variability of the SFGL. Stable isotope un-mixing of the bed source suggests that the SFGL has varying levels of carbon quality seasonally and annually, in which non-equilibrium conditions stem from extreme depositional events. Coupling stable isotope mass balance and SFGL fractionation processes into water quality modeling frameworks, reduced uncertainty of the C budget by nearly 60%, suggesting algal sloughing constitutes nearly 40% of the total organic C budget, shifting the balance from dissolved C to particulate C dominated. Time series analysis of the eight year dataset suggest nitrogen dynamics in the SFGL dominated stream were consistent with existing conceptual models when algal biomass is the prominent organic matter source in the SFGL, but contradicts conventional wisdom in winter through late spring when abiotic sorption appears prominent. The development of a new numerical model to simulate the fluvial N budget couples this new conceptual model of SFGL stream N dynamics to isotope mass-balances and C dynamics in order to provide a comprehensive management tool for restoration engineers. Meta-analysis and upscaling of results for regional to global scales will enable researchers to place the role of the SFGL in a broader context.

Key words: Surficial Fine-Grained Laminae, stream, hydrology, biogeoechemistry, model

William I Ford III
Student Signature
6-03-2014
Date

CONTROL OF THE SURFICIAL FINE-GRAINED LAMINAE UPON STREAM CARBON AND NITROGEN CYCLE

By

William Isaac Ford III

Dr. James F Fox
Director of Thesis

Dr. Yi-Tin Wang
Director of Graduate Studies

6-03-2014
Date

ACKNOWLEDGEMENTS

This work benefited greatly from contributions of my Dissertation committee, fellow graduate students, and laboratory technicians and staff. First and foremost, I'd like to thank my Dissertation advisor, Dr. James Fox, for his support, camaraderie and mentorship throughout my undergraduate and graduate studies that have made me a stronger scientist and engineer, while also providing an example of how to be an excellent mentor. I'd like to thank members of my dissertation committee: Dr. Lindell Ormsbee, Dr. Yi-Tin Wang, Dr. Mark Coyne, and my outside examiner Dr. Carmen Agouridis as these instructors aided both my research and graduate education greatly. Further, I'd like to thank the numerous graduate and undergraduate researchers that aided with sample collection and processing as well as laboratory staff at the Environmental Research and Training Lab, the University of Kentucky Stable Isotope Lab, the University of Arkansas Stable Isotope Lab, and the Kentucky Geological Survey Lab.

I'd also like to thank my family for their integral role throughout my academic career. My wife, Calah, was extremely patient and supportive throughout the dissertation process. My parents provided support and encouragement throughout my academic career and pushed me to work hard and to make ethical decisions.

Finally, I'd like to thank the College of Engineering, the National Science Foundation, and the Kentucky Science and Engineering Foundation for providing financial support for my graduate studies and data collection.

TABLE OF CONTENTS

LIST OF TABLES

LIST OF FIGURES

Chapter 1: Introduction

Text extract with permission from Fox, J., Ford, W., Strom, K., Villarini, G., Meehan, M. 2014. Benthic Control upon the Morphology of Transported Fine Sediment in a Low-Gradient Stream. *Hydrological Processes*. 28 (11): 3776-3788.

Copyright © 2014 John Wiley & Sons, Ltd.

The surficial fine-grained laminae, or SFGL, is a continually changing, biologically active, thin ephemeral layer that often blankets the surface of the streambed. The SFGL is composed of organic and inorganic fine sediments that are loosely packed and high in water content with a bulk density on the order of 1.1g cm^{-3}. In low-order streams, this thin fluvial layer tends to range from 1-10mm in thickness (Droppo and Stone, 1994). The SFGL shows prominence as a sediment source to the stream water, especially at the onset of a hydrologic event due to its loose structure and relatively low critical shear stress (Russo and Fox, 2012). During the falling limb of the hydrograph, aggregated sediments are deposited back to the SFGL, and the structure of the temporary storage zone redevelops. It is now recognized that during the low discharge, baseflow periods in between hydrologic events that the structure of the SFGL is partially built by biological activity in the benthos. Autotrophs including filamentous algae and diatoms colonize within the surface sediment (Battin et al., 2003; Garcia-Aragon et al., 2011). During photosynthesis, the autotrophs secrete extracellular polymeric substances (or EPS). Algal EPS is primarily acid polysaccharides secreted from the cell membrane that act as a gluey substance and holds sediment particles together (Kies et al., 1996). Heterotrophic bacteria metabolize carbon within autotrophs and deposited sediment organic matter and in turn produce a network of secreted EPS fibrils. EPS fibrils are cohesive colloids on the order of 10nm in diameter that form a structural matrix within the SFGL (Defarge et al., 1996; Droppo and Amos, 2001). The net result is the presence of a biofilm within the surface sediment that provides the structure of SFGL through a bridging and binding matrix of EPS originated from filamentous algae, diatoms and microbial production (Smith and Underwood, 1998; Yallop et al., 2000; Battin et al., 2003; Gerbersdorf et al., 2008; Gerbersdorf et al., 2009; Garcia-Aragon et al., 2011).

This dissertation will explore the role of SFGL on stream biogeochemistry through investigation of fluvial C and N cycles. Chapter 2 develops a conceptual particulate organic carbon model for SFGL controlled streams that couples hydrodynamics, sediment, and biogeochemical processes to quantify the significance of autochthonous carbon in the SFGL. Thereafter, the model is tested and verified in a study stream, and the behavior of the SFGL at varying timescales is discussed. Chapter 3 explores the temporal statistical distribution of transported sediment carbon utilizing statistical distribution fitting analysis of the aforementioned model output. Chapter 4 presents a new metric, utilizing a data driven stable isotope approach, to assess the quality and quantity of SFGL carbon seasonally and in response to a high magnitude flood disturbance. The utility of the stable isotopes to provide insight on carbon quality and quantity prompted the development of a stable isotope sub-model in Chapter 5 to further constrain uncertainty present in the fluvial organic carbon budget. An Empirical Mode Decomposition analysis is performed in Chapter 6 to test traditional assumptions regarding the fluvial N budget in low gradient ag-disturbed streams. New mechanisms governing fate and transport of fluvial N are utilized to develop a new fluvial N model in Chapter 7 utilizing a conceptually-based couple modeling framework, and a new numerical scheme.

References

Battin, T.J., Kaplan, L.A., Newbold, J.D. and Hansen, C.M.E. 2003. Contributions of microbial biofilms to ecosystem processes in stream mesocosms, Nature 426, 439-442.

Defarge C., Trichet J., Jaunet A-M., Robert M., Tribble J. and Sansone F.J. 1996. Texture of microbial sediments revealed by cryo-scanning electron microscopy: Journal of Sedimentary Research, v. 66, p. 935–947.

Droppo I, Stone M. 1994. In-channel surficial fine grained sediment lamina. Part I: Physical Characteristics and formational processes. Hydrological Processes 8:101-111.

Droppo, I.G., and Amos, C.L. 2001. Structure, stability, and transformation of contaminated lacustrine surface fine-grained laminae. Journal of Sedimentary Research, Vol. 71, No. 5, pp 717-726.

Garcia-Aragon, J., Droppo, I.G., Krishnappan, B.G., Trapp, B. and Jaskot, C. 2011. Erosion characteristics and floc strength of Athabasca River cohesive sediments: towards managing sediment-related issues, J Soils Sediments 11:679–689.

Gerbersdorf SU, Jancke T, Westrich B, Paterson DM 2008. Microbial stabilization of riverine sediments by extracellular polymeric substances. Geobiology 6:57–69.

Gerbersdorf SU, Bittner R, Lubarsky H, Manz W, Paterson DM 2009. Microbial assemblages as ecosystem engineers. J Soils Sediments 9:640–652.

Kies, L., Fast, T., Wolfstein, K., Hoberg, M. L., 1996. On the role of algae and their exopolymers in the formation of suspended particulate matter in the Elbe estuary (Germany). Archives Hydrobiologica Special Issues on Advanced Limnology 47, 93-103.

Russo J, Fox J. 2012. The role of the surface fine-grained laminae in low-gradient streams: A model approach. Geomorphology. DOI: 10.1016/j.geomorph.2012.05.012

Smith D.J. and Underwood J.C. 1998 Exopolymer production by intertidal epipelic diatoms. Limnol Oceanogr 43(7):1578–1591.

Yallop ML, Paterson DM, Wellsbury P 2000. Interrelationships between rates of microbial production, exopolymer production, microbial biomass and sediment stability in biofilms of intertidal sediments. Microb Ecol 39:116–127.

Copyright © William Isaac Ford III 2014

Chapter 2: Modeling Fine Particulate Organic Carbon Fate and Transport

Adapted with permission from Ford, W., Fox, J. 2014. Model of Particulate Organic Carbon Transport in an Agriculturally Impacted Stream. *Hydrological Processes*. 28 (3): 662-675.

Copyright © 2014 John Wiley & Sons, Ltd.

2.1 SUMMARY

The present contribution focuses on modeling the total particulate organic carbon (POC) and benthic POC transport from a lowland stream impacted by agricultural land-use. A mass balance, reach scale model is verified that accounts for water, sediment and POC transport, sediment and POC temporary storage and exchange with the streambed, and production and degradation of carbon pools in the benthos. We found that the POC load is highly variable during individual hydrologic events and is influenced by transport of mixed carbon sources including upland, streambank and benthic POC sources. Benthic POC stocks and transport were found to vary seasonally and annually but are in a state of long-term equilibrium. Equilibrium is governed by negative feedback mechanisms whereby high POC export due to extreme hydrologic events and high frequency hydrologic events reduces benthic POC stocks and inhibits benthic POC growth. Benthic POC accounted for 4 tC y^{-1} or 22% of the total annual POC loading in the stream's main stem and 8.9 tC y^{-1} or 48% of the POC yield for the entire watershed. These results suggest that further attention should be given to benthic-derived POC when budgeting stream ecosystem carbon for low-order stream systems.

2.2 INTRODUCTION

The fluvial transport of particulate organic carbon (POC) in streams and rivers has received recent attention due to its potential impact on regional and global carbon budgets (Cole et al., 2007; Oeurng et al., 2011) and its influence on downstream aquatic ecosystem functioning (Tank et al., 2010). POC in streams originates from different sources including terrestrial-derived, or allochthonous, carbon from plant litter, soil organic matter and soil detritus and aquatically-derived, or autochthonous, carbon from phytoplankton and benthic production (Hope et al., 1994).

Literature results tend to support the concept that low order streams are dominated by POC from soil carbon origin while high order rivers are dominated by autochthonous carbon associated with phytoplankton production (Gao et al., 2007; Gomez et al., 2003; Helie and Hillaire-Marcel, 2006; Masiello and Druffel, 2001). Small, steep gradient streams have been found to provide a conduit for old refractory OM from upland hillslopes and gullies (Gomez et al., 2003; Masiello and Druffel, 2001). When considering large rivers, it is recognized that the high water residence time provides the conditions for autochthonous POC *via* phytoplankton production (Gao et al., 2007; Helie and Hillaire-Marcel, 2006).

Notwithstanding the importance of soil erosion derived POC transport in small steep systems or phytoplankton production in large rivers, most streams are part of larger networks in which upland carbon is transferred to streams which thereafter transform the allochthonous inputs and promote downstream autochthonous production. While terrestrial inputs of POC to streams has been heavily researched, the in-stream biogeochemical fate and transport associated with POC in streams is not well understood (Alvarez-Cobellas et al., 2010). The result is the disappearance of chemical and isotopic signatures of POC due to complex transformations during transfer from land to the marine environment (Gao et al., 2007).

To further constrain POC source, fate and transport in inland waters, we place emphasis on low-order, lowland stream systems that are impacted by agricultural land-uses. Lowland stream systems are characterized by low stream and hillslope gradients that promote temporary storage of mobilized fluvial sediment within the streambed of the channel (Walling et al., 2006). The low-order nature of these systems promotes

autochthonous benthic processes, as opposed to phytoplankton production, due to the high velocities and shallow water depth (Allan, 1995; Naiman and Bilby, 1998). Nutrient and sunlight conditions support a benthic system dependent upon streambed stored soil carbon, which contrasts, for example, streams draining forested lands where the benthic POC cycle is heavily dependent upon leaf inputs and summer canopy (Tank et al., 2010; Webster et al., 1999). As a result there is prominence of a fine benthic layer that is subjected to both physical and microbiological alterations. Sediments are actively eroded and deposited (Fox et al., 2010, Walling et al., 2006) with erosion and scour of the streambed occurring at low and moderate flows and net deposition occurring during high flows (Russo and Fox, 2012). Algal production and heterotrophic decomposition are governing processes impacting POC and depend on light availability, temperature and nutrient supply (Rutherford et al., 2000).

A conceptual understanding of the processes impacting benthic POC suggests a coupled biologic and hydrologic control upon POC transport. An understanding of benthic POC suggests seasonal variability due to biologic controls of algal production during light available, high temperature warmer seasons and continued heterotrophic decomposition and benthic POC losses in cooler months when algal production is low (Naiman and Bilby, 1998). While much work has been performed to understand seasonal variability of benthic algal biomass in general (Biggs, 1996; Cox, 1990; Francoeur et al., 1999), few studies have quantified the resultant signal upon the POC load. The hydrologic control of POC transport has primarily focused on the importance of high flow events to transport the majority of the carbon load (Masiello and Druffel, 2001; Dalzell et al., 2005). Some studies have focused on the high variability associated with POC transport as a function of hydrology (Dalzell et al., 2007; Oeurng et al., 2011). It is plausible that the hydrologic control in lowland stream systems will impact POC transport on a number of time-scales associated with seasonal hydrology down to flow acceleration and deceleration during individual hydrologic events.

The objective of this paper is to quantify POC transport in a low-order, lowland stream system that is impacted by agricultural land-uses. We place specific emphasis on the transport of benthic POC, which to our knowledge has not been explicitly estimated in studies that focus on POC transport from low-order stream systems. To meet our goal,

field data is collected and mass-balance sediment and particulate carbon models are calibrated and validated that allows study of POC transport from the lowland stream system to assess variation of carbon transport during individual hydrologic events, seasonally and annually. Results enable discussion of the (i) coupled hydrologic and biologic controls upon POC transport for the system and (ii) the overall significance of benthic POC transport within the system.

2.3 STUDY SITE

The study watershed was the Upper South Elkhorn watershed (HUC 5100205270, 61.8 km^2) located within the Kentucky River Basin (18,000 km^2) in the Bluegrass physiographic region of central Kentucky, USA (see Figure 1). The South Elkhorn watershed was chosen for this study due to its lowland morphology and high background nutrient loads resulting from agricultural and urban land-use practices that promote temporary storage and accrual of carbon in the streambed. Slopes across the watershed were generally low. High sinuosity of the stream channel further reduced the slope along the stream corridor. The streambed is bedrock controlled and characterized by local heterogeneity, e.g., zones of pronounced fluvial storage in the stream bed. Evidence of streambank erosion of the cohesive banks was found to exist based on visual observation of fluvial undercutting and scars.

Agriculture with intermittent forest (57%) and urban/suburban (43%) landuses were prominent. Urban and agricultural land-uses have been shown to have significantly higher background levels of nitrogen compared to undisturbed systems (Mulholland et al., 2008). Measurements of nitrogen and phosphorous levels in the stream water showed an average of 2.34 $mgNO_3^- L^{-1}$ and 0.22 $mgP L^{-1}$. These levels exceed thresholds proposed by Dodds et al. (2002) of 0.04$mgN L^{-1}$ and 0.03$mgP L^{-1}$, above which chlorophyll levels were found to be significantly higher. Hence, production of autochthonous carbon is not limited by nutrients in the stream system. Benthic algae was assumed dominant as compared to phytoplankton since the South Elkhorn is a small, low-

order system with an average water depth of 0.38m, and low suspended sediment concentrations (average of 12mg L^{-1}) at low flow.

2.4 METHODS

Figure 2 illustrates the modeling framework used to estimate sediment and carbon transport in the stream. The stream was divided into six sub-reaches, using 30 minute time intervals so that speed of propagation of the numerical scheme was on the same order of magnitude as the speed of transported POC. The South Elkhorn Creek was modeled continuously over a five year simulation period.

2.4.1 Data Collection and Analysis

Suspended sediment samples and POC samples were collected from the watershed outlet at baseflow and for moderate and high flow storm events for model verification. Sediment samples were collected using an automated pump sampler. After collection, samples were brought back to the lab and filtered using Glass Microfibre Whatman filters (Cat No. 1822-047), which retain sediments greater than 1.2 microns. Filtered samples were dried in an oven at 103°C for a minimum of 24 hours to provide estimates of sediment concentration in streamwater. *In situ* suspended sediment traps were used to collect spatially and temporally integrated samples for transported POC measurements (Phillips et al., 2000). Phillips et al. (2000) highlights the use of the traps for obtaining representative, integrated samples of carbon content for streams. Samples were collected on a weekly basis from March of 2006 through December of 2009. Samples with clogged sediment traps and inadequate sample weight were not analyzed further due to potential biasing during collection. In total, 104 POC samples were collected and analyzed. In the lab, samples were centrifuged in a high volume rotor to concentrate solids. The concentrated sample was freeze dried to remove any remaining water, wet sieved to retain the fine fraction (<53 μm), centrifuged and freeze dried again, then ground to a fine powder (Fox, 2009). Powdered samples were weighed into silver capsules that were subsequently acidified repeatedly with 6% sulfurous acid in order to remove carbonate phases (Verardo et al., 1990). Samples were analyzed using a Costech

4010 elemental analyzer. Average standard deviation for the sample of the elemental standard (acetanilide) was 0.82% for %C.

2.4.2 Inputs and Parameterization

Model inputs and parameterization were accomplished by measurements in the field and analysis of values reported in the literature for agriculturally impacted streams. Table 1 compiles model inputs and parameters used in the water flow and sediment transport models. Table 2 compiles model inputs and parameters used in POC growth and decomposition models.

2.4.2.1 Measured Inputs and Parameters

Water flowrate was available from United States Geological Survey gage #32503289000 located at the outlet of the watershed. Flow depth, H, was approximated as a function of flowrate using a power function where c_1 and c_2 are the empirically determined coefficients. The stream channel bathymetry measurements including width, B, stream gradient, S, channel bank side slope, z, and streambank height, H_{bank}, were reported in Fox et al. (2010) and Russo and Fox (2012) for the South Elkhorn creek and were measured using a laser level and rod. Stream lengths were delineated using geospatial analysis in a geographical information system. Bulk density of the streambanks, ρ_{sbanks}, was estimated using the United States National Resources Conservation Service soils database for the region. The percentage of the streambed that contained an active layer is denoted by *% Cover* and was estimated using 57 measurements collected on a grid in a representative reach. Sediment depth, d_{sed}, was measured using a ruler at the 57 in-stream locations. The fraction of transport sediments <53 μm, FF, was measured using a particle size distribution analysis of transported sediments. Settling velocity of fine sediments, W_s, was calculated for the average particle size of 30 μm for non-spherical particles (Dietrich, 1982). Carbon content of fine soil organic matter, SOM, $C_{F\text{-}SOM}$, coarse SOM, $C_{C\text{-}SOM}$, and fine bank sediment, $C_{F\text{-}Bank}$ were measured in previous studies for the watershed (Fox et al., 2010). Maximum light intensity measurements, I_{max}, were calculated at the streambed using the Beer-Lambert law and solar radiation data from the National Renewable Energy Laboratory (Dunlap et al., 2001).

2.4.2.2 Literature-based Inputs and Parameters

The critical shear stress of streambed sediment, τ_{cr}, was based on a mean value of biologically active surface sediments at various stages of biostabilization (Droppo et al., 2001). τ_{cr} of the streambanks was based on cohesive sediments with low density vegetation (Millar and Quick, 1998). Streambed bulk density, ρ_{sbed}, and active layer depth, d_{Bio}, were parameterized from streams with surficial streambed sediments as a prominent source with similar upland agricultural and soil conditions (Droppo and Stone, 1994). A number of accepted, reported values were also used to parameterize the carbon content and stock of POC pools, including algae, C_{Algae}, (Gosselain et al., 2000), allochthonous leaf litter, $C_{det\text{-}leaf}$, (Schlesinger, 2000), and benthic leaf litter detritus, $SC_{Detritus}$, (Richardson, 1992). Fixed light intensity and temperature inputs for benthic algae modeling were based on values reported in the literature for agriculturally impacted streams (Rutherford et al., 2000; Martin et al., 2006; Chapra et al., 2008). These inputs included light saturation, I_k, minimum growth temperature, T_{min}, maximum growth temperature, T_{max}, optimum growth temperature, T_{opt}, density dependence coefficient, P_{sat}, temperature coefficient, Pk_{resp}, and reference temperature, T_{ref}. Decomposition rates of carbon pools were parameterized based on our meta-analysis of *in-situ* field studies reported in the literature. One stage of decomposition was parameterized for the benthic algae pool, $DEC_{C\text{-}Algae}$, given that filamentous algae are labile and generally 2-200 microns in diameter (Alvarez and Guerrero, 2000; Jackson and Vollaire, 2007; Sinsabaugh et al., 1994; Webster et al., 1999; Yoshimura et al., 2008). Two stages of decomposition were parameterized for leaf litter including decomposition of coarse litter, $DEC_{C\text{-}LD}$, and intermediate litter, $DEC_{Med\text{-}LD}$, (Alvarez and Guerrero, 2000; Jackson and Vollaire, 2007; Minshall et al., 1983; Rier et al., 2007; Short et al., 1980; Sinsabaugh et al., 1994; Webster et al., 1999; Yoshimura et al., 2008). Decomposition of soil organic matter, $DEC_{B\text{-}SOM}$, from the uplands and fine POM less than 53 µm in the streambed, $DEC_{B\text{-}LD}$ and $DEC_{B\text{-}Algae}$, were parameterized based on results from Six and Jastrow (2002) and Webster et al. (1999), respectively.

2.4.3 Model Equations

2.4.3.1 Water and Sediment Transport Models

Water flowrate was modeled at each node in Figure 1 using the drainage-area ratio method (Emerson et al., 2005). The mass balance of suspended sediment was formulated as

$$SS_i^j = SS_{i-1}^j + E_{i\ Bank}^{\ j} + E_{i\ Bed}^{\ j} - D_i^j + Q_{i\ SSin}^{\ j}\Delta t - Q_{i\ SSout}^{\ j}\Delta t \ , \quad (1)$$

where, SS (kg) is the suspended sediment in the water column, E (kg) is the erosion from streambank and streambed sources, D (kg) is deposition to the bed, Q_{SS} (kg s^{-1}) is suspended sediment transported into and out of the modeled reach, and Δt (s) was the time step. Source erosion was modeled to be potentially limited by shear resistance, the transport carrying capacity of the fluid, and supply of the erosion source. These processes are modeled for both the streambed and the streambanks as

$$E_i^{\ j\ I} = \min\left[k\left(\tau_{i\ f}^{\ j} - \tau_{cr}^{\ I}\right)\rho_S^I SA^I \Delta t, T_{i\ C}^{\ j} - SS_{i-1}^j, S_{i-1}^{\ j\ I}\right], \quad (2)$$

where, (I) represents the sediment source, k (m^{-1}) is the erodibility coefficient, τ_f (Pa) is the shear stress of the fluid at the centroid of the erosion source, τ_{cr} (Pa) is the critical shear stress of the erosion source, ρ_s (kg m^{-3}) is the bulk density of the sediment source, SA (m^2) is the surface area of the erosion source, T_c (kg) is the transport carrying capacity and S (kg) is the sediment supply. In Equation (2), the erodibility coefficient and fluid shear stress were parameterized following the method of Hanson and Simon (2001). T_c was estimated using a Bagnold like expression (Chien and Wan, 1999) as

$$T_{i\ C}^{\ j} = c^{j}{}_{TC}\frac{\left(\tau_{i\ f}^{\ j}\right)^2}{W_s}L^j\Delta t \ , \quad (3)$$

where c_{TC} (s^{-1}) was the transport capacity coefficient, W_s (m s^{-1}) was the particle settling velocity, and L (m) was the length of the reach. Deposition of sediment to the streambed was estimated as

$$D_i^j = \frac{W_s\Delta t}{k_p H_i^j}\left[SS_{i-1}^j - T_{i\ C}^{\ j}\right], \quad (4)$$

where k_p was the concentration profile coefficient, and H (m) was the water column height. S of the banks was assumed infinite, however the supply of sediment in the streambed was budgeted as

$$S_{i\ Bed}^{j} = S_{i-1\,Bed}^{j} - E_{i\ Bed}^{j} + D_{i}^{j}. \quad (5)$$

2.4.3.2 POC Model

There are three primary pools of POC in the streambed which were modeled as

$$POC_{i\ Bed}^{j} = POC_{i\ B-Algae}^{j} + POC_{i\ B-SOM}^{j} + POC_{i\ B-LD}^{j}, \quad (6)$$

where $POC_{B\text{-}Algae}$ (kgC) is the mass of POC from algae in the active benthic layer, $POC_{B\text{-}SOM}$ (kgC) is the mass of POC from SOM in the active benthic layer, and $POC_{B\text{-}LD}$ (kgC) is the mass of POC from decomposing leaf litter in the active layer. The mass balance of $POC_{B\text{-}Algae}$ was modeled as

$$POC_{i\ B-Algae}^{j} = POC_{i-1\,B-Algae}^{j} + A_{i\ Algae}^{j} - DEC_{i\ B-Algae}^{j} POC_{i-1\,B-Algae}^{j} \Delta t - POC_{i\ Adj}^{j}, \quad (7)$$

where A_{Algae} (kgC) represents algae accrual in the benthic layer, $DEC_{B\text{-}Algae}$ (s^{-1}) is the rate at which benthic algal POC is decomposed, and POC_{Adj} (kgC) is the mass of the POC from algae lost due to erosion and deposition dynamics in the active benthic layer. Decomposition rates were assumed to vary proportionally with heterotrophic bacterial growth (e.g., White et al., 1991). Algal POC was modeled following from the benthic algae model for agriculturally impacted streams developed by Rutherford et al. (2000) and subsequently used in a number of streamwater quality models (e.g., WASP, Martin et al., 2006; and QUAL2K, Chapra et al., 2008). The algal POC was

$$A_{i\ Algae}^{j} = DEC_{C-Algae} SA_{Bed} \Delta t^{2} \left(F_{i}^{j} + P_{i-1}^{j} + P_{i\ Col}^{j} - \mathrm{Re}\, s_{i}^{j} - Scour_{i}^{j} \right), \quad (8)$$

where, $DEC_{C\text{-}Algae}$ (s^{-1}) is the decomposition rate of the algal mat, F (kgC m^{-2} d^{-1}) is the carbon fixation rate, P (kgC m^{-2} d^{-1}) is the biomass accrual rate in the algal mat, P_{col} (kgC m^{-2} d^{-1}) is the algal colonization rate, Res (kgC m^{-2} d^{-1}) is the respiration rate of the algal mat, and $Scour$ (kgC m^{-2} d^{-1}) is the carbon eroded from the algal mat. Algal scour was modeled using the shear and supply limited conditions similarly to the method discussed for erosion of the streambed and streambank sediments. SOM in the benthic boundary layer was modeled similarly to benthic algal carbon but included both coarse and fine carbon pools. The POC was modeled as

$$POC_{i\ B-SOM}^{j} = POC_{i-1\,B-SOM}^{j} + POC_{i\ D(SOM)}^{j} + DEC_{C-SOM}\,POC_{i-1\,C-SOM}^{j}\,\Delta t - POC_{i\ E(SOM)}^{j} \pm POC_{i\ Adj}^{j} - DEC_{i\ B-SOM}^{j}\,POC_{i-1\,B-SOM}^{j}\,\Delta t \quad (9)$$

where $POC_{D\,(SOM)}$ (kgC) is the mass of POC associated with fine SOM being deposited to the benthic layer , $DEC_{C\text{-}SOM}$ (s^{-1}) is the decomposition rate of coarse SOM, $POC_{C\text{-}SOM}$ (kgC)is the mass of coarse POC in SOM, $POC_{E\,(SOM)}$ (kgC) is the mass of POC associated with fine SOM being eroded from the benthic layer, $DEC_{B\text{-}SOM}$ (s^{-1}) is the decomposition rate of fine benthic SOM, and $POC_{C\text{-}SOM}$ (kgC) is the mass of POC in the benthic layer associated with fine SOM. Unlike algae, POC_{adj} in the benthic SOM mass balance can be a source of SOM because material below the active layer is assumed to be SOM. Although the South Elkhorn is primarily a human disturbed system, with light canopy cover, intermittent forest areas provide autumnal leaf litter inputs to the stream, thus POC from fine benthic leaf detritus ($POC_{B\text{-}LD}$) was accounted for in the modeling framework using a similar mass balance approach to SOM and algae. Since the particle size of leaf litter is larger than that of a soil particle or algae, leaf detritus (LD) was operationally defined to go through two stages of decomposition before entering the fine benthic pool. The fine benthic LD pool was adjusted for deposition and erosion similar to algae.

2.4.4 Model Calibration and Validation

Parameters in the sediment transport and POC models were calibrated and validated using the collected data. The sediment data was used within the Einstein approach to calculate sediment flux at the cross section at the watershed outlet (Yalin 1977; Graf 1984; Chang, 1988; Raudkivi 1990; Chien and Wan 1999). Sediment transport model calibration and validation followed closely the method outlined for the South Elkhorn Watershed by Russo and Fox (2012). Briefly, the governing mass balance equation of the sediment transport model, sediment inflow, Q_{SSin}, was modeled using a quadratic relationship and a coefficient, c_3. The transport carrying capacity, C_{TC} and c_3, were calibrated to ensure modeled and measured sediment loads matched and that the sediment bed was in long term equilibrium. A high and low transport capacity were used since spatial heterogeneity of the stream bed and variation of particle settling velocity impact transport carrying capacity at different water depths (Russo and Fox, 2012). Global calibration of the parameters did not result in long term streambed equilibrium for

all reaches, thus parameters were adjusted in each reach to satisfy the equilibrium condition. Goodness-of-fit of simulated and measured sedigraphs was based on visual observations as well as percent difference and correlation coefficient metrics. The transported POC data were integrated measurements over the period of approximately one week; thus, transported POC yields (CY_{weekly}) were used to compare modeled to measured results. The calibration parameters for the POC model included the algal critical shear stress (τ_{cr}), algal respiration rate (P_{resp}), and algal colonization rate (P_{col}). τ_{cr} was calibrated within an appropriate range for various stages of biostabilization reported in Droppo et al. (2001). P_{resp} and P_{col} were calibrated within ranges published within Rutherford et al. (2000) for agriculturally impacted streams (see Rutherford et al. (2000) Table 3 and Figure 5). Visual observations (Figure 4) as well as percent difference and correlation coefficient metrics were also used to compare goodness-of-fit of measured and modeled carbon yields.

2.5 RESULTS

2.5.1 Model Performance

Sediment and carbon models were coupled to study POC source, fate and transport in the South Elkhorn watershed. Model performance in calibration and validation was assessed for both the sediment and carbon models. The sediment transport model was calibrated and validated using measured sediment flux at the watershed outlet. Model performance for the sediment transport component is shown in Figure 3. Two types of events were used for calibration and validation including: low flow and moderate hydrologic events (Figure 3a-g); and high discharge hydrologic events (Figure 3h-k). Peak flow and sediment yield estimates for each event are provided in Figure 3. Four low flow and three high flow events were used for calibration while three low flow and one high flow event were used for validation. Visually, the sediment transport model results match the sediment discharge peaks measured with the transported data. Some over- or under-estimation is noticed in the results but the model captures the dynamics of the measured sediment in general. The coefficient of determination and percent difference metrics for the sediment transport model results (see Table 3a) suggests the model performs good to very good overall. Calibration and validation results for *CY* are

observed in Figure 4. Differences in measured and modeled *CY*--or model residuals--(Figure 4a) are generally low, with some over-or-under estimation observed. The sum of residuals is less than 1%, or 0.5 tC, for the 104 yields measured in this study. Modeled *CY* (Figure 4c) tends to agree very well in terms of measured *CY* (Figure 4b) for both high and low hydrologic events. Coefficient of determination and percent difference metrics (see Table 3b) also suggest very good model performance overall.

2.5.2 Results for Individual Hydrologic Events

Figure 5 includes model results of water discharge and transported sediment carbon content, C_T, (Figure 5a) and the distribution of sediment and carbon sources (Figure 5b) over a six month time span. Sources include fractions, f_{ci}, from (i) the uplands and tributaries that inflow to the modeled stream section, (ii) the streambank sediments that erode to the stream channel, and (iii) the streambed source which includes the sum of previously deposited upland carbon, leaf litter and detritus, and autochthonous carbon from benthic algae. Values of C_T and f_{ci} fluctuate rapidly resulting from the complexity of multiple sources (see Figure 5b). During a given event, source contributions from streambed sediments ranged from 0 to 96% of the particulate flux; upland sediments from 4 to 100%; and streambank sediments from 0 to 36%. Streambed or upland sediments were the dominant fraction during all phases of individual hydrologic events; with the streambanks as a secondary contributory. Generally, results show that as Q increases, C_T decreases, and the fraction of carbon from banks and the uplands increase. Consequently, at low flows, C_T is more enriched, and the fraction originating from the bed is larger than that of the banks or upland source.

2.5.3 Results for the Five Year Simulation Period

Model results over the entire five year simulation period (Figure 6) are shown in order to highlight seasonal and annual results of the lowland stream system with respect to transported carbon. Streamwater discharge at the watershed outlet, Q (m^3s^{-1}), sediment discharge, Q_{ss} (kg s^{-1}), the average depth of fluvial sediment deposited in the streambed, d_i (cm), the particulate organic carbon content in the streambed, C_{Bed} (gC/100g sediment), and transported carbon content at the exit of the modeled stream section, C_T (gC/100g sediment), are provided in Figure 6. C_{Bed} and C_T results varied seasonally, as seen in

Figure 6d-e. Seasonally averaged values and standard deviations of C_T over the five year simulation were 2.83±0.59, 2.54±0.34, 2.94±0.54, and 3.12±0.95 gC/100g sediment for winter, spring, summer and fall, respectively. Generally, C_T and C_{Bed} increased from late-spring to early fall and began to recede in mid-fall to mid-spring.

Annual variation of C_{Bed} and C_T also resulted from the model simulation and is illustrated in Figure 6d-e. In 2007 and 2008, the occurrence of hydrologic events during the late-spring and summer was not pronounced (Figure 6a), with C_T increasing steadily. C_T ranged from 2.0 to 4.4 gC/100g sed in 2007 and 2.4 to 4.7 gC/100g sed in 2008. In contrast, during the late-spring and summer of 2009 there was a relatively high density of hydrologic events (Figure 6a) during which C_T ranged from 2.8 to 3.4 gC/100g sediment; hence the range of C_T was reduced by more than 50%. Model results show abrupt shifts in C_T and C_{Bed} during extreme events. This is most evident in the high magnitude storm event during September, 2006. Immediately following the event, a 0.65 gC/100g sediment shift in C_{Bed} and C_T was simulated. Simultaneously, a 0.5 cm aggradation of the streambed was simulated. There is visual evidence in Figure 6 that the magnitude of the peak annual events were associated with changes in C_{Bed}, C_T and d_i, e.g., peak flows during 2008 and 2010.

2.5.4 Fluvial POC Budget

Annual and seasonal POC yields were calculated from results of the five year continuous simulation to assess the source contributions and timing of transported carbon. The total POC yield from the watershed was 18.4 tC y^{-1} and 0.3 tC $km^{-2}y^{-1}$ when normalized by the watershed area. Benthic POC accounted for 4 tC y^{-1} or 22% of the total annual POC loading. POC exported from the watershed was found to be distributed seasonally. Fall and winter had the highest POC yields of 6.7 tC $season^{-1}$ and 6.2 tC $season^{-1}$, respectively. The high fall loading reflects high flows combined with high carbon content of the streambed, and the high winter loading reflects the high density of hydrologic events.

Analysis of exported carbon showed that relatively high flow conditions transported the majority of the POC load. We operationally defined a large hydrologic event as a rainfall event with a 1.5 month return period generating a peak water

discharge, Q_{peak}, exceeding 2.5 cms. 90 percent of flows occurred below this threshold. Based on this definition, large hydrologic events transported 87% of the POC load and occurred less than 10 percent of the time.

2.6 DISCUSSION

2.6.1 Hydrologic and Biologic Control of POC Transport

Stored fine sediments in the streambed of the lowland, agriculturally impacted streams provide a matrix for carbon transfer including autochthonous carbon production and POC degradation. To this end, the importance of including the biologic control of water temperature and light availability on benthic POC within lowland systems becomes evident. However, we point out that the hydrologic control is at least as important when considering time scales that include individual hydrologic events, seasonal variation and annual variation in the lowland stream system.

Results show that during individual hydrologic events, the POC load is highly variable in terms of its signature and is heavily influenced by hydrologic processes that initially erode and thereafter deposit temporarily stored carbon in the streambed. While individual hydrologic events produce high short-term variability of the POC load, it is evident that the streambed sediment depth is in a state of long-term equilibrium balanced by erosion and scour during low-to moderate-events with net deposition during high flow events (Russo and Fox, 2012). The implication of the hydrologically controlled streambed in a state of long-term equilibrium is that the benthic boundary layer is able to become temporarily developed and also be in a state of long-term equilibrium. Long term equilibrium is governed by erosion-deposition dynamics in which carbon accrues at the streambed surface during hydrologically inactive periods and can either be eroded during small-moderate events or buried by sediment deposits during large events, controlling the accrual of benthic algal biomass.

The long-term benthic POC equilibrium is intermittent with seasonal and annual variability. Seasonal variation of C_{Bed} with dependence on biologic processes tends to agree with published theory and results regarding the seasonal variability of benthic algal biomass (Biggs, 1996; Cox, 1990; Francoeur et al., 1999). However, for the lowland

stream system, the hydrologic control should be further highlighted. C_{Bed} for a hypothetical model scenario that was simulated with no exchange of POC between the water column and the streambed, i.e., no benthic erosion or deposition is shown in Figure 7. Note that the hypothetical condition is indicative of an equilibrium streambed that neglects the influence of temporary storage—for example the condition assumed for steeper gradient systems (Gomez et al., 2003; Masiello and Druffel, 2001) that could potentially be erroneously extrapolated to lowland systems. For reference, the calibrated model condition is also included in Figure 7. In general the accumulation of autochthonous carbon and increase of C_{Bed} is simulated in the hypothetical and reference cases. However, the C_{Bed} decrease in the late-fall and winter is underestimated for the hypothetical case when benthic erosion and deposition are not present. The result is that the streambed is not equilibrated in the long-term with respect to C_{Bed}. Thus, the importance of bed erosion and deposition controlled by watershed hydrology upon maintaining carbon equilibrium in the streambed is highlighted.

The importance of benthic carbon as a POC source and the existence of the equilibrium streambed motivated further analysis of the behavior of benthic POC export from the system. Table 4 shows the distribution of POC exported over the modeled time period. Over the five year simulation period, benthic POC export exhibits low seasonal variability and constitutes 24, 17, 29 and 18% of the particulate carbon load in the winter, spring, summer and fall, respectively (see Table 4). The low seasonal variability of benthic POC in the long-term reflects the combined effects of seasonal temperature variation and seasonal hydrologic variability for the temperate climate (MAT=12.7 °C) with moderate rainfall (MAP=1160 mm). For example, 30 to 40% of the particulate carbon load is transported in the winter (see Table 4) when the occurrence of high flow hydrologic events is high but the streambed tends to be depleted in terms of its benthic carbon load. In the summer, approximately 10% of the particulate carbon load is transported (see Table 4) because the occurrence of high flow hydrologic events tends to be low but at the same time the bed is enriched in benthic POC. The result is that benthic POC constitutes 24% of the particulate carbon load in the winter and 29% of the particulate carbon load in the summer, exhibiting low seasonal variability over the entire five year simulation period.

Annual variability was also low for benthic carbon transport, which is reported in Table 5. Year-to-year comparison shows that 3.5, 2.7, 3.9, 7.4 and 1.8 tC y^{-1} was transported as benthic carbon during 2006, 2007, 2008, 2009 and 2010, respectively. Further, during the simulation period, the annual variability that did exist for benthic POC export was attributed to variation in the total POC load (see Table 5), and the contribution of the total POC load that was of benthic POC origin exhibited a low variability of 22(±7)% overall. Results for individual years are provided in Table 5.

The long-term equilibrium of the lowland stream system with respect to benthic POC export is not governed by simple one-step processes but rather is the result of negative feedback mechanisms whereby high short-term and seasonal variability in hydrology is balanced by feedbacks from the biology of the streambed. For example, the event in September 2006 eroded the streambed during the rising limb and peak of the hydrograph and flushed benthic POC out of the watershed. The single event transported 0.4 tC out of the modeled stream section suggesting a positive feedback mechanism where high flow brings high benthic POC. However, the long-term response of the system suggests a negative feedback. Flushing of the streambed and thereafter deposition of upland derived SOC to the streambed in the falling limb of the hydrograph produced a clock-resetting event for the benthos. The streambed needed to reestablish an autochthonous pool of carbon, which did not occur until the following summer 2007. The carbon load associated with the benthic POC pool was very low throughout winter 2007 (see Table 6). Thus, the export of benthic POC for the time period was consistent with the long-term averages.

As a second example of negative feedback mechanisms whereby high short-term and seasonal variability in hydrology is balanced by biological feedbacks is seen in 2007 and 2008. The occurrence of hydrologic events during the summer of 2007 and summer of 2008 was low. The lack of transport during these time periods produced decreased transport of benthic POC and again suggests a positive influence of hydrology on benthic POC export where low flow brings reduced benthic carbon loading. However, because the benthic carbon production rate increases with increasing biomass (Rutherford et al., 2000), the benthos was able to become highly developed with respect to its autochthonous carbon pool. In turn, transport of benthic POC during the hydrologic

events in the fall and winter seasons was high, providing a negative feedback and the export of benthic POC for the time period was consistent with the long-term averages.

The long-term equilibrium of the lowland stream system suggests stability of the system in the face of short-term and seasonal hydrologic variability. However, the response of these lowland systems to instabilities imposed by drastic disturbances, e.g., aggressive urbanization or agricultural practices, or climate changes has yet to be investigated.

2.6.2 Fluvial POC Budget

The annual POC yield falls within the range of POC yields reported from other mild gradient systems. A review by Hope et al. (1994) shows POC yields ranging two orders of magnitude from 0.05 to 4.3 tC $km^{-2}y^{-1}$. Watersheds were generally temperate and boreal forests ranging from <1 km^2 to 3,000,000 km^2. Generally, POC yields were <1 tC $km^{-2}y^{-1}$ for watersheds smaller than 100 km^2. More recent studies such as Guo and MacDonald (2006), and Oeurng et al. (2011) have quantified POC yields at 1.2 and 0.32 tC $km^{-2}y^{-1}$ in their respective systems. Guo and Macdonald (2006) was performed in the Yukon River, 855,000 km^2, containing vast alpine and arctic regions. Oeurng et al. (2011) was performed in a large agricultural watershed, 1110 km^2, in south-west France. High flows transporting the majority of the carbon agrees well with Dalzell et al. (2007) which states that 71% and 85% of the total annual organic carbon load was exported in flow events occurring less than 20% of the time. The study was performed in an 850 km^2 agricultural watershed in west central Indiana, USA.

Benthic POC was a major source of transported POC and accounted for 22% of the total annual POC loading in the South Elkhorn. The model simulation was performed for the 9 km main stem of the South Elkhorn only and benthic POC in the tributaries was not modeled as an input to the model domain. An upper bound to autochthonous derived carbon can be estimated for the entire watershed by also considering the tributaries. We extrapolated benthic carbon transport rates using streambed surface area values estimated in a geographical information system and found that 8.9 tC y^{-1} or as much as 48% of the POC yield originates from in-stream benthic POC for the watershed. The benthic POC yield for the lowland stream system is shown to make up a substantial portion of the total

particulate carbon yield whether considering just the third order main stem of the South Elkhorn or the entire watershed. The result tends to question conventional wisdom, which places low-order stream systems as soil organic carbon (SOC) dominated. Prevailing theory tends to categorize small and large stream systems as end-members in which low-order streams are dominated by transport of old, refractory carbon that originated from soils while high-order rivers are dominated by transport of labile, autochthonous carbon that originated from the water column (Masiello and Druffel, 2001; Gomez et al., 2003; Helie and Hillaire-Marcel, 2006; Gao et al., 2007). Here, it is obvious that lowland stream systems similar to the South Elkhorn do not explicitly fit an end-member relationship based on stream scale when considering the benthic origin of a substantial portion of exported carbon.

It is perhaps logical that past research has considered low-order streams draining agricultural lands, such as the South Elkhorn, as SOC dominated. Surely, soil erosion and sediment yields from agriculturally impacted streams have been historically high the past century and have been the topic of intense research and best management practice implementation (Toy et al., 2002, Ch 1). However, in developed countries, erosion control strategies are now more strictly enforced and their use is highly motivated with the intent to maintain the fertility of farmlands and promote crop production. Thus, a shift in the functioning of low-order streams draining agricultural lands with respect to their carbon export is conceivable. As erosion control strategies are improved, SOC loss from agricultural lands will continue to be reduced but dissolved inorganic nitrogen and phosphorus will continue to be exported from the land surface to the streams as runoff. In turn, benthic carbon production will stay relatively high and perhaps dominate the POC load. Since organic nitrogen (ON) and organic phosphorus (OP) behave similarly to OC, high benthic production will likely promote substantial uptake of inorganic N and P, and higher fluxes of benthic ON and OP. Likewise, since OC stock and quality is important for decomposing organisms, permanent removal of N and P from the systems could help mitigate excess DIN and DIP. The scenario sheds further importance on benthic POC in lowland systems and raises a number of questions with regards to the sensitivity of its production and transport as impacted by disturbances such as climate forcing and the redistribution of croplands. The idea is particularly worthy of note when

considering that lowland watershed systems represent the majority of the food producing land masses in the world, and perhaps the production of autochthonous, stream-derived carbon from streams draining these lands has been underestimated.

2.6.3 Further Investigation

The results of this study suggest that benthic carbon production and degradation and its feedback with hydrology should be considered in studies of POC source, fate and transport in inland waters. Further, a conceptual model of POC origin in streams and rivers should more explicitly consider factors that might impact benthic POC, such as stream gradient, watershed gradient, land-use and land management in addition to stream order. Analysis of drastic disturbances and climate change scenarios for local and regional carbon budgets should also account for the fate the benthic carbon source.

One specific area of further investigation is study of benthic POC and its interaction with hydrology and erosion control strategies in other watershed systems. For example, the effect of erosion control on POC export has been highlighted for organic-rich peatland catchments of the United Kingdom (Evans et al., 2006; Hope et al., 1997; Pawson et al., 2008; Worall et al., 2003). POC flux in actively eroding peatlands behave similarly to steep gradient systems in that they export high OC loads and can become the most significant component of OC export in the watershed system (Pawson et al., 2008). Erosion control *via* revegetation of gullies minimizes the flux of POC by promoting fluvial deposits onto gully floors and streamside fans and in turn brings into question the peatland systems as a net source or sink of carbon to the atmosphere (Evans et al., 2006). While benthic POC growth and degradation might be perceived as small in the organic rich peatland streams relative to organic rich loads, their contribution might further constrain the source/sink question for watersheds with erosion control.

A second specific area of further investigation is integration of our modeling framework with detailed biogeochemistry studies of organic matter (OM) composition and degradation rates of POC pools, particularly the finest pool (FPOM, d<53µm). In the present study, we parameterized decomposition rates of carbon pools using a meta-analysis of *in-situ* field studies rather than directly measuring composition of OM (e.g., cellulose content, lignin content and phenol type). Our indirect accounting of chemical

and physical OM composition for POC pools is reasonable given that most pools are well constrained. Coarse leaf litter, moderate leaf litter, and coarse filamentous algae are labile carbon sources for macroinvertabrates and heterotrophic communities, decomposing on the order of 10^{-3} to 10^{-2} d^{-1} (Alvarez and Guerrero, 2000; Jackson and Vollaire, 2007; Minshall et al., 1983; Rier et al., 2007; Short et al., 1980; Sinsabaugh et al., 1994; Webster et al., 1999; Yoshimura et al., 2008). FPOM pools are considered to be more recalcitrant (e.g., higher lignin and cellulose contents) resulting from utilization of labile components (Yoshimura et al., 2008). Algal and leaf litter derived FPOM have decomposition rates of 10^{-3} d^{-1} and SOM decomposes on the order of 10^{-5} d^{-1} (Webster et al., 1999; Six and Jastrow, 2002). However, the FPOM pool remains a topic of uncertainty. Some studies suggest that flocculation of labile dissolved OM or sloppy feeding of CPOM can generate labile FPOM with low lignin contents, and the FPOM can have higher decomposition rates than larger size classes (Jackson and Vollaire 2007; Webster et al., 1999). Measuring chemical composition and degradation rates of FPOM is particularly difficult given the heterogeneity of sources and lack of methodological approaches (Tank et al., 2010). Further research that constrains FPOM will allow us to estimate the far-reaching implications of FPOM fate with respect to downstream water quality. For example, high nitrate loadings in Midwestern agricultural watersheds can potentially be offset by headwater-derived labile benthic FPOM, which fuels microbially mediated denitrification processes (Griffiths et al., 2012). Conversely, less attractive impacts could result from downstream transport of abundant labile FPOM, including high turnover and degassing of carbon to the atmosphere.

List of Inputs and Parameters	**Description**
% Cover	Percentage of streambed covered with fine fluvial deposits
Δt	Model Timestep
B	Width of the streambed
c_1	Scale coefficient for empirical determination of flow depth

c_2	Power coefficient for empirical determination of flow depth
c_3	Scale coefficient for sediment inflow
C_{Algae}	Carbon content of benthic algae
C_{Anoxic}	Carbon content of sediments in below the active layer
C_{Dep}	Carbon content of deposited sediment
$C_{det\text{-}C\text{-}SOM}$	Carbon content of coarse SOM from uplands
$C_{det\text{-}leaf}$	Carbon content from detrital leaf material
$C_{F\text{-}Bank}$	Carbon content of fine bank sediments
$C_{F\text{-}SOM}$	Carbon content of fine SOM from the uplands
$C_{T\ initial}$	Carbon content of initially transported sediments
C_{TCHigh}	Transport carrying capacity for high flows
C_{TCLow}	Transport carrying capacity for low flows
$CY_{B\text{-}Algae}$	Carbon yield from the benthic algae source
CY_{Banks}	Carbon yield from the bank source
CY_{Bed}	Carbon yield from the bed source
$CY_{B\text{-}LD}$	Carbon yield from the leaf detritus source
$CY_{B\text{-}SOM}$	Carbon yield from the benthic SOM source
CY_T	Total particulate carbon yield
$CY_{Upland\text{-}SOM}$	Carbon yield of upland SOM source
d_{Bio}	Depth of the biologically active layer
$DEC_{B\text{-}Algae}$	Decomposition rate of benthic algae
$DEC_{B\text{-}LD}$	Decomposition rate of benthic leaf detritus
$DEC_{B\text{-}SOM}$	Decomposition rate of benthic SOM
$DEC_{C\text{-}Algae}$	Decomposition rate of coarse algae
$DEC_{C\text{-}LD}$	Decomposition rate of coarse algae
$DEC_{Med\text{-}LD}$	Decomposition rate medium step size of leaf detritus
d_{sed}	Depth of the sediment layer
FF	Fraction of transported sediments <53µm
G	Acceleration due to gravity
H_{bank}	Bankfull depth
I_k	Light saturation parameter

L	Length of a given stream reach
P_{col}	Algal colonization rate
$P_{initial}$	Initial algal biomass
Pk_{resp}	Temperature coefficient
P_{max}	Maximum fixation rate
$POC_{fines\ initial}$	Initial mass of fine POC in streambed
P_{resp}	Respiration rate of algal biomass
P_{sat}	Density dependence coefficient
S	Stream gradient
$SC_{Detritus}$	Standing crop of benthic detritus
SY_{Bank}	Sediment yield from the bank source
SY_{Bed}	Sediment yield from the bed source
$SY_{Uplands}$	Sediment yield from the upland hillslope source
T_{max}	Maximum growth temperature
T_{min}	Minimum growth temperature
T_{opt}	Optimum growth temperature
T_{ref}	Reference temperature
W_s	Particle settling velocity for 30µm diameter particle
Z	Slope of the streambanks
P	Density of water
$\rho_{s\ algae}$	Bulk density of the algae
ρ_{sbank}	Bulk density of the bank sediments
ρ_{sbed}	Bulk density of the bed sediments
$\tau_{cr\ algae}$	Critical shear stress of algae
τ_{crbank}	Critical shear stress of the streambank
τ_{crbed}	Critical shear stress of the streambed

2.7 CONCLUSIONS

Results suggest that the streambed of the lowland, agriculturally impacted stream provides a matrix for POC source and transfer dictated by hydrologic forcing coupled with autochthonous carbon production and degradation. We found that the hydrologic control is at least as important as the biologic control, and their coupling results in POC variability for individual hydrologic events, seasonally and annually. High variability resulted for individual events primarily due to hydrologic timing of streambed, streambank and upland POC sources. Seasonal POC variability was attributed to growth and decomposition of carbon, and the benthic POC stock varied annually. Despite both seasonal and annual variability, transported benthic POC from the stream remained fairly constant in the long term. We found that this long term equilibrium of POC was attributed to extreme hydrologic events resetting the active benthic layer and periodic dense hydrologic activity that inhibit benthic growth. Thus, an increase in hydrologic forcing and in turn POC export is balanced by a reduction in benthic POC transport thereafter to produce negative feedbacks in the system. The negative feedbacks imply that budgeting of benthic POC transport from low order systems cannot be constrained using a single variable (e.g., flow regime or water temperature), but rather require coupled modeling or dense datasets. A second implication is that the sensitivity of the negative feedbacks governing benthic POC transport to drastic disturbances (e.g., climate forcing, aggressive upland practices) requires further study.

Results of the fluvial carbon budget suggest that benthic POC accounted for 4 tC y^{-1} or 22% of the total annual POC loading in the main South Elkhorn's main stem and 8.9 tC y^{-1} or 48% of the POC yield for the entire watershed. The substantial transport of benthic POC from the system questions conventional wisdom, which places low-order stream systems as soil organic carbon dominated. A shift in the carbon functioning of low-order streams draining agricultural lands is implied as erosion control strategies are implemented. Under erosion control, agricultural soil loss is reduced but dissolved nutrients in runoff can remain high and promote benthic POC production. The transport carrying capacity of starved streamwater is able to detach and carry streambed sediments and in turn the increasing importance of benthic POC transport is conceivable. This in-stream contribution is highlighted herein; however, further study of these processes in

other systems and upscaling to larger land masses is needed to account for the benthic POC contribution to the inland freshwater carbon cycle.

2.8 REFERENCES

Allan JD. 1995. *Stream Ecology: Structure and Function of Running Waters*. Chapman & Hall: New York.

Alvarez-Cobelas M, Angeler D, Sa´nchez-Carrillo S, Almendros G. 2010. A worldwide view of organic carbon export from catchments. *Biogeochemistry* 107:275-293 DOI: 10.1007.s10533-010-9553-z.

Alvarez S, Guerrero M. 2000. Enzymatic activities associated with decomposition of particulate organic matter in two shallow ponds. *Soil Biology and Biochemistry* 32:1941-1951.

Biggs B. 1996. Patterns in benthic algae of streams. In *Algal Ecology*, Stevenson RJ, Bothwell ML, Lowe RL. (eds). Academic Press: New York; 31-56.

Chang H. 1988. *Fluvial Processes in River Engineering.* Krieger Publishing Company: Malabar, Florida.

Chapra S, Pelletier G, Tao H. 2008. QUAL2K: A Modeling Framework for Simulating River and Stream Water Quality, Version 2.11: Documentation and Users Manual. Civil and Environmental Engineering Dept., Tufts University, Medford, MA.

Chien N. Wan Z. 1999. *Mechanics of sediment transport.* ASCE: Reston, Virginia; 446.

Cole J, Prairie Y, Caraco N, McDowell W, Tranvik L, Striegl R, Duarte C, Kortelainen P, Downing J, Middelburg J, Melack J. 2007. Plumbing the global carbon cycle: Intergrating inland waters into the terrestrial carbon budget. *Ecosystems* 10:171-184.

Cox E. 1990. Studies on the algae of a small softwater stream. I. Occurrence and distribution with particular reference to the diatoms. *Archiv für Hydrobiologie Supplement* 83:525-552.

Dalzell B, Filley T, Harbor J. 2005. Flood pulse influences on terrestrial organic matter export from an agricultural watershed. *J. Geophys. Res.* 110.

Dalzell B, Filley T, Harbor J. 2007. The role of hydrology in annual organic carbon loads and terrestrial organic matter export from a Midwestern agricultural watershed. *Geochimica et Cosmochimica Acta* 71:1448-1462.

Dietrich W. 1982. Settling velocity of natural particles. *Water Resources Research* 18(6):1615-1626.

Dodds W, Smith V, Lohman K. 2002. Nitrogen and phosphorus relationships to benthic algal biomass in temperate streams. *Can. J. Fish. Aquat. Sci.* 59:865–74.

Droppo I, Lau Y, Mitchell C. 2001. The effect of depositional history on contaminated bed sediment stability. *The Science of the Total Environment* 266:7-13

Droppo I, Stone M. 1994. In-channel surficial fine grained sediment laminae. Part I: Physical Characteristics and formational processes. *Hydrological Processes* 8:101-111

Dunlap M, Marion W, Wilcox S. 2001. Solar radiation data manual for flat-plate and concentrating collectors, Report no. NREL/ TP-463–5607, Golden (CO): National Renewable Energy Laboratory.

Emerson D, Vecchia A, Dahl A. 2005. Evaluation of drainage-area ratio method used to estimate streamflow for the Red River of the North Basin, North Dakota and Minnesota. In *U.S. Geological Survey Scientific Investigations Report* 2005–5017.

Evans M, Warburton J, and Yang J. 2006. Eroding blanket peat catchments: Global and local implications of upland organic sediment budgets. *Geomorphology* 79: 45-57.

Fox J. 2009. Measurements of sediment transport processes in forested watersheds with surface coal mining disturbance using carbon and nitrogen isotopes. *Journal of the American Water Resources Association* 45(5): 1273-1289.

Fox J, Davis C, Martin D. 2010. Sediment source assessment in a lowland watershed using nitrogen stable isotopes. *Journal of American Water Resources Association* 46:1192-1204.

Francoeur S, Biggs B, Smith R, Lowe R. 1999. Nutrient limitation of algal biomass accrual in streams: seasonal patterns and a comparison of methods. *J. N. Am. Benthol. Soc.* 18:242–260.

Gao Q, Tao Z, Yao G, Ding J, Liu Z, Liu K. 2007. Elemental and isotopic signatures of particulate organic carbon in the Zengjiang River, southern China. *Hydrological Processes* 21:1318-1327.

Gomez B, Trustrum N, Hicks D, Rogers K, Page M, Tate K. 2003. Production, storage, and output of particulate organic carbon: Waipaoa River basin, New Zealand. *Water Resources Research* 39(6): ESG2-1-ESG2-8.

Gosselain V, Hamilton P, Descy J. 2000. Estimating phytoplankton carbon from microscopic counts: an application for riverine systems. *Hydrobiologia* 438:75-90.

Graf W. 1984. *Hydraulics of Sediment Transport*. Water Resources Publications, LLC.

Guo L, Macdonald R. 2006. Source and transport of terrigenous organic matter in the upper Yukon River: Evidence from isotope ($\delta^{13}C$, $\delta^{14}C$, and $\delta^{15}N$) composition of dissolved, colloidal, and particulate phases. *Global Biogeochem. Cycles* 20.

Hanson G, Simon A. 2001. Erodibility of cohesive streambeds in the loess area of the midwestern USA. *Hydrological Processes* 15(1):23–38.

Helie J, Hillaire-Marcel C. 2006. Sources of particulate and dissolve organic carbon in the St Lawrence River: isotopic approach. *Hydrological Processes* 20:1945-1959.

Hope D, Billett M, Cresser M. 1994. A review of the export of carbon in river water: fluxes and processes. *Environ. Pollut.* 84:301–324.

Hope D, Billett M, Cresser M. 1997. Exports of organic carbon from two river systems in NE Scotland. *J. Hydrol*. 193: 61-82.

Jackson C, Vallaire S. 2007. Microbial activity and decomposition of fine particulate organic matter in a Louisiana cypress swamp. *J. N. Am. Benthol. Soc.* 26(4):743-753.

Martin J, Ambrose R, Wool T. 2006. WASP7 Benthic Algae—Model Theory and User's Guide. U.S. Environmental Protection Agency, Athens, GA.

Masiello C, Druffel E. 2001. Carbon isotope geochemistry of the Santa Clara River. *Global Biogeochem. Cycles* 15(2):407-416.

Millar R, Quick M. 1998. Stable width and depth of gravel-bed rivers with cohesive banks. *Journal of Hydraulic Engineering* 124(10):1005-1013.

Minshall G, Petersen R, Cummins K, Bott T, Sedell J, Cushing C, Vannote R. 1983. Interbiome comparison of stream ecosystem dynamics. *Ecological Monographs* 53(1):2-25.

Mulholland P, Helton A, Poole G, Hall R, Hamilton S, Peterson B, Tank J, Ashkenas L, Cooper L, Dahm C, Dodds W, Findlay S, Gregory S, Grimm N, Johnson S, McDowell W, Meyer J, Valett H, Webster J, Arango C, Beaulieu J, Bernot M, Burgin A, Crenshaw C, Johnson L, Niederlehner B, O'Brien J, Potter J, Sheibley R, Sobota D, Thomas S. Stream denitrification across biomes and its response to anthropogenic nitrate loading. *Nature* 452:202-206.

Naiman R, Bilby R. 1998. *River ecology and management: lessons from the Pacific coastal ecoregion.* Springer Verlag: New York.

Oeurng C, Sauvage S, Sanchez-Perez J. 2011. Assessment of hydrology, sediment and particulate organic carbon yield in a large agricultural catchment using the SWAT model. *Journal of Hydrology* 401:145-153.

Pawson R, Lord D, Evans M, Allott T. 2008. Fluvial organic carbon flux from an eroding peatland catchment, southern Pennines, UK. *Hydrol. Earth Syst. Sci.* 12:625-634.

Phillips J, Russell M, Walling D. 2000. Time-integrated sampling of fluvial suspended sediment: a simple methodology for small catchments. *Hydrological Processes* 14:2589-2602.

Raudkivi A. 1990. *Loose Boundary Hydraulics*. Pergamon Press.

Richardson J. 1992. Coarse particulate detritus dynamics in small montane streams of the southwestern British Columbia. *Can. J. Fish. Aquat. Sci.* 49: 337–346.

Rier S, Kuehn K, Francoeur S. 2007. Algal regulation of extracellular enzyme activity in stream microbial communities associated with inert substrata and detritus. *J. N. Am. Benthol. Soc.* 26(3):439–449.

Russo J, Fox J. 2012. The role of the surface fine-grained laminae in low-gradient streams: A model approach. *Geomorphology* In press. DOI: 10.1016/j.geomorph.2012.05.012

Rutherford J, Scarsbrook M, Broekhuizen N. 2000. Grazer control of stream algae: modeling temperature and flood effects. *Journal of Environmental Engineering* 126:331–339.

Schlesinger W. 2000. Carbon sequestration in soils: some cautions amidst optimism. *Agriculture, Ecosystems and Environment* 82:121-127.

Short R, Canton S, Ward J. 1980. Detrital processing and associated macroinvertebrates in a Colorado mountain stream. *Ecology* 61(4):728-732.

Sinsabaugh R, Osgood M, Findlay S. 1994. Enzymatic models for estimating decomposition rates of particulate detritus. *J. N. Am. Benthol. Soc.* 13(2):160-169.

Six J, Jastrow J. 2002. Soil organic matter turnover. In *Encyclopedia of Soil Science*, Lal R. (eds). Boca Raton, FL; 936–942.

Tank J, Rosi-Marshall E, Griffiths N, Entrekin S, Stephen M. 2010. A review of allochthonous organic matter dynamics and metabolism in streams. *J. N. Am. Benthol. Soc.* 29:118–146.

Thurman E. 1985. *Organic geochemistry of natural waters.* Nijhoff/Junk.

Toy T, Foster G, Renard K. 2002. *Soil erosion: Processes, predictions, measurements, and control.* John Wiley & Sons: New York.

Verardo D, Froelich P, and McIntyre A. 1990. Determination of organic carbon and nitrogen in marine sediments using the Carlo Erba NA-1500 analyzer. *Deep Sea Res. Part A* 37: 157–165.

Walling D, Collins A, Jones P, Leeks G, Old G. 2006. Establishing fine-grained sediment budgets for the Pang and Lambourn LOCAR catchments. *Journal of Hydrology* 330:126-141.

Webster J, Benfield E, Ehrman T, Schaeffer M, Tank J, Hutchens J, D'Angelo D. 1999. What happens to allochthonous material that falls into streams? A synthesis of new and published information from Coweeta. *Freshwater Biology* 41:687-705.

White P, Kalff J, Rasmussen J, Gasol J. 1991. The effect of temperature and algal biomass on bacterial production and specific growth rate in freshwater and marine habitats. *Microbial Ecology* 21:99-118.

Worall F, Reed M, Warburton J, Burt T. 2003. Carbon budget for a British upland peat catchment. *The Science of the Total Environment* 312: 133-146.

Yalin M. 1990. *Mechanics of Sediment Transport*. Pergamon Press.

Yoshimura C, Gessner M, Tockner K, Furumai H. 2008. Chemical properties, microbial respiration, and decomposition of coarse and fine particulate organic matter. *J. N. Am. Benthol. Soc.* 27:664–673.

2.9 TABLES AND FIGURES

Table 1. Inputs and parameterization of the sediment transport sub-model.

Parameters	Reach 1	Reach 2	Reach 3	Reach 4	Reach 5	Reach 6	Units
B	8.5	8.5	8.5	8.5	8.5	8.5	m
z	2	2	2	2	2	2	$m\ m^{-1}$
L	1687	1074	1233	1442	1229	2102	m
Δt	1800	1800	1800	1800	1800	1800	s
ρ	1000	1000	1000	1000	1000	1000	$kg\ m^{-3}$
g	9.81	9.81	9.81	9.81	9.81	9.81	$m\ s^{-2}$
S	$4.4*10^{-4}$	$4.4*10^{-4}$	$4.4*10^{-4}$	$4.4*10^{-4}$	$4.4*10^{-4}$	$4.4*10^{-4}$	$m\ m^{-1}$
τ_{crbank}	2	2	2	2	2	2	Pa
τ_{crbed}	0.17	0.17	0.17	0.17	0.17	0.17	Pa
ρ_{sbank}	1400	1400	1400	1400	1400	1400	$kg\ m^{-3}$
ρ_{sbed}	1100	1100	1100	1100	1100	1100	$kg\ m^{-3}$
H_{bank}	2.50	2.50	2.50	2.50	2.50	2.50	m
% Cover	74	74	74	74	74	74	%
C_{TCHigh}	$6*10^{-9}$	$7*10^{-9}$	$7*10^{-9}$	$7*10^{-9}$	$7*10^{-9}$	$7*10^{-9}$	$m^{1.5}kg^{-0.5}s^{-1}$
C_{TCLow}	$1*10^{-9}$	$2.7*10^{-9}$	$2*10^{-9}$	$2*10^{-9}$	$2*10^{-9}$	$2*10^{-9}$	$m^{1.5}kg^{-0.5}s^{-1}$
W_s	$3.5*10^{-4}$	$3.5*10^{-4}$	$3.5*10^{-4}$	$3.5*10^{-4}$	3.510^{-4}	$3.5*10^{-4}$	$m\ s^{-1}$
d_{sed}	$5.5*10^{-2}$	$5.5*10^{-2}$	$5.5*10^{-2}$	$5.5*10^{-2}$	$5.5*10^{-2}$	$5.5*10^{-2}$	m
c_1	0.22	0.22	0.22	0.22	0.22	0.22	-------
c_2	0.58	0.58	0.58	0.58	0.58	0.58	-------
c_3	$1X10^{-5}$	$3X10^{-6}$	0.002	0.014	$1X10^{-6}$	1.1	-------
FF	0.46	0.46	0.46	0.46	0.46	0.46	gg^{-1}

Table 2. Inputs and parameterization for the in-stream carbon model.

Parameters	Values	Units
$C_{T\ initial}^{(A)}$	1.8	gC 100gOM^{-1}
$C_{F\text{-}Bank}^{(A)}$	1.6	gC 100gOM^{-1}
$C_{Anoxic}^{(A)}$	1.8	gC 100gOM^{-1}
$C_{F\text{-}SOM}^{(A)}$	1.8	gC 100gOM^{-1}
$C_{Dep}^{(A)}$	1.8	gC 100gOM^{-1}
$C_{Algae}^{(B)}$	41	gC 100gOM^{-1}
$C_{det\text{-}leaf}^{(B)}$	50	gC 100gOM^{-1}
$C_{det\text{-}C\text{-}SOM}^{(A)}$	4	gC 100gOM^{-1}
$\rho_{s\ algae}^{(B)}$	1100	kg m^{-3}
$POC_{fines\ initial}^{(A)}$	1527	kgC
$P_{col}^{(C)}$	1*10^{-4}	kgC m^{-2} d^{-1}
$P_{max}^{(Bav)}$	2.4*10^{-3}	kgC m^{-2} d^{-1}
$I_k^{(B)}$	230	µmol m^{-2} s^{-1}
$T_{min}^{(B)}$	5	^{o}C
$T_{opt}^{(B)}$	20	^{o}C
$T_{max}^{(B)}$	30	^{o}C
$P_{sat}^{(B)}$	2.5*10^{-3}	kgC m^{-2}
$P_{resp}^{(C)}$	0.13	d^{-1}
$Pk_{resp}^{(B)}$	1.05	------
$T_{ref}^{(B)}$	20	^{o}C
$\tau_{cr\ algae}^{(C)}$	0.35	Pa
$d_{Bio}^{(B)}$	5*10^{-3}	m
$SC_{Detritus}^{(B)}$	1.6*10^{-2}	kgC m^{-2}
$DEC_{B\text{-}SOM}^{(Bav)}$	3*10^{-5}	d^{-1}
$DEC_{C\text{-}Algae}^{(Bav)}$	2.6*10^{-3}	d^{-1}
$DEC_{B\text{-}Algae}^{(Bav)}$	1.3*10^{-3}	d^{-1}
$DEC_{C\text{-}LD}^{(Bav)}$	1.5*10^{-2}	d^{-1}
$DEC_{Med\text{-}LD}^{(Bav)}$	2.6*10^{-3}	d^{-1}
$DEC_{B\text{-}LD}^{(Bav)}$	1.3*10^{-3}	d^{-1}

$^{(A)}$ = Parameter measured or estimated in study
$^{(B)}$ = Parameter obtained from literature (^{Bav} denotes an average literature value)
$^{(C)}$ = Calibration Parameter.

Table 3. Statistical results for (a) the sediment transport model and (b) in-stream carbon model.

(a) Sediment Transport Model	% Diff	R^2
Calibration	2.52	0.73
Validation	-20.8	0.87
Total	-2.2	0.72
(b) POC Model	% Diff	R^2
Calibration	8.79	0.94
Validation	-1.61	0.95
Total	7.07	0.94

Table 4. (a) Sediment and (b) carbon budgets seasonally averaged for the five year simulation period. *t* denotes metric tonnes. Abbreviations are found in the "List of parameters"

(a)	Winter (t/season)	Spring (t/season)	Summer (t/season)	Fall (t/season)	Annual Total (t/y)
SY_{Bed}	100.4±50.8	57.9±22.4	23.8±17.4	77.8±61.9	259.9±96.7
SY_{Bank}	63.3±44.2	32±14.2	14.6±11.7	55.5±50.1	165.3±79.4
$SY_{Uplands}$	125.8±109.2	105±99.8	20.8±20.8	180.1±245.2	431.8±297.2
(b)	Winter (tC/season)	Spring (tC/season)	Summer (tC/season)	Fall (tC/season)	Annual Total (tC/y)
CY_{Bed}	3.2±1.7	1.7±1.0	0.8±0.6	2.6±1.9	8.2±3.6
$CY_{B\text{-}SOM}$	1.6±0.8	1.0±0.4	0.4±0.3	1.3±1.1	4.4±1.6
$CY_{B\text{-}Algae}$	1.5±1	0.7±0.6	0.4±0.3	1.2±1	3.8±2.1
$CY_{B\text{-}LD}$	$3*10^{-5}$±$1*10^{-5}$	$3*10^{-5}$±$1*10^{-5}$	$2*10^{-5}$±$1*10^{-5}$	$3*10^{-5}$±$3*10^{-5}$	$1*10^{-4}$±$4*10^{-5}$
$CY_{Upland\text{-}SOM}$	2.1±1.7	1.9±1.8	0.4±0.4	3.3±4.4	7.6±5.1
CY_{Banks}	0.9±0.6	0.5±0.2	0.2±0.2	0.9±0.8	2.6±1.2

Table 5. Total annual POC yields delineated for each carbon source

Carbon Source	2006 (tC y^{-1})	2007 (tC y^{-1})	2008 (tC y^{-1})	2009 (tC y^{-1})	2010 (tC y^{-1})
$CY_{B\text{-}SOM}$	6.0	3.3	4.2	6.2	2.4
$CY_{Uplands\text{-}SOM}$	16.1	2.7	6.5	7.8	5.1
$CY_{B\text{-}Algae}$	3.5	2.7	3.9	7.4	1.8
$CY_{B\text{-}LD}$	$1.3*10^{-4}$	$7.6*10^{-5}$	$7.9*10^{-5}$	$1.6*10^{-4}$	$6.7*10^{-5}$
CY_{Banks}	4	1.7	2.3	3.7	1.2
CY_{T}	29.5	10.3	16.9	25.0	10.5

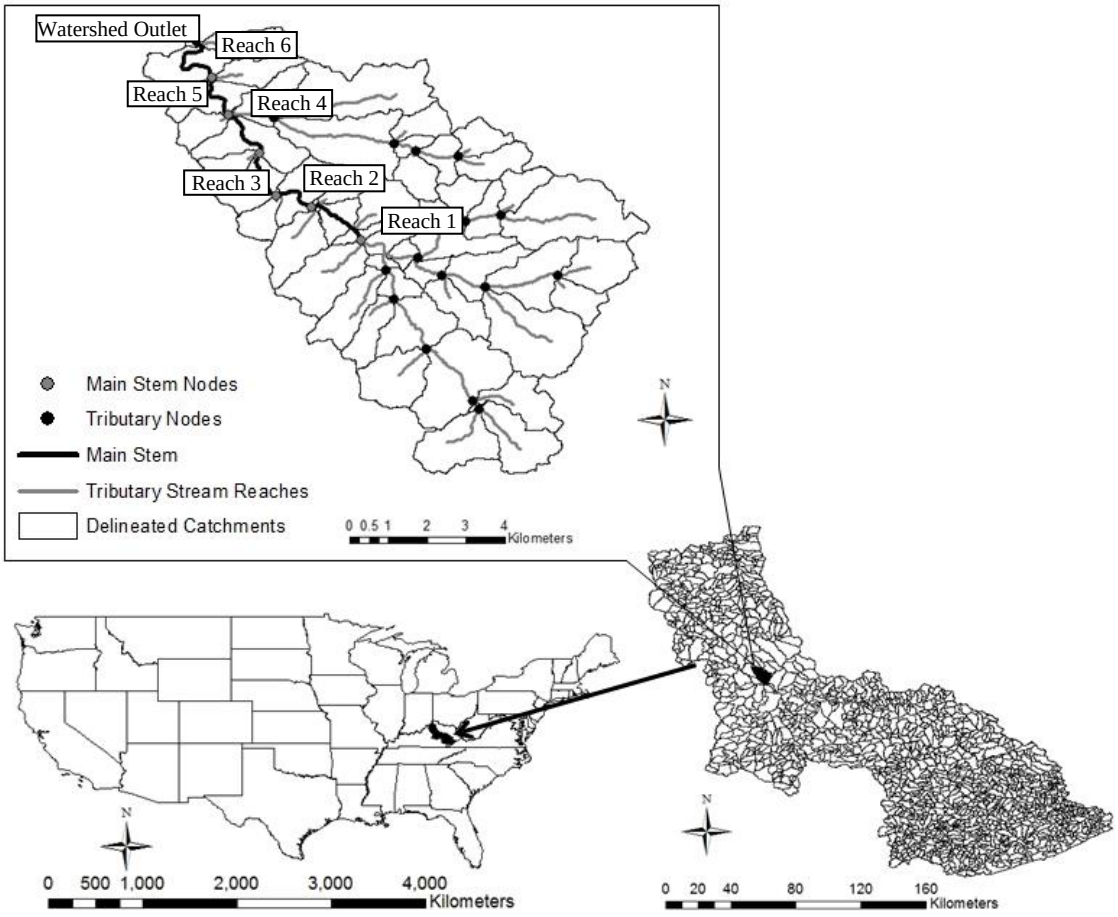

Figure 1. The Upper South Elkhorn watershed (61.8 km^2) located within the Kentucky River Basin, U.S.A.

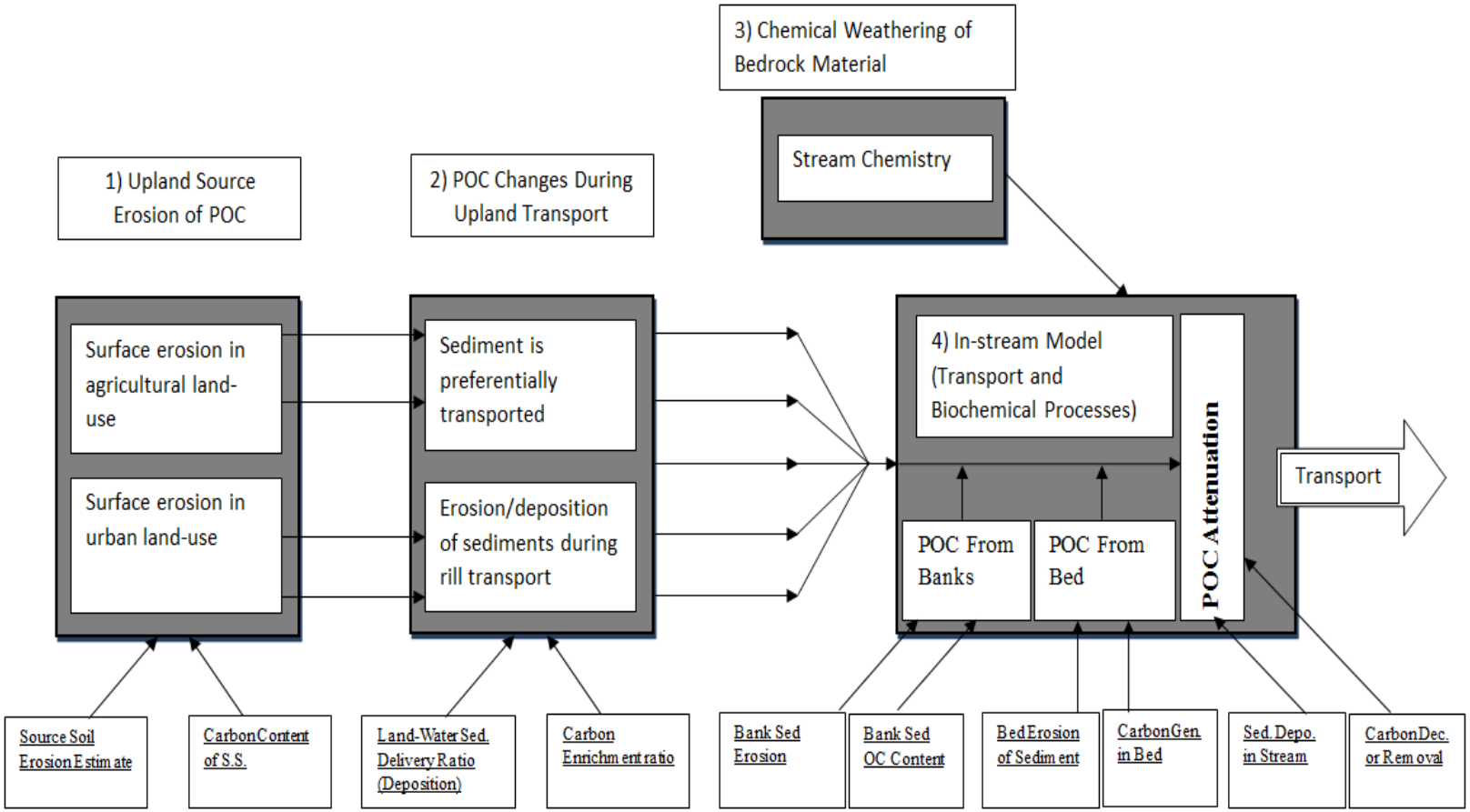

Figure 2. Modeling framework for analysis of POC fate and transport at a watershed scale.

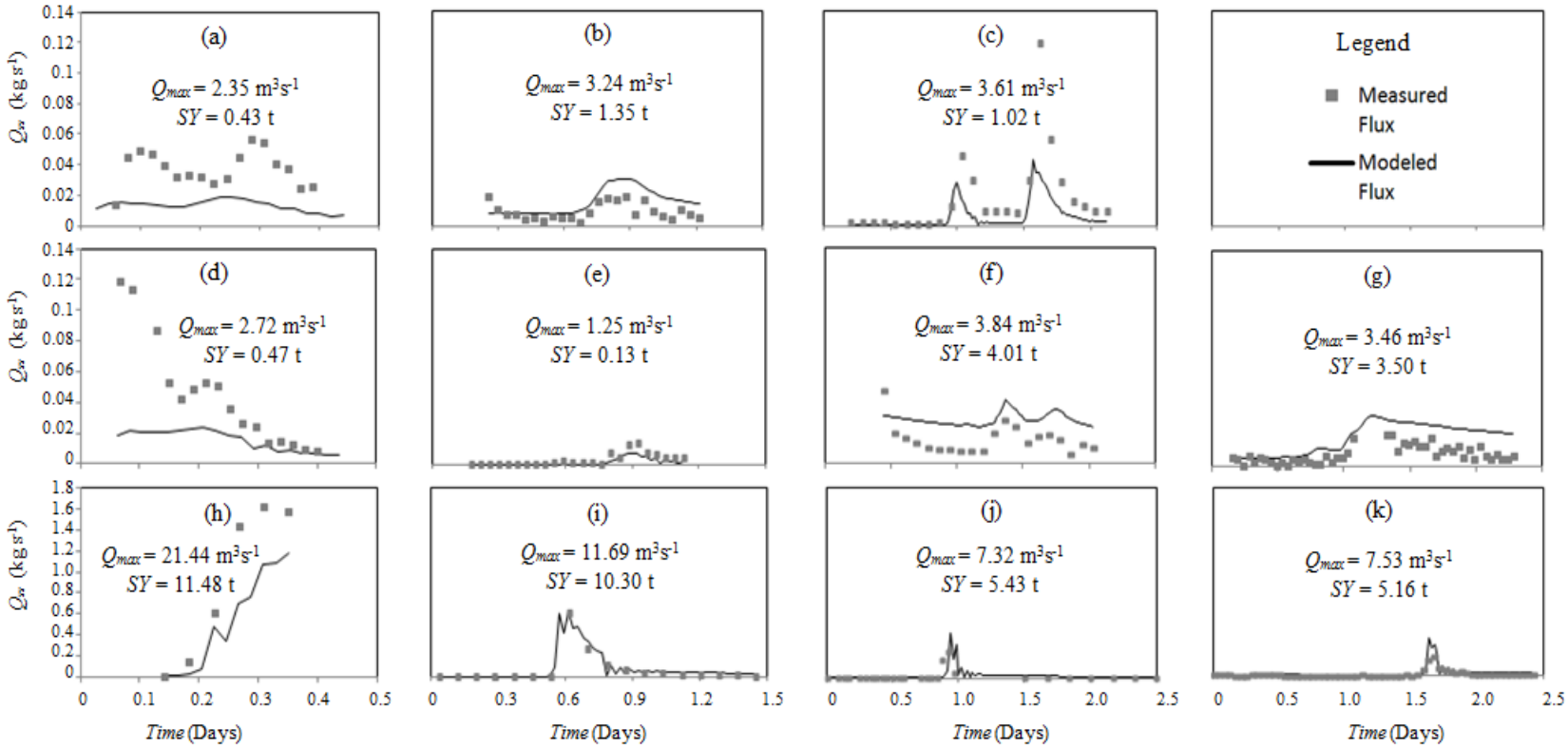

Figure 3. Model Performance: (a-d) Depict calibration results for low flows and moderate events. (e-g) Depict validation for low flows and moderated events. (h-j) Depict calibration for high flow events. And (k), depicts validation for high flow events.

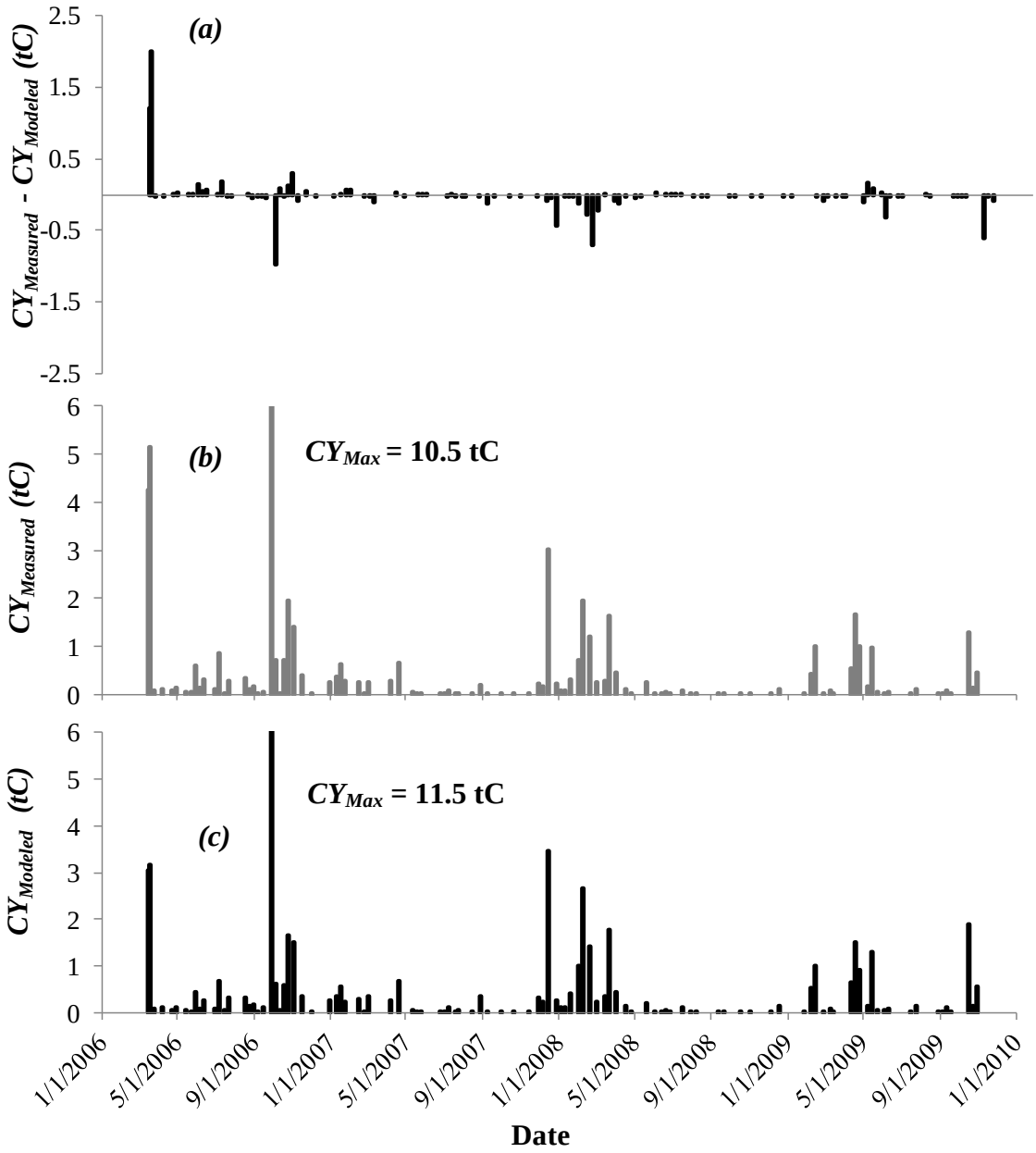

Figure 4. (a) Residuals of weekly *CY*, (b) measured transported organic carbon yield per event and (c) modeled transported organic carbon yield per event.

(a)

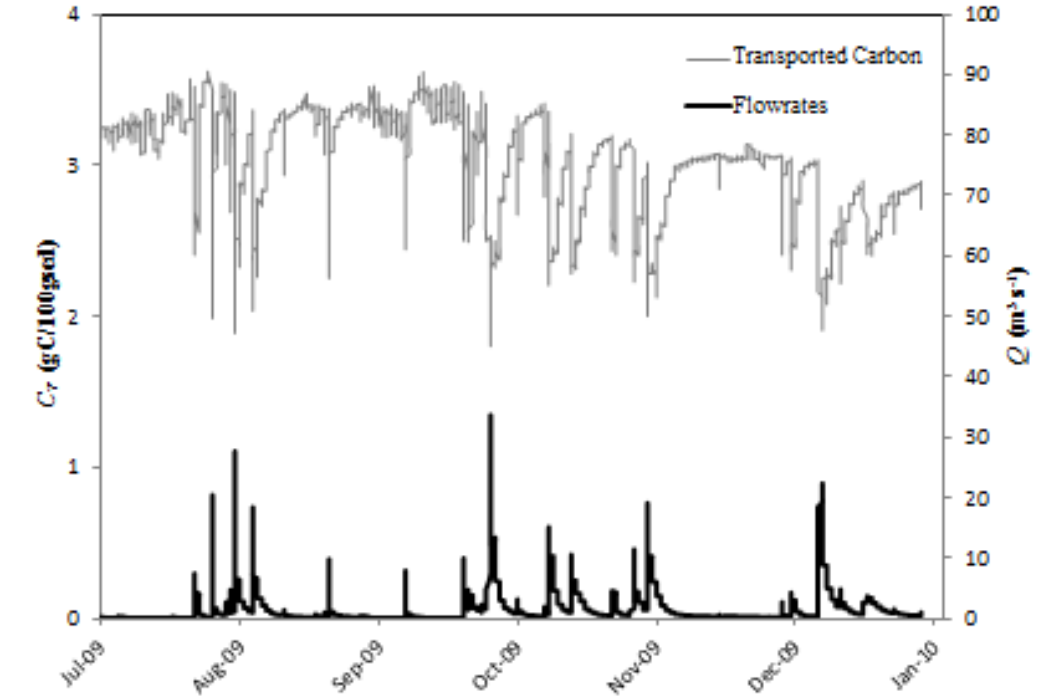

(b)

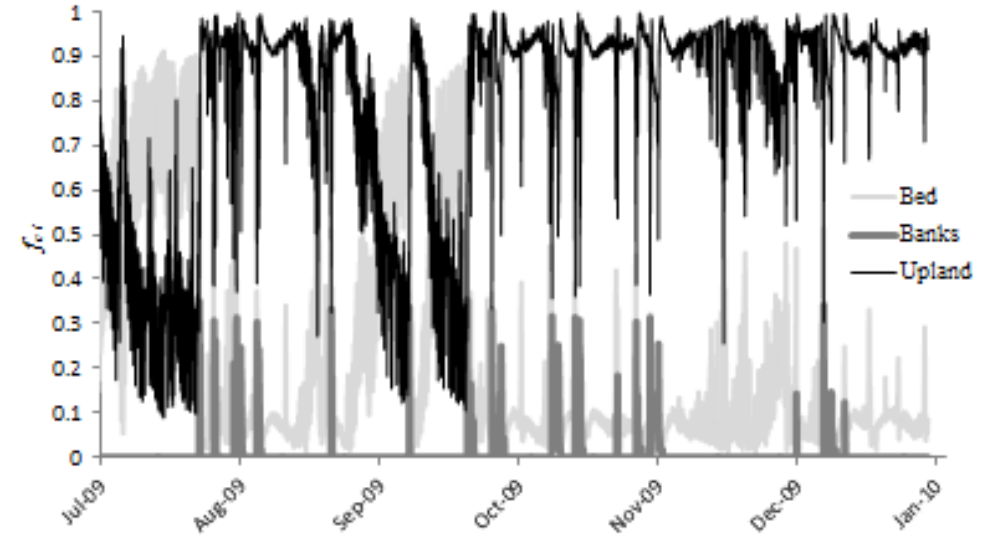

Figure 5. (a) c_T and (b) f_{ci} for 2009.

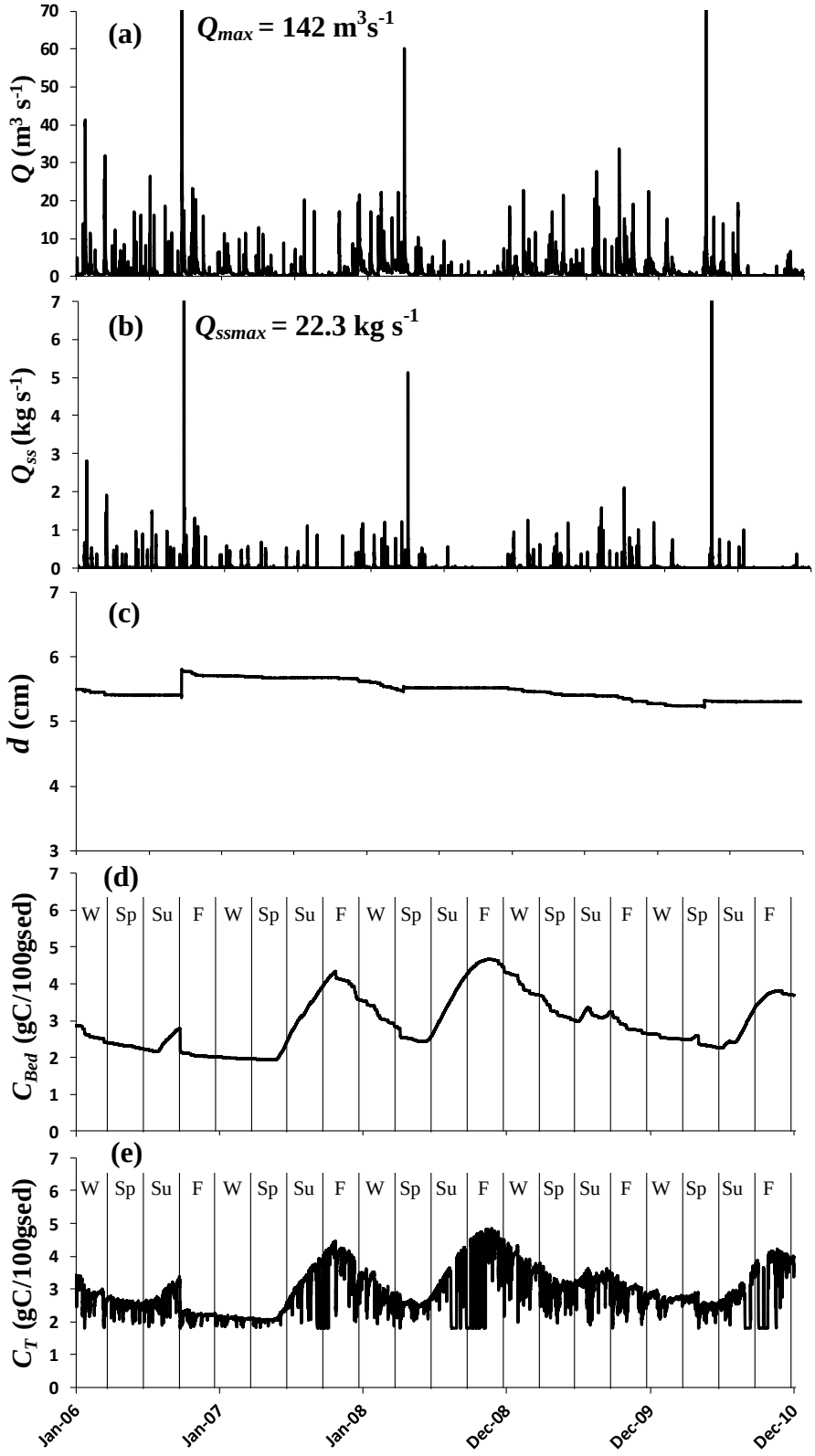

Figure 6. (a) Streamwater discharge, (b) sediment discharge, (c) streambed depth, (d) streambed carbon, and (e) transported carbon over the five year simulation period.

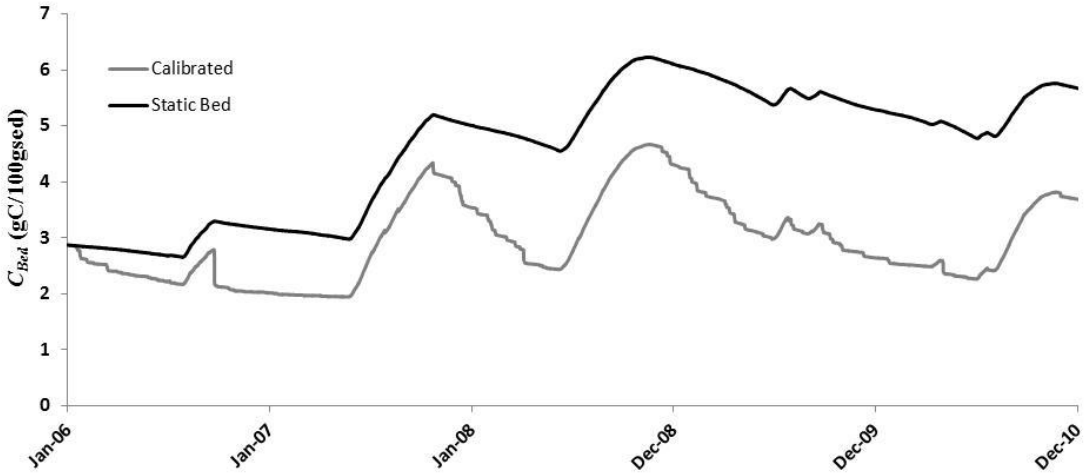

Figure 7. Calibrated and static bed conditions for the in stream POC model.

Copyright © William Isaac Ford III 2014

Chapter 3: Control of the SFGL on the transported FPOC Statistical Distribution

Adapted with permission from Ford, W., Fox, J. 2014. Benthic control on the statistical distribution of transported sediment carbon in a low-gradient stream. *Journal of Hydrology*. In Press.

Copyright © 2014 Elsevier

3.1 SUMMARY

Results from a numerical model that simulates particulate organic carbon source, fate and transport were used to generate the statistical distribution of transported sediment carbon in a low-gradient, agriculturally-impacted stream over a five-year model simulation. Results suggest that the statistical distribution of transported sediment carbon is Gamma distributed (RMSEA=0.066) for the low-gradient stream. The distributional form of transported sediment carbon is governed by seasonal variability of temporarily stored benthic carbon and the relative contributions of benthic, bank and upland carbon sources. Results of the study suggest that shape and skew of the Gamma distribution are governed by biological activity (i.e., autochthonous production and decomposition) of the streambed. Analysis was performed to examine how field sampling factors, including flow conditions during sampling, sampling frequency, and the sampling temporal domain including event, seasonal and annual variability, capture the statistical distribution of transported sediment carbon. Contrary to conventional wisdom, sampling flow conditions and sampling frequency showed little impact on the sampled distribution of transported sediment carbon, which reflects the amalgamation of streambank and upland carbon sources on the stream bed in this low-gradient stream. Annual variability, i.e., wet and dry years, and seasonal variability were needed to adequately capture the statistical distribution of transported sediment carbon, which reflects the stochastic nature of the hydrologic regime annually and the seasonal variability of biological processes. The results provide a testable hypothesis, and a sampling design approach, for the statistical distribution of transported sediment carbon in low-gradient systems where benthic biological processes are prominent.

3.2 INTRODUCTION

Organic carbon associated with fine sediment particles and sediment aggregates is now recognized to promote benthic carbon cycling at local stream scales, fuel heterotrophic bacteria that can transform and remove nutrients from the streamwater, and have significant implications for carbon budgeting at regional and global scales (Arango et al., 2007; Cole et al., 2007; Arango and Tank, 2008; Battin et al., 2009; Alvarez-Cobelas et al., 2010; Tank et al., 2010; Akamatsu et al., 2011; Findlay et al., 2011; Newcomer et al., 2012; Ford and Fox, 2014). However, recent literature suggests that reliable estimates of sediment carbon in streams is lacking, and a number of studies point to the need for transported sediment carbon (gC $100gSed^{-1}$) data to help reduce uncertainty in carbon budget assessments and to predict the composition of benthic carbon in downstream river reaches (Dalzell et al., 2005; Cole et al, 2007; Battin et al., 2009; Alvarez-Cobelas et al., 2010; Akamatsu et al., 2011). Of particular recent interest are streams that are low-gradient and agriculturally-impacted in which riparian canopy removal and high nutrient inputs from fertilizers promote benthic autotrophic production, and low stream and hillslope gradients promote pronounced benthic sediment storage (Walling et al., 2006; Battin et al., 2009; Russo and Fox, 2012; Ford and Fox 2014). Low-gradient, agriculturally-impacted streams are now recognized to play a dominant role in freshwater carbon cycling and associated downstream water quality due to the net large land masses they cover and their high nutrient loads that promote in-stream carbon cycling (Alexander et al., 2008; Mulholland et al., 2008; Griffiths et al., 2012). In this paper, we focus on analyzing transported sediment carbon, symbolized here as C_T, over a five year time period in a low-gradient, agriculturally-impacted stream. Specifically, we examine the statistical distribution of C_T exported from the watershed over the five-year period and investigate the importance of field sampling design factors on representing the statistical distribution of C_T.

While the statistical distributions of water (Nash, 1994; Segura et al., 2013) and sediment (Parker and Troutman, 1989; Benkhaled et al., 2013) transported in streams have been heavily investigated historically in hydrology research, less emphasis has been placed on the statistical distribution of C_T. The body of knowledge surrounding the

statistical distribution of C_T has tended to center around transported carbon quality in small, steep mountainous streams due to the fact that steep systems can export high carbon loads over relatively short distances (Masiello and Druffel, 2001). Research of steep streams over the past decade has tested the hypothesis that C_T follows a bimodal distribution in which sources of carbon enriched biogenic sediments, i.e., surface soils with relatively short residence times, are activated during low flows, sources of carbon depleted geogenic sediments, i.e., deep soils or bedrock, are mobilized during high flows, and in-stream sources are neglected as a result of low storage and autochthonous production (Masiello and Druffel, 2001; Lyons et al., 2002; Gomez et al., 2003; Coynel et al., 2005; Leithold et al., 2006; Hilton et al., 2008; Blair et al., 2010; Gomez et al., 2010; Hatten et al., 2012). A definition sketch of C_T in small mountainous rivers is provided in Figure 1a. Theoretically, C_T will be unimodal if either a single carbon source is reflected (e.g., biogenic source), heterogeneous source mixing occurs under different flow regimes, or if two carbon sources have similar carbon concentrations. A bimodal distribution is expected when different flow regimes preferentially erode and transport a unique source such as high flows erode and transport deep geogenic sources while low flows erode and transport surface soils. To our knowledge, no studies have examined the statistical distribution of C_T in low-gradient, agriculturally-impacted streams despite the fact that numerous studies have measured C_T data and calculated statistical moments, i.e., mean, variance, skewness, and kurtosis, for low-gradient streams (Munson and Carey, 2004; Dalzell et al., 2005; Dalzell et al., 2007; Schuster et al., 2008; Oeurng et al., 2011; Owens and Shipitalo, 2011; Griffiths et al., 2012).

It is recognized that the statistical distribution of C_T in streams will reflect the carbon sources and their relative contributions to the fluvial carbon load. Further, the C_T distribution reflects both carbon quantity and carbon quality because carbon sources have different levels of bioavailability and organic matter compositions. For lowland systems, newly generated benthic carbon is a higher quality source than terrestrial carbon as a result of higher energy per unit mass and less recalcitrant carbon-compounds such as lignin and cellulose (Thorp and Delong, 2002; Lane et al., 2013). We hypothesize for low-gradient systems that a unimodal distribution will exist because algal biomass varies seasonally and will be integrated with bank and upland carbon in the streambed as

suggested in Figure 1b. The lowland system transports heterogeneous source contributions of upland, bank and benthic carbon in which the benthic source is an amalgamation of previously deposited and newly generated carbon (Ford and Fox, 2014). A unimodal C_T distribution is further promoted when carbon distributions of bank, upland and bed sources overlap. The transport of soil and streambank originated carbon and its imprint upon the C_T distribution in low-gradient streams is expected to be analogous to steep streams in that carbon rich surface sediments will be eroded from the uplands during moderate hydrologic events while depleted, lower quality carbon from deeper soils and streambank sources will be transported during high magnitude hydrologic events (Toy et al., 2002; Jacinthe et al., 2009; Kim et al., 2010). However, the impact of temporarily stored and generated streambed sediment carbon upon the statistical distribution of C_T is less predictable as streambed carbon is expected to show variability across numerous time scales (Cole et al., 2007; Battin et al., 2009; Griffiths et al., 2012; Ford and Fox, 2014). The make-up of streambed sediment carbon will reflect recent hydrologic events that deposit sediment to the streambed, heterotrophic bacterial decomposition and autotrophic production of organic carbon that varies seasonally in the streambed, and longer-term hydrologic variability that has been shown to impact streambed carbon annually (White et al., 1991; Rutherford et al., 2000; Ford and Fox, 2014). The complexity added to carbon transport in low-gradient, agriculturally-impacted streams *via* the streambed source and the instantaneous nature of C_T sampling suggests the need for estimating the statistical distribution of C_T using population estimates that encompass event, seasonal, and annual variability.

Due to the fact that the statistical distribution of C_T has not been examined in low-gradient agriculturally-impacted streams, questions remain regarding an appropriate field sampling routine to estimate the statistical moments of C_T (e.g., statistical mean, variance, skewness, and kurtosis). Review of past literature suggests that few studies have specifically focused on measuring C_T, however numerous studies measure C_T to support broader environmental studies, e.g. particulate organic carbon (POC) flux estimates under varying flow conditions, and foodweb studies. Sampling protocol for C_T varies widely; however factors including flow conditions, temporal domain and sampling frequency are considered important in most studies. With regard to flow conditions,

recent studies have placed a heavy emphasis on C_T during high flows (Masiello and Druffel 2001; Worall et al., 2003; Dalzell et al., 2005; Dalzell et al., 2007; Oeurng et al., 2011; Owens and Shipitalo, 2011) with only a few studies assessing the importance of C_T at low flows (e.g. Griffiths et al., 2012). The temporal domain also has been varied with multi-year and single-year datasets used equally to estimate C_T (Cuffney and Wallace, 1988; Lyons et al., 2002; Gomez et al., 2003; Worall et al., 2003; Sharma and Rai, 2004; Leithold et al., 2006; Aldrian et al., 2008; Zhang et al., 2009; Oeurng et al., 2011; Owens and Shipitalo, 2011). Further, some studies have used sampling routines from a single season while others sample during multiple seasons (Carey et al., 2005; Dalzell et al., 2005; Guo and Macdonald, 2006; Waterloo et al., 2006; Pawson et al., 2008; Galy et al., 2008). Finally, sampling frequency has been widely inconsistent with samples obtained daily to monthly (Sharma and Rai., 2004; Guo and Macdonald 2006; Waterloo et al., 2006; Aldrian et al., 2008; Zhang et al., 2009; Oeurng et al., 2011).

Our objective was to examine the statistical distribution of C_T in a low-gradient stream and thereafter test how presumed important sampling factors capture the overall C_T distribution. To represent the C_T population, we model C_T continuously over a five year time period for a low-gradient, agriculturally-impacted stream using a watershed-scale model that couples carbon source, fate and transport. We considered that a watershed-scale model was needed to simulate the population of C_T due to the complexity of upland, streambank, and streambed carbon sources that can be reflected in C_T *via* event, seasonal and annual scales (Alvarez-Cobelas et al., 2010; Ford and Fox, 2014). Using results of the continuous model simulation, the C_T statistical distribution was examined using frequency analysis and a suite of probabilistic models that were tested to find the best statistical fit. We then perform a statistical analysis to assess how sampling flow conditions, temporal domain and sampling frequency impact the distribution of C_T. The factors are examined by systematically drawing subsets of the C_T population from the continuous numerical model results, fitting the probability model to the C_T population subsets, and statistically comparing the statistical C_T distributions from the subsets to the parent C_T distribution from the entire five year population.

3.3 METHODS

In the following sections, the methods are described for generating the parent statistical distribution of C_T, testing presumed important sampling factors, fitting a probabilistic model to each histogram and non-parametric statistical methods used to compare the parent distribution to the sub-sampled distributions. The parent statistical distribution of C_T was generated using a watershed-scale numerical model that couples source, fate and transport over a five year time period for a low-gradient, agriculturally-impacted stream. The numerical model was calibrated and validated using an extensive longitudinal C_T dataset, the results of which were recently published in Ford and Fox (2014). The simulation was performed from 2006 to 2010 for the South Elkhorn Creek watershed (61.8 km^2), which is characterized by low stream and hillslope gradients, a biogeochemically active streambed, eroding streambanks, high nutrient loads and cohesive upland soils (Fox et al., 2010; Russo and Fox, 2012; Ford and Fox, 2014). A 30 minute temporal timestep and five year duration of the model was simulated in order to adequately represent the C_T population. The simulation timeframe was the same period as the calibration dataset. The model was not extended beyond the calibration timeframe as it included simulation of hydrologic events with various magnitudes, seasonal variability, and multiple wet and dry years as well as a year with an extreme storm event.

The South Elkhorn watershed (61.8 km^2) is located within the Kentucky River Basin, USA (see Figure 2). Elevations range from 254 to 317 meters above sea level and average streambed gradients (4.4×10^{-4} m m^{-1}) are low, promoting pronounced fluvial storage. The stream channel is bedrock controlled, and evidence of erosion from the cohesive banks was found to exist based on visual observation of fluvial undercutting and scars. Land cover is predominantly agriculture (57%), predominantly pasture and rangeland, and urban (43%) which promote high nitrogen and phosphorus levels in the stream associated with fertilizer applications on upland hillslopes and weathering of underlying Ordovician limestone. NO_3 concentrations in the watershed ranged from 0.23 to 5.9 mgN/L-NO_3 and dissolved phosphorus ranged from 0.1 to 0.42 mgP/L. Hence nutrients were assumed non-rate limiting since accepted thresholds for rate-limiting conditions are 0.04mgN/L and 0.03mgP/L for DIN and DP, respectively (Dodds et al.,

2002). The present approach should be utilized with caution for systems where nutrients are potentially rate-limiting. In this case, additional sub-models may be needed to account for these limitations.

3.3.1 Continuous Model of C_T

The continuous process-based numerical model for C_T couples previously published sediment transport and benthic algal biomass numerical models and uses empirical data from the South Elkhorn for parameterization and calibration including flowrate, water temperature, light intensity, C_{upland}, C_{bank}, and C_T (Rutherford et al., 2000; Russo and Fox, 2012; Ford and Fox, 2014). The equations for sediment transport provide the basis for a C_T model since carbon is one component of transported sediment. The mass balance of sediment was modeled as

$$SS_i^j = SS_{i-1}^j + E_i^j{}_{Bank} + E_i^j{}_{Bed} - D_i^j + Q_i^j{}_{SSin}\Delta t - Q_i^j{}_{SSout}\Delta t \quad , \tag{1}$$

where, (i) represents the time step, (j) represents the reach identifier, SS (kg) is sediment in the water column, E (kg) is the erosion from streambank and streambed sources, D (kg) is deposition to the bed, Q_{SS} (kg s^{-1}) is suspended sediment transported into and out of the modeled reach, and Δt (s) was the time step. Source erosion in the South Elkhorn was modeled to be limited by shear resistance, the transport carrying capacity of the fluid, and supply of the erosion source (Russo and Fox, 2012). These processes are modeled for both the streambed and the streambanks as

$$E_i^{jI} = \min\left[k\left(\tau_i^j{}_f - \tau_{cr}^I\right)\rho_S^I SA^I \Delta t, T_i^j{}_C - SS_{i-1}^j, S_{i-1}^j{}^I\right], \tag{2}$$

where, (I) represents the sediment source, k (m^{-1}) is the erodibility coefficient, τ_f (Pa) is the shear stress of the fluid at the centroid of the erosion source, τ_{cr} (Pa) is the critical shear stress of the erosion source, ρ_s (kg m^{-3}) is the bulk density of the sediment source, SA (m^2) is the surface area of the erosion source, T_c (kg) is the transport carrying capacity and S (kg) is the sediment supply. The transport capacity of the fluid estimates the energy available to transport sediments and was estimated using a Bagnold-like expression (see Russo and Fox, 2012). Sediment deposition to the streambed was modeled as

$$D_i^j = \frac{W_s \Delta t}{k_p H_i^j}\left[SS_{i-1}^j - T_i^j{}_C\right], \tag{3}$$

where W_s was the sediment settling velocity (m s^{-1}), k_p was the concentration profile coefficient, and H (m) was the water column height. The d_{50} (median particle diameter) of sediment aggregates transported in-stream is fairly homogenous across the simulation period, as shown in Fox et al. (2013), hence a single settling velocity was used in the simulation. The sediment simulation was calibrated utilizing collected suspended sediment samples at the watershed outlet and the assumption that streambed depth is in a long-term equilibrium, based on eight years of visual observations in the watershed. Calibration data was collected utilizing ISCO automated grab samplers for events of varying magnitudes and durations (Russo and Fox, 2012; Ford and Fox, 2014). Output from the model included sediment loads as well as sediment fractions from bank, bed, and upland sources.

The C_T model was formulated to simulate inputs and outputs of sediment carbon, erosion/deposition of carbon in the streambed, fixation of CO_2 into organic carbon, and decomposition by heterotrophs. C_T was estimated continuously as

$$C_{i\ T}^{j} = C_{i\ Bed}^{j} f_{i\ Bed}^{j} + C_{Upland} f_{i\ upland}^{j} + C_{Banks} f_{i\ Banks}^{j} \quad (4)$$

where C is specified for each carbon source and f is the fraction of total sediment originating from each source. f was calculated for each time step and reach using results of Equation (1), and were then input to Equation (4). Special emphasis was placed on modeling the streambed carbon source since its signature can vary in time. C of the streambed, C_{bed}, was modeled as

$$C_{i\ Bed}^{j} = \frac{POC_{i\ Bed}^{j}}{S_i^j} \times 100 \text{ (gC/100gSed)}, \quad (5)$$

where POC_{Bed} is the mass of particulate organic carbon in the bed. POC_{Bed} was budgeted continuously to originate from in-stream algal production, soil organic matter and decomposing leaf detritus. For example, the algal pool was modeled as

$$POC_{i\ Bed-Algae}^{j} = POC_{i-1\,Bed-Algae}^{j} + A_{i\ Algae}^{j} - DEC_{i\ Bed-Algae}^{j} POC_{i-1\,Bed-Algae}^{j} \Delta t - POC_{i\ Adj}^{j} \text{ (gC)}, \quad (6)$$

where A_{Algae} (kgC) represents epilithic algae accrual in the benthic layer, $DEC_{Bed\text{-}Algae}$ (s^{-1}) is the rate at which benthic algal POC is decomposed, and POC_{Adj} (kgC) is the mass of the POC from algae lost due to erosion and deposition dynamics in the active benthic

layer (Ford and Fox, 2014). A_{Algae} is limited by temperature, light availability, and biomass population-level consequences (Rutherford et al., 2000). Microbial decomposition rates of POC were assumed to vary proportionally with heterotrophic bacterial growth, and subsequently as a function of temperature (White et al., 1991). Mass balances similar to Equation (6) were performed for soil organic matter and leaf detritus carbon in the streambed as described in Ford and Fox (2014). Russo and Fox (2012) and Ford and Fox (2014) detail inputs and parameterization procedures for the sediment transport and POC submodels, respectively. To help calibrate the C_T sub-model we collected transported sediment samples at the watershed outlet weekly for approximately five years. *In situ* sediment trap samplers were used since they provide a representative spatial and temporal averaged measure of the elemental sediment carbon signature during the duration of its field deployment (Phillips et al., 2000). Samples were analyzed using a Costech 4010 elemental analyzer. Average standard deviation for the sample of the elemental standard (acetanilide) was 0.82% for percent carbon. Our dynamic model of the benthos and sediment transport processes coupled with the aforementioned calibration methods allowed us to account for the disconnectivity in sediment delivery from upland catchments and temporary retention in the main-stem (Fryirs, 2013). The model was calibrated to ensure that between-event, seasonal and annual variability was well represented as described in Ford and Fox (2014).

Sediment carbon eroded and transported from upland soils, C_{Upland}, can vary spatially across a hillslope or with depth in the soil column. Similarly, bank sediment carbon, C_{Bank}, can vary spatially within a watershed based on bank height, flood history and land-use. To better capture uncertainty of sediment carbon sources beyond that of previous modeling efforts, upland soil organic carbon (SOC) and bank sediment variability were included. The descriptive statistics, e.g., mean and standard deviation, of the upland and bank sediments were estimated using collected and published data (NRCS, 2006; Fox et al., 2010).

C_{upland} represents the ratio of the SOC standing stock to mass of sediment in a given control volume. The standing stock of upland SOC (kg m^{-3}) was estimated using the published Natural Resources Conservation Service (NRCS) SOC data which has been

rasterized on a 2 minute grid cell and provides organic carbon content and bulk density with depth (NRCS, 2006). The SOC stock to a depth, *y*, is given as

$$SOC_{Stock} = \int_0^y \rho_B SOC(y)dy \,, \tag{7}$$

where, ρ_B is the bulk density of the soil, and *SOC(y)* is the equation describing the organic carbon profile (gC gsed^{-1}). Maximum erosion depth in the uplands was set to 10 cm, which reflects the maximum rill erosion depth for the South Elkhorn. SOC profiles were parameterized using organic matter profiles in the region and are provided in Table 1 (MacDonald et al., 1983). Spatial heterogeneity of C_{Bank}, was measured at five cross sections (three main stem, and two tributary) on three occasions in 2007 and 2008 (Fox et al., 2010). Vegetation was scraped off the bank surface and approximately 20 grams of sample were collected. Samples were collected at 15, 30 and 45 cm above the water surface at each of the five sampling locations. For each site, the 15, 30 and 45 cm samples were pooled to create a homogenized, or average, value of C_{Bank}. Samples were analyzed using a Costech 4010 elemental analyzer. Average standard deviation for the sample of the elemental standard (acetanilide) was 0.82% for percent carbon.

Accounting for carbon variability also relied on estimating POC source mixing during transport (Fox and Papanicolaou, 2008). It is reasonable to assume both C_{Bank} and C_{Upland} transported in the stream can be approximated by normal distributions, since, by the central limit theorem (Olkin et al., 1994), the transported signature will be indicative of a heterogeneous mixture of carbon erosion from a large number of sites (*n*) that amalgamate in the stream channel. Thus, regardless of the parent distribution of C_{Bank} and C_{Upland} , the distribution of their mean, or amalgamated in-stream signature, can be approximated as

$$D(X_{bar})^K \rightarrow N(\mu_x^K, \frac{\sigma_x^{K\,2}}{n}) \,, \tag{8}$$

where, *K* is the source identifier (i.e., bank and upland carbon sources), $D(X_{bar})$ denotes the distribution of the mean, μ_x is the mean of the source population, σ_x is the standard deviation of the source population, and *n* is the number of sites from which a source is eroded. The term standard error of the mean ($\sigma_x/n^{1/2}$) was used to denote the standard deviation of the distribution of the mean. As *n* goes to infinity, the variance goes to zero

and the mean can be used as a best approximation of the distribution. To approximate *n*, we assumed that the number of sites eroded for bank and upland soil carbon is approximately equal to the average mass of transported source carbon divided by the mass of the samples analyzed.

3.3.2 Statistical Analysis

The statistical analysis was conducted in three stages as follows: (1) A probabilistic model was selected and fit to the parent, 5 year C_T results using goodness-of-fit criteria and model parameters were estimated. (2) The probabilistic model was fit separately to the C_T results from each sampling test described in Table 2 and model parameters and statistical moments were estimated. (3) Statistical results from the 28 sampling tests were compared to the parent 5 year probabilistic model using tests for non-normal populations.

In order to select and fit a probability model for C_T, a series of distributions were tested against the C_T distribution including the Gamma, Normal, Weibull and Lognormal distributions. The Gamma distribution was chosen as the statistical model to best represent C_T based on the results of the continuous model simulation because it is bounded at zero, has inherent skewness, and provided the best fit to the data. Choice of the Gamma distribution also had the advantage for future research in that it is a well-known model that is easy to use and is found in all major statistical modeling packages. The Gamma distribution has a density function of

$$f(x) = \frac{1}{\Gamma(k)\theta^k} x^{k-1} e^{-\frac{x}{\theta}}, \tag{9}$$

where, Γ was the gamma function, k was the shape parameter, θ was the scale parameter, and x was the variable to be modeled, in this case C_T. All parameters and variables must be greater than zero or else the density equals zero. Likewise, Γ was defined as

$$\Gamma(k) = (k-1)! \tag{10}$$

Since our C_T values have a minimum restriction of the carbon content of bank sediments, a surrogate function that shifts C_T close to zero was used as

$$g(C_T) = C_T - C_{T,\min}, \tag{11}$$

where, $C_{T,min}$ was the lowest bin value generated in a frequency analysis, or the lowest observed C_T value. Substituting $g(C_T)$ in Eqn (11) for x in Eqn (9), the frequency distribution for C_T is obtained as

$$f(g(C_T)) = \frac{1}{\Gamma(k)\theta^k} g(C_T)^{k-1} e^{-\frac{g(C_T)}{\theta}}, \quad (12)$$

After examining the parent statistical distribution of C_T, we performed a statistical analysis to assess how presumed important factors during sampling impact the sampled distribution of C_T. Tests were conducted for varying flow conditions, sampling frequencies and temporal domains as outlined in Table 2. Tests 1 through 8 were designed to investigate the importance of sampling across a range of flow conditions with Tests 1 through 4 representing low, moderate and high flows and Test 5 through 8 representing low and moderate flows only (Q<2.5 m^3s^{-1}, where Q is the volumetric flowrate). The high flow threshold was determined based on an understanding of sediment transport processes in the system, in which flows above 2.5 m^3s^{-1} have a higher energy to entrain and transport sediments and more pronounced connectivity with the uplands (Russo and Fox, 2012). Tests 9 through 16 were designed to investigate the importance of single year (i.e., a dry year in 2008 in tests 9 through 12 and a wet year in 2009 in tests 13 through 16) versus multi-year sampling tests. Tests 17 through 28 were designed to investigate the samples obtained during specified seasons with three tests specified for each season. Winter was defined as Dec. 22-March21st, spring was defined as March 22nd to June 21st, summer was defined as June 22nd to September 21st, and fall was defined as September 22nd to December 21st. All investigations included variation of sampling frequency. For example, weekly, biweekly, fortnightly (i.e., once every two weeks), and monthly sampling frequencies were tested for the total flow regime factor in tests 1, 2, 3 and 4, respectively.

For both the parent distribution and 28 subset test distributions, statistical analysis was used to develop histograms, fit Gamma model parameters and estimate statistical moments. Histograms for the parent distributions and each of the sampling test scenarios were generated using the readily available statistical software, *R (Version 2.15.0)*. For the parent distribution, 15 bins were used since over 80,000 data points were generated during the continuous simulation. For the 28 subset tests, bin sizes were selected in the

statistical software according to the Freedman-Diaconis rule, which establishes bin size as a function of sample size and interquartile range (Freedman and Diaconis, 1981). A minimum chi-squared estimation technique (Olkin et al., 1994), using the chi-square test statistic, was used to determine the optimum shape and scale parameters for the parent distribution and each of the 28 sampling tests. Randomization tests and the root mean square error of approximation (RMSEA) were used to assess goodness-of-fit between measured histograms and modeled distributions based on accepted metrics (Steiger, 2007; Hooper et al., 2008). For the parent distribution, the sample size was too large to perform a randomization test, thus only RMSEA was used. For randomization tests, Monte-Carlo simulations were performed to generate required statistical measures. Hypothesis testing, in which p-values generated from randomization tests were compared against a 0.05 significance level, suggested statistical equivalence if p-values exceed the significance level, contrary to the majority of statistical tests. RMSEA values less than or equal to 0.1 suggested sufficient model fit to the measured frequency distribution (Hooper et al., 2008). Using the optimum shape and scale parameters, mean, standard deviation, skewness, and excess kurtosis (normalizing for kurtosis of the normal distribution) were estimated for C_T as follows (Olkin, 1994)

$$E(C_T) = k\theta + C_{T,Min}, \tag{13}$$

$$Var(C_T) = k\theta^2, \tag{14}$$

$$Skew(C_T) = \frac{2}{\sqrt{k}}, \tag{15}$$

$$Kur(C_T) = \frac{6}{k}. \tag{16}$$

In order to assess the 28 tests in Table 2 against the C_T parent five year distribution, non-parametric statistical tests for non-normal populations were used. To test for equality of variances, Levene's test was used. The computed test statistic, denoted by *W*, is tested against an F distribution assuming a 5% significance level. To test for statistically identical distributions, the Mann-Whitney U test, or Wilcoxon rank sum test, was used assuming a 5% significance level. Although the Wilcoxon rank sum test doesn't explicitly test for differences in central measure of tendency, combining results of the Wilcoxon and Levene's tests allowed assessment of equality of the central measure of

tendency for two non-identically distributed datasets with statistically equivalent variances (EPA, 2006).

3.4 RESULTS

C_T is highly variable in the South Elkhorn Creek at low flows ranging from 2 to 5 gC100gSed^{-1} and C_T variability decreases towards a constant value of approximately 3 gC100gSed^{-1} as stream peak flow (Q_{pk}) increases (see Fig 3a). Instantaneous C_T over the simulation period shows high variability associated with hydrologic event, seasonal and annual temporal scales (see Fig 3b). Hydrologic event variability results in instantaneous C_T peaks on the order of 3 gC100gSed^{-1}. Seasonal variability shows longer-term temporal oscillations, albeit variable in magnitude annually, which tend to coincide with water temperature oscillations that reflect seasons (see Fig 3c). Reflection of temperature's seasonal variability in the C_T time-series is somewhat expected in the biologically active benthos since the algal pool is dependent upon light availability and temperature (Rutherford et al., 2000) and decomposition from the algal pool to the fine sediment carbon pool is a function of temperature (White et al., 1990; Ford and Fox, 2014). Intuitively, the result might suggest that temperature alone is a reliable predictor of C_T. However, we found that regression of C_T as a function of water temperature alone yielded poor correlation (R^2<0.2), which again reflects the overall complexity of the benthic and hydrologic controlled stream system and dynamic nature of coupled processes operating at event, seasonal and annual scales.

The model simulation over the five-year period showed that C_T is impacted by both the seasonality from temperature dependent algal growth and decomposition, and hydrologic variability operating at event and annual scales. High event variability of C_T can be attributed to short term variability in the flow regime in which low flows have available energy to erode the bed source while moderate and high flows receive heavy inputs from upland soils and scour the cohesive streambanks (Russo and Fox, 2012). Annual variability stems from the density and magnitude of hydrologic events during the growing season, i.e. late spring, summer and early fall (see Fig 3d), which in turn impact the accrual of algae in the benthic source. This is evidenced by the depleted C_T peak in

2009, a growing season with dense hydrologic activity, relative to 2008, a growing season with relatively dry hydrologic conditions.

Figure 4 compares the results of the five-year C_T frequency distribution to models of common probabilistic distributions including Gamma, Normal, Lognormal and Weibull. From visual inspection, it's evident that the Gamma probability and cumulative density functions are most closely aligned with the C_T data distributions. The Gamma model thus generates the best statistical fit for both the cumulative (CDF) and probability density functions (PDF). The Gamma distribution provides more flexibility through the shape (k) and scale (θ) parameters and subsequently provides the best RMSEA values for both the CDF and PDF.

Figure 4 also displays the frequency histogram of C_T for the five year simulation as well as the Gamma model fit. With regards to the histogram, the peak, or mode, of the data occurred in the 2.6-2.8 $gC100gSed^{-1}$ bin. The left tail of the histogram ranged from 1.8-2.6 $gC100gSed^{-1}$ while the right tail ranged from 2.8-4.9 $gC100gSed^{-1}$. The histogram is characterized by a steep left-hand tail, a long right-hand tail and slight skew, which are indicative of a Gamma distribution (Olkin et al., 1994). A Gamma model with k and θ of 3.12 and 0.39 respectively, was fit to the histogram. Moment estimates for the best-fit model are also displayed in Figure 4. An RMSEA value of 0.066 was obtained, denoting a good fit based on stringent criterion for the RMSEA global fit index (Steiger, 2007; Hooper et al., 2008).

Results for the simulated statistical distribution of C_T in the South Elkhorn suggest that the temporal distribution of C_T is reflective of the variability of sediment carbon sources. Distributions of the carbon sources as well as C_T are shown in Figure 5. The median and inner-quartile range of C_T, 2.83 and 2.55-3.34 $gC100gsed^{-1}$, respectively, suggest that the benthic source was the primary contributor since C_{Bank} and C_{upland} average 1.6 and 2.36 $gC100gsed^{-1}$, respectively. The steep left tail of the distribution is attributed to the infrequent occurrences of bank and upland erosion, which primarily occur during high magnitude events with a return interval greater than one month (Russo and Fox, 2012; Ford and Fox, 2014). The magnitude of right skew, excess kurtosis and values of the shape and scale parameters for the C_T distribution were governed by median values of the seasonal C_{Bed} distributions and overlap between their inner quartile ranges. With

regards to skew, median values varied from 2.76 gC100gsed^{-1} during spring to 4.27 gC100gsed^{-1} in fall which was nearly twice that of the difference between C_{Bank} and C_{upland} hence the distribution experienced a fairly strong right skew. Further, the high overlap between the inner quartile ranges in all seasons dampened the level of excess kurtosis. These coupled source interactions govern the level of shape and scale parameters of the Gamma distribution.

Figures 6 through 8 display the histograms for C_T for the 28 sampling tests. Table 2 provides a comprehensive summary of all tests, shape and scale parameters of the generated Gamma distributions, RMSEA and randomization tests used to assess goodness-of-fit, descriptive statistics (i.e. mean, standard deviation, skewness and excess kurtosis), and acceptance or rejection of Levene's test and the Mann-Whitney U test.

Results of the study show that sampling at different frequencies, e.g. biweekly, weekly or monthly sampling tests, produced comparable distributions. For example, histograms in tests 1 through 4 in Figure 6, which correspond to biweekly, weekly, fortnightly and monthly sampling for all flow conditions, display similar peaks and tails in which all histograms appear to be Gamma distributed. The histogram results are further supported by values reported in Table 2, in which sampling frequencies had small discrepancies between model parameters and descriptive statistics in tests 1 through 4. Similarly, varying sampling frequency for low and moderate flows (tests 5-8), 2008 (tests 9-12) and winter sampling tests (tests 26-28) did not generate pronounced differences in Gamma parameters or descriptive statistics. Sampling frequency tests in 2009 (tests 13-16), spring (tests 17-19), summer (tests 20-22) and fall (tests 23-26) do show some small differences in Gamma parameters, descriptive statistics and statistical tests when varying sampling frequency. The small differences in Gamma model parameters is likely an artifact of the methodological approach as the impact of a single event will have more pronounced impacts on smaller sample sizes.

Figure 6 shows the distributions for testing flow conditions in low, moderate and high flow regimes in tests 1 through 4 as compared to low to moderate flows only in tests 5 through 8. No major disparities were observed between sampling at low flow conditions versus incorporating high flow conditions. Likewise, based on Table 2, values for mean, variance, skewness and kurtosis are all very close with the small differences

being attributed to high flows contributing C_T that is typically depleted compared to the benthic carbon source. The shape and scale parameters were close to the parent distribution model across tests 1 through 8. Somewhat surprisingly, the sampling tests that only sampled low to moderate flows generated Gamma model parameters closer to that of the parent Gamma model. Based on goodness-of-fit criteria, tests 1 through 8 had high p-values for the randomization test and low RMSEA values, denoting good fit, except for one. The biweekly test for low to moderate flows was on the border of being a good fit based on RMSEA criteria and a poor fit based on the randomization p-value. For tests 1 through 8, statistical results in Table 2 show that variances were equivalent to that of the parent distribution. However, the Mann-Whitney test rejected that the sampling scenario distributions in tests 1 through 8 were identical to the parent distribution, which points out the slight difference in the central measure of tendency. As an example from Table 2, Test 1 (biweekly frequency with all flow regimes) has an expected mean of 3.31 whereas the parent distribution has an expected mean of 3.02.

Figure 7 provides histogram results for testing the C_T distributional dependence of single-year sampling in tests 9 through 16 with multi-year sampling in tests 1 through 4. In general, single-year tests 9 through 12 from 2008 (dry year) and single-year tests 13 through 16 from 2009 (wet year) did not adequately capture the range, variability, and likeness of the overall parent distribution compared to the multi-year tests. The single-year tests from both 2008 and 2009 were found to have significant goodness-of-fit to Gamma distributions (except for test 9), however in 2008 the shape and scale parameters differed vastly from the parent distribution and in 2009 shape and scale parameters varied with sampling frequency and did not adequately represent those of the parent distribution (see Table 2).

Figure 8 (tests 17 through 28) displays the C_T histograms for the seasonal sampling tests. Sampling C_T in a single season did a poor job of capturing the parent C_T distribution. Generally, winter and spring were observed to be Gamma distributed and generated acceptable goodness-of-fit statistics with optimized Gamma models but did not approximate the five year parent distribution parameters well. Summer and fall gave poor goodness-of-fit statistics to optimized Gamma models. Results of Levene's test suggest that summer and winter tests best estimated the variance of the parent distribution

while the Mann-Whitney test suggests that spring tests best represent the central measure of tendency of the distribution. However, none of the seasonal tests adequately represented all components of the parent distribution.

3.5 DISCUSSION

Results of this study suggest that C_T for low-gradient, agriculturally-impacted streams is Gamma distributed and supports the hypothesis that upland eroded soil carbon, streambank eroded carbon, and temporarily stored and generated streambed carbon are reflected in a unimodal statistical distribution of C_T. The steep left tail of the C_T distribution reflects the small contribution of bank carbon and stems from flow and transport capacity limitations that preferentially export upland and benthic carbon sources (Ford and Fox, 2014; Russo and Fox, 2012). Further, the humped peak of the C_T distribution in Figure 4 reflects both the decreasing variability in C_T with increasing flow (Figure 3d), in which the transport capacity of the fluid is increasingly satisfied by upland sediment carbon as flow increases, as well as the heavy presence of upland carbon in C_{Bed}. Further, results from Figure 5 suggest that the skewed right-tail of the C_T distribution results from an amalgamation of the seasonal distributions of C_{Bed}. C_{Bed} is governed by the coupled interaction of the hydrologic flow regime (see Figure 3d) and variations in the biological processes associated with temperature fluctuations (see Figure 3b). As can be seen in Figure 5, summer and fall distributions are the most carbon enriched stemming from high autochthonous accrual during warm months. Further, C_{Bed} distributions in the fall and winter have the largest variance stemming from high annual variability of autochthonous build up during the summer and varying levels of hydrologic activity during fall and winter. The limited range and depleted carbon values associated with the spring distribution is attributed to winter flows wiping out the autochthonous pool in the bed coupled with the inability of that pool to redevelop until summer.

The Gamma distribution found for C_T for the low-gradient agriculturally-impacted stream in this study differs from past research performed in small mountainous rivers in which studies have tested the hypothesis that C_T follows a bimodal distribution (Hatten et al., 2012). Low-gradient agriculturally-impacted streams are expected to be of

high significance in this discussion because they are extensive and amalgamate to form large river systems that actively cycle carbon, e.g. the Mississippi River basin (Griffiths et al., 2012). To this end, this study complements the growing body of knowledge surrounding C_T distributions that leads to an understanding of how transported sediment carbon impacts the dissolved phases of nutrients and carbon as well as downstream ecosystem processes. This study suggests the C_T distribution becomes skewed to the right as a result of a biologically active streambed source, in which the level of skew is dependent upon the level of carbon accrual in streambed sediments. While our study suggests that C_T from low-gradient agriculturally-impacted streams follows a Gamma distribution, knowledge from steep mountainous rivers suggests that small differences in watershed characteristics can drastically impact the distribution. For example, a synthesis by Hatten et al. (2012) highlights steep mountainous rivers in violation of the bimodal C_T distribution as a result of differing geogenic and biogenic source characteristics coupled with differences in source contributions to C_T. Further research should investigate the distribution of C_T in systems with varying watershed characteristics, e.g., basin size, to expand current knowledge of how the distribution varies across watershed gradients.

To assess the potential transferability of the Gamma distribution to other low-gradient, temperate, agriculturally-impacted systems, we performed a sensitivity analysis. Ten scenarios, indicative of realistic watershed conditions in other low-gradient systems, were simulated and C_T frequency distributions were compared to statistical Gamma models. The ten scenarios included enriched and depleted soil and bank carbon conditions, as well as varying levels of benthic carbon production and decomposition (see Table 3). Values of algal growth and decomposition dynamics were obtained from the literature for similar agriculturally-impacted systems (see Rutherford et al., 2001; Ford and Fox, 2014). The ranges used for upland and bank sources were obtained in the study site but are comparable to values obtained in other ag-systems in the region (e.g., Jacinthe et al., 2009 in northeast Ohio). Results in Figure 9 suggest that Gamma models significantly represent the frequency distribution for most of the scenarios with the exception of scenarios 6, 8 and 10. Interestingly, scenarios 6, 8, and 10 coincide with either very low benthic carbon production or very low decomposition rates; the results of

which further support our hypothesis that benthic biological activity governs the shape and form of the statistical distribution of C_T and that a system with biologically active benthos will result in a right-tailed unimodal distribution of C_T resembling Gamma. Results suggest that regardless of parameterization, unimodal C_T distribution will exist in similar systems as a result of amalgamation, or mixing, of sources within the benthos that reduces the opportunity for multiple modes. The contrasting findings of a bimodal distribution for sampling routines in the fall occurs as a result of two distinct sources, i.e., a depleted upland and bank sediment carbon source that is transported at moderate-high flows, and an enriched, autochthonous dominated benthic source that is transported at low flows. This result would suggest the potential for a bimodal distribution when there is a distinct disconnect between the uplands and the streambed, which is atypical at annual or multi-annual scales in low-gradient systems. Results of this study add to the growing body of knowledge that the C_T distribution is governed by source variability and provides a testable hypothesis in low-gradient systems that C_T is Gamma distributed. Further study of C_T distributions from other low-gradient streams is needed to verify the hypothesis suggested here. Likewise, further work is needed to incorporate organic rich catchments where allocthonous C is enriched and in-stream carbon is negligible (e.g. streams draining peat catchments and wetlands).

While studies have highlighted the importance of sampling routines that emphasize high flow conditions to adequately capture sediment and carbon export (Meybeck et al., 2003; Dalzell et al., 2005; Dalzell et al., 2007; Duvert et al., 2011), few studies have investigated an appropriate sampling routine for capturing the statistical distribution of C_T. Results of this study suggest that there is no major disparity between sampling routines with and without high flow considerations for a two year sampling duration, and that both represent the parent system distribution well. This result contradicts conventional wisdom that measurements of carbon during high flows should be emphasized (Dalzell et al., 2005; Oeurng et al., 2011). Physically, sampling at low to moderate flow conditions for the C_T distribution is adequate for the low-gradient stream because sediment carbon is dominated by the bed source during this flow regime (Russo and Fox 2012; Ford and Fox 2014). These temporarily stored bed sediments retain and integrate the carbon signatures of all sediment sources since extremely high flows result

in deposition of recalcitrant carbon from the uplands and streambanks. Although it's not intuitive, measuring suspended carbon at low-moderate flows in this system is appropriate because it captures the full range of C_T. Further, solely sampling high flow conditions can bias the C_T distribution resulting from over sampling the depleted C_T signature transported from the upland soils.

Multi-year tests best represented the parent distribution relative to single year tests. Two year distributions (see Figure 6 and Table 2) best represented the shape and scale parameters as well as the descriptive statistics since both wet and dry years were represented. Sampling from a dry (2008) or wet (2009) year alone is not recommended for the C_T distribution due to their ineffectiveness at generating equivalent distributions and shape and scale parameters to that of the parent distribution. Generally, 2008 tests poorly represented the kurtosis, shape and scale parameters of the parent statistical distribution as a result of C_{Bed} going through an undisturbed growth phase coupled with preferential erosion of the bed source which promotes a more uniform distribution (Ford and Fox, 2014; Russo and Fox, 2012). Further, 2009 tests poorly captured the range and the shape and scale parameters due to dense hydrologic forcing of benthic carbon that prevents C_T from reaching its maximum state. Although two year datasets represented the parent distribution well, results of this study suggest that longer temporal domains are advised if feasible since mean values for the parent and sampling distributions were slightly different (<10%).

Results of this study suggest that sampling in a single season poorly represents the parent Gamma distribution. Physical and biological variables govern seasonal variability of C_T. Autochthonous carbon production enriches the signature in late spring, summer and early fall, evidenced by the increased C_T value observed during these periods in Figure 3b, as a function of temperature (Figure 3c) and light availability (Ford and Fox, 2014). Decomposition of OM depletes the signature in late fall, winter and early spring (Figure 3b) resulting from higher rates of decomposition relative to production. High flows from late fall through spring flush the benthic algal material and provide stronger connectivity between the upland carbon and the stream channel (Figure 3d). These processes are reflected in the C_T distributions as can be seen in Figure 8 (Tests 17-28). For example, fall tests show a bimodal-like distribution in which the peak associated with

the 4.5-5 gC 100gsed^{-1} bin stems from the algal enriched streambed source, whereas the peak associated with the 3-3.5 gC 100gsed^{-1} bin stems from mixing of the upland SOM source with the benthic source.

Results of this study suggest that frequency of the sampling routine is inconsequential in that sampling on a monthly timescale generates an equivalent distribution to a biweekly, weekly or fortnightly timescale. Recent studies have highlighted the need to sample at a higher resolution to capture C_T (Waterloo et al., 2006; Oeurng et al., 2011), while more traditional studies suggest use of a monthly or fortnightly interval is sufficient (Hope et al., 1994). Results from this study support the latter which is significant for low-gradient, agriculturally-impacted streams because sample collection and analysis at high frequencies can become expensive and time consuming. While this result can be potentially applied to similar watershed systems, it should be used with caution for watersheds with differing characteristics (e.g., steep-gradient systems lacking prominent storage zones).

3.6 CONCLUSIONS

Based on the modeling and statistical analysis results, the statistical distribution of C_T for low-gradient streams is hypothesized as Gamma distributed and the hypothesis that the statistical distribution is reflective of the upland, streambank and streambed carbon sources is confirmed. To adequately capture this distribution, we suggest that sampling of C_T be performed over a multi-year duration in which datasets incorporate wet and dry hydrologic regimes and all seasons. Frequency and flow regime are ultimately inconsequential and sampling of low-moderate conditions on a fortnightly-monthly timescale will adequately capture the distribution of C_T. Results of this study are limited to systems with comparable watershed characteristics including low stream and hillslope gradients, temperate climate, bedrock controlled streambeds with fine fluvial sediment deposits, and high nutrient loads in the overlying water column. The present study provides new information of the statistical distribution of C_T and provides results that lead towards guidance for C_T sampling protocol in lowland watersheds for researchers interested in estimating carbon export from streams for regional and global carbon budgets, carbon supply and variability for stream quality assessment and modeling. Further, although this study focuses on the distribution of transported sediment carbon, ongoing research is being conducted to constrain the distribution of other important nutrients including nitrogen and phosphorus.

3.7 REFERENCES

Akamatsu, F., Konayashi, S., Amano, K., Nakanishi, S., Oshima, Y., 2011. Longitudinal and seasonal changes in the origin and quality of transported particulate organic matter along a gravel-bed river. Hydrobiologia, 669, 183-197.

Aldrian, E., Chen, C.T.A., Adi, S., Prihartanto, Sudiana, N., Nugroho, S.P., 2008. Spatial and seasonal dynamics of riverine carbon fluxes of the Brantas catchment in East Java. J. Geophys. Res., 113, 1-13.

Alexander, R.B., Smith, R.A., Schwarz, G.E., Boyer, E.W., Nolan, J.V., Brakebill, J.W., 2008. Differences in phosphorus and nitrogen delivery to the Gulf of Mexico from the Mississippi River Basin. Evironmental Science and Technology, 42, 822-830.

Alvarez-Cobelas, M., Angeler, D., Sa´nchez-Carrillo, S., Almendros, G., 2010. A worldwide view of organic carbon export from catchments. Biogeochemistry 107, 275-293.

Arango, C.P., Tank, J.L., 2008. Land use influences the spatiotemporal controls on nitrification and denitrification in headwater streams. J.N. Am. Benthol. Soc., 27(1), 90-107.

Arango, C.P., Tank, J.L., Schaller, J.L., Royer, T.V., Bernot, M.J., David, M.B., 2007. Benthic organic carbon influences denitrification in streams with high nitrate concentration. Freshw. Biol., 52, 1210-1222.

Battin, T.J., Kaplan, L.A., Findlay, S., Hopkinson, C.S., Marti, E., Packman, A.I., Newbold, J.A., Sabater, F., 2009. Biophysical controls on organic carbon fluxes in fluvial networks. Nat. Geosci., 1, 95-100.

Benkhaled, A., Higgins, H., Chebana, F., Necir, A., 2013. Frequency analysis of annual maximum suspended sediment concentrations in Abiod wadi, Biskra (Algeria). Hydrological Processes, doi: 10.1002/hyp.9880.

Blair, N.E., Leithold, E.L., Brackley, H., Trustrum, N., Page, M., Childress, L., 2010. Terrestrial sources and export of particulate organic carbon in the Waipao sedimentary system: Problems, progress and processes. Mar. Geol., 270, 108-118.

Carey, A.E., Gardner, C.B., Goldsmith, S.T., Lyons, W.B., Hicks D.M., 2005. Organic carbon yields from small, mountainous rivers, New Zealand. Geophys. Res. Lett., 32, L15404.

Cole, J., Prairie, Y., Caraco, N., McDowell, W., Tranvik, L., Striegl, R., Duarte, C., Kortelainen, P., Downing, J., Middelburg, J., Melack, J., 2007. Plumbing the global carbon cycle: Intergrating inland waters into the terrestrial carbon budget. Ecosystems, 10, 171-184.

Coynel, A., Etcheber, H., Abril, G., Maneux, E., Dumas, J., Hurtrez, JE., 2005. Contribution of small mountainous rivers to particulate organic carbon input in the Bay of Biscay. Biogeochemistry, 74, 151-171.

Cuffney, T.F., Wallace, J.B., 1988. Particulate organic matter export from three headwater streams: discrete versus continuous measurements. Can. J. Fish. Aquat. Sci., 45, 2010-2016.

Dalzell, B., Filley, T., Harbor, J., 2005. Flood pulse influences on terrestrial organic matter export from an agricultural watershed. J. Geophys. Res., 110, G02011.

Dalzell, B., Filley, T., Harbor, J., 2007. The role of hydrology in annual organic carbon loads and terrestrial organic matter export from a Midwestern agricultural watershed. Geochim. Cosmochim. Acta, 71, 1448-1462.

Dodds, W., Smith, V., Lohman, K., 2002. Nitrogen and phosphorus relationships to benthic algal biomass in temperate streams. Canadian Journals of Fisheries and Aquatic Sciences, 59, 865-874.

Duvert, C., Gratiot, N., Nemery, J., Burgos, A., Navratil, O., 2011. Sub-daily variability of suspended sediment fluxes in small mountainous catchments- implications for community-based river monitoring. Hydrol. Earth Syst. Sci., 15, 703-713.

FAO-UNESCO, 2006. Soil Map of the World, digitized by ESRI. Soil climate map, USDA-NRCS, Soil Science Division, World Soil Resources, Washington D.C. Soil Pedon database, USDA-NRCS National Soil Survey Center, Lincoln, NE.

Fryirs, K., 2013. (Dis)Connectivity in catchment sediment cascades: a fresh look at the sediment delivery problem. Earth Surf. Process. Landforms, 38, 30-46.

Findlay, S.E.G., Mulholland, P.J., Hamilton, S.K., Tank, J.L., Bernot, M.J., Burgin, A.J., Crenshaw, C.L., Dodds, W.K., Grimm, N.B., McDowell, W.H., Potter J.D., Sobota, D.J., 2011. Cross-stream comparison of substrate-specific denitrification potential. Biogeochemistry, 104, 381-392.

Ford, W.I., Fox, J.F., 2014. Model of particulate organic carbon transport in an agriculturally impacted stream. Hydrol. Process., 28(5), DOI: 10.1002/hyp.9569

Fox, J.F., Papanicolaou, A.N., 2008. Application of the spatial distribution of nitrogen stable isotopes for sediment tracing at the watershed scale. J. Hydrol.,358, 46-55.

Fox, J., Ford, W., Strom, K., Villarini, G., Meehan, M., 2013. Benthic control upon the morphology of transported fine sediments in a low-gradient stream. Hydrological Processes, doi: 10.1002/hyp.9928.

Freedman, D., Diaconis, P., 1981. On the histogram as a density estimator: L_2 theory. Z. Wahrscheinlichkeitstheorie verw. Gebiete, 57, 453-476.

Galy, V., France-Lanord, C., Lartiges, B., 2008. Loading and fate of particulate organic carbon from the Himalaya to the Ganga-Brahmaputra delta. Geochim. Cosmochim. Acta, 72, 1767-1787.

Gomez, B., Trustrum, N., Hicks, D., Rogers, K., Page, M., Tate, K., 2003. Production, storage, and output of particulate organic carbon: Waipaoa River basin, New Zealand. Water Resour. Res., 39(6), ESG2-1-ESG2-8.

Gomez, B., Baisden, W.T., Rogers, K.M., 2010. Variable composition of particle-bound organic carbon in steepland river systems. J. Geophys. Res., 115, F04006.

Griffiths, N.A., Tank, J.L., Royer, T.V., Warrner, T.J., Frauendorf, T.C., Rosi-Marshall, E.J., Whiles, M.R., 2012. Temporal variation in organic carbon spiraling in Midwestern agricultural streams. Biogeochemistry, 108, 149-169.

Guo, L., Macdonald, R., 2006. Source and transport of terrigenous organic matter in the upper Yukon River: Evidence from isotope ($\delta^{13}C$, $\delta^{14}C$, and $\delta^{15}N$) composition of dissolved, colloidal, and particulate phases. Global Biogeochem. Cycles, 20, GB2011.

Hatten, J.A., Goni, M.A., Wheatcroft, R.A., 2012. Chemical characteristics of particulate organic matter from a small, mountainous river system in the Oregon Coast Range, USA. Biogeochemistry, 107, 43-66.

Hilton, R.G., Galy, A., Hovius, N., 2008. Riverine particulate organic carbon from an active mountain belt: importance of landslides. Global Biogeochem. Cycles, 22, GB1017.

Hooper, D., Coughlan, J., Mullen, M., 2008. Structural Equation Modelling: Guidelines for Determining Model Fit. Electronic Journal of Business Research Methods, 6(1), 53-60.

Hope, D., Billett, M., Cresser, M., 1994. A review of the export of carbon in river water: fluxes and processes. Environ. Pollut., 84, 301–324.

Jacinthe, P.A., Lal, R., Owens, L.B., 2009. Application of stable isotope analysis to quantify retention of eroded carbon in grass filters at the North Appalachian experimental watersheds. Geoderma, 148, 405-412.

Kim, J.-H., Zarzycka, B., Buscail, R., Peterse, F., Bonnin, J., Ludwig, W., Schouten, S., Shinninghe Damste, J.S., 2010. Contribution of river-borne soil organic carbon to the Gulf of Lions (NW Mediterranean). Limnol. Oceanogr., 55(2), 507-518.

Lane, C.S., Lyon, D.R., Ziegler, S.E. 2013. Cycling of two carbon substrates of contrasting lability by heterotrophic biofilms across a nutrient gradient of headwater streams. Aquat Sci, 75, 235-250, DOI: 10.1007/s00027-013-0269-0

Leithold, E.L., Blair, N.E., Perkey, D.W., 2006. Geomorphologic controls on the age of particulate organic carbon from small mountainous and upland rivers. Global Biogeochem. Cycles, 20, GB3022.

Lubowski, R.N., Vesterby, M., Bucholtz, S., Baez, A., Roberts M.J., 2006. Major uses of land in the United States, 2002. Economic Information Bulletin Number 13. Economic Research Service, United States Department of Agriculture, Washington.

Lyons, W.B, Nezat, C.A., Carey, A.E., Hicks, D.M., 2002. Organic carbon fluxes to the ocean from high-standing islands. Geology, 30, 443-446.

Masiello, C., Druffel, E., 2001. Carbon isotope geochemistry of the Santa Clara River. Global Biogeochem. Cycles, 15(2), 407-416.

McDonald, H.P., 1983. Soil Survey of Jessamine and Woodford Counties, Kentucky, Volumes 40-41. United States. Soil Conservation Service, Kentucky Agricultural Experiment Station, Kentucky. Dept. for Natural Resources and Environmental Protection. 94 pgs.

Meybeck, M., Laroche, L., Durr, H.H., Syvitski, J.P.M., 2003. Global variability of daily total suspended solids and their fluxes in rivers. Global and Planetary Change, 39, 65-93.

Mulholland, P. J., Helton, A. M., Poole, G. C., Hall, R. O., Hamilton, S. K., Peterson, B. J., Tank, J. L., Ashkenas, L. R., Cooper, L. W., Dahm, C. N.; Dodds, W. K., Findlay, S., Gregory, S. V., Grimm, N. B., Johnson, S. L., McDowell, W. H., Meyer, J. L., Valett, H. M.; Webster, J. R., Arango, C., Beaulieu, J. J., Bernot, M. J., Burgin, A. J., Crenshaw, C., Johnson, L., Merriam, J., Niederlehner, B. R., O'Brien, J. M., Potter, J. D., Sheibley, R. W., Sobota, D. J., Thomas, S. M., 2008. Excess nitrate from agricultural and urban areas reduces denitrification efficiency in streams. Nature,.452, 202–205.

Munson, S.A., Carey, A.E., 2004. Organic matter sources and transport in an agriculturally dominated temperate watershed. Appl. Geochem., 19, 1111-1121.

Nash, D.B., 1994. Effective sediment-transporting discharge from magnitude-frequency analysis. J.Geol., 102.

Newcomer, T.A., Kaushal, S.S., Mayer, P.M., Shields A.R., Canuel, E.A., Groffman, P.M., Gold, A.J., 2012. Influence of novel organic carbon sources on denitrification in forest, degraded urban and restored streams. Ecol. Monogr., 82(4), 449-466.

Oeurng, C., Sauvage, S., Sanchez-Perez, J., 2011. Assessment of hydrology, sediment and particulate organic carbon yield in a large agricultural catchment using the SWAT model. J. Hydrol., 401, 145-153.

Olkin, I., Gleser, L.J., Derman, C., 1994. Probability Models and Applications, second ed. MacMillan, New York.

Owens, L.B., Shipitalo, M.J., 2011. Sediment-bound and dissolved carbon concentration and transport from a small pastured watershed. Agric. Ecosyst. Environ., 141, 162-166.

Parker, R.S., Troutman, B.M., 1989. Frequency Distribution of Suspended Sediment Loads. Water Resources Research, 25(7), 1567-1574.

Pawson, R., Lord, D., Evans, M., Allott, T., 2008. Fluvial organic carbon flux from an eroding peatland catchment, southern Pennines, UK. Hydrol. Earth Syst. Sci., 12, 625-634.

Phillips, J., Russell, M., Walling, D., 2000. Time-integrated sampling of fluvial suspended sediment: a simple methodology for small catchments. Hydrological Processes, 14, 2589–2602.

Russo, J., Fox, J., 2012. The role of the surface fine-grained laminae in low-gradient streams: A model approach. Geomorphology, 171-172, 127-138.

Rutherford, J., Scarsbrook, M., Broekhuizen, N., 2000. Grazer control of stream algae: modeling temperature and flood effects. J. Environ. Eng., 126, 331–339.

Schuster, P.F., Shanley, J.B., Marvin-Dipasquale, M., Reddy, M.M., Aiken, G.R., Roth, D.A., Taylor, H.E., Krabbenhoft, D.P., DeWild, J.F., 2008. Mercury and organic carbon dynamics during runoff episodes from a Northeastern USA watershed. Water Air Soil Pollut., 187, 89-108.

Segura, C., Lazzati, D., Sankarasubramanian, A., 2013. The use of broken power-laws to describe the distributions of daily flow above the mean annual flow across the conterminous US. Journal of Hydrology, doi: http://dx.doi.org/10.1016/j.jhydrol.2013.09.016.

Sharma, P., Rai, S.C., 2004. Streamflow, sediment and carbon transport from a Himalayan watershed. *J. Hydrol.*, 289, 190-203.

Steiger, J.H., 2007. Understanding the limitations of global fit assessment in structural equation modeling. Pers. Individ. Dif., 42, 893-898.

Tank, J.L., Rosi-Marshall, E.J., Griffiths, N.A., Entrekin, S.A., Stephen, M.L., 2010. A review of allochthonous organic matter dynamics and metabolism in streams. J. North Am. Benthol. Soc., 29(1), 118-146.

Thorp, J.H., Delong, M.D., 2002. Dominance of autochthonous carbon in food webs of heterotrophic rivers. Oikos, 96(3), 543-550.

Toy, T., Foster, G., Renard, K., 2002. Soil erosion: Processes, predictions, measurements, and control. John Wiley & Sons, New York.

Trimmer, M., Grey, J., Heppell, C.M., Hildrew A.G., Lansdown, K., Stahl, H., Yvon-Durocher, G., 2012. River bed carbon and nitrogen cycling: State of play and some new directions. Sci. Total Environ., DOI: 10.1016/j.scitotenv.2011.10.074

U.S. Environmental Protection Agency (U.S. EPA). Data Quality Assessment: Statistical Methods for Practitioners. EPA/240/B-06/003. Washington, DC: Office of Environmental Information, 2006.

Walling, D., Collins, A., Jones, P., Leeks, G., Old, G., 2006. Establishing fine-grained sediment budgets for the Pang and Lambourn LOCAR catchments. J. Hydrol., 330, 126-141.

Waterloo, M.J., Oliveira, S.M., Drucker, D.P., Nobre, A.D., Cuartas, L.A., Hodnett, M.G., Langedijk, I., JAns, W.W.P., Tomasella, J., Araujo, A.C., Pimentel, T.P.,

Estrada, J.C.M., 2006. Export of organic carbon in run-off from an Amazonian rainforest blackwater catchment. Hydrol. Process., 20, 2581-2597.

White, P., Kalff, J., Rasmussen, J., Gasol, J., 1991. The effect of temperature and algal biomass on bacterial production and specific growth rate in freshwater and marine habitats. Microb. Ecol., 21, 99-118.

Worall, F., Reed, M., Warburton, J., Burt, T.. 2003. Carbon budget for a British upland peat catchment. Sci. Total Environ., 312, 133-146.

Zhang, X., Zhao, X., Liang, W., 2009. Profile distribution and storage of soil organic carbon and total nitrogen under conservation tillage in Northwest Liaoning, China. American-Eurasian Journal of Sustainable Agriculture, 3(4), 630-636.

3.8 TABLES AND FIGURES

Table 1. Soil data from the South Elkhorn watershed. Average ± one standard deviation for C_{Bank} is 1.6± 0.3% and the top 10 cm of C_{Upland} is 2.6± 1.8%.

Soil Type	Average Depth (cm)	OM(%)	C_{upland}(%)
Fairmount (76KY-230-1)	14.0	7.15	4.15
	35.6	3.40	1.97
Donerail Silt Loam (76Ky-113-2)	16.5	3.28	1.90
	53.3	0.81	0.47
	97.8	0.59	0.34
	143.5	0.49	0.28
Lowell Silt Loam (72KY-57-1)	14.0	3.66	2.12
	34.3	1.25	0.73
	49.5	0.70	0.41
	69.9	0.53	0.31
	92.7	0.43	0.25
	119	0.41	0.24
Lowell Silt Loam (72KY-120-3)	10.2	2.14	1.24
	27.9	0.99	0.57
	48.3	0.48	0.28
	71.1	0.38	0.22
	90.2	0.36	0.21
	106.7	0.34	0.20
	120.7	0.38	0.22

Table 2. Sampling routines, best fit Gamma model parameters, goodness-of-fit indices, descriptive statistics and statistical comparison to the parent distribution.

Routine	Sampling Timeframe	Time Interval	Flow Condition	Shape (k)	Scale (θ)	[1]Rand. Test P-value	[2]RMSEA	Mean (gC/100 gSed)	Variance (gC/100 gSed)	Skewness	Excess Kurtosis	Mann-Whitney	Levene's
Dist.	2006-2010	30 minute	All	3.12	0.39		0.07	3.02	0.47	1.13	1.92		
1	2008-2009	Biweekly	All	3.46	0.38	0.12	0.06	3.31	0.50	1.08	1.74	Reject	Accept
2	2008-2009	Weekly	All	3.58	0.35	0.88	0.00	3.26	0.45	1.06	1.68	Reject	Accept
3	2008-2009	Fortnightly	All	3.47	0.35	0.98	0.00	3.22	0.43	1.07	1.73	Reject	Accept
4	2008-2009	Monthly	All	3.49	0.36	0.99	0.00	3.26	0.45	1.07	1.72	Reject	Accept
5	2008-2009	Biweekly	Low-Mod.	3.37	0.39	0.01	0.11	3.39	0.54	1.06	1.68	Reject	Accept
6	2008-2009	Weekly	Low-Mod.	3.52	0.38	0.72	0.00	3.34	0.51	1.07	1.71	Reject	Accept
7	2008-2009	Fortnightly	Low-Mod.	3.26	0.39	0.78	0.00	3.29	0.51	1.11	1.84	Reject	Accept
8	2008-2009	Monthly	Low-Mod.	3.34	0.39	1.00	0.00	3.31	0.52	1.09	1.80	Reject	Accept
9	2008	Biweekly	All	1.99	0.75	0.01	0.15	3.49	1.12	1.42	3.02	Reject	Reject
10	2008	Weekly	All	2.26	0.62	0.39	0.05	3.40	0.87	1.33	2.66	Accept	Reject
11	2008	Fortnightly	All	1.93	0.71	0.88	0.00	3.36	0.96	1.44	3.12	Accept	Accept
12	2008	Monthly	All	2.14	0.66	0.88	0.00	3.41	0.93	1.37	2.81	Accept	Accept
13	2009	Biweekly	All	3.79	0.23	0.08	0.09	3.27	0.20	1.03	1.58	Reject	Reject
14	2009	Weekly	All	3.29	0.25	0.90	0.00	3.24	0.21	1.10	1.82	Reject	Reject
15	2009	Fortnightly	All	3.15	0.28	0.98	0.00	3.28	0.25	1.13	1.91	Reject	Reject
16	2009	Monthly	All	2.35	0.39	0.99	0.00	3.32	0.36	1.30	2.55	Accept	Accept
17	[3]Spring	Biweekly	All	2.96	0.23	0.45	0.00	2.89	0.16	1.16	2.03	Accept	Reject
18	[3]Spring	Weekly	All	1.71	0.30	0.95	0.00	2.91	0.15	1.53	3.50	Accept	Reject
19	[3]Spring	Fortnightly	All	1.78	0.33	0.95	0.00	2.99	0.19	1.50	3.37	Accept	Reject
20	[3]Summer	Biweekly	All	4.00	0.31	0.00	0.27	3.22	0.37	1.00	1.50	Reject	Reject
21	[3]Summer	Weekly	All	3.70	0.35	0.08	0.22	3.28	0.45	1.04	1.62	Reject	Accept
22	[3]Summer	Fortnightly	All	2.54	0.47	0.07	0.33	3.40	0.56	1.26	2.36	Reject	Accept
23	[3]Fall	Biweekly	All	2.37	0.82	0.00	0.30	3.94	1.59	1.30	2.53	Reject	Reject
24	[3]Fall	Weekly	All	2.01	0.92	0.25	0.17	3.85	1.70	1.41	2.99	Reject	Reject
25	[3]Fall	Fortnightly	All	1.88	0.88	0.40	0.12	3.64	1.44	1.46	3.20	Accept	Accept
26	[3]Winter	Biweekly	All	1.73	0.62	0.23	0.13	3.57	0.66	1.52	3.47	Reject	Accept
27	[3]Winter	Weekly	All	1.91	0.52	0.47	0.00	3.50	0.53	1.45	3.13	Reject	Accept
28	[3]Winter	Fortnightly	All	1.82	0.54	0.98	0.00	3.49	0.54	1.48	3.30	Reject	Accept

[1]Readings of 0.00 denote values <0.005. [2]All seasonal routines were conducted in 2008-2009. [3]RMSEA<0.1 denotes acceptable fit for Gamma distributions. Mann-Whitney test is accepted if the location of the distribution is significantly equivalent to the parent distribution. Levene's test is accepted if variance of the distribution is equivalent to that of the parent distribution.

Table 3. Model sensitivity analysis scenarios to test the transferability to other low-gradient, agriculturally disturbed systems. A_{Max} is the maximum fixation rate, A_{Resp} is the respiration rate of the algal mat, $\tau_{cr\text{-}algae}$ is the critical shear stress of the algal mat, DEC_{CPOM} is the decomposition rate of the algal mat, and DEC_{FPOM} is the decomposition rate of fine particulate carbon.

Scenario	C_{Upland} (gC gSed^{-1})	C_{Bank} (gC gSed^{-1})	A_{Max} (kgC m^{-2}d^{-1})	A_{resp} (d^{-1})	$\tau_{cr\text{-}algae}$ (Pa)	DEC_{CPOM} (d^{-1})	DEC_{FPOM} (d^{-1})
Calibration	0.024	0.016	$2.4\text{x}10^{-3}$	0.13	0.35	$8\text{x}10^{-3}$	$4.2\text{x}10^{-3}$
Enriched $C_{Bank,Upland}$	0.042	0.021	$4\text{x}10^{-3}$	0.09	1	$8\text{x}10^{-3}$	$5\text{x}10^{-3}$
Enriched C_{Upland}, Depleted C_{Bank}	0.042	0.010	$4\text{x}10^{-3}$	0.09	1	$8\text{x}10^{-3}$	$5\text{x}10^{-3}$
Depleted $C_{Bank,Upland}$	0.018	0.010	$4\text{x}10^{-3}$	0.09	1	$8\text{x}10^{-3}$	$5\text{x}10^{-3}$
High Algae	0.030	0.016	$7.7\text{x}10^{-3}$	0.15	2	$8\text{x}10^{-3}$	$5\text{x}10^{-3}$
Low Algae	0.030	0.016	$0.4\text{x}10^{-3}$	0.03	0.1	$8\text{x}10^{-3}$	$5\text{x}10^{-3}$
Fast Decomposition	0.030	0.016	$4\text{x}10^{-3}$	0.09	1	$15\text{x}10^{-3}$	$10\text{x}10^{-3}$
Slow Decomposition	0.030	0.016	$4\text{x}10^{-3}$	0.09	1	$1\text{x}10^{-3}$	$0.4\text{x}10^{-3}$
High Algae, Fast Decomposition	0.030	0.016	$7.7\text{x}10^{-3}$	0.15	2	$15\text{x}10^{-3}$	$10\text{x}10^{-3}$
Low Algae, High $C_{Bank,Upland}$	0.042	0.021	$0.4\text{x}10^{-3}$	0.03	0.1	$8\text{x}10^{-3}$	$5\text{x}10^{-3}$

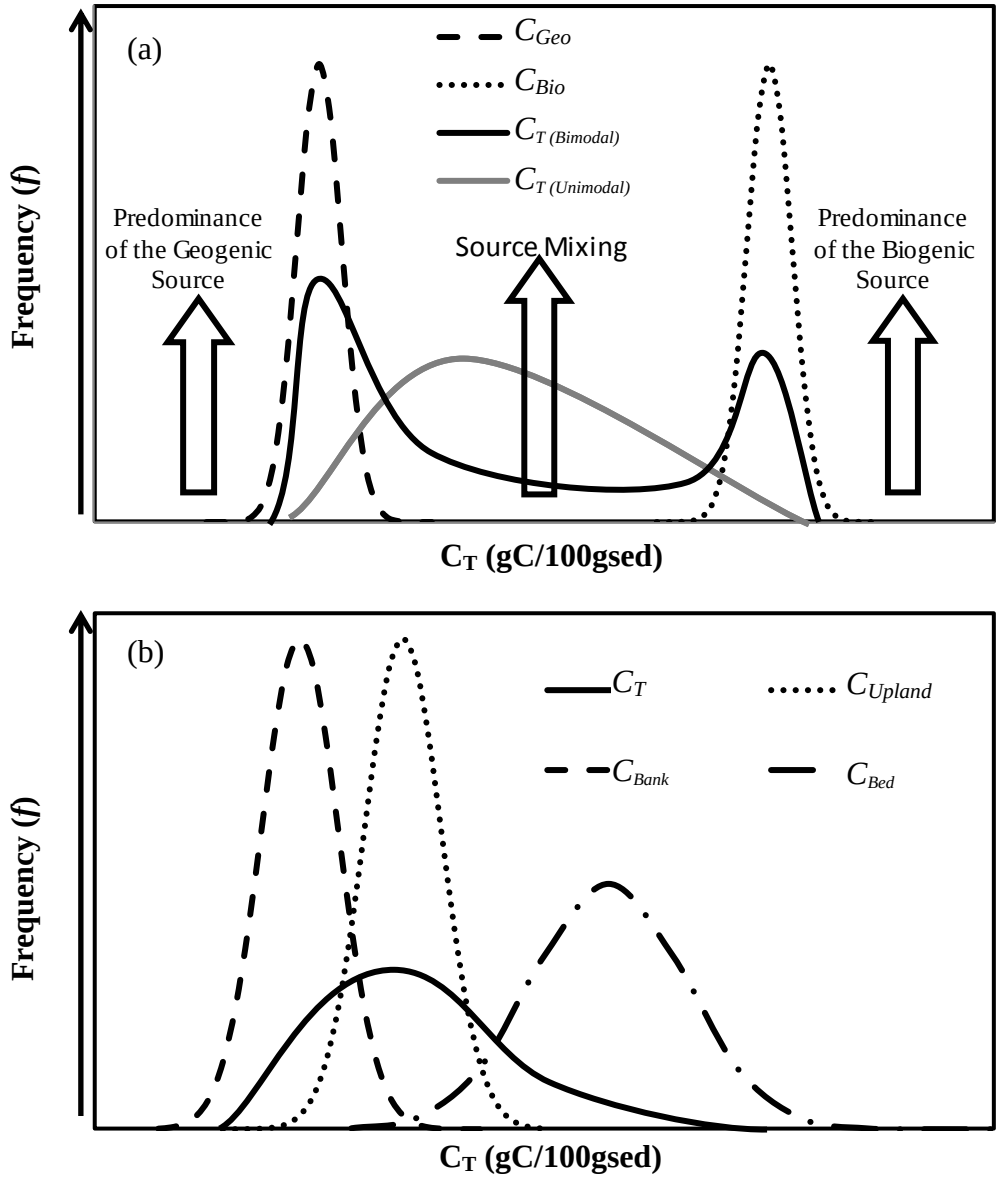

Figure 1. Definition sketch for a hypothetical C_T probability density function in (a) small mountainous rivers and (b) low-gradient, biologically active agricultural streambeds.

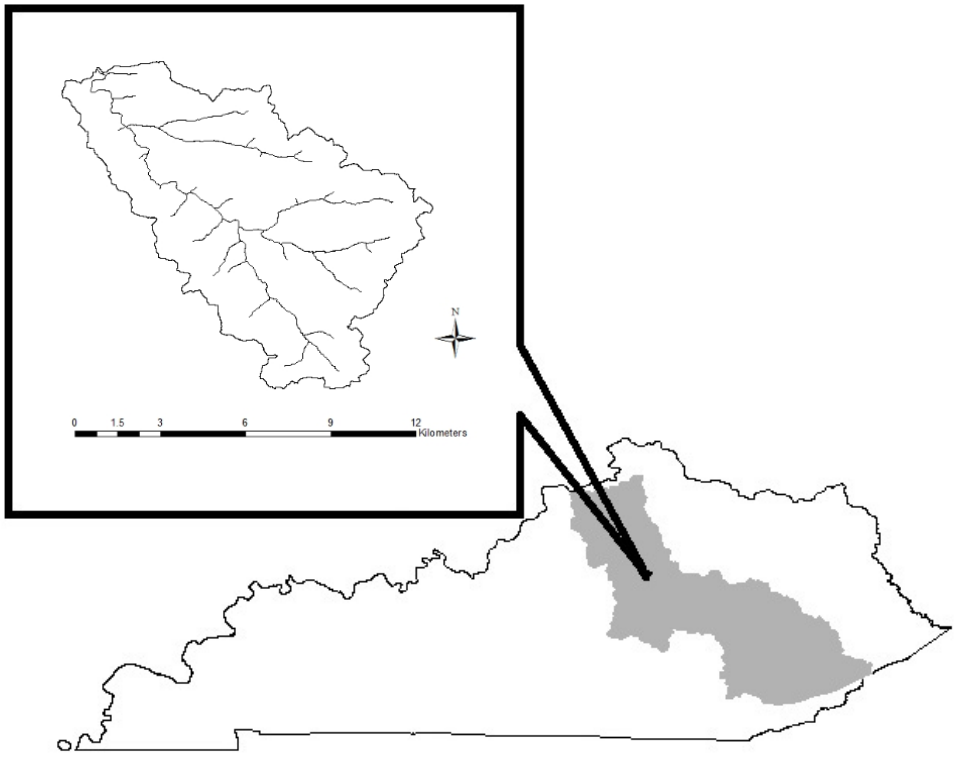

Figure 2. South Elkhorn watershed located in Central Kentucky, USA. Model domain for the statistical distribution of C_T

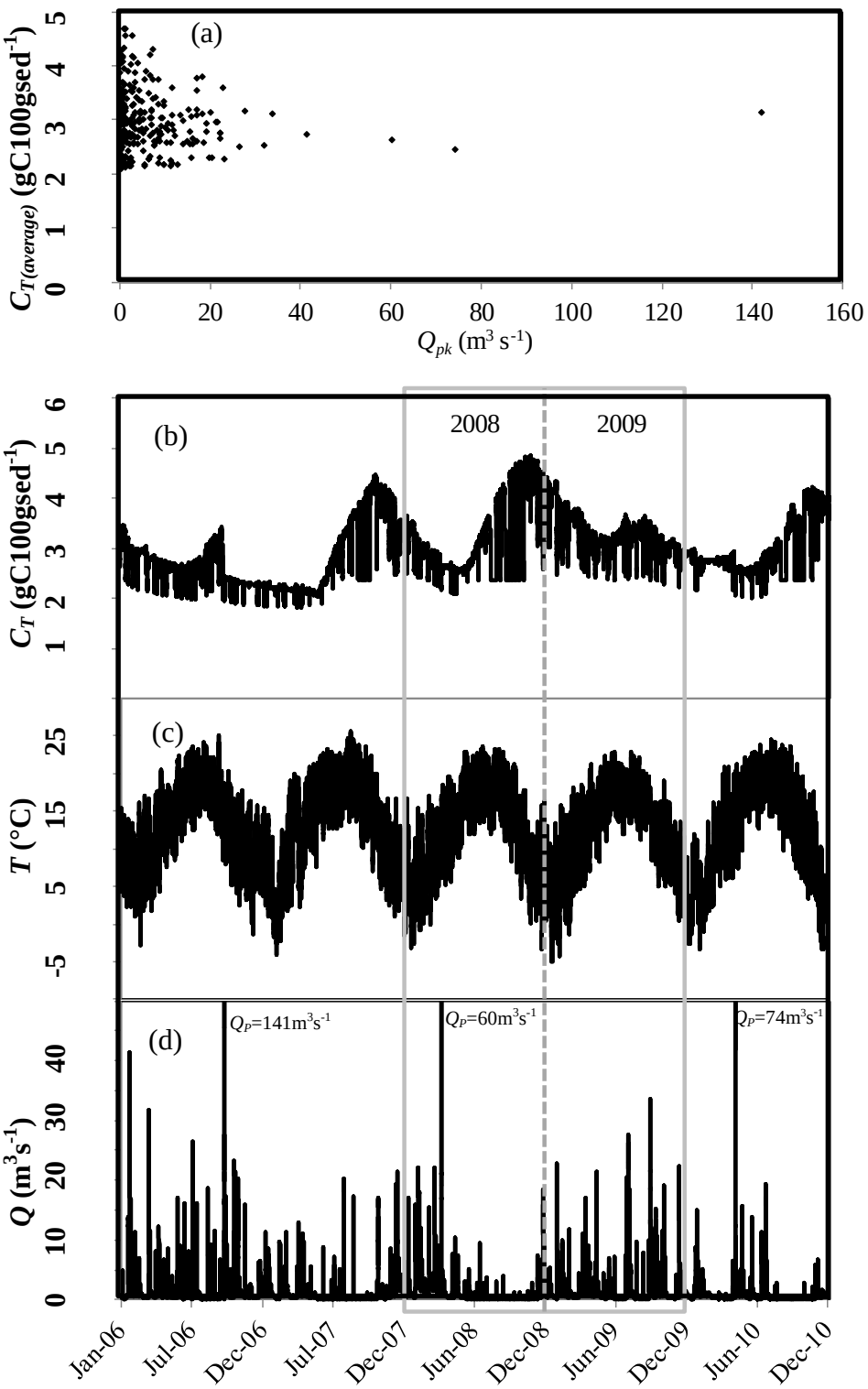

Figure 3. Model outputs for (a) peak weekly flow vs. weekly averaged C_T and continuous model results of (b) carbon content of transported sediments, (c) streamwater temperature and (d) instantaneous stream water flowrate.

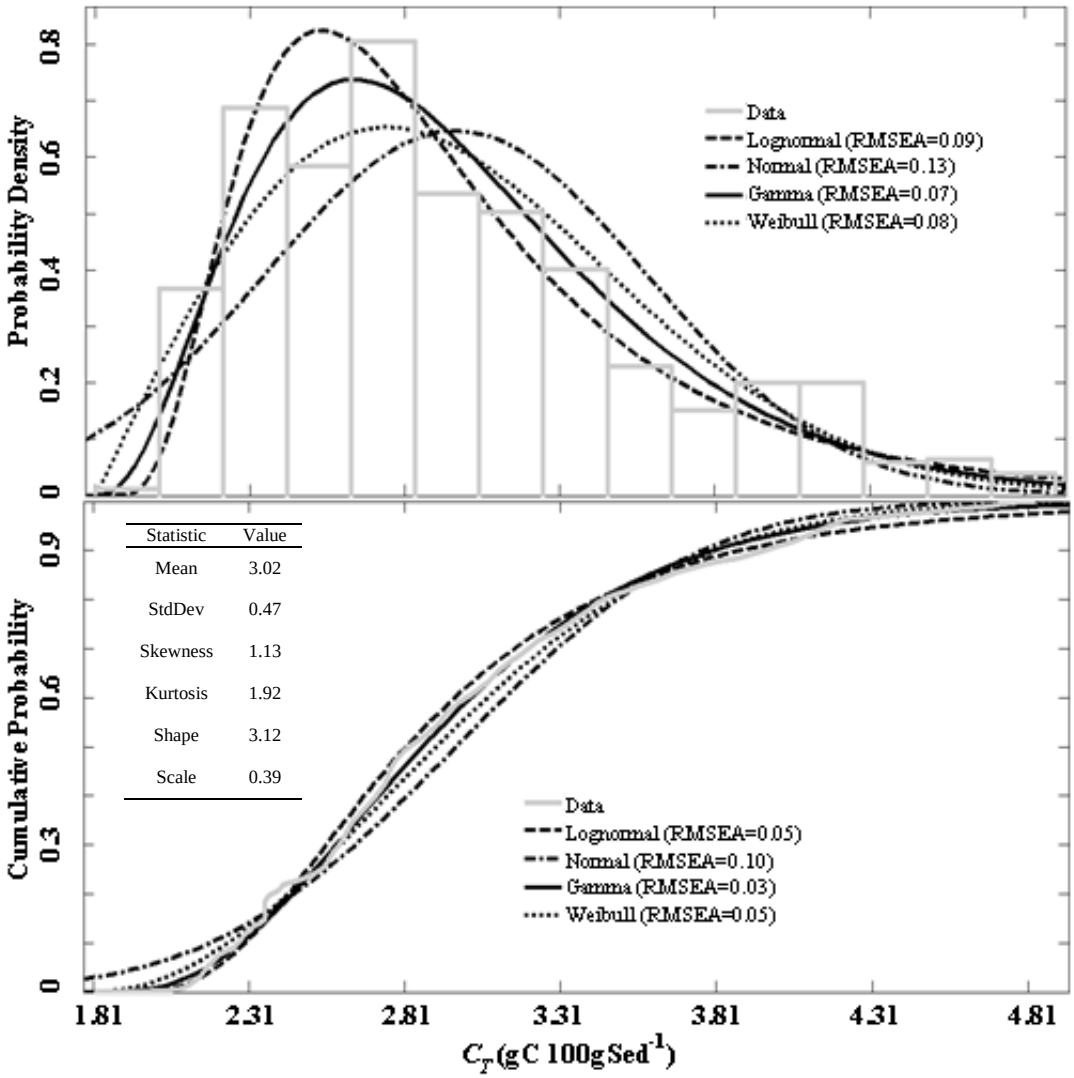

Figure 4. Goodness-of-fit for statistical distributions to the frequency distribution of the process-based numerical model. For the selected Gamma model, moment estimates and best fit parameters are provided in the table.

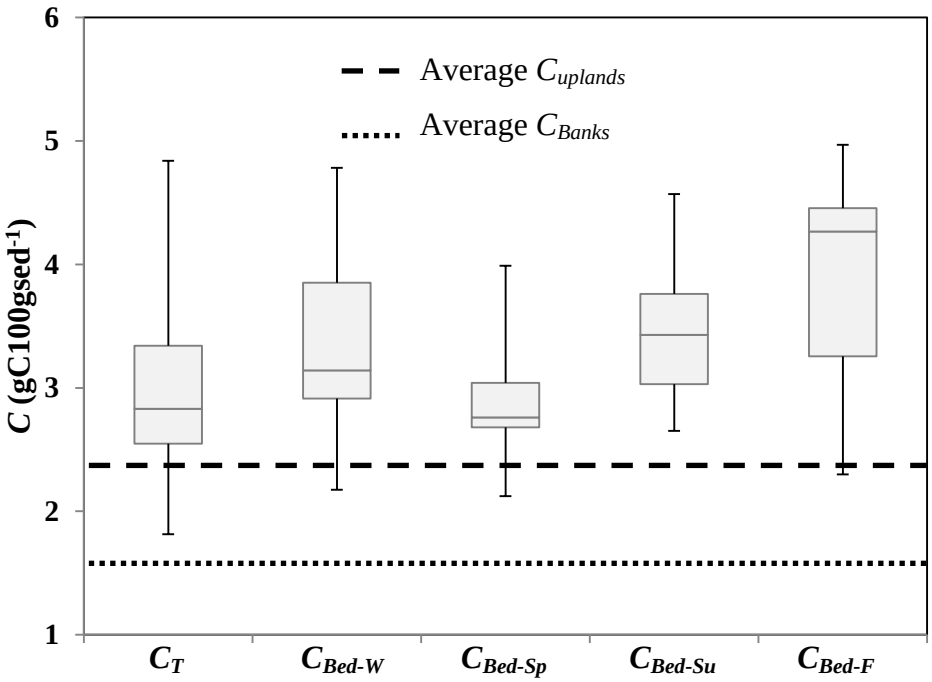

Figure 5. Denotes the minimum, 25th percentile, median, 75th percentile and maximum for population of transported carbon, CT, and seasonal distributions of benthic carbon CBed with lines denoting the mean value of upland, Cupland, and bank, CBank, carbon sources. The seasonal abbreviations in the above figure represent winter (W), spring (Sp), summer (Su), and fall (F).

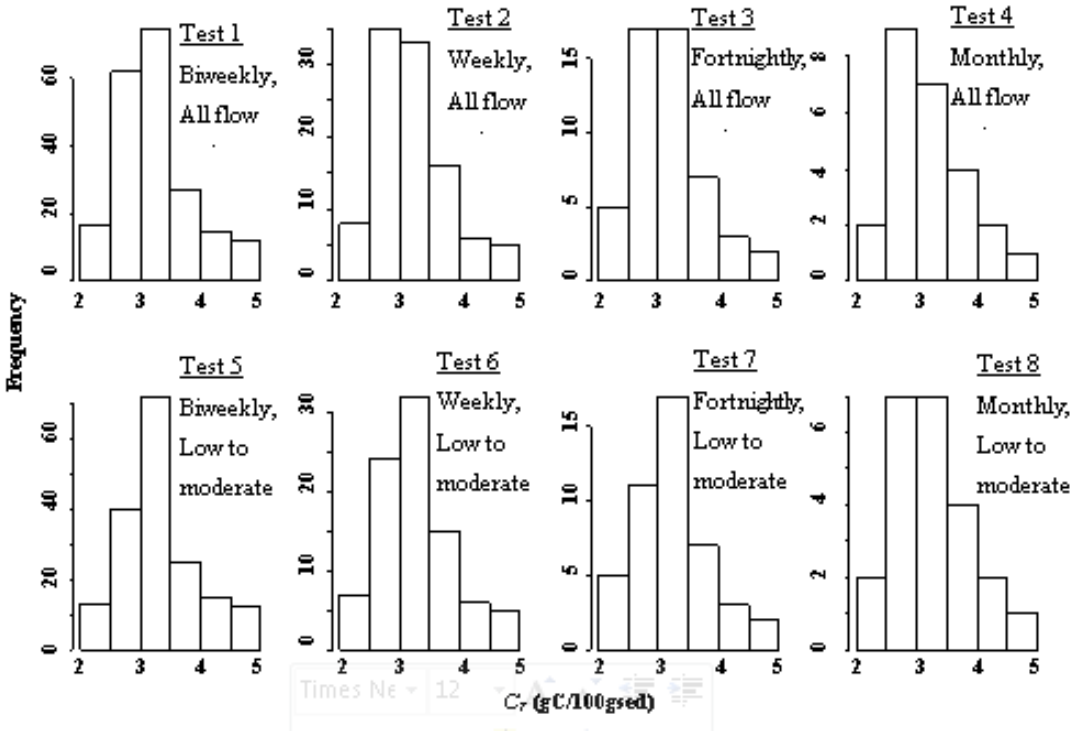

Figure 6. Results of C_T distribution for sampling tests of all flow regimes (1-4) versus low-moderate flows (5-8).

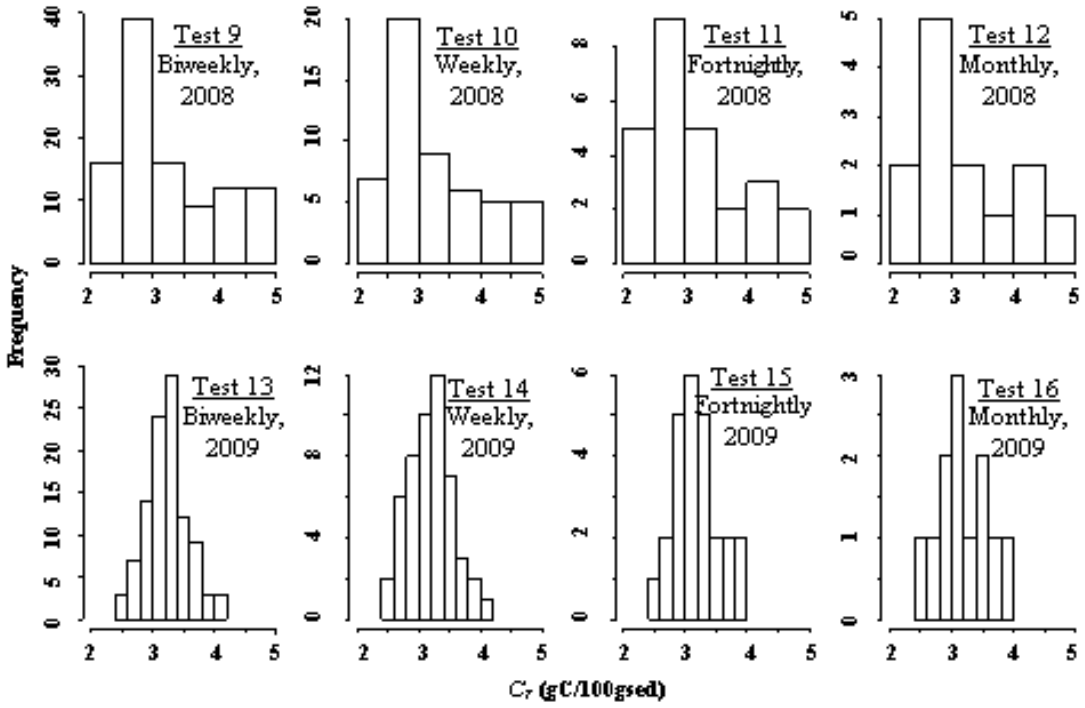

Figure 7. Results of C_T distribution for single year (Tests 9-16) sampling tests.

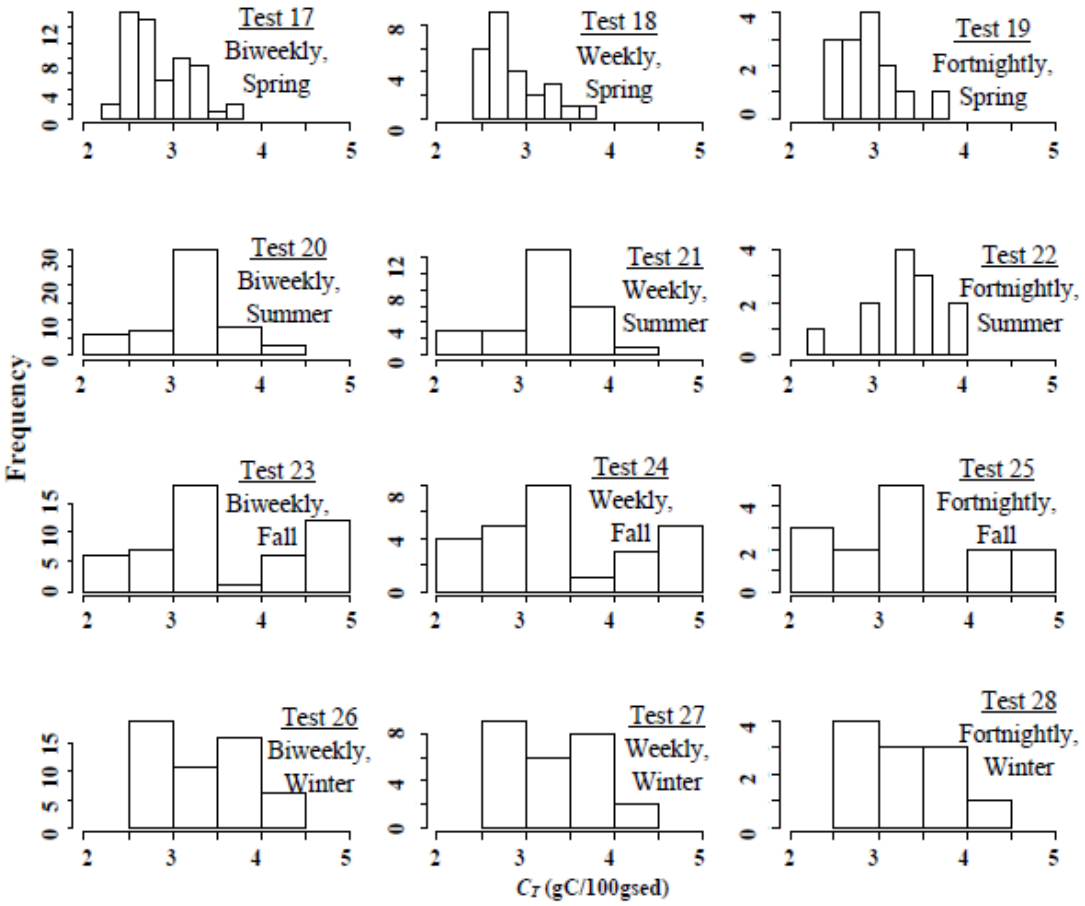

Figure 8. Results of C_T distribution for testing seasonal sampling (Tests 17-28).

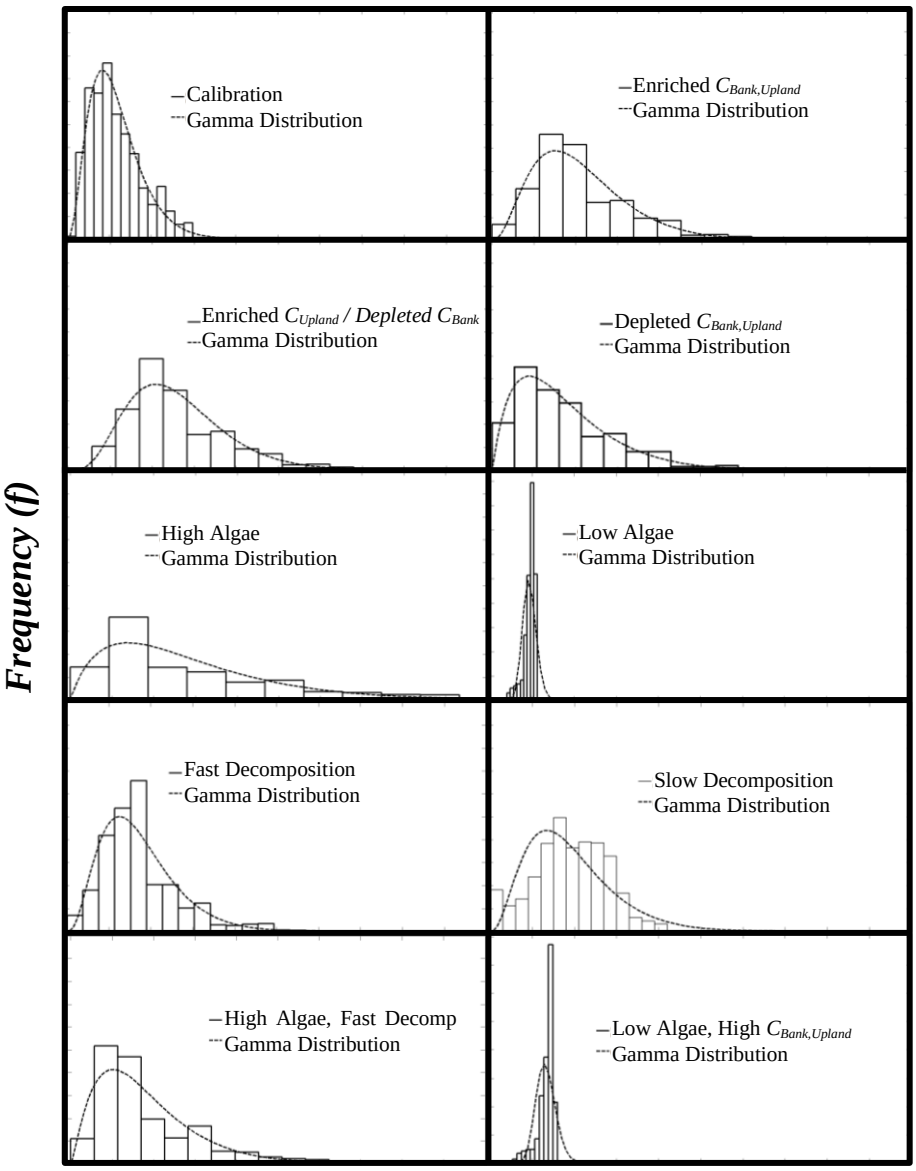

Figure 9. Model sensitivity analysis to assess transferability of Gamma distribution to other low-gradient, temperate watersheds.

Copyright © William Isaac Ford III 2014

Chapter 4: Assessment of Carbon Quality and Quantity Following an Extreme Flood

Adapted with permission from Ford, W., Fox, J., Rowe, H. 2014. Impact of Extreme Hydrologic Disturbances upon the Sediment Carbon Quality in Agriculturally-impacted Temperate Streams. *Ecohydrology*. Accepted.

Copyright © 2014 John Wiley & Sons Ltd.

4.1 SUMMARY

The impact of extreme hydrologic disturbances on the quality of fine particulate organic carbon (FPOC) associated with sediments in low-gradient, agriculturally-impacted streams remains poorly understood despite the significance of the FPOC pool to benthic food webs, organic matter budgets and nutrient cycles. We estimated immediate and long-term impacts of an extreme flow disturbance on FPOC quality using a five year dataset of the stable carbon isotopic signature and a new metric for carbon quality. Results of the study show that the stable isotopic signature of sediment carbon is significantly enriched in the year following the extreme event, which reflects the streams response to accrual of degraded soil carbon. Further, our FPOC metric was found to be inversely proportional to the isotopic signature, suggesting an immediate shift of the benthic ecosystem to lower quality carbon that is retained for more than one year before recovering to the pre-disturbance state. Following recovery, results show that the benthic ecosystem exports FPOC with quality that oscillates seasonally—the lowest quality observed in late spring and the highest quality in late fall. Although studies have addressed the response of high quality algal biomass to fluvial shearing, this study is the first to assess the response of high quality FPOC to an extreme hydrologic disturbance characterized by sediment deposition in an agriculturally-impacted stream.

4.2 INTRODUCTION

The quality of sediment carbon associated with fine particulate organic carbon (FPOC) plays important roles in energy food webs, nutrient cycling, and organic matter budgets (Arango et al., 2007; Cole et al., 2007; Arango and Tank, 2008; Battin et al., 2009; Findlay et al., 2011; Griffiths et al., 2012; Newcomer et al., 2012; Trimmer et al., 2012). Specifically, the impact of extreme hydrologic disturbances have been highlighted in that they can mobilize and transport high loads of FPOC, yet little is known about FPOC quality following such events (Gomez et al., 2003; Dalzell et al., 2007; Akamatsu et al., 2011; Ford and Fox, 2012). FPOC is a heterogeneous mixture of degraded terrestrial and aquatic coarse POC and aggregated colloidal dissolved organic carbon, CDOC, in which the composite quality is a function of the chemical composition, e.g., lignin content (Hope et al., 1994; Yoshimura et al., 2008; Marcarelli et al., 2011). Of particular interest is FPOC in small, low-gradient agricultural stream ecosystems in which streams transport high nutrient and sediment loads and in-stream carbon production is pronounced (Mulholland et al., 2008; Ford and Fox, 2012; Russo and Fox, 2012; Griffiths et al., 2012). In addition, the systems are expansive, covering large landmasses such as in the food producing Midwestern U.S. (Lubowski et al., 2006; Griffiths et al., 2012). Low DOC concentrations, open canopies and low stream and hillslope gradients in these systems promote large zones of temporary storage in which fluvial carbon sources are dominated by soil organic matter (SOM) derived from decomposed terrestrial plant litter as well as autochthonous algae (Walling et al., 2006; Mulholland et al., 2008; Lyon and Ziegler, 2009; Lane et al., 2013; Ford and Fox, 2012).

Terrestrial litter and litter derived SOM is readily accepted as a lower quality source of organic matter relative to algal carbon. Decomposition rates for terrestrial material have been shown to be orders of magnitude lower than that of in-stream derived carbon (Enriquez et al. 1993; Webster et al., 1999; Six and Jastrow, 2002). Further, studies have shown that algal carbon has more energy per unit mass as compared to allochthonous carbon (Thorp and Delong, 2002). The lower quality of allochthonous SOM stems from higher contents of more complex, recalcitrant carbon

compounds, such as lignin and cellulose while algal biomass is composed primarily of highly labile neutral sugars such as glucose (Vieira and Myklestad, 1986; Waite et al., 1995; Lane et al., 2013). A recent study by Yoshimura et al. (2008) suggests that lignin contents in fine detrital algae are nearly half that of terrestrial derived fine sediment. Currently there is debate as to whether small fluxes of high quality FPOC or large fluxes of low quality FPOC drive benthic metabolic processing. A recent synthesis by Marcarelli et al. (2011) discusses the importance of both and highlights the current disconnect between studies that quantify organic matter budgets and organic matter quality. As a result there is a need for quantitative metrics that can distinguish FPOC quality for food web studies while also quantifying source contributions for FPOC budgets.

Metrics of FPOC quality are scarce due to high uncertainties present in transported FPOC measurements that stem from poor temporal data resolution, lacking methodological approaches, dynamic source mixtures of transported FPOC and poor constraint of benthic FPOC composition (Yoshimura et al., 2008; Tank et al., 2010; Battin et al., 2009; Alvarez-Cobelas, 2012). The dynamic nature of the benthic carbon source has recently been recognized to be governed by coupled biological and physical processes in which streambed FPOC is not uniformly distributed spatially or temporally (Droppo and Stone, 1994; Russo and Fox, 2012; Ford and Fox, 2012; Trimmer et al., 2012; Ford and Fox, in Review). To better constrain spatiotemporal variability of FPOC, hydrodynamic processes must be tightly coupled to biogeochemical measures of FPOC. Mass balance sediment transport models have been successfully used to estimate contributions of bank, bed and upland sources in FPOC budgets (Ford and Fox, 2012), however the chemical properties of FPOC such as carbon content, C:N ratio, and lignin contents have been shown to have distinctively different chemical properties from their parent source material which can mask the overall quality of the FPOC mixture (Dalzell et al., 2005; Yoshimura et al., 2008). A partial solution has been recently recognized in that stable carbon isotope signatures, $\delta^{13}C$, have been used to successfully partition sources of FPOC (Phillips and Gregg, 2003; Fox and Papinicolaou, 2007; Mukundan et al., 2010).

Unlike other chemical signatures, $\delta^{13}C$ is reflective of FPOC sources since small isotopic shifts are associated with decomposition (Sharp, 2007). $\delta^{13}C$ signatures of FPOC have been used to apportion sources of carbon over the past decade in small stream ecosystems (Bellanger et al., 2004; Fox and Papanicolaou, 2007; Fox, 2009; Jacinthe et al., 2009; Schindler Wildhaber et al., 2012), large rivers and lakes (Bird et al., 1998; Helie and Hillaire-Marcel, 2006; Bonn and Rounds, ; Kendall et al., 2001; Chen and Jia, 2009; Gao et al., 2007) and coastal waterbodies (Martinotti et al., 1997; Sigleo and Macko, 2002 Gu et al. 2011; Sarma et al., 2012). Despite its abundant use, studies using $\delta^{13}C$ in small streams to characterize source contributions have assumed an inert stream channel in which $\delta^{13}C$ signatures of exported FPOC are reflective of upland soil organic carbon (SOC) sources derived from C3 and C4 plants, with $\delta^{13}C$ signatures of -24 to -29‰ and -10 to -14 ‰, respectively (Smith and Epstein, 1971; Onstad et al., 2000; Palmer et al., 2001; Fox and Papanicolaou, 2007; Fox, 2009; Jacinthe et al., 2009; Brunet et al., 2011). Recent recognition of the importance of streambeds for FPOC dynamics would suggest that in-stream derived algal sources should also be considered in apportioning source analysis (Cole et al., 2007; Battin et al., 2009; Ford and Fox, 2012). The potential of $\delta^{13}C$ to apportion algae and upland sources for quality is realized because in low-gradient streams $\delta^{13}C$ of algae have significantly depleted $\delta^{13}C$ values relative to SOC ranging from -28 to -42‰ (Onstad et al., 2000; Palmer et al., 2001; Dalzell et al. 2007; Sakamaki and Richardson, 2011; Schindler Wildhaber et al., 2012).

Synthesizing current knowledge of $\delta^{13}C$ of FPOC sources with knowledge of FPOC dynamics in streams suggests that apportioning high quality, in-stream derived carbon from low quality, soil derived carbon in the FPOC pool can be accomplished by coupling ambient measures of $\delta^{13}C$ with estimates of sediment source contributions. For a streambed under typical disturbance conditions, FPOC quality fluctuates seasonally as a function of biologic growth, decomposition and hydrologic dynamics (White et al., 1991; Rutherford et al., 2000; Ford and Fox, 2012; Griffiths et al., 2012).

With the efficacy of $\delta^{13}C$ for estimating quality implied, of paramount interest in this study is the long-term response of FPOC quality to extreme hydrologic

disturbances and the extent that they can shift the streambed into dis-equilibrium. A growing body of knowledge has shown tighter connectivity of the stream channel with the uplands during high magnitude storm events in which excessive sediment loads from upland hillslopes smother the streambed, suggesting bed resetting to low-quality FPOC (Gomez et al., 2003; Russo and Fox, 2012; Ford and Fox, 2012). Of higher ambiguity is the long-term recovery of high quality, autochthonous FPOC. Recovery of high quality FPOC is dependent upon resilience of benthic algal communities following extreme flow disturbances with the level of resilience and recovery reflecting the magnitude of the disturbance, frequency, season of occurrence, and type of disturbance, e.g., deposition vs. shear (Peterson, 1996). We hypothesize that the extreme storm disturbance will generate poor FPOC quality with subsequent periods of disequilibrium as algal recovery will be stunted by heavy deposition of fine sediments to the streambed surface.

The objective of this paper was to assess FPOC quality following an extreme event in a low-gradient agriculturally-impacted stream ecosystem using ambient measurements of δ^{13}C of transported sediments and sediment transport model results to provide a new metric of FPOC quality based on the contributions of different carbon sources to the FPOC load. We collected five years of fluvial sediment, approximately weekly, from two sites and analyzed the sediment for $\delta^{13}C$ of FPOC in a low-gradient agriculturally-impacted stream with both autochthonous and recalcitrant FPOC sources. The FPOC quality metric that was applied in this paper estimates the ratio of algal carbon to recalcitrant SOC in benthic and transported FPOC using $\delta^{13}C$ to differentiate the sources. We applied our metric to estimate FPOC quality during and after an extreme hydrologic event using an extensive five year dataset of $\delta^{13}C$ of FPOC from two locations in the stream study site.

4.3 METHODS

4.3.1 Study Site

The low-gradient agriculturally-impacted South Elkhorn stream located in Kentucky, USA (Figure 1) was selected as the study site to test our hypothesis due to (i) the importance of autochthonous, high quality carbon as well as low quality soil carbon transported to the stream ecosystem and (ii) the occurrence of an extreme hydrologic event during our five year sampling period.

The South Elkhorn is a mixed-landuse, agricultural and urban impacted stream with relatively low gradients and gradual hillslopes in the Bluegrass Region of central Kentucky, USA. The land-use impact, low-gradient topography, and temperate climate lead to longitudinal variability in FPOC composition in the streambed in which warm temperatures and high light availability in summer through fall promote autochthonous growth of in-stream derived FPOC. Moderate and high flows in winter and spring subsequently flush or bury labile FPOC, depositing recalcitrant FPOC from the uplands (Fox et al., 2010; Ford and Fox, 2012; Russo and Fox, 2012). The mixture of high and low quality carbon from autochthonous and terrestrial sources, respectively, makes the low-gradient study site indicative of low-gradient agricultural streams covering large landmasses such as in the food producing Midwestern U.S (Griffiths et al., 2012).

An extreme event occurred in the South Elkhorn basin during the sampling period. The storm-of-record for the South Elkhorn occurred September 23rd 2006 when approximately 145 mm of rain fell in a 24 hour period with a peak hourly intensity of 56mm/hour. The peak flowrate measured at USGS gauging station 03289000 was 145 m^3s^{-1}, which was nearly twice the peak flow of any other storm event over the five year data collection period. Previous models of sediment and carbon dynamics in the study watershed suggest that low quality terrestrial FPOC from the uplands blanketed the streambed source during the event (Russo and Fox, 2012; Ford and Fox, 2012).

Sediment FPOC was collected for five years, approximately weekly, from two sites shown in Figure 1 and analyzed for its stable carbon isotope signature. Figure 1

displays the study site, sampling locations, and locations of bank sediment collection sites. Site 1 drains 32.8 km^2 of predominantly urban lands (55% urban and 45% ag) *via* 28.4 km of stream reaches (14.8 km of first order and 13.6 km of second order streams). Site 2 drains 61.8 km^2 of predominantly agricultural land use (43% urban and 57% ag) *via* 54.3 km of stream reaches (25.9 km of first order, 19.6 km of second order and 8.8 km of third order streams).

4.3.2 Five Year Dataset of $\delta^{13}C$

In order to assess the FPOC quality in the time frame prior to, during and following an extreme event, we measured the stable carbon isotopic signature ($\delta^{13}C$) of transported FPOC, symbolized as $\delta^{13}C_T$, and the carbon content of fine sediment, symbolized as C_T, over a five year time period in the South Elkhorn Creek. *In situ* sediment trap samplers (Phillips et al., 2000) were installed at the longitudinal midpoint (Site 1) and outlet (Site 2) of the watershed to collect temporally and spatially integrated $\delta^{13}C_T$ and C_T samples. The samples were collected on a weekly basis over a five year period from spring 2006 to winter 2010. 185 samples were collected at Site 1 and 189 samples were collected at Site 2. Sediment trap samples were removed from the analysis if trap inlets were clogged or buried by large sediment deposits or debris during sample collection or if C_T was below that of the source end members. After filtering, 146 samples were obtained from Site 1 and 150 were obtained from Site 2.

In addition to collection of the in-stream transported sediments that include a mixture of high quality, autochthonous FPOC and lower quality soil-derived FPOC, sediment samples were collected to estimate FPOC sources. Samples were collected during storm events in spring, 2006 to help constrain the carbon isotopic and elemental signature of transported upland soils. Samples were collected in three tributaries (see T1, T2 and T3 in Fig 1). The tributary samples are also described in Fox et al. (2010). In total, 11 additional samples were collected and analyzed (see Table 1). Bank sediment samples were collected to estimate the carbon isotopic and elemental signature of bank-derived FPOC. Vegetation was removed from the bank surface and approximately 20 grams of sample were collected (see Fox et al., 2010

for full explanation of bank sampling methods). Samples were collected at 15, 30 and 45 cm above the water surface at each site and pooled. In total, 15 samples were collected from 5 different sites (BS-1-BS-5) in 2007 and 2008 (see Table 1).

Each sediment trap sample was brought back to lab, centrifuged, decanted and freeze dried to remove dissolved components. Bank samples were dried in an oven at 45° Celsius. For samples greater than 0.5 grams, subsamples were obtained and wet-sieved on a 53 μm sieve. All samples were then ground for stable carbon isotope analysis. To remove carbonate phases, samples were acidified repeatedly using 6% sulfurous acid (Verardo et al., 1989). Samples were analyzed using a Costech 4010 elemental analyzer interfaced with a Thermo Finnigan Conflo III device and connected to a Thermo Finnigan Delta Plus XP isotope ratio mass spectrometer. Isotopic results were reported in terms of delta notation defined in Equation (1).

$$\delta^{13}C = \left(\frac{R_{Sample}}{R_{Standard}} - 1\right) * 1000 \quad (1)$$

where R_{Sample} is the $^{13}C/^{12}C$ ratio of the samples and $R_{Standard}$ is the $^{13}C/^{12}C$ ratio of the universal standard, Vienna Pee Dee Belemnite (VPDB). The carbon elemental signature, *C*, was reported as a percentage of the mass of carbon relative the mass of sediment. Average standard deviation for the samples were 0.04‰ for $\delta^{13}C$ and 0.82% for *C*. Average standard deviations of standards were 0.04‰ for $\delta^{13}C$ and 0.82% for *C*. Standard deviations are based on averages from all analytical runs in which standards and samples were analyzed in three or more replications.

4.3.3 New FPOC Quality Metric: R_{qual}

The FPOC quality metric, symbolized as R_{qual}, was formulated using $\delta^{13}C$ and applied in this paper to estimate the ratio of labile autotrophic FPOC to recalcitrant terrestrial derived FPOC. R_{qual} of a given sediment mixture can be estimated using Equation (2).

$$R_{qual-Mixture} = \frac{\sum_{i=1}^{n} X_{AS,i}^{C}}{\sum_{j=1}^{m} X_{TS,j}^{C}}, \quad (2)$$

where, X^C denotes a fraction of FPOC in a sediment mixture from a given source, *AS* and *TS* represent the autochthonous sources and terrestrial sources, *i* and *j* are indices, and *n* and *m* are the total number of autochthonous and terrestrial sources. R_{qual} in Equation (2) provides a quantitative measure of quality in which R_{qual} values between 0 and 1 correspond to terrestrial FPOC dominance, i.e., lower quality carbon, while R_{qual} values greater than 1 correspond to autochthonous FPOC dominance, i.e., higher quality carbon. For streams, the terrestrial FPOC sources can include a heterogeneous mixture of soils eroded at different depths as well as decomposed leaf litter and detritus. Similarly, autochthonous FPOC can originate from detrital benthic algae and decomposed macrophytes.

We apply the use of the $\delta^{13}C$ tracer for the FPOC sources in the South Elkhorn to estimate $R_{qual.}$ for the low quality bank and upland FPOC sources and high quality algal streambed FPOC source (i.e., $X^C_{AS,i}$ and $X^C_{TS,j}$ in Equation 2). It's recognized that the streambed source for South Elkhorn Creek is composed of both previously deposited terrestrial sediment FPOC and high quality algal FPOC (Russo and Fox, 2012; Ford and Fox, 2012), hence $X_{AS}{}^C$ in the streambed can be separated utilizing an isotope tracer mass balance model as

$$X^C_{AS-Bed} = \frac{\delta^{13}C_{Bed} - \delta^{13}C_{TS,U}}{\delta^{13}C_{AS} - \delta^{13}C_{TS,U}}, \tag{3}$$

where, $\delta^{13}C_{Bed}$ is the composite streambed sediment carbon isotopic signature, $\delta^{13}C_{TS,U}$ is the carbon isotopic signature of the upland terrestrial source, and $\delta^{13}C_{AS}$ is the carbon isotopic signature of the autochthonous algal source. $X^C{}_{TS,U}$ in the streambed can be estimated based on the condition that the summation of the fractions equals unity. $\delta^{13}C_{Bed}$ was estimated using a similar mass balance for the transported carbon isotopic signature and the identity that X^C of the source equals the sediment source fraction multiplied by the ratio of carbon content of the source to carbon content of the transported sediment signature. $\delta^{13}C_{Bed}$ was estimated as

$$\delta^{13}C_{Bed} = \frac{C_T\delta^{13}C_T - C_{TS,Ba}X^S_{TS,Ba}\delta^{13}C_{TS,Ba} - C_{TS,U}X^S_{TS,U}\delta^{13}C_{TS,U}}{C_T - C_{TS,Ba}X^S_{TS,Ba} + C_{TS,U}X^S_{TS,U}}, \tag{4}$$

where, C is the carbon content of the different sources, X^S is the fraction of sediment associated with each source, Ba represents the terrestrial bank source, and T represents the composite transported FPOC mixture.

Equations (2), (3) and (4) were parameterized and solved utilizing the previously described $\delta^{13}C$ and C data that were collected, results of a published sediment transport model and parameterization ranges from the literature. Sediment fractions from bank and upland sources, $X_{TS,Ba}$, and $X_{TS,U}$ (see Figure 2b-c) were estimated using results from a sediment transport model in which fractions were modeled at T1 and T2 using a mass-balance approach that incorporates erosion/deposition dynamics as well as shear, supply and transport capacity limitations (see Russo and Fox, 2012; Ford and Fox, 2012). $C_{TS,Ba}$, and $\delta^{13}C_{TS,Ba}$ were measured at five locations in the study reach in which values are reported in Table 1, the average value was used for model parameterization. $C_{TS,U}$ and $\delta^{13}C_{TS,U}$ were constrained using measurements at three tributaries (Table 1) and high flow events in the main stem as these values represent a larger contribution from the upland soils (see Figure 3); the average value was used for model parameterization. $\delta^{13}C_{AS}$ was assumed constant during the five year period and was estimated using values derived from a lowland agricultural watershed and assuming that decomposition results in a fractionation of 2‰ (Dalzell et al. 2007; Hill and Mcquaid, 2009). Table 2 summarizes the ranges for all $\delta^{13}C$ and C values and the final parameterized values.

4.3.4 Statistical Analysis

Carbon transported in South Elkhorn Creek has been previously shown to be non-normally distributed (Ford and Fox, *in Review*). Hence, non-parametric tests were needed to estimate if temporal and spatial variability was present in the dataset. Independence of individually collected samples was assumed and tests were performed in the statistical package *R Version 2.15.0* to estimate temporal and spatial variability. The Wilcoxon-rank sum test for two samples (or the Mann-Whitney U test) was used to estimate if means between Site 1 and Site 2 were significantly different (α=0.05). The Kruskal-Wallis one-way analysis of variance test was used to

estimate if significant differences in seasonal and annual distributions were present (α=0.05).

4.4 RESULTS

Figure 4a plots the five year dataset for $\delta^{13}C_T$ for Sites 1 and 2 from the main stem of the South Elkhorn stream ecosystem. Pronounced temporal dynamics in the longitudinal dataset of $\delta^{13}C_T$ are observed in Fig 4a including an instantaneous increase of $\delta^{13}C_T$ following the extreme event in late September 2006. Thereafter, a steady, increase of $\delta^{13}C_T$ occurs through summer of 2007 followed by a rapid decrease of $\delta^{13}C_T$ in fall of 2007. Following 2007, periodic seasonal fluctuations of $\delta^{13}C_T$ with more gradual annual decreases from 2008 to 2010 are visually observed in Fig 4a. $\delta^{13}C_T$ ranges from -24.5 to -28.8‰ for Site 1 and -24.4 to -28.6‰ for Site 2. Annual distributions were found to have statistically different locations (χ^2=153.3, df=4, P=2.2x10^{-16}) with means for 2006 (-26.2‰) and 2007 (-25.8‰) exhibiting significantly increased values compared to 2008 (-26.9‰), 2009 (-27.11‰) and 2010(-27.35‰). As is evident, average values of $\delta^{13}C_T$ were inversely proportional to time from 2007 to 2010 at both sites. The impact of the September 2006 extreme event are clearly evident in that $\delta^{13}C_T$ signatures for 2007 average around 0.5‰ higher than averages from any other year in the study. Locations of seasonal distributions were also found to be statistically different (χ^2=8.7, df=3, P=0.033) supporting the seasonal oscillations seen visually in Fig 4a. Seasonal means for winter (-26.9‰), spring (-26.6‰), summer (-26.7‰) and fall (-26.5‰) support that there are deviations with some years having more pronounced seasonal deviations relative to others. For example, $\delta^{13}C_T$ in 2008 is fairly static seasonally with little enrichment or depletion of the signature observed which starkly contrasts 2010 where the signature experienced enrichment from -28.5‰ to -26.1‰ during winter and spring and depletion from -26.1‰ to -28.8‰ during summer and fall. As a final note on $\delta^{13}C_T$, high between-event variability was observed for both sites with differences between consecutive data points as large as 3‰.

Figure 4b plots $\delta^{13}C_T$ seasonal and annual means for Sites 1 and 2, and visually little differences are seen supporting the concept that FPOC transport

processes are similar throughout the main stem of South Elkhorn Creek and the sites can be treated as replicates. Regressing annual and seasonal means for Site 1 against Site 2 generates a high coefficient of determination (R^2=0.93) and a slope of 1 (see Fig 4b). Results of the Mann-Whitney U test revealed that the distributions were not significantly different (P=0.5831) suggesting spatial variability was not pronounced. Samples were pooled from Site 1 and Site 2 to assess longitudinal variability.

Figure 4c plots results of $\delta^{13}C_{Bed}$ estimated using Equation (4) for Sites 1 and 2 for the five year temporal duration. $\delta^{13}C_{Bed}$ shows similar temporal trends as $\delta^{13}C_T$, albeit more pronounced fluctuations since the storm-derived contribution of FPOC from the upland soils and streambanks are removed from the $\delta^{13}C$ signal. $\delta^{13}C_{Bed}$ shows increase following the September 2006 event, restabilization of the signature in late 2007, and seasonal oscillations more clearly than $\delta^{13}C_T$. The improved observations of $\delta^{13}C$ streambed dynamics for the $\delta^{13}C_{Bed}$ decomposed signal relative to $\delta^{13}C_T$ are particularly evident during the 2008, 2009 and 2010 seasonal oscillations as removal of upland and bank sources allow unmasking of streambed signature which exhibits biologic control. The range of isotopic signatures of $\delta^{13}C_{Bed}$ for Site 1 and Site 2 were -22.9 to -29.13‰ and -22.3 to -29.12‰ respectively. Similar to $\delta^{13}C_T$, seasonal (χ^2=18.2, df=3, P=0.004) and annual (χ^2=149.28, df=4, P=2.2x10^{-16}) variability were statistically significant.

Figure 4d plots $\delta^{13}C_{Bed}$ seasonal and annual means for Sites 1 and 2, and visually little differences are seen. Similar to $\delta^{13}C_T$, $\delta^{13}C_{Bed}$ at Sites 1 and Site 2 were not found to be significantly different supporting the concept that FPOC processes are similar at the sites and the sites can be treated as replicates. Regressing annual and seasonal means of Site 1 against Site 2 generated a high coefficient of determination (R^2=0.93) and a slope of 0.99 (Fig 4d). Further the Mann-Whitney U test revealed no significant differences between distributions at Site 1 and Site 2 (P=0.06).

In order to include uncertainty in our analysis of the decomposed $\delta^{13}C_{Bed}$ signal via Equation (4), Figure 5 displays the sensitivity of $\delta^{13}C_{Bed}$ for the parameterization range reported in Table 2. For high and low-end variability of $\delta^{13}C_{Bed}$, longitudinal trends are consistent with that observed for the final parameterized results in Fig 4c. The $\delta^{13}C$ enrichment following the September 2006

event has a small range of variability and shows clear enrichment for both low and high simulations. With regard to seasonal fluctuations in the $\delta^{13}C_{Bed}$ signature, low end variability had more pronounced oscillations while high-end variability had similar signatures to $\delta^{13}C_T$.

Figure 6 provides results of R_{qual} for transported and streambed FPOC for all sampling points when $\delta^{13}C_T$ was measured from 2006 to 2010. Visually it is noticed that R_{qual} distinguishes between periods of low and high quality longitudinally associated with the September 2006 extreme event and the later re-stabilization period. R_{qual} is inversely proportional to the $\delta^{13}C$ values shown in Fig 4a,c, which reflects the low quality associated with higher $\delta^{13}C$ signatures of upland and bank sources and higher quality associated with lower $\delta^{13}C$ signatures of autochthonous sources. Generally, R_{qual} ranges from 0-2.07 for benthic FPOM and 0-1.41 for transported FPOM with averages of 0.33 and 0.19 respectively. These averages correspond to algae derived FPOC constituting 25% of benthic and 16% of transported pools. Immediately following the storm event in September, 2006 $R_{qual\text{-}T}$ and $R_{qual\text{-}Bed}$ shift close to zero suggesting poor quality. As evidence in Figure 6, quality of benthic and transported FPOC remains low through much of 2007 before it starts to increase in late fall. From 2008 to 2010 $R_{qual\text{-}T}$ has an increasing annual trend with some seasonal oscillations while $R_{qual\text{-}Bed}$ maintains a fairly stable annual average with more prevalent seasonal oscillations. Low quality coincides with enriched carbon isotopic values while high quality coincides with depleted isotopic values (see Fig 4).

4.5 DISCUSSION

4.5.1 Impact of Extreme Flow Disturbance on FPOC Quality

Results of this study support the hypothesis that the extreme flow disturbance generates disequilibrium conditions in which benthic, as well as transported FPOC quality is dampened for an extended period of time. For the two seasons prior to the extreme disturbance, R_{qual} results suggest that benthic FPOC has an average of 12% labile high quality carbon. Subsequently, in the two seasons following the high

magnitude disturbance a major shift in the $\delta^{13}C$ signatures and low estimates of R_{qual} were observed, suggesting a shift to recalcitrant upland soil and streambank sediment derived benthic carbon in which only 6.5 % of the benthic FPOC was labile autochthonous material. Quality remains low until late 2007 when results suggest that algal FPOC is able to reestablish and comprise on average 35% of the FPOC pool during late fall and winter. Thereafter, in 2008 to 2010 FPOC quality oscillates seasonally about an annual mean, suggesting reestablishment of a quasi-equilibrium state in which algal FPOC stocks accrue during warm, dry periods, i.e., late spring through early fall, and are depleted during cool, wet periods, i.e., late fall through early spring, which generally agrees with previous study of carbon dynamics in the stream ecosystem (Ford and Fox, 2012).

Results of this study suggest that the response of $\delta^{13}C$ and FPOC quality estimated *via* R_{qual} to the extreme flow disturbance reflects coupled disturbances of the sediment and algal pools. Enriched signatures of $\delta^{13}C$ and depleted R_{qual} values following the September, 2006 event suggest that high deposits of fine silts and clay from upland soils blanket the streambed, resetting the bed to low quality FPOC. This observation adds to the traditional as well as growing body of knowledge that high flows promote pronounced connectivity of the stream channel and upland hillslopes (Ferguson 1988; Whiting, 2002; Milan, 2012). Burial of the algal pool by fine sediment deposits coupled with the timing of the high magnitude disturbance result in enriched values of $\delta^{13}C$ and poor FPOC quality for much of 2007. Stunted recovery of FPOC quality is suggested to stem from smothering existing algal biomass with fine sediment deposits, limiting light and oxygen for biological growth. Peterson (1996) suggested a similar process for benthic dominated stream systems with high potential for upland derived loads during events. Further, since the extreme event in the South Elkhorn Creek occurs during the fall, lower ambient light availability and milder temperatures create unfavorable conditions for development of a new algal mat (e.g., Biggs 2000). The result is that algal biomass is unable to regenerate until the following growing season with significant contributions to the FPOC pool becoming prominent at the end of the year since algal FPOC requires senescence and decomposition of the algal mat (Ford and Fox, 2012).

Although numerous studies have investigated the response of algal biomass to excessive fluvial shear (Peterson, 1996; Matthei et al., 2003; Riseng et al., 2004; Davis et al., 2013), less research has studied algal and FPOC quality recovery following extensive deposition and smothering of the algal pool (Peterson, 1996). This study agrees with the limited number of studies that have shown stunted recovery of algal biomass following burial from sediment deposits (Steinman et al., 1990, Steinman et al., 1991; Peterson, 1996). To this end this study provides the first *in situ* approach to understanding recovery periods of high quality FPOC following extreme hydrologic events.

4.5.2 Implications of FPOC Quality

The longitudinal variation of FPOC quality as impacted by extreme hydrologic events observed in this study has important implications for sediment-derived carbon budgets and nutrient fate. The importance of high quality, algal carbon to the FPOC budget has been highlighted in detail in Ford and Fox (2012). Results of this study show the highly variable nature of transported FPOC quality. This study highlights low FPOC quality for in-stream and transported sediments during periods following extreme storm events as well as spring and summer under quasi-equilibrium conditions. Further, high FPOC quality occurs during late fall and into winter stemming from optimal conditions for autotrophic growth during summer and fall. Seasonal variability of FPOC quality has implications for nutrient fate as recent studies in agriculturally-impacted stream ecosystems have highlighted that denitrifying heterotrophic microbes are enhanced by the availability of high quality organic carbon, high NO_3^- concentrations and zones of low oxygen availability (Arango et al., 2007; Arango and Tank, 2008; Findlay et al., 2011; Newcomer et al., 2012). We suggest that linking transported R_{qual} to *in situ* and laboratory studies of denitrification rates could be further implemented into nitrogen models that simulate streambed denitrification to better understand nitrogen removal.

4.5.3 Ability of $\delta^{13}C$ and R_{qual} to Reflect FPOC Quality

Results of this study support the concept that the $\delta^{13}C$ signature of transported FPOC can be used to as a metric for the quality of FPOC. The carbon stable isotope works well at discriminating quality since high vs. low quality FPOC sources have distinctive isotopic signatures. The proposed approach is supported in that the literature parameterized model of R_{qual} suggests an average algal FPOC contribution of 16% to the transported load, which is within the range found in a previously published carbon fate and transport model for the system (Ford and Fox, 2012). R_{qual} fulfills a current need to better constrain quality of FPOC longitudinally (e.g. seasonal, annual and event based variability), as is evidenced by Figure 6. R_{qual} appears an effective measure of quality in that it clearly differentiates between labile and recalcitrant pools and quantifies their contributions to the FPOC mixture which aids in fulfilling the disconnect present between studies of organic matter budgets and organic matter quality (Marcarelli et al., 2011).

Despite our perceived usefulness of R_{qual}, some limitations exist that provide avenues for further research. Currently, R_{qual} assumes high or low quality depending on substrate type; however bio-stabilization of recalcitrant SOM has been recognized to improve its bioavailabilty (Lane et al., 2013). Future improvements to R_{qual} are needed to incorporate these recent advancements in sediment aggregate composition in which the surface area of transported sediment can be higher during summer months due to algal and bacterial excretion of exopolymeric substances that result in aggregation of recalcitrant SOM particles (Fox et al., 2013). Further, this current study assumes the stable isotopic signature of algal FPOC is conservative over the five year study. Variability in the isotopic signature of the DIC source or the assimilatory fractionation could impact the isotopic composition of algae. Coupling a DIC isotope submodel to this method could help to further constrain uncertainty in estimating sediment FPOC quality. Finally, the current application of R_{qual} provided in this study is limited to low-gradient agricultural streams with cohesive upland soils and streambanks and in-stream derived algal carbon as governing organic carbon sources.

4.6 CONCLUSIONS

Findings of this study suggest the effectiveness of utilizing ambient measures of $\delta^{13}C$ to understand the impact of extreme storm disturbances on sediment carbon quality in agriculturally-impacted stream ecosystems. Results of $\delta^{13}C_T$ show a pronounced enrichment of the isotopic signature immediately following the extreme hydrologic disturbance indicative of low quality soil FPOC, in which the signature remains enriched until the following fall. Similarly, results of $\delta^{13}C_{Bed}$ show similar impacts stemming from the extreme disturbance with more pronounced seasonal oscillations observed during the years following recovery of the isotopic signature. Further, results of this study show that R_{qual} is inversely proportional to $\delta^{13}C$, hence benthic FPOC quality was found to be poor and remain poor for a year following the extreme disturbance before recovering to pre-disturbance levels. $\delta^{13}C$ data and estimates of R_{qual} suggest the importance of timing and magnitude of deposition events on both instantaneous and long-term FPOC quality. The findings of this study are significant as climate change models project increased frequency of extreme events during fall and winter seasons in the Midwestern United States (Christensen et al., 2007). Future applications of R_{qual} across watershed gradients should be performed in order to incorporate other organic carbon fractions, e.g., C4 plants and geogenic organic matter, in order to strengthen the applicability of the metric.

4.7 REFERENCES

Akamatsu, F., Konayashi, S., Amano, K., Nakanishi, S., Oshima, Y., 2011. Longitudinal and seasonal changes in the origin and quality of transported particulate organic matter along a gravel-bed river. Hydrobiologia, 669, 183-197.

Alvarez-Cobelas, M., Angeler, D., Sa´nchez-Carrillo, S., Almendros, G., 2010. A worldwide view of organic carbon export from catchments. Biogeochemistry 107, 275-293.

Arango, C.P., Tank, J.L., 2008. Land use influences the spatiotemporal controls on nitrification and denitrification in headwater streams. J.N. Am. Benthol. Soc., 27(1), 90-107.

Arango, C.P., Tank, J.L., Schaller, J.L., Royer, T.V., Bernot, M.J., David, M.B., 2007. Benthic organic carbon influences denitrification in streams with high nitrate concentration. Freshw. Biol., 52, 1210-1222.

Battin, T.J., Kaplan, L.A., Findlay, S., Hopkinson, C.S., Marti, E., Packman, A.I., Newbold, J.A., Sabater, F., 2009. Biophysical controls on organic carbon fluxes in fluvial networks. Nat. Geosci., 1, 95-100.

Bellanger, B., Huon, S., Velasquez, F., Valles, V., Girardin, C., Mariotti, A. 2004. Monitoring soil organic carbon erosion with $\delta^{13}C$ and $\delta^{15}N$ on experimental field plots in the Venezuelan Andes. Catena, 58, 125-150.

Biggs, J.F. 2000. Eutrophication of streams and rivers: dissolved nutrient-chlorophyll relationships for benthic algae. J. N. Am. Benth. Soc., 19(1), 17-31.

Bird, M.I, Robinson, R.A.J., Win Oo, N., Maung, A., Lu, X.X., Higgitt, D.L., Swe, A., Tun, T., Lhaing Win, S., Sandar Aye, K., Mi Mi Win, K., Hoey, T.B. 2008. A preliminary estimate of organic carbon transport by the Ayeyarwady (Irrawaddy) and Thanlwin (Salween) Rivers of Myanmar. Quartenary International, 186, 113-122.

Bonn, B.A. Rounds, S.A. 2010. Use of stable isotopes of carbon and nitrogen to identify sources of organic matter to bed sediments of the Tualatin River, Oregon. USGS Scientific Investigations Report, 2010-5154, 58p.

Brunet, F., Potot, C., Probst, A., Probst, J.-L. 2011. Stable carbon isotope evidence for nitrogenous fertilizer impact on carbonate weathering in a small agricultural watershed. Rapid Commun. Mass Spectrom., 25, 2682-2690, DOI:10.1002/rcm.5050.

Chen, F., Jia, G. 2009. Spatial and seasonal variations in $\delta^{13}C$ and $\delta^{15}N$ of particulate organic matter in a dam-controlled subtropical river. River Res. Applic., 25, 1169-1176.

Christensen, J.H., B. Hewitson, A. Busuioc, A. Chen, X. Gao, I. Held, R. Jones, R.K. Kolli, W.-T. Kwon, R. Laprise, V. Magaña Rueda, L. Mearns, C.G. Menéndez, J. Räisänen, A. Rinke, A. Sarr and P. Whetton, 2007. Regional Climate Projections. In: *Climate Change 2007: The Physical Science Basis. Contribution of Working Group I to the Fourth Assessment Report of the Intergovernmental Panel on Climate Change*, Solomon, S., D. Qin, M. Manning, Z. Chen, M. Marquis, K.B. Averyt, M. Tignor and H.L. Miller (eds.). Cambridge University Press, Cambridge, United Kingdom and New York, NY, USA.

Cole, J., Prairie, Y., Caraco, N., McDowell, W., Tranvik, L., Striegl, R., Duarte, C., Kortelainen, P., Downing, J., Middelburg, J., Melack, J., 2007. Plumbing the global carbon cycle: Intergrating inland waters into the terrestrial carbon budget. Ecosystems, 10, 171-184.

Dalzell, B., Filley, T., Harbor, J., 2007. The role of hydrology in annual organic carbon loads and terrestrial organic matter export from a Midwestern agricultural watershed. Geochim. Cosmochim. Acta, 71, 1448-1462.

Davis, J.M., Baxter, C.V., Minshall, G.W., Olson, N.F., Tang, C., Crosy, B.T. 2013. Climate-induced shift in hydrological regime alters basal resource dynamics in a wilderness river ecosystem. Freshwater Biology, 58, 306-319, DOI: 10.1111/fwb.12059.

Droppo, I., Stone, M. 1994. In-channel surficial fine grained sediment laminae. Part I: Physical Characteristics and formational processes. Hydrological Processes, 8, 101-111

Enriquez, S., Duarte, C.M., Sand-Jensen, K. 1993. Patterns in decomposition rates among photosynthetic organisms: the importance of detritus C:N:P content. Oecologia, 94, 457-471.

Findlay, S.E.G., Mulholland, P.J., Hamilton, S.K., Tank, J.L., Bernot, M.J., Burgin, A.J., Crenshaw, C.L., Dodds, W.K., Grimm, N.B., McDowell, W.H., Potter J.D., Sobota, D.J., 2011. Cross-stream comparison of substrate-specific denitrification potential. Biogeochemistry, 104, 381-392.

Ford, W.I., Fox, J.F., 2012. Model of particulate organic carbon transport in an agriculturally impacted stream. Hydrol. Process., In Press DOI: 10.1002/hyp.9569

Ford, W.I., Fox, J.F., 2012. Statistical distribution of transported sediment carbon is a low-gradient stream. J. Hydrol., In Review

Fox, J.F., Papanicolaou, A.N. 2007. The use of carbon and nitrogen isotopes to study watershed erosion processes. Journal of the American Water Resources, 43(4), 1047-1064

Fox, J., Davis, C., Martin, D. 2010. Sediment source assessment in a lowland watershed using nitrogen stable isotopes. Journal of American Water Resources Association, 46, 1192-1204.

Fox, J., Ford, W.I., Strom, K., Villarini, G., Meehan, M. 2013. Benthic control upon the morphology of transported fine sediments in a low-gradient stream. Hydrological Processes, In Press, DOI: 10.1002/hyp.9928.

Fox, J. 2009. Measurements of sediment transport processes in forested watersheds with surface coal mining disturbance using carbon and nitrogen isotopes. *Journal of the American Water Resources Association,* 45(5), 1273-1289.

Gao, Q., Tao, Z., Yao, G., Ding, J., Liu, Z., Liu, K. 2007. Elemental and isotopic signatures of particulate organic carbon in the Zengjiang River, southern China. Hydrological Processes, 21, 1318-1327.

Gomez, B., Trustrum, N., Hicks, D., Rogers, K., Page, M., Tate, K., 2003. Production, storage, and output of particulate organic carbon: Waipaoa River basin, New Zealand. Water Resour. Res., 39(6), ESG2-1-ESG2-8.

Griffiths, N.A., Tank, J.L., Royer, T.V., Warrner, T.J., Frauendorf, T.C., Rosi-Marshall, E.J., Whiles, M.R., 2012. Temporal variation in organic carbon spiraling in Midwestern agricultural streams. Biogeochemistry, 108, 149-169.

Gu, B., Schelske, C.L., Waters, M.N. 2011. Patterns and controls of seasonal variability of carbon stable isotopes of particulate organic matter in lakes. Oecologia, 165, 1083-1094, DOI: 10.1007/s00442-010-1888-6.

Helie, J., Hillaire-Marcel, C. 2006. Sources of particulate and dissolve organic carbon in the St Lawrence River: isotopic approach. Hydrological Processes, 20, 1945-1959.

Hill, J.C., Mcquaid, C.D. 2009. Variability in the fractionation of stable isotopes during degradation of two intertidal red algae. Estuarine, Coastal and Shelf Science, 82, 397-405.

Hope, D., Billett, M., Cresser, M., 1994. A review of the export of carbon in river water: fluxes and processes. Environ. Pollut., 84, 301–324.

Jacinthe, P.A., Lal, R., Owens, L.B., 2009. Application of stable isotope analysis to quantify retention of eroded carbon in grass filters at the North Appalachian experimental watersheds. Geoderma, 148, 405-412.

Kendall, C., Silva, S.R., Kelly, V.J. 2001. Carbon and nitrogen isotopic compositions of particulate organic matter in four large river systems across the United States. Hydrological Processes, 15, 1301-1346, DOI: 10.1002/hyp.216.

Lane, C.S., Lyon, D.R., Ziegler, S.E. 2013. Cycling of two carbon substrates of contrasting lability by heterotrophic biofilms across a nutrient gradient of headwater streams. Aquat Sci, 75, 235-250, DOI: 10.1007/s00027-013-0269-0

Lubowski, R.N., Vesterby, M., Bucholtz, S., Baez, A., Roberts M.J., 2006. Major uses of land in the United States, 2002. Economic Information Bulletin Number 13. Economic Research Service, United States Department of Agriculture, Washington.

Lyon, D.R., Ziegler, S.E. 2009. Carbon cycling within epilithic biofilm communities across a nutrient gradient of headwater streams. Limnol. Oceanogr., 54, 439-449.

Marcarelli, A.M., Baxter, C.V., Mineau, M.M., Hall, R.O. 2011. Quantity and quality: unifying food web and ecosystem perspectives on the role of resource subsidies in freshwaters. Ecology, 92(6), 1215-1225.

Martinotti, W., Camusso, M., Guzzi, L., Patrolecco, L., Pettine, M. 1997. C,N and their stable isotopes in suspended and sedimented matter from the Po estuary (Italy). Water, Air, Soil Pollution, 99, 325-332.

Matthei, C.D., Guggelberger, C., Huber, H. 2003. Local disturbance history affects patchiness of benthic river algae. Freshwater Biology, 48, 1514-1526.

Milan, D. 2012. Geomorphic impact and system recovery following an extreme flood in an upland stream: Thinhope Burn, northern England, UK. Geomorphology, 138, 319-328.Mukundan, R., Radcliffe, D.E., Ritchie, J.C., Risse, L.M., McKinley, R.A. 2010. Sediment fingerprinting to determine the source of suspended sediment in a southern piedmont stream. J. Envrion. Qual., 39, 1328-1337, DOI: 10.2134/jeq2009.0405.

Mulholland, P., Helton, A., Poole, G., Hall, R., Hamilton, S., Peterson, B., Tank, J., Ashkenas, L., Cooper, L., Dahm, C., Dodds, W., Findlay, S., Gregory, S., Grimm, N., Johnson, S., McDowell, W., Meyer, J., Valett, H., Webster, J., Arango, C., Beaulieu, J., Bernot, M., Burgin, A., Crenshaw, C., Johnson, L., Niederlehner, B., O'Brien, J., Potter, J., Sheibley, R., Sobota, D., Thomas, S. 2008. Stream denitrification across biomes and its response to anthropogenic nitrate loading. Nature, 452, 202-206.

Newcomer, T.A., Kaushal, S.S., Mayer, P.M., Shields A.R., Canuel, E.A., Groffman, P.M., Gold, A.J., 2012. Influence of novel organic carbon sources on denitrification in forest, degraded urban and restored streams. Ecol. Monogr., 82(4), 449-466.

Onstad, G.D., Canfield, D.E., Quay, P.D., Hedges, J.L. 2000. Source of particulate organic matter in rivers from the continental USA: lignin phenol and stable carbon isotope compositions. Geochemica et Cosmochimica, 64(20), 3359-3546.

Palmer, S.M., Hope, D., Billett, M.F., Dawson, J.J.C., Bryant, C.L. 2001. Sources of organic and inorganic carbon in a headwater stream: evidence from carbon isotope studies. Biogeochemistry, 52, 321-338.

Peterson, C. G. (1996) Response of benthic algal communities to natural physical disturbance. Pages 375-402, In (R. J. Stevenson, M. L. Bothwell, & R. L. Lowe, editors) Algal Ecology: Freshwater Benthic Ecosystems. Academic Press, San Diego.

Phillips, D.L., Gregg, J.W. 2003. Source partitioning using stable isotopes: coping with too many sources. Oecologia, 136, 261-269, DOI: 10.1007/s00442-003-1218-3.

Riseng, C.M., Wiley, M.J., Stevenson, R.J. 2004. Hydrologic disturbance and nutrient effects on benthic community structure in Midwestern US streams: a covariance structure analysis. J. N. Am. Benthol. Soc., 23(2), 309-326.

Russo, J., Fox, J., 2012. The role of the surface fine-grained laminae in low-gradient streams: A model approach. Geomorphology, 171-172, 127-138.

Rutherford, J., Scarsbrook, M., Broekhuizen, N., 2000. Grazer control of stream algae: modeling temperature and flood effects. J. Environ. Eng., 126, 331–339.

Sakamaki, T., Richardson, J.S. 2011. Biogeochemical properties of fine particulate organic matter as an indicator of local and catchment impacts on forested streams. J. App. Eco., 48, 1462-1471, DOI: 10.1111/j.1365-2664.02038.x.

Sarma V.V.S.S., Arya, J., Subbaiah, Ch.V., Naidu, S.A., Gawade, L., Kumar, P.P, Reddy, N.P.C. 2012. Stable isotopes of carbon and nitrogen in suspended matter and sediments from the Godavari estuary. J. Oceanogr., 68, 307-319, DOI: 10.1007/s10872-012-0100-5.

Schindler Wildhaber, Y., Liechti, R., Alewell, C. 2012. Organic matter dynamics and stable isotope signature as tracers of the sources of suspended sediment. Biogeosciences, 9, 1985-1996, DOI: 10.5194/bg-9-1985-2012.

Sharp, Z. 2007. Principles of stable isotope geochemistry. Prentice Hall, New Jersey. 360p.

Sigleo, A.C., Macko, S.A. 2002. Carbon and nitrogen isotopes in suspended particles and colloids, Chesapeake and San Francisco Estuaries, U.S.A. Estuarine, Coastal and Shelf Science, 54, 701-711.

Six, J., Jastrow, J. 2002. Soil organic matter turnover. In *Encyclopedia of Soil Science*, Lal R. (eds). Boca Raton, FL; 936–942.

Smith, B.N., Epstein, S. 1971. Two categories of $^{13}C/^{12}C$ ratios for higher plants. Plant Physiol., 47, 380-384.

Steinman, A.D., McIntire, C.D. 1990. Recovery of lotic periphyton communities after disturbance. Environmental Management, 14, 589-604.

Steinman, A.D., Mulholland, P.J., Palumbo, A.V., Flum, T.F., DeAngelis, D.L. 1991. Resistance of lotic ecosystems to a light elimination disturbance: a laboratory stream study. Oikos, 58, 80-90.

Tank, J.L., Rosi-Marshall, E.J., Griffiths, N.A., Entrekin, S.A., Stephen, M.L., 2010. A review of allochthonous organic matter dynamics and metabolism in streams. J. North Am. Benthol. Soc., 29(1), 118-146.

Thorp, J.H., Delong, M.D. 2002. Dominance of autochthonous carbon in food webs of heterotrophic rivers. Oikos, 96(3), 543-550.

Trimmer, M., Grey, J., Heppell, C.M., Hildrew A.G., Lansdown, K., Stahl, H., Yvon-Durocher, G., 2012. River bed carbon and nitrogen cycling: State of play and some new directions. Sci. Total Environ., DOI: 10.1016/j.scitotenv.2011.10.074

Vieira, A.A.H. Myklestad, S. 1986. Production of extracellular carbohydrate in cultures of Ankistrodesms densus. J. Plankton Res., 8, 985-994.

Waite, A.M., Olson, R.J., Dam, H.G., Passow, U. 1995. Sugar-containing compounds on the cell surfaces of marine diatoms measured using concanavalin A and flow cytometry. J. Phycol., 31, 925-933.

Walling, D., Collins, A., Jones, P., Leeks, G., Old, G., 2006. Establishing fine-grained sediment budgets for the Pang and Lambourn LOCAR catchments. J. Hydrol., 330, 126-141.

Webster, J., Benfield, E., Ehrman, T., Schaeffer, M., Tank, J., Hutchens, J., D'Angelo, D. 1999. What happens to allochthonous material that falls into streams? A synthesis of new and published information from Coweeta. Freshwater Biology, 41, 687-705.

White, P., Kalff, J., Rasmussen, J., Gasol, J., 1991. The effect of temperature and algal biomass on bacterial production and specific growth rate in freshwater and marine habitats. Microb. Ecol., 21, 99-118.

Yoshimura, C., Gessner, M., Tockner, K., Furumai, H. 2008. Chemical properties, microbial respiration, and decomposition of coarse and fine particulate organic matter. J. N. Am. Benthol. Soc., 27, 664–673.

4.8 TABLES AND FIGURES

Table 1. $\delta^{13}C$ and C measured from streambank and tributary sources in the watershed.

Site Identifier	*Sampling Date*	*C(gC 100gSed^{-1})*	*$\delta^{13}C$*
BS-1	10/15/2007	1.55	-23.86
	3/12/2008	1.20	-24.82
	7/24/2008	1.04	-24.39
BS-2	10/26/2007	1.82	-24.38
	3/31/2008	1.57	-25.36
	7/23/2008	1.25	-25.23
BS-3	10/11/2007	1.94	-24.31
	3/12/2008	2.05	-25.16
	7/29/2008	1.80	-26.06
BS-4	10/12/2007	1.88	-24.94
	3/13/2008	1.52	-25.51
	7/24/2008	1.64	-25.92
BS-5	10/15/2007	1.87	-24.46
	3/13/2008	1.48	-24.99
	7/24/2008	1.61	-25.60
	Minimum	1.04	-26.06
	Maximum	2.05	-23.86
	Mean	1.61	-25.00
T-1	3/15/2006	2.50	-26.82
	3/17/2006	2.88	-27.17
	4/7/2006	4.07	-25.86
	4/13/2006	3.17	-26.40
T-2	3/15/2006	3.45	-27.60
	3/17/2006	4.37	-26.48
	4/13/2006	3.95	-26.51
T-3	3/15/2006	2.50	-26.67
	3/17/2006	2.68	-27.02
	4/7/2006	2.24	-26.67
	4/13/2006	2.25	-26.01
	Minimum	2.24	-27.17
	Maximum	4.37	-25.86
	Mean	3.10	-26.66

Table 2. Parameterization range values for the R_{qual} model.

Parameters	Range	Optimal Value	Units
X_{Ba},X_{Bed},X_U [(A)]	0 to 1	Event Specific	--
C_{Ba} [(A)]	1.04 to 2.05	1.6	gC 100gSed^{-1}
C_U [(A)]	2.24to 3.84	3.1	gC 100gOM^{-1}
$\delta^{13}C_{Ba}$ [(A)]	-23.9 to -26.1	-25	‰
$\delta^{13}C_U$ [(A)]	-25.7 to -27.4	-26.5	‰
$\delta^{13}C_{Alg}$ [(B)]	-28 to -42	-30.4	‰

(A) = Parameter measured or estimated in study
(B) = Parameter obtained from literature

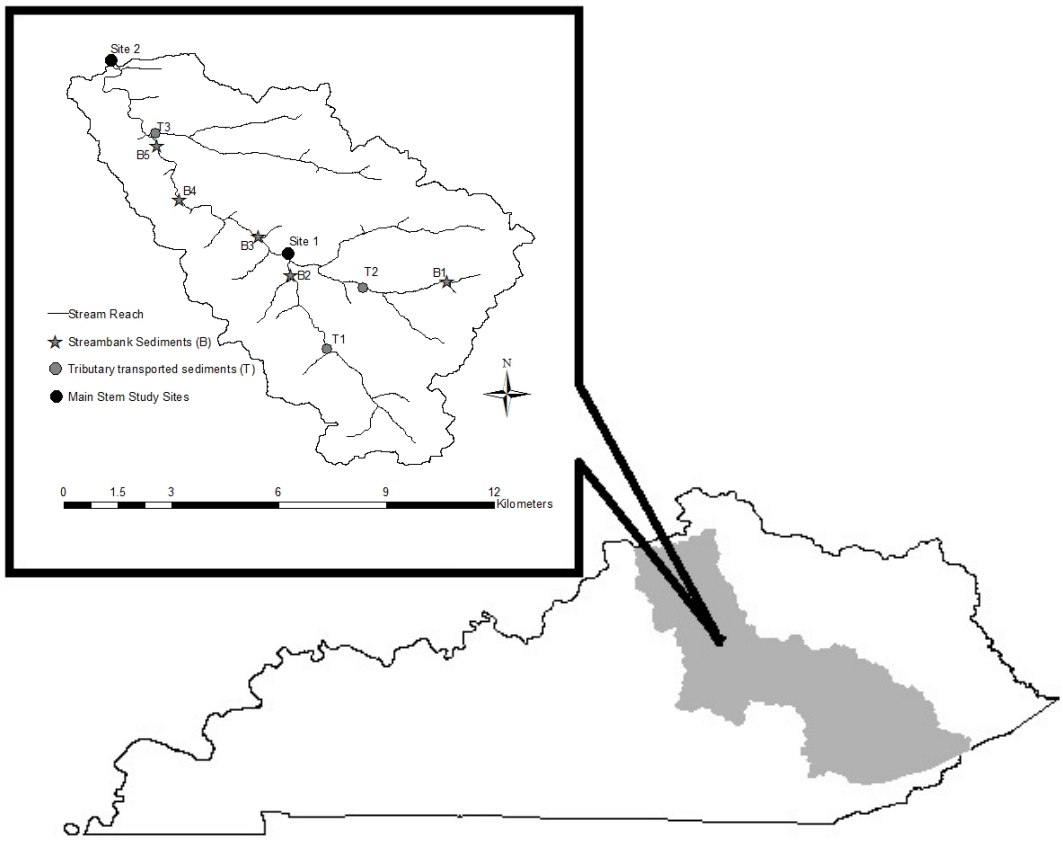

Figure 1. South Elkhorn study site and location with site for sample collection

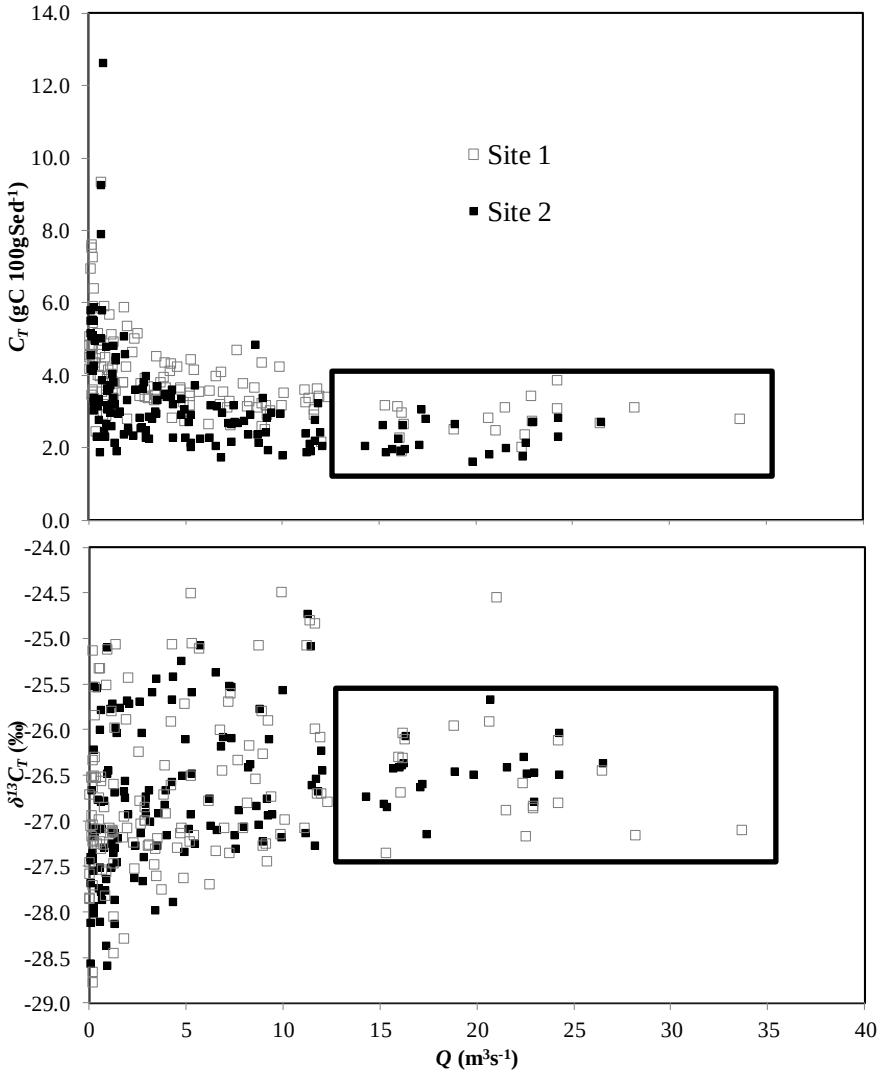

Figure 2. Scatterplot $\delta^{13}C_T$ and C_T vs. Flowrate (Q) at the watershed outlet for main stem study sites. The bounded range represents the likely composite value for $\delta^{13}C$ of upland sediments.

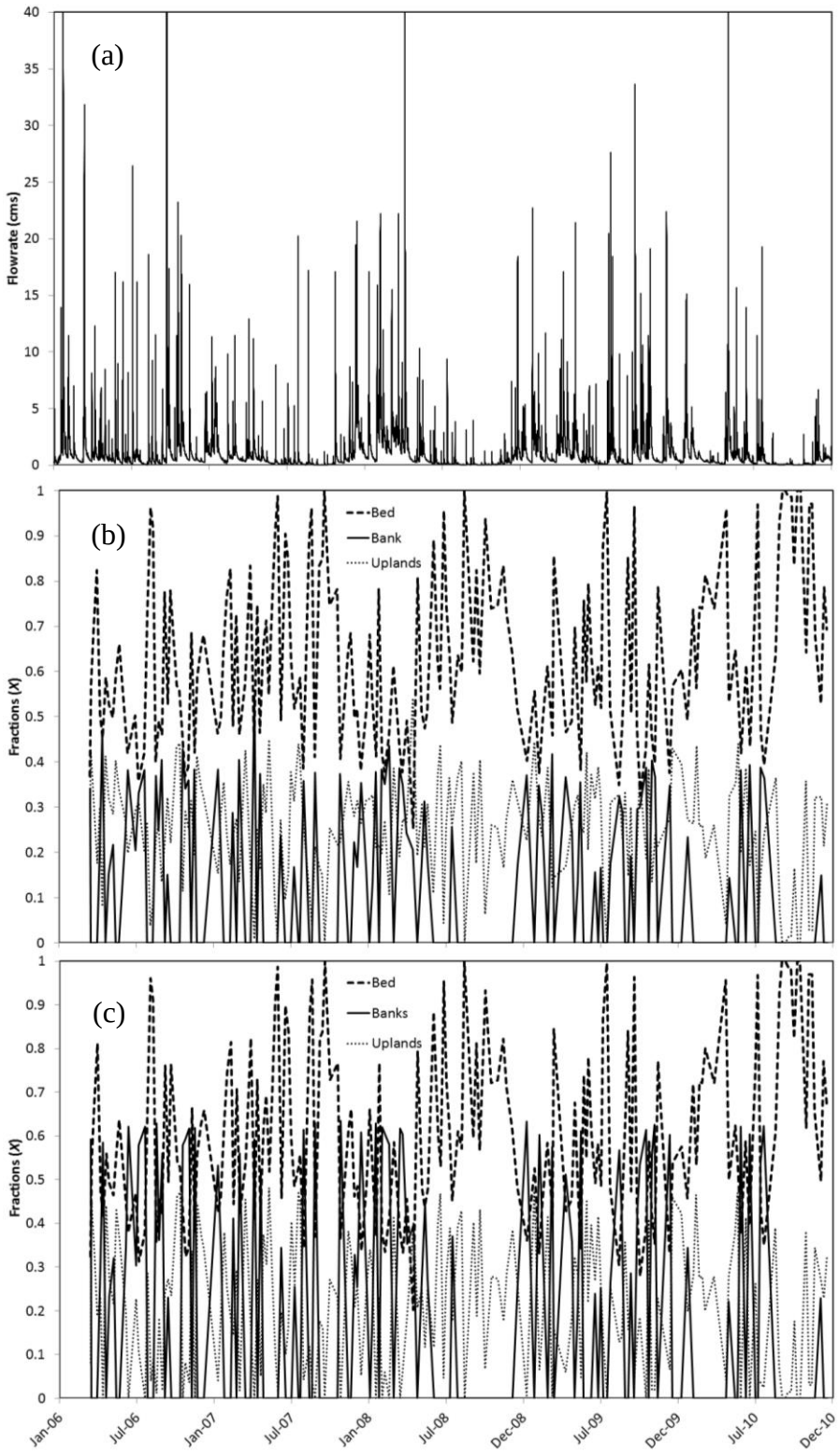

Figure 3. (a)Flowrate measured at the watershed outlet and sediment source fractions for (b) Site 1 and (c) Site 2.

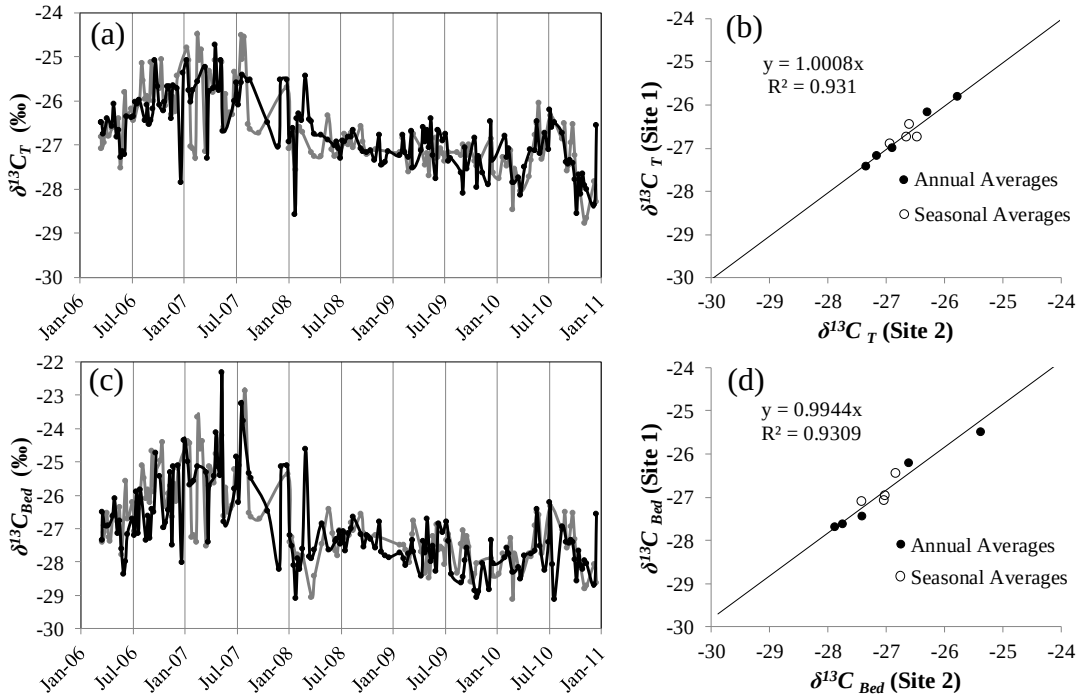

Figure 4. (a) $\delta^{13}C_T$ over five year temporal duration; (b) spatial comparison of $\delta^{13}C_T$ for sites 1 and 2; (c) $\delta^{13}C_{Bed}$ for five year temporal duration; and (d) spatial comparison of $\delta^{13}C_{Bed}$ for sites 1 and 2.

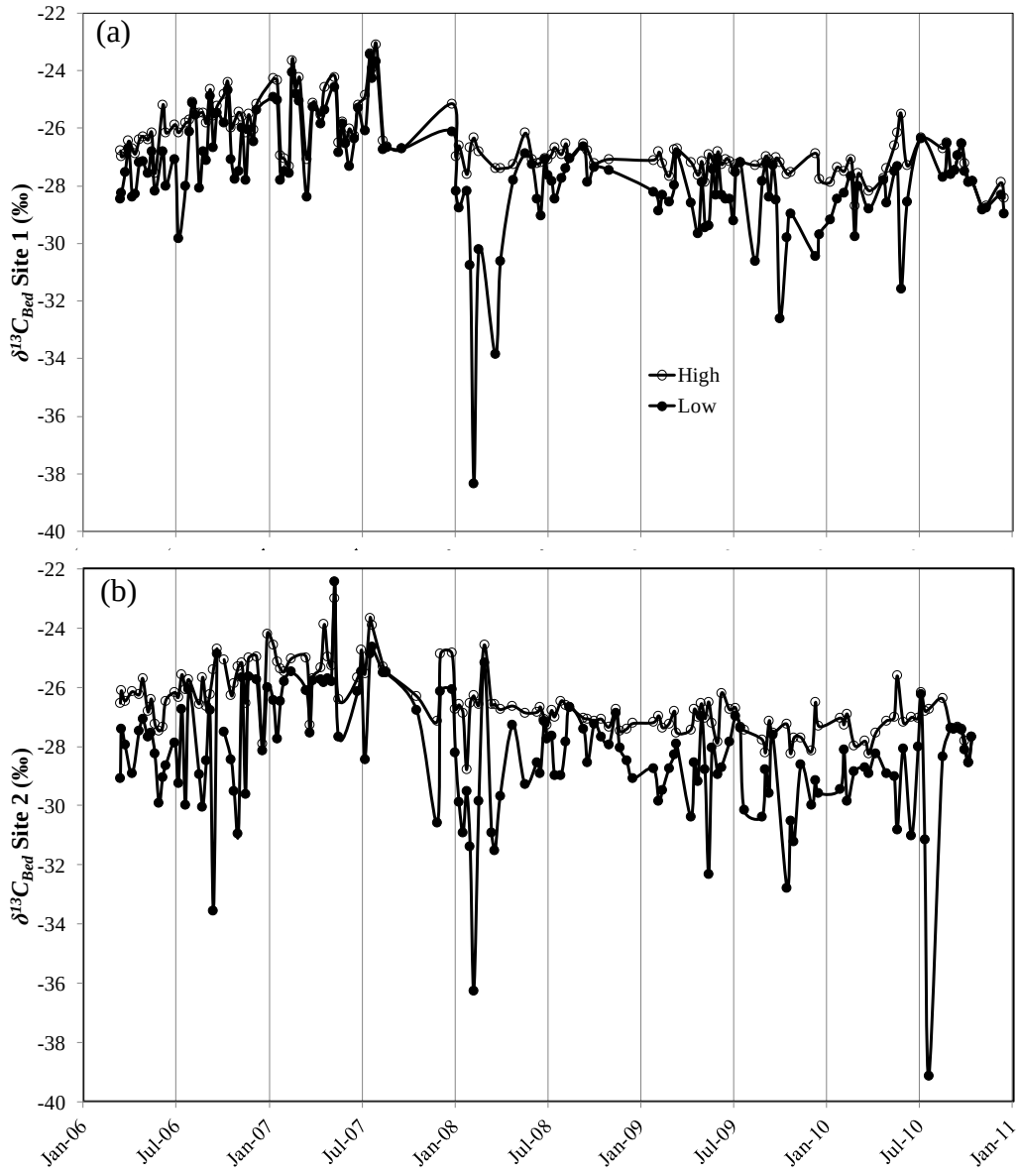

Figure 5. Variability of $\delta^{13}C_{Bed}$ for (a) Site 1 and (b) Site 2.

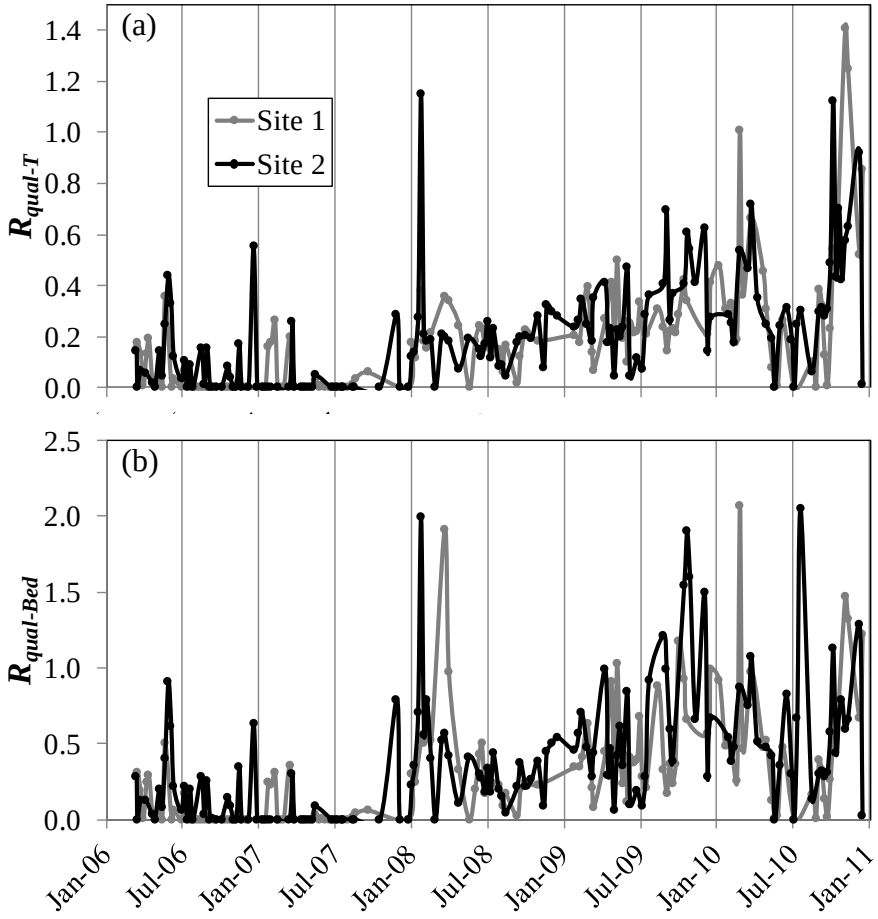

Figure 6. Five year results for (a) R_{qual-T} and (b) $R_{qual-Bed}$.

Copyright © William Isaac Ford III 2014

Chapter 5: Watershed-Scale Stable Isotope Simulation of the Fluvial Organic Carbon Budget using the ISOFLOC model

5.1 SUMMARY

A new numerical model termed ISOFLOC is presented to simulate the fluvial organic carbon budget in watersheds where hydrologic, sediment transport, and biogeochemical processes are coupled to control benthic and transported carbon composition and flux. One innovation of ISOFLOC is the formulation of new stable carbon isotope model subroutines that include isotope fractionation processes in order to estimate carbon isotope source, fate and transport. A second innovation is the coupling of transfers between carbon pools, including benthic produced algal carbon (APOC), fine particulate and dissolved organic carbon (FPOC and DOC), and particulate and dissolved inorganic carbon (PIC and DIC), to simulate the carbon cycle in a comprehensive manner beyond that of existing watershed water quality models. ISOFLOC is tested and verified in a low-gradient, agriculturally-impacted stream. Results of a global sensitivity analysis suggest high sensitivity of algal parameters in ISOFLOC, facilitating uncertainty reduction of 60% for APOC flux. Further, results of the calibration highlight tightened coupling of APOC, FPOC, and DIC pools in ISOFLOC captures C dynamics at event, seasonal and annual timescales, suggesting the potential transferability of ISOFLOC. Results of the application suggest temporal variability of APOC can shift the stream system from net autotrophic, to net heterotrophic at seasonal timescales. Finally, results for the fluvial organic carbon budget show that inclusion of APOC sloughing shifts the balance of organic carbon flux from dissolved to particulate dominated, contradicting conventional wisdom of fluvial organic carbon transport and suggesting a need to reassess fluvial organic carbon transport in highly autotrophic systems.

5.2 INTRODUCTION

Fluvial carbon budgets at the watershed-scale remain poorly constrained due to the fact that physical and biogeochemical processes alter the composition of carbon species during transit from source to sink [Cole et al., 2007; Battin 2009; Butman and Raymond, 2011]. Of particular interest are low-order streams where high nutrient loads from agriculture and urban land uses, low stream and hillslope gradients, and low canopy cover promote pronounced autochthonous benthic carbon processing and thus in-stream carbon production and turnover that is on the same order or greater than allocthonous C inputs [Mulholland et al., 2008; Tank et al., 2010; Griffiths et al., 2012; Alvarez-Cobelas et al., 2012]. For these systems, dissolved organic (DOC), particulate organic (POC), dissolved inorganic (DIC) and particulate inorganic (PIC) are the primary pools of the fluvial C budget [Hope et al., 1994]. Specifically, the organic fraction has been highlighted to have significant implications for water quality since in-stream transformations and fluxes impact trophic state of the system, benthic food webs, and nutrient and oxygen levels [Marcarelli et al., 2011]. The motivation of the present study is to improve water quality modeling technology for estimating watershed-scale fluvial organic carbon budgets in low-gradient, agriculturally impacted streams where autochthonous benthic carbon processes play a substantial role in the C cycle. We introduce the isotope-based fluvial organic carbon, or ISOFLOC, model, which simulates elemental and isotopic carbon production, transformations, and fluxes in-streams with pronounced benthic C cycling.

Synthesizing current understanding of processes that will impact the fluvial organic carbon budget alludes to the complexity of the low-gradient agriculturally disturbed stream (see Figure 1). Autotrophic algal biomass assimilates DIC and temporarily fixes it as algal POC, herein referred to as APOC. APOC can either be decomposed to fine POC (FPOC) or DOC, respired to DIC through heterotrophic respiration, or advected downstream *via* sloughing (i.e., physical detachment). FPOC is an amalgamation of carbon contained in silt and clay sized particles eroded from upland soils, streambanks, and generated within the stream channel either from breakdown of coarse POC or aggregation of DOC. FPOC is subjected to similar physical and biogeochemical forcing as APOC including further decomposition, respiration, and

downstream transport. DOC is predominantly composed of soil leachates from the upland subsurface seepage but can also contain leachates from APOC and FPOC. Inorganic carbon composition directly impacts newly generated organic matter and can reflect levels of respiration and dissolution from the streambed. PIC can be dissolved to DIC or precipitated depending on *pH* conditions, and DIC composition is dependent upon in-stream OC respiration, dissolution of PIC and gaseous exchange with the atmosphere.

Currently available watershed-scale water quality models have attempted to estimate some fluxes and transformations of the organic carbon budget depicted in Figure 1; however a model that is formulated to consider organic carbon detachment and advection as well as growth and turnover processes characteristic of streams with autotrophic cycling has not been developed previously. Watershed-scale water quality models applicable to water, sediment, C, and nutrient loadings to streams such as SWAT, AnnAGNPS, and SPARROW, tend to be focused on upland production and routing using 1-D hydrologic and sediment transport subroutines. SWAT and AnnAGNPS neglect in-stream contributions; suggesting carbon composition is a function of upland soil carbon and erosion dynamics only [Bingner et al., 2011; Neitsch et al., 2011; Oeurng et al., 2011]. SPARROW utilizes a heavily empirical regression model coupled with semi-theoretical growth and first-order decay reactions for organic carbon to simulate TOC composition at watershed outlets; however SPARROW does not adequately account for temperature dependent decomposition processes or exchange processes between carbon pools [White et al., 1991; Shih et al., 2010; Ford and Fox, 2014].

A second class of water quality models including AQUATOX, QUAL2K, and WASP are more heavily focused on water quality in-stream and have been applied to low order streams at the watershed-scale, although perhaps often erroneously given that these models are formulated to simulate C and nutrient transformations typical of large, slow moving water bodies. AQUATOX, QUAL2K, and WASP conceptualize the benthos as a two layer, 1 mm aerobic and 10 cm anaerobic, well-mixed system that receives inputs from detrital carbon of varying quality, i.e., labile algal detritus, refractory detritus, and non-reactive detritus [DiToro, 2001; Wool et al., 2006; Chapra et al., 2008; Park and Clough, 2012]. An underlying assumption of these models is that POC is contained solely in the anaerobic layer under steady state, thus the models ignore the impact of fluvial

erosion on benthic carbon composition, which is typical of streams. Further, the aerobic layer is typically much larger than 1 mm in streams resulting from fluid and algal growth and decomposition coupled with oxygen advection into the loosely compacted, neutrally buoyant surface fine-grained laminae (SFGL), or active layer [Droppo and Stone, 1994; Droppo et al., 2001; Walling et al., 2006; Russo and Fox, 2012; Ford and Fox, 2014].

A lack of watershed-scale water quality models applicable to streams with pronounced autochthonous cycling suggests new model formulations are needed that account for upland carbon loading, simulate inter-pool transfer, continuously simulate the carbon composition of the benthos, account for algal growth and turnover, and simulate the impacts of advection. Therefore, the present work aims to enhance the water quality modeling technology for fluvial organic carbon budgets through incorporation of the model feedbacks shown in Figure 1. Specifically, we account for and couple the aforementioned physical and biogeochemical processes. Further, we place emphasis on estimating the contribution of sloughed APOC to downstream fluxes, as few studies to our knowledge have incorporated this flux as a component of POC budgets. In part, this can be attributed to a lack of technology to calibrate shear resistance of algal biomass at the watershed-scale, as most algal sloughing models have focused on the process scale [Graba et al., 2010; Fovet et al., 2012; Graba et al., 2013].

It is well recognized that the physical and biogeochemical process rates impacting DOC, POC, and APOC fate and transport at the watershed-scale can produce a numerical modeling environment that is highly parameterized. In an effort to assist with model parameterization of physical and biogeochemical rates, we introduce the use of stable carbon isotopes within our watershed-scale water quality modeling. $\delta^{13}C$ is the isotopic signature of a carbon pool and reflects the ratio of ^{13}C to ^{12}C atoms in a given sample as

$$\delta^{13}C_{Sample} = \left(\frac{(^{13}C/^{12}C)_{Sample}}{(^{13}C/^{12}C)_{VPDB}} - 1 \right) \times 1000 \ , \qquad (1)$$

where δ is the standard isotope notation, and *VPDB* is the reference standard Vienna Pee Dee Belemnite. Measuring and modeling of $\delta^{13}C$ of carbon pools provides an extra set of source and transformation equations to water quality studies and thus carbon stable isotopes have been heavily applied in recent years, primarily within data-driven approaches. $\delta^{13}C$ measurements of FPOC have been used to apportion sources of carbon

in aquatic systems ranging from small streams to coastal waterbodies [Fox and Papanicolaou, 2007; Fox, 2009; Kendall et al., 2010; Schindler Wildhaber et al., 2012; Sarma et al., 2012]. Source apportionment studies have placed heavy emphasis on the ability of $\delta^{13}C$ to differentiate soil organic carbon (SOC) sources derived from C3 and C4 plants due to their significantly different $\delta^{13}C$ signatures of -24 to -29‰ and -10 to -14 ‰, respectively [Smith and Epstein, 1971; Onstad et al., 2000; Palmer et al., 2001; Fox and Papanicolaou, 2007; Fox, 2009; Jacinthe et al., 2009; Brunet et al., 2011].

Despite the recognized power of $\delta^{13}C_{FPOC}$, few studies have incorporated isotopes into catchment scale hydrologic models [McGuire and McDonnel, 2008]. The few studies that have implemented stable isotope technology in water quality modeling have focused on either nutrients (e.g., nitrogen cycling in Fox et al., 2010), or short timescales (e.g., diel cycling of DIC in Tobias and Bohlke, 2011). Synthesizing recent insights suggests $\delta^{13}C_{FPOC}$ can help constrain the fluvial organic carbon budget since $\delta^{13}C_{FPOC}$ is effective at tracing C sources, and is sensitive to isotope fractionation processes. With regard to source tracing, $\delta^{13}C$ values of autochthonous and allochthonous sources have been shown to be statistically differentiable with $\delta^{13}C$ ranges of -28 to -42‰ and -10 to -29‰ respectively [Onstad et al., 2000; Palmer et al., 2001; Dalzell et al. 2007; Sakamaki and Richardson, 2011; Schindler Wildhaber et al., 2012]. With regard to in-stream transformations, large isotope fractionations of the DIC pool during assimilation (0-20‰), and low isotope fractionation during decomposition of organic carbon (0-2‰) suggest $\delta^{13}C_{FPOC}$ can help constrain parameters associated with APOC assimilation [Jacinthe et al., 2009; Dubois et al., 2010].

Our goal is to advance watershed-scale, water quality modeling for estimating the fluvial organic carbon budget in low-gradient systems characterized by high nutrient loads and a thin, active SFGL layer. To do this, we introduce the isotope-based fluvial organic carbon, or ISOFLOC, model. ISOFLOC couples existing one-dimensional hydraulics and sediment transport, benthic algae, and FPOC mass-balance models to new DIC and $\delta^{13}C$ mass-balance sub-models that include isotope fractionation processes. ISOFLOC is tested and applied in a small, low-gradient, agriculturally disturbed watershed with prominent autochthonous cycling. Model evaluation techniques including sensitivity analysis, model calibration and validation, and uncertainty analysis

are conducted for the model testing application. An eight year longitudinal dataset of carbon content (C_{FPOC}) and the stable carbon isotopic composition ($\delta^{13}C_{FPOC}$) of fine transported sediments are utilized to assist with evaluating the modeling framework. Results of the fluvial organic carbon budget are provided for APOC, FPOC, and DOC pools to extend our understanding of streams with prominent autochthonous cycling.

5.3 METHODS

5.3.1 ISOFLOC Model Formulation

Figure 2 provides a flowchart summarizing connectivity of the sub-models in ISOFLOC. Water and sediment transport subroutines provide the basis for advective transport of dissolved and particulate carbon phases. Reaction equations for APOC, and FPOC and DIC are simulated simultaneously in ISOFLOC to estimate coupled feedbacks between the different pools. Organic carbon pools simulated in ISOFLOC include DIC, DOC, APOC and FPOC, which are characteristic of low-gradient, agriculturally and urban disturbed systems. In the following, we describe the formulation for the total elemental inorganic and organic phases, then we describe the new isotope mass balance formulations.

DIC as well as DOC advects with water streamflow and reacts with the benthic pools in the streambed. Advection of DIC and DOC is modeled in ISOFLOC using model input of volumetric water flowrate, Q_i^j, for a given spatial reach, *j*, and timestep, *i*, and Q_i^j can be modeled using data-driven, conceptual, or process-based hydrologic models calibrated for the watershed. DIC fate in a given reach is modeled to account for reactions with the streambed. Assimilation and respiration impart changes to the DIC composition, which are modeled utilizing a mass balance for *DIC* (kgC) as

$$DIC_i^j = DIC_{i-1}^j + DIC_{in_i}^{\ j} - DIC_{out_i}^{\ j} + (Dis_i^j + Inv_i^j + \mathrm{Re}s_i^j - Fix_i^j - \mathrm{Pr}e_i^j)SA_{Bed}\Delta t - Eva_i^j \quad (2)$$

where, *in* represents the advective upstream influx of DIC, *out* represents the advective downstream outflux of DIC, *Inv* (kgC m^{-2} d^{-1}) is the rate of CO_2 invasion from the atmosphere due to excess atmospheric CO_2 partial pressures, *Dis* (kgC m^{-2} d^{-1}) is the rate of particulate carbonate dissolution in the stream bed, *Pre* (kgC m^{-2} d^{-1}) is the

precipitation rate of new particulate carbonate material, and *Eva* (kgC) is the mass of CO_2 evasion from the stream channel to the atmosphere due to excess stream CO_2 partial pressures. Evasion from the stream channel is modeled using a reach-scale model of evasion based on Wallin et al. [2013] as

$$Eva_i^j = \frac{\left((P_{CO2-Water} - P_{CO2-Atm}) \times k_{Hi}{}^j \times .012\right) \times w_{CO2} \times V_{Wateri}{}^j}{H_i^j} \times \Delta t \,, \qquad (3)$$

where, k_H (mol CO_2/L atm) is the Henry's law coefficient and varies as a function of temperature [Masters and Ela, 2008], P_{CO2} (atm) is the partial pressure of CO_2, w_{CO2} (m s^{-1}) is the gas transfer velocity, and Δt is the model timestep. The coefficient, 0.012 (kgC/mol CO_2), accounts for the atomic mass of carbon present in aqueous CO_2. Partial pressure of CO_2 in the water is modeled utilizing carbonate equilibrium kinetics [Masters and Ela 2008; Doctor et al., 2008]. The model assumes that if CO_2 is not super saturated, assimilation is the sole removal process of DIC since an influx of atmospheric CO_2 will make the water acidic, favoring algal production over calcium precipitation. For the invasion rate, CO_2 is assumed to diffuse from the atmosphere to the stream until P_{CO2} is equal to that of the atmosphere (e.g. until it reaches saturation conditions). With regards to DOC, reactions with the streambed were neglected since labile autochthonous carbon from algal exudates generally make up a small portion of transported DOC and are typically turned over very quickly in small streams [Johnson, 2008]. Therefore, DOC concentrations (kgC m^{-3}) are multiplied by streamwater *Q* at the watershed outlet to estimate the mass flux of DOC at each time step.

The formulation for benthic algae (APOC) growth and fate accounts for algal DIC fixation during growth, C lost from the algal pool during respiration and decomposition, and algal transport from the benthic region due to sloughing [Rutherford et al., 2001; Ford and Fox, 2014]. *APOC* (kgC) is simulated as

$$APOC_i^j = APOC_{i-1}^j + (Fix_i^j + APOC_i^j{}_{Col} - \mathrm{Re}s_i^j - DEC_{APOC\,i}{}^j) SA_{Bed} \Delta t - Slough_i^j \,, \qquad (4)$$

where, *Fix* (kgC m^{-2} d^{-1}) is the carbon fixation rate, $APOC_{col}$ (kgC m^{-2} d^{-1}) is the algal colonization rate, *Res* (kgC m^{-2} d^{-1}) is the respiration rate of the algal mat, DEC_{APOC} (kgC m^{-2} d^{-1}) is the breakdown rate of coarse algae to fine sediment algae and are assumed to vary proportionally with heterotrophic bacterial growth [e.g., White et al., 1991], and

Slough (kgC) is the carbon eroded from the algal mat. Algal sloughing is modeled using shear and supply limited conditions as

$$Slough_i^j = \min\left[k\left(\tau_{i\,f}^{\,j} - \tau_{cr}^{APOC}\right)\rho_S^{APOC} SA_{Bed}\Delta t, APOC_i^j\right], \quad (5)$$

where, k (m^{-1}) is the erodibility coefficient, τ_f (Pa) is the shear stress of the fluid at the centroid of the erosion source, τ_{cr} (Pa) is the critical shear stress of the erosion source, ρ_s (kg m^{-3}) is the bulk density of the source, and SA (m^2) is the surface area of the erosion source. Sloughed algae is assumed to be exported from the watershed, since algal material is relatively neutrally buoyant and would not be expected to settle out of suspension during flow conditions that would induce sloughing.

POC includes fine and coarse carbon pools that are mixed with inorganic particles and aggregates which reside in the streambed as a heterogeneous matrix of sediments. For this reason, sediment transport mechanics provide the basis for POC transport and temporary storage. Simulation of sediment transport of fine sediment is specifically formulated in ISOFLOC for a class of streams with SFGL following the formulation by Russo and Fox [2012] as

$$SS_i^j = SS_{i-1}^j + E_{i\,Bank}^{\,j} + E_{i\,Bed}^{\,j} - D_i^j + Q_{i\,SSin}^{\,j}\Delta t - Q_{i\,SSout}^{\,j}\Delta t \ , \quad (6)$$

where, SS (kg) is the suspended sediment in the water column, E (kg) is the erosion from streambank and streambed sources, D (kg) is deposition to the bed, Q_{SS} (kg s^{-1}) is suspended sediment transported into and out of the modeled reach, and Δt (s) is the time step. Source erosion is modeled to be potentially limited by shear resistance, the transport carrying capacity of the fluid, and supply of the erosion source. These processes are modeled for both the streambed and the streambanks as

$$E_i^{\,j\,I} = \min\left[k\left(\tau_{i\,f}^{\,j} - \tau_{cr}^{I}\right)\rho_S^I SA_I\Delta t, T_{i\,C}^{\,j} - SS_{i-1}^j, S_{i-1}^{\,j\,I}\right], \quad (7)$$

where, (I) represents the sediment source, T_c (kg) is the transport carrying capacity and S (kg) is the sediment supply. In Equation (2), the erodibility coefficient and fluid shear stress are parameterized following the method of Hanson and Simon [2001]. T_c is estimated using a Bagnold like expression [Chien and Wan, 1999] as

$$T_{i\,C}^{\,j} = c^{\,j}{}_{TC}\frac{\left(\tau_{i\,f}^{\,j}\right)^2}{w_s}L^j\Delta t \ , \quad (8)$$

where c_{TC} (s^{-1}) is the transport capacity coefficient, w_s (m s^{-1}) is the particle settling velocity, and L (m) is the length of the reach. Deposition of sediment to the streambed is estimated as

$$D_i^j = \frac{w_s \Delta t}{k_p H_i^j}\left[SS_{i-1}^j - T_i^{j}{}_C\right], \tag{9}$$

where k_p is the concentration profile coefficient, and H (m) is the water column height. S of the banks is assumed infinite, however the supply of sediment in the streambed is budgeted as

$$S^{j}{}_{i\ Bed} = S_{i-1\,Bed}^j - E^{j}{}_{i\ Bed} + D_i^j + Gen_i^j . \tag{10}$$

where, Gen (kg) is the mass of inorganic fine sediment generated from APOC. The dynamic benthic FPOC composition is simulated as a function of erosion/deposition dynamics, production of algal FPOC from APOC decomposition, and heterotrophic breakdown of FPOC pools in the benthos. FPOC concentration in the streambed $C_{FPOC\text{-}Bed}$ is modeled continuously as

$$\begin{aligned} C^{j}{}_{i\ FPOC-Bed} = \Big(&\frac{C^j_{i-1\,FPOC-Bed} * S^j_{i-1\,Bed}}{100} + \frac{D_i^j C_{Upland} - E^{j}{}_{i\ Bed} C^j_{i-1\,FPOC-Bed}}{100} \\ &+ \left(DEC_{APOC\,i}^{\ j} - DEC^{j}{}_{i\ FPOC-Algae} - DEC^{j}{}_{i\ FPOC-upland}\right) SA_{Bed}\Delta t\Big) * 100 / S^{j}{}_{i\ Bed} \end{aligned}, \tag{11}$$

where $DEC_{FPOC\text{-}Algae}$ (kgC m^{-2} d^{-1}) is the rate at which algal FPOC is decomposed, $DEC_{FPOC\text{-}Algae}$ (kgC m^{-2} d^{-1}) is the rate at which upland soil derived FPOC is decomposed, and C (%) is the percentage carbon of a given sediment carbon source. Transported FPOC concentration ($C_{FPOC\text{-}T}$) is estimated by multiplying carbon weighted fractions for the total suspended carbon load, derived from the sediment transport model, by C of each source.

Stable carbon isotope mass balances with carbon advection as well as the potential for isotope fractionation during reactions are simulated in ISOFLOC for APOC, DIC and FPOC pools. The isotopic signature of a particular carbon pool, given in terms of δ notation defined in Eqn (1), is simulated as

$$\delta^{13}C_i^j = \delta^{13}C_{i-1}^j X^{C\,j}_{\ i-1} + \sum \delta^{13}C_{inputs_i}^{\ j} X^{C\ \ j}_{inputs_i} - \sum \delta^{13}C_{outputs_i}^{\ j} X^{C\ \ j}_{outputs_i} - \sum \varepsilon_{frac_i}^{\ j} \ln\left(f_{frac_i}^{\ j}\right), \tag{12}$$

where, X^C represents the fraction of carbon in a given pool and is parameterized using outputs from the aforementioned sediment and mass-balance elemental models, ε is the enrichment factor during an isotopic fractionation process and Rayleigh-type models are used to simulate fractionation (Sharp et al., 2007). In Rayleigh fractionation, $\varepsilon_{A\text{-}B}$ is defined as

$$\varepsilon_{A-B} = \left[\frac{(^{13}C/^{12}C)_A}{(^{13}C/^{12}C)_B} - 1 \right] \times 1000 \tag{13}$$

where A is the product and B is the reactant in equation (12). f is the fraction of a substrate remaining after the isotope fractionation process occurs and is derived from the appropriate elemental model. Implementing known inputs, outputs and fractionation processes for APOC, DIC and FPOC into equations (12,13), the isotopic submodel for APOC is simulated as

$$\begin{aligned} \delta^{13}C_{APOC\,i}^{\;\;j} = {} & \delta^{13}C_{APOC\,i-1}^{\;\;j} X_{APOC\,i-1}^{C\;\;j} - \delta^{13}C_{Slough_i}^{\;\;j} X_{Slough_i}^{C\;\;j} + \delta^{13}C_{Fix\,i}^{\;\;j} X_{Fix\,i}^{C\;\;j} \\ & - \varepsilon_{\mathrm{Res}} \ln(f_{\mathrm{Res}\,i}^{\;\;j}) - \varepsilon_{DEC(APOC)} \ln(f_{DEC(APOC)_i}^{\;\;j}) \end{aligned}, \tag{14}$$

where, $\delta^{13}C_{Fix}$ is a function of $\delta^{13}C_{DIC}$ and the fractionation imparted by algal assimilation. $\delta^{13}C_{DIC}$ is estimated as

$$\begin{aligned} \delta^{13}C_{DIC\,i}^{\;\;j} = {} & \delta^{13}C_{DIC\,i-1}^{\;\;j} X_{DIC\,i-1}^{C\;\;j} + \delta^{13}C_{DIC-in\,i}^{\;\;j} X_{DIC-in\,i}^{C\;\;j} - \delta^{13}C_{DIC-out\,i}^{\;\;j} X_{DIC-out\,i}^{C\;\;j} \\ & + \delta^{13}C_{\mathrm{Res}\,i}^{\;\;j} X_{\mathrm{Res}\,i}^{C\;\;j} + \delta^{13}C_{Dis\,i}^{\;\;j} X_{Dis\,i}^{C\;\;j} + \delta^{13}C_{Inv\,i}^{\;\;j} X_{Inv\,i}^{C\;\;j} \\ & - \varepsilon_{Eva} \ln(f_{Eva\,i}^{\;\;j}) - \varepsilon_{Fix\,i}^{\;\;j} \ln(f_{Fix\,i}^{\;\;j}) - \varepsilon_{\mathrm{Pre}} \ln(f_{\mathrm{Pre}\,i}^{\;\;j}) \end{aligned}, \tag{15}$$

where, ε_{Fix} varies temporally and spatially since previous studies have shown that enrichment factors at low concentrations of aqueous CO_2 are significantly lower than at high aqueous CO_2 concentrations [e.g., Riebesell et al., 2000]. While the relationship between partial pressure of CO_2 and ε_{Fix} is still not clearly defined [Bade et al., 2006], the present version of ISOFLOC assumes an exponential decay for ε_{Fix} as a function of the inverse of C_{DIC} since findings of Riebesell et al. [2000] suggests low sensitivity of ε_{Fix} at moderate-high C_{DIC} and a steep decline for decreasing DIC at low C_{DIC}, reminiscent of an exponential decay relationship. The threshold was utilized as a calibration parameter (Table 3). $\delta^{13}C_{FPOC\text{-}Bed}$ is simulated as

$$\delta^{13}C_{FPOC-Bed_i}{}^{j} = \delta^{13}C_{FPOC-Bed_{i-1}}{}^{j} X^{C}_{FPOC-Bed_{i-1}}{}^{j} - \delta^{13}C_{E_i}{}^{j} X^{C\,j}_{E\,i} + \delta^{13}C_{D_i}{}^{j} X^{C\,j}_{D\,i}$$
$$+ \delta^{13}C_{DEC(APOC)_i}{}^{j} X^{C}_{DEC(APOC)_i}{}^{j} - \varepsilon_{DEC(FPOC-Alg\,ae)} \ln(f_{DEC(FPOC-Alg\,ae)_i}{}^{j}) \cdot$$
$$- \varepsilon_{DEC(FPOC-Upland)} \ln(f_{DEC(FPOC-Upland)_i}{}^{j})$$

(16)

The isotopic signature of fine transported sediment ($\delta^{13}C_{FPOC\text{-}T}$) is estimated using a simple mass balance that calculates the carbon weighted average of source contributions and their associated isotopic signatures (i.e., $\delta^{13}C_{FPOC\text{-}Bed}$, $\delta^{13}C_{Upland}$, and $\delta^{13}C_{Bank}$).

5.3.2 Model Application

To test the new ISOFLOC model formulation, an eight year simulation was performed for the South Elkhorn watershed, a low gradient, agricultural and urban impacted, temperate system (62 km^2) in the Bluegrass Region of central Kentucky (see Figure 3). Agricultural (57%) and urban (43%) land uses promote high nutrient loads and pronounced benthic algae production in the South Elkhorn, and transported sediments are predominantly silt and clay sized particles [Fox et al., 2014]. In general, sediment erosion rates in the uplands are low in the ag-dominated watershed due to the fact that the region is heavily conserved, pristine horse farms that support the equine industry. However, the watershed experienced pronounced anthropogenic disturbances in 2006-2007 associated with urbanization and construction (Figure 3), as well as natural high flow disturbance events and pronounced sediment transport throughout 2006. Watershed model setup and troubleshooting was aided by previous knowledge gained from modeling upland and streamflow hydrology in the watershed with data driven methods and the Hydrologic Simulations Program Fortran (HSPF) model, sediment transport modeling in the South Elkhorn, and particulate carbon and nutrient modeling in the watershed [Fox et al., 2010; Russo, 2010; Ford, 2011; Russo and Fox, 2012]. For ISOFLOC testing, modeling of the benthos focused on the main-stem due to the high residence times and favorable conditions for autochthonous production and decomposition (e.g., shallow water depths, low velocities, and open canopy). Inflow of water, sediment and carbon constituents was accounted for in tributaries upstream of the main stem and laterally along the main stem utilizing empirical and physically based

relationships that were previously calibrated in the aforementioned studies. The model was simulated at a 30 minute timestep in six equivalently sized reaches over the eight year period to ensure the speed of propagation of the numerical scheme was on the same order of magnitude as constituent transport time.

Table 1 shows the model parameterization for the South Elkhorn application of ISOFLOC which was accomplished through field-based measurements, appropriate ranges from comparable streams and watersheds, and model calibration. For the DIC elemental mass balance an average pH of weekly collected estimates at two sites along the main stem of the study site was used and was measured with a Hach meter. $C_{DIC\text{-}in}$ was measured from GF-F (0.7 µm) filtered grab samples collected monthly for nine months at two tributaries and two main stem locations using a UIC Carbon Dioxide Coulometer CM5014. Speciation constants, K_1 and K_2, were obtained assuming chemical equilibrium at 25°C since variability associated with temperature fluctuations is small in freshwater streams [Masters and Ela, 2008]. The average gas transfer velocity, w_{CO2}, was parameterized using ranges of low-order streams in the Midwestern U.S. [Butman and Raymond, 2011]. $P_{CO2\text{-}Atm}$ was assumed spatially homogenous and reflects recent estimates [Wallin et al., 2013]. *Pre* and *Dis* were parameterized using results of a DIC mass balance model application in a low-order agricultural stream [Tobias and Buhlke, 2011]. DOC in the system was measured from GF-F (0.7 µm) filtered grab samples collected monthly for nine months at two tributaries and two main stem locations using a Teledyne Tekmar Torch TOC analyzer. Results suggest the conservative nature of DOC in-stream since measurements in the main stem fall between tributary end-members at both high and low flow conditions. Further, DOC concentrations did not show major temporal trends; hence an average concentration was used to estimate the DOC flux and the ranges for the main stem are provided in Table 1.

C_{APOC} was parameterized from elemental signatures of riverine algal biomass [Gosselain et al., 2000]. Physical parameters of the algal mat, ρ_{Algae} and τ_{cr}^{algae}, were parameterized using ranges for laboratory studies of SFGL [Droppo and Stone, 1994]. Rates and thresholds for algal production and respiration, i.e., P_{Col}, P_{Max}, I_K, T_{Min}, T_{opt}, T_{max}, P_{sat}, P_{resp}, Pk_{resp} and T_{ref}, were based on a synthesis of measurements from autochthonous dominated stream ecosystems and model parameterization in a similar

low-order, agricultural watershed [see Rutherford et al., 2001 and references within]. Meta-analysis of *in situ* field studies reporting decomposition of CPOC and FPOC was performed to provide ranges for breakdown rates of OC, i.e., DEC_{APOC}, $DEC_{FPOC\text{-}Algae}$, $DEC_{FPOC\text{-}Upland}$ [Sinsabaugh et al., 1994; Webster et al., 1999; Alvarez and Guerrero, 2000; Jackson and Vallaire, 2007; Yoshimura et al., 2008]. C_{Upland} and C_{Bank} were measured in the watershed using transported sediment samples collected at high flows and grab samples from scouring banks respectively and analyzed through combustion on an elemental analyzer.

With regard to the stable isotope mass balance model, enrichment of algae during decomposition, $\varepsilon_{DEC\text{-}APOC}$, was assumed analogous to fractionations associated with terrestrial organic matter decomposition and was parameterized using values observed in soil carbon profiles in a watershed with similar characteristics [Jacinthe et al., 2009]. $\varepsilon_{Assim\text{-}Max}$ was parameterized using results of a DIC mass balance model application in a similar, low-order agricultural stream [Tobias and Bohlke, 2011]. For DIC, $\delta^{13}C_{DIC\text{-}IN}$ was measured using 0.45 µm filtered grab samples that were acid-digested with 5% phosphoric acid, and analyzed on a GC column interfaced with an IRMS, similar to the method discussed in Doctor et al. [2008]. $\delta^{13}C_{Dis}$ and $\delta^{13}C_{Inv}$ were estimated using well accepted values for carbonate minerals, the dissolution source, and atmospheric CO_2 ,the invasion source [Finlay, 2003; Sharp et al., 2007]. $\varepsilon_{Evasion}$ was parameterized conservatively using estimates from a headwater stream where evasion is a dominant mechanism in DIC dynamics [Doctor et al., 2008]. $\delta^{13}C_{Upland}$ and $\delta^{13}C_{Bank}$ were measured in the watershed using transported sediment samples collected at high flows and grab samples from scouring banks respectively and analyzed on an isotope ratio mass spectrometer (IRMS). Enrichment of FPOC during decomposition, $\varepsilon_{DEC\text{-}FPOC}$, was assumed analogous to fractionations associated with terrestrial organic matter decomposition and was parameterized using values observed in soil carbon profiles in a watershed with similar characteristics [Jacinthe et al., 2009].

Eight years of semi-weekly elemental and isotopic signatures of transported FPOC were utilized to test the sensitivity and calibrate/validate the numerical model. Temporally and spatially integrated transported sediment samples were collected utilizing *in situ* sediment trap samplers [Phillips et al., 2000]. The samples are collected

approximately weekly, with a total of 327 samples collected from 2006-2013. Samples were brought back to the lab, centrifuged, decanted, frozen, freeze dried, wet sieved to isolate the fines fraction, ground, acidified with 6% sulfurous acid, and analyzed on a Costech elemental analyzer interfaced with a GC column and IRMS [Verardo et al., 1990; Rowe et al., 2002]. Samples that were too small to wet sieve or samples in which the sediment trap inlet was clogged in the field were removed from the evaluation dataset. In total, 209 samples were available for model evaluation, of which 157 were used for model calibration and 52 were used for validation. Selection of the calibration and validation dataset was performed randomly. For elemental and isotopic signatures, standard deviations of reference materials were 0.82% and 0.04‰, respectively, while standard deviations of unknowns were 0.07 % and 0.04‰, respectively.

Sensitivity of parameters impacting the fluvial organic carbon budget was tested through a global sensitivity analysis of ISOFLOC. Nominal range values for the potentially sensitive variables were plotted against the average isotopic signature of transported fine sediments for the calibration period, $\delta^{13}C_{FPOC\text{-}T(av)}$(see Table 1). $\delta^{13}C_{FPOC\text{-}T(av)}$ was utilized as the response variable because (1) we were interested in understanding the new stable isotope technology, (2) $\delta^{13}C_{FPOC\text{-}T(av)}$ was used as a calibration dataset since it has been previously shown to have seasonal and annual oscillations at the watershed outlet indicative of source variability and in-stream processes, and (3) the impact of highly non-linear feedbacks between physical and biological processes, and subsequently parameters, on $\delta^{13}C_{FPOC\text{-}T(av)}$ are not intuitive and the sensitivity analysis helped better understand these linkages. To apportion sensitivity of the output from the elemental and isotopic model parameters, a Monte Carlo based (global) approach was implemented. Distributions of the inputs were assumed uniform as is typical for an exploratory analysis [Salteli et al., 2004]. In total, 23 parameters were tested and approximately 700 simulations were performed. Average $\delta^{13}C_{FPOC\text{-}T(av)}$ was used as the response variable to maintain consistency with the calibration dataset. Coefficients of determination and scatter plots (Figure 3) were generated to qualitatively understand the influence of each input to the output dataset.

Calibration of the model was performed utilizing manual calibration techniques in which sensitive parameters were tuned iteratively to generate a statistically sufficient fit

to the calibration dataset. Average literature values were used for parameters that were insensitive. To account for surficial erosion during the period of upland disturbance between 2006 and 2008 the $\delta^{13}C_{Upland}$ and C_{Upland} was calibrated to fit the shift observed in the data. A $\delta^{13}C_{Upland}$ of -24‰ and C_{Upland} of 1.3% was used from 5-30-2006 through 12-31-2007 generated the best model fit. Visual and numerical goodness-of-fit metrics [Moriasi et al., 2007] were used for calibration, including time series plots for both elemental and isotopic signatures, Nash Sutcliffe Efficiency (NSE), ratio of the root mean square error to the standard deviation of measured data (RSR), and percent bias (PBIAS). Further, the ability to capture between event variability was tested for the model evaluation period using scatter plots of differences between datapoints. Points that plotted in the I or III quadrant suggest the model adequately captured between event variability whereas points that plotted in the II or IV quadrant suggest low accuracy at capturing between event variability. In terms of the statistical metrics, the model was deemed acceptable if the model fit provided a better approximation then the data mean trend.

5.4 RESULTS

5.4.1 ISOFLOC Model: Sensitivity Analysis

The average $\delta^{13}C$ value of transported fine sediment for the five year simulation ($\delta^{13}C_{FPOC\text{-}T(av)}$) is plotted against potentially sensitive model parameters (e.g. τ^{cr}_{algae}) in Figure 4. Correlations between parameters and outputs were weak due to the high non-linearity of the model as observed in the coefficient of determination values. Negative relationships were observed between τ^{cr}_{algae}, P_{resp}, DEC_{APOC}, C_{DIC}, $\varepsilon_{Assim\text{-}max}$ and $\delta^{13}C_{FPOC\text{-}T(av)}$ while positive relationships were observed between P_{max}, $\delta^{13}C_{DIC}$, $DEC_{FPOC\text{-}Algae}$ and $\delta^{13}C_{FPOC\text{-}T(av)}$. All other parameters showed little to no sensitivity based on visual observation of flat slopes for regression lines and no pronounced funneling effects (e.g., $DEC_{FPOC\text{-}Algae}$ has low variability at high decomposition rates and high variability at low decomposition rates). Results of the sensitivity show that numerous processes represented in ISOFLOC influence the output of $\delta^{13}C_{FPOC\text{-}T(av)}$ which is reflective of the sensitivity of $\delta^{13}C_{FPOC}$ to sources and the highly coupled nature of physical and biogeochemical processes impacting fluvial organic carbon.

One parameter in the sensitivity analysis that was of particular interest is τ^{cr}_{algae}, which shows a shift in the response of the minimum value for $\delta^{13}C_{FPOC\text{-}T(av)}$ from -26‰ to -30‰ occurring at 0.7 Pa. τ^{cr}_{algae} was the only parameter to generate such a pronounced shift in the response variable. The reason that $\delta^{13}C_{FPOC\text{-}T(av)}$ output by the model is so sensitive to the inherent shear stress of the algae to resist detachment is due to the linkage of biological and physical processes in the benthic algal layer. Holding all other parameters constant, low critical shear stress conditions, e.g., 0.3 Pa, produces relatively high rates of algal sloughing and in turn pronounced algal growth towards equilibrium resulting in net DIC assimilation by algae of 94 tC/yr and an average $\delta^{13}C_{APOC}$ of -27‰. High critical shear stress conditions, e.g., 1.3 Pa, produces relatively low algal sloughing rates and less algal growth resulting in net DIC assimilation by algae of 51tC/yr and an average $\delta^{13}C_{APOC}$ of -31‰. The dependence of $\delta^{13}C_{FPOC\text{-}T(av)}$ upon τ^{cr}_{algae} reflects the complexity of the coupled physical and biogeochemical processes and shows the utility of the isotope subroutines. Isotope fractionation associated with the preferential uptake of the lighter ^{12}C is less pronounced during low τ^{cr}_{algae} conditions when DIC assimilation by algae is high, but isotope fractionation is more pronounced during high τ^{cr}_{algae} conditions when DIC assimilation by algae is low and algae can prefer ^{12}C atoms from the large DIC pool.

Similarly to τ^{cr}_{algae}, APOC parameters, i.e., P_{resp}, P_{max}, and DEC_{APOC}, show sensitivity to $\delta^{13}C_{FPOC\text{-}T(av)}$ stemming from effects of net accrual of DIC. Increasing P_{max} increases standing stock of algal biomass and fixation, resulting in fuller assimilation of the isotopically enriched DIC signature. Increasing P_{resp} and DEC_{APOC} decrease standing stocks of algal biomass, allowing for more preference of the ^{12}C isotope. Related is the sensitivity of the DIC parameters, i.e., $\varepsilon_{Fix\text{-}max}$, $\delta^{13}C_{DIC}$, and C_{DIC}, in which increases in $\varepsilon_{Fix\text{-}max}$ and C_{DIC} result in more depleted values of $\delta^{13}C_{FPOC\text{-}T(av)}$ due to larger fractionations being able to occur from the DIC pool to the APOC mat. Increasing $\delta^{13}C_{DIC}$ has a nearly linear effect on the $\delta^{13}C_{FPOC\text{-}T(av)}$ since it has no significant impact on the processes, it is primarily shifting the signature by a constant which is evidenced by the relatively high R^2.

Decomposition parameters, DEC_{APOC} *and* $DEC_{FPOC\text{-}Algae}$, show pronounced funneling effects, i.e., decreasing $\delta^{13}C_{FPOC\text{-}T(av)}$ variability with increasing parameter

values for $DEC_{FPOC\text{-}Algae}$ and increasing $\delta^{13}C_{FPOC\text{-}T(av)}$ variability with decreasing parameter values for DEC_{APOC}. High decomposition of the APOC mat and low decomposition of the algal FPOC result in more pronounced accrual of algal biomass in the FPOC pool. As the algal FPOC pool decreases, variability of the isotopic signature will be driven by heterogeneous mixtures of bank and upland sediments. Conversely, as the algal FPOC increases, variability of the isotopic signature of algae is incorporated into the $\delta^{13}C_{FPOC\text{-}T(av)}$ which can range from -13.2 to -34.5‰ depending on the level of preferential assimilation of ^{12}C.

5.4.2 ISOFLOC Model: Calibration/Validation

Visual observation of scatterplots and time series of transported sediment carbon suggest good agreement between modeled and measured $\delta^{13}C_{FPOC}$ and C_{FPOC} results on an event, seasonal and annual basis (see Fig 5 and Tab 1). In this manner, the model shows the ability to capture variability associated with timing of hydrologic events, carbon erosion-deposition dynamics, and temporal variability of the benthic biological processes. For example, annual variability of peaks in transported carbon correspond to the varying degrees of hydrologic events during the growing season while seasonality results from the coupled effects of growth and decomposition processes in the benthos and event-to-event variability is shown to result from heterogeneous source contributions in which low flows predominantly scour the streambed source while moderate to high flows provide more significant contributions from bank and upland sources. Thus, visually the model shows the ability to capture variability of transported organic carbon at numerous temporal scales for the watershed.

Quantitatively, the model performed well and all statistical metrics provide acceptable fit for both calibration and validation periods for C_{FPOC} and for the calibration for $\delta^{13}C_{FPOC}$ (see Tab 2). Low values of NSE and high values of RSR for the validation period stem from three datapoints that had large deviations from measured data relative to the data range. ISOFLOC model results show periodic over/under estimation of C_{FPOC} and $\delta^{13}C_{FPOC}$. Pronounced over estimation of the C_{FPOC} was observed during the growing season of 2007, coinciding with the watershed disturbances (see Fig 3). During 2006-2007 there are pronounced upland land-use change disturbances and dense high-

magnitude hydrologic disturbances promoting sediment transport. $\delta^{13}C$ of transported sediment are relatively high during this time period ranging from -24 to-26‰ and reflecting deep soil source or bank source ($\delta^{13}C$ ranges from -24 to -25‰ for soils at depth and banks). On the contrary, $\delta^{13}C$ is relatively low in 2008-2013 when watershed disturbance was not so pronounced with $\delta^{13}C$ of transported sediment ranging from -26 to -30 ‰ and more reflective of surface soils ($\delta^{13}C$ ~-26 to -27‰) and algal biomass ($\delta^{13}C$ ranges from -30 to -40‰ for algae). Model prediction of event-to-event variability is also impacted during this period (see Fig 6). Model performance from 2006-2007 did not estimate between event variability in either dataset as well as results from 2008-2013, which did capture between event variability very well. Linear regression of the scatter plots show that for 2008-2013 the coefficient of determination for the elemental and isotopic model results are 0.38 and 0.15 respectively with slopes of 1.0 and 0.6 respectively. Further for 2006-2007 the coefficient of determination for the elemental and isotope signatures are 0.07 and 0.03 respectively with slopes of 0.3 and -0.2 respectively.

5.4.3 ISOFLOC Model: Fluvial Organic Carbon Budget

Seasonal and annual estimates of carbon yields are provided in Table 3. For the calibrated model solution, approximately 0.84 tC km^{-2} yr^{-1} of sloughed algae, 0.31 tC km^{-2} yr^{-1} of FPOC, and 0.93 tC km^{-2} yr^{-1} of DOC is exported from the watershed. Sloughing was generally highest in fall and spring and lowest in summer and winter. The years with high density of hydrologic events (2006 and 2009) had the highest mass of sloughed algae while the year with the summer drought (2008) had the lowest. FPOC and DOC were highest in winter and fall and lowest in spring and summer. Yields of benthic uptake and respiration of aqueous CO_2 were 8.6 tC km^{-2} yr^{-1} and 7.6 tC km^{-2} yr^{-1} respectively. Overall, respiration and assimilation were highest during spring and summer and significantly lower in fall and winter. Uptake outweighs respiration in every season of every year except for the fall season during 2007, 2008 and 2010.

We placed particular emphasis on the time varying nature of the algal carbon pool due to the magnitude of its contribution to the total organic load for this system (i.e., 41% of the fluvial organic carbon load) and its lack of inclusion in previous studies at the

watershed scale. Model results for the temporal source and transport of algal biomass are provided in Figure 7. Time series of benthic algal biomass are provided for 2006, a year with at least one pronounced high flow event during each of the four seasons. Peak algal biomass for the system is 450 gC m^{-2} (surface area of the bed covered in algae) and typically occurs between June and August while most depleted conditions occur in January and February. Algal biomass oscillates seasonally as a function of light and temperature variability. High magnitude events in spring or summer briefly deplete algal biomass with pre-disturbance levels being met, or exceeded within two to three weeks since the system conditions are conducive to pronounced growth during non-rate limiting conditions from temperature, light, or population consequences. Conversely, in fall and winter, high sloughing significantly reduces the ability of benthic stocks to return to pre-disturbance levels as a result of light and temperature limitations on biological growth of algae in the fall and winter.

5.5 DISCUSSION

5.5.1 Fluvial Organic Carbon Budget

The importance of understanding the fluvial organic carbon budget and in particular algal biomass and sloughing dynamics is recognized for the low-gradient, agriculturally impacted watershed. Results of this study suggest that sloughed algae accounts for 41% of the organic carbon loading in the watershed. Despite comprising an extremely small amount of the overall sediment budget (<10%), the enriched carbon contents of algal biomass are responsible for a large contribution of the carbon load during high flows, as evidenced by shifts in the algal stock during large events (see Fig 7). While overall fluxes of TOC (2.1 tC km^{-2} yr^{-1}), DOC (0.93 tC km^{-2} yr^{-1}), and POC (1.2 tC km^{-2} yr^{-1}) fall within ranges reported in the literature [see review by Alvarez-Cobellas et al., 2012], our results suggest that the inclusion of the sloughing component can shift the balance of majority share of TOC export from DOC to POC. Exclusion of sloughed algae suggests that 75% of TOC is DOC and 25% is POC which agrees well with a recent synthesis of catchments in the United States, i.e., 75% DOC and 25% POC [Alvarez-Cobellas et al., 2012, supplementary Table 2]. However, when including the algal component for the South Elkhorn watershed, 44% of TOC is transported as DOC

and 56% as POC. The influence of algal biomass suggests a need to be more inclusive of benthic algae sloughing fluxes in watershed and regional scale models to determine its contribution to TOC export at different scales and how it is attenuated during transit. The magnitude of the algal flux has potentially significant implications for receiving water bodies downstream of low-gradient systems since deposition of labile material can potentially promote heterotrophic induced oxygen depletion [Ohte et al., 2007; Stringfellow et al., 2009]. While these studies have focused on phytoplankton, we see a need to focus on benthic production that is amalgamated from small streams as a contributor to hypoxia in downstream water bodies as well since low-order streams make up a high percentage of the total drainage network.

In addition to the downstream implications of APOC flux, results of the study provide watershed scale assessment of trophic state, which has significant implications for water quality within the stream channel. The significance of system trophic state is intrinsically linked to water quality through its impacts on benthic food webs, nutrient removal, and streamwater oxygen conditions. As a whole, the system is autotrophic (i.e., net primary production, NPP, or the difference between uptake and respiration, is greater than zero), which agrees with studies in similar mid-west ag streams [e.g Griffiths et al., 2012]. Of particular interest were the estimated heterotrophic conditions occurring in fall of 2007, 2008, 2010, 2012 and 2013. The time-varying trophic state stems from the coupled physical and biogeochemical processes in which low fluvial shear stresses associated with small hydrologic events in fall of 2007, 2008, 2010, 2012 and 2013 limit scour of algal biomass promoting pronounced respiration, and limited production due to coupled population, temperature and light limitations. Further work should investigate the implications of time-varying trophic state on nutrient uptake and removal dynamics as well as streamwater oxygen conditions. Further, the few systems that have provided a long-term assessment of trophic state have utilized diel variations in % saturation of dissolved oxygen (DO) time series at a specified location to estimate net uptake and respiration rates of in-stream biota [Dodds, 2007]. The modeling approach herein provides a new, watershed-scale, assessment of time-varying trophic state and adds another datapoint to the sparse literature.

5.5.2 Model Advancement

Our results suggest that coupling numerical models of POC and DIC dynamics with isotopic mass balances provide model feedbacks that allow for a unique calibration of the water quality modeling framework that may not have been realized otherwise. Results of the sensitivity analysis suggest that the response variable, $\delta^{13}C_{FPOM}$, is uniquely sensitive to the critical shear stress of algae since it requires a shear stress exceeding 0.7 Pa to attain an average $\delta^{13}C_{FPOM}$ lower than -26. Low critical shear stresses result in over-estimation of algal assimilation as the algal mat tries to achieve its maximum population. Over-assimilation of DIC causes depleted DIC concentrations in which carbon assimilation can become limited to diffusion from the atmosphere. Under these low concentrations, isotopic signatures of the algal mat become enriched because isotopic fractionation of the lighter ^{12}C atoms is less pronounced. Since seasonality of FPOM is reflective of the algae signature, under low critical shear stress of algae, an appropriate calibration fit was not possible.

In addition, the new isotope routine adds strength in calibration since it adds more equations than unknowns and because it significantly reduces uncertainty in model parameters. Sensitivity analysis results for the South Elkhorn model suggest that the additional isotope sub-model only adds two additional sensitive parameters that are not sensitive components of the elemental model [see sensitivity analysis of the elemental model reported in Ford and Fox, 2014]. As seen in the methods, the isotope sub-routine adds three equations to the total model formulation suggesting that for this system the isotope sub-model adds more equations than unknowns. Further application of the model is needed in other systems to assess whether the sensitivity analysis reported here can be generalized for watersheds with similar characteristics. To further display the ability of the isotope routine to constrain uncertainty in the organic carbon budget, we provide a multi-objective based uncertainty evaluation of the Monte Carlo simulations [van Griensven et al., 2003; Rode et al., 2007]. Model simulations were assumed to provide sufficient fit based on visual observation. The uncertainty range for C_{FPOC} and $\delta^{13}C_{FPOC}$ datasets are shown in Table 8. When using the additional stable isotope routine, uncertainty of FPOC flux was not reduced significantly however algal biomass sloughing uncertainty was reduced by 60%. The result suggests the need for caution when

calibrating solutions using solely C_{FPOC} without simultaneously budgeting feedbacks from the carbon source. The novel approach of tightened coupling of DIC and POC phases can be easily implemented into future models, and results of this study show the strength of calibration using stable isotope and elemental data. The results of this study need to be further tested in other watershed systems to assess the transferability for the fluvial organic carbon budget.

5.5.3 Modeling Needs and Limitations

Despite the major advancements of the model and its ability to capture variability at different timescales, results suggest some needs for future improvements and future research in this area. First, the inability of the numerical model to simulate the shift of the isotopic and elemental signatures in October 2006, the subsequent return to pre-disturbance conditions (see Fig 5), and between event variability from 2006-2007 (see Fig 6) suggest poor performance during non-equilibrium streambed conditions. Non-equilibrium conditions for 2006-2007 stem from upland construction in the watershed and dense, high-magnitude hydrologic activity throughout 2006 (see Fig 3). High magnitude flows, coupled with disturbed upland soils promote pronounced deposition to the streambed, burying existing SFGL and APOC [Russo and Fox, 2012]. As evidenced by the shift in the calibration data to enriched δ^{13}C values, soil carbon eroded from the uplands during this period is predominantly deep, depleted FPOC, which is less bioavailable than APOC or surface soil FPOC. As a result, it's conceivable that heterotrophic bacterial pools are subject to non-equilibrium conditions following the deposition events as they are sensitive to carbon quality. Further, over-prediction of C_T during the 2007 growing season suggests that extensive deposition limits accrual of algal biomass for a full growing season, which has been previously hypothesized to occur as a result of limited light, oxygen and nutrient delivery to existing stocks of algal biomass buried under sediment deposits [Peterson, 1996]. Further research is needed in the laboratory and field to inform and help develop sub-models that can simulate these non-equilibrium benthic processes.

In addition to limitations associated with modeling streambed disequilibrium, a limitation is possible regarding the equilibrium conditions of the stable isotope

subroutine. Although the stable isotope routine has major advantages associated with its ability to trace sources of carbon, and help us develop the unique calibration discussed within, the Rayleigh formulations have limitations associated with representing non-equilibrium conditions as highlighted in Maggi and Riley [2010]. Further work is needed to assess potential alternatives to represent dis-equilibrium conditions for watershed–scale models and to gain a more process based understanding of disequilibrium conditions. That said, we do not have reliable fractionation datasets to parameterize the transient processes associated with the non-equilibrium type model, so this work should move forward in concert with laboratory and field studies of transient isotope fractionation in freshwater studies. Nevertheless, we see here advancement in water quality modeling by including the isotopes, and future research in this area will be welcomed.

5.6 CONCLUSIONS

ISOFLOC and its innovative features, including the stable carbon isotope model subroutines and the coupling of transfers between carbon pools, provide a stream carbon modeling framework that estimate useful carbon source, fate and transport results for hydrologists and ecologists. The following conclusions of this study are:

1. Global sensitivity analysis suggest that benthic rates, including algal growth, critical shear stress of algae, and algal decomposition, are the most sensitive parameters impacting the isotope subroutines in ISOFLOC. Adjusting the benthic rates during calibration and matching observed and model isotopic signatures reduces uncertainty in ISOFLOC by 60%.
2. Results of transported elemental and isotopic carbon signatures from ISOFLOC and observed samples show good to very good agreement on event, seasonal and annual time scales. The result suggests that the tightened coupling of DIC and POC phases and the strength of the stable isotope calibration may be useful in future stream applications such as assessing ‘hot-moments’ of nutrient biotransformations, seasonal hypoxia in receiving water bodies, and large-scale annual C budgets.

3. Calibrated model results from the eight year simulation estimate that the total fluvial organic carbon flux is divided into 40% algal carbon, 15% fine particulate carbon, and 45% dissolved carbon. Inclusion of the algal pool into the total fluvial organic carbon flux shifts the stream from dissolved-dominated to particulate-dominated. The result questions traditional views of the dominant phase of transported carbon in previous reported studies where algal particulate carbon flux is not considered and dissolved carbon is suggested to dominate.
4. The algal carbon pool is found to be impacted by both physical and environmental stream variables and has a strong linkage with fine particulate organic carbon through the algal decomposition process. Due to these linkages, model results suggest that the timing of hydrologic events can shift the functioning of the stream from autotrophic to heterotrophic.

We qualify the use of ISOFLOC for stream systems where benthic carbon processes are dominated by autochthonous production and decomposition. Although not included herein, rate limiting nutrient conditions can be easily implemented, and the model parameterization can account for shifts in stream-bed gradients. The usefulness of ISOFLOC in contrasting systems where leaf litter drives benthic biological processes, e.g., forested systems, is not intuitively obvious. Further, limitations surrounding parameterization of transient processes associated with dis-equilibrium fractionation models and streambed disequilibrium need further investigation, and we welcome future contributions in these areas.

5.7 REFERENCES

Alvarez-Cobelas, M., D. Angeler, S. Sa´nchez-Carrillo, G. Almendros (2012), A worldwide view of organic carbon export from catchments, Biogeochem., 107, 275-293, doi: 10.1007.s10533-010-9553-z.

Alvarez, S., M. Guerrero (2000), Enzymatic activities associated with decomposition of particulate organic matter in two shallow ponds, Soil Biology and Biochemistry, 32, 1941-1951.

Bade, D.L., M.L. Pace, J.J. Cole, S.R. Carpenter, (2006), Can algal photosynthetic inorganic carbon isotope fractionation be predicted in lakes using existing models?, Aquat. Sci., 68, 142-153, doi:10.1007/s00027-006-0818-5.

Battin, T.J., L.A. Kaplan, S. Findlay, C.S. Hopkinson, E., Marti, A.I. Packman, J.A. Newbold, F. Sabater, (2009), Biophysical controls on organic carbon fluxes in fluvial networks, Nat. Geosci., 1, 95-100, doi:10.1038/ngeo101.

Bingner, R., F.D. Theurer, Y. Yuan, (2011), AnnAGNPS technical processes, USDA-ARS, Version 5.2.

Brunet, F., C. Potot, A. Probst, J.-L. Probst, (2011), Stable carbon isotope evidence for nitrogenous fertilizer impact on carbonate weathering in a small agricultural watershed, Rapid Commun. Mass Spectrom., 25, 2682-2690, doi:10.1002/rcm.5050.

Butman, D., P.A. Raymond, (2011), Significant efflux of carbon dioxide from streams and rivers in the United States, Nat. Geosci., doi:10.1038/ngeo1294.

Chapra, S., G. Pelletier H. Tao (2008), QUAL2K: A Modeling Framework for Simulating River and Stream Water Quality, Version 2.11: Documentation and Users Manual, Civil and Environmental Engineering Dept., Tufts University, Medford, MA.

Chien, N, Z. Wan (1999), Mechanics of sediment transport, ASCE: Reston, Virginia.

Cole, J., Y. Prairie N. Caraco W. McDowell, L. Tranvik, R. Striegl, C. Duarte, P. Kortelainen, J. Downing, J. Middelburg, J. Melack, (2007), Plumbing the global carbon cycle: Intergrating inland waters into the terrestrial carbon budget, Ecosystems, 10, 171-184, doi: 10.1007/s10021-006-9013-8.

Dalzell, B., T. Filley, J. Harbor, (2007), The role of hydrology in annual organic carbon loads and terrestrial organic matter export from a Midwestern agricultural watershed, Geochimica et Cosmochimica Acta, 71, 1448-1462, doi: 10.1016/j.gca.2006.12.009.

DiToro, D.M., (2001), Sediment Flux Modeling, John Wiley and Sons, Hoboken, New Jersey.

Doctor, D.H., C. Kendall, S.D. Sebestyen, J.B. Shanley, N. Ohte, E.W. Boyer, (2008), Carbon isotope fractionation of dissolved inorganic carbon (DIC) due to outgassing of carbon dioxide from a headwater stream, Hydrological Processes, 22, 2410-2423, doi: 10.1002/hyp.6833.

Dodds, W.K., (2007), Trophic state, eutrophication and nutrient criteria in streams, Trends in Ecology and Evolution, 22(12), 669-676, doi: 10.1016/j.tree.2007.07.010.

Droppo, I., Y. Lau, C. Mitchell, (2001), The effect of depositional history on contaminated bed sediment stability, The Science of the Total Environment, 266,7-13.

Droppo, I., M. Stone, (1994), In-channel surficial fine grained sediment laminae. Part I: Physical Characteristics and formational processes,. Hydrological Processes, 8, 101-111, doi: 10.1002/hyp.3360080202.

Dubois, K.D., D. Lee, J. Veizer, (2010), Isotopic constraints on alkalinity, dissolved organic carbon, and atmospheric carbon dioxide fluxes in the Mississippi River, Journal of Geophysical Research, 115, G02018, doi: 10.1029/2009JG001102.

Ford, W.I., J.F. Fox, (2014), Model of particulate organic carbon transport in an agriculturally impacted stream, Hydrol. Process., 28(3), 662-675, doi: 10.1002/hyp.9569.

Ford, W.I., (2011), Particulate organic carbon fate and transport in a lowland temperate watershed, M.S. thesis, Dep. of Civil Engineering, University of Kentucky, Lexington, Kentucky.

Fovet, O., G. Belaud, X. Litrico, S. Charpentier, C. Bertrand, A. Dauta, C. Hugodot, (2012), Modelling periphyton in irrigation canals, Ecological Modeling, 221, 1153-1161, doi: 10.1016/j.ecolmodel.2010.01.002.

Fox, J.F., A.N. Papanicolaou, (2007), The use of carbon and nitrogen isotopes to study watershed erosion processes, Journal of the American Water Resources, 43(4), 1047-1064, doi: 10.1111/j.1752-1688.2007.00087.x.

Fox, J., (2009), Measurements of sediment transport processes in forested watersheds with surface coal mining disturbance using carbon and nitrogen isotopes, Journal of the American Water Resources Association, 45(5), 1273-1289.

Fox, J., C. Davis D. Martin (2010), Sediment source assessment in a lowland watershed using nitrogen stable isotopes, Journal of American Water Resources Association, 46, 1192-1204, doi: 10.1111/j.1752-1688.210.00485.x.

Fox, J., W.I. Ford, K. Strom, G. Villarini, M. Meehan, (2014), Benthic control upon the morphology of transported fine sediments in a low-gradient stream, Hydrological Processes, In Press, DOI: 10.1002/hyp.9928.

Gosselain, V., P. Hamilton, J. Descy, (2000), Estimating phytoplankton carbon from microscopic counts: an application for riverine systems, Hydrobiologia, 438, 75-90.

Graba, M., F.Y. Moulin, S. Bouletreau, F. Garabetian, A. Kettab, O. Eiff, J.M. Sanchez-Perez, S. Sauvage, (2010), Effect of near-bed turbulence on chronic detachment of epilithic biofilm: Experimental and modeling approaches, Water Resources Research, 46, W11531, doi: 10.1029/2009WR008679.

Graba, M., S. Sauvage, F.Y. Moulin, G. Urrea, S. Sabater, J.M. Sanchez-Perez, (2013), Interaction between local hydrodynamics and algal community in epilithic biofilm, Water Research, 47, 2153-2163, doi: 10.1016/j.watres.2013.01.011.

Griffiths, N.A., J.L. Tank, T.V. Royer, T.J. Warrner, T.C. Frauendorf, E.J. Rosi-Marshall, M.R. Whiles, (2012), Temporal variation in organic carbon spiraling in Midwestern agricultural streams, Biogeochemistry, 108, 149-169, doi: 10.1007/s10533-011-9585-z.

Hanson, G., A. Simon (2001), Erodibility of cohesive streambeds in the loess area of the midwestern USA, Hydrological Processes, 15(1),23–38.

Hope, D., M. Billett M. Cresser (1994), A review of the export of carbon in river water: fluxes and processes, Environ. Pollut., 84,301–324, doi: 10.1016/0269-7491(94)90142-2.

Jacinthe, P.A., R. Lal, L.B. Owens, (2009), Application of stable isotope analysis to quantify retention of eroded carbon in grass filters at the North Appalachian experimental watersheds, Geoderma, 148, 405-412, doi: 10.1016/j.geoderma.2008.11.013.

Jackson, C., S. Vallaire, (2007), Microbial activity and decomposition of fine particulate organic matter in a Louisiana cypress swamp, J. N. Am. Benthol. Soc., 26(4), 743-753, doi: 10.1899/07-020R1.1.

Johnson, L.T., (2008), The influence of land use on the role of dissolved organic carbon and nitrogen in stream nutrient processing, PhD Dissertation, Biological Sciences, University of Notre Dame.

Kendall, C., M.B. Young, S.R. Silva, (2010), Applications of stable isotopes for regional to national-scale water quality and environmental monitoring programs. in Isoscapes: Understanding movement, pattern and processs on earth through isotope mapping, p. 89-111, Springer, New York.

Maggi, F., W.J. Riley, (2010), Transient competitive complexation in biological kinetic isotope fractionation explains nonsteady isotopic effects: Theory and application to denitrification in soils, Journal of Geophysical Research, 114, G04012.

Marcarelli, A.M., C.V. Baxter, M.M. Mineau, R.O. Hall, (2011), Quantity and quality: unifying food web and ecosystem perspectives on the role of resource subsidies in freshwaters, Ecology, 92(6), 1215-1225.

McGuire, K., J. McDonnell, (2008), Stable isotope tracers in watershed hydrology, Chapter 11, in Stable Isotopes in Ecology and Environmental Science, Second Edition, 334-374, John Wiley and Sons, Hoboken, New Jersey.

Moriasi, D.N., J.G. Arnold, M.W. Van Liew, R.L. Bingner, R.D. Harmel, T.L. Veith, (2007), Model evaluation guidelines for systematic quantification of accuracy in watershed simulations, Transactions of the ASABE, 50(3), 885-900, doi: 10.13031/2013.23153.

Mulholland, P., A. Helton, G. Poole, R. Hall, S. Hamilton, B. Peterson, J. Tank, L. Ashkenas, L. Cooper, C. Dahm, W. Dodds, S. Findlay, S. Gregory, N. Grimm, S. Johnson, W. McDowell, J. Meyer, H. Valett, J. Webster, C. Arango, J. Beaulieu, M. Bernot, A. Burgin, C. Crenshaw, L. Johnson, B. Niederlehner, J. O'Brien, J. Potter, R. Sheibley, D. Sobota, S. Thomas, Stream denitrification across biomes and its response to anthropogenic nitrate loading, Nature, 452, 202-206, doi: 10.1038/nature06686.

Neitsch, S.L., J.G. Arnold, J.R. Kiniry, J.R. Williams, (2011), Soil and Water Assessment Tool Theoretical Documentation Version 2009, Texas Water Resources Institute Technical Report No. 406, College Station, Texas.

Oeurng, C., S. Sauvage, J. Sanchez-Perez, (2011), Assessment of hydrology, sediment and particulate organic carbon yield in a large agricultural catchment using the SWAT model, Journal of Hydrology, 401,145-153, doi: 10.1016/j.jhydrol.2011.02.017.

Ohte, N., S. Silva, C. Kendal, C. Kratzer, R. Dahlgren, D. Doctor, (2007), Sources and transport of algae and nutrients in a Californian river in a semi-arid climate, Freshwater Biology, 2007, 12, 2476-2493, doi: 10.1111/j.1365-2427.2007.01849.x.

Onstad, G.D., D.E. Canfield, P.D. Quay, J.L. Hedges, (2000), Source of particulate organic matter in rivers from the continental USA: lignin phenol and stable carbon isotope compositions, Geochemica et Cosmochimica, 64(20), 3359-3546, doi: 10.1016/s0016-7037(00)00451-8.

Palmer, S.M., D. Hope, M.F. Billett, J.J.C. Dawson, C.L. Bryant, (2001), Sources of organic and inorganic carbon in a headwater stream: evidence from carbon isotope studies, Biogeochemistry, 52, 321-338.

Park, R.A., J.S. Clough, (2012), AQUATOX (Release 3.1) Modeling environmental fate and ecological effects in aquatic ecosystems, U.S. EPA, Washington, DC.

Peterson, C. G. (1996), Response of benthic algal communities to natural physical disturbance, Pages 375-402, In Algal Ecology: Freshwater Benthic Ecosystems. Academic Press, San Diego, CA.

Phillips, J., M. Russell, D. Walling, (2000), Time-integrated sampling of fluvial suspended sediment: a simple methodology for small catchments, Hydrological Processes 14:2589-2602, doi: 10.1002/1099-1085(2001015)14:14<2589::aid-hyp94>3.0co;2-d.

Riebesell, U., S. Burkhardt, A. Dauelsber, B. Kroon, (2000), Carbon isotope fractionation by a marine diatom: dependence on the growth-rate-limiting resource, Marine Ecology Progress Series, 193, 295-303.

Rode, M., U. Suhr, G. Wriedt, (2007), Multi-objective calibration of a river water quality model-Information content of calibration data, Ecological Modeling, 204, 129-142, doi: 10.1016/j.ecolmodel.2006.12.037.

Rowe, H.D., R.B. Dunbar, D.A. Mucciarone, G.O. Seltzer, P.A. Baker, S. Fritz, (2002), Insolation, moisture balance and climate change on the South American altiplano since the last glacial maximum, Climatic Change, 52, 175-199.

Russo, J. P., (2010), Investigation of surface fine grained laminae, streambed, and streambank processes using a watershed scale hydrologic and sediment transport model, M.S. thesis, Dep. Civil and Engineering, University of Kentucky, Lexington, Kentucky.

Russo, J., J. Fox, (2012), The role of the surface fine-grained laminae in low-gradient streams: A model approach, Geomorphology, 171-172, 127-138, doi: 10.1016/j.geomorph. 2012.05.012

Rutherford, J., M. Scarsbrook, N. Broekhuizen, (2000), Grazer control of stream algae: modeling temperature and flood effects, Journal of Environmental Engineering, 126, 331–339, doi: 10.1061/(ASCE)0733-9372(2000)126:4(331).

Sakamaki, T., J.S. Richardson, (2011), Biogeochemical properties of fine particulate organic matter as an indicator of local and catchment impacts on forested streams, J. App. Eco., 48, 1462-1471, doi: 10.1111/j.1365-2664.02038.x.

Saltelli, A., S. Tarantola, F. Campolongo, M. Ratto, (2004), Sensitivity Analysis in Practice. A Guide to Assessing Scientific Models, John Wiley and Sons, Hoboken, New Jersey.

Sarma, V.V.S.S., J. Arya, Ch.V. Subbaiah, S.A. Naidu, L. Gawade, P.P. Kumar, N.P.C Reddy, (2012), Stable isotopes of carbon and nitrogen in suspended matter and sediments from the Godavari estuary, J. Oceanogr., 68, 307-319, doi: 10.1007/s10872-012-0100-5.

Schindler Wildhaber, Y., R. Liechti, C. Alewell, (2012), Organic matter dynamics and stable isotope signature as tracers of the sources of suspended sediment, Biogeosciences, 9, 1985-1996, doi: 10.5194/bg-9-1985-2012.

Sharp, Z., (2007), Principles of stable isotope geochemistry, Prentice Hall, New Jersey.

Shih, J., R.B. Alexander, R.A. Smith, E.W. Boyer, G.E. Schwarz, S. Chung, (2010), An initial SPARROW model of land use and in-stream controls on total organic carbon in streams of the conterminous United States, U.S. Geological Survey Open-File Report, p. 22.

Sinsabaugh, R., M. Osgood, S. Findlay (1994), Enzymatic models for estimating decomposition rates of particulate detritus, J. N. Am. Benthol. Soc. 13(2), 160-169, doi: 10.2307/1467235.

Smith, B.N., S. Epstein, (1971), Two categories of $^{13}C/^{12}C$ ratios for higher plants, Plant Physiol., 47, 380-384.

Stringfellow, W., J. Herr, G. Litton, M. Brunell, S. Borglin, J. Hanlon, C. Chen, J. Graham, R. Burks, R. Dahlgren, C. Kendall, R. Brown, N. Quin, (2009), Investigation of river eutrophication as part of a low dissolved oxygen total maximum daily load implementation, Water Science and Technology, 59.1, doi: 10.2166/wst.2009.739.

Tank, J., E. Rosi-Marshall, N. Griffiths, S. Entrekin, M. Stephen, (2010), A review of allochthonous organic matter dynamics and metabolism in streams, J. N. Am. Benthol. Soc., 29, 118–146, doi: 10.1899/08-170.1.

Tobias, C., J.K. Bohlke, (2011), Biological and geochemical controls on diel dissolved inorganic carbon cycling in a low-order agricultural stream: implications for reach scales and beyond, Chemical Geology, 283, 18-30, doi: 10.1016/j.chemgeo.2010.12.012.

van Griensven, A., W. Bauwens, (2003), Multiobjective autocalibration for semidistributed water quality models, Water Resources Research, 39(12), 1348, doi: 10.1029/2003WR002284.

Verardo, D.J., P.N. Froelich, A. McIntyre, (1990), Determination of organic carbon and nitrogen in marine sediments using the Carlo Erba NA-1500 Analyzer, Deep-Sea Research, 37(1), 157-165, doi: 10.1016/0198-0149(90)90034-s.

Wallin, M.B., T. Grabs, I. Buffam, H. Laudon, A. Agren, M.G. Oquist, K. Bishop, (2013), Evasion of CO_2 from streams- The dominant component of the carbon export through the aquatic conduit in a boreal landscape, Global Change Biology, 19(3), 785-797, doi: 10.1111/gcb.12083.

Walling, D., A. Collins, P. Jones, G. Leeks, G. Old, (2006), Establishing fine-grained sediment budgets for the Pang and Lambourn LOCAR catchments, Journal of Hydrology, 330,126-141, doi: 10.1016/j.jhydrol.2006.04.015.

Webster, J., E. Benfield, T. Ehrman, M. Schaeffer, J. Tank, J. Hutchens, D. D'Angelo, (1999), What happens to allochthonous material that falls into streams? A synthesis of new and published information from Coweeta, Freshwater Biology, 41, 687-705, doi: .10.1046/j.1365-2427.1999.00409.x.

White, P., J. Kalff, J. Rasmussen, J. Gasol, (1991), The effect of temperature and algal biomass on bacterial production and specific growth rate in freshwater and marine habitats, Microbial Ecology, 21, 99-118.

Wool, T.A., R.B. Ambrose, J.L. Martin, E.A. Comer, (2006), Water Quality Analysis Simulation Program (WASP), Version 6, U.S. EPA, Washington, DC.

Yoshimura, C., M. Gessner, K. Tockner, H. Furumai, (2008), Chemical properties, microbial respiration, and decomposition of coarse and fine particulate organic matter, J. N. Am. Benthol. Soc., 27, 664–673, doi: 10.1899/07-106.1.

5.8 TABLES AND FIGURES

Table 1. Inputs and parameterization for the South Elkhorn Application of ISOFLOC.

Parameters	Nominal Range	Calibrated Value	Units
Elemental Mass Balance Model			
pH	7-8.5	7.2	-------
$C_{DIC\text{-}IN}$	10-60	50	mgC L^{-1}
K_1	$4.47*10^{-7}$	$4.47*10^{-7}$	-------
K_2	$4.68*10^{-11}$	$4.68*10^{-11}$	-------
$P_{CO2\text{-}Atmosphere}$	380	380	ppm
w_{CO2}	$3.47\text{-}6.94*10^{-5}$	$5.31*10^{-5}$	m s^{-1}
Pre	$0\text{-}6.67*10^{-8}$	$3.32*10^{-8}$	kgC m^{-2} s^{-1}
Dis	$0\text{-}1.67*10^{-8}$	$8.37*10^{-9}$	kgC m^{-2} s^{-1}
C_{DOC}	1.1-1.7	1.4	mgC L^{-1}
C_{APOC}	0.41	0.41	gC $gSed^{-1}$
p_{algae}	1100	1100	kg m^{-3}
τ_{cr}^{algae}	0.2-2	1.3	Pa
P_{col}	$1*10^{-6}\text{-}1*10^{-4}$	$1*10^{-4}$	kgC $m^{-2}d^{-1}$
P_{Max}	$0.4\text{-}7.7*10^{-3}$	$2.4*10^{-3}$	kgC $m^{-2}d^{-1}$
I_K	230	230	µmol$m^{-2}s^{-1}$
T_{min}	5	5	°C
T_{opt}	20	20	°C
T_{max}	30	30	°C
P_{sat}	$2.5*10^{-3}$	$2.5*10^{-3}$	kgC m^{-2} d^{-1}
P_{resp}	0.025-0.15	0.13	d^{-1}
Pk_{resp}	1.05	1.05	-------
T_{ref}	20	20	°C
DEC_{APOC}	$0.1\text{-}1.5*10^{-2}$	$0.2*10^{-2}$	d^{-1}
$DEC_{FPOC\text{-}Algae}$	$0.01\text{-}1*10^{-2}$	$0.15*10^{-2}$	d^{-1}
$DEC_{FPOC\text{-}Upland}$	$0.1\text{-}1*10^{-4}$	$0.5*10^{-4}$	d^{-1}
C_{Upland}	0.02-0.04	0.024	gC $gSed^{-1}$
C_{Bank}	0.0104-0.0205	0.016	gC $gSed^{-1}$
Stable Isotope Mass Balance Model			
$\varepsilon_{DEC\text{-}APOC}$	0-2	1	‰
$\varepsilon_{Assimilation\text{-}Max}$	15-25	20	‰
$c_{\varepsilon\text{-}Assim}$	-------	0.002	-------
$\delta^{13}C_{DIC\text{-}IN}$	-10- -15	-13.5	‰
$\delta^{13}C_{Dis}$	5- -8	-1	‰
$\delta^{13}C_{Inv}$	-7- -9	-8	‰
$\varepsilon_{Evasion}$	0-4	2	‰
$\delta^{13}C_{Bank}$	-23.9- -26.1	-25	‰
$\delta^{13}C_{Upland}$	-25.7- -27.4	-26.5	‰
$\varepsilon_{DEC\text{-}FPOC}$	0-2	1	‰

Table 2. Goodness-of-fit indices for the optimum model fit to the five year calibration datasets of C_{FPOC} and $\delta^{13}C_{FPOC}$.

Metric	C_{FPOC}	$\delta^{13}C_{FPOC}$
	Calibration	
NSE	0.44	0.04
RSR	0.75	0.98
PBIAS	-0.9%	0.1%
	Validation	
NSE	0.1	-0.4
RSR	0.95	1.2
PBIAS	-8.2%	0.5%

Table 3. Fluvial organic carbon budget results for the five year modeling study in the South Elkhorn Watershed using the ISOFLOC model.

Sloughed Algae Flux (tC)									
	2006	2007	2008	2009	2010	2011	2012	2013	Total
Winter	17.0	12.5	10.5	9.9	2.4	8.7	12.6	12.9	86.6
Spring	8.0	6.6	10.1	24.4	22.6	31.3	0.8	16.6	120.4
Summer	7.7	3.3	0.7	14.6	4.5	3.8	3.5	35.9	74.1
Fall	39.3	13.3	1.5	39.0	2.2	19.2	8.9	13.1	136.5
Total	72.1	35.8	22.8	88.0	31.8	62.9	25.8	78.4	**417.6**
FPOC Flux (tC)									
	2006	2007	2008	2009	2010	2011	2012	2013	Total
Winter	12.8	2.3	10.5	6.1	2.7	6.5	3.7	6.3	50.8
Spring	2.3	1.2	7.3	5.1	7.8	10.3	0.3	3.6	37.9
Summer	2.2	0.7	0.2	3.5	1.1	0.8	1.1	9.4	19.0
Fall	12.9	4.7	0.5	11.8	0.6	6.0	2.5	8.4	47.2
Total	30.1	8.9	18.5	26.4	12.2	23.6	7.5	27.7	**154.9**
DOC Flux (tC)									
	2006	2007	2008	2009	2010	2011	2012	2013	Total
Winter	22.4	16.6	29.4	18.9	12.2	21.3	18.4	20.8	159.9
Spring	10.6	8.2	18.0	18.8	15.8	25.4	4.3	16.3	117.5
Summer	7.9	3.7	2.0	10.2	4.7	5.7	5.2	20.6	60.1
Fall	27.7	15.7	3.7	26.1	4.9	19.9	9.4	13.8	121.2
Total	68.5	44.2	53.2	74.1	37.6	72.4	37.3	71.5	**458.8**
Benthic Respiration (tC)									
	2006	2007	2008	2009	2010	2011	2012	2013	Total
Winter	12.6	16.7	3.8	13.6	11.9	10.9	30.3	10.2	109.8
Spring	138.7	173.8	123.6	142.3	162.5	122.5	184.3	149.7	1197.3
Summer	241.0	246.5	249.4	231.3	246.3	239.9	233.8	211.1	1899.2
Fall	39.6	89.9	92.8	43.5	78.1	65.0	73.0	75.0	556.9
Total	431.9	526.8	469.6	430.7	498.7	438.3	521.3	446.1	**3763.3**
Benthic Uptake (tC)									
	2006	2007	2008	2009	2010	2011	2012	2013	Total
Winter	26.7	32.6	13.3	28.9	22.2	23.2	53.5	21.6	222.0
Spring	172.1	198.0	159.7	184.8	203.5	174.4	198.6	193.1	1484.3
Summer	249.0	249.5	250.6	244.9	250.3	240.9	235.5	245.8	1966.6
Fall	66.5	85.2	78.0	63.3	63.6	68.7	65.7	70.3	561.1
Total	514.2	565.4	501.6	521.9	539.5	507.2	553.2	530.9	**4234.0**

Table 4. Uncertainty evaluation for the South Elkhorn ISOFLOC simulation including results of a single objective uncertainty evaluation utilizing C_{FPOC} and the added constraint from a multi objective uncertainty evaluation utilizing C_{FPOC} and $\delta^{13}C_{FPOC}$

Metric	*Range using single-objective C_{FPOC-T} Calibration*	*Range using multi-objective C_{FPOC-T} and $\delta^{13}C_{FPOC-T}$ Calibration*
APOC Flux	0.32-5.5 tC km^{-2} yr^{-1}	0.32-2.4 tC km^{-2} yr^{-1}
FPOC Flux	0.28-0.35 tC km^{-2} yr^{-1}	0.28-0.34 tC km^{-2} yr^{-1}

Figure 1. Reach-scale conceptual model of the fluvial carbon cycle in low-gradient, bedrock controlled temperate streams. DOC, DIC, POC and PIC flow into the stream reach from upland sources. The complexity of the system is realized as coupled physical and biogeochemical processes including erosion, sloughing, deposition, flocculation/aggregation, invasion, assimilation, decomposition, precipitation, and dissolution, impact the composition and quantity of the different carbon phases. Downstream advection and evasion to the atmosphere are primary means of flux out of the stream reach.

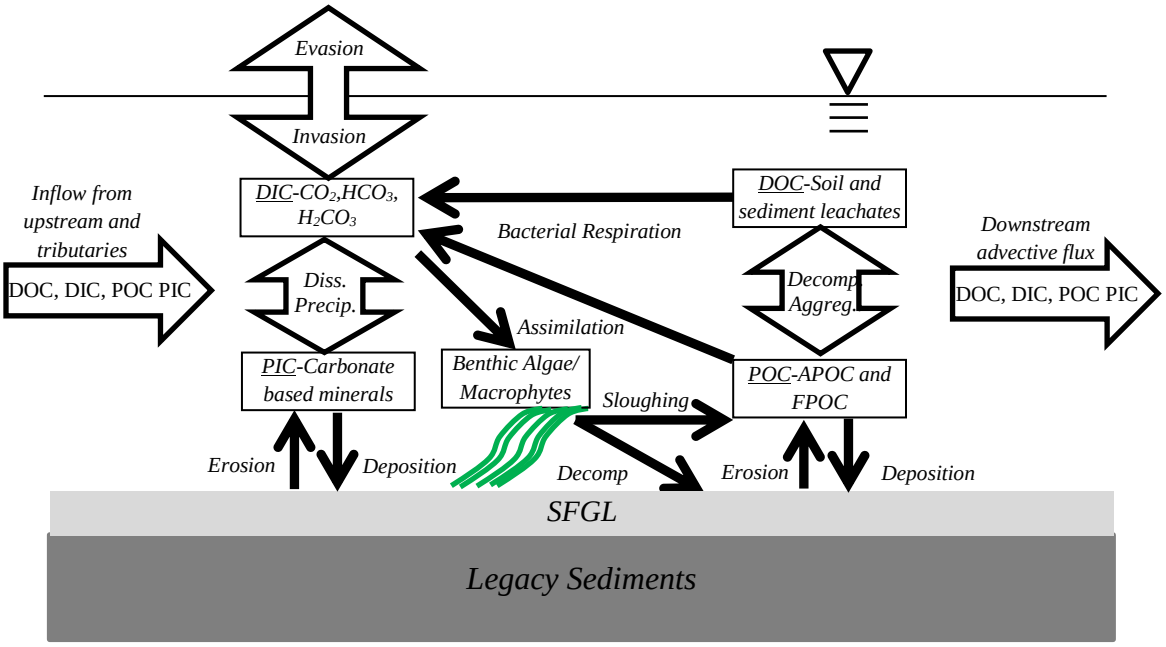

Figure 2. Model flowchart for the organic carbon budget. Hydrologic models provide inputs to a hydraulic sediment transport model that simulates fluvial fluxes of sediment and associated source contributions. Simultaneously the carbon model is simulated for DIC, DOC, and POC cycling within the river channel. Particulate organic carbon generation during autotrophic growth is incorporated into the bed source of the sediment transport model, while results of sediment fractions and fluxes feed into the carbon model. The carbon sub-model results are fed into the carbon isotope model which is then utilized to parameterize the elemental carbon model. Calibration and validation datasets for flow, sediment concentration, and carbon elemental and isotopic signatures (shown at the right) are used to verify the model simulations.

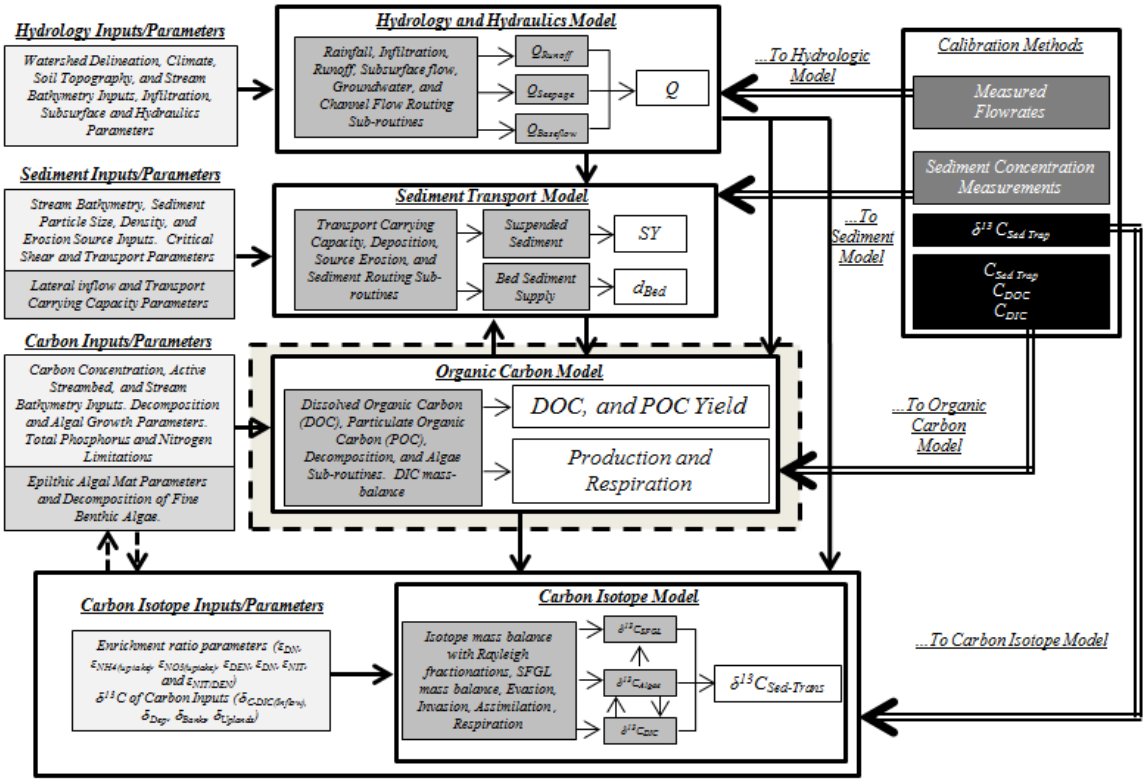

Figure 3. The left side of the figure shows the location of the study site in the Kentucky River Basin, and the modeling domain for the main stem of the South Elkhorn watershed. The right side of the figure shows visual evidence of construction that occurred from 2006-2007 at various locations in the watershed. Heavy construction promoted erosion of deep, $\delta^{13}C$ enriched soils that are brought to the surface during the construction process.

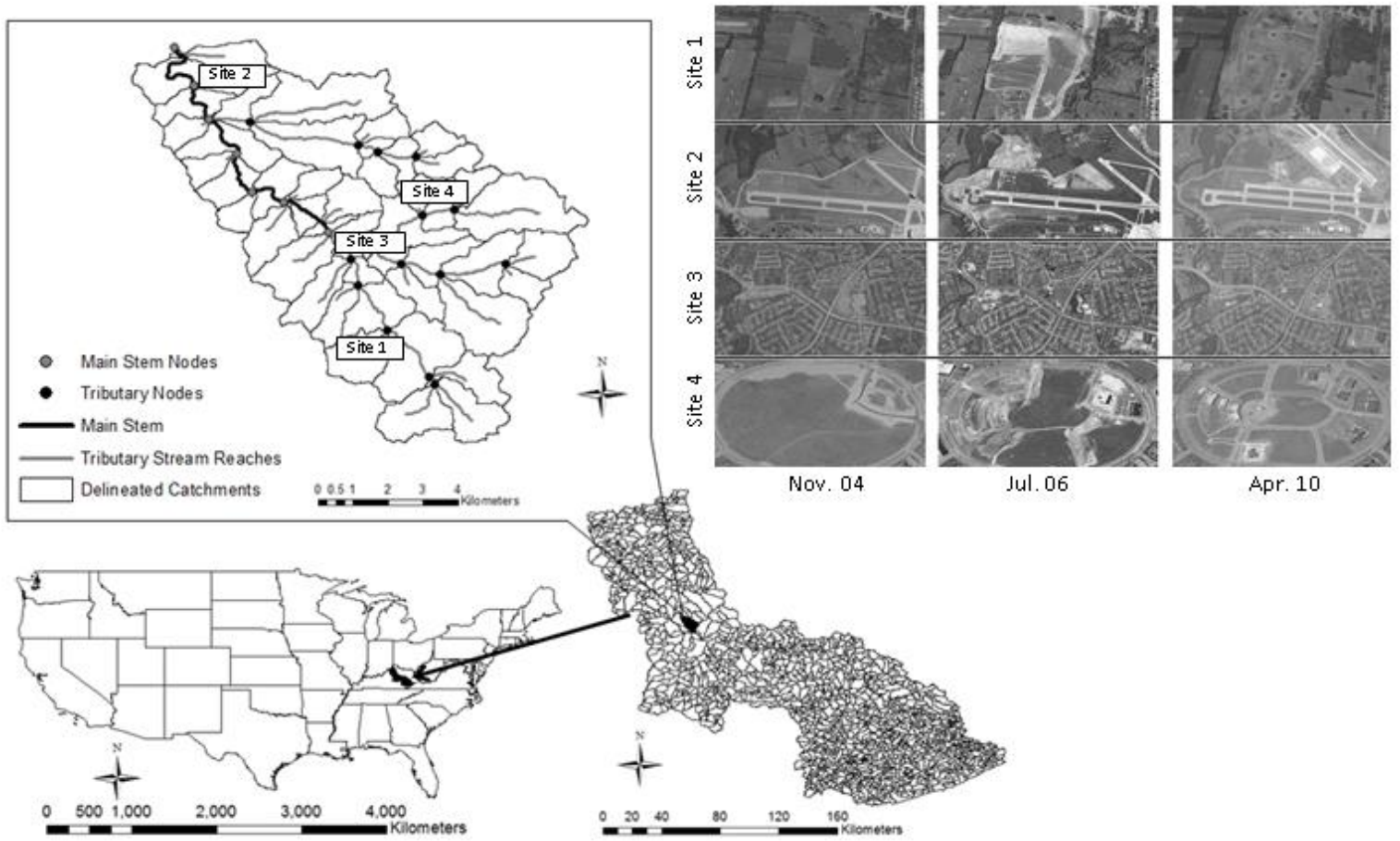

Figure 4. Sensitivity analysis of the ISOFLOC model displays the response of $\delta^{13}C_{FPOC}$ to model parameters. The values plotted the average specified parameter value for that run.

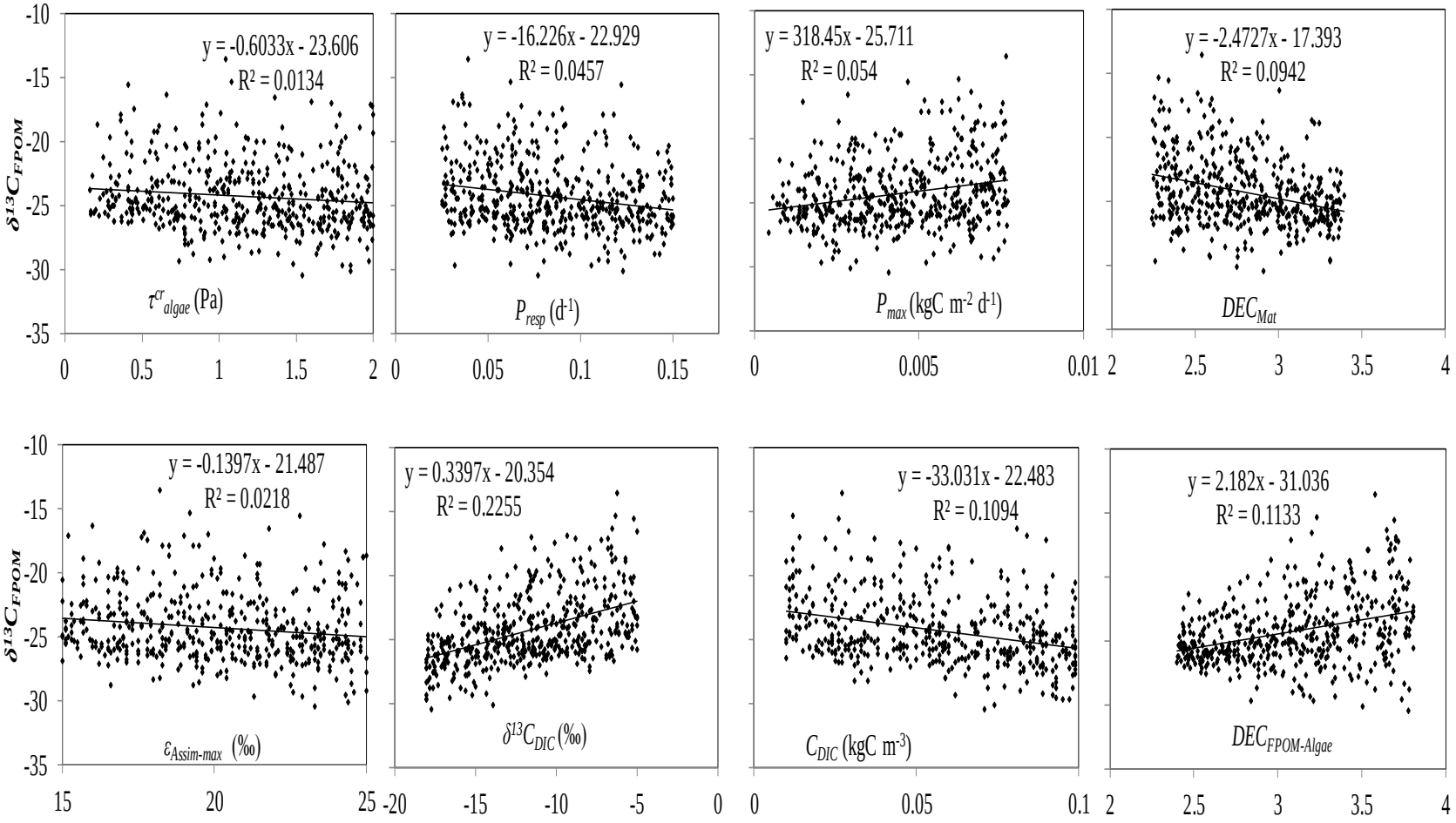

Figure 5. Calibration results of the elemental and isotope models are presented for time series (a-b) and scatterplots of measured vs. modeled data (c-d) for the eight year simulation. Figure 5a-b shows that in general both the elemental and isotope models capture annual, seasonal and between event variability. For the isotope model, plotting measured vs. modeled yields some over under estimation but relatively little bias. For the elemental model, some over/under estimation is also observed and the model does show some bias towards over-estimation especially during the growing season of 2007, which was the year following the high magnitude disturbances and during the construction.

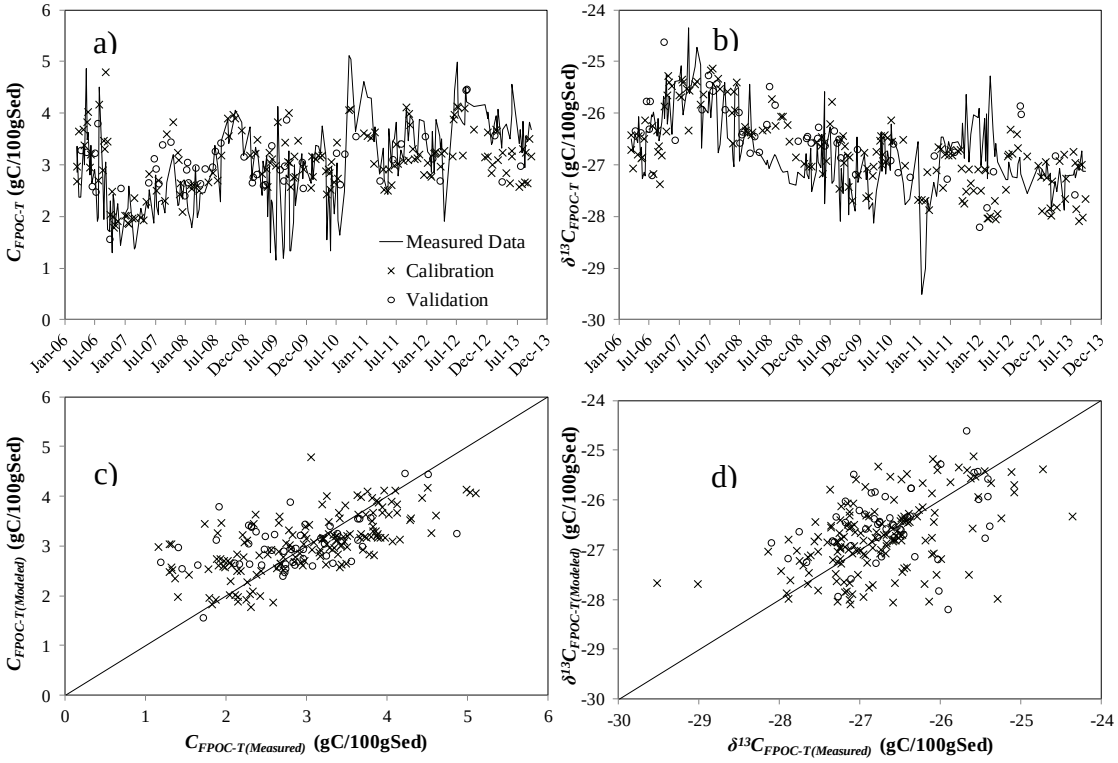

Figure 6. Event variability for the elemental (a-b) and isotope (c-d) models. Plotted values are deviations between calibration points for measured (y-axis) vs. modeled (x-axis). Points that plot in first and third quadrants indicate the model adequately captures between-event variability. Points that plot in the second and fourth quadrants indicate that the model does not capture between event variability. As is evident, during 2006-2007, when upland disturbance and high magnitude events are pronounced, the between event variability points plot predominantly in the second and fourth quadrants. Conversely, for years following the natural and anthropogenic disturbances (e.g. 2008-2013) both models appear to capture between event variability well, with most points plotting in the first and third quadrants.

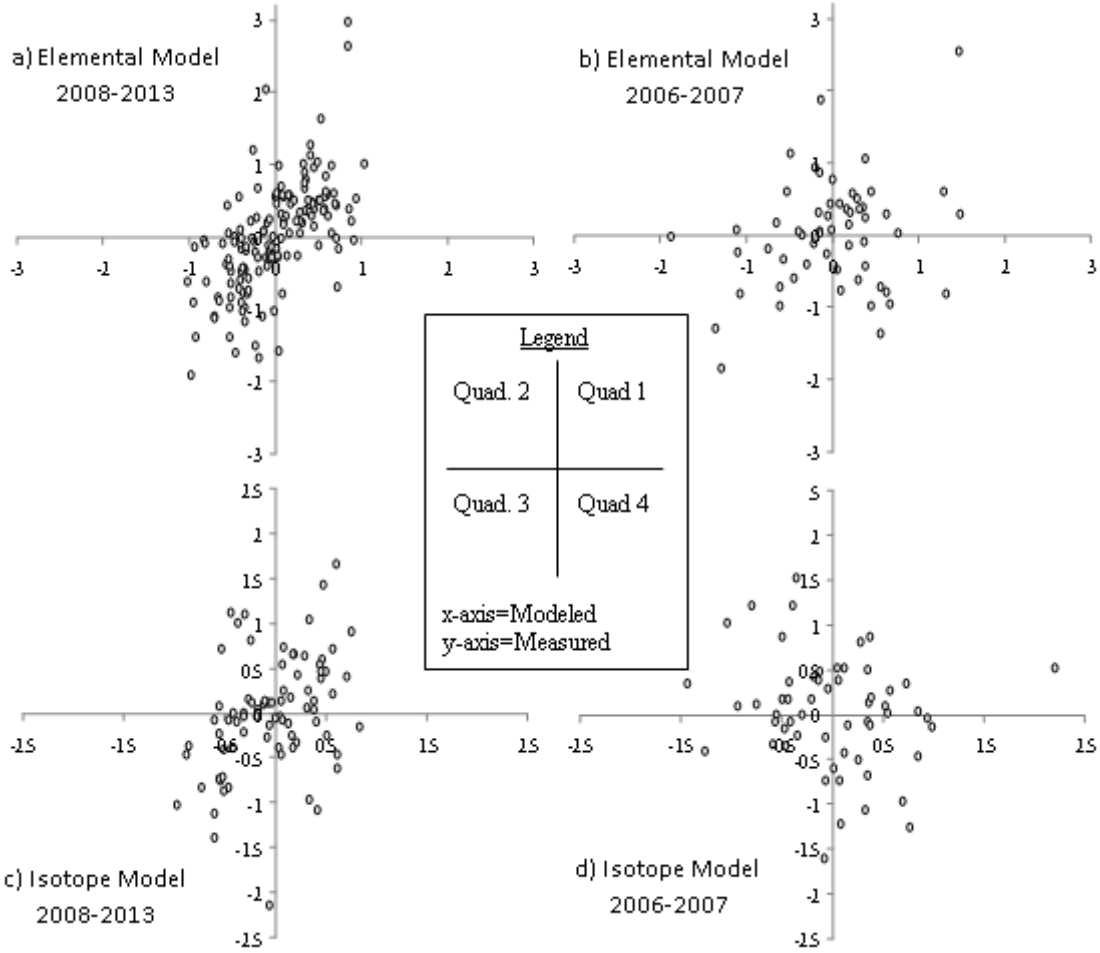

Figure 7. Simulations of standing stock of algal biomass, *B*, and volumetric water flowrate at the watershed outlet during 2006. High magnitude events occurring in spring, summer, fall and winter were prominent in 2006. Occurrence of high magnitude events in fall and winter deplete and limit recovery of *B*, while *B* in spring and summer typically return to pre-disturbance states within 2-3 weeks following the high magnitude flow disturbance.

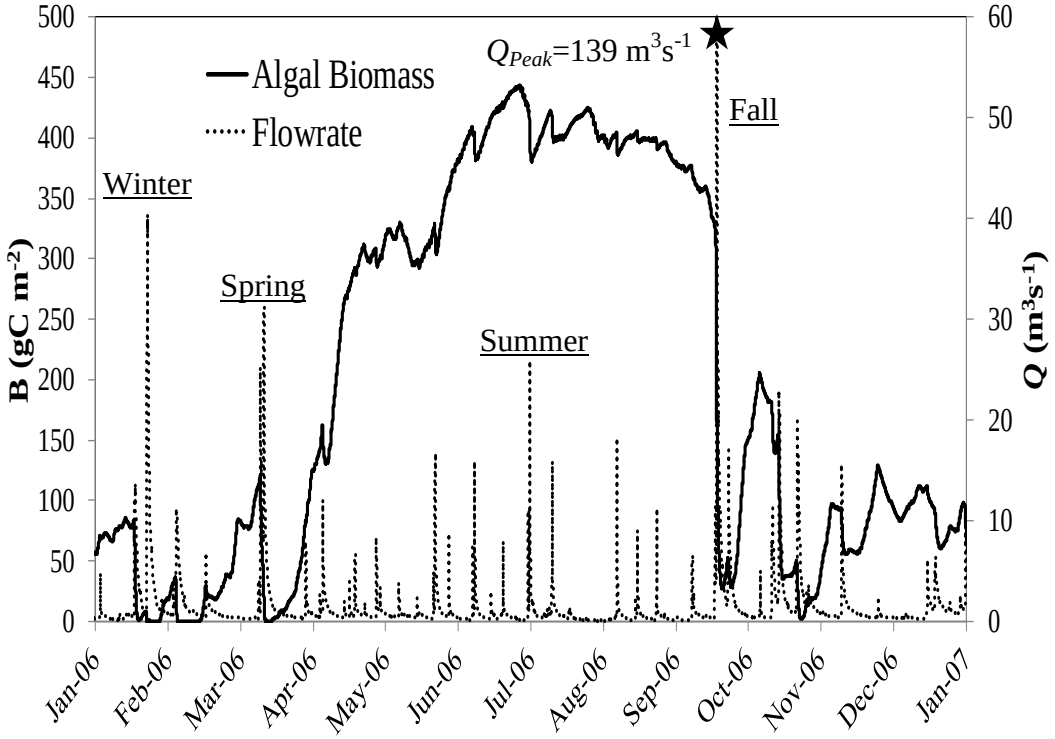

Copyright © William Isaac Ford III 2014

Chapter 6: Testing Assumptions for Nitrogen Fate in a Low-Gradient, Agriculturally Disturbed Stream

6.1 SUMMARY

Assumptions surrounding the stream N cycle in agriculturally disturbed watersheds suggest biologically mediated removal and transformation of dissolved and particulate N are analogous to processes occurring in pristine forested systems and point to tight, complex linkages between C and N processes. Despite the significance of these systems, little work has been conducted in streams characterized by surficial fine-grained lamina (SFGL) despite their spatial extent in low-gradient streams. The objective of the present study was to test prevailing assumptions for stream N cycling in a low-gradient ag-disturbed watershed utilizing an extensive eight year dataset of ambient transported particulate N and C measurements and a fourteen month pilot dataset for dissolved constituents. Both elemental and stable isotope signatures were analyzed for particulate and dissolved phases, and Empirical Mode Decomposition (EMD) of the time-series datasets was performed to overcome stationarity and distributional assumptions of more traditional methods. Removal of short term oscillations via the EMD analysis isolated seasonal signatures of the SFGL allowing interpretation of benthic fluctuations. Results suggest agreement with prevailing assumptions in late spring through fall, when autotrophic growth and decomposition dynamics govern tight coupling between in-stream C and N dynamics resulting in significant temporary sequestration of DIN, and providing labile C sources for benthic denitrification in the SFGL. Conversely in winter through mid-spring, when NO_3 loadings from upland fertilizer application and delivery of upland sediments by high flow storm events are pronounced, results suggest decoupling of C and N cycles in which increases in sediment N instantaneously coincide with decreases in transported NO_3 and sediment C. The result is attributed to abiotic sorption as the mechanism for transient storage of NO_3 during this period, analogous to processes occurring in B horizon soils with the presence of variably charged sesquioxides. The potential implications are significant in that NO_3 sorption suggests a potential retardation of NO_3 loadings downstream, and also provides a site for denitirification under low NO_3

conditions in summer when heterotrophs have to compete with autotrophs for streamwater DIN, to some degree autocorrecting for high anthropogenic loadings.

6.2 INTRODUCTION

Mechanisms controlling source, fate and transport of N in agricultural and urban disturbed watersheds (<100km^2) have received increasing attention over the past decade as a result of the deleterious impacts of anthropogenic N loadings on drinking water quality and eutrophic/hypoxic conditions in receiving waterbodies (Alexander et al., 2008; Galloway, 2008; Seitzinger, 2008; Xue et al., 2009; French et al., 2012; Trimmer et al., 2012). Despite the environmental significance, studies of N in human disturbed streams have assumed in-stream dynamics are consistent with the conceptual model developed for small, pristine, forested streams where nutrient loads are small, hillslopes and streambeds have steep gradients and organic matter dynamics are governed by allochthonous sources (Peterson et al., 2001; Bernhardt et al., 2005; Mulholland et al., 2008; Sebestyen et al., 2014). Conversely, agriculturally and urban disturbed watersheds, which are dominant throughout the mid-western U.S., are characterized by fine sediment surface soils, mild streambed gradients that promote transient sediment storage, and high background nutrient loadings and low canopy cover that promote autotrophic benthic algae as the dominant organic matter source (Walling et al., 2006; Griffiths et al., 2012; Ford and Fox, 2014a). The aforementioned characteristics of mid-western ag and urban watersheds promote formation of a thin, advection dominated, biologically active surface fine-grained lamina (SFGL) layer which is comprised of a heterogeneous mixture of autotrophic algae, heterotrophic bacteria and fine sediment aggregates, effectively integrating erosion/deposition and biogeochemical sediment processes (Droppo and Stone, 1994; Droppo et al., 2001; Russo and Fox, 2012; Fox et al., 2014; Zahraeifard et al., 2014). The contrasting watershed characteristics suggests a need to test the status quo for in-stream N cycling in low-gradient human disturbed systems characterized by SFGL.

The emerging conceptual model of N dynamics in SFGL dominated, ag-disturbed streams stem from a critical review by Birgand (2007) and a large scale tracer study of headwater streams by Mulholland et al. (2008), and point to hydrodynamics and benthic

mediated biological redox reactions driving dissolved inorganic N, or DIN (i.e., NH_4^+ and NO_3^-), attenuation and exchange between dissolved and particulate phases *via* assimilation, ammonification, nitrification and denitrification. Hydrodynamics are the physical drivers for transport of dissolved and particulate solutes into and out of stream reaches and transient storage zones associated with the SFGL (Battin et al., 2003; Russo and Fox, 2012; Zhareifiard et al., 2014). Assimilation denotes the biotic fixation of DIN, NH_4 and NO_3, into microbial biomass, i.e., amino and nucleic acids, and is dominated by primary production in the aforementioned streams, as opposed to heterotrophic fixation (Birgand, 2007; Kendall, 2007; Ford and Fox, 2014a). Ammonification is the bacterial mineralization of organic nitrogen to ammonium in which fate is determined by reassimilation rates by benthic biota, indirect nitrification, and regeneration via advection into the water column. Nitrification is the oxidation of ammonium to nitrate through a two-step process including oxidation to nitrite, NO_2, followed by rapid oxidation to NO_3 and can occur from advection of the overlying water column into the SFGL, i.e., direct nitrification, or can occur following mineralization of organic matter, i.e., indirect nitrification. Denitrification, or the dissimilatory reduction of NO_3 into gaseous nitrogen, is performed by facultatively anaerobic, heterotrophic organisms that can occur in either deep diffusion dominated zones where oxygen is low, or in localized anoxic pockets, e.g., within algal mats, where sharp gradients in dissolved oxygen profiles occur over short distances (Birgand, 2007; Gu et al., 2007; Findlay et al., 2011; Harvey et al., 2013).

Assumptions surrounding the N cycle in ag-disturbed streams include coupled C and N processes and the significance of biotic processes in hyporheic zones. Three primary avenues in which C and N are assumed coupled are during assimilation and immobilization of algal biomass, nitrification, and denitrification. Coupled assimilation of C and N occurs during photoautotrophic algal growth, and has been suggested to have significant implications for downstream delivery, or in-stream retention through degradation of detrital algae (Birgand et al., 2007; Godwin et al., 2009). Nitrification rates of chemoautotrophic bacteria are dependent upon ammonium mineralization of labile carbon and in N limited systems will be inversely related to C content since labile C stimulates competition from heterotrophic bacteria, however for ag systems where N is typically non rate-limiting nitrification is assumed to increase with labile carbon content

due to the enhanced mineralization rates (Butturini et al., 2000; Arango and Tank, 2008). Denitrification rates are assumed to increase with labile carbon availability and high NO_3 concentrations characteristic of agriculturally disturbed streams (Arango et al., 2007; Arango and Tank, 2008; Findlay et al., 2011; Newcomer et al., 2012). Despite existence of conceptual models, recent advancements have been made in ag-disturbed streams regarding the role of the hyporheic zone, suggesting that uncertainty in the conceptual model is still pronounced (Gu et al., 2007; Zarnetske et al., 2011; Baker et al., 2012; Zarnetske et al., 2012; Harvey et al., 2013). Further, while abiotic processes have been included for cationic ammonium, biological transformations have generally been assumed to be the primary mechanisms impacting in-stream fate of the NO_3 anion thus neglecting processes such as sorption as a potential mechansim for transient storage (Hantush, 2007).

While the prevailing assumptions regarding biologically mediated redox reactions of N in agriculturally disturbed streams have gained general acceptance and prompted inclusion into widely accepted numerical model decision making tools, the assumptions remain untested using long-term, comprehensive, ambient datasets that can be used to infer stream N dynamics. Rather, methods to measure biotic fluxes and transformations have relied on laboratory and field analyses of ambient samples, and stream augmentation approaches. Bench-scale laboratory sediment core experiments and *in situ* mesocosms have been used extensively to estimate N transformation rates, however they have shown to bias results in that they do not adequately simulate vertical advective fluxes into substrates, hence underestimating delivery of solutes to biota, and they only provide a point sample of processes (Birgand, 2007; Turlan et al., 2007). Reach-scale *in situ* studies have utilized conservative and non-conservative tracer injections (e.g., dye tracing, bromide, $^{15}N\text{-}NO_3$) to characterize solute storage potential and in-stream fate, however the expense and labor intensive nature of the approaches limit temporal domain to a few weeks (Mulholland et al., 2008; Baker et al., 2012). Ambient point measurements of upstream and downstream reaches have been coupled with mass-balance calculations to estimate uptake, however these processes don't account for regeneration from the pore water, thus over-estimating rates (Seitzinger et al., 2002, Trimmer et al., 2012). Finally, ambient point measurements of sediment N have

provided little fruitful insight as a result of the added complexity of sediment source variability (Kendall et al., 2001; Akamatsu et al., 2011). Collectively, studies have placed heavy emphasis on sampling during presumed periods including late spring through fall when biological processes are most pronounced and less in winter through mid-spring when autotrophic and heterotrophic pools are temperature limited (Birgand, 2007; Sebestyen et al., 2014). In addition to methodological limitations from measurements, time-series analysis of hydrologic and water quality data have primarily utilized Fourier based approaches that assume parametric, linear and stationary characteristics of constituent datasets, despite recent findings that contradict those assumptions for transported constituents in ag-disturbed streams (Machiwal and Jha, 2012; Ford and Fox, 2014b).

The previous N measurements methods mentioned in the foregoing discussion have been pioneering to substantiate the existence and importance of nutrient spiraling and its connectivity to OM processes in streams. However, the current assumption of coupled biological processes as controlling the N cycle in agriculturally-disturbed streams has been untested using long-term, ambient datasets that can be used to infer stream N dynamics. The objective of the present study was to test existing assumptions regarding the conceptual model of stream N dynamics in agriculturally-disturbed watersheds by (i) collecting an extensive long-term dataset (8 years) of temporally and spatially integrated transported sediment samples in a low-gradient ag-disturbed system controlled by SFGL, (ii) investigating dissolved and particulate phases for both C and N species transported in-stream, and (iii) performing a data driven Empirical Mode Decomposition (EMD) time-series analysis that overcomes limiting assumptions of the traditional Fourier analysis to understand drivers of seasonal fluctuations. Long-term assessments throughout the year are needed in order to overcome existing limitations of the aforementioned methods to study N dynamics, and to provide duplicates of seasonal processes that encompass a range of hydrodynamic and climate conditions. Ambient measures of dissolved and particulate phases for C and N provide an avenue to test recent findings of coupled C and N processes and to more tightly understand biogeochemical reactions causing exchange between dissolved and particulate pools. Finally, the EMD analysis overcomes simplifying limitations of the Fourier analysis including stationarity

and parametric distributions of analyzed data (Haung et al., 1998). Our results contradict conventional wisdom regarding prevailing assumptions of N conceptual models during timeframes that have been overlooked when studying nitrogen dynamics in ag-disturbed systems.

6.3 METHODS

In order to test existing assumptions regarding the stream N cycle in human disturbed watersheds we collected and analyzed an extensive dataset following the Quality Assurance Project Plan for site selection, sample collection protocol, sample analysis and handling, laborartory analysis, blanks and replicates, and post-analysis processing. The methodological approach can be summarized as a five-step procedure as follows:

1) Study Site: A mixed use, bedrock controlled watershed in the Bluegrass Region of Central Kentucky characterized by intermittent SFGL storage in first and second order tributaries and perennial storage in the main stem as well as high nutrient loadings (Russo and Fox, 2012; Ford and Fox, 2014a).
2) N Sources: We collected samples spatially in first and second order tributaries and at upstream and downstream sites of the main stem in order to evaluate inputs and sources of C and N at different spatial scales. To characterize potential particulate N and C sources we collected sediment from streambanks, benthic algal biomass growing on the streambed surface, and transported sediment samples at first order tributary sites to characterize upland sources. Further to characterize dissolved phases, a fourteen month pilot dataset for dissolved solutes were collected in order to better understand fluctuations in the sediment N data.
3) Transported Stream N: Spatially and temporally integrated sediment trap samples that capture heterogenous mixtures of transported SFGL, bank, and upland hillslope sediments during stormflows were collected at upstream and downstream boundaries of the main stem in order to capture variability of in-stream processes occurring in tributaries and main-stem sites. An eight year timeframe, 2006-2013, was conducted in the South Elkhorn watershed in order to

encompass a range of hydrologic and climate conditions, which drive in-stream N variability, and to have replicates of seasonal processes. To characterize dissolved phases, a fourteen month pilot dataset for dissolved solutes were collected from the main stem.

4) Biogeochemical Analyses: For the present study we focus on analyzing elemental concentrations and isotopic signatures of sources and mixture samples for both dissolved and particulate phases as they are sensitive to sources of C and N, as well as biogeochemical transformations in the SFGL.
5) Statistical Analyses: Finally, our analytical experimental method consisted of performing an Empirical Mode Decomposition (EMD) time-series analysis, a purely data driven approach without limiting assumption of the traditional Fourier analysis, as well as investigating the statistical distributions of elemental and isotopic signatures in order to test our hypothesis.

We provide full description of our methods in the following sub-sections.

6.3.1 Study Site

The South Elkhorn watershed (Figure 1), 62 km^2, was chosen as the study site to investigate SFGL function due to extensive knowledge of landuse, flow, sediment and carbon dynamics in the system, the highly productive nature of the streambed, and spatial and temporal variability of the dynamic benthos (Fox et al., 2010; Russo and Fox, 2012; Ford and Fox, 2014a; Ford and Fox, 2014b; Fox et al., 2014; Ford et al., 2014). The SE is a mixed-use, agriculturally and urban disturbed watershed located in the Bluegrass Region of Central Kentucky. Agricultural land use (57%) is dominated by pristine horse farms while urban land use (43%) is primarily residential and commercial. Precipitation, and subsequently streamflow, is driven by stormflows, producing 1150 mm/year of precipitation and an average streamwater flowrate of 1.2 m^3s^{-1}. Soils in the watershed are predominantly silty clay loams, hence fine sediments are a significant component of the transported load having an average particle diameter of ~20μm (Fox et al., 2014). The SE watershed has 53 perennial stream reaches, of which 27 are first order, 13 are second

order and 13 are third order. Transported sediments in-stream reflect a heterogeneous mixture of benthic, bank and upland sources in which benthic sediments are prominent during low-moderate flows, streambank sediments are prominent at moderate to high flows, and upland sediments are pronounced at high flows (Russo and Fox, 2012). Streambeds are bedrock controlled with limited karst, in which fine sediments cover ~75% of the streambed. The SFGL is comprised of a heterogenous mixture of upland sediments deposited from the uplands on the receding limb of the hydrograph and newly generated autochthonous material in the benthos (Fox et al., 2010; Russo and Fox, 2012; Ford and Fox, 2014a). Visual observation of the system over the eight year study suggests that SFGL is intermittent in the first and second order stream reaches and perennial in the main-stem of the watershed. The algal contributions significance is recognized in that recent estimates from the system suggest algal biomass can constitute a combined 80% of the POC flux, while constituting less than 10% of the total sediment load (Ford and Fox, 2014a; Ford and Fox, 2014b). Cohesive streambanks coupled with densely compacted legacy sediments limit the prominence of hyporheic flow.

Non-rate limiting production of algal biomass in-stream is supported by measurements of high bioavailable N and P in the system. NO_3 concentrations in stream reaches range from 0.23 to 5.9 mgN/L-NO_3 and dissolved phosphorus ranges from 0.1 to 0.42 mgP/L which exceeds thresholds for rate-limiting nutrient conditions of algal growth of 0.04mgN/L and 0.03mgP/L (Dodds et al., 2002). High background levels of phosphorus stem from a mixture of dissolution of phosphatic limestone and fertilizer application, while N primarily stems from fertilizer application. Suggested fertilizer application rates for cool-season grasses in the region vary depending on stock of horse pastures and time of year (Murdock and Ritchey, 2012-AGR-1). For cool season grasses, low-stocking pastures suggest late-fall, and late-summer applications, while high-stocking pastures suggest late-winter, mid-spring, and late-summer applications. Further, for lawns and turf in urban settings, fall applications are suggested for cool season grasses and late-spring to mid-summer applications are suggested for warm season grasses.

6.3.2 Field Sample Collection and Preparation

Transported sediment samples were collected at two main-stem sites for eight years (2006-2013) including MS-1, the main-stem outlet, and MS-2, the main-stem inlet, in order to characterize how SFGL processes differ between tributaries (i.e., first and second order reaches) and the main-stem (third order reaches). Measurements of transported fine sediment during storm events were collected utilizing *in situ* sediment traps (Phillips et al., 2000). The traps collect a spatially and temporally integrated sample, which have been shown to provide a statistically representative measure of the chemical signature for the <53µm size class. Sediment traps were replaced weekly in the field with clean sediment traps and were cleaned using phosphorus free soap and deionized, deoxygenated (DIDO) water. Samples were collected in five gallon buckets and stored in a refrigerated space for at least 48 hours to ensure sedimentation from the water column. Samples were brought to a steady state by decanting, centrifuging, freezing and freeze drying to remove remaining water. The bulk sample was sub-sampled depending on mass, wet sieved to retain the fines fraction, brought to a steady state, ground, weighed into silver capsules, and acidified with 6% sulfurous acid to remove carbonate phases (Verardo et al., 1990; Fox, 2007; Ford and Fox, 2014a).

Temporal variability of benthic C and N processes stems from variability of watershed and climate variables. The eight year timeframe (2006-2013), encompasses a range of scales including event, seasonal, and annual scales (Figure 1). Temporal variability in temperature and precipitation are expected to be the important meteorological variables driving benthic C and N variability (Ford and Fox, 2014b). Seasonal temperature oscillations stem from the humid subtropical climate in which peaks occur during warm summers and valleys occur during mild winters. Seasonal flow oscillations stem from antecedent moisture conditions in which warm, dry summers limit connectivity between upland hillslopes and the stream channel, reducing baseflow as well as surface runoff during storms; and cool, wet winters promote high antecedent moisture conditions, higher baseflow, and more pronounced surface runoff associated with connectivity between upland hillslopes and the stream channel. Longer-term wet and dry conditions are present during the timeframe as evidence by the prolonged low flows during summers of 2007 and 2008 and the high flows during summer of 2009. Finally,

high magnitude events, i.e., September 2006 event with a Q_{Peak}=138m^{3}s^{-1}, have been shown to have prolonged impacts on benthic composition in the South Elkhorn (Ford et al., 2014).

6.3.3 Source Characterization

To characterize potential sources including upland and bank sediments as well as algal biomass, additional samples were collected. Four months of transported sediment data were collected in first order tributaries, June-September 2013, at an agriculturally dominated tributary (TA-1) and an urban dominated tributary (TU-1) in order to help characterize the upland hillslope source. Samples were processed analogous to the sediment trap samples in the main-stem. Bank sediment samples were collected on five separate occasions in 2007-2008 by scraping vegetation from eroding bank sites and obtaining 20 grams of sediment at 15, 30, and 45 cm above the water surface during low flows (Fox et al., 2010). Samples were homogenized, subsampled, wet sieved to retain the fines fraction, brought to a steady state, ground, weighed into silver capsules, and acidified with 6% sulfurous acid to remove carbonate phases. Grab samples of algal biomass were collected in the field at each of the study sites on three separate occasions in summer 2013, brought back to the lab, freeze dried, subsampled, and weighed into silver capsules. Samples were not acidified since the content of PIC relative to POC was assumed negligible.

To further understand in-stream biogeochemical processes mediated through benthic sediments and benthic algal biomass, a fourteen month pilot dataset of dissolved constituents was collected from four first order tributaries, two ag and two urban, two second order tributaries, one ag and one urban, and the transported sediment monitoring sites on the third order main stem (Figure 1 and Table 1). Samples were collected for a range of flow conditions in which each season had at least one base flow period and one storm flow represented. Discrete sample collection was conducted using 1L sterilized ISOCHEM bottles that were rinsed *in situ* before sample collection. Duplicates and blanks were taken bimonthly (approximately ten percent of the samples).

6.3.4 Laboratory Analysis

Isotopic and chemical signatures of dissolved and particulate phases were measured from the collected transported sediment and source samples in order to assess in-stream fate and of N processes in the SFGL dominated streambed. Samles were prepared and analyzed utilizing protocol in the Quality Assurance Project Plan (QAPP, Appendix 1). Particulate samples were analyzed for elemental compositions, *FPOC* and *FPN*, and their isotopic signatures, $\delta^{13}C_{FPOC}$ and $\delta^{15}N_{FPN}$, by combusting samples at 980°C on a Costech Elemental Analyzer, passing the gas stream through a Gas Chromatograph (GC) column to a Thermo Finnigan Delta-Plus Isotope Ratio Mass Spectrometer (IRMS). The elemental reference was acetanilide (%C=71.09%; %N=10.36%), and isotopic references were DORM ($\delta^{13}C$=-19.59‰; $\delta^{15}N$=12.46‰), and CCHIX ($\delta^{13}C$=-16.6‰; $\delta^{15}N$=3.5‰).

Dissolved samples were filtered in the laboratory using GF-B and GF-F Whatman filters. Splits for dissolved phosphorus (DP), dissolved organic carbon (DOC), dissolved inorganic carbon (DIC), nitrate (NO_3), ammonium (NH_4), $\delta^{15}N_{NH4}$, and $\delta^{15}N_{NO3}/\delta^{18}O_{NO3}$ were obtained. DP, DOC, and DIC samples, which were analyzed according to standard operating procedure in the QAPP at the Kentucky Geological Survey Laboratory, showed fairly conservative behavior spatially and temporally suggesting little sensitivity to in-stream processes, hence they were excluded from the analysis. Further, ammonium concentrations, measured on a Varion 40 spectroscopy system, were generally below detectable limits (0.02mgN_{NH4} L^{-1}); however NO_3 concentrations were high, and showed pronounced spatial and temporal variability. NO_3 concentrations (N_{NO3}) were measured at the Kentucky Geological Survey Laboratory utilizing an Ion Chromatograph. Relative percent difference for replicates was less than 10% and reference standards (HPLC grade reagants) were guaranteed to ±10% of their theoretical concentration. Stable isotopic signatures of NO_3 ($\delta^{15}N_{NO3}$ and $\delta^{18}O_{NO3}$) were measured using a bacterial denitrification method consistent with the USGS Reston Stable Isotope Laboratory method discussed in Coplen et al. (2012) and analyzed on a Finnigan Delta^{Plus} CF-IRMS interfaced with a GC-column. Reference standards for the analysis were N3 (19.975 µM KNO_3, $\delta^{15}N$=4.7‰ and $\delta^{18}O$=25.6‰), USGS 32 (19.7 µM KNO_3, $\delta^{15}N$=180 ‰ and $\delta^{18}O$=25‰), USGS 34 (20 µM KNO_3, $\delta^{15}N$=-1.8‰ and $\delta^{18}O$=-27.9‰), USGS 35 (20 µM KNO_3, $\delta^{15}N$=2.7‰ and $\delta^{18}O$=57.5‰).

6.3.5 Statistical Analysis

We performed an exploratory time series analysis on the eight year datasets of sediment carbon and nitrogen constituents and explanatory variables, i.e., flow and water temperature. Time series were assumed to be non-linear, non-stationary and their distributions non-parametric (see Ford and Fox, 2014a; Ford and Fox, 2014b). Empirical mode decomposition, EMD, was used to decompose the time series into intrinsic mode functions, IMFs (Haung et al., 1998; Wu et al., 2007). EMD was selected as the preferred method for the analysis since there are no limiting assumptions about the dataset, it can be applied to a wide class of signals and it is uses an *a posteriori* approach which is ideal for an exploratory analysis. Further, it overcomes linearity assumptions of a Fourier spectra analysis. IMFs are a finite series of amplitude and frequency modulated, oscillatory functions in which your lowest frequency IMF is identified as the base trend and the highest frequency trend is considered noise for well-sampled datasets (Wu et al., 2007). EMD is conducted utilizing a six step iterative procedure in which (1) local maxima and minima are identified in the time series, (2) cubic spline interpolation signals are computed to create upper and lower envelopes, (3) upper and lower envelopes are averaged, (4) the average envelope is subtracted from the signal (related to the current iteration), (5) the process is repeated until the averaged envelope converges to a stated threshold, (6) the resulting IMF is subtracted from the original dataset to create a new time series and steps 1-5 are repeated until all extremes are removed. In general the dataset X(t) can be represented as

$$X(t) = \sum_{i=1}^{n} c_i + r_n$$

where c_i are the IMFs, and r_n is the residual noise following the coarsest frequency trend.

We compiled a previously published code in Matlab that overcomes limitations of the original framework by incorporating modifications for identifying local maxima and minima, end point considerations, stopping criteria and IMF removal (Rato et al., 2008). We performed statistical significance tests to test the hypothesis that IMFs of the dataset are statistically different from white noise IMFs (Wu et al., 2007). A log-log plot of

variance versus mean period was plotted for each IMF and tested against a confidence interval for white noise (Wu and Huang, 2004). Month to month trends are not expected for the environmental variables in this study, hence a monthly period was used as the basis for noise and negative linear relationship of log(Var) vs. log (Period) with a slope of -1 was plotted with upper and lower bounds for the confidence interval being represented with $\log_{10}(\text{Var}) \pm \log_{10}(3)$. IMFs of the dataset that plot outside the specified variance range are statistically differentiable from white noise and thus have some physical meaning. Herein, we define quasi-seasonal variability as statistically significant IMFs with oscillations that have an average period of approximately one year or less, annual variability as statistically significant IMFs with oscillations having an average period between 2-8 years, and long-term variability as the residual noise IMF.

To test covariance between chemical and isotopic signatures of sediment C and N, a covariance table (Table 3) was generated utilizing the coefficient of determination statistic for both main-stem sites. Relationships with high R^2 values were further explored utilizing scatterplots. For exploratory spatial analysis more traditional statistical approaches were utilized. Box and whisker plots were generated for both sediment and dissolved constituents. The central measure of tendency was represented by the median value of the dataset, min and max values of the box represent 25^{th} and 75^{th} percentiles of the dataset and the whiskers represent min and max values of the dataset. Additionally, histograms for sediment data were generated since sample numbers were large enough to investigate the distribution. Histogram bin sizes were generated using the Freedman-Diaconis rule (Freedman and Diaconis, 1980).

6.4 RESULTS

6.4.1Source Data Results

Results show that dissolved nitrate varied considerably for tributaries throughout the fourteen month sampling duration (Table 1 and Figures 2 and 3). Median N_{NO3} was significantly higher in agricultural tributaries as compared to urban tributaries at both high flows ($N_{NO3\text{-}AG}$= 5 mgN/L and $N_{NO3\text{-}Urban}$= 2.5 mgN/L) and low flows ($N_{NO3\text{-}AG}$= 3.2

mgN/L and $N_{NO3\text{-}Urban}$= 2.5 mgN/L). Median $\delta^{15}N_{NO3}$ values did not show distinct gradients between ag and urban tributaries, but were substantially higher at low flows (7-8 ‰) as compared to high flows (5-6 ‰). Median $\delta^{18}O_{NO3}$ values did not show distinct gradients with regard to land use or flow regime. With regard to temporal variability of nitrate at low flows, which is indicative of a groundwater nitrate source from upland soils, N_{NO3} showed distinct seasonal patterns for both ag and urban tributaries with peak values occurring in late winter-early spring (3-6 mg/L), and minimum concentrations in early-mid fall (0.5-1.5 mgN/L). Inversely, $\delta^{15}N_{NO3}$ and $\delta^{18}O_{NO3}$ from ag and urban tributaries show increases with decreasing N_{NO3} for the ag site and fairly static signatures in the urban site, except for summer when NO_3 deposition from the atmosphere is a potential source (i.e., $\delta^{18}O_{NO3} > 15$).

Results in Table 2 provide measured values of elemental (*FPOC*, *FPN*, *C:N*) and isotopic signatures ($\delta^{13}C$ and $\delta^{15}N$) for potential sediment sources to the SFGL, i.e., benthic algae, fine bank sediments, and transported fine sediments from agricultural and urban tributaries. Relative to other sediment sources, average benthic algae is higher in *FPOC* (27.9 gC/100gSed^{-1}), and *FPN* (2.5 gN/100gSed^{-1}), lower in $\delta^{13}C$ (-37.8 ‰) and has an average $\delta^{15}N$ (5.0 ‰) and *C:N* (12.4). Bank sediments are lower in *FPOC* (1.6 gC/100gSed^{-1}), *FPN* (0.2 gN/100gSed^{-1}), *C:N* (10.3), and higher in $\delta^{13}C$ (-25.0 ‰) and $\delta^{15}N$ (6.9 ‰). Fine transported sediment from ag tributaries, have average values of *FPOC* (4.7 gC/100gSed^{-1}), *FPN* (0.41 gN/100gSed^{-1}), $\delta^{13}C$ (-28.0 ‰) and $\delta^{15}N$ (4.8 ‰) and high *C:N* (11.9), with urban tributaries having slightly lower values of *FPOC* (4.0 gC/100gSed^{-1}), *FPN* (0.3 gN/100gSed^{-1}),and $\delta^{15}N_{FPN}$ (3.3 ‰), and slightly higher values of *C:N* (13.3) and $\delta^{13}C$ (-26.9). The highest variability is present in the algal signatures, however only *C:N* and $\delta^{15}N$ have ranges that overlap with signatures of other sources.

6.4.2 Main-stem Data Results

Results of the one year data collection effort for dissolved solutes in the main-stem (Figures 2 and 3) show periods of conservative and non-conservative NO_3^- transport through the stream channel. With regard to the flow regime, baseflow N_{NO3} is highest in the tributaries and decreases with increasing stream order. Inversely, average baseflow

$\delta^{15}N_{NO3}$ signatures are lowest in the tributaries and increase with increasing stream order. On average, $\delta^{18}O_{NO3}$ does not show the same trend and appears fairly conservative spatially. During stormflows, all chemical signatures appear conservative spatially in that values in the mainstem fall between tributary end-members. With regard to seasonality, N_{NO3} in the main stem generally falls between tributary end-members in the winter and spring, when concentrations are high, and below tributary end-members in the summer and fall, when concentrations are low. High concentrations during winter and spring are reflective of fertilization of pasture/rangeland grasses in late fall/early winter coupled with saturated soil conditions that promote high connectivity of the stream channel and upland hillslopes (Murdock and Ritchey, 2012). Low concentrations in summer and fall are reflective high autotrophic and terrestrial production which reduces downstream fluvial nitrate losses. $\delta^{15}N_{NO3}$ signatures generally fall between tributary end-members in summer and above tributary end-members in Fall, Winter and Spring. $\delta^{18}O_{NO3}$ signatures generally fall between tributary end members in all seasons however signatures in summer periodically fall below tributary end-members. Isotopic signatures, $\delta^{15}N_{NO3}$ from 3-12 ‰ and $\delta^{18}O_{NO3}$ from 0-15 ‰, suggest a mixture of nitrified ammonium fertilizer, soil mineralization, and manure/septic waste as NO_3 sources in the stream (French et al., 2012).

Results of the distributional forms for transported sediment chemical signatures at upstream (MS-2) and downstream (MS-1) sites (Figure 4) show that autochthonous SFGL processes are similar in the main stem and tributary reaches and slight deviations reflect degradation state of the SFGL source as opposed to contributions from bank sources. As seen in the box and whisker plots of transported fine sediment in Figure 4, median *FPOC*, *FPN* and *C:N* show distinct decreases reflective of degraded sediment C and N at the downstream site relative to the upstream site. Median $\delta^{13}C_{FPOC}$ at upstream and downstream main-stem sites are equivalent and reflect similar contributions from terrestrial and algal C sources. The increased median for $\delta^{15}N_{FPN}$ at the downstream site relative to the upstream site reflects the increase in $\delta^{15}N_{NO3}$ from the upstream to the downstream site. Cumulatively this would suggest that long residence of algae from upstream sources in the main stem SFGL cause depletion of *FPOC*, *FPN* and *C:N* signatures in the main-stem of the watershed and that additional sediment is generated

through autotrophic processes in the main stem that, at least to some degree, offset degradation of tributary algae, as evidenced by $\delta^{13}C_{FPOC}$ reflecting comparable amounts of autochthonous carbon in upstream and downstream reaches and $\delta^{15}N_{FPN}$ reflecting DIN isotopic signatures.

Transported *FPOC* and *FPN* have high covariance at both upstream and downstream sites, however higher deviation from the linear relationship for *FPOC* as a function of *FPN* at the downstream site reflect periods of decoupling for *FPOC* and *FPN* (Table 3 and Figure 5). *FPOC* and *FPN* at upstream and downstream sites have a strong positive linear relationship with no other pair of chemical signatures having a R^2 greater than 0.3. Deviations from the linear relationship increase with increasing values of *FPOC* and *FPN*. Further, the variability at these higher values is more pronounced at the downstream main-stem as compared to the upstream main-stem site as evidenced by the slightly lower R^2 value of 0.79 as opposed to 0.81 respectively. This deviation from the linear covariance is observed in the raw *FPOC* and *FPN* time series data in spring of 2008 when you see a pronounced fluctuation (increase and decrease) for *FPN* but a gradual increase for *FPOC*.

6.4.3 EMD Analysis Results

Results from the EMD analysis of the eight year raw dataset show that quasi-seasonal fluctuations in explanatory variables, e.g., temperature and flowrate, are not in phase with chemical signatures of C and N suggesting competition between biologic and hydrodynamic processes. Statistically significant quasi-seasonal variability was observed from the EMD analysis (see Figure 6 and 7) for streamwater temperature (T), streamwater flowrate (lnQ), fine particulate organic carbon at upstream and downstream boundaries of the main-stem ($FPOC_{MS-2}$ and $FPOC_{MS-1}$), the carbon to nitrogen atomic ratio at the upstream boundary of the main-stem ($C{:}N_{MS-2}$), the stable isotopic signature of fine particulate organic carbon at upstream and downstream boundaries of the main-stem ($\delta^{13}C_{FPOC}{}^{MS-2}$and $\delta^{13}C_{FPOC}{}^{MS-1}$), and the stable isotopic signature of fine particulate nitrogen at upstream and downstream boundaries of the main-stem ($\delta^{15}N_{FPN}{}^{MS-2}$and $\delta^{15}N_{FPN}{}^{MS-1}$). For explanatory variables, local maximums and minimums generally

occurred in mid-summer and early winter respectively for *T* and late winter and early fall respectively for *lnQ*. Local maximums and minimums for *FPOC* and *C:N* at the upstream site occur in late-fall and spring respectively, with *FPOC* seasonality being slightly less pronounced at the upstream site as opposed to the downstream site. The stable isotopic signature of *FPOC* is inversely consistent with *FPOC* and *C:N* in that local maximums and minimums occur in spring and late-fall respectively. Stable isotopic signatures of *FPN* at the upstream site have local maximums in late-fall/early-winter and minimums in late spring. Stable isotopic signatures of *FPN* at the downstream site has a unique quasi-seasonal oscillation in which two local maximums (fall, and spring) and two local minimums (winter and summer) occur in a single year.

Further, results of the study show that nitrate fluctuations are reflected in transported FPN at both upstream and downstream sites. As previously mentioned, transported FPN did not have any statistical significant seasonal IMFs, hence results of quasi-seasonal IMFs for the stable isotope signature of FPN at both upstream and downstream sites ($\delta^{15}N_{FPN}{}^{MS\text{-}1}$ and $\delta^{15}N_{FPN}{}^{MS\text{-}2}$) was plotted alongside the spatially averaged isotopic signature of transported nitrate ($\delta^{15}N_{NO3}$) during low flow conditions (Figure 8). From visual inspection of Figure 8 there are two distinct oscillations of $\delta^{15}N_{NO3}$ occuring from January to May and May through September. The peak in late winter visually coincides with a fluctuation in the $\delta^{15}N_{FPN}{}^{MS\text{-}1}$ IMF but not with the $\delta^{15}N_{FPN}{}^{MS\text{-}2}$ IMF. The second peak in the $\delta^{15}N_{NO3}$ data, which is similar to temperature in that it peaks in July, is reflected in the $\delta^{15}N_{FPN}{}^{MS\text{-}1}$ and $\delta^{15}N_{FPN}{}^{MS\text{-}2}$ IMFs but lagged by multiple months.

6.5 DISCUSSION

6.5.1 Seasonal OM Variability

Results of transported sediment C in the main-stem provide a consistent depiction of in-stream OM dynamics in the SFGL of low-gradient agriculturally disturbed streams which reflects autotrophic production, heterotrophic decomposition, and sediment transport dynamics. Seasonal biological and physical behavior of the heterogeneous SFGL layer is reflected in quasi-seasonal fluctuations of *FPOC* in which two carbon end-

members, including algae and terrestrial SOC, control timing of carbon maxima, approximately 5 gC/100gSed, and minima, approximately 2 gC/100gSed (Figure 6 and 7). Carbon maxima in late-fall are indicative of a particulate C store originating from in-stream algal C. Carbon minima in spring are reflective of a more recalcitrant terrestrial SOC source (Table 2). The C maxima agree well with high temperatures in late-spring through late-fall, as evidenced by positive values in temperature IMFs, coupled with dampened connectivity between upland hillslopes and the stream channel during storm events, as evidenced by the negative values for flowrate IMFs, which promote favorable conditions for algae production and heterotrophic bacterial decomposition (White et al., 1991; Rutherford et al., 2001). Further, the time difference between peak temperature IMFs in summer and FPOC IMFs in fall suggests a time lag between algal C stock and FPOC stocks due to heterotrophic decomposition. The time lag is reminiscent of results found for a previous modeling study in the system in which the lag between peak algal biomass and peak *FPOC* stems from continued breakdown of algal biomass which enriches the SFGL layer in algal FPOC until late fall (Ford and Fox, 2014a). Conversely, winter periods and spring C minima reflect SOC input to the streambed and low algal C production. Low temperatures in late-fall through late-spring, as evidenced by negative values of the seasonal temperature IMF, coupled with high connectivity between uplands and hillslopes, as evidenced by the positive values for the seasonal flowrate IMF, provides flow and temperature limited conditions for algal biomass in which heterotrophic decomposition of the algal *FPOC* outweighs inputs from the coarse algal mat (Ford and Fox, 2014a). Further, inputs of terrestrial SOC are high during this time period since higher upland and stream channel connectivity and higher magnitude storm events promote pronounced upland sediment loading which is subsequently deposited to the SFGL on the receding limb of a storm event (Russo and Fox, 2012). Stable C isotope results provide further support for the two C source end-member hypothesis because *FPOC* and $\delta^{13}C_{FPOC}$ are inversely related, e.g., FPOC maxima correspond with $\delta^{13}C_{FPOC}$ minima, which reflects the low $\delta^{13}C$ signatures (-35‰) of algae and high $\delta^{13}C$ signatures (-26‰) of terrestrial SOC.

Comparison of carbon results for upstream and downstream sites suggests similar SFGL processes throughout the fluvial system, albeit seasonal processes seem more

pronounced at the downstream site as a result of higher SFGL residence times in the main-stem. Generally *FPOC* at upstream and downstream sites have similar results for the EMD analysis suggesting that the aforementioned seasonal growth and decomposition mechanisms, as well as SOC inputs, are prominent throughout main-stem and tributary stream reaches. The lack of distinct seasonality during some seasons for *FPOC* at the upstream site (e.g., 2009) is reflective of the lower deposition and SFGL residence time upstream of MS-2 relative to SFGL storage in the main stem. Decreases in expected values of *C:N* and *FPOC* from upstream to downstream, as shown in Figure 4, suggest higher contributions of bank sediment carbon in the transported load which agrees with previous studies of sediment and carbon transport in the system (Russo and Fox, 2012; Ford and Fox, 2014a).

6.5.2 Seasonal N Variability: Late Spring-Fall

Results of dissolved and particulate N phases from late-spring through fall suggest tight coupling of SFGL C and N processes associated with algal production and OM decomposition that are consistent with current understanding of ag-disturbed stream N dynamics. N dynamics, as reflected by *FPN*, suggest SFGL algal assimilation as the pathway for transient removal of NO_3 from the water column from summer through fall because *FPN* increases coincide with *FPOC* increases. Despite noise of the *FPN* dataset resulting in statistically insignificant IMFs at a seasonal timescale, visual inspection of the raw *FPN* datasets at both upstream and downstream sites suggest that algal production and degradation cause increases in *FPN* through fall, reminiscent of the aforementioned *FPOC* processes. The time difference between the $\delta^{15}N_{NO3}$ and $\delta^{15}N_{FPN}$ IMFs for both upstream and downstream sites (Figure 8) is reminiscent of the time lag between temperature and *FPOC*. Further, spatially averaged dissolved results in Figure 3, i.e., N_{NO3}, $\delta^{15}N_{NO3}$ and $\delta^{18}O_{NO3}$, further support prominence of algal assimilation in spring and summer since both $\delta^{15}N_{NO3}$ and $\delta^{18}O_{NO3}$ are high relative to subsurface fertilizer derived NO_3 (~7‰ during high flows) and N_{NO3} is decreasing during this period suggesting uptake associated with biotic assimilation (Kendall et al., 2007; Sebestyen et al., 2014). This result suggests that the time varying nature of NO_3 is incorporated into

the benthic sediment $\delta^{15}N$ signature through algal growth and decomposition which is consistent with current understanding of ag-disturbed benthic OM dynamics (Birgand, 2007; Ford and Fox, 2014a). Coupled nitrification/denitrification, heterotrophic mediated processes, and subsequent regeneration to the water column appear prominent in fall since: $\delta^{15}N_{NO3}$ shows an abrupt increase suggesting N isotope fractionation; $\delta^{18}O_{NO3}$ values decrease reminiscent of $\delta^{18}O_{H2O}$=-6‰ suggesting pronounced nitrification of mineralized ammonium; and N_{NO3} remains relatively static suggesting denitrification isn't impacting total N_{NO3}. The timing of this process supports recent findings in Southwestern Michigan where low NO_3 concentrations stimulate coupled nit/den in fall (Arango and Tank, 2008).

6.5.3 Seasonal N Variability: Winter-Mid Spring

While results suggest seasonal N cycling in late-spring through fall is consistent with current understanding of stream N dynamics, existing theory does not adequately explain fluctuations in winter through mid-spring, suggesting alternative governing mechanisms. As is clearly seen for 2008 and 2010 in the far left column of Figure 6, SFGL C decreases during winter and spring while SFGL N shows an increase and $\delta^{15}N_{FPN}$ shows an increase more reflective of fertilizer N and subsurface NO_3 sources. Further, results of Figure 8 suggest that NO_3 and sediment N dynamics at the downstream site are tightly linked from Jan-May since $\delta^{15}N_{FPN}$ at the downstream site and spatially averaged $\delta^{15}N_{NO3}$ have increasing and decreasing fluctuations that are in phase, i.e., there is no apparent timelag. Decreasing FPOC during winter and spring, as a result of influxes of sediments from upland hillslopes with low C and N contents and limited algae accrual in the SFGL, would suggest that the fluctuations in FPN are not reflective of biological processes including autotrophic and bacterial production. Conversely, the temporal variability would suggest that results are governed by abiotic processes that have previously been overlooked in traditional assumptions of stream N cycling in ag streams for winter through mid-spring.

Deviations from traditional biologic assumptions regarding the stream N cycle during winter and spring are further evidenced by the spatial variability of *FPN* and NO_3

in the study watershed. The SFGL in first and second order stream reaches does not have prominence of *FPN* production during winter and spring since there are decreasing gradients in the *FPN* time-series and no statistically significant secondary seasonal fluctuations for $\delta^{15}N_{FPN}$. Covariance analysis of *FPOC* and *FPN* (Table 3 and Figure 5) would tend to suggest that C and N processes are more tightly coupled in the tributaries of the watershed as evidenced by the higher R^2 values and less bias at high *FPOC* and *FPN* values at the upstream site relative to the downstream site, which suggests that biotic processes impact C and N similarly. Spatial variability of streamwater N_{NO3} support FPN production in the main stem coincides with attenuation of NO_3 during winter and spring as evidenced by lower NO_3 concentrations at the downstream site relative to the upstream site in winter and early spring (Figure 3). Since this time period coincides with pronounced delivery and deposition of upland sediments to the SFGL in the main stem (Russo et al., 2012), it's reasonable to deduce that the mechanism driving N exchange between dissolved and particulate phases is an abiotic process associated with upland terrestrial material.

Taken together, spatiotemporal variability in *FPN* and NO_3^- support NO_3 adsorption as a likely mechanism for transient storage in the SFGL, which has previously been neglected as a component of fluvial N cycles. Adsorption is defined as the inter-molecular attractive force causing adhesion of an anionic molecule to a positively charged solid surface, e.g., fine sediment particles. Adsorption to fine sediment particles has typically relied on the presence of variably charged sesquioxides, e.g., iron, aluminum, or manganese oxides, that can coat surfaces of permanent, negatively charged clay and silt sized particles (Eick et al., 1999; Hamdi et al., 2013). Sesquioxides typically accumulate in the B soil horizon, i.e., the silty-clay layer, through the process of illuviation, which is prominent in the Inner Bluegrass Region (USDA, 2004). A recent study of physical sediment aggregate composition in the South Elkhorn watershed suggests B horizon soils are a prominent source of fine sediments to the stream channel (having a d_{50} of transported sediments = 20 μm) which reflects soil surveys in the region in which soils are predominantly silty-clay loam (Fox et al., 2014). The high delivery of silty-clay loam soils to the main-stem of the SFGL during high magnitude storm events supports that sesquioxides are prominent in the SFGL during winter to spring. The

presence of sesquioxides coupled with rapid assimilation of NO_3^- in the main stem SFGL provides evidence of in-stream adsorption as a prominent mechanism for FPN and NO_3^- variability during winter-spring. High NO_3^- concentrations (>2 mg L^{-1} N-NO_3) further support prominence of sorption in winter-spring since adsorption capacity of a solid adsorbent (e.g, SFGL) increases with increasing adsorbate (e.g., NO_3^-) concentration (Foo and Hamed, 2010). To our knowledge, no studies have suggested NO_3 sorption as a significant mechanism for DIN storage in stream sediments, highlighting the novelty of the present contribution.

While NO_3^- sorption has been neglected in fluvial systems, studies of NO_3^- sorption in similar agricultural soils, and anion adsorption of other macronutrients in streams, namely phosphorus (P), provide further support of NO_3^- sorption in the SFGL. NO_3 sorption in agricultural soils with pronounced B horizons have only recently been recognized to be a mechanism for temporary NO_3 removal, minimizing the leaching of the pollutant to ground and surface waters (Eick et al., 1999; Hamdi et al., 2013). Research in soils over the past decade has found NO_3 sorption to be most pronounced when anion exchange capacity is high, e.g., low pH, highly weathered soils with the presence of variable charge sesquioxides, and cation exchange capacity is low, such as when humic substances from organic matter are low (Eick et al., 1999; Panuccio et al., 2001; Martinez-Villegas et al., 2004; Donn and Menzies, 2005; Wong and Wittwer, 2009; Hamdi et al., 2013). Analogous to the soil system, the SFGL during winter and spring has similar conditions as evidenced by high delivery of upland hillslope sediments to the SFGL which are low humic soils with sesquioxides. Conversely, in summer and fall when organic carbon content is pronounced due to accrual of algal biomass in the SFGL the sorption mechanism is likely small. Unlike NO_3^-, anion adsorption of phosphate, PO_4^{-3}, has become readily accepted as a mechanism of in-stream fate for reach-scale conceptual models and numerical model of in-stream P cycling (Withers and Jarvie, 2008; Agudelo et al., 2011). P sorption uptake rates, in some instances, have been estimated to outweigh that of algal assimilation (Withers and Jarvie, 2008 and references within). Similarly to soil nitrate sorption, sorption potential of the adsorbent (e.g., SFGL) is dependent upon adsorbate concentration, pH, redox conditions, and OM composition further qualifying the SFGL as a potential site for NO_3 sorption.

Further work is needed to test NO_3^- sorption capacity of SFGL sediments at a process-scale, both in the laboratory and field. While such an undertaking is beyond the scope of this study, we provide compelling evidence that SFGL conditions in winter-spring provide favorable conditions for NO_3^- sorption and should be considered in the conceptual framework for fluvial N cycling. To provide some quantitative evidence of the significance of adsorption as a driving mechanism for transient storage, we provide a back-of-the-envelope estimate of the potential sorption capacity in the main-stem of the SFGL assuming that the 0.2gN $100gSed^{-1}$ increase in 2008, a year in which sorption appears prominent, occurs over a two month span in late-winter, early spring. Our liberal estimate suggests that $8 \cdot 10^3$ μg N m^{-2} h^{-1} could potentially be adsorbed to the SFGL during 2008, which is equivalent to the average rate of biological nitrate uptake measured in agricultural streams during peak production (Mulholland et al., 2008).

The sorption hypothesis proposed herein brings into question the current state of knowledge of N cycling in agriculturally disturbed streams, suggesting a need to reassess N budgets in systems with pronounced SFGL zones and high nutrient levels. Current state of knowledge on N cycling in ag streams only consider biotic processes, i.e., ammonification, assimilation, nitrification, and denitrification, as governing mechanisms for fluvial N cycling, analogous to pristine forested systems where NO_3 concentrations are low and storage is not pronounced (Peterson et al., 2001; Birgand, 2007; Mulholland et al., 2008). Perhaps this has been, in part, an artifact of emphasis being placed on N dynamics in hyporheic dominated stream systems where neutrally charged, porous sand and gravel sized particles are the dominant benthic substrates and sesquioxides will be low relative to SFGL soils (Trimmer et al., 2012). Future assessments of fluvial N budgets in SFGL streams need to consider sorption as a mechanism for transient storage since it has significant implications for nitrogen removal via temporary sequestration, permanent removal through denitrification and nutrient availability to biota.

6.6 CONCLUSIONS

Results of the statistical time-series analysis for the eight year ambient measurements of sediment N agree with existing stream N theory during late-spring

through fall when algal OM dynamics control SFGL composition and disagree in winter through mid-spring stemming from the abiotic adsorption of NO_3 to variably charged mineral coatings on deposited sediments from the uplands. While results suggest that adsorption rates have the potential to be on the same order of magnitude as uptake rates, process based models are needed to help constrain these estimates and provide ranges over years with varying levels of adsorption. The significance of the previously unrecognized transient storage zone is recognized in that it has the potential to promote permanent removal *via* heterotrophic denitrification and biotic assimilation under supply limited periods and it provides controlled release of NO_3 to downstream water bodies, which is significant under high loading conditions. While our findings potentially suggest a paradigm shift in stream-N theory for low-gradient, ag-disturbed streams, further work is needed in other SFGL dominated systems to support or refute the hypothesis proposed herein and bench-scale experiments are needed to test adsorption isotherms in the laboratory utilizing SFGL sediments during the specified timeframes.

6.7 REFERENCES

Agudelo, S.C., Nelson, N.O., Barnes, P.L., Keane, T.D., Pierzynski, G.M. 2011. Phophorus adsorption and desorption potential of stream sediment and field soils in agricultural watersheds. J. Environ Quality. 40:144-152.

Akamatsu, F., Konayashi, S., Amano, K., Nakanishi, S., Oshima, Y., 2011. Longitudinal and seasonal changes in the origin and quality of transported particulate organic matter along a gravel-bed river. Hydrobiologia, 669, 183-197.

Alexander, R.B., Smith, R.A., Schwarz, G.E., Boyer, E.W., Nolan, J.V., Brakebill, J.W., 2008. Differences in phosphorus and nitrogen delivery to the Gulf of Mexico from the Mississippi River Basin. Evironmental Science and Technology, 42, 822-830.

Arango, C.P., Tank, J.L., 2008. Land use influences the spatiotemporal controls on nitrification and denitrification in headwater streams. J.N. Am. Benthol. Soc., 27(1), 90-107.

Arango, C.P., Tank, J.L., Schaller, J.L., Royer, T.V., Bernot, M.J., David, M.B., 2007. Benthic organic carbon influences denitrification in streams with high nitrate concentration. Freshw. Biol., 52, 1210-1222.

Baker, D.W., Bledsoe, B.P., Price, J.M. 2012. Stream nitrate uptake and transient storage over a gradient of geomorphic complexity, north-central Colorado, USA. *Hydrological Processes*. 26: 3241-3252.

Battin TJ, Kaplan LA, Newbold JD, Hansen CME. 2003. Contributions of microbial biofilms to ecosystem processes in stream mesocosms. *Nature* 426: 440-442.

Bernhardt ES, Likens GE, Hall RO Jr, Buso DC, Fisher SG, Burton TM, Meyer JL, McDowell WH, Mayer MS, Bowden WB, Findlay SEG, MacNeale KH, Steltzer RS, Lowe WH. 2005. Can't see the forest for the stream? In-stream processing and terrestrial nitrogen exports. BioScience 55:219–230.

Birgand F.; Skaggs, R. W.; Chescheir, G. M.; Gilliam, J. W. Nitrogen removal in streams of agricultural catchments—a literature review. *Critical Reviews in Environmental Science and Technology*. 2007, 37, 381-487.

Butturini A, Battin TJ, Sabater F. 1999. Nitrification in stream sediment biofilms: the role of ammonium concentration and DOC quality. *Water Research*, 34(2): 629-639.

Coplen, T.B., Qi, Haiping, Révész, Kinga, Casciotti, Karen, and Hannon, J.E., 2012, Determination of the $\boldsymbol{\delta}^{15}$N and $\boldsymbol{\delta}^{18}$O of nitrate in water; RSIL lab code 2900, chap. 17 ***of*** Stable isotope-ratio methods, sec. C ***of*** Révész, Kinga, and Coplen, T.B. eds., Methods of the Reston Stable Isotope Laboratory (slightly revised from version 1.0 released in 2007): U.S. Geological Survey Techniques and Methods, book 10, 35 p., available only at http://pubs.usgs.gov/tm/2006/tm10c17/. (Supersedes version 1.0 released in 2007.)

Dodds, W., Smith, V., Lohman, K., 2002. Nitrogen and phosphorus relationships to benthic algal biomass in temperate streams. Canadian Journals of Fisheries and Aquatic Sciences, 59, 865-874.

Donn, M.J., Menzies, N.W. 2005. Simulated rainwater effects on anion exchange capacity and nitrate retention in Ferrosols. *Australian Journal of Soil Research*. 43: 33-42.

Droppo I, Stone M. 1994. In-channel surficial fine grained sediment lamina. Part I: Physical Characteristics and formational processes. *Hydrological Processes* 8:101-111

Droppo, I.G., Lau, Y.L., Mitchell C. 2001. The effect of depositional history on contaminated bed sediment stability. Science of the Total Environment. 266: 7-13.

Eick, M.J., Brady, W.D., Lynch, C.K. 1999. Charge properties and nitrate adsorption of some acid southeastern soils. *J Environ. Qual*. 28: 138-144.

Findlay, S.E.G., Mulholland, P.J., Hamilton, S.K., Tank, J.L., Bernot, M.J., Burgin, A.J., Crenshaw, C.L., Dodds, W.K., Grimm, N.B., McDowell, W.H., Potter J.D., Sobota, D.J., 2011. Cross-stream comparison of substrate-specific denitrification potential. Biogeochemistry, 104, 381-392.

Foo, K.Y., Hamed, B.H. 2010. Insights into the modeling of adsorption isotherm systems. *Chemical Engineering Journal*. 156: 2-10.

Ford, W.I., Fox, J.F., 2014a. Model of particulate organic carbon transport in an agriculturally impacted stream. Hydrol. Process., 28(5), DOI: 10.1002/hyp.9569

Fox J, Davis C, Martin D. 2010. Sediment source assessment in a lowland watershed using nitrogen stable isotopes. *Journal of American Water Resources Association* 46:1192-1204.

Fox, J., Ford, W., Strom, K., Villarini, G., Meehan, M., 2013. Benthic control upon the morphology of transported fine sediments in a low-gradient stream. Hydrological Processes, doi: 10.1002/hyp.9928.

Fox, J.F., Papanicolaou, A.N. 2007. The use of carbon and nitrogen isotopes to study watershed erosion processes. *Journal of American Water Resources Association*. 43(4): 1047-1064.

Freedman, D., Diaconis, P., 1981. On the histogram as a density estimator: L_2 theory. Z. Wahrscheinlichkeitstheorie verw. Gebiete, 57, 453-476.

French C, Rock L, Nolan K, Tobin J, Morrisey A. 2012. The potential for a suite of isotope and chemical markers to differentiate sources of nitrate contamination: A review. *Water Research* 46: 2023-2041.

Galloway, J. N.; Townsend, A. R.; Erisman J. W.; Bekunda, M.; Cai, Z.; Freney, J. R.; Martinelli, L. A.; Seitzinger, S. P.; Sutton, M. A. Transformation of the nitrogen cycle: recent trends, questions, and potential solutions. *Science.* 2008, 320, 889-892.

Godwin, C.M., Arthur, M.A., Carrick, H.J. 2009. Periphyton nutrient status in a temperate stream with mixed land-uses: implication for watershed nitrogen storage. *Hydrobiologia*. 623: 141-152.

Griffiths, N.A., Tank, J.L., Royer, T.V., Warrner, T.J., Frauendorf, T.C., Rosi-Marshall, E.J., Whiles, M.R., 2012. Temporal variation in organic carbon spiraling in Midwestern agricultural streams. Biogeochemistry, 108, 149-169.

Gu, C., Hornberger, G.M., Mills, A.L., Herman, J.S., Flewelling, S.A. 2007. Nitrate reduction in streambed sediments: effects of flow and biogeochemical kinetics. *Water Resources Research*. 43: W12413.

Hamdi, W., Gamaoun, F., Pelster, D.E., Seffen, M. 2013. Nitrate sorption in an agricultural soil profile. *Applied and Environmental Soil Science,* 1-7.

Hantush, M.M. 2007. Modeling nitrogen-carbon cycling and oxygen consumption in bottom sediments. *Advances in Water Resources*. 30: 59-79.

Harvey, J.W., Bohlke, J.K., Voytek, M.A., Scott, D., Tobias, C.R. 2013. Hyporheic zone denitrification: Controls on effective reaction depth and contribution to whole-stream mass balance. *Water Resources Research*. 49: 6298-6316.

Huang, N.E., Shen, Z., Long, S.R., Wu, M.C., Shih, H.H., Zheng, Q., Yen, N., Tung, C.C., Liu, H.H. 1998. The empirical mode decomposition and the Hilbert spectrumfor nonlinear and non-stationary time series analysis. *Proceedings: Mathematical, Physical and Engineering Sciences*. 454(1971): 903-995.

Kendall, C., Silva, S.R., Kelly, V.J. 2001. Carbon and nitrogen isotopic compositions of particulate organic matter in four large river systems across the United States. Hydrological Processes, 15, 1301-1346, DOI: 10.1002/hyp.216.

Kendall, C., Elliott, E.M., and Wankel, S.D., 2007. Tracing anthropogenic inputs of nitrogen to ecosystems, Chapter 12, In: R.H. Michener and K. Lajtha (Eds.), Stable Isotopes in Ecology and Environmental Science, 2nd edition, Blackwell Publishing, p. 375-449.

Machiwal, D., Jha, M.K. 2012. Hydrologic Time Series Analysis: Theory and Practice. Springer.

Martinez-Villegas, N., Flores-Velez, L.Ma., Dominguez, O. 2004. Sorption of lead in soil as a function of pH: a study case in Mexico. *Chemosphere*. 57:1537-1542.

Mulholland P, Helton A, Poole G, Hall R, Hamilton S, Peterson B, Tank J, Ashkenas L, Cooper L, Dahm C, Dodds W, Findlay S, Gregory S, Grimm N, Johnson S, McDowell W, Meyer J, Valett H, Webster J, Arango C, Beaulieu J, Bernot M, Burgin A, Crenshaw C, Johnson L, Niederlehner B, O'Brien J, Potter J, Sheibley R, Sobota D, Thomas S. Stream denitrification across biomes and its response to anthropogenic nitrate loading. *Nature* 452:202-206.

Murdock, L., Ritchey, E. 2012. Lime and Nutrient Recommendations 2012-2013. Cooperative Extensive Service- UK College of Ag.

Newcomer, T.A., Kaushal, S.S., Mayer, P.M., Shields A.R., Canuel, E.A., Groffman, P.M., Gold, A.J., 2012. Influence of novel organic carbon sources on denitrification in forest, degraded urban and restored streams. Ecol. Monogr., 82(4), 449-466.

Panuccio, M.R., Muscolo, A., Nardi, S. 2001. Effect of humic substances on nitrogen uptake and assimilation in two species of pinus. *Journal of Plant Nutrition*. 24(4-5): 693-704.

Peterson, B.J., W.M. Wollheim, P.J. Mulholland, J.R. Webster, J.L. Meyer, J.L. Tank, E. Marto˜, W.B. Bowden, H.M. Valett, A.E. Hershey, W.H. McDowell, W.K. Dodds, S.K. Hamilton, S. Gregory, and D.D. Morrall, 2001. Control of Nitrogen Export From Watersheds by Headwater Streams. Science 292(5514):86-90.

Phillips J, Russell M, Walling D. 2000. Time-integrated sampling of fluvial suspended sediment: a simple methodology for small catchments. *Hydrological Processes* 14:2589-2602.

Rato, R.T., Ortigueira, M.D., Batista, A.G. 2008. On the HHT, its problems, and some solutions. *Mechanical Systems and Signal Processing*. 22: 1374-1394.

Russo J, Fox J. 2012. The role of the surface fine-grained laminae in low-gradient streams: A model approach. *Geomorphology* In press. DOI: 10.1016/j.geomorph.2012.05.012

Rutherford, J., Scarsbrook, M., Broekhuizen, N., 2000. Grazer control of stream algae: modeling temperature and flood effects. J. Environ. Eng., 126, 331–339.

Sebestyen, S.D., Shanley, J.B., Boyer, E.W., Kendall, C., Doctor, D.H. 2014. Coupled hydrological and biogeochemical processes controlling variability of nitrogen species in streamflow during autumn in an upland forest. *Water Resources Research*. In Press.

Seitzinger, S.P., J.A. Harrison, J.K. Bo¨hlke, A.F. Bouwman, R. Lowrance, B. Peterson, C. Tobias, and G. Van Drecht, 2006. Denitrification Across Landscapes and Waterscapes: A Synthesis. Ecological Applications 16:2064-2090.

Seitzinger, S. 2008. Out of reach. *Nature*, 45:162-163.

Trimmer, M., Grey, J., Heppell, C.M., Hildrew A.G., Lansdown, K., Stahl, H., Yvon-Durocher, G., 2012. River bed carbon and nitrogen cycling: State of play and some new directions. Sci. Total Environ., DOI: 10.1016/j.scitotenv.2011.10.074

Turlan, T., Birgand F., Marmonier, P. 2007. Comparative use of field and laboratory mesocosms for in-stream nitrate uptake measurement. *Ann. Limnol.-Int J. Lim.* 43(1): 41-51.

USDA. 2004. Soil Survey of Warren County, Kentucky.

Verardo, D.J., Froelich, P.N., McIntyre, A. 1990. Determination of organic carbon and nitrogen in marine sediments using the Carlo Erba NA-1500 Analyzer. *Deep-Sea Research*. 37 (1): 157-165.

Walling D, Collins A, Jones P, Leeks G, Old G. 2006. Establishing fine-grained sediment budgets for the Pang and Lambourn LOCAR catchments. *Journal of Hydrology* 330:126-141.

White P, Kalff J, Rasmussen J, Gasol J. 1991. The effect of temperature and algal biomass on bacterial production and specific growth rate in freshwater and marine habitats. *Microbial Ecology* 21:99-118.

Withers, P.J.A., Jarvie, H.P. 2008. Delivery and cycling of phosphorus in rivers: A review. *Science of the Total Environment*. 379-395.

Wong, M.T.F., Wittwer, K. 2009. Positive charge discovered across Western Australian wheatbelt soils challenges key soil and nitrogen management assumptions. *Australian Journal of Soil Research*. 47:127-135.

Wu, Z., Huang, N.E. 2004. A study of the characteristics of white noise using the empirical mode decomposition method.

Wu, Z., Huang, N.E., Peng, C. 2007. On the trend, detrending, and variability of nonlinear and nonstationary time series. *Proceedings of the National Academy of Sciences*. 104(38): 14889-14894.

Xue D, Botte J, Baets BD, Accoe F, Nestler A, Taylor P, Cleemput OV, Berglund M, Boechkx P. 2009. Present limitations and future prospects of stable isotope methods for nitrate source identification in surface- and groundwater. *Water Research* 43: 1159-1170.

Zahraeifard, V, Deng Z, Malone R. 2014. Modelling spatial variations in dissolved oxygen in fine-grained streams under uncertainty. *Hydrological Processes,* In Press.

Zarnetske, J.P., Haggerty, R., Wondzell, S.M., Baker, M.A. 2011. Dynamics of nitrate production and removal as a function of residence time in the hyporheic zone. *Journal of Geophysical Research*. 116: G01025.

Zarnetske, J.P., Haggerty, R., Wondzell, S.M., Bokil, V.A., Gonzalez-Pinzon, R. 2012. Coupled transport and reaction kinetics control the nitrate source-sink function of hyporheic zones. *Water Resources Research*. 48: W11508.

6.8 TABLES AND FIGURES

Table 1. Dissolved DIN, in terms of NO_3-N, collected in the South Elkhorn watershed from September 2012 through November 2013. Data was collected under a range of flow conditions. N is in mgN L^{-1} and isotope signatures are in ‰.

Date	Flow Regime[1]	MS-1			MS-2			SU			SA			TU-1			TU-2			TA-1			TA-2		
		N	δ15N	δ18O	N	δ15N	δ18O	N	δ15N	δ18O	N	δ15N	δ18O	N	δ15N	δ18O	N	δ15N	δ18O	N	δ15N	δ18O	N	δ15N	δ18O
9/18/2012	Moderate	1.0	8.9	8.1	1.1	9.0	10.2							0.6	7.8	30.0				1.3	9.7	7.7			
10/23/2012	Low	0.3	12.2		0.5	11.4								1.4	7.4	-1.8				0.7	11.0				
11/13/2012	Low	0.2	7.8	4.0	0.7	7.9	2.9							1.2	7.1	5.7				1.6	8.0	3.4			
12/20/2012	High	0.8	6.0	2.5	0.5	5.6	2.8							0.4	5.5	8.0				2.4	3.7	4.0			
12/21/2012	High	1.3	4.5	0.2	2.6	5.0	3.4							2.2	6.3	1.4				2.8	3.1	3.0			
2/20/2013	Low	2.4	8.9	7.9	2.6	9.6	8.1							2.3	7.4	8.4				5.5	7.1	6.2			
3/25/2013	High	3.0	6.1	3.2	3.1	6.0	3.3	2.6	7.0	5.0	3.3	4.1	6.2	2.7	3.6	1.4	1.3	6.0	16.0	5.9	5.3	4.0	4.8	10.8	4.8
4/22/2013	Moderate	3.2	6.0	5.7	3.3	3.3	1.7							2.8	4.9	5.7				5.9	2.8	3.6			
5/28/2013	Low	2.1	9.2	7.0	1.9	8.8	5.1	1.9	10.3	9.3	1.8	9.9	10.7	1.9	6.0	2.0	1.8	10.1	7.3	2.7	8.0	8.6	2.4	7.5	7.6
7/1/2013	Moderate				2.7	11.6	12.3							2.9	14.2	16.5				4.9	6.4	7.0			
7/29/2013	Low	2.7	7.9	5.8	2.7	9.0	7.4	2.7	8.7	3.8	2.5	7.9	3.2	2.6	7.4	6.2	2.2	10.9	8.8	2.9	6.5	8.0	2.7	8.2	8.0
9/6/2013	Low	2.3	8.1	5.6	2.3	6.8	0.9							2.6	6.7	4.3				3.6	6.2	5.0			
10/16/2013	Low	2.5	9.5	7.2	2.3	8.8	3.7							2.8	8.6	7.5				3.7	5.2	4.8			
11/11/2013	Low	2.9	5.9	2.5	3.1	8.0	4.9	2.4	7.7	3.2	3.5	7.1	3.1	2.5	7.1	6.1	1.8	8.1	4.5	5.0	4.1	2.0	3.4	3.7	1.9

[1]Low flows denote a Q<1 cms, moderate flows denote a 1cms< Q< 2.5cms, and high flows denote a Q>2.5 cms.

Table 2. Chemical and isotopic signatures of sediment sources. Values are reported as an average ± standard deviation of the data.

Chemical Signature	Benthic Algae (n=12)	Banks (n=15)	Ag Tributary (n=11)	Urban Tributary (n=9)
FPOC (gC 100gsed^{-1})	27.9 ± 7.12	1.61 ± 0.29	4.69± 0.87	3.99 ± 0.59
FPN (gN 100gsed^{-1})	2.45 ± 1.11	0.18 ± 0.03	0.41 ± 0.05	0.30 ± 0.05
C:N	12.4 ± 3.48	10.3 ± 0.39	11.9 ± 0.70	13.26 ± 0.97
$\delta^{13}C$ (‰)	-37.8 ± 5.50	-25.0 ± 0.64	-28.0 ± 0.23	-26.9 ± 0.51
$\delta^{15}N$ (‰)	4.95 ± 1.60	6.85 ± 0.51	4.75 ± 0.28	3.26 ± 0.92

Table 3. Linear covariance analysis for chemical signatures at MS-1 and MS-2. Values represent coefficient of determination (R^2) assuming linear covariance.

MS-1	***FPOC***	***FPN***	***C:N***	***$\delta^{13}C$***	***$\delta^{15}N$***
FPOC	1				
FPN	0.79	1			
C:N	0.01	0.15	1		
$\delta^{13}C$	0.28	0.26	0.05	1	
$\delta^{15}N$	0.01	0.00	0.03	0.02	1
MS-2	***FPOC***	***FPN***	***C:N***	***$\delta^{13}C$***	***$\delta^{15}N$***
FPOC	1				
FPN	0.81	1			
C:N	0.00	0.06	1		
$\delta^{13}C$	0.10	0.10	0.01	1	
$\delta^{15}N$	0.10	0.03	0.08	0.01	1

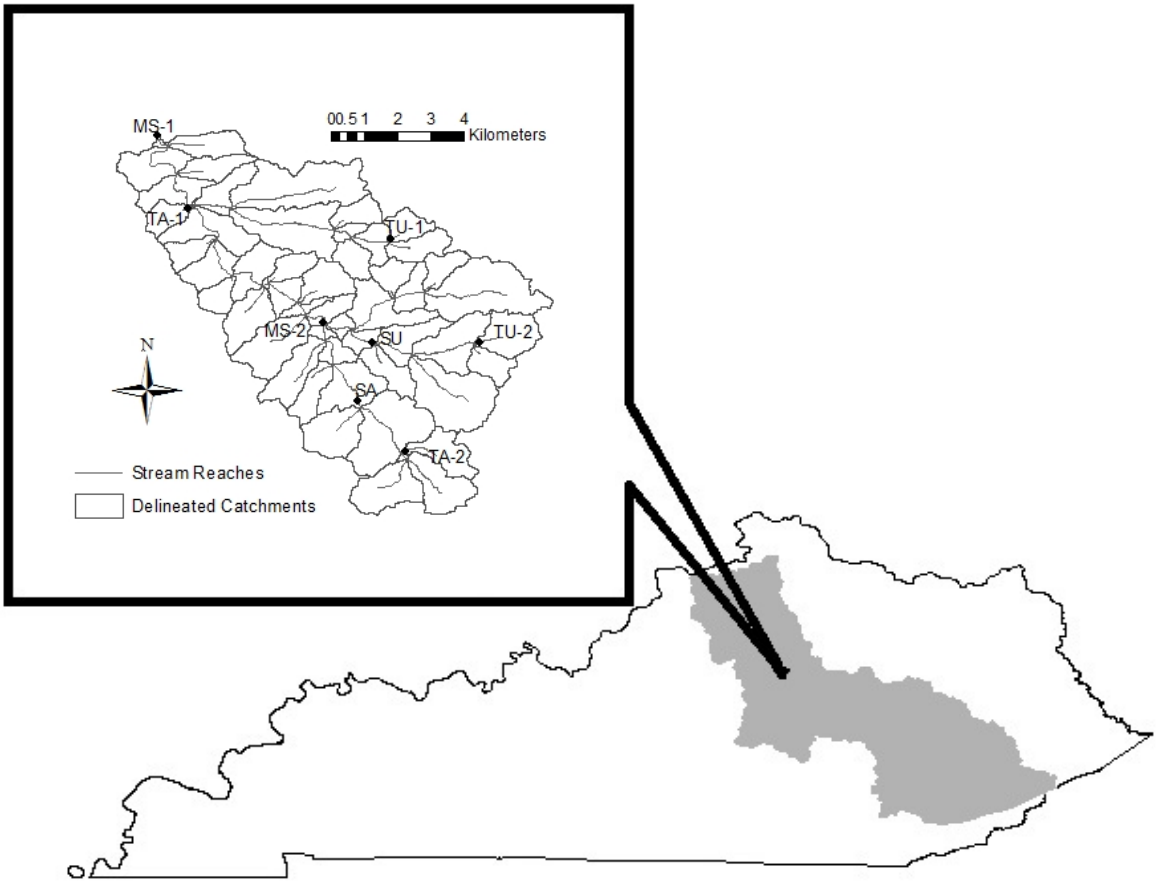

Figure 1. South Elkhorn watershed, located in the Bluegrass Region of Central Kentucky. Map displays watershed boundaries, tributary-scale delineation, stream network, and site identifiers for monitored sites.

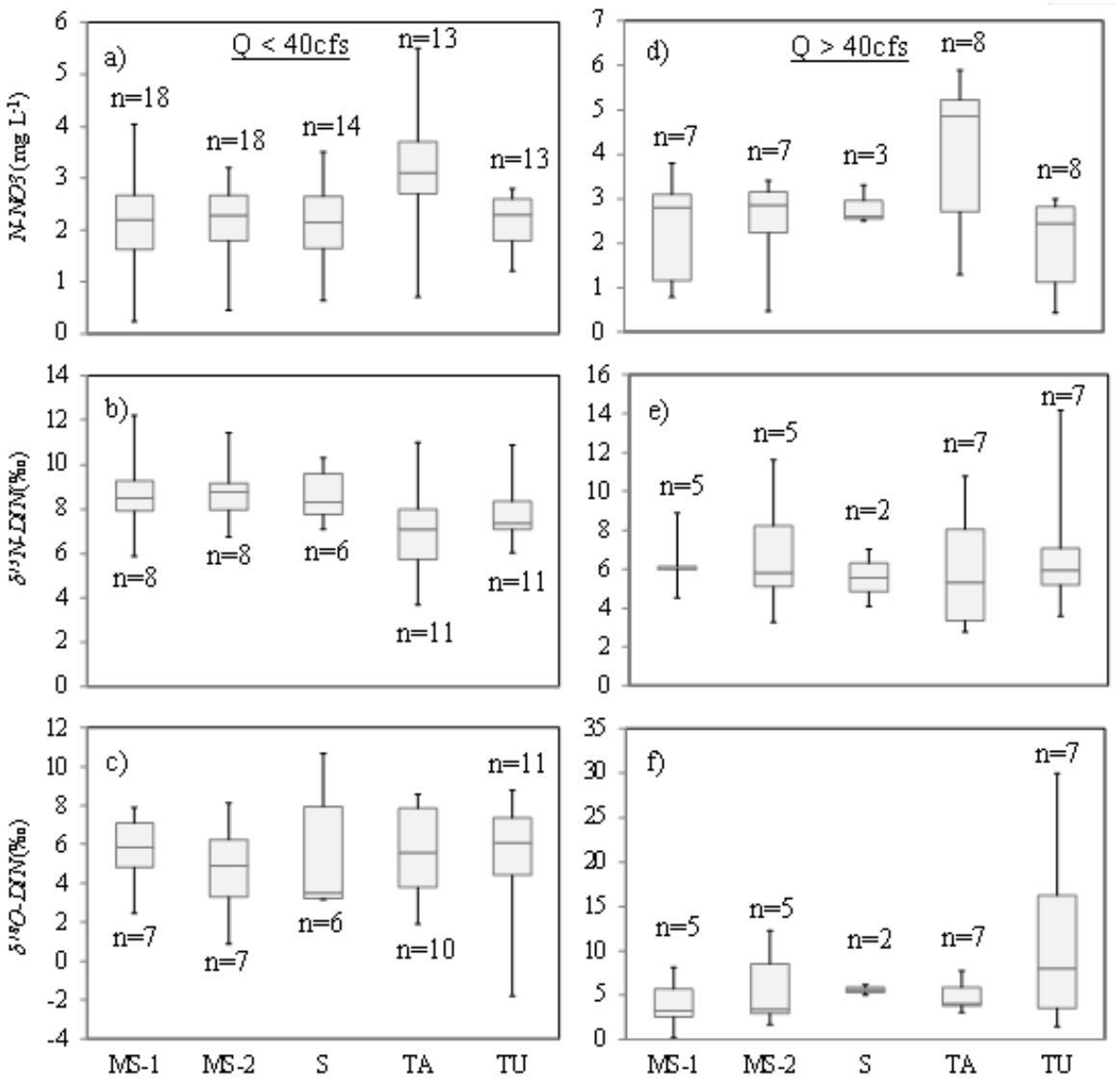

Figure 2. Box and whisker plots displaying spatial variability of NO_3 concentrations and isotopic signatures at tributary and main-stem monitoring sites in the South Elkhorn watershed. Plots on the left (a-c) represent base-flow condtions (Q<40 cfs) while plots on the right (d-f) represent high flow conditions (Q>40cfs).

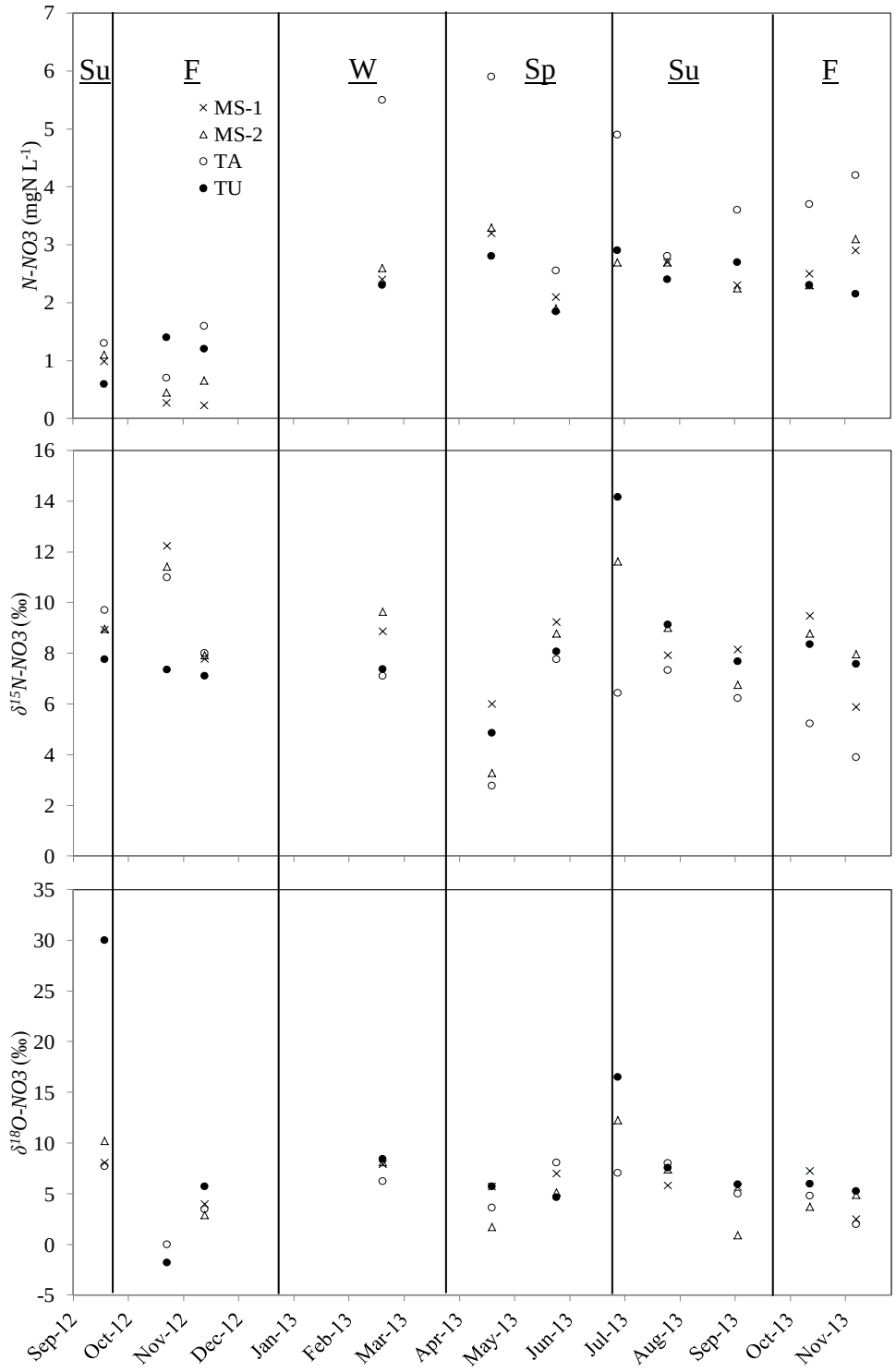

Figure 3. Spatial variability of DIN during individual sampling periods at low flows. Su = Summer, F = Fall, W=Winter, Sp=Spring.

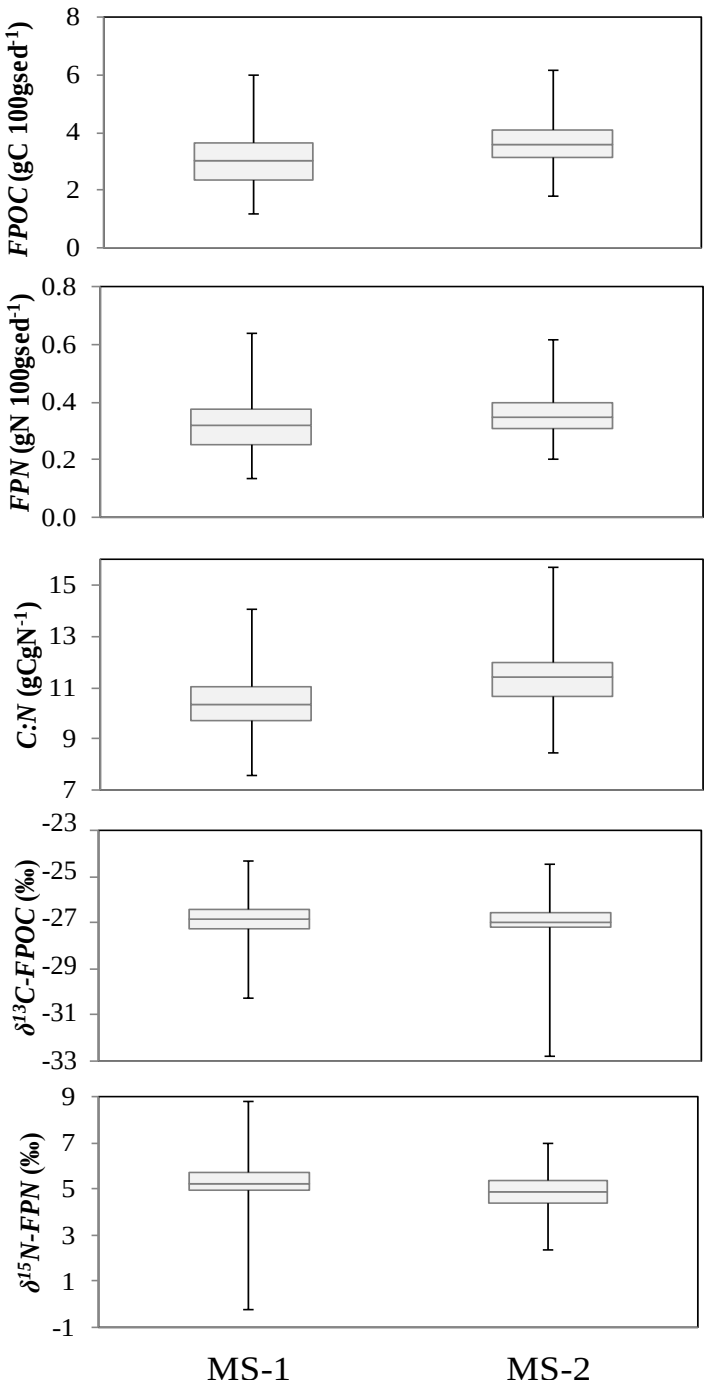

Figure 4. Box and whisker plots displaying spatial variability of sediment sources of FPOC (a), FPN (b), C:N (c), δ13C (d), and δ15N (e). Tributary sediment samples weren't included since measurements only encompass a six month timeframe (hence seasonal variability is not captured).

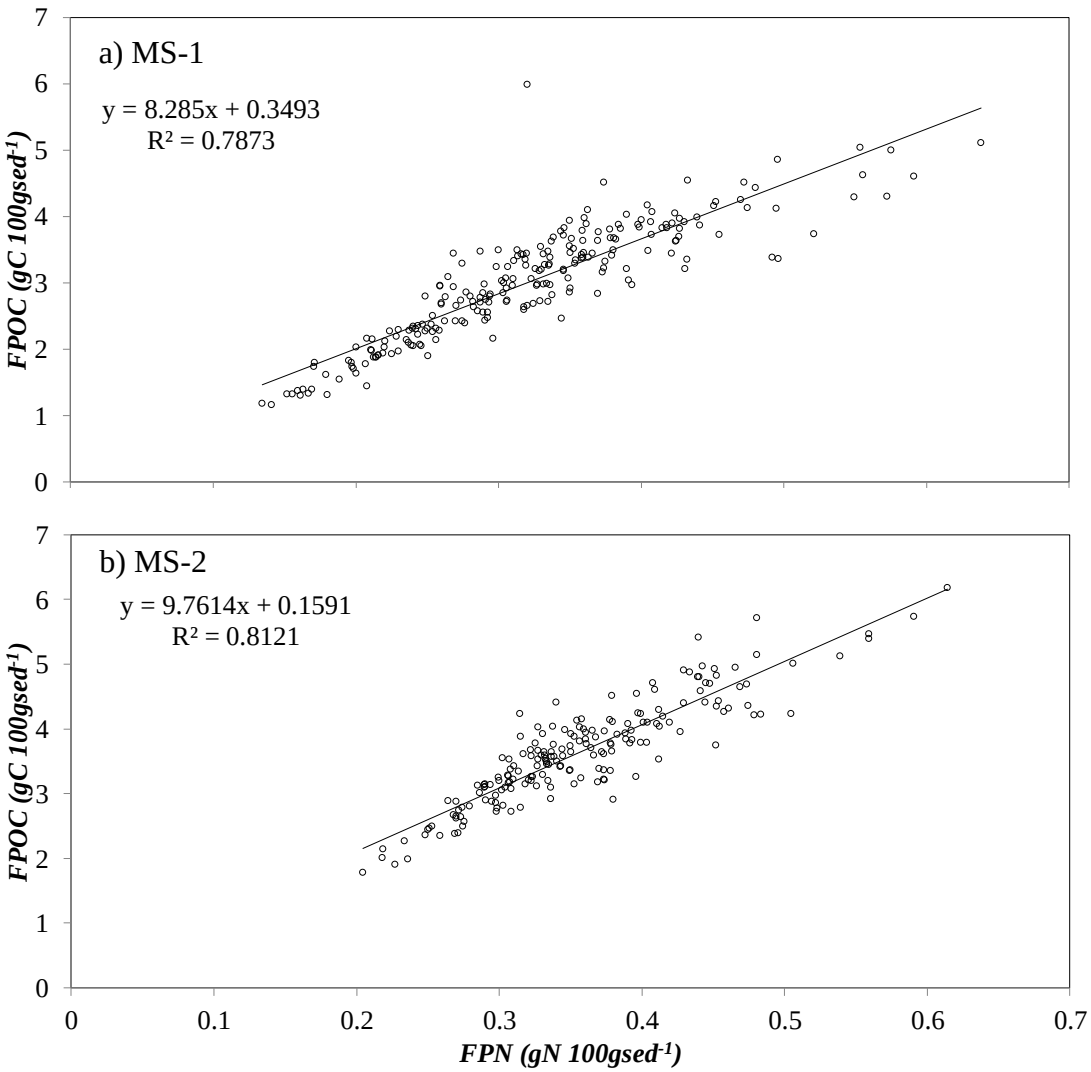

Figure 5. Scatterplots of FPOC as a function of FPN at (a) MS-1 and (b) MS-1. Results show positive linear covariance between the two chemical signatures at both sites. Further, results show increasing error/deviation from the linear trend with increasing values.

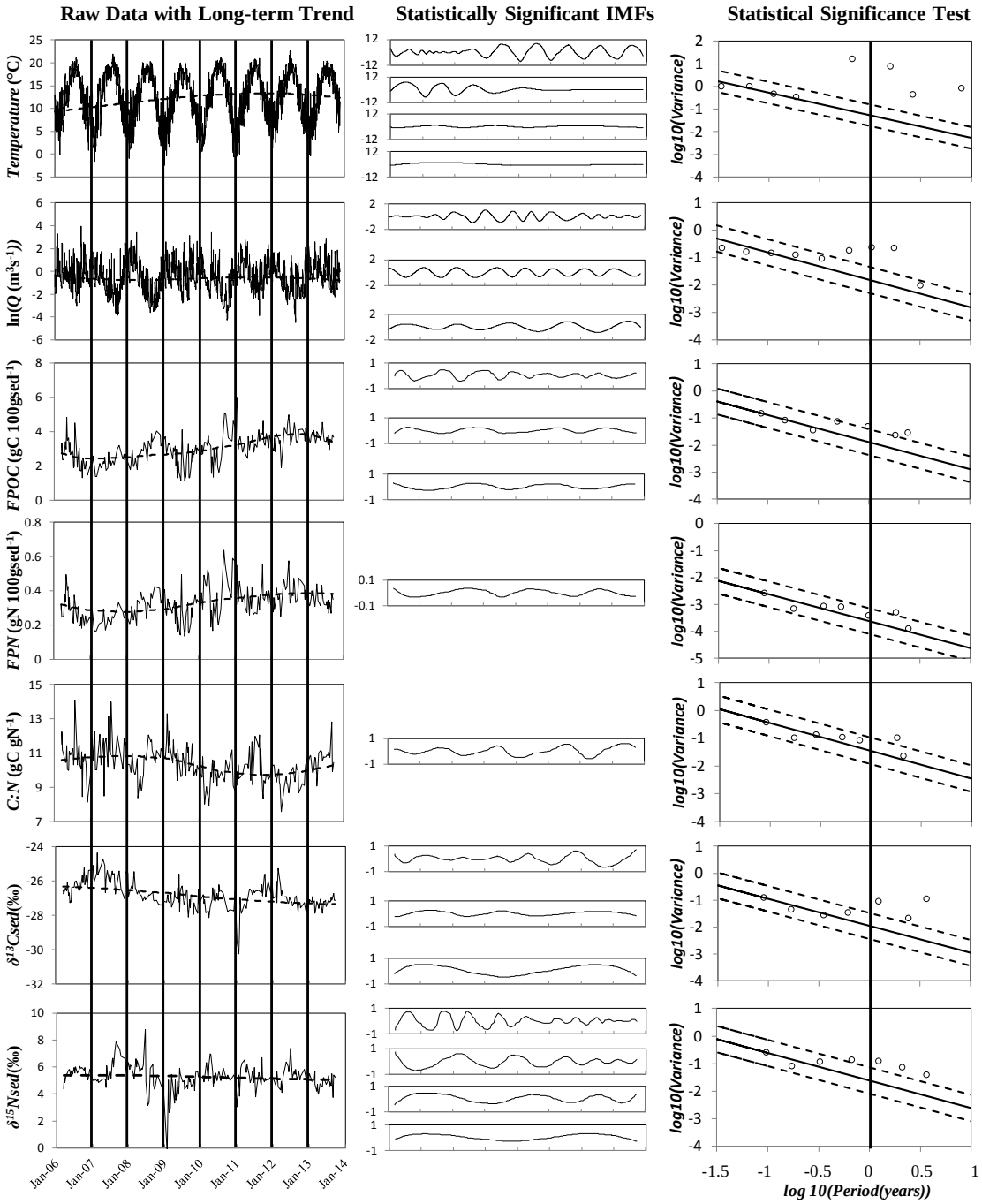

Figure 6. Eight year timeseries of sediment nitrogen and potential explanatory variables (FPOC, d13Csed, and log transformed flowrate) at site MS-1, statistically significant IMFs from the EMD analysis, and the statistical significance test.

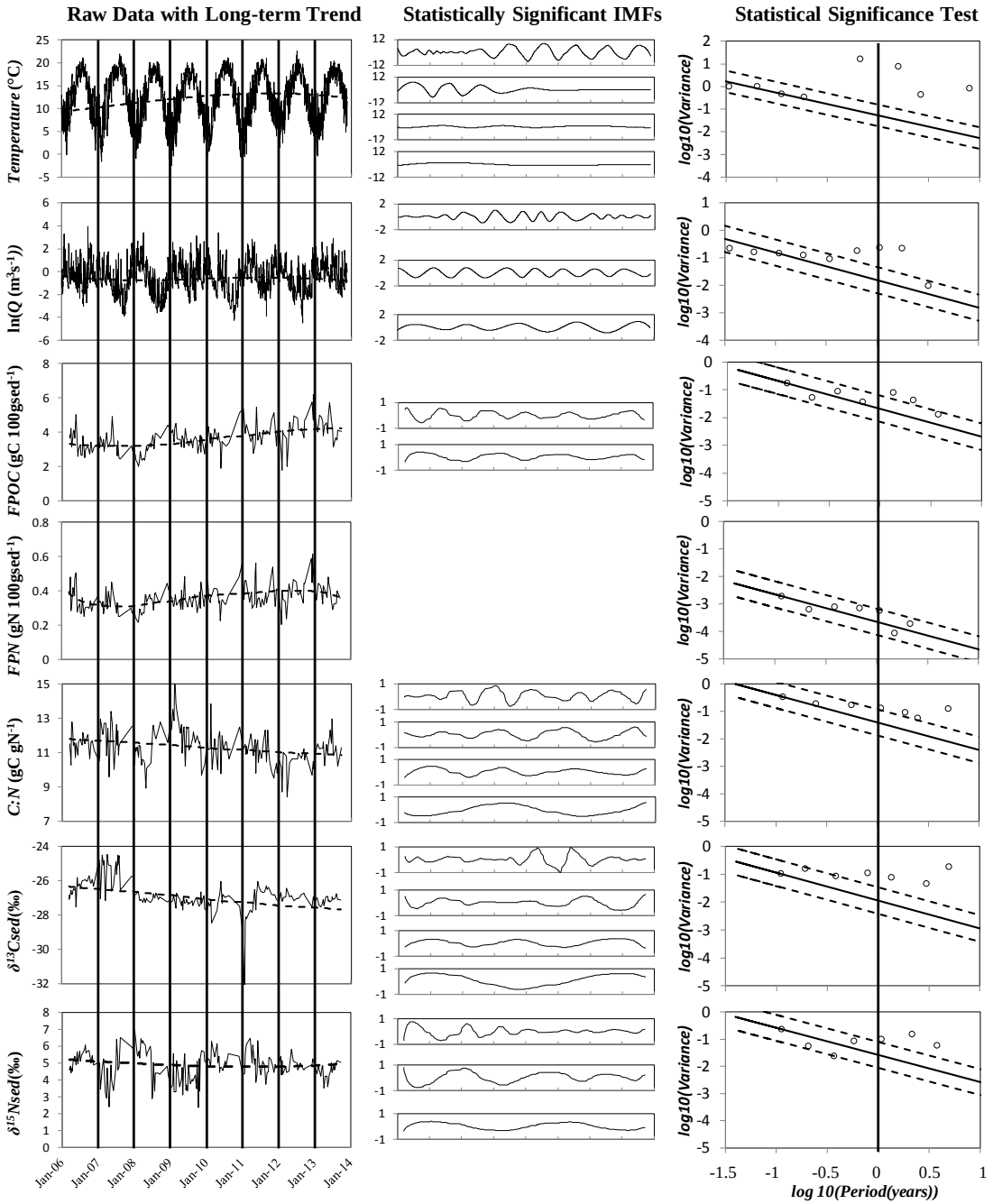

Figure 7. Eight year timeseries of sediment nitrogen and potential explanatory variables (FPOC, d13Csed, and log transformed flowrate) at site MS-2, statistically significant IMFs from the EMD analysis, and the statistical significance test.

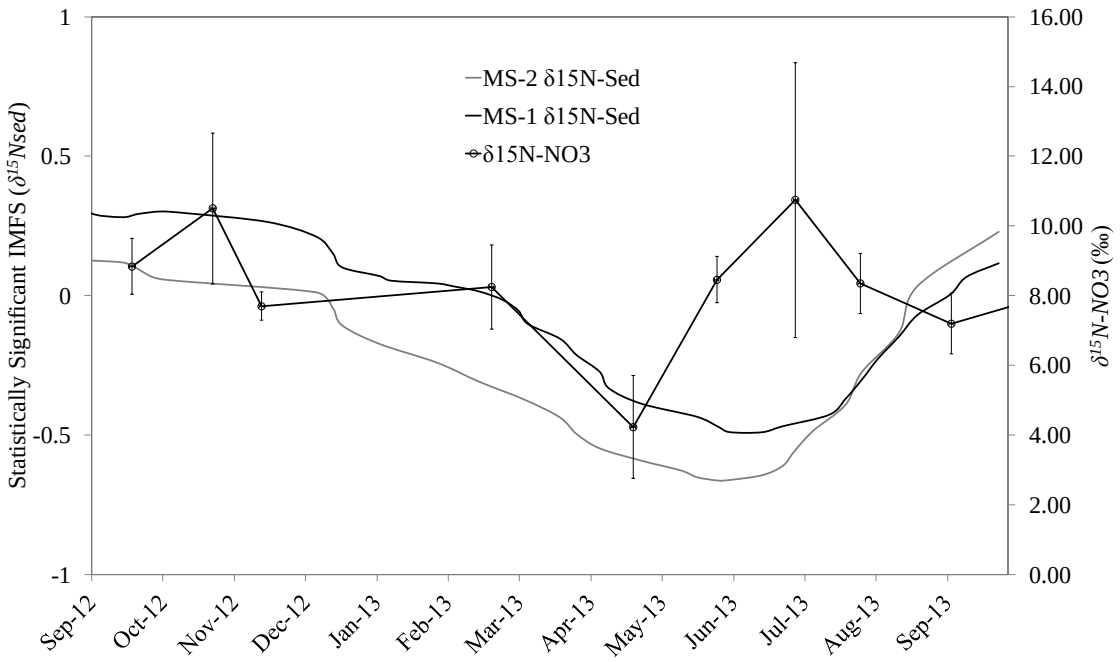

Figure 8. Overlapping streamwater and sediment N data from September 2012 through October 2013 is displayed. The sum of statistically significant IMFs for $\delta^{15}N_{Sed}$ are plotted on the left y-axis for sites MS-1 and MS-2 and the average $\delta^{15}N_{NO3}$ signature is plotted on the right y-axis with standard deviations. Results show that multipeak oscillations of the streambed source are governed by the DIN source. The spatially averaged $\delta^{15}N_{NO3}$ signatures shown in Figure 4 were plotted against statistically significant IMFs for $\delta^{15}N_{FPN}$ for both MS-1 and MS-2 for the one year of overlapping data collection.

Copyright © William Isaac Ford III 2014

Chapter 7: Development an SFGL Nitrogen Model to Simulate the Fluvial Nitrogen Budget: TRANSFER

7.1 SUMMARY

To improve water quality modeling technology for in-stream N in systems characterized by a thin flocculent, advection dominated, sediment layer (i.e., the SFGL) we introduce TRANSFER (Technology for Removable Annual Nitrogen in Streams for Ecosystem Restoration). The objective of the present study was to evaluate the efficacy of elemental and stable isotope routines in TRANSFER to constrain uncertainty surrounding the fluvial N budget. Transported measures of fine particulate nitrogen (FPN) are utilized as the response variable in the model due to its sensitivity to reflect biotic processes and source signatures, and its efficacy at integrating in-stream processes. Eight years of transported FPN data was collected at the watershed outlet of a low-gradient SFGL dominated stream utilizing temporally and spatially integrated sediment trap samples. Samples were analyzed for FPN content, C_{FPN}, and the isotopic signature $\delta^{15}N_{FPN.}$ Results of the study suggest that C_{FPN} is sensitive to the C:N ratio of algal biomass, NH_4 concentrations in the surface water are sensitive to nitrification rates and NO_3 concentrations are sensitive to denitrification rates suggesting that the tight coupling of the C and N processes in TRANSFER promote a unique calibration for the fluvial N cycle. Further, $\delta^{15}N_{FPN}$ was found to be most sensitive to the isotopic signature of NO_3 in the surface water which suggests that TRANSFER has the potential to constrain in-stream processes while also apportioning sources of dissolved constituents providing a more comprehensive assessment of the watershed scale fluvial N budget. Results of the average annual nitrogen budget suggest that approximately 11% of inflowing DIN is removed through transient and permanent DIN removal pathways. Notwithstanding the significance of the findings, further work is needed to evaluate the transferability of the approach to other stream systems and to test the impact of previously neglected stream N processes on the fluvial N budget.

7.2 INTRODUCTION

Dissolved inorganic nitrogen (DIN) concentrations of streamwater runoff from agriculturally impacted and urban watershed systems is well recognized as an environmental concern with regard to hypoxia and anoxia of rivers, lakes and estuaries, prompting new regulations and on-going debate regarding DIN reduction methods (Galloway et al., 2008; Seitzinger, 2008; Conley et al., 2009). Agricultural and urban systems often occur in lowland settings, characterized by mild watershed and stream gradients that cause significant storage of sediments in the stream channel and development of a thin aerobic biological layer known as the surficial fine-grained lamina (Droppo and Stone, 1994; Walling et al., 2006; Fox et al., 2010). In turn, increased fine sediments and sediment carbon in the SFGL has been shown to increase nitrogen (N) transformations, including assimilation by biota and nitrification and denitrification rates (Birgand, 2007; Arango and Tank, 2008; Mulholland et al., 2008). The latter evidence supports the concept of a negative feedback mechanism whereby increased DIN loading gives way to decreasing fluxes relative to DIN inputs, e.g. increased transformations, implying that sediments in disturbed stream systems can variably attenuate inputs of N pollution. While the general behavior of N cycling in agriculturally- and urban-impacted stream systems is generally understood, quantifying DIN transport, transformation and removal has remained a difficult task. There remains a need to provide advancement in methods and models to study in-stream nitrogen fate and transport that are validated by long-term *in situ* studies of the annual stream nitrogen budget (Birgand, 2007; Trimmer et al., 2012).

The pools and biological reactions governing fate and transport of reactive N in stream ecosystems have been studied extensively across landuse gradients (Peterson et al., 2001; Bernhardt et al., 2005; Arango and Tank, 2008; Mulholland et al., 2008). The primary pools of active nitrogen in the stream include nitrate (NO_3^-) and ammonium (NH_4^+) in streamwater, sediment nitrogen (SN) in the streambed associated with microbial biomass, detritus and organic matter from eroded soils, and NO_3^- and NH_4^+ in the streambed. In streams, nitrite, NO_2, is transient and is quickly oxidized to NO_3 by nitrite oxidizing bacteria. DIN is exchanged between streambed sediments and the

overlying streamwater. NH_4^+ and NO_3^- enter the stream from the land surface and are transported downstream as DIN. DIN is taken up by microorganisms in the bed *via* biological assimilation, and ammonium is transferred to nitrate *via* direct nitrification. Regeneration is the release of DIN back to the streamwater and is the result of mineralization, whereby released DIN is either recycled or transported downstream. DIN is removed from the system *via* denitrification in anoxic sediments and transport of eroded organic nitrogen from the streambed.

Nitrogen research in agricultural streams over the past decade has placed increased emphasis on the role of carbon dynamics on nitrogen transformations. With regard to sediment, agricultural streams promote favorable conditions for in-stream production of algal biomass and accrual of algal sediments in the SFGL, which has previously been highlighted as a prominent temporary benthic carbon store and would subsequently promote transient nitrogen storage (Griffiths et al., 2012; Ford and Fox, 2014). Further, high carbon quality and quantity, e.g., algal biomass, has been highlighted as a fuel source for heterotrophic denitrification processes in anaerobic environments, and as a labile source of ammonium for chemoautotrophic nitrification (Butturini et al., 1999; Arango et al., 2007; Arango and Tank, 2008; Newcomer et al., 2012). Despite these recent advancements, few studies have attempted to couple these innovations within a water quality modeling framework that simulates the annual nitrogen budget.

Further, increased emphasis has been placed on methodological approaches to quantify reaction rates and differentiate sources of dissolved and particulate N phases. In this light, ambient measures of the stable isotopic signature ($\delta^{15}N$) of N phases has been implemented with varying success for DIN and sediment source apportionment (Kendall et al., 2001; Xue et al., 2009; Akamatsu et al., 2011; French et al., 2012). The occurrence of isotopic fractionation, or the preferential utilization of light ^{14}N isotope, makes pure fingerprinting assessments difficult, however may potentially be useful for constraining processes where fractionation is prevalent (Kendall et al., 2007). In the stream nitrogen cycle, measured $\delta^{15}N$ of each nitrogen phase (i.e., org-N, NO_3^- and NH_4^+) provides an extra equation in the set of biogeochemical reactions being solved for nitrogen mass balance. Despite the increased use of stable isotope technology for water quality

assessments, few studies have utilized them in hydrologic water quality modeling frameworks to help constrain estimates of source and fate (McGuire and McDonnell, 2008).

The present study aims to improve water quality modeling technology to simulate the fluvial N budget, including permanent and temporary removal of streamwater DIN through a coupled numerical modeling framework. TRANSFER, **T**echnology for **R**emovable **A**nnual **N**itrogen in **S**treams **F**or **E**cosystem **R**estoration, is presented and tested utilizing an eight year ambient dataset of transported sediment nitrogen. Results of the study provide an exploratory calibration for the testbed application in order to highlight the sensitivity of different sub-models in TRANSFER. An annual nitrogen budget is provided to determine the role of the SFGL in net DIN removal.

7.3 METHODS

7.3.1 Model Formulation

TRANSFER couples hydrologic, sediment, organic carbon, and nitrogen dynamics in a low-gradient, ag-disturbed stream in order to better constrain estimates of source, fate and transport of nitrogen (see model framework in Figure 1). TRANSFER builds upon the ISOFLOC model (Chapter 5) which tightly couples hydrology, sediment, and organic carbon processes to simulate the fluvial organic carbon budget (see Chapters 2 and 5 for details on hydrologic, sediment and C sub-models). N modeling builds upon a previously published N mass-balance model (Fox et al., 2010) in which the algal sediment growth is explicitly coupled to DIN dynamics and terms to account for stream biogeochemical reactions. Adsorption for NH_4 is neglected as a result of low ammonium concentrations in the test basin, but can be easily added for site specific conditions.

DIN and DON advect with water streamflow and react with the benthic pools in the streambed. Advection of DIN and DON is modeled in TRANSFER using model input of volumetric water flowrate, Q_i^j, for a given spatial reach, j, and timestep, i, and Q_i^j can be modeled using data-driven, conceptual, or process-based hydrologic models calibrated for the watershed. Concentrations of dissolved constituents are assumed to be well mixed vertically and laterally, as well as within the modeled reach segment (1-d black box approach). Further, since the SFGL is an advection dominated layer

(Zahraeifard et al., 2014), we account for the SFGL pore-water pool separate from the surface water. Conceptually the pore-water pool is quiescent in the streamwise direction (i.e., no x-directional flow), and a vertically hydrodynamic storage zone (Battin et al., 2003). The highly compacted diffusion dominated bottom layer is neglected since DIN penetration will be low and little labile carbon sources are present for denitrifying bacteria.

DIN transport in a stream reach is modeled to account for streamwise and vertical advective exchange with SFGL porewater, in which dispersive fluxes are neglected in the streamwise direction since reach averaged advective fluxes will be much higher than dispersive fluxes at upstream and downstream boundaries. Further, vertical diffusive fluxes have been shown to be orders of magnitude lower than vertical advection in rough bed flumes (Reidenbach et al., 2010). We assumed reactions in the streamwater were negligible since turbidity was low (i.e., periphyton was the predominant algal pool as opposed to phytoplankton) and bacterial communities are assumed to be prominent in the SFGL. The mass-balance is simulated using a one-dimensional black box approach. A cutoff for vertical advection is specified by the user, which produces well-mixed surface and pore water conditions above the specified flow, and isolates the pore-water pool from surface water below the specified flow. A high and low flow condition is utilized because (1) under high flows algal mats will be vertically expanded, as opposed to lying flat on the SFGL surface, which facilitates advective exchange; (2) turbulent mixing with the benthos is governed by instantaneous vertical velocity, which will be governed by small roughness elements, e.g., SFGL skin friction, at low flows, and larger roughness elements, e.g., bedforms, at high flows; (3) energy containing eddies are drastically different at low and high flows, which has been shown to drastically impact sediment transport carrying capacity in SFGL streams (Russo and Fox, 2012). For the scenario when flow is greater than the advection threshold, total DIN in the stream at a specified spatial and temporal step is estimated as

$$DIN_{Tot\,i}^{\;j\;X} = DIN_{Sur\,i-1}^{\;j\;\;X} + DIN_{Pore\,i-1}^{\;j\;\;X} + R_i^{\,j\,X}{}_{Tot} + [\underbrace{Q_{out\,i-1}^{\;j-1} C_{DIN\,i-1}^{Sur\;j-1\,X} + Q_{Trib\,i}^{\;j} C_{DIN\,i}^{Trib\;j\,X}}_{Inflow}) \underbrace{- Q_{out\,i}^{\;j} C_{DIN\,i}^{Tot\;j\,X}}_{\text{Outflow}}]\Delta t \quad (1)$$

where, *Sur* denotes the surface water pool, *Pore* denotes the pore water pool, *Trib* denotes tributaries draining uplands in a specified reach, *DIN* is the mass of a specified

DIN species *X* (NO3 or NH4), *C* is the concentration of a specified DIN phase for the given water pool. Since the system is well-mixed, surface and pore water pools at the end of the timestep are assumed equal to the total *DIN* concentration. Thus *DIN* for the surface water and pore water is modeled as

$$DIN_{Sur_i}^{\ j\ X} = C_{DIN\,i}^{Tot\ j\ X} * V_{Sur_i}^{\ j} \tag{2}$$

and

$$DIN_{Pore_i}^{\ j\ X} = C_{DIN\,i}^{Tot\ j\ X} * V_{Pore_i}^{\ j} \tag{3}$$

where, *DIN* is the mass of DIN for specified phase, *V* is the volume of water in a specified pool and is estimate using the a mass balance considering inflows and outflows for surface water and the following for pore water.

$$V_{Pore_i}^{\ j} = \frac{(\rho_{Dry} - \rho_{SFGL})S_i^j}{\rho_{fluid}\rho_{SFGL}} \tag{4}$$

where, ρ_{Dry} is the dry bulk density of the SFGL material, ρ_{SFGL} is the *in situ* saturated bulk density, ρ_{Fluid} is the bulk density of water and *S* is the SFGL sediment supply. Further, if flow is below a specified threshold, *DIN* is modeled in the surface and pore water pools disjointly as

$$DIN_{Sur_i}^{\ j\ X} = DIN_{Sur_{i-1}}^{\ j\ \ X} + R_i^{j\ X}_{\ Sur} + [\underbrace{Q_{out_{i-1}}^{\ j-1} C_{DIN\,i-1}^{Sur\ j-1\ X} + Q_{Trib_i}^{\ j} C_{DIN\,i}^{Trib\ j\ X}}_{Inflow} \underbrace{- Q_{out_i}^{\ j} C_{DIN\,i}^{Sur\ j\ X}}_{\text{Outflow}}]\Delta t \tag{5}$$

and

$$DIN_{Pore_i}^{\ j\ X} = DIN_{Pore_{i-1}}^{\ j\ \ X} + R_i^{j\ X}_{\ Pore}, \tag{6}$$

where, the pore-water pool has no advective exchange with the overlying surface water.

R is modeled to include biotic and abiotic processes including assimilation, regeneration, nitrification, denitrification, sorption and desorption as

$$R_i^{j\ X}_{\ Pool} = Min_{Net_i}^{\ j\ NH4} \pm c_{DN\,i}^{\ j} \Delta t - Assim_i^{j\ X} - R_{Den_i}^{\ j} SA_{Bed} \Delta t - Sorp_i^{j\ NO3-} + Desorp_i^{j\ NO3-}$$

where, *X* denotes the DIN phase (NH_4 or NO_3), *in* represents the advective upstream and lateral influx of DIN, *out* represents the advective downstream outflux of DIN, *X* represent the DIN species, i.e., NH_4 or NO_3 (NO_2 is neglected since it is an intermediate step), Min_{Net} is the net mass of ammonium generated in the pore-water pool from organic matter mineralization, *Assim* (kgN) is the mass of algae assimilated to algal biomass.

Assimilation is assumed to first be satisfied by the fraction of mineralized ammonium availabile (see below), then nitrate in the pore water, and finally nitrate loosely adsorbed to sediments. c_{DN} represents the direct nitrification rate and is assumed to be zero since ammonium is not present in the surface water, c_{DEN} is the rate (kgN/s) of denitrification in the SFGL (kgN/s), and *Sorp/Desorp* represents abiotic uptake and regeneration of DIN from the water column. Net mineralization is modeled as a function of total mineralized ammonium from coarse and fine algal pools, mass that is instantaneously assimilated by nitrifying chemoautotrophs, and the mass assimilated by photoautotrophic algae as

$$Min_{Net\,i}^{\ j} = Min_i^j - IN_i^j S_i^j \Delta t - Assim_i^{j\,NH4} \quad (7)$$

where, *Min* is the mass mineralized and is quantified as the sum of mineralization of the coarse algal pool and fine algal pool as

$$Min_i^j = \mathrm{Re}\, s_{i\ Mat}^{j\,CO2} c_{Min-algae} + Min_{SFGL\ i}^{Algae\,j} \quad (8)$$

where, *Res* is the carbon respired during the given timestep, $c_{min\text{-}algae}$ is the mass of N atoms mineralized per C atom respired, and $Min_{SFGL}^{\ Algae}$ is the mass mineralized from the SFGL algal pool and is varied as a function of temperature (White et al., 1991). Oxic conditions in the SFGL are assumed to be satisfied for nitrification, thus indirect nitrification rates are modeled using results of Arango and Tank, 2008 that suggest sediment exchangeable NH_4 availability and FPOC content are the primary drivers of rates as opposed to streamwater NH_4. The power function for indirect nitrification, *IN* (kgN kgSed^{-1} s^{-1}) is modeled as

$$IN_i^j = \beta_{IN} (FPOC_i^j)^{\alpha_{IN}} \quad (9)$$

where, *FPOC* (kgC kgSed^{-1}) is the carbon content of SFGL sediments derived from Ford and Fox (In Review), α_{IN} is the exponent calibration coefficient for indirect nitrification, and β_{IN} is the minimum indirect nitrification rate, in which we assumed *IN* rates were on the same order of magnitude as *DEN* rates. Since mineralized NH_4 is extremely labile and can be assimilated immediately we assume that all remaining mineralized NH_4, following satisfaction of the *IN* rates, is re-uptaken by the benthos to satisfy assimilation requirements of the microbial community, with the remainder being regenerated to the water column, or stored in the pore water pool depending on flow conditions.

Denitrification is impacted by NO_3 concentration, sediment C content and temperature; however the functional form of how these processes co-vary is not well understood. Arango and Tank (2008) found sediment C content to be the best descriptive variable in ag-disturbed streams, therefore denitrification rates, *DEN* (kgN kgSed^{-1} s^{-1}) is modeled using a power function as

$$DEN_i^j = \beta_{Den} FPOC_i^{j\,\alpha_{Den}} \quad (10)$$

where, α_{Den} is the exponent calibration coefficient for denitrification, and β_{Den} is the minimum denitrification rate. α_{Den} and β_{Den} were calculated using a min and max range, Mulholland et al. (2008), and over a range of carbon contents derived from Arango and Tank (2008). Nitrification/denitrification rates are coupled when N_{NO3} concentrations fall below 0.15 mgL^{-1}, and denitrification rates are otherwise satisfied by the surface water pool (Seitzinger et al., 2006; Birgand, 2007; Arango and Tank, 2008).

While sorption/desorption has typically been considered for ammonium, low concentrations in ag streams deter ammonium sorption and is henceforth neglected. Conversely, the SFGL modeled herein support favorable conditions for NO_3 sorption, and thus it is considered in the modeling framework. Since the physical adsorption process is rapid and is assumed to reach equilibrium within the modeled timestep, a non-linear Freundlich adsorption isotherm model is used to get the total mass adsorped during a specified timestep, seen in Goldberg et al. (2007), as

$$Sorp_{SFGL\ i}^{Equil\ j} = S_{Upland_i}^{\ j} K_{Fr-NO3} (C_{NO3-Surface_{i-1}}^{\ j})^n \quad (11)$$

where, $Sorp_{SFGL}^{\ Equil}$ is the equilibrium mass of sorption for a specified mass of an adsorbing substrate, $K_{Fr\text{-}NO3}$ is the Freundlich constant for NO_3, *C* is the concentration of NO_3 in the surface water, and *n* is the empirical coefficient to account for non-linearity. To estimate the sorption/desorption, a mass balance for $N_{SFGL}^{\ Sorp}$ was simulated continuously as

$$N_{SFGL\ i}^{Sorp\ j} = N_{SFGL\ i-1}^{Sorp\ j} + Sorp_i^{j\ NO3} - Desorp_i^{j\ NO3} - E_i^j \left(\frac{Sorp_{SFGL\ i-1}^{Equil\ j}}{S_{i-1}^j}\right) \quad (12)$$

where, *Sorp* and *Desorp* are calculated at each timestep to satisfy the equilibrium requirements.

PN includes fine and coarse nitrogen pools comprised primarily of benthic algal biomass and fine particulate sediment particles and aggregates from upland sediment sources (Ford and Fox, 2014). The emphasis of the low-gradient, human disturbed system suggests relatively minor inputs from leaf litter and detritus since much of that material is turned over *in situ*, and fluxes to streambeds or to suspended loads are small relative to algae and FPOC.

$$Slough_i^j = \min\left\lfloor k\left(\tau_{i\ f}^{\ j} - \tau_{cr}^{APN}\right)\rho_S^{APN} SA_{Bed}\Delta t, A_i^j\right\rfloor. \quad (13)$$

where, k (m^{-1}) is the erodibility coefficient, τ_f (Pa) is the shear stress of the fluid at the centroid of the erosion source, τ_{cr} (Pa) is the critical shear stress of the erosion source, ρ_s (kg m^{-3}) is the bulk density of the source, SA (m^2) is the surface area of the erosion source, and A is the coarse algal biomass which equals APOC divided by 0.42 (the carbon content of algae). Sloughed algae is assumed to be exported from the watershed, since algal material is relatively neutrally buoyant and would not be expected to settle out of suspension during flow conditions that would induce sloughing. To model nitrogen content of coarse algal biomass (*APN*) a mass balance mirroring that of algal carbon (Ford and Fox, 2014) was formulated as

$$APN_i^j = APN_{i-1}^{\ j} + (Assim_i^j - Min_{Mat\ \ i}^{Algae^j} - DEC_{Mat\ \ i}^{Algae^j})SA_{Bed}\Delta t - Slough_{Mat-N\ i}^{\ \ j}, \quad (14)$$

where, $Slough_{Mat\text{-}N}$ (kgN) is the nitrogen scouredfrom the algal mat (see Ford and Fox, In Review). Assimilation of DIN is non-rate limiting and is modeled as follows.

$$Assim_i^j = \frac{Fix_i^j + APOC_{i\ Col}^{\ j}}{C:N_{Assim}}, \quad (15)$$

where, Fix (kgN m^{-2} d^{-1}) is the carbon fixation rate, $APOC_{col}$ (kgN m^{-2} d^{-1}) is the algal carbon colonization rate, and $C{:}N_{Assim}$ is the atomic carbon to nitrogen ratio of newly assimilated algae, and *Min* is the mineralization rate of algal biomass to DIN. Adsorption of nitrate is neglected since organic matter typically has a slight negative charge which would repulse the nitrate anion.

Sediment transport mechanics provide the basis for PN transport and temporary storage. Simulation of sediment transport of fine sediment is specifically formulated in TRANSFER for a class of streams with SFGL following the formulation by Russo and Fox (2012) as

$$SS_i^j = SS_{i-1}^j + E_{i\ Bank}^j + E_{i\ Bed}^j - D_i^j + Q_{i\ SSin}^j \Delta t - Q_{i\ SSout}^j \Delta t \ , \quad (16)$$

where, *SS* (kg) is the suspended sediment in the water column, *E* (kg) is the erosion from streambank and streambed sources, *D* (kg) is deposition to the bed, Q_{SS} (kg s^{-1}) is suspended sediment transported into and out of the modeled reach, and Δt (s) is the time step. Source erosion is modeled to be potentially limited by shear resistance, the transport carrying capacity of the fluid, and supply of the erosion source. These processes are modeled for both the streambed and the streambanks as

$$E_i^{j\,I} = \min\left[k\left(\tau_{i\ f}^j - \tau_{cr}^I\right)\rho_S^I SA_I \Delta t, T_{i\ C}^j - SS_{i-1}^j, S_{i-1}^{j\ I}\right], \quad (17)$$

where, (*I*) represents the sediment source, T_c (kg) is the transport carrying capacity and *S* (kg) is the sediment supply. In Equation (2), the erodibility coefficient and fluid shear stress are parameterized following the method of Hanson and Simon (2001). T_c is estimated using a Bagnold like expression (Chien and Wan, 1999) as

$$T_{i\ C}^j = c^j{}_{TC} \frac{\left(\tau_{i\ f}^j\right)^2}{w_s} L^j \Delta t \ , \quad (18)$$

where c_{TC} (s^{-1}) is the transport capacity coefficient, w_s (m s^{-1}) is the particle settling velocity, and *L* (m) is the length of the reach. Deposition of sediment to the streambed is estimated as

$$D_i^j = \frac{w_s \Delta t}{k_p H_i^j}\left[SS_{i-1}^j - T_{i\ C}^j\right], \quad (19)$$

where k_p is the concentration profile coefficient, and *H* (m) is the water column height. *S* of the banks is assumed infinite, however the supply of sediment in the streambed is budgeted as

$$S_{i\ Bed}^j = S_{i-1\,Bed}^j - E_{i\ Bed}^j + D_i^j + Gen_i^j \, . \quad (20)$$

where, *Gen* (kg) is the mass of inorganic fine sediment generated from algae. Benthic FPN composition is simulated as a function of erosion/deposition dynamics, production of algal FPN from APN decomposition, and mineralization rates to ammonium. Mass of nitrogen in the SFGL relative to the supply of sediment in the at a given timestep is modeled as a function of the two available pools as

$$C_{SFGLi}^{N\ j} = \frac{N_{SFGLi}^{\ j}}{S_{SFGLi}^{\ j}} = \frac{N_{SFGL\ i}^{Upland^j}}{S_{SFGL\ i}^{Upland^j}} f_{SFGL}^{Upland} + \frac{N_{SFGL\ i}^{Algae^j}}{S_{SFGL\ i}^{Algae^j}} f_{SFGL}^{Algae}, \quad (21)$$

where C is the concentration (kgN kgsed^{-1}), N is the mass of nitrogen associated with the specified SFGL source and is modeled for upland sediments and algal sediments separately as

$$N_{SFGL\ i}^{Upland^j} = N_{SFGL\ i-1}^{Upland^j} + D_i^j C_N^{Upland} + Sorp_i^j - Desorp_i^j - E_i^j C_{SFGL\ i}^{Upland^j} * f_{SFGL}^{Upland}, \quad (22)$$

$$N_{SFGL\ i}^{Algae^j} = N_{SFGL\ i-1}^{Algae^j} + DEC_{Mat\ i}^{Algae^j} - Min_{SFGL\ i}^{Algae^j} - E_i^j C_{SFGL\ i}^{Algae^j} * f_{SFGL}^{Algae}, \quad (23)$$

where DEC_{Mat}^{Algae} (kgC m^{-2} d^{-1}) is the rate at which algal FPN is mineralized to NH_4^+, and N (%) is the percentage nitrogen of a given sediment carbon source. Transported FPN concentration ($N_{FPN\text{-}T}$) is estimated by multiplying carbon weighted fractions for the total suspended carbon load, derived from the sediment transport model, by N of each source. Further, depositional fluxes are assumed to occur on the receding limb of a hydrograph (e.g., flow deceleration) hence it is assumed that all benthic and bank samples have been flushed and sediments are primarily coming from the uplands.

Stable nitrogen isotope mass balances with nitrogen advection as well as the potential for isotope fractionation during reactions are simulated in TRANSFER for APN, DIN and FPN pools. The isotopic signature of a particular carbon pool, given in terms of δ notation as

$$\delta_i^j = \delta_{i-1}^j X_{i-1}^j + \sum \delta_{inputs_i}^{\ j} X_{Inputs_i}^{\ j} - \sum \delta_{outputs_i}^{\ j} X_{outputs_i}^{\ j} - \sum \varepsilon_{frac_i}^{\ j} \ln(f_{frac_i}^{\ j}), \quad (24)$$

where, X represents the fraction of an element in a given pool and is parameterized using outputs from the aforementioned sediment and mass-balance elemental models, ε is the enrichment factor during an isotopic fractionation process and Rayleigh-type models are used to simulate fractionation (Sharp et al., 2007). In Rayleigh fractionation, $\varepsilon_{A\text{-}B}$ is defined as

$$\varepsilon_{A-B} = \left[\frac{(^{15}N/^{14}N)_A}{(^{15}N/^{14}N)_B} - 1 \right] \times 1000 \quad (25)$$

where A is the product and B is the reactant. f is the fraction of a substrate remaining after the isotope fractionation process occurs and is derived from the appropriate elemental

model. Implementing known inputs, outputs and fractionation processes for APN, DIN and FPN into equations (24, 25), the isotopic submodel for APN is simulated as

$$\begin{aligned}\delta^{15}N_{APN\,i}^{\ j} = {} & \delta^{15}C_{APN\,i-1}^{\ j} X_{APN\,i-1}^{C\ j} - \delta^{15}N_{APN\,i-1}^{\ j} X_{Slough_i}^{N\ j} + \delta^{15}N_{Assim\,i}^{\ j} X_{Assim\,i}^{N\ j} \\ & - \varepsilon_{Min(APN)} \ln(f_{Min(APN)_i}^{\ j}) - \varepsilon_{DEC(APN)} \ln(f_{DEC(APN)_i}^{\ j})\end{aligned}, \quad (26)$$

where, f denotes the fraction remaining from the total mass of N in the reach during the timestep to provide a conservative estimate of fractionation. This assumption is feasible since the temporal discretization is high (30 minutes) relative to the time step that we are simulating (e.g., event-based, seasonal, annual)

For DIN we continuously account for the stable isotopic composition of nitrate ($\delta^{15}N_{NO3}$) in the stream channel. $\delta^{15}N_{NO3}$ is modeled as

$$\begin{aligned}\delta^{15}N_{NO3\,i}^{\ j} = {} & \delta^{15}N_{NO3\,i-1}^{\ j} X_{NO3\,i-1}^{N\ j} + \delta^{15}N_{NO3-in\,i}^{\ j} X_{NO3-in\,i}^{N\ j} - \delta^{15}N_{NO3\,i-1}^{\ j} X_{NO3-out_i}^{N\ j} \\ & + \delta^{15}N_{Reg\,i}^{\ j} X_{Reg\,i}^{N\ j} + \delta^{15}N_{Desorp_i}^{\ j} X_{Desorp_i}^{N\ j} + \delta^{15}N_{DN\,i}^{\ j} X_{DN\,i}^{N\ j} \\ & - \varepsilon_{Sorp} \ln(f_{Sorp_i}^{\ j}) - \varepsilon_{Assim\,i}^{\ j} \ln(f_{Assim\,i}^{\ j}) - \varepsilon_{DEN} \ln(f_{DEN\,i}^{\ j})\end{aligned}, \quad (27)$$

Finally, we provide $\delta^{15}N$ of FPN in the SFGL as it is effectively an integrator of DIN and Algae signatures providing an integrated measure of in-stream processes, and hence is used as a response variable for model evaluation. The mass balance for $\delta^{15}N_{SFGL}$ is modeled as

$$\begin{aligned}\delta^{15}N_{SFGL\,i}^{\ j} = {} & \delta^{15}N_{SFGL\,i-1}^{\ j} X_{FPOC-Bed\,i-1}^{N\ j} - \delta^{15}N_{E\,i}^{\ j} X_{E\,i}^{N\,j} + \delta^{15}N_{DEC(APN)_i}^{\ j} X_{DEC(APN)_i}^{N\ j} + \delta^{15}N_{D\,i}^{\ j} X_{D\,i}^{N\,j} \\ & + \delta^{15}N_{Sorp_i}^{\ j} X_{Sorp_i}^{N\ j} - \varepsilon_{Desorp} \ln(f_{Desorp_i}^{\ j}) - \varepsilon_{Min(SFGL-Algae)} \ln(f_{Min(SFGL-Algae)_i}^{\ j})\end{aligned}, \quad (28)$$

The nitrogen stable isotopic signature of suspended sediment ($\delta^{15}N_{FPN\text{-}T}$) is estimated using a simple mass balance that calculates the nitrogen weighted average of source contributions and their associated isotopic signatures (i.e., $\delta^{15}N_{SFGL}$, $\delta^{15}N_{Upland}$, and $\delta^{15}N_{Bank}$).

7.3.2 Model Application

The potential for TRANSFER to constrain the fluvial nitrogen budget was tested utilizing an eight year dataset from a stream in which sediment and FPOC dynamics has previously been modeled (See QAPP for data QAQC procedures). In order to test TRANSFER we collected temporally and spatially integrated sediment trap samples

(Phillips et al., 2000) at the watershed outlet of the South Elkhorn watershed. Further isotopic and elemental signatures of NO_3 were collected at the watershed outlet and tributaries in order to parameterize the model (Ford and Fox, In Prep). The South Elkhorn Creek Watershed (62 km^2) model domain is provided in Figure 2. The watershed was chosen for its topographic, land use, and geologic features, which are characteristic of the small agriculturally-impacted streams producing hypoxia and anoxia problems in the Gulf of Mexico, as well as previous research experience in the watershed. There are 53 perennial reaches in our model domain of which 27 are first order, 13 are second order and 13 are third order. The reaches are fed by numerous ephemeral streams, ditches and gullies throughout the watershed. Instantaneous volumetric flow ranges from around 3 cfs during base flow to 5000 cfs during extreme events with an average instantaneous flow of 44 cfs. Average annual sediment loads for the system is 861 t y^{-1} of which 775 t y^{-1} are transported during events and 86 t y^{-1} are transported at baseflow (Russo and Fox, 2012). The underlying geology of the Bluegrass Region where the watershed is located promotes high background levels of phosphorus in-stream ranging between 100 to 420 μgP/L. These levels far exceed minimum thresholds for autochthonous growth (Dodds et al., 2002) and produce N:P ranges (5:1 to 17:1) that are well below N:P ratios of autochthonous OM in Midwestern United States agriculturally-impacted streams, which are approximately 32:1.

Some simplifying assumptions were made to test the efficacy of the stable isotope routine in transfer to constrain the fluvial N budget including neglecting sorption/desorption since the process is not yet well understood in streambeds for nitrate, and subsequently isotopic fractionations are poorly constrained (Kendall, 1998). Further we neglect the pore-water model since it's assumed that advection into and out of the SFGL will be high promoting well mixed conditions, however temporary residence of mineralized N is considered to facilitate biotic reuptake and indirect nitrification. We neglect fractionations associated with organic matter breakdown as its well understood that fractionations associated with decomposition are relatively small, i.e., on the order of 1-2‰ (Kendall et al., 2007). Further we neglect the contributions of coupled nitrification and dentrification since measured values in the watershed never fall below the required

threshold of 150µg L^{-1} (Seitzinger et al., 2006; Arango and Tank, 2008; Mulholland et al., 2008).

The stable isotopic signature of transported sediment nitrogen, $\delta^{15}N_{FPN\text{-}T}$ (‰), and elemental composition of transported sediment nitrogen, $C_{FPN\text{-}T}$ (gN 100gsed^{-1}), were utilized as response variables for the model performance. We calibrated the model through a multi-objective processes, based on the sensitivity of different components in the model to the response variables. Values for calibrated parameters are reported in Table 1. Manual calibration techniques were used generate acceptable visual fit with time-series of modeled and measured data. An extensive model evaluation (i.e., global sensitivity analysis, calibration/validation statistics, and uncertainty analysis), was outside the scope of the study since the objective was to determine the efficacy of the proposed model to simulate different components of the nitrogen budget and is a future need, when the sorption mechanism is better understood, to quantify model uncertainty and performance.

7.3.3 Inputs and Parameterization

Parameterization ranges of the numerical model, as well as the calibrated solution are provided in Table 1. All parameters surrounding sediment or carbon dynamics are generated from a previously calibrated sediment and fluvial organic carbon model. All decomposition and mineralization rates of N were parameterized analogous to that of FPOC from the previously calibrated FPOC model since C and N sediment dynamics are tightly linked in the SFGL (Chapter 6). The carbon to nitrogen atomic ratio of assimilated algal biomass ($C{:}N_{Assim}$) and initial isotopic signatures of the algal mat were parameterized based on point sample measurements within the stream channel, which were subsequently ground and combusted on an elemental analyzer interfaced with an IRMS. Further, elemental N and $\delta^{15}N$ values of bank and upland sediments were characterized based on samples collected in the watershed (see Fox et al., 2010). Concentrations and $\delta^{15}N$ values of streamwater nitrate were derived from tributary measurements over the course of a fourteen month sampling period. Average values were used to determine if in-stream processes governed seasonal variability of

downstream measurements of $\delta^{15}N_{NO3}$ and $N_{NO3.}$ Exponent coefficients for the nitrification and denitrification models (α_{IN} and α_{DEN}) were assumed to be equal to one since previous studies of nitrification and denitrification in agricultural based streams in Michigan have shown that processes vary linearly with sediment organic carbon content (Arango and Tank, 2008). Rates of nitrification and denitrification were assumed to have comparable ranges, and vary over three orders of magnitude (10^2-10^4 µgN m^{-2} h^{-1}), which is consistent with rates in ag-streams (Arango and Tank, 2008; Mulholland et al., 2008). Isotopic enrichment values (i.e., ε_{Assim} and ε_{Den}) were generated from average values derived from the literature (Wada, 1980; Heaton, 1986; Montoya and McCarthy, 1995; Kendall, 1998; Neboda et al., 2003; Kendall et al., 2007; Fox et al., 2010). Enrichment factors were not varied during model simulation since isotopic signature of transported sediments is insensitive to uncertainty in enrichment factors (Fox et al., 2010).

7.4 RESULTS AND DISCUSSION

Results of the study suggest that a three-step model evaluation should be used to constrain the stream fluvial N budget in TRANSFER (Figure 3), in which *C:N* ratio of assimilated algal biomass is fit the $C_{FPN\text{-}T}$, rates of nitrification/denitrification are adjusted to satisfy streamwater ammonium and nitrate concentrations, and the isotopic signature of inflowing DIN is adjusted to fit $\delta^{15}N_{FPN\text{-}T}$. As evidenced in Figure 3, sediment, carbon and nitrogen model inputs are initially provided to the model. A local sensitivity analysis was performed and it was observed that the *C:N* ratio of assimilated algal biomass was the most sensitive parameter for the $C_{FPN\text{-}T}$. Conversely, little sensitivity was observed in the $\delta^{15}N_{FPN\text{-}T}$ dataset under varying *C:N* assimilation ratios, suggesting that the elemental model can be calibrated in isolation of the isotopic model. Hence the *C:N* ratio for assimilated algae was adjusted and model output was checked against the calibration dataset, $C_{FPN\text{-}T}$. The optimized visual calibration for $C_{FPN\text{-}T}$ is observed in Figure 4. Generally some over/under estimation is observed, however the model captures dynamics well at event-multiannual timescales. The ability of the model to capture dynamics at different timescales suggests the efficacy of the model to simulate both seasonal and annual budgets for the stream N cycle. Further, the ability of the C:N ratio of assimilated

algae to constrain signature of sediment FPN suggests the efficacy of tightly coupling sediment, carbon and nitrogen dynamics in the SFGL. While recent research has highlighted that C and N dynamics are coupled in agriculturally disturbed streambeds, TRANSFR is unique in that most models neglect the coupled assimilation/degradation C and N processes in the SFGL and have not been shown to adequately simulate benthic N processes at multi-annual timescales (DiToro, 2001; Aragno and Tank, 2008; Trimmer et al., 2012; Ford and Fox, In Prep).

As observed in Figure 3, following calibration of assimilation rates, nitrification rates were adjusted to satisfy realities of streamwater NH_4 concentrations. With regard to NH_4 concentrations, previous data collection in the watershed suggests NH_4 concentrations are below detectable limits (0.02mg/L) in the main-stem of the watershed throughout the year (Ford and Fox, In Prep). For the model application, an inflowing NH_4 concentration of 0.01 mg/L was assumed, i.e., half the detection limit, and sensitivity analysis suggests that regeneration of NH_4 from the bed, and thus indirect nitrification rates, was the most sensitive component of the surface water NH_4 concentrations (see QAPP in Appendix 1 for details on NH_4 analysis method and detection limits). Nitrification rates were adjusted within their parameterization range in order to satisfy the condition that median NH_4 concentrations in the overlying surface water were less than the detection limit for NH_4. The resulting indirect nitrification rate for the system was observed to be on the order of 10^4 $\mu gN\ m^{-2}\ h^{-1}$ which is on the high end for nitrification rates characteristic of agricultural streams (Arango and Tank, 2008). The advection dominated nature of the SFGL provides an oxic layer, and high FPOC content, thus supplying high volumes of sediment derived ammonium (Ford and Fox, 2014; Zahraeifard et al., 2014). The result is that favorable conditions for chemoautotrophic nitrification are present, suggesting high regeneration capacity of the SFGL to the streamwater in summer and fall when mineralization is pronounced.

Similarly to nitrification, denitrification rates were constrained utilizing realities of NO_3 concentrations measured in the study watershed. Results from Ford and Fox (In Prep) highlight that NO_3 concentrations fluctuate seasonally in the main-stem, with high values in late fall through mid-spring and low values in summer and early fall when in-stream production is pronounced. Further, spatial variation with increasing stream order

suggests that concentrations were highest in first order streams and lowest in the third-order main-stem. The South Elkhorn application of TRANSFER suggests that denitrification had a pronounced impact on the average NO_3 concentration of the surface water annually and seasonally. Denitrification rates in low-gradient ag-streams generally range from 10^2 to 10^4µgN m^{-2} h^{-1} (Mulholland et al., 2008). For a low denitrification rate, (~10^2 µgN m^{-2} h^{-1}) results suggest that average concentration of NO_3 are relatively static in the long-term (i.e., 3mg L^{-1}) and do not have pronounced variation from reach to reach. Conversely, utilizing a high dentirification rate (~10^4 µgN m^{-2} h^{-1}), average concentrations in Reach 1 were 2.7 mg L^{-1} and Reach 6 were 2.5 mg L^{-1} suggesting signification attenuation of NO_3 in the main stem. Denitrification rates were thus modeled to be on the order of 10^3 µgN m^{-2} h^{-1} and varied temporally as a function of FPOC content in order to satisfy temporal and spatial constraints of the measured nitrate concentrations, which is on the middle to high end of denitrification rates reported in the literature (Arango and Tank, 2008; Mulholland et al., 2008). The oxic nature of the SFGL would suggest that denitrification rates would be low, contradicting results of the model calibration. However denitrification potential in hot spots, or localized zones of anoxic substrates with high organic matter content, e.g., a thick filamentous algal mat, have the potential to account for more than half of the denitrification capacity supporting the findings of the model calibration (Findlay et al., 2011).

While the elemental model and streamwater concentrations of N phases were effective at constraining uptake, nitrification and denitrification rates, results of the calibration for the $\delta^{15}N_{FPN\text{-}T}$ dataset suggest time-varying NO_3 isotopic signature highlighting the sensitivity of $\delta^{15}N_{FPN\text{-}T}$ as a potential NO_3 fingerprinting tool. Preliminary sensitivity analysis of the isotope model in TRANSFER suggests that the most sensitive parameter, when calibrating $\delta^{15}N_{FPN\text{-}T}$, was the isotopic signature of $\delta^{15}N_{NO3}$. Varying the isotopic signature over the range of values found in tributaries in the study system (3-15‰) provided a high and low end bound for the calibration data. Assuming a static isotopic signature (Figure 5a) results suggest the model performs well for 2006 through early-2008 and overestimates the measured data from mid-2008 through 2013. The good fit between measured and modeled data in 2006-2007 in Figure 5a suggests uptake of NO_3 with an isotopic signature of 12‰, reflective of a mixture of

manure, soil derived nitrate, and fertilizers in surface water sources (Kendall et al., 2007; Xue et al., 2009; French et al., 2012). The poor fit in 2009-2013 coincides with a period of increasing organic matter quality and stock in the streambed (see accrual of $C_{FPN\text{-}T}$ in Figure 4 and Ford and Fox, In Review). The higher density of algal carbon (average $\delta^{15}N$=5‰) in the SFGL of tributaries will produce NO_3 to the surface water that will decrease the $\delta^{15}N$ signature of the inflowing NO_3 to the main stem and subsequently get integrated into the bed. This process is likely to be prominent during periods of high uptake (e.g., spring through early fall) when the proportion of mineralized algal NO_3 to inflowing upland NO_3 will be high. For this reason, $\delta^{15}N$ of NO_3 coming into the stream reach was adjusted in 2009-2013 to 10‰ in order to provide a more accurate depiction of the surface water DIN source. The resulting calibration with the time-varying isotopic signature is provided in Figure 5b, and the revised $\delta^{15}N_{NO3}$ signature provides good agreement between measured and modeled $\delta^{15}N_{FPN\text{-}T}$ in 2009-2013.

Notwithstanding the improved performance, modeled $\delta^{15}N_{FPN\text{-}T}$ during 2008 is approximately 2-5‰ higher than measured data, potentially suggesting an alternative NO_3 source during the 2008 growing season. The 2008 growing season (spring-fall) was uncharacteristically dry relative to other years in the model domain. Under drought conditions, stream connectivity with upland fertilizers will be less pronounced, hence soil mineralized ammonium (δ^{15}N=4-6%) will have a more distinct fingerprint on the NO_3 signature. Simultaneously, similar to 2009-2013, algal biomass in tributaries was pronounced in 2008 (Chapter 4; δ^{15}N=2-7%) and will constitute a significant portion of the main-stem inflowing NO_3 since manure and fertilizer delivery via surface flow and seepage will be dampened by the drought. As a result, a $\delta^{15}N_{NO3}$ signature of 4 during drought conditions in 2008 provided the best fit of measured and modeled $\delta^{15}N_{FPN}$.

These results collectively suggest that $\delta^{15}N_{FPN\text{-}T}$ in TRANSFER has the potential to act as a fingerprinting tool to continuously track prominent δ^{15}N signatures from DIN from year to year, which can subsequently quantify proportions of NO_3 from differing sources. This innovation could be particularly useful in pre and post assessment of restoration efforts in order to determine the behavior of the system following nutrient mitigation. Further work is needed in systems with contrasting DIN sources to the test the validity of the source tracing hypothesis since $\delta^{15}N_{DIN}$ data was unavailable for 2008.

Collectively results of the model performance suggest that the novel model innovations of coupling C and N processes with stable isotope signatures of transported sediments can help constrain in-stream processes and upland source contributions, thus highlighting the SFGL as an integrator of watershed N processes.

As a final note, an average annual nitrogen budget was generated from the calibrated model in order to quantify the role of the SFGL in net annual DIN removal (Table 2). Results of the model predict that the SFGL removes 11% (0.2 tN km^{-2} yr^{-1}) of inflowing nitrogen in the main-stem of the watershed via temporary and permanent removal pathways, reducing upland nitrogen inputs from 1.9 to 1.7 tN km^{-2} yr^{-1}. Of the fraction that is removed, approximately 50% is removed permanently *via* denitrification and 50% is temporarily removed and flushed from the system in the form of sloughed algae. The ability of the SFGL to remove 11% of the total NO_3 load suggests the effectiveness at low flows, since high flows in winter, during dormant biological activity, will transport the majority of the DIN. Further work is needed at a process scale in order to test and apply the sorption mechanism discussed in the methods in order to quantify its role as a transient storage mechanism. While this study emphasized development and a calibration procedure for the TRANSFER model, future work is needed to provide a more robust model evaluation, i.e., global sensitivity analysis, calibration/validation statistics, and uncertainty analysis, to provide bounds for the fluvial nitrogen budget.

7.5 CONCLUSIONS

Results of this study suggest that TRANSFER can be an effective modeling tool to simulate the fluvial nitrogen budget in low-gradient agriculturally disturbed steams. Results of the study suggest that utilizing transported FPN as a response variable provides a unique calibration for DIN assimilation associated with the tight coupling of TRANSFER to sediment and carbon models. Further the depleted NH_4 concentrations, typical of streams in the region, facilitate calibration of regeneration rates, while NO_3 concentrations assist in calibration of denitrification rates. The additional stable isotope response variable is sensitive to the isotopic signature of streamwater DIN, suggesting that TRANSFER can potentially act as a fate and fingerprinting model. TRANSFER has

the potential to be applied by both practitioners and scientists alike for restoration design as well as pre and post assessment, total N and NO_3 TMDLs, and behavioral analysis of N dynamics in a system.

7.6 REFERENCES

Akamatsu, F., Konayashi, S., Amano, K., Nakanishi, S., Oshima, Y., 2011. Longitudinal and seasonal changes in the origin and quality of transported particulate organic matter along a gravel-bed river. Hydrobiologia, 669, 183-197.

Arango, C.P., Tank, J.L., 2008. Land use influences the spatiotemporal controls on nitrification and denitrification in headwater streams. J.N. Am. Benthol. Soc., 27(1), 90-107.

Arango, C.P., Tank, J.L., Schaller, J.L., Royer, T.V., Bernot, M.J., David, M.B., 2007. Benthic organic carbon influences denitrification in streams with high nitrate concentration. Freshw. Biol., 52, 1210-1222.

Battin TJ, Kaplan LA, Newbold JD, Hansen CME. 2003. Contributions of microbial biofilms to ecosystem processes in stream mesocosms. *Nature* 426: 440-442.

Bernhardt ES, Likens GE, Hall RO Jr, Buso DC, Fisher SG, Burton TM, Meyer JL, McDowell WH, Mayer MS, Bowden WB, Findlay SEG, MacNeale KH, Steltzer RS, Lowe WH. 2005. Can't see the forest for the stream? In-stream processing and terrestrial nitrogen exports. BioScience 55:219–230.

Birgand F.; Skaggs, R. W.; Chescheir, G. M.; Gilliam, J. W. Nitrogen removal in streams of agricultural catchments—a literature review. *Critical Reviews in Environmental Science and Technology*. 2007, 37, 381-487.

Butturini A, Battin TJ, Sabater F. 1999. Nitrification in stream sediment biofilms: the role of ammonium concentration and DOC quality. *Water Research*, 34(2): 629-639.

Conley, D. J.; Paerl, H. W.; Howarth, R. W.; Boesch, D. F.; Seitzinger, S. P.; Havens, K. E.; Lancelot, C.; Likens, G. E. Controlling Eutrophication: Nitrogen and Phosphorus. *Science*. 2009, 323, 1014-1015.

DiToro, D.M., (2001), Sediment Flux Modeling, John Wiley and Sons, Hoboken, New Jersey.

Droppo I, Stone M. 1994. In-channel surficial fine grained sediment lamina. Part I: Physical Characteristics and formational processes. *Hydrological Processes* 8:101-111

Findlay, S.E.G., Mulholland, P.J., Hamilton, S.K., Tank, J.L., Bernot, M.J., Burgin, A.J., Crenshaw, C.L., Dodds, W.K., Grimm, N.B., McDowell, W.H., Potter J.D., Sobota, D.J., 2011. Cross-stream comparison of substrate-specific denitrification potential. Biogeochemistry, 104, 381-392.

Ford, W.I., Fox, J.F., 2014. Model of particulate organic carbon transport in an agriculturally impacted stream. Hydrol. Process., 28(5), DOI: 10.1002/hyp.9569

Fox J, Davis C, Martin D. 2010. Sediment source assessment in a lowland watershed using nitrogen stable isotopes. *Journal of American Water Resources Association* 46:1192-1204.

French C, Rock L, Nolan K, Tobin J, Morrisey A. 2012. The potential for a suite of isotope and chemical markers to differentiate sources of nitrate contamination: A review. *Water Research* 46: 2023-2041.

Galloway, J. N.; Townsend, A. R.; Erisman J. W.; Bekunda, M.; Cai, Z.; Freney, J. R.; Martinelli, L. A.; Seitzinger, S. P.; Sutton, M. A. Transformation of the nitrogen cycle: recent trends, questions, and potential solutions. *Science.* 2008, 320, 889-892.

Goldberg S, Criscenti LJ, Turner DR, Davis JA, Cantrell KJ. 2007. Adsorption-Desorption Processes in subsurface reactive transport modeling. *Vadose Zone Journal*, 6: 407-435.

Griffiths, N.A., Tank, J.L., Royer, T.V., Warrner, T.J., Frauendorf, T.C., Rosi-Marshall, E.J., Whiles, M.R., 2012. Temporal variation in organic carbon spiraling in Midwestern agricultural streams. Biogeochemistry, 108, 149-169.

Montoya, J.P. and J.J. McCarthy, 1995. Isotopic Fractionation During Nitrate Uptake by Phytoplankton Grown in Continuous Culture. Journal of Plankton Research 17(3):439-464.

Kendall, C., 1998. Tracing nitrogen sources and cycling in catchments. *In:* C. Kendall and J.J. McDonnell (Editors), Isotope Tracers in Catchment Hydrology, Elsevier, Amsterdam, pp. 519-576.

Kendall, C., Silva, S.R., Kelly, V.J. 2001. Carbon and nitrogen isotopic compositions of particulate organic matter in four large river systems across the United States. Hydrological Processes, 15, 1301-1346, DOI: 10.1002/hyp.216.

Kendall, C., Elliott, E.M., and Wankel, S.D., 2007. Tracing anthropogenic inputs of nitrogen to ecosystems, Chapter 12, In: R.H. Michener and K. Lajtha (Eds.), Stable Isotopes in Ecology and Environmental Science, 2nd edition, Blackwell Publishing, p. 375-449.

McGuire, K., J. McDonnell, (2008), Stable isotope tracers in watershed hydrology, Chapter 11, in Stable Isotopes in Ecology and Environmental Science, Second Edition, 334-374, John Wiley and Sons, Hoboken, New Jersey.

Montoya, J.P. and J.J. McCarthy, 1995. Isotopic Fractionation During Nitrate Uptake by Phytoplankton Grown in Continuous Culture. Journal of Plankton Research 17(3):439-464.

Mulholland P, Helton A, Poole G, Hall R, Hamilton S, Peterson B, Tank J, Ashkenas L, Cooper L, Dahm C, Dodds W, Findlay S, Gregory S, Grimm N, Johnson S, McDowell W, Meyer J, Valett H, Webster J, Arango C, Beaulieu J, Bernot M, Burgin A, Crenshaw C, Johnson L, Niederlehner B, O'Brien J, Potter J, Sheibley R, Sobota D, Thomas S. Stream denitrification across biomes and its response to anthropogenic nitrate loading. *Nature* 452:202-206.

Needoba, J.A., N.A. Waser, P.J. Harrison, and S.E. Calvert, 2003. Nitrogen Isotope Fractionation in 12 Species of Marine Phytoplankton During Growth on Nitrate. Marine Ecology Progress Series 255:81-91.

Newcomer, T.A., Kaushal, S.S., Mayer, P.M., Shields A.R., Canuel, E.A., Groffman, P.M., Gold, A.J., 2012. Influence of novel organic carbon sources on denitrification in forest, degraded urban and restored streams. Ecol. Monogr., 82(4), 449-466.

Peterson, B.J., W.M. Wollheim, P.J. Mulholland, J.R. Webster, J.L. Meyer, J.L. Tank, E. Marto˜, W.B. Bowden, H.M. Valett, A.E. Hershey, W.H. McDowell, W.K. Dodds, S.K. Hamilton, S. Gregory, and D.D. Morrall, 2001. Control of Nitrogen Export From Watersheds by Headwater Streams. Science 292(5514):86-90.

Phillips J, Russell M, Walling D. 2000. Time-integrated sampling of fluvial suspended sediment: a simple methodology for small catchments. *Hydrological Processes* 14:2589-2602.

Reidenbach MA, Limm M, Hondzo M, Stacey MT. 2010. Effects of bed roughness on boundary layer mixing and mass flux across the sediment water interface. *Water Resources Research*, 46: W07530.

Russo J, Fox J. 2012. The role of the surface fine-grained laminae in low-gradient streams: A model approach. *Geomorphology* In press. DOI: 10.1016/j.geomorph.2012.05.012

Seitzinger, S.P., J.A. Harrison, J.K. Bo¨hlke, A.F. Bouwman, R. Lowrance, B. Peterson, C. Tobias, and G. Van Drecht, 2006. Denitrification Across Landscapes and Waterscapes: A Synthesis. Ecological Applications 16:2064-2090.

Seitzinger, S. 2008. Out of reach. *Nature*, 45:162-163.

Sharp, Z. 2007. Principles of stable isotope geochemistry. Prentice Hall, New Jersey. 360p.

Trimmer, M., Grey, J., Heppell, C.M., Hildrew A.G., Lansdown, K., Stahl, H., Yvon-Durocher, G., 2012. River bed carbon and nitrogen cycling: State of play and some new directions. Sci. Total Environ., DOI: 10.1016/j.scitotenv.2011.10.074

Wada E. 1980. Nitrogen isotope fractionation and its significance in biogeochemical processes occurring in marine environments. In: Marine Chemistry, E.O. Goldberg, Y. Horibe and K. Saruhashi (Editors). Uchida Rokahuko Publishing Company, Tokyo, pp. 375-398.

Walling D, Collins A, Jones P, Leeks G, Old G. 2006. Establishing fine-grained sediment budgets for the Pang and Lambourn LOCAR catchments. *Journal of Hydrology* 330:126-141.

White P, Kalff J, Rasmussen J, Gasol J. 1991. The effect of temperature and algal biomass on bacterial production and specific growth rate in freshwater and marine habitats. *Microbial Ecology* 21:99-118.

Xue D, Botte J, Baets BD, Accoe F, Nestler A, Taylor P, Cleemput OV, Berglund M, Boechkx P. 2009. Present limitations and future prospects of stable isotope methods for nitrate source identification in surface- and groundwater. *Water Research* 43: 1159-1170.

Zahraeifard, V, Deng Z, Malone R. 2014. Modelling spatial variations in dissolved oxygen in fine-grained streams under uncertainty. *Hydrological Processes,* In Press.

7.7 TABLES AND FIGURES

Table 1. TRANSFER model inputs and parameterization for the South Elkhorn model application.

Parameters	Nominal Range	Calibrated Value	Units
Elemental Mass Balance Model			
$C{:}N_{Assim}$	8-16	11	gC gN^{-1}
$C_{FPN\text{-}Upland}$	0.15-0.25	0.2	gN $100gSed^{-1}$
$C_{FPN\text{-}Banks}$	0.14-0.22	0.18	gN $100gSed^{-1}$
α_{IN}	$3{\cdot}10^{-9}$-$3{\cdot}10^{-7}$	$3{\cdot}10^{-7}$	-------
α_{DEN}	$3{\cdot}10^{-9}$-$3{\cdot}10^{-7}$	$6{\cdot}10^{-8}$	-------
β_{IN}	-------	1	-------
β_{DEN}	-------	1	-------
$N\text{-}NO_3$	2-3.6	3.0	mgN L^{-1}
$N\text{-}NH_4$	0-0.02	0.01	mgN L^{-1}
Stable Isotope Mass Balance Model			
ε_{DEN}	5-15	11.5	‰
$\varepsilon_{Fix\text{-}NO3}$	0-10	6.3	‰
$\delta^{15}N_{NO3\text{-}06\text{-}07}$	3-15	12	‰
$\delta^{15}N_{NO3\text{-}08\text{-}13}$	3-15	10	‰
$\delta^{15}N_{Banks}$	6-7.5	6.5	‰
$\delta^{15}N_{Uplands}$	4-12	-----	‰
$\delta^{15}N_{Mat\text{-}Initial}$	2-7	5	‰

Table 2. Average annual fluvial nitrogen budget for sediment and dissolved nitrogen pools including algae, fine particulate nitrogen, NO_3 and NH_4. Further, permanent removal, via denitrification is quantified to assess its significance at an annual scale.

Nitrogen Pool	Input (tN km^{-2} yr^{-1})	Annual Yield (tN km^{-2} yr^{-1})
NO_3	1.9	1.7
NH_4	$9 \cdot 10^{-3}$	$6 \cdot 10^{-3}$
FPN	---------	0.03
Sloughed Algae	---------	0.08
Denitrification	---------	0.08

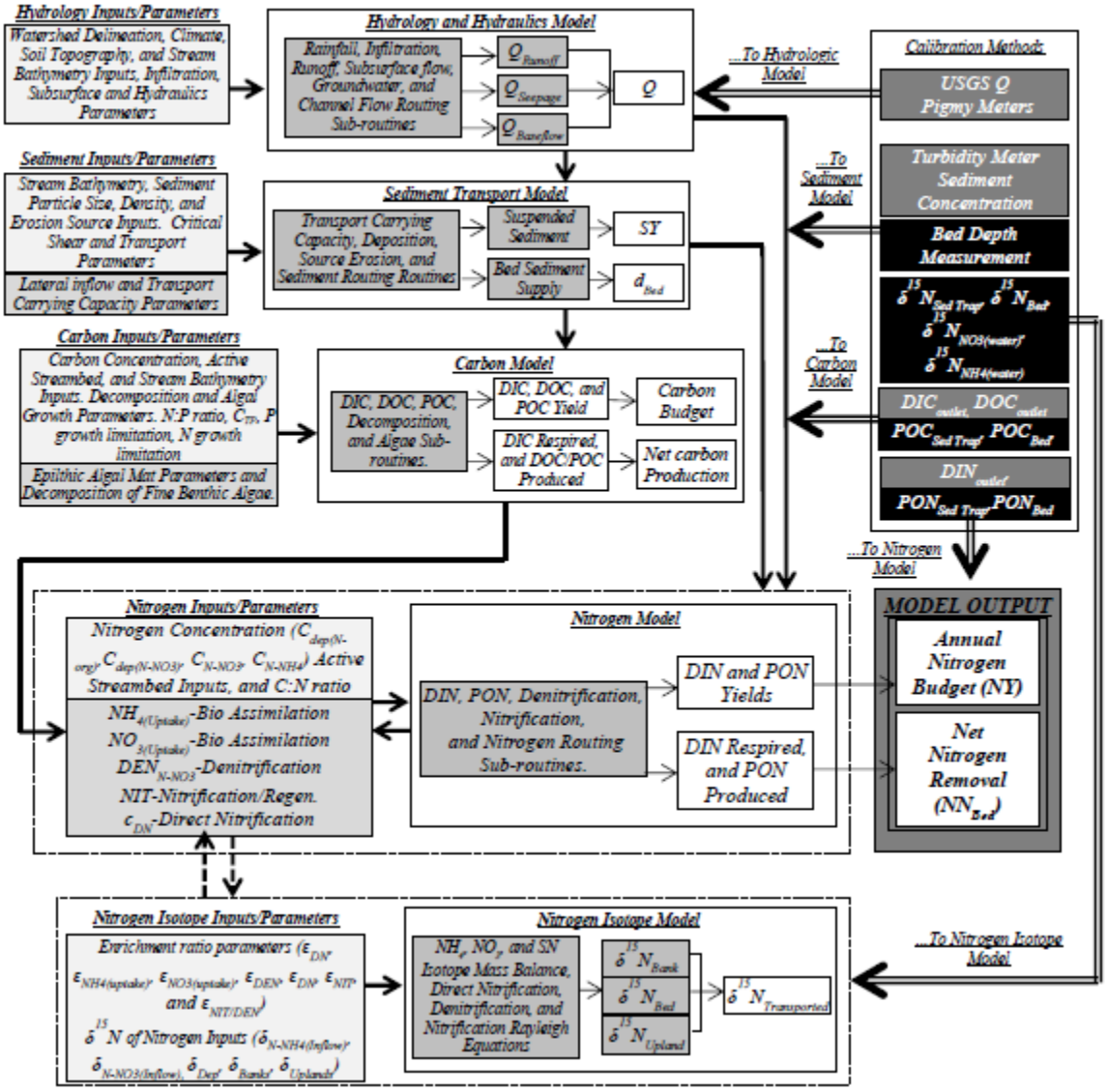

Figure 1. TRANSFER modeling framework including inputs and outputs and calibration data.

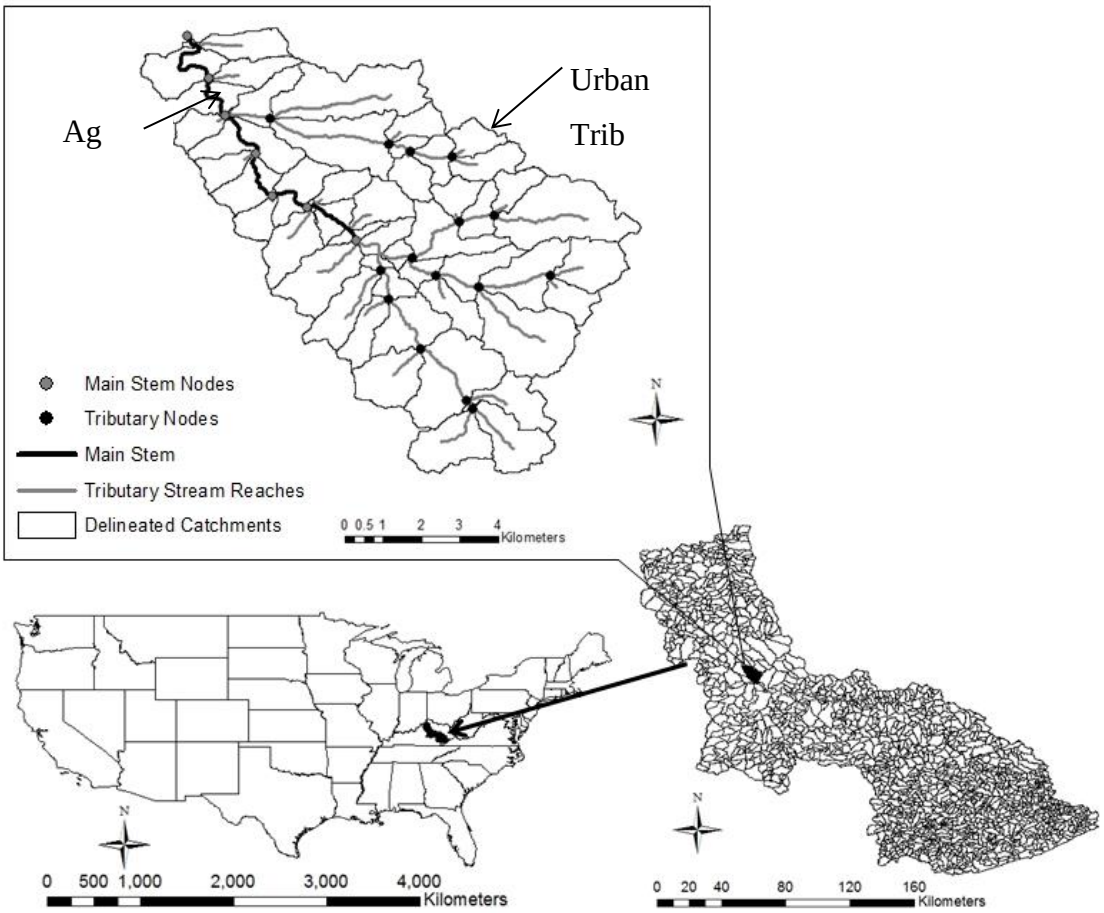

Figure 2. Model Domain for the South Elkhorn Watershed including the main stem modeling domain, monitored tributary reaches.

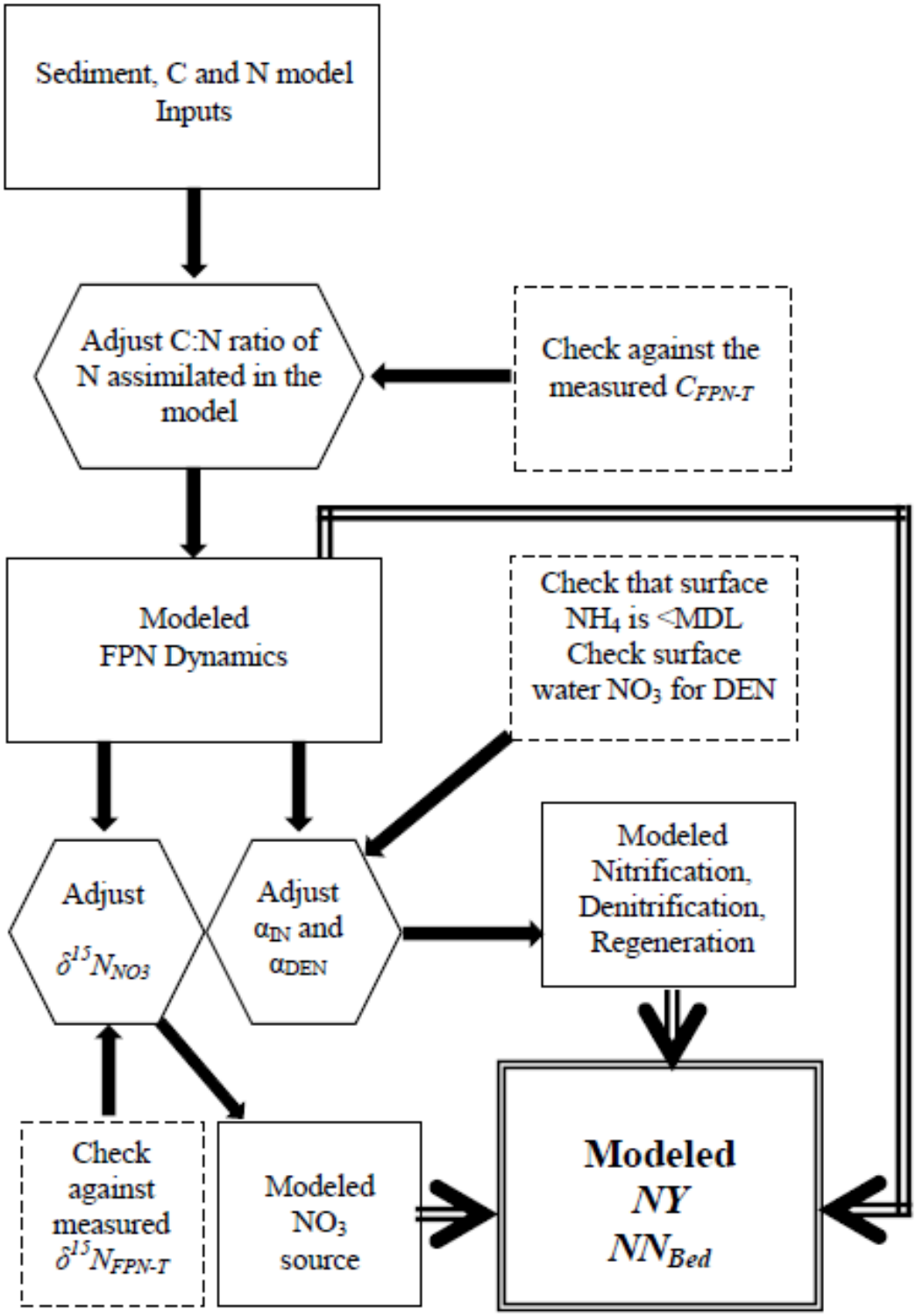

Figure 3. Calibration procedure for TRANSFER in the test application

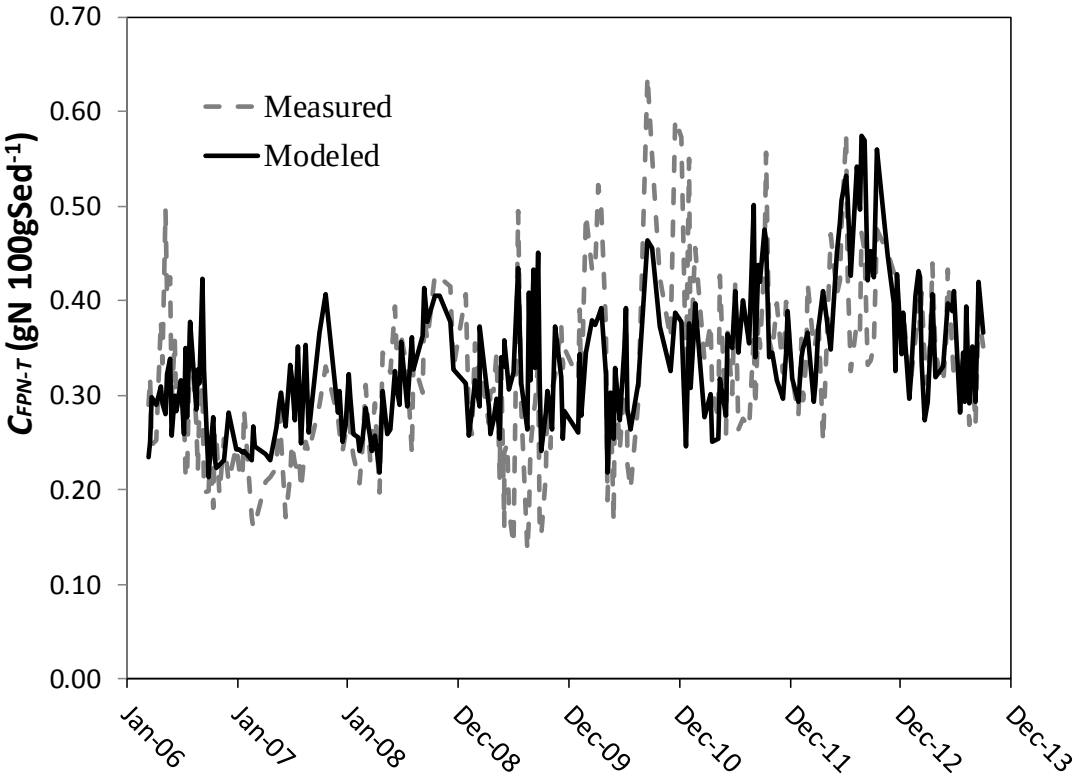

Figure 4. Calibration of C_{FPN-T} is attained by constrain the biological assimilation rate, which is parameterized from the fluvial C model in TRANSFER.

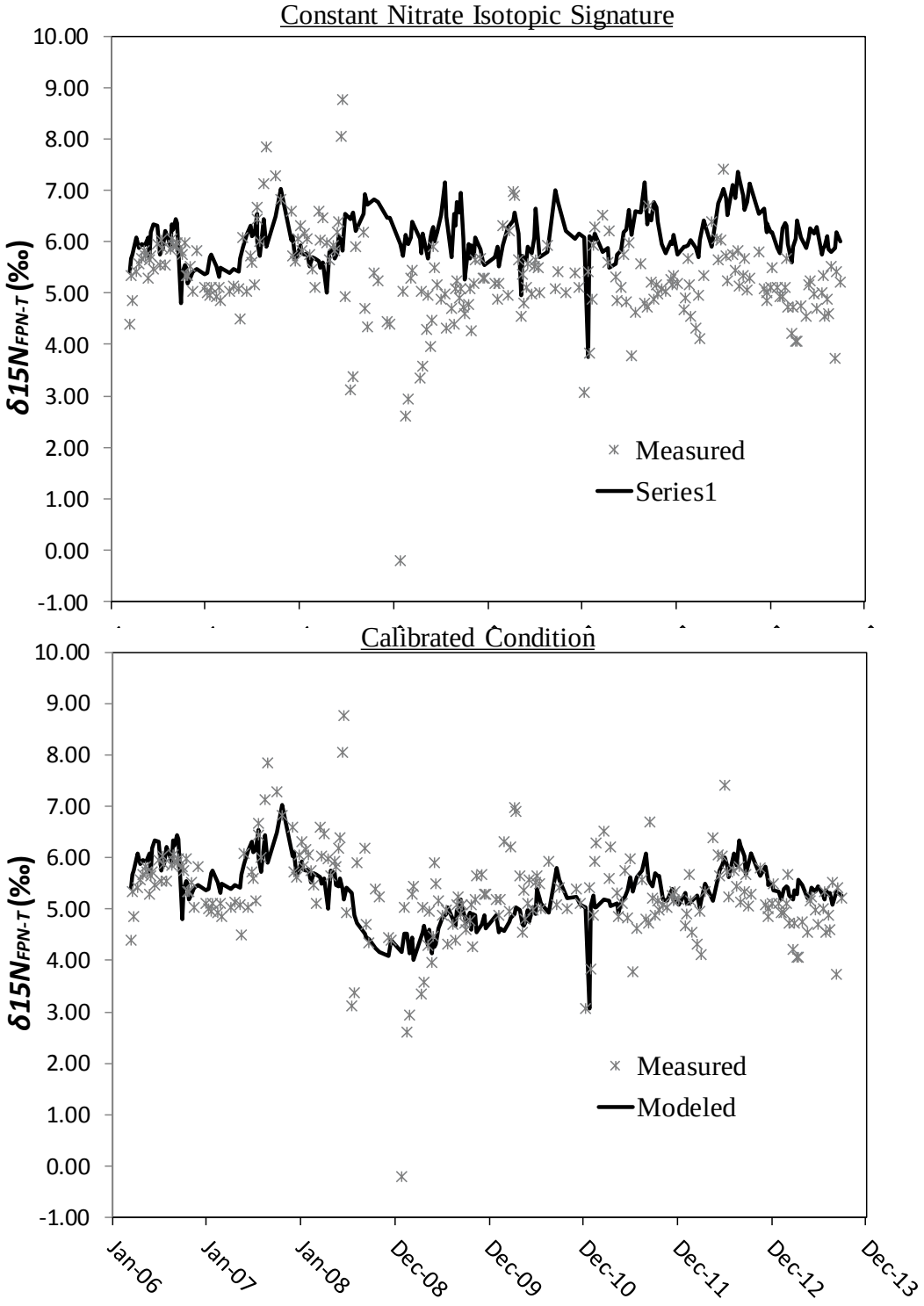

Figure 5. Results of the calibration for $\delta^{15}N_{FPN\text{-}T}$ for (a) a constant nitrate isotopic signature and (b) separate signatures for 2006-2007 and 2008-2013. Sensitivity of $\delta^{15}N_{FPN\text{-}T}$ to $\delta^{15}N_{NO3}$ suggests that TRANSFER can can potentially trace sources of NO_3.

Copyright © William Isaac Ford III 2014

Chapter 8: Conclusions

To summarize, results of this dissertation aimed to unmask the coupled hydrodynamic and biogeochemical behavior of the SFGL in a low-gradient ag-stream as it pertains to stream C and N cycles. The following list summarizes the main findings:

- Particulate organic carbon dynamics in SFGL streams are driven by autotrophic growth and decomposition mechanisms in which hydrodynamic variability at different timescales impacts the level of accrual.
- The statistical distribution of transported sediment carbon in low-gradient ag-streams is Gamma distributed, as a result of benthic growth and decomposition mechanisms governing shape and scale parameters of the statistical model.
- Extreme hydrodynamic disturbances induce short-term disequilibrium benthic processes (on the order of 2-3 years), in which carbon quality and quantity vary seasonally thereafter.
- Implementation of stable isotope technology into the fluvial organic carbon budget modeling framework reduces uncertainty in algal sloughing estimates by nearly 60%. The resulting budget suggests that inclusion of sloughed algal biomass into fluvial OC budget shifts the system from dissolved to particulate dominance which contradicts conventional wisdom.
- Carbon and nitrogen processes are tightly coupled in the SFGL during late spring to early fall when SFGL composition is dominated by autotrophic organic matter, with a slightly negative charge. Decoupling of C and N cycles in winter and early spring is suggested to occur as a result of NO_3 adsorption associated with delivery of recalcitrant, variably charged minerals to the SFGL during late fall and winter.
- We provide a fully coupled numerical modeling framework to simulate the fluvial N budget in low-gradient SFGL dominated streams. Results of the calibration suggest the efficacy of TRANSFER to constrain both in-stream biogeochemical reactions upland nitrate sources, which stems from the ability of SFGL sediments to integrate the isotopic signature through algal growth decompositions dynamics.

Results and modeling frameworks developed herein are applicable to streams and rivers characterized by the SFGL, i.e., low-order systems with low stream and hillslope gradients and high influxes of bioavailable nutrients, promoting pronounced temporary storage and biotic processes. Synthesizing current studies that investigate SFGL would support its prominence in the Southeastern and Midwestern United States, as well as parts of western and eastern Canada suggesting that the SFGL constitutes large land-masses across North America. For systems draining organic rich uplands, e.g., peat catchments or wetlands, results and models in this study should be utilized with caution as upland organic matter can drive fluvial C and N cycling. Similarly, for steep forested systems, leaf litter and detritus governs benthic stream dynamics and autochthounous material is less pronounced due to high canopy cover. Notwithstanding these limitations, the process-based nature of the modeling framework that couples hydrodynamics, sediment transport and biogeochemical cycles, provides flexibility in model parameterization; hence providing scientists and engineers with a starting point to assess fluvial C and N cycling in systems with contrasting watershed characteristics and anthropogenic disturbances. The ambient sediment data collection method proposed herein is a feasible sampling approach since *in situ* samplers are inexpensive and can be built by entry-level researchers, chemical signatures (%C, %N, C:N, $\delta^{13}C$, and $\delta^{15}N$) can be analyzed from a single sample, and sample costs are ~$20/sample when shipped to a stable isotope laboratory. Further work should test the transferability of methods and results proposed herein across spatiotemporal gradients.

Copyright © William Isaac Ford III 2014

APPENDICES

Appendix 1: Quality Assurance Project Plan for Data Collection

Quality Assurance Project Plan

Project Title: South Elkhorn Nitrogen Research

River Basin: Kentucky River

Sub-Catchment: South Elkhorn Creek

Organization: University of Kentucky

Project Co-Managers:

William Ford
Signature Date

Jimmy Fox (Primary)
Signature Date

Carmen Agouridis
Signature Date

Project Laboratory Manager

Jason Backus (KGS)
Signature Date

Erik Pollock (ASIL)
Signature Date

Chris Romanek (UKSIL)
Signature Date

Project Advisors

Lindell Ormsbee
Signature Date

Yitin Wang
Signature Date

Chris Romanek
Signature Date

Section A: Project Management and Objectives
A.1) Distribution List

William Ford
Graduate Associate Department of Civil Engineering
University of Kentucky
161 O.H. Raymond Bldg
Lexington, Kentucky 40506-0281
Phone: 859-494-9464
wiford2@g.uky.edu

Dr. Jimmy Fox
Department of Civil Engineering
University of Kentucky
161 O.H. Raymond Bldg
Lexington, Kentucky 40506-0281
Phone: 859-257-8668
jffox@engr.uky.edu

Dr. Carmen Agouridis
Department of Biosystems and Agriculture Engineering
University of Kentucky
207 C.E. Barnhart Building
Lexington, Kentucky 40546
Phone: 859-257-3000
carmen.agouridis@uky.edu

Dr. Chris Romanek
Department of Earth and Environmental Sciences
University of Kentucky
121 Washington Avenue
Lexington, Kentucky 40506-0053
Phone: 859-257-1952
c.romanek@uky.edu

Jason Backus
Kentucky Geological Survey
University of Kentucky
366 Mining and Minerals Building
Lexington, Kentucky 40506-0107
Phone: 859-257-5500
jbackus@uky.edu

Erik Pollock
University of Arkansas Stable Isotope Laboratory
University of Arkansas
850 W Dickson Street
Fayetteville, Arkansas 72701
Phone: 479-575-4506
epolloc@uark.edu

Dr. Lindell Ormsbee
Kentucky Water Resources Research Institute
University of Kentucky
233 Mining and Minerals Building
Lexington, Kentucky 40506-0281
Phone: 859-257-6329
lormsbee@engr.uky.edu

Dr. Y.T. Wang
Department of Civil Engineering
University of Kentucky
161 O.H. Raymond Bldg
Lexington, Kentucky 40506-0281
Phone: 859-257-5937
ywang@engr.uky.edu

A.2) Project Organization

A.2.1) Roles and Responsibilities, Communication Pathways, and Organizational Chart

The roles and responsibility of the involved parties are detailed below. Figure 1 provides the organizational chart of the project including roles of the associated party and lines representing propagation of information in the project.

William Ford
Graduate Assistant Department of Civil Engineering
University of Kentucky
Role: Graduate Research Associate and Co-Principal Investigator
Responsibilities: Manager of the project, QAPP Development, Transport data to KGS lab and mail to Stable Isotope Lab, Insure data meets all quality requirements, Analyze sediment elemental and stable isotope samples, Perform post-analysis and work to publish dataset

Dr. Jimmy Fox
Department of Civil Engineering
University of Kentucky
Role: Co-Principal Investigator, Primary advisor to the graduate student
Responsibility: Co-manager of the project, Advisor to graduate student and assists with post-analysis and publication of data

Dr. Carmen Fox
Department of Biosystems and Ag. Engineering
University of Kentucky
Role: Co-Principal Investigator
Responsibility: Co-manager of the project

Dr. Chris Romanek
Department of Earth and Environmental Sciences
University of Kentucky
Role: Graduate Student Ph.D. Committee Member, Lab manager of University of Kentucky Stable Isotope Lab.
Responsibility: Advisor to graduate student, Assists with operation of the Elemental Analyzer and Isotope Ratio Mass Spectrometer in the UKSIL.

Jason Backus
Kentucky Geological Survey
University of Kentucky
Role: Lab manager at the Kentucky Geological Survey Laboratory
Responsibility: Performs analysis of streamwater constituent concentrations, Insure proper quality control measures are taken and all protocol are met

Erik Pollock
University of Kentucky Stable Isotope Laborartory
University of Arkansas
Role: Lab Manager of Arkansas Stable Isotope Lab
Responsibility: Performs analysis of streamwater $\delta^{15}N_{NO3}$, Insure proper quality control measures are taken and all protocol are met

Dr. Lindell Ormsbee
Kentucky Water Resources Research Institute
University of Kentucky
Role: Graduate Student Ph.D. Committee Member
Responsibility: Advisor to graduate student

Dr. Y.T. Wang
Department of Civil Engineering
University of Kentucky
Role: Graduate Student Ph.D. Committee Member
Responsibility: Advisor to graduate student

A.2.2) Special Training Requirements and Certification

No special training requirements are required to perform the procedures outlined in this QAPP. The project/data manager has been trained by advisors and laboratory personnel on all of the procedures he will perform, and the project manager will oversee undergraduate students that collect probe data and sediment trap samples. The project manager will visit and learn all laboratory procedures performed in the two labs (KGS and ASIL) that lab work is to be contracted out to.

A.3) Project Planning/ Problem Definition

A.3.1) Project Definition

Environmental Questions and Problems

High dissolved inorganic nitrogen (DIN) loadings from agriculturally and urban impacted stream systems have been highlighted as a governing factor for hypoxic and anoxic conditions in rivers, lakes and estuaries. Hypoxic conditions stem from nuisance algal blooms that deplete the oxygen supply during respiration. Increasing agricultural and urban land use has prompted new regulatory debate to mitigate the impacts (Turner and Rabalais, 1991; Turner and Rabalais, 1994; Diaz and Rosenberg, 1995; Rabalais et al., 1996; Vitousek et al., 1997; Galloway et al., 2008; Seitzinger, 2008; Conley et al., 2009). Increased regulatory action requires tighter

constraint and management of the nitrogen cycle at the watershed scale, which has recently been highlighted as one of the major challenges facing engineers (NAE, 2008).

In fluvial environments, nitrogen occurs primarily as DIN (i.e. nitrate, NO_3, or ammonium, NH_4^+) or particulate nitrogen (PN). The in-stream fate of nitrogen is governed by coupled physical and biological processes. DIN loadings are impacted by flow variability, fertilization and manure, assimilation rate by stream biota, regeneration from the streambed, and coupled nitrification/denitrification processes. Similarly, particulate nitrogen (PN) is impacted by erosion and deposition dynamics, ammonification of organic matter, and assimilation rates.

A need exists to collect ambient measurements of nitrogen phases in the field because laboratory methods do not adequately capture the complex hydrodynamic and biogeochemical processes occurring and numerical models require input and verification data. Collection of an annual dataset of sediment, carbon, phosphorus and nitrogen constituents for water and sediment matrices (Table 1) can aid in understanding inputs, outputs and in-stream processing of nitrogen. Understanding these processes can help to constrain assimilation, nitrification and denitrification rates with the goal of tighter constraint of the stream nitrogen budget. Samples that are collected at high spatial and temporal resolution can help to identify changes in inputs with flow conditions and seasons as well as differences in land use. One of the major questions that we expect this dataset to answer is the extent that bed sediments remove DIN (either through temporary storage or permanent denitrification) from the water column. Here, the isotopic signature of nitrogen for sediment and water constituents are used because it has been shown to be highly sensitive to fractionation processes (Kendall, 1998). Coupling these measurements with elemental concentrations can help disseminate whether assimilation or denitrification is the primary driver for downstream changes in the streamwater DIN loads and at what times of the year these processes are important.

Table 0-1) Summary of Project Data Needs

Analyte	Sample Frequency	Sample Location	Number of Samples
NH_4	Monthly	2 main stem and 4 tribs	82
NO_3	Monthly	2 main stem and 4 tribs	102
DIC	Monthly	2 main stem and 4 tribs	56
DOC	Monthly	2 main stem and 4 tribs	58
DP	Monthly	2 main stem and 4 tribs	56
P	Hourly	Lexington Airport	Continuous
V	Monthly	2 tributaries	Continuous
Q	Continuous 5 minute data	1 main stem	Continuous
C	Event, Weekly, Monthly	2 main strem and 4 tribs	576 (ISCO) 184(Depth integrated)
H	Continuous 5 minute data	2 tributaries	Continuous
Turb	Continuous 5 minute data	1 main stem and 2 tribs	Continuous
Temp	Continuous 5 minute data	2 main sites and 4 tribs	Continuous
$\delta^{15}N_{NO3}$	Monthly	2 main stem and 4 tribs	102
$\delta^{15}N_{NH4}$	Monthly	2 main stem and 4 tribs	82
$\delta^{15}N_{Sed}$	Weekly	2 main stem	104
POC_{Sed}, PN_{Sed}	Weekly	2 main stem	104
Temp, pH, DO, Cond.	Weekly	2 main stem and 4 tribs	184

Full names of the analytes in the above table are ammonium, nitrate, dissolved inorganic carbon, dissolved organic carbon, dissolved phosphorus, precipitation, velocity, flowrate, sediment concentration, flow depth, turbidity, temperature, stable nitrogen isotopic signature of nitrate, stable nitrogen isotopic signature of ammonium, stable nitrogen isotopic signature of transported sediment, particulate organic carbon, particulate nitrogen, temperature, pH, dissolved oxygen and conductivity respectively.

Due to the complexities of nitrogen processes in-stream, and the high expense in collecting high resolution streamwater constituent data, mathematical models, coupled with the aforementioned datasets, can be used as an alternative. Current modeling efforts have been unsuccessful at constraining the stream nitrogen budget as a result of (1) models that don't fully depict the physical system by neglecting the shallow surficial fine sediment layer where biological production and decomposition is prominent and (2) the inability to restrict model uncertainty as a result of highly variable parameters. A partial solution comes from the realization that organic matter in-stream provides a substrate that can enhance removal of DIN from the water column through biogeochemical processes (Arango and Tank, 2008; Findlay et al., 2011; Newcomer et al., 2012). However, quantifying the importance of organic matter deposits as a site of nitrogen removal from streams is lacking and needs to be better constrained.

The objective of this project is to collect constituents of phosphorus, carbon, sediment and nitrogen in order to (1) understand how nitrogen is actively cycled in the streambed sediments of low-order, human disturbed systems, (2) generate a data-based nitrogen budget for the stream nitrogen cycle, and (3) provide an input and calibration dataset for a deterministic nitrogen model. These objectives are motivated by the increasing concern of hypoxic/anoxic conditions that occur in the Gulf of Mexico (Zhou et al., 2010). As a result of excessive nitrogen and phosphorus loads, Kentucky is one of the primary contributors to this problem (Alexander et al., 2008) making it a critical area to assess the function of these streams and reduce uncertainty associated with DIN loadings. To help constrain the budget we plan to collect data of elemental and isotopic signatures of relevant constituents and build a coupled physical and biological modeling framework to constrain the stream nitrogen budget (see Figure 2 for a detailed flow chart of the modeling framework). With regard to the model, data collected during the project will serve as (1) inputs into the hydrologic, sediment, carbon, nitrogen and nitrogen isotope sub-models, (2) be used as calibration and validation for each of the submodels. Detailed spatial and temporal datasets of DIN concentrations and their associated $\delta^{15}N$ signatures will help to better understand nitrogen transfer and removal in streambeds. Simultaneously we also need to continue to collect transported sediment signatures to gain a better understanding of how the DIN signatures are correlated to the transported signatures. Since nitrogen assimilation, nitrification and denitrification processes are significantly impacted by organic carbon cycling; carbon phases in sediment and streamwater are needed. Likewise since carbon assimilation is potentially limited by nutrient availability, bioavailable phosphorus concentrations are needed to

ensure non-rate limiting growth conditions. Preliminary water data was collected at two main stem sites (T1 and T2 in Figure 4) and two small tributaries (F1 and F2 in Figure 4) in order to fine tune an appropriate sampling design for sampling of streamwater constituents. The rationale for the sampling design is discussed in detail in section B.1.

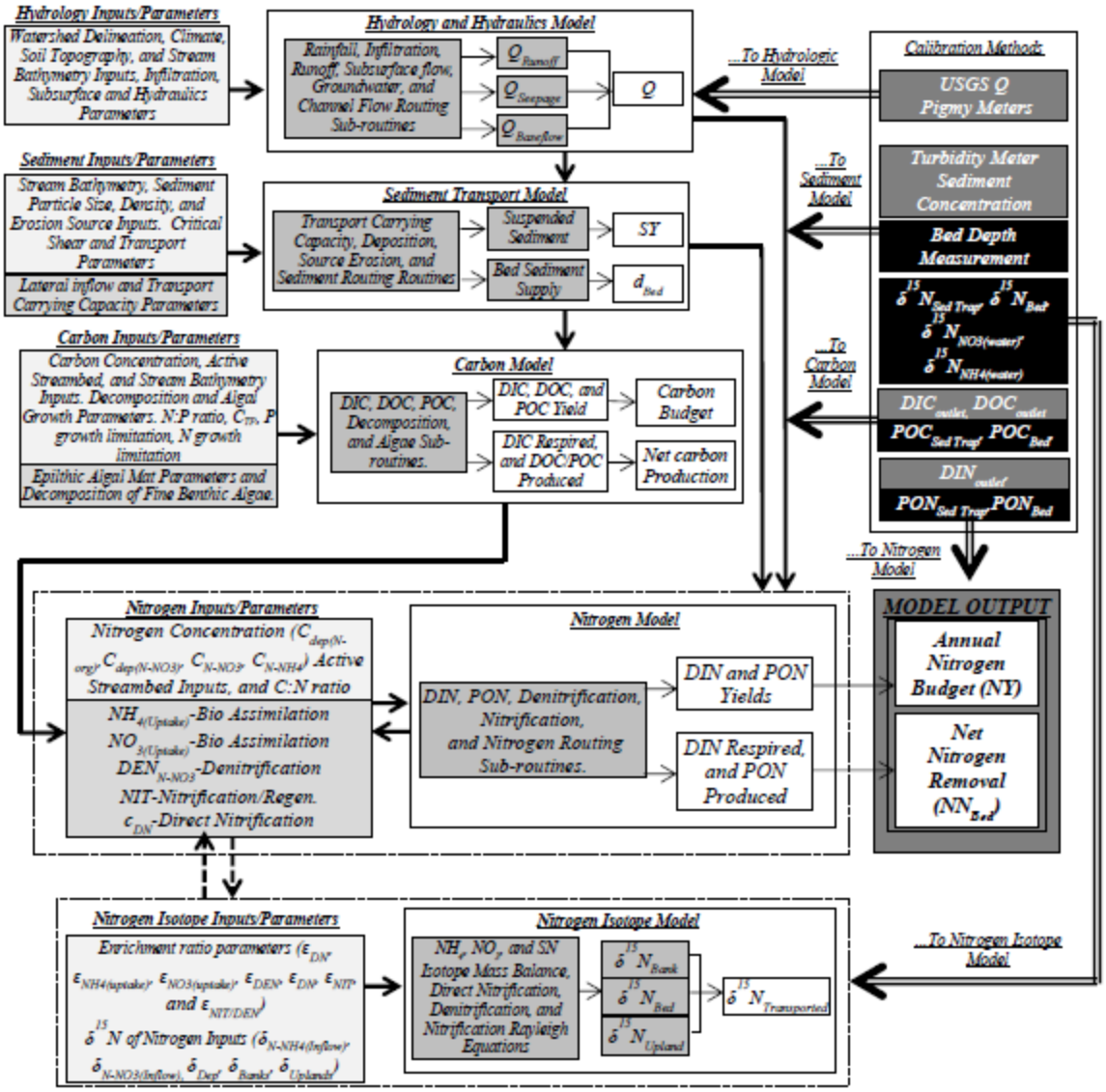

Figure 2. TRANSFER modeling framework including inputs and outputs and calibration data.

Study Watershed

The study site for this project is the Upper South Elkhorn Watershed, located in the Kentucky River Basin (Figure 3). The watershed is primarily located in Fayette County but also extends into Jessamine and Woodford counties. The watershed contains a USGS Gauging station (USGS 03289000) at the watershed outlet and a NOAA weather station (Lexington Bluegrass Airport) directly outside the watershed (Figure 4). The study site drains approximately 62 km^2 consisting of agricultural (57%) and urban (43%) land uses. The main stem of the watershed is third order and is approximately 10 km long (Figure 4). The watershed is characterized by low stream and hillslope gradients coupled with high stream sinuosity. This promotes zones of pronounced temporary sediment storage, estimated at 74% of the stream bed (Fox et al., 2010; Ford and Fox 2012; Russo and Fox 2012). The streambed is controlled by Ordovician limestone (predominantly calcium carbonate with high phosphorus contents), limiting the influence of upwelling and downwelling processes. The presence of pastureland and suburban areas with limestone bedrock promotes high background concentrations of bioavailable phosphorus and nitrogen (see *Previous Monitoring*). Light canopy cover, moderate temperatures and shallow flow depths promote dominance of benthic autochthonous production (Ford and Fox, 2012).

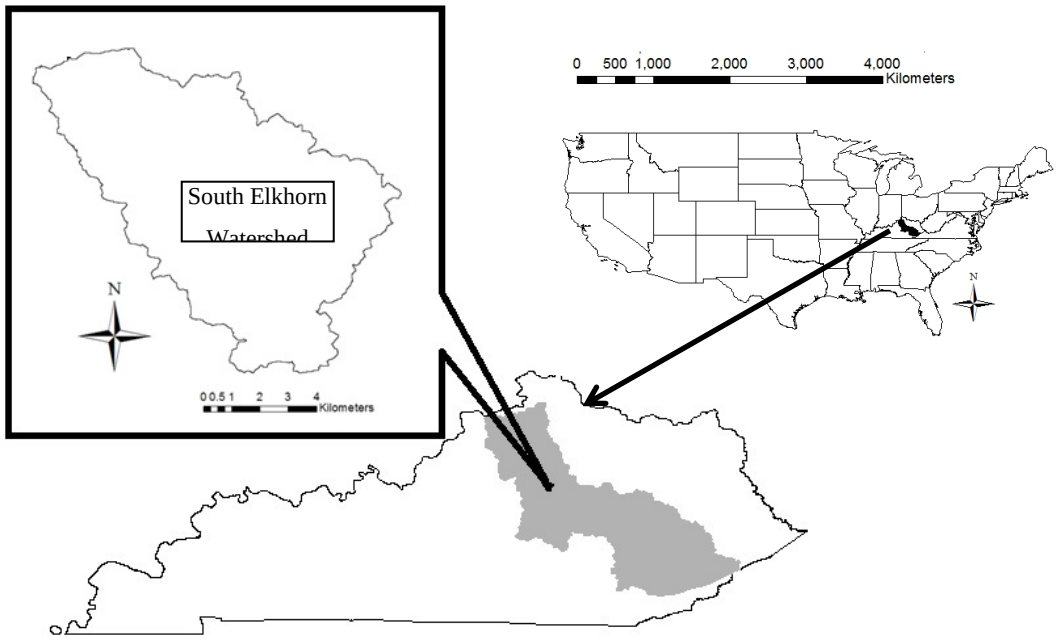

Figure 1) Geographic Location of the South Elkhorn Watershed

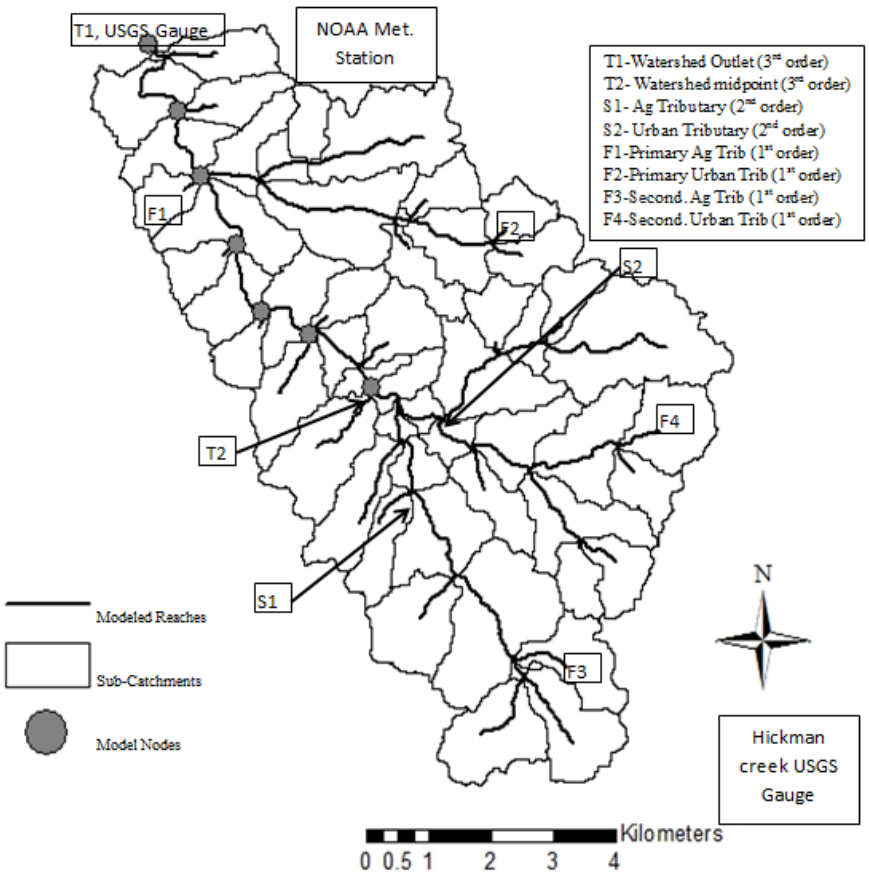

Figure 2) Historic Modeling and Sampling Locations

Previous Monitoring

The South Elkhorn watershed has been heavily monitored since 2006. Figure 5 details all previously collected data for the South Elkhorn including temporal and spatial domains. Preliminary, monthly nutrient concentration and isotope data (e.g. NO_3, NH_4, $\delta^{15}N_{NO3}$, DIC, DOC, DP) was collected from 2010-present. Weekly sampling of organic carbon content (TOC), particulate nitrogen (TN), $\delta^{15}N$ and $\delta^{13}C$ of fine sediment, C:N ratio, depth integrated sediment concentration, pH, DO, Temperature, and Conductivity has been conducted as part of a continued longitudinal study. Point samples of $\delta^{15}N$ of bank and bed sediments have been collected to classify the sources (see Fox et al., 2010). Further, point samples of sediment concentration have been collected during storm events varying in magnitude and duration. Continuous, five minute flowrate, stage and precipitation data have been obtained at the watershed outlet using the USGS gauging station since the beginning of the sampling period. Additionally, deductive numerical sub-models have been derived from a conceptual understanding of the system and published in refereed journals, including sediment transport (Russo and Fox, 2012), particulate organic carbon (Ford and Fox, 2012) and a nitrogen elemental and isotope model (Fox et al., 2010). Generally, the behavior of the system in terms of sediment and sediment carbon is fairly well understood, with model calibration/validation procedures yielding strong goodness-of-fit criteria to measured data in the system.

Figure 6 depicts the results of the calibrated sediment transport and carbon sub-models at the outlet of the watershed (T1). Briefly, results of the sediment model suggest a dynamic, long-term equilibrium in which low-moderate flows scour the sediment bed and high flows deposit excessive sediment loads during the receding limb of the storm event as evidenced by 6a-6c. POC dynamics are governed by biological growth and decomposition of autochthonous material, and sediment transport and erosion/deposition dynamics (Figure 6d-6e). Inorganic and organic dissolved phases of carbon and dissolved phosphorus have also been collected from September 2012 through February 2013 (Figure 6f-h) and were used to help refine the sampling schedule.

The results of the nitrogen dataset are not well understood due to the complexities of the nitrogen cycle. The following outlines some preliminary results observed from data collection of nitrogen concentrations and isotopic signatures in streamwater and sediment constituents.

Up to this point ammonium concentrations in the measured reaches have been below detectable limits.

Nitrate concentrations show distinct seasonality with high concentrations in the late fall and winter and lower concentrations in the spring and summer (Figure 7a).

With regard to spatial variability concentrations decrease with increasing catchment size during low flows suggesting assimilation and removal during these periods. However during higher flows concentrations in T1 and T2 generally fall between the end members of the first order tributaries F1 and F2.

$\delta^{15}N_{NO3}$ results suggest that at higher flows, downstream signatures generally fall between the tributary end-members. Also, as concentration of nitrate increases, the $\delta^{15}N_{NO3}$ signature decreases to around 5 ‰ (i.e. there is seasonality to the signature).

$\delta^{15}N_{NO3}$ shows enrichment occurring with increasing catchment size during the baseflow event but not the low flow event occurring a month later. This could suggest that a different process (one with a more significant fractionation) occurred to the water in transit during the baseflow sample (e.g. coupled nitrification/denitrificaiton vs. assimilation).

Figure 7e depicts the longitudinal trend of ambient measurements of the sediment nitrogen stable isotope signature from T1 and T2. Although the time series appears highly variable, both sites show pronounced seasonal trends and spatial variability. Conversely, data for the elemental signature of sediment nitrogen (Figure 7d) tends to show only the spatial variability and no pronounced seasonal trends.

Based on visual inspection the timing of the nitrogen peaks for $\delta^{15}N_{Sed}$ coincides with that of $\delta^{15}N_{NO3}$.

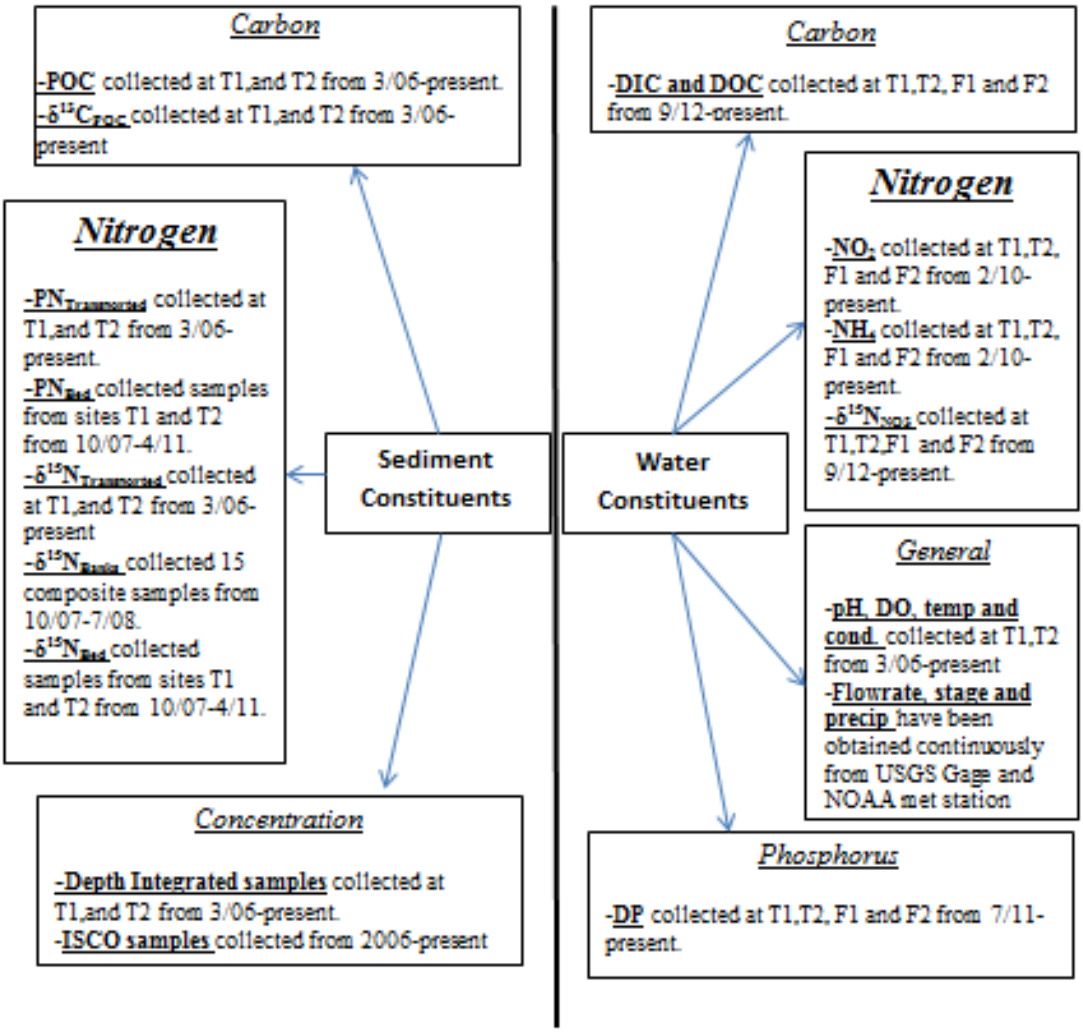

Figure 5) Schematic of previous sample collection efforts from 2006-present.

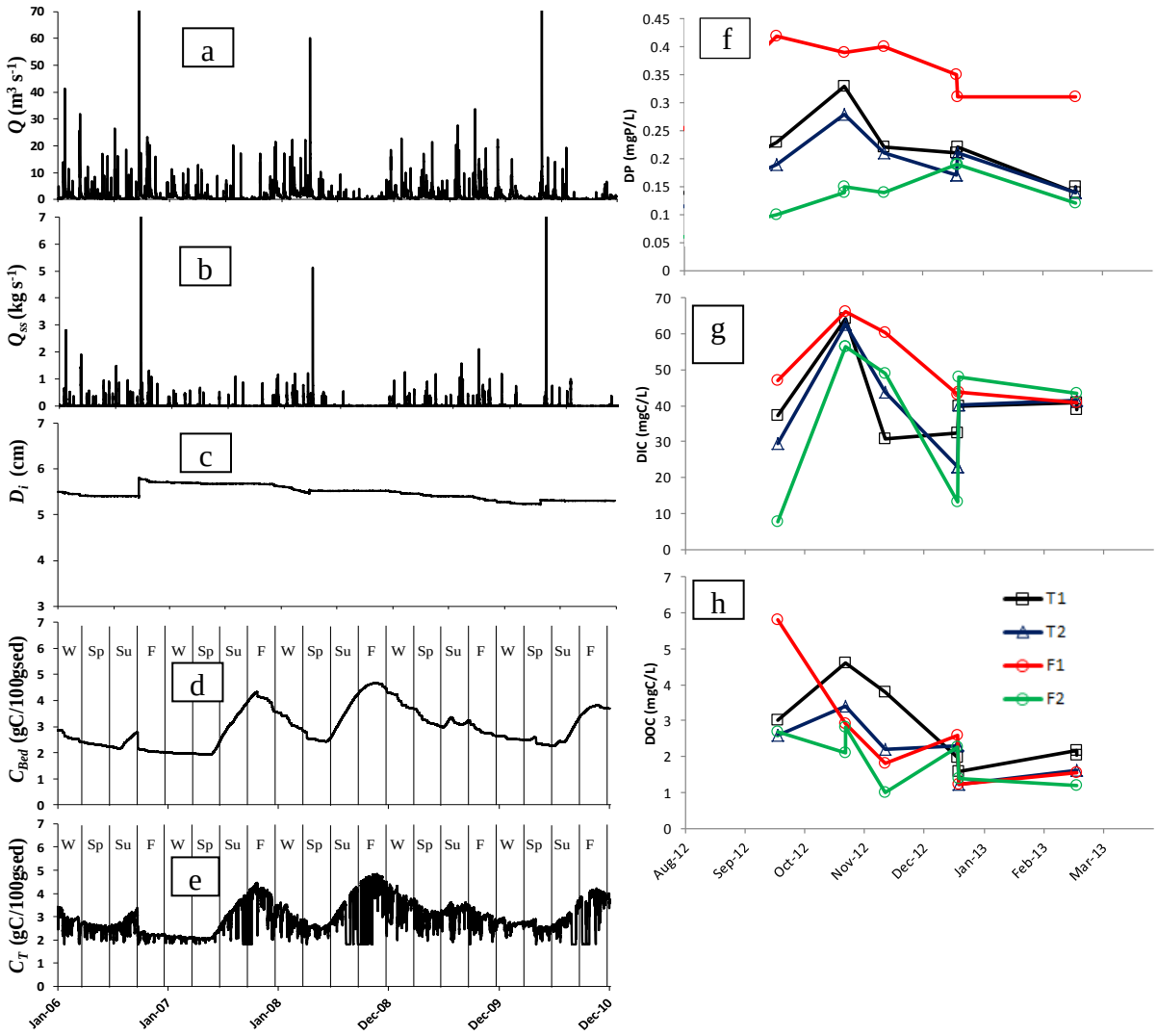

Figure 3) Results of water flow (Q), sediment (Qss) bed depth (D), carbon content of bed sediments (C_{Bed}), carbon content of transported sediments (C_T), dissolved phosphorus (DP), dissolved inorganic carbon (DIC) and dissolved organic carbon (DOC).

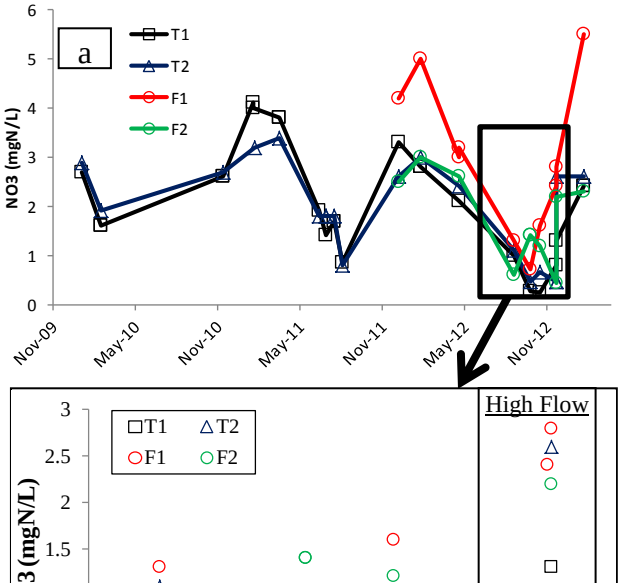

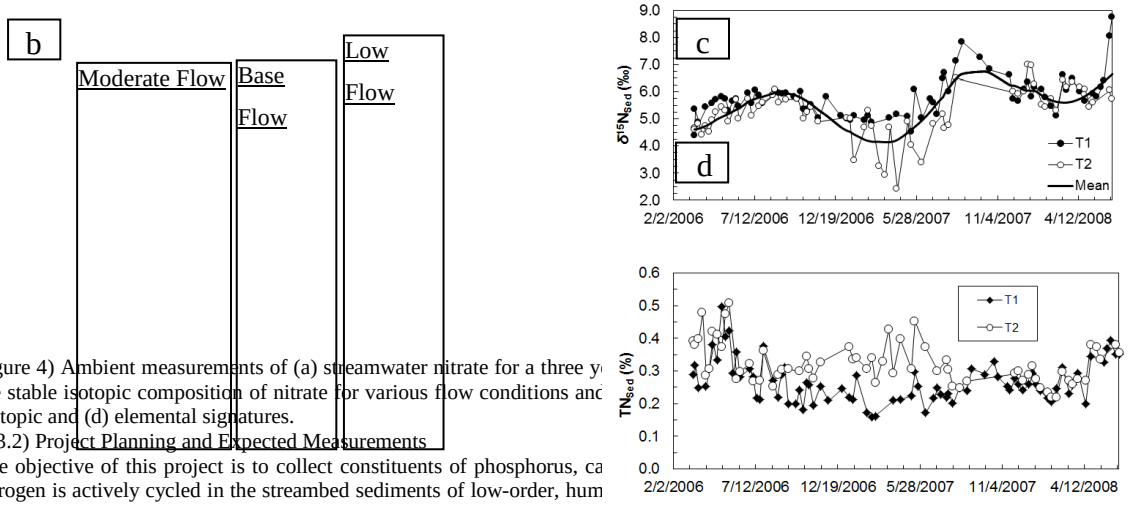

Figure 4) Ambient measurements of (a) streamwater nitrate for a three y the stable isotopic composition of nitrate for various flow conditions and isotopic and (d) elemental signatures.

A.3.2) Project Planning and Expected Measurements

The objective of this project is to collect constituents of phosphorus, ca nitrogen is actively cycled in the streambed sediments of low-order, hum for the stream nitrogen cycle, and (3) provide an input and calibration dataset for a deterministic nitrogen model. The project quality objectives are outlined in section A.4. Sampling, analytical and data review activities are discussed briefly in the following subsections, but are detailed in Part B, with Table 1 summarizing the data collection needs defined during the planning process between the project manager and the primary advisor. Additional, non-analytical, inputs are discussed in section A.4.1.3. Data collection needs stem from the model input and calibration needs observed in Figure 2. Final products and deliverables from the project are outlined in section C.5.

1) Ammonium

Grab samples will be collected at each of the surface water data acquisition stations. These samples will be analyzed for Ammonium. Refer to Section A.6.2 for sampling schedules. Refer to Section B for sample analysis and acquisition methodology.

2) Nitrate

Grab samples will be collected at each of the surface water data acquisition stations. These samples will be analyzed for Nitrate. Refer to Section A.6.2 for sampling schedules. Refer to Section B for sample analysis and acquisition methodology.

3) Dissolved Inorganic Carbon

Grab samples will be collected at each of the surface water data acquisition stations. These samples will be analyzed for Dissolved Inorganic Carbon. Refer to Section A.6.2 for sampling schedules. Refer to Section B for sample analysis and acquisition methodology.

4) Dissolved Organic Carbon

Grab samples will be collected at each of the surface water data acquisition stations. These samples will be analyzed for Dissolved Organic Carbon. Refer to Section A.6.2 for sampling schedules. Refer to Section B for sample analysis and acquisition methodology.

5) Dissolved Phosphorus

Grab samples will be collected at each of the surface water data acquisition stations. These samples will be analyzed for Dissolved Phosphorus. Refer to Section A.6.2 for sampling schedules. Refer to Section B for sample analysis and acquisition methodology.

6) Precipitation

Precipitation data will be obtained continuously at hour intervals using rainfall records available from NOAA for the Lexington Airport. Average rainfall depths for the subwatersheds upstream of each sampling locations will be determined using standard NOAA protocols. No approved EPA method exists for the measurement of precipitation data. Precipitation data will also be obtained from 2 USGS gauging stations (located at the watershed outlet and in an adjacent system). Refer to section A.5 for treatment of secondary data.

7) Fluid Velocity

Fluid Velocity will be obtained from the tributaries using a propellometer at each of the tributaries where sediment concentration is measured. Refer to section A.6.2 for sampling schedules. Refer to section B for sample analysis and acquisition methodology.

8) Flowrate Measurements

Flowrate will be obtained from a USGS gauging station at the watershed outlet. Refer to section A.5 for treatment of secondary data.

9) Sediment Concentration

Suspended sediment samples will be collected at a specified point using Teledyne ISCOs for storm events at the watershed outlet and two tributaries. Depth integrated sediment samples will be collected during weekly (sediment trap) field sampling and during monthly (grab) field sampling. Samples will be brought back to the lab and analyzed for Total Suspended Solids. Refer to section A.6.2 for sampling schedules. Refer to section B for sample analysis and acquisition methodology. A relationship will also be established between TSS and Turbidity to simulate continuous estimates of sediment concentration.

10) Stage

Stage data will be collected at all wadable sites during field visits using a meter stick. The measurements will be made at repeatable locations (e.g. on the front left side of a t-post that is embedded in the streambed) and will measure the distance from the streambed to the water surface.

11) Turbidity

Turbidity measurements will be collected continuously at the two primary tributaries and at the watershed outlet. YSI 600 OMS V2 sondes and YSI 6136 turbidity samplers will be utilized to generate continuous 5 minute measurements. Refer to Section B for sample field acquisition methodology.

12) Temperature

Temperature measurements will be collected continuously at the two primary tributaries and at the watershed outlet. YSI 600 OMS V2 sondes and a thermistor of sintered metallic oxide will be utilized to generate continuous 5 minute measurements. Refer to Section B for sample field acquisition methodology.

13) $\delta^{15}N$ of Nitrate

Grab samples will be collected at each of the surface water data acquisition stations. These samples will be analyzed for $\delta^{15}N_{NO3}$. Refer to Section A.6.2 for sampling schedules. Refer to Section B for sample analysis and acquisition methodology.

14) $\delta^{15}N$ of Ammonium

Grab samples will be collected at each of the surface water data acquisition stations. These samples will be analyzed for $\delta^{15}N_{NH4}$. Refer to Section A.6.2 for sampling schedules. Refer to Section B for sample analysis and acquisition methodology.

15) $\delta^{15}N$ of Transported Sediment, POC and PN

Sediment traps will be placed at the two main stem sites to gather spatially and temporally integrated sediment samples. These samples will be analyzed for $\delta^{15}N$ of Transported Sediment, POC and PN using an elemental analyzer that is interfaced with an Isotope Ratio Mass Spectrometer.

16) Field Parameters

Four different field parameters will be measured at each sampling location. These include water temperature, pH, dissolved oxygen, and specific conductance. These parameters will be measured using a Hach meter during weekly field visits and monthly grab sample visits.

A.4) Project Quality Objectives and Measurement Performance Criteria

All data collected in support of the project will follow standard operating procedures, EPA protocols for *Quality Assurance Project Plans, EPA-505-B-04-900A, 2005* and the *Kentucky Ambient/Watershed Water Quality Monitoring Standard Operating Procedure Manual, 2005.* The latter document provides both quality objectives and criteria (e.g Appendix F – Quality Control Design) which are applicable to both field parameters (i.e. water temperature, specific conductance, pH, and dissolved oxygen) as well as phosphorus grab samples (i.e. nutrients) that will be collected as part of this study. Further, analysis of isotope samples will follow *EPA-Sip/OP.1* which outlines the quality objectives criteria for carbon and nitrogen elemental/isotopic analysis.

A.4.1) Development of Project Quality Objectives Using the Systematic Planning Process

A.4.1.1) Problem Statement

The problem statement is outlined in section A.3.1.

A.4.1.2) Goals of the Study

The primary hypothesis of the study is that $\delta^{15}N$ of DIN and SN can be used to constrain the stream nitrogen budget. Alternatively we hypothesize that the $\delta^{15}N$ measurements don't improve uncertainty in the nitrogen model however the nitrogen budget is still improved by coupling flow, sediment, and carbon processes to for nitrogen inputs. Additional goals of the study include closing the stream nitrogen stable isotope budget in agricultural watersheds by using ambient isotopic measurements of streamwater DIN and of sediment nitrogen.

A.4.1.3) Information Inputs

See section A.3.2 for the analytical inputs needed to fill gaps missing in the Problem Statement. Additional inputs needed for the study includes geospatial data for the watershed including land cover maps, digital elevation models, soil type data, and road maps.

A.4.1.4) Study Boundaries

The proposed dataset will be collected over a 12 month timeframe within a 62 km^2 study basin. Sediment transport and water quality inputs will be collected at the 1 km^2 scale to understand tributary inputs. Intermediate tributaries and main stem sites will be collected to understand spatial variability in the watershed. Sampling was designed around current knowledge and data gaps. See section A.3.1 for justification of the sampling design and timing found in section A.6.

A.4.1.5) Analytical Approach

Samples collected from Sites 1 and 2 in Figure 4 will represent integrated measurements of all upstream activity with Site 1 containing 57% ag and 43% urban. Site 2 represents predominantly urban upstream land use. Site 3 will represent small (~1 km^2) agricultural tributaries, and Site 4 will represent small urban tributaries. Site 5 represents intermediate sized (~10 km^2) agricultural tributaries, and Site 6 will represent intermediate sized urban tributaries. The parameters of interest and there use are outlined in Table 1.

A.4.1.6) Performance or Acceptance Criteria

Detailed information on data quality indicators, performance activities and performance criteria of each analyte can be found in section A.4.2.

A.4.1.7) Detailed Plan for Obtaining Data

See section B.1 for the detailed tasks of collecting data and the attached appendices for data collection methods and analytical procedures.

A.4.2) Measurement Performance Criteria

Measurement Performance Criteria (MPC) are quantified for each analytical process in the below tables in order to address issues associated with (1) precision, (2) accuracy and bias, (3) sensitivity and quantitation limits, (4) representativeness, (5) comparability and (6) completeness (see EPA-505-B-04-900A). The first 4 MPCs are addressed in Tables 2 and 3. Completeness is addressed using the checklist found in Table 4. The completeness form is a tool that provides project managers with a comprehensive checklist of deliverables used to verify the quality of the data through rigorous documentation of the sample collection and analytical procedures. With regard to comparability, samples will be taken from the exact same location each time by staking sampling locations with t-posts that are driven into the streambed. Although Method Detection Limits (MDL) and Quatitation limits (QL) are not clearly defined here, they are defined for each analysis in section A.6.1.

Table 0-2) QC Sample or Measurement Performance Activity

Analyte	**Lab Precision**	**Overall Precision**	**Lab Accuracy/ Bias**	**Overall Accuracy/ Bias**	**Sensitivity**
Ammonium	Standard Duplicates	Sample Duplicates	Standards/ Blanks	Equipment Blank	Based on Instrument
Nitrate	Standard Duplicates	Sample Duplicates	Standards/ Blanks	Equipment Blank	Based on Instrument
Dissolved Inorganic Carbon	Standard Duplicates	Sample Duplicates	Standards/ Blanks	Equipment Blank	Based on Instrument
Dissolved Organic Carbon	Standard Duplicates	Sample Duplicates	Standards/ Blanks	Equipment Blank	Based on Instrument
Dissolved Phosphorus	Standard Duplicates	Sample Duplicates	Standards/ Blanks	Equipment Blank	Based on Instrument
Sediment Concentration	Balance/ Analytical Standard	Sample Duplicates	Standards/ Blanks	Equipment Blank	N/A
$\delta^{15}N$ of Nitrate	Standard Duplicates	Sample Duplicates	Calibrate to strandard	Blanks	Based on Standards
$\delta^{15}N$ of Ammonium	Standard Duplicates	Sample Triplicates	Calibrate to standard	Blanks	Based on Standards
$\delta^{15}N$ of Transported Sediment	Standard Duplicates	Sample Triplicates	Calibrate to standard	Blanks	See EPA SIP/OP.01
POC of Transported Sediment	Standard Duplicates	Sample Triplicates	Calibrate to standard	Blanks	See EPA SIP/OP.01
PN of Transported Sediment	Standard Duplicates	Sample Triplicates	Calibrate to standard	Blanks	See EPA SIP/OP.01

Table 0-3) Measurement Performance Criteria

Analyte	**Lab Precision**	**Overall Precision**	**Lab Accuracy/ Bias**	**Overall Accuracy/ Bias**	**Sensitivity**
Ammonium	RPD ≤10%	RPD≤10%	Standard ±10% Blank <MDL	<MDL	0.05-1 ppm
Nitrate	RPD ≤10%	RPD ≤10%	Standard ±10% Blank <MDL	<MDL	0-40mg/L
Dissolved Inorganic Carbon	RSD≤0.2%	RPD≤10%	Standard 11.7-12.1%C Blank <7 Coulomb	<7 Coulomb	<1-10,000 micrograms
Dissolved Organic Carbon	RPD ≤10%	RPD ≤10%	Standard ±10% Blank <MDL	<MDL	50ppb - 30,000ppm
Dissolved Phosphorus	RPD ≤10%	RPD ≤10%	Standard ±10% Blank <MDL	<MDL	0.05-1mg/L
Sediment Concentration	Balance <0.5mg Standard ±15%	>50mg/L RPD<20% ≤50mg/L ±10mg/L	Standard ±10% Blank <10mg/L	<10mg/L	>10mg/L
δ15N of Nitrate	±0.4‰	±0.4‰	N/A	No peak	0-+54‰
δ15N of Ammonium	±0.25‰	±0.25‰	N/A	No peak	-1.8-+180‰
δ15N of Transported Sediment	±0.5‰	±0.5‰	Standard ±0.5‰ Blank No peak	No peak	0.5-10 Volts
POC of Transported Sediment	SD ±10%	SD ±10%	Standard ±10% Blank No peak	No peak	0-50%
PN of Transported Sediment	SD ±10%	SD ±10%	Standard ±10% Blank No peak	No peak	0-10%

Table 0-4) Completeness Checklist (from EPA-505-B-04-900A)

Item	Description	Verification (completeness)	Validation (conformance to specifications)
Planning Documents/Records			
1	Approved QAPP	**X**	
2	Contract	**X**	
4	Field SOPs	**X**	
5	Laboratory SOPs	**X**	
Field Records			
6	Field logbooks	**X**	**X**
7	Equipment calibration records	**X**	**X**
8	Chain-of-Custody Forms	**X**	**X**
9	Sampling diagrams/surveys	**X**	**X**
10	Geophysics reports	**X**	**X**
11	Relevant Correspondence	**X**	**X**
12	Change orders/deviations	**X**	**X**
13	Field audit reports	**X**	**X**
14	Field corrective action reports	**X**	**X**
Analytical Data Package			
15	Cover sheet (laboratory identifying information)	**X**	**X**
16	Case narrative	**X**	**X**
17	Internal laboratory chain-of-custody	**X**	**X**
18	Sample receipt records	**X**	**X**
19	Sample chronology (i.e. dates and times of receipt, preparation, & analysis)	**X**	**X**
20	Communication records	**X**	**X**
21	Project-specific PT sample results	**X**	**X**
22	LOD/LOQ establishment and verification	**X**	**X**
23	Standards Traceability	**X**	**X**
24	Instrument calibration records	**X**	**X**
25	Definition of laboratory qualifiers	**X**	**X**
26	Results reporting forms	**X**	**X**
27	QC sample results	**X**	**X**
28	Corrective action reports	**X**	**X**
29	Raw data	**X**	**X**
30	Electronic data deliverable	**X**	**X**

A.5) Secondary Data Evaluation

The secondary data, sources, uses, and limitations are summarized in Table 5. Meteorological data including air temperature and precipitation will be used as inputs into the hydrologic and carbon models. These parameters are important because precipitation drives surface runoff and temperature has an impact on evapotranspiration and biological processes. The data will be obtained from a NOAA, National Weather Service (NWS) station located at the Lexington Bluegrass Airport (see Figure 4). The data is discretized temporally at an hourly timestep. A limitation of the data set is that it is located just outside the watershed boundary and may induce error since rainfall doesn't occur uniformly in a basin.

Flowrate at the outlet of the watershed will be used to aid in calibration of the hydrologic model. The USGS gauging station is located at the watershed outlet and has no known limitations (see Figure 4). The estimates are collected continuously at a five minute interval.

Geospatial maps are needed to assess spatial variability of land use, slope and soil type. This information is used as an input for the hydrologic model. Geospatial USGS data including Digitial Elevation Models (DEMs) and National Land Cover Datasets (NLCD) will be used for the sub-basin in question. USDA converges of soils in the region will be utilized. A potential limitation exists in the resolution of the data needing to match the resolution of the model.

Previously published transported sediment (Fox et al., 2010; Russo and Fox, 2012; Ford and Fox, 2012) and bank sediment (Fox et al., 2010) data will be used to assist in model parameterization. Elemental and isotopic signatures of transported sediments were collected using integrated sediment trap samplers. Bank samples were collected at three different depths and pooled to determine average signatures. The data was analyzed using appropriate QC as discussed in this QAPP.

Table 0-5) Secondary data sources, use and limitations

Data type	**Source**	**Data uses relative to current project**	**Factors affecting the reliability of data and limitations on data use**
Meteorological	National Weather Service	Input into hydrologic and Carbon models	Located just outside the watershed boundary
Flowrate at watershed outlet	USGS	Calibration of hydrologic model.	No known limitations.
Digital Elevation Models	USGS	Delineation of watersheds, estimates of upland hillslopes.	Resolution isn't high enough to accurately depict streambed slopes
Landcover Data	USGS-NLCD	Determine the % land use of each sub-basin. Inputs into the hydrologic model	No known limitations
Soils Data	USDA	Needed as an input for the hydrologic model	No known limitations
Carbon Model	Ford and Fox, 2012.	Used as an input for the nitrogen model.	Does not currently include growth/decompostition processes in small tributary streambeds.
Sediment Transport Model	Russo and Fox, 2012.	Used as an input for the nitrogen model.	Needs further refinement in terms of sediment inputs from small tributaries.
Sediment trap data	Fox et al., 2010	Used as tributary input for the sediment, carbon, nitrogen and nitrogen isotope models	Data was collected at the watershed outlet during high flows which assumes those sources are transported during these events
Bank Sediment data	Fox et al., 2010	Used as input for the sediment, carbon, nitrogen and nitrogen isotope models	No known limitations

A.6) Project Overview and Schedule

A.6.1) Project Overview (Outcome of Project Scoping Activities)

Table 6 provides a detailed overview of the project data needs, the laboratory method detection limit (MDL) and the quantitation limit (QL). The MDL is a statistically derived detection limit that represents a 99% confidence level that the reported signal is different from a blank sample and the QL is the minimum concentration of an analyte that can be routinely identified and quantified above the method detection limit. The QL is optimally defined as 10*MDL but can be as low as 3*MDL (see EPA-505-B-04-900A). The analytical procedures and labs were chosen as a result of proximity, temporal and economic feasibility balanced with the desired project quality criteria discussed in section A.4.

Table 0-6) Overview of project data needs, quantitation limits and method detection limits.

Analyte	**Quantitation Limit (QL)**	**Method Detection Limit (MDL)**
Ammonium	0.06 mg/L	0.02 mg/L
Nitrate	0	0
Dissolved Inorganic Carbon	N/A	N/A
Dissolved Organic Carbon	0.9 mg/L	0.3 mg/L
Dissolved Phosphorus	0.06 mg/L	0.02 mg/L
Sediment Concentration	30 mg/L	10 mg/L
δ15N of Nitrate	0.5 Volts	0 Volts
δ15N of Ammonium	0.5 Volts	0 Volts
δ15N of Transported Sediment	0.5 Volts	0 Volts
POC of Transported Sediment	N/A	N/A
PN of Transported Sediment	N/A	N/A

A.6.2) Project Schedule

The below project schedule addresses particular tasks needed to satisfy the sampling procedure described in Task B.1.1. Generally, samples will be collected over a year (February 2013-January 2014) and analysis and subsequent data implementation will be conducted the following 4 months (February 2014-May 2014). The project schedule activities, responsible parties, timeframe of the proposed activity, deliverables and deliverable due dates are addressed in Table 7.

Table 0-7) Project Scheduling Summary

Activity	**Responsible parties**	**Activity Timeframe**	**Deliverable(s)**	**Deliverable due date**
Sample collection-Surface Water	William Ford	Feb 2013-Jan 2014	Field notes	Feb 2014
Sample collection-Sediment Traps	Undergraduate Researchers	Feb 2013-Jan 2014	Field notes	Feb 2014
Sample collection- Sediment Load	William Ford/ Undergraduate Researchers	Feb 2013-Jan 2014	Field notes	Feb 2014
Surface Water Sample Analysis	Jason Backus/ Erik Pollock/ William Ford	Feb 2013-Jan 2014	Report of Analyses for each sample run	Feb 2014
Sediment Trap Sample Preparation	Undergraduate Researchers	Feb 2013-Jan 2014	Laboratory Procedure Spreadsheet	Feb 2014
Sediment Trap Elemental/Isotope Analysis	William Ford/ Dr. Romanek	Feb 2014	Report of Analyses for each sample run	Mar 2014
Sediment Load Sample Analysis	Undergraduate Researchers/ William Ford	Feb 2013-Jan 2014	Report of Analyses for each sample run	Feb 2014
Data Validation	William Ford	Mar 2013- Feb 2014	QAQC Report	Mar 2014
Incorporartion into modeling Framework	William Ford	February 2014-May 2014	Dissertation Research	May 2014

Section B: Measurement/ Data Acquisition

B.1) Sampling Tasks

B.1.1) Sampling Process Design and Rationale

B.1.1.1) Location of Environmental Samples

To generate the desired spatial variability and to assess the importance of watershed scale, samples will be obtained from the sites depicted in Figure 4 in section A.3.2. Four first order streams with drainage areas on the order of 1 km^2 (2 predominantly agricultural and 2 predominantly urban), two second order streams with a drainage area of around 10 km^2 (1 predominantly agricultural and 1 predominantly urban) and 2 third order sites, (1 at the watershed longitudinal midpoint and the other at the watershed outlet) will be monitored. Site selection was motivated by understanding nutrient and carbon inputs from urban and agricultural lands *via* the small tributaries and to assess how alterations occur during downstream transport under various flow conditions.

Sites on the order of 1 km^2 were chosen since they produce stream lengths on the order of 100 meters long. These sites have been identified as important zones for ammonium uptake and transformation (Peterson et al., 2001). During preliminary analysis, trends were noticed in multiple constituents going from lower to higher order systems. To help verify this trend an intermediate (2^{nd} order) set of watersheds was introduced. Finally, the main stem sites offer integration of the two prominent land uses with one site containing predominantly urban drainage and the other is ag dominated.

Site selection was determined based on the following criteria which was obtained from the Kentucky Ambient/Watershed Water Quality Monitoring SOP Manual

Sampler Safety- Expensive sampling equipment will be used to sample sediment load (i.e. the turbidity and ISCO samplers), hence safety of samplers is of the utmost importance. Sites were generally located in 'out of site' secluded areas and lines will be buried.

Accessibility- Sites selected were generally easily accessible from a nearby road in which a parking spot is readily available.

Proximity to a current hydrological Station- The South Elkhorn watershed was partially chosen as the test bed for this study as it has a USGS gauging station 03289000 on the main stem and a meteorological station on the watershed border.

Transport time to laboratories- The South Elkhorn watershed is a short drive (approximately 4 miles) from the University of Kentucky Hydraulics and KGS labs.

Conformation of stream reach sampled- Stream reaches of sampling sites were generally straight riffle sections. This also allows for wading during higher flows to obtain grab samples.

Reach mixing- Monitored stream sections appeared to be well mixed with homogenous pH, DO, and temperature readings in the area surrounding the sampling site.

Backwater effect- Sampling locations were setup upstream of major tributaries (or upstream of the main stem for the small tributaries) to avoid backwater effects.

Other factors- Site safety and authorization to sample from landowners were considered during the site selection process.

B.1.1.2) Scheduling, Number of Samples and Sampling Design Rationale

To meet the desired objectives of the project, the samples mentioned in Table 1 will be collected. Note, that within a given season the order of sampling can be rearranged since hydrologic conditions are highly unpredictable. Therefore, a generic 12 month sampling routine is proposed. The following subsections detail the scheduling, number of samples and design rationale (e.g. why the sample design was selected for each data type). Table 8 displays a summary schedule for water and sediment samples collected throughout the project.

Ammonium- Ammonium samples will be collected once/season at baseflow for all 8 sites suggested. Ammonium samples will also be collected once/season at 8 sites for high flows. In addition, subsurface seepage will be sampled on the receding limb of the hydrograph at the 4 first order sites (F1-F4) for the two largest storm events. 5 blanks and 5 duplicates will also be taken. Preliminary samples suggest that little to no ammonium is present in the sampled stream reaches; however seasonal checks are needed to ensure. Likewise, storm events need to be closely monitored since the majority of transported nitrogen occurs during these periods. A total of ***82*** samples will be collected.

Nitrate- Nitrate samples will be collected once/season at baseflow for all 8 sites suggested. Additionally, nitrate samples will be collected at 4 sites (T1,T2,F1,F2) once per season during baseflow to get additional seasonal and spatial data. Nitrate samples will also be collected once/season at 8 sites for high flows. In addition, subsurface seepage will be sampled on the receding limb of the hydrograph at the 4 first order sites (F1-F4) for the two largest storm events. 7 blanks and 7 duplicates will be taken. Preliminary samples suggest that nitrate is abundant during all seasons and that both seasonal and spatial variability may be important in governing nitrate transport and removal at baseflow. Likewise, storm events need to be closely monitored since the majority of transported nitrogen occurs during these periods. A total of ***102*** samples will be collected.

Dissolved Inorganic Carbon- DIC samples will be collected twice per season at baseflow for three sites (T1, F1, F2) since the signature of the main stem remains fairly constant (based on preliminary results). DIC will also be collected once per season during high flows at T1, F1, and F2. In addition, subsurface seepage will be sampled on the receding limb of the hydrograph at T1,F1 and F2 during the two largest events. 7 blanks and 7 duplicates will be collected. Collection of DIC will help to constrain the stream carbon cycle for the system, which will assist in parameterization of the nitrogen model. Preliminary results suggest that the tributaries represent DIC end members with the main stem site falling somewhere in between depending on flow conditions. A total of ***56*** samples will be collected.

Dissolved Organic Carbon- DOC samples will be collected twice per season at baseflow for four sites (T1, T2, F1, F2) since the signature of shows an increasing trend with increasing drainage area during low flows (based on preliminary results which are consistent with textbook knowledge). DOC will also be collected once per season during high flows at two small tributaries (F1,F2). This results from preliminary storm event data that suggest the DOC signature is consistent throughout the watershed at high flows. In addition, subsurface seepage will be sampled on the receding limb of the hydrograph at F1 and F2 during the two largest events. 7 blanks and 7 duplicates will be collected. Collection of DOC will help to constrain the stream carbon cycle, which will ultimately assist in parameterization of the nitrogen model. A total of ***58*** samples will be collected.

Dissolved Phosphorus- DP samples will be collected twice per season at baseflow for three sites (T1, F1, F2) since the signature of the main stem is fairly constant(based on preliminary results). DP will also be collected once per season during high flows at T1, F1, and F2. In addition, subsurface seepage will be sampled on the receding limb of the hydrograph at T1,F1 and F2 during the two largest events. 7 blanks and 7 duplicates will be collected. Collection of DP will help to constrain the stream carbon cycle since it can provide rate limiting conditions for carbon growth, which will ultimately assist in parameterization of the nitrogen model. Preliminary

results suggest that the tributaries represent DP end members with the main stem site falling somewhere in between depending on flow conditions. A total of ***56*** samples will be collected.

Precipitation- Precipitation will be ***obtained continuously at 1 hour intervals*** from NOAA for the Lexington Bluegrass Airport rain gage. Precipitation data is needed as an input for the hydrologic model.

Fluid Velocity- Fluid velocity will be obtained at the small tributaries, during a range of flows (ideally ***8 storm events*** of varying magnitude) to develop a stage discharge relationship. This will help develop continuous flowrate estimates from the small tributaries.

Flowrate Measurements- Flowrate measurements will be ***obtained continuously at 5 minute intervals***. Flowrates are needed for calibration of the hydrologic model.

Sediment Concentration- Sediment concentrations will be collected for an additional 6-8 storm events using the ISCO automated samplers at three sites (T1, F1, F2) to calibrate the YSI meters. A total of ***576*** samples will be collected. Further, sediment concentration will also be measured using a depth integrated sampler during monthly stream water sampling and weekly sediment trap sampling. A total of ***184*** samples will be collected.

Stage- Stage will be measured at each sampling location during field visits and will be ***obtained continuously at 5 minute intervals*** using bubblers attached to an ISCO (see section B.1.2) at three sites (T1,F1, F2). Stage is a surrogate measurement for discharge and will eventually be utilized to calibrate the hydrologic model.

Turbidity- Turbidity measurements will be ***obtained continuously at 5 minute intervals*** utilizing a YSI probe discussed in section B.1.2. Three stations will be monitored (T1, F1, F2). Turbidity can be used as a surrogate for sediment concentration (Rasmussen, 2009) hence, in combination with flow, we can generate continuous sediment loads at the watershed outlet and the two tributaries allowing a stronger calibration of the sediment transport model.

Temperature- Air temperature will be ***obtained continuously at 1 hour intervals*** from NOAA for the Lexington Bluegrass Airport. Air temperature is needed as an input for the hydrologic model. Water temperature will be ***obtained continuously at 5 minute intervals*** utilizing a YSI probe discussed in section B.1.2. Three stations will be monitored (T1, F1, F2). Continuous water temperature data is important for biological processes in stream and will be used for the carbon growth and decomposition models.

$\delta^{15}N$ of Nitrate- $\delta^{15}N$ of Nitrate samples will be collected once/season at baseflow for all 8 sites suggested. Additionally, $\delta^{15}N$ of nitrate samples will be collected at 4 sites (T1,T2,F1,F2) once per season during baseflow to get additional seasonal and spatial data. Nitrate samples will also be collected once/season at 8 sites for high flows. In addition, subsurface seepage will be sampled on the receding limb of the hydrograph at the 4 first order sites (F1-F4) for the two largest storm events. 7 blanks and 7 duplicates will be taken. Preliminary samples suggest that nitrate is abundant during all seasons and that both seasonal and spatial variability may be important in governing nitrate transport and removal at baseflow. Likewise, storm events need to be closely monitored since the majority of transported nitrogen occurs during these periods. A total of ***102*** samples will be collected.

$\delta^{15}N$ of Ammonium- $\delta^{15}N$ of Ammonium samples will be collected once/season at baseflow for all 8 sites suggested. $\delta^{15}N$ of Ammonium samples will also be collected once/season at 8 sites for high flows. In addition, subsurface seepage will be sampled on the receding limb of the hydrograph at the 4 first order sites (F1-F4) for the two largest storm events. 5 blanks and 5 duplicates will also be taken. Preliminary samples suggest that little to no ammonium is present in the sampled stream reaches; however seasonal checks are needed to ensure. Likewise, storm events need to be closely monitored since the majority of transported nitrogen occurs during these periods. A total of ***82*** samples will be collected..

$\delta^{15}N$ of Transported Sediment, POC and PN- Weekly sediment trap samples from the two main stem sites will be analyzed using an elemental analyzer interfaced with an IRMS for $\delta^{15}N$, POC and PN. A single sample can be used to generate the suite of parameters. These data can be used to calibrate and validate the carbon and nitrogen models and provide temporally and spatially integrated measures of sediment bound transported constituents. A total of ***104*** samples will be collected.

Field Parameters- Field parameters, including pH, conductivity, temperature and DO will be measured using a Hach probe (see section B.1.2) during each field visit. These general field parameters help to further classify the stream reaches and are potentially important independent variables for nitrogen constituents. A total of ***184*** measurements will be taken.

Table 8) Summary of the monthly sampling routine. Refer to Figure 4 for the site locations. * Samples collected on a weekly basis.

Constituent	Flow	Winter-1	Winter-2	Winter-3	Spring-1	Spring-2	Spring-3	Summer-1	Summer-2	Summer-3	Fall-1	Fall-2	Fall-3
NH_4	Base	All sites			All sites			All sites			All sites		
	Storm		All sites			All sites			All sites			All sites	
	Seepage		F1-F4						F1-F4				
NO_x	Base	All sites		T1, T2,F1,F2	All sites		T1, T2,F1,F2	All sites		T1, T2,F1,F2	All sites		T1, T2,F1,F2
	Storm		All sites			All sites			All sites			All sites	
	Seepage		F1-F4						F1-F4				
DIC	Base	T1,F1,F2		T1,F1,F2	T1,F1,F2		T1,F1,F2	T1,F1,F2		T1,F1,F2	T1,F1,F2		T1,F1,F2
	Storm		T1,F1,F2			T1,F1,F2			T1,F1,F2			T1,F1,F2	
	Seepage		T1,F1,F2						T1,F1,F2				
DOC	Base	T1,T2,F1,F2		T1,T2,F1,F2	T1,T2,F1,F2		T1,T2,F1,F2	T1,T2,F1,F2		T1,T2,F1,F2	T1,T2,F1,F2		T1,T2,F1,F2
	Storm		F1,F2			F1,F2			F1,F2			F1,F2	
	Seepage		F1,F2						F1,F2				
DP	Base	T1,F1,F2		T1,F1,F2	T1,F1,F2		T1,F1,F2	T1,F1,F2		T1,F1,F2	T1,F1,F2		T1,F1,F2
	Storm		T1,F1,F2			T1,F1,F2			T1,F1,F2			T1,F1,F2	
	Seepage		T1,F1,F2						T1,F1,F2				
$\delta^{15}N_{NO3}$	Base	All sites		T1, T2,F1,F2	All sites		T1, T2,F1,F2	All sites		T1, T2,F1,F2	All sites		T1, T2,F1,F2
	Storm		All sites			All sites			All sites			All sites	
	Seepage		F1-F4						F1-F4				
$\delta^{15}N_{NH4}$	Base	All sites			All sites			All sites			All sites		
	Storm		All sites			All sites			All sites			All sites	
	Seepage		F1-F4						F1-F4				
C	Base	*All sites	*All sites	*All sites	*All sites	*All sites	*All sites	*All sites	*All sites	*All sites	*All sites	*All sites	*All sites
	Storm	T1,F1,F2	T1,F1,F2		T1,F1,F2	T1,F1,F2		T1,F1,F2	T1,F1,F2		T1,F1,F2	T1,F1,F2	
	Seepage	T1,F1,F2	T1,F1,F2		T1,F1,F2	T1,F1,F2		T1,F1,F2	T1,F1,F2		T1,F1,F2	T1,F1,F2	
$*\delta^{15}N_{Sed}$	Flow Integrated	T1,T2	T1,T2	T1,T2	T1,T2	T1,T2	T1,T2	T1,T2	T1,T2	T1,T2	T1,T2	T1,T2	T1,T2
$*POC_{Sed}$ PN_{Sed}	Flow Integrated	T1,T2	T1,T2	T1,T2	T1,T2	T1,T2	T1,T2	T1,T2	T1,T2	T1,T2	T1,T2	T1,T2	T1,T2

B.1.1.3) Design Assumptions

The following assumptions are associated with the selected sample design.

Selected tributaries are representative of their respective land use across the watershed.

Since urban and ag practices are fairly homogenous across the watershed, this is justifiable.

It's assumed that the sampling design frequency is sufficient to capture seasonal variation in key constituents.

Based on results of Ford and Fox, *in progress* monthly sampling frequency is adequate to capture the distribution of the population.

It is assumed that the detailed sampling of the 4 storm events will be sufficient for providing a representative range of flow conditions and that each storm event sampled is representative of storm events occurring in the season.

By only sampling ammonium once per season at base flow we assume that the seasonal value is constant.

This is reasonable because ammonium concentrations are representative of upland practices which generally aren't varying drastically on a short time scale.

Assumes that no significant land use changes will occur over the sampling duration.

We will monitor for development or changing land use practices.

By sampling using grab sample methods, it is assumed dissolved constituents are uniformly distributed in the water column.

Diffusion and well mixed streamwater promote uniformity with depth.

B.1.1.4) Validation of Nonstandard Methods

No nonstandard methods are required for this project.

B.1.2) Sampling Procedures and Requirements

The following sections describe the procedures and requirements to collect samples in the field and deliver them to the laboratory. Standard operating procedures (SOPs) and reference material can be found in the Reference and Appendix sections.

B.1.2.1) Sample Collection Procedures

The following subsections outline the procedures used to collect samples used in this project.

Ammonium, Nitrate, Dissolved Inorganic Carbon, Dissolved Organic Carbon, Dissolved Phosphorus, $\delta^{15}N$ of Nitrate, $\delta^{15}N$ of Ammonium - The direct method for streams (EPA #EH-01) will be utilized to sample NH_4^+, NO_3, DIC, DOC, DP, $\delta^{15}N_{NH4,NO3}$ at each site. After the bottle is rinsed in the stream water, the sample is collected by placing the bottle under the water surface with the opening pointing upstream. The sampler will remain downstream of the container and the sample will be collected in a downstream to upstream motion without disturbing the substrate.

Precipitation- Data will be collected from the NOAA website monthly and stored in an appropriate database (discussed in section B.5).

Fluid Velocity- In-stream vertical velocity profiles will be measured for a range of flows at quarter, half and three quarter stations in the stream cross-section using a Gurley Pigmy propeller meter. Operation of the Gurley meter will follow manufacturer specifications (Gurley, 2004).

Flowrate Measurements- Data will be collected from the NOAA website monthly and stored in an appropriate database (discussed in section B.5).

Sediment Concentration- Sediment concentration will be collected using an automated pump sampler to collect dense concentration data during storm events. Methods for probe measurement, i.e., programming and operation, will follow manufacturer specifications (Teledyne, 2009). Further, an isokinetic-depth integrated sampler will be used to estimate sediment concentrations at fixed stations using accepted USGS methods for sample collection (USGS, 2003).

Stage- Stage will be measured at quarter, half and three quarter stations in the stream cross-section and average stage will be reported for each site. Stage is collected continuously at T1, F1 and F2 using Teledyne ISCO Bubbler Modules (see Teledyne-Bubbler Document in the Appendix).

Turbidity and Temperature- Turbidity and temperature will be sampled in the field using a YSI 600 OMS Multiparameter Sonde with a 6136 Turbidity probe. Methods for probe measurement and calibration will follow manufacturer specifications (YSI, 2011). The probe will be maintained weekly in the field and calibrated once per month in the lab.

$\delta^{15}N$ of Transported Sediment, POC and PN- Sediment trap samplers will be left in the field for a week at a time to generate a spatially and temporally integrated measure of $\delta^{15}N$ of Transported Sediment, POC and PN. Briefly, at the front of the trap (inlet) a 4mm diameter inlet tube allows acceleration of fluid into a 98mm diameter test section. The increase in area results in sedimentation, and subsequent trapping of fine sediments. The fluid exits the test section through another 4mm tube. This method was originally published in Phillips et al. (2000) and has been utilized for published studies in the watershed selected for this project (Fox et al., 2010; Ford and Fox, 2012).

Field Parameters- DO, conductivity, pH and water temperature will be sampled in the field using a Hach handheld meter with the appropriate probes. Methods for probe measurement and calibration will follow manufacturer specifications (Hach, 2006). The probes will be calibrated prior to and after sampling.

B.1.2.2) Sample Containers, Volume and Preservation

In the field, bulk samples will be collected for the suite of water quality parameters (NH_4^+, NO_3, DIC, DOC, DP, $\delta^{15}N_{NH4,NO3}$) in pre-cleaned I-Chem, wide mouth, 1000 mL, HDPE, plastic bottles (which are EPA approved for water quality sample collection). For collection containers of sediment and sediment trap samples see the following sub-headings. Differing trains of thought are present on whether samples should be filtered in the field or in the lab. Field conditions are uncontrollable; hence there are numerous routes in which the sample can become contaminated. Therefore, for this study, samples will be collected (unfiltered) in the field and brought back to the lab immediately for filtration. Based on the sample collection guide from the USDA (Turk, 2003) samples that are most susceptible to degradation are ones that have high suspended solids (which are relatively low based on previous TSS analysis at baseflow) or samples analyzed for trace constituents. Samples will be filtered using Whatman Glass Fiber 0.7µm, 47mm filters and then separated into their respective splits for analysis (see the following subheadings). The total require volume of samples (see below) is 815 mL, hence the 1000 mL bottle will provide plenty of extra sample in case of a spill. During transport of water quality samples back to the lab, the samples are placed in zip lock bags to avoid contamination and then placed in a cooler to refrigerate the sample to 4^0C.

Ammonium- Filtered ammonium samples are poured into pre-cleaned 250mL glass amber I-CHEM bottles and subsequently acidified using 10-15 drops of concentrated sulfuric acid H_2SO_4 (see KGS 4500-NH_3-F which stems from standard methods) to a pH<2. Samples are then refrigerated to 4^0C and have a holding time of 28 days. For the NH_4 split a minimum of 100 mL of the sample is needed.

Nitrate, Dissolved Inorganic Carbon, Dissolved Phosphorus- Filtered nitrate, DIC and DP samples are poured into pre-cleaned 250mL HDPE I-CHEM bottles without acid preservation (see KGS 9056, KGS DIC SOP, and KGS D515/ASTM D515). Samples are then refrigerated to 4°C and have a holding time of 28 days. For the NO_3, DIC, DP split, a minimum of 150 mL of sample is needed.
Dissolved Organic Carbon- Filtered nitrate samples are poured into pre-cleaned 40mL I-CHEM VOA/TOC vials (Part # IC-360040) and preserve with 1ml/L of phosphoric acid, H_3PO_4 (see KGS 9060/Standard Methods for Examination of Water and Wastewater Method 5310-B). Samples are then refrigerated to 4°C and have a holding time of 28 days. For the DOC split a minimum of 40 mL of sample is needed with no headspace.
Sediment Concentration- Depth integrated suspended sediment samples will be collected in pint, plastic containers, of which about ¾ is filled with sample. Automated samplers will collect 750 mL of sample in 1000 mL plastic bottles (see Teledyne ISCO manual). The samples will be stored in coolers at 4°C until they can be refrigerated at 4°C in the UK hydraulics lab. Holding times are up to 7 days as per EPA 160.2.
$\delta^{15}N$ of Nitrate- Filtered $\delta^{15}N_{NO3}$ samples are poured into pre-cleaned 125 mL HDPE I-CHEM bottles without acid preservation (USGS RSIL, 2003a). Samples are then refrigerated to 4^0C and have a holding time of 4 weeks. For the NO_3, DIC, DP split, a minimum of 125 mL of sample is needed.
$\delta^{15}N$ of Ammonium- Filtered $\delta^{15}N_{NH4}$ samples are poured into 2 pre-cleaned 250 mL HDPE I-CHEM bottles without acid preservation. Although the protocol calls for preservation with acid, samples are not acidified since the concentration is not important and microbes have been filtered out. Samples are then refrigerated to 4°C and have a holding time of 28 days. For the $\delta^{15}N_{NH4}$ split, 400 mL of sample is needed.
$\delta^{15}N$ of Transported Sediment, POC and PN- Samples are collected in a sediment trap as described in Phillips et al. (2000). Approximately 8L of a sediment/water mixture is poured into clean 5 gallon buckets. The samples are preserved by refrigerating at 4°C to minimize microbial transformations. Samples are spun down and de-watered to a steady (freeze-dried) state as quickly as possible.
Precipitation, Fluid Velocity, Flowrate Measurements, Stage, Turbidity,Temperature, Field Parameters- Not applicable.

B.1.2.3) Equipment/Sample Containers Cleaning and Decontamination Procedures

All sample containers for water quality and sediment analysis will be new, pre-cleaned, disposable equipment and does not require decontamination. For bottles, and containers used to collect sediments and for the filtration apparatus in the KGS and UK hydraulics lab, standard decontamination procedures for equipment cleaning and decontamination (KDOW, 2005) will be followed.

B.1.2.4) Field Equipment Calibration, Maintenance, Testing and Inspection Procedures

Equipment Calibration- The only non-analytical equipment that needs calibration is the Teledyne ISCO automated grab sampler. Lines for the automated grab sampler will periodically be replaced and the program will be calibrated to ensure that the appropriate volume of sample is obtained. Procedures outlined in the manufacturer's manual will be followed. The date of line replacement and calibration will be denoted in the "South Elkhorn TSS and Turbidity Fieldbook" discussed in B.1.2.6.
Maintenance, Testing and Inspection-Before sampling all equipment will be inspected to ensure it has been cleaned and is in proper working condition. Sampling will be done on an event-by-event basis (this includes baseflow sampling) and will be somewhat unpredictable with regard to timing. Sampling failure can only be ascertained after an event, and as such, any opportunity for capturing samples from a particular event will have passed. Therefore, after each event, all equipment will be thoroughly inspected to ascertain if failure occurred, and if so, the nature of the failure. Information concerning the failure will be recorded in the Equipment Maintenance/Failure Log (which stems from the corrective actions response log--Figure 12. Steps will then be taken to repair or replace the equipment. Additional monitoring equipment will be available for replacement if any equipment fails in the UK Hydraulics Laboratory.
Responsible person- William Ford, Graduate Student, University of Kentucky.

B.1.2.5) Sampling Supply Inspection and Acceptance Procedures

B.1.2.5.1) Supplies for cleaning equipment

Simple Green All-Purpose Cleaner (Phosphate free)---Lowes/Home Depot
Special precaution will be taken not to contaminate the cleaner by using designated bottles for the cleaner.
Acetone Optima*, High purity mobile phase for HPLC and/or extraction solvent for GC applications---Fischer Scientific
Reagent lot numbers will be recorded for their use duration in a laboratory notebook.
Special precaution will be taken not to contaminate the reagent by using designated bottles for the reagent.
Note: If any supplies are known to have become contaminated they will be removed and new supplies will be utilized. Any such incident will be documented accordingly.

B.1.2.5.2) Responsible persons for checking supplies and implementing protocol-

William Ford, Graduate Student, University of Kentucky.
Undergraduate Students, University of Kentucky

B.1.2.6) Field Documentation Procedures

Grab Samples- For collection of grab samples a notebook titled "South Elkhorn Streamwater Sampling/Nutrient Sampling Fieldbook" will be utilized. Each collection site will get its own section of the notebook and will denote the following characteristics.
A visual schematic of the sampling site including significant objects and the sampling location
Further columns in the notebook will be used to denote the following stream measurements.
Sample Date/Time
Site ID
pH
DO
Temp
Conductivity
Comments (e.g. site conditions, any problems or abnormalities)
Fluid Velocity- Fluid velocity and flow depth measurements will be logged on the Fluid Velocity Sample Collection Log (Figure 8).

Sediment Concentration- To keep up with sediment concentration sampling in the field, a notebook called "South Elkhorn TSS and Turbiditiy Sampling Fieldbook" will be used. Sediment concentrations will be collected using two methods as discussed before, and each will have their own section of the notebook.
Depth Integrated Sediment Samples
Site
Date/Time
Flow depth
Comments (e.g. Problems with sampler, site conditions)
Automated Sampler (Teledyne ISCO)
Site
Date/Time
Bottles Replaced (Y or N)
Data Uploaded (Y or N)
Samples Obtained (Y or N)
Sampling Problems (e.g. No trigger, dead battery, some samples not full, etc)
Depth of nozzle from bed (z^*)
For the Automated sampler a separate maintenance section will be appointed to the notebook for maintenance of the sampler in the field.
Stage- Stream stage measurements will be logged on the Stream Stage Sample Collection Log (Figure 9).
Sediment Trap Samples- For collection of sediment trap samples a notebook titled "South Elkhorn Weekly Sediment Trap Fieldbook" will be utilized. Each collection site will get its own section of the notebook and will denote the following characteristics.
A visual schematic of the sampling site including significant objects and the sampling location
Further columns in the notebook will be used to denote the following stream measurements.
Sample Date/Time
Site ID (Carried throughout the Analysis Procedure)
Condition of the tube (e.g. clogged, clear, rotated, raised off bed)
Depth of the tube after installation
pH
DO
Temp
Conductivity
Comments (e.g. site conditions, any problems or abnormalities)
B.2) Analytical Tasks
B.2.1) Sample Preparation for Analysis
Methods used to prepare samples for analytical procedures need to be documented to understand potential sources of error. For preparation procedures see the Appendix section the SOPs in the Appendix section.
B.2.2) Analytical SOPs
The following table provides a summary of the analytical SOPs used in this document. For more detailed information on how to perform any of the analytical procedures, please refer to the Appendix or Reference sections.

Table 0-8) Analytical Standard Operating Procedure Summary

Analyte	**SOP Ref.**	**Title and Date**	**Definitive or Screening Data**	**Modified for Project? Y/N**
Ammonium	KGS 4500-NH_3-F/ SMEWW-Method 4500-NH_3-F	KGS- Ammonium as Nitrogen in Water, January 2009 (Derived from "Standard Methods for the Examination of Water and Wastewater", 1998, pg.4-108)	Definitive	N
Nitrate	KGS 9056/ ASTM vol. 11.01 D4327	KGS- Ion Chromatography of Water, January 2009 (Derived from "Standard Test Method for Anions in Water by Chemically Suppressed Ion Chromatography", 1996)	Definitive	N
Dissolved Inorganic Carbon	KGS DIC	Dissolved Inorganic Carbon SOP, January 2009. (Derived from UIC Carbon Dioxide Coulometer Application Note 1 and 3)	Definitive	N
Dissolved Organic Carbon	KGS 9060/ SMEWW-Method 5310-B	Total/Dissolved Organic Carbon in Water, January 2012 (Derived from "Standard Methods for the Examination of Water and Wastewater", 1998, pg.4-108)	Definitive	N
Dissolved Phosphorus	KGS D515/ ASTM vol. 11.01 D515	KGS- Total Phosphorus in Water, April 2011. (Derived from "Standard Methods for the Examination of Water and Wastewater", 1998, pg. 24)	Definitive	N

Analyte	SOP Ref.	Title and Date	Definitive or Screening Data	Modified for Project? Y/N
Fluid Velocity	GPI (2004)	Gurley Precision Instruments Hydrological Equipment Operation and Maintenance Guide, 2004	Definitive	N
Sediment Concentration	EPA 160.2	Residue, Non-Filterable (Gravimetric, Dried at 103-105°C), 1971.	Definitive	N
Stage	Teledyne (2011)	730 Bubbler Module Installation and Operation Guide, 2011	Definitive	N
Turbidity	YSI (2006)	6-series Multiparameter Water Quality Sondes, 2006	Definitive	N
Temperature	YSI (2006)	6-series Multiparameter Water Quality Sondes, 2006	Definitive	N
$\delta^{15}N$ of Nitrate	Coplen et al. (2012)	Determination of the $\delta^{15}N$ and $\delta^{18}O$ of nitrate in water; RSIL lab code 2900, chap. 17 of Stable isotope-ratio methods. Revised in 2012	Definitive	Y-See revised analytical SOP in Appendix 11
$\delta^{15}N$ of Ammonium	Hannon and Bohlke (2008)	Determination of the $\delta(^{15}N/^{14}N)$ of ammonium (NH_4+) in water: RSIL lab code 2898, chap. C15 of Révész, Kinga, and Coplen, Tyler B., eds., Methods of the Reston Stable Isotope Laboratory: U.S. Geological Survey, Techniques and Methods, 10–C15, 30 p., 2008.	Definitive	Y-See revised analytical SOP in Appendix 12
$\delta^{15}N$ of Transported Sediment	EPA SIP/OP.01	Analysis of Environmental Samples Using Continuous Flow Gas Isotope Ratio Mass Spectrometry, January 1999.	Definitive	Y-See revised analytical SOP in Appendix 13
POC, PN of Transported Sediment	EPA SIP/OP.01	Analysis of Environmental Samples Using Continuous Flow Gas Isotope Ratio Mass Spectrometry, January 1999.	Definitive	Y-See revised analytical SOP in Appendix 13
Temp, pH, DO, Conductivity	Hach (2006)	HACH HQ Series Portable Meters User Manual, Edition 5, 2006	Definitive	N

B.2.3) Field Analytical Instrument Calibration Procedures

B.2.3.1) Instruments Requiring Calibration

YSI turbidity probe

The YSI 600 OMS Sonde with a 6136 Turbidity probe will be used to determine turbidity continuously in the streamwater. Sonde calibration is site dependent and will likely be an iterative process. Preliminarily the plan is to calibrate the probe monthly, but maintain on a weekly basis and check for deviation from the calibrated values bimonthly using a field meter.

Hach ph, DO, and conductivity probes

The Hach session156 Portable Multiparameter Meter will be used to determine conductivity, dissolved oxygen, and pH content. The meter will be calibrated in the laboratory before and after each series of field testing. The meter will be calibrated approximately halfway through each sampling event. All post-calibration measurements will be recorded in the calibration log for that instrument. Initial and post-calibration values will be compared and any substantial discrepancies in both the calibration log and on the appropriate field data sheet will be notes.

B.2.3.2) Instrument Calibration Methods

Turbidity probe calibration

Acceptable standards for use with the YSI turbidity probe are detailed in Standard Methods for the Treatment of Water and Wastewater (Section 2130B). YSI 6073G is a 123NTU Formazin standard purchased from Fondriest. Two point calibration is used in which the zero point is Deionized organic free water and the second point is the 123 NTU standard. Calibration steps are:

Open up the Ecowatch software to perform the calibration.

Select the 2-point option to calibrate the turbidity probe using only two calibration standards (One clear water-0 NTU, One formazin standard 123 NTU).

Immerse the sonde in the 0 NTU standard and press enter.

The screen will display real-time readings that will allow determination of reading stabilization.

Pressing enter will confirm the first calibration.

Place the sonde in the second turbidity standard and input the correct turbidity value in NTU and press enter.
After the readings have stabilized press enter to confirm the calibration (make sure to record the value that the probe stabilized at for both calibration points).
Conductivity probe calibration
Hach's Conductivity probe uses a 1000 µS/cm (at 25 °C) NaCl standard solution. For typical applications with conductivity of 0–10,000 µS (10 mS/cm), calibrate with this standard to achieve the accuracy specified for the meter. Calibration steps are:
Make sure the meter is in Conductivity Reading mode.
Place the probe in the conductivity standard. Agitate the probe to dislodge bubbles in the cell. Avoid resting the probe on the bottom or side of the container.
Press CAL. Icons that represent the active navigation keys will appear in the lower part of the display. The meter will recall the most recent type of calibration. Look at the units field to see what kind of calibration is active.
Scroll to the preferred units using the UP or DOWN ARROWS.
Use the number keys to change the numeric value, if desired. The value entered must be the standard's conductivity value at a reference temperature of 25 °C. (Note: All Hach standards have the conductivity value corresponding to the 25 °C reference temperature printed on their labels. It is not necessary to fill up the numeric entry screen before moving on. To clear the numeric display, press CE.)
When the value and units are correct, press ENTER to calibrate on the standard. The meter automatically corrects the calibration measurement to the 25 °C reference temperature using the NaCl-based, non-linear temperature coefficient.
The meter will return to Conductivity Reading mode when the calibration is finished.

pH and temperature probe calibration
Prepare three pH buffers according to the electrode instruction manual. Choose from 1.68, 4.01, 7.00 (or 6.86), 10.01, and 12.45 pH buffers. (Note: Use a 6.86 or 7.0 pH buffer for the mid-range buffer.)
Turn the instrument on. From the pH Reading mode, press CAL. CAL and flashing ? will appear in the upper display area, along with Standard and 1.
Place the pH electrode in one of the buffers.
Press READ. The instrument will automatically recognize the calibration buffer value. The temperature and pH values will be updated until a stable reading is reached. [(Note: The pH values for the buffers are given for 25 °C. If the calibration buffer temperature is not 25 °C, the pH values displayed for the buffers will reflect the correct pH value for the calibration buffer temperature.) (Note: If the meter is measuring in pH mode, it automatically moves to the next calibration step when the reading stabilizes (indicated by three beeps). If measuring in mV mode, the meter beeps three times when the reading stabilizes. Press ENTER to accept the reading.)]
When the reading has stabilized or been accepted, the standard number will change to 2.
Remove the probe from the first buffer and rinse with deionized water. Place the probe in the second buffer.
Press READ. The temperature and pH values will be updated until a stable reading is reached.
When the reading has stabilized or been accepted, the standard number will change to 3. (To accept this calibration after two points, press EXIT. Press ENTER to accept the calibration or EXIT to cancel the calibration without saving it.)
Remove the probe from the second buffer and rinse with deionized water. Place the probe in the third buffer.
Press READ. The temperature and pH values will be updated until a stable reading is reached.
When the reading has stabilized or been accepted, the slope value and the Store and ? icons will appear.
To save the calibration and return to the reading mode, press ENTER. To exit the calibration without saving it and return to the reading mode, press EXIT.

DO probe calibration
Secure the probe cable to the calibration and storage chamber by wrapping cable through the bottom of the chamber lid before filling with water. (Note: Avoid completely filling the lower part of the calibration chamber with water.)
Prepare the calibration and storage chamber by holding it under water and squeezing it a couple of times to pull a small amount of water into the lower chamber through the inlet. Alternately, open the bottom of the chamber and insert a water-soaked sponge.
Insert the DO probe into the calibration and storage chamber. The tip of the probe must not be flooded with water or be holding a drop of water on the membrane.
Allow at least ten minutes for the atmosphere in the chamber to reach a steady state. [(Note: Gently squeezing the lower chamber a couple of times to force water-saturated air into the probe chamber will speed up stabilization. Avoid squeezing liquid water into the chamber.) (Note: Keep the DO probe at a uniform temperature. When holding the probe, do not touch the metallic button on the side of the probe. The button is a thermistor that senses temperature. An inaccurate calibration will result if the temperature of the thermistor is different from the probe membrane.)]
Press the DO key to put the meter in DO Reading mode.
Press the CAL key located in the lower left corner of the keypad.
The display will show 100%. Press the ENTER key. The stabilizing icon will appear while the meter completes the calibration.
When the calibration is complete, the meter will return to the reading mode. Press the EXIT key during the calibration sequence to back out of the calibration routine, one screen at a time, without completing a calibration. (Note: If the CAL and ? icons flash after calibration, the calibration failed and needs to be repeated.)
B.2.3.3) Calibration Apparatus
Calibration for the YSI meter will be conducted in manufacturer provided calibration containers. For the Hach probes the calibration apparatus includes the containers for the calibration standards that are supplied by the manufacturer.
B.2.3.4) Calibration Standards
Turbidity Standard
126 NTU Formazin polymer-based standard.
Conductivity standard
1000 µS/cm (at 25 °C) NaCl standard solution
pH and temperature probe calibration
1.68, 4.01, 7.00 (or 6.86), 10.01, and 12.45 pH buffers

DO probe calibration
De-ionized, organic free water within the calibration storage chamber.
B.2.3.5) Calibration Frequency
The YSI turbidity probe will be calibrated at least once per month. In addition, every other week the probe will be tested against standards in the field to check if the probe has undergone extensive drift or fouling. The Hach multimeter probes will be calibrated prior to and after each sampling trip. No midpoint calibration will be performed due to time constraints of bringing samples back to the lab for filtration and preservation.
B.2.3.6. Personnel Responsible for Calibration and Inspection
William Ford and Undergraduate Students at the University of Kentucky Hydraulics Lab will be responsible for calibration and inspection procedures.
B.2.3.7. Documentation of Calibration Procedures
The YSI turbidity meter calibration and maintenance procedure will be documented in the "South Elkhorn TSS and Turbidity Fieldbook". Calibration dates, readings during bimonthly field checks, condition of the YSI meter, and readings during calibration process will be recorded in the fieldbook. Calibration procedures will similarly be documented in the "South Elkhorn Weekly Sediment Trap Fieldbook".
B.2.4) Lab Analytical Instrument Calibration Procedures
All laboratory analytical instrument calibration procedures are detailed in the SOP references found in the Appendix. All analytical instruments were chosen in order that they meet the required QLs specified in this QAPP.
B.2.5) Analytical Instrument and Equipment Maintenance, Testing and Inspection Procedures
For maintenance, testing and inspection procedures for all laboratory instruments please refer to the analytical SOPs referenced in Table 9 and subsequently found in the Appendix section. For field based analytical instruments, the manufacturers manual was used to insure the instruments were maintained, tested and inspected properly before and after measurements were taken. Any problems with the instrumentation will be clearly noted in the field notebooks associated with the specific instrument (section B.2.3.7). The instrumentation will be secured in the UK Hydraulics laboratory. Spare parts are available in case of probe failure.
B.2.6) Analytical Supply Inspection and Acceptance Procedures
B.2.6.1) Supplies for Analytical Procedures
The following discuss the supplies and acceptance procedures for analytical equipment in the three laboratories. For the KGS and ASIL labs protocol provided in the Appendix section and outlined in Table 9 will provide the supply Inspection and Acceptance Procedures.
Kentucky Geological Survey Analytical Procedures
Refer to Table 9/Appendices for the Ammonium, Nitrate, DIC, DOC, and DP SOPs for all supplies, reagents and laboratory procedures to ensure availability and freeness from target analytes and interferences.
Arkansas Stable Isotope Lab Analytical Procedures
Refer to Table 9/Appendices for the $\delta^{15}N$ of Ammonium and $\delta^{15}N$ of Nitrate SOPs for all supplies, reagents and laboratory procedures to ensure availability of supplies and cleanliness.
Hydraulics Lab Analytical Procedures
TSS Analysis
Forceps
Graduated Cylinder
Filtration Apparatus
Sediment Trap Sample Preparation Procedure
Plastic Pitcher
Siphon
HDPE 125 mL bottles
750 mL plastic centrifuge bottles
250 mL centrifuge bottles
<53 mircon mesh sieves
Sample grinding
Metal Spatula
$\delta^{15}N$ of NH_4 Sample preparation Procedure
HDPE 250 mL bottles
Forceps
UK Stable Isotope Lab Analytical Procedures
Sediment Trap Sample Analysis
Metal Spatula
Forceps
Note: If any supplies are known to have become contaminated they will be removed and new supplies will be utilized or decontaminated appropriately. Any such incident will be documented accordingly.
B.2.6.2) Responsible persons for checking supplies and implementing protocol
Jason Backus, KGS Lab, University of Kentucky.
Erik Pollock, ASIL, University of Arkansas.
William Ford, Graduate Student, University of Kentucky.
Chris Romanek, UKSIL, University of Kentucky.
Undergraduate Students, University of Kentucky

B.3) Sample Collection Documentation, Handling, Tracking, and Custody Procedures
B.3.1) Sample Collection Documentation
On-site and off-site analytical documentation procedures are discussed in section B.5. Further, refer to section B.1.2.6 for information about field documentation. This section addresses container identification labels, the required sample identification information and an example.

B.3.1.1) Sample Identification

Measurements requiring labeled containers include ammonium, nitrate, DIC, DOC, DP, TSS, $\delta^{15}N$ of ammonium and nitrate, and sediment trap samples.

Field Container Labeling-During field sampling, the following information will be filled out and placed on each sample container used.

Site_____
Analysis_____
Collector_____
Date/Time_____

Laboratory Labels- Upon returning to the laboratory each sample brought in needs to be logged in (section 3.2) and given an appropriate, traceable Sample ID. New sample containers, or field sampling containers (depending on the analyte) will be labeled using the following.

Site_____
Sample ID_____
Analysis_____
Collector_____
Date/Time_____
Grab/Composite_____
Preservation_____

B.3.1.2) Sample Label Protection

To protect the sample labels, clear, waterproof tape will cover all labels to prevent bleeding of ink, or tearing of the label.

B.3.2) Sample Handling and Tracking System

Samples will be entered into a log book whenever they come into the UK Hydraulics lab and will be given a unique sample identification number. The sampling number system will denote the analytical run, the site, the sample number associated with that site, and information about the sample matrix (e.g. filtered, ground, bulk sample etc.). For example, a sample that was collected from T1 during January that is a field duplicate and is filtered would be labeled "J-T1-02-F". Further information about the samples, such as the analysis being conducted, can be found on the analyte specific sample container (see section B.3.1). A key will be kept in the lab book to help identify what each component means.

Procedures used for internal laboratory tracking are discussed in the SOPs found in the Appendix section. Typically the sample ID provided upon arrival at the UK hydraulics lab will be used throughout analytical procedure in order to minimize confusion. Further, specific laboratory storage procedures for each analyte are discussed in the SOPs found in the Appendix section.

B.3.2.1) Sample Handling

Sampling Organization: University of Kentucky, Department of Civil Engineering
Laboratory: UK Hydraulics Lab, UKSIL, KGS Lab, ASIL
Method of sample delivery (shipper/carrier): Carried /Shipped (UPS overnight)
Number of days from reporting until sample disposal: Maximum Holding Time/Project duration

Activity	**Organization and title or position of person responsible for the activity**
Sample labeling	William Ford/Undergraduate students- University of Kentucky, Department of Civil Engineering.
COC form completion	William Ford- University of Kentucky, Department of Civil Engineering
Packaging	William Ford- University of Kentucky, Department of Civil Engineering
Shipping coordination	William Ford- University of Kentucky, Department of Civil Engineering
Sample receipt, inspection, & log-in	Jason Backus- Kentucky Geological Survey Erik Pollock- University of Arkansas Stable Isotope Lab William Ford- University of Kentucky, Department of Civil Engineering
Sample custody and storage	Jason Backus- Kentucky Geological Survey Erik Pollock- University of Arkansas Stable Isotope Lab
Sample disposal	Jason Backus- Kentucky Geological Survey (SOPs state retention time) Erik Pollock- University of Arkansas Stable Isotope Lab (SOPs states retention time)

Table 0-9) Sample Handling Process

B.3.2.2) Sample **Delivery**

Samples analyzed at the Kentucky Geological Survey or UK Stable Isotope Lab will be carried by William Ford, or an undergraduate assistant. Samples sent to the Arkansas Stable Isotope Lab, water samples will be shipped in insulated containers with ice packs (to keep samples cooled to 4^{o}C) each month after sample collection. If storm events are sampled, the samples won't be shipped until all samples from a given event are obtained. Samples will be shipped overnight using UPS. Sample delivery groups (SDGs) of 20 or less will be used (EPA-505-B-04-900A). Chain of custody forms will be used to denote when samples are shipped and received (see section B.3.3). No hazardous materials will be shipped during the course of this project.

B.3.3) Sample Custody

To document sample handling, the following procedure will be used for chain of custody.

Person collecting samples will complete the respective Fieldbook log.

Person relinquishing packaged samples to carrier will sign Chain-of-Custody form and obtain signature of the representative of the carrier.

Transported package will include a copy of the Samples Collection Log, Equipment Maintenance/Failure Log (if necessary) and the Chain-of-Custody form.
Person receiving transported samples will obtain signature of representative of carrier and sign Chain-of-Custody form.
Laboratory personnel will sign Chain-of-Custody form to acknowledge receipt of samples.
Laboratory personnel will sign Chain-of-Custody form when samples are disposed.
The Database Manager will keep a copy of the Chain-of-Custody form.

The forms used for Chain of Custody are seen in Figure 10 and 11. This form is applicable to all analysis performed in this project.
B.4) Quality Control Samples
B.4.1) Sampling Quality Control Samples
B.4.1.1.) Water Quality Parameters and DIN Stable Isotope Parameters
To ensure QC of field based methods, field blanks and field duplicates will be collected every other sample run (e.g. approximately 1/16 samples) which adheres to the suggestion of 5% (KDOW, 2006). Blanks will consist of De-ionized water and will be carried to each site and will be processed identically to the other samples. Duplicate samples will be collected from each sampling site at least once during the sampling routine. For confidentiality purposes blanks and duplicates will not be explicitly labeled as that, instead the sample identification number will be used as identification and the sample log in book, which links the sample to the sample identification number, will not be available to off-site lab managers.
B.4.1.2) Sediment Concentration
Blanks and replicates of sediment concentration samples in the field are not feasible due to the nature of the sampling regime (e.g. sediment concentrations can change rapidly thus both depth integrated and automated sampling would not be unable to collect a "duplicate" sample).
B.4.1.3) $\delta^{15}N$, $\delta^{13}C$ of Transported Sediment, POC and PN
Sediment trap samples are integrated samples and are collected at a fixed point the stream. It's not feasible to collect duplicates and impossible to collect blanks for these samples.
B.4.2) Analytical Quality Control Samples
Analytical control samples for KGS Lab procedures are well defined and have been fine-tuned by the lab operator. The QC procedures are found in the Appendix SOPs. Analytical QC samples for tasks performed at the UKSIL, UK hydraulics lab, and ASIL are outlined in the following subsections.
B.4.2.1) Sediment Concentration
Blanks will be established by running a known volume of deionized water through the filtration device and measuring the resulting TSS. This measurement is performed to ensure that no contamination occurs during the analytical procedure and that the scale is working properly. If the blank is greater than the MDL then the test will be rerun and all equipment will be checked accordingly. Sample splits will be conducted 1/10 samples. During this process a homogenized sample will be split into two equal volumes and if the resultant TSS concentration is greater than 10% different the test will be rerun with the next sample, the previous data will be red flagged in the database and lab notebooks.
B.4.2.2) $\delta^{15}N$ of Nitrate
Deionized water was utilized as a Blank. Standards for the analysis were 20µM KNO_3, IAEA (International Atomic Energy Agency) N3 (19.975 µM N-KNO_3, $\delta^{15}N$=4.7‰ and $\delta^{18}O$=25.6‰), USGS 32 (19.7 µM KNO_3, $\delta^{15}N$=180 ‰ and $\delta^{18}O$=25‰), USGS 34 (20 µM KNO_3, $\delta^{15}N$=-1.8 ‰ and $\delta^{18}O$=-27.9‰), USGS 35 (20 µM KNO_3, $\delta^{15}N$=2.7‰ and $\delta^{18}O$=57.5‰). Duplicates and blanks were taken bimonthly from the field. For isotope analysis, splits are taken for ten percent of the samples.
B.4.2.3) $\delta^{15}N$ of Ammonium
Samples were run in triplicate to verify precision of the instrument and repeatability of the diffusion procedure. Field blanks and field duplicates were collected bimonthly. Two pure ammonium sulfate reagants $(NH_4)_2SO_4$ were used as reference materials; USGS 25 with a $\delta^{15}N$=-30.41‰, and USGS26 with a $\delta^{15}N$=+53.7‰. The reference materials are used to calibrate each sample run. Standard deviations of the reference material samples were used to determine if performance criteria for the sample run were met.
B.4.2.4) $\delta^{15}N$, $\delta^{13}C$ of Transported Sediment, POC and PN
Standard deviations of the instrument are established by injecting a reference gas for carbon and nitrogen. Further, linearity is established by injecting the reference gas at different concentrations and calculating the change in the isotopic signature over the change in voltage. Since a single sample is used to obtain all 4 parameters and a range of isotopic values needs to be established, two isotopic standards and one elemental standard will be used. A template has been established (see Section 3.5) for a typical sample run. The instrument is warmed up by running equipment blanks to ensure background concentrations are low and a set of standards to ensure that the instrument is working appropriately. During the analysis, around $1/4^{th}$ of the run is standards. One out of every ten samples is run in triplicate to establish a standard deviation of the data and to test homogeneity and processing of the samples.
B.5) Data Management Tasks
B.5.1) Project Documentation and Records
The purpose of this section is to detail all records that will be generated encompassing all aspects of the project. Section B.5.1 details lists the documents and records that will be generated in this project. Section B.5.2 will detail package deliverable documents for sample collection and field measurement, on-site analytical, and off-site analytical data deliverable documents. Section B.5.3 will discuss procedures for manual and electronic data recording and storage and provide templates for the appropriate forms. Section B.5.4 describes handling and management of data from generation to its final use and storage. Section B.5.5 discusses the procedures for tracking, control, storage, archival, retrieval and security of the data.
B.5.1.1) Sample Collection and Field Measurements
The following provides a comprehensive list of records and documents that will be generated for the sample collection and field measurements
Field data collection (Section B.1.2.6)
Chain of custody records (Section B.3.3)
Sampling instrument calibration/maintenance logs (Section B.2.3.2)
Sampling locations and their associated schematic (Section B.1)
Sampling plan (Section B.1)

Sampling notes (See Field book discussion in section B.1.2.6)
Corrective action/ Failure reports (Figure 12)
Data Exclusion Reports (See section D.2 for reasons to exclude data)
Documentation of methods deviations (See section D.2 for occurrence of deviations from QAPP methods)
Electronic Data Deliverables (Section B.5.3)
Meteorological Data from field (Section A.5)
Continuous Stream Data (Section A.5 and A.3.2)
Sampling Instrument Maintenance and Calibration Logs (See Field book discussion in section B.1.2.6, calibration in section B.2.3 and maintenance in section B.2.5)

B.5.1.2) Analytical Records

The following provides a comprehensive list of records and documents that will be generated for analytical records.

Chain of Custody records (Section B.3.3)
Preparation and Analysis forms (logbooks) (For field logbooks see previous section, for analytical logbooks see section B.5.3).
Raw data and tabulated data summary forms, standard QC checks, QC samples (See section B.5.3 for raw analytical data forms, see Data review section D for tabulate data summary information).
Sample Chronology (Section B.5.3).
Corrective action/ Failure reports (Figure 12)
Documentation of methods deviations (See section D.2 for occurrence of deviations from QAPP methods)
Electronic Data deliverables (Section B.5.3).
Instrument Calibration Records (Section B.2.3)
Laboratory Sample Identification Number (Section B.3.1.1)
Reporting Forms, completed with actual results (Section B.5.2)
Signatures for laboratory sign-off (COC forms)

B.5.1.3) Project Data Assessment Records

Field Sampling Audit Checks (Section C.1.1)
Analytical Audit Checks (Section C.1.1)
Data Review Reports (Section D)
Corrective action/Failure reports (Figure 12)

B.5.2) Data Package Deliverables

B.5.2.1) Sample Collection and Field Measurements Data Package Deliverables

Grab samples shall be logged into the specified field manual along with analytical data including, pH, DO, temp and conductivity. Velocity shall be logged using the fluid velocity sample collection log (Figure 8). Stage should be logged using the stage sample collection log (Figure 9). Data should be input electronically into a database immediately after returning from the field (Section B.5.3).

B.5.2.2) On-site Analysis Data Package Deliverables

All raw data generated from on-site analysis shall be recorded manually on the lab analysis or logbook sheets (see section B.5.3). The data will be uploaded to a spreadsheet electronically for storage.

B.5.2.3) Off-site Laboratory Package Deliverables

Laboratory Records shall consist of the monthly analysis reports as prepared by the Kentucky Geological Survey laboratory and the Arkansas Stable Isotope laboratory. Analysis of samples should be completed and reported within one month of receipt of the samples.

B.5.3) Data Reporting Formats

B.5.3.1) Sample Collection and Field Measurements

Data collected in the field will be recorded manually into fieldbooks or onto data sheets (section B.3.1 and Figures 8 and 9). If data needs to be corrected, it shall be marked out with a straight line and written above the marked out section (room permitting). All original data and corrections need to be initialed by the sampler. Collected data will be transformed from raw forms into usable data forms by transcribing the data into an EXCEL spreadsheet via electronic import. Chain of Custody forms (Figure 10) will be filled out in concert with fieldbooks and will be uploaded to the electronic database upon receipt of the completed form.

B.5.3.2) Procedural alterations and data exclusions

Raw forms for corrective actions, data exclusion and method deviations forms (Figures 10-14) should be filled out during the collection and analytical process. Thereafter, the template will be used to import a soft copy of the reports.

B.5.3.3) Analytical instrument maintenance and calibration

Raw fieldbook data for instrument maintenance and calibration will be electronically transcribed into an EXCEL spreadsheet using the template in Figure 15. The spreadsheet will be emailed to co-managers immediately after entering the data and stored on a UK engineering server.

B.5.3.4) Secondary Data

Continuous data will be collected electronically from the NOAA Lexington Bluegrass airport using the template in Figure 16. Turbidity, flow, stage, precipitation and temperature will be collected continuously in the stream channel at three sites and logged using the template found in Figure 17.

B.5.3.5) On-site laboratory analytical procedures

Upon entry into the lab, each sample will be logged in using Figure 18. For samples sent to other labs, the Chain of custody forms will be used to track their location after the carrier takes them out of the lab. For samples analyzed by William Ford and the undergraduate researchers the samples progress will be tracked with the form in Figure 21. On-site laboratory analysis will be recorded using raw data forms found in Figures 19-23. This includes the TSS analysis (Figure 19), preparation work for $\delta^{15}N$, $\delta^{13}C$, TOC, TN and C:N of the sediment traps(Figures 20-21) and the associated EA/IRMS analysis templates (Figure 22-23), and preparatory work for $\delta^{15}N$ of streamwater ammonium (Figure 24). All forms will be transcribed in their associated template and saved in separate folders for organizational purposes.

Surface Water Data Acquisition
Fluid Velocity Sample Collection Log

Date: _____
Site ID: _____
Section: _____
Start Time: _____
End Time: _____

Technicians: _____
Signatures: _____

Site	Flow Depth (m)	Velocity(m/s)	Comments

Figure 5) Fluid Velocity Sample Collection Log

Surface Water Data Acquisition
Stream Stage Sample Collection Log

Date: _____
Site ID: _____
Section: _____
Start Time: _____
End Time: _____

Technicians: _____
Signatures: _____

Site	Flow Depth (m)	Comments

Figure 6) Stream Stage Sample Collection Log

Page 1 of _______

South Elkhorn Watershed Project
CHAIN OF CUSTODY RECORD

REQUEST ID:

SAMPLING LOCATI0N:

Date/Time	SAMPLE IDENTIFICATION	MATRIX	NUMBER of CONTAINERS	PRESERVATION/ TREATMENT	ANALYSIS REQUESTED *A- Add D- Delete X- Select*		LAB USE ONLY
Date: __/__/__ Time: ___:___ MILITARY	ID# __ __ __ __ __ __ __ __	☐ WATER __Surface __Ground __Storm ☐ SOIL ☐ SEDIMENT ☐ OTHER	__ Glass, 1000 mL __ Plastic, 1000 mL __ Glass, 250 mL __ Plastic, 250 mL __ Plastic, 125 mL __ ISCO __ Glass, 60 mL __ Vial, 40 mL __ Vacutainer Other:	__ ICE __ H2SO4 __ HNO3 __ HCl __ H3PO4 __ RAW __ FILTERED __ GROUND	__ NH4 __ NO3 __ DIC __ DOC __ DP __ δ15N NH4 __ δ15N N03 __ δ15N Sediment __ δ13C Sediment	__ POC __ PN OTHER	LAB ID: COMMENTS:
Date: __/__/__ Time: ___:___ MILITARY	ID# __ __ __ __ __ __ __ __	☐ WATER __Surface __Ground __Storm ☐ SOIL ☐ SEDIMENT ☐ OTHER	__ Glass, 1000 mL __ Plastic, 1000 mL __ Glass, 250 mL __ Plastic, 250 mL __ Plastic, 125 mL __ ISCO __ Glass, 60 mL __ Vial, 40 mL __ Vacutainer Other:	__ ICE __ H2SO4 __ HNO3 __ HCl __ H3PO4 __ RAW __ FILTERED __ GROUND	__ NH4 __ NO3 __ DIC __ DOC __ DP __ δ15N NH4 __ δ15N N03 __ δ15N Sediment __ δ13C Sediment	__ POC __ PN OTHER	LAB ID: COMMENTS:
Date: __/__/__ Time: ___:___ MILITARY	ID# __ __ __ __ __ __ __ __	☐ WATER __Surface __Ground __Storm ☐ SOIL ☐ SEDIMENT ☐ OTHER	__ Glass, 1000 mL __ Plastic, 1000 mL __ Glass, 250 mL __ Plastic, 250 mL __ Plastic, 125 mL __ ISCO __ Glass, 60 mL __ Vial, 40 mL __ Vacutainer Other:	__ ICE __ H2SO4 __ HNO3 __ HCl __ H3PO4 __ RAW __ FILTERED __ GROUND	__ NH4 __ NO3 __ DIC __ DOC __ DP __ δ15N NH4 __ δ15N N03 __ δ15N Sediment __ δ13C Sediment	__ POC __ PN OTHER	LAB ID: COMMENTS:

Sampler's Signature:

Relinquished by:	Date:	Recieved by:	Date:
Representing:	Time:	Laboratory:	Time:

Archiving/Disposal (Notes/Dates):

Signature

Figure 7) Chain of Custudy Form (Cover)

REQUEST ID:

CONTINUATION PAGE _____ of _____

Date/Time	**SAMPLE IDENTIFICATION**	**MATRIX**	**NUMBER of CONTAINERS**	**PRESERVATION/ TREATMENT**	**ANALYSIS REQUESTE** *A- Add D- Delete X- Select*	**LAB USE ONLY**
Date: __/__/__ Time: ___:___ MILITARY	ID# __ __ __ __ __ __ __ __ __	☐ WATER __Surface __Ground __Storm ☐ SOIL ☐ SEDIMENT ☐ OTHER	__ Glass, 1000 mL __ Plastic, 1000 mL __ Glass, 250 mL __ Plastic, 250 mL __ Plastic, 125 mL __ ISCO __ Glass, 60 mL __ Vial, 40 mL __ Vacutainer Other:	__ ICE __ H2SO4 __ HNO3 __ HCl __ H3PO4 __ RAW __ FILTERED __ GROUND	__ NH4 __ POC __ NO3 __ PN __ DIC OTHER __ DOC __ DP __ δ15N NH4 __ δ15N NO3 __ δ15N Sediment __ δ13C Sediment	LAB ID: COMMENTS:
Date: __/__/__ Time: ___:___ MILITARY	ID# __ __ __ __ __ __ __ __ __	☐ WATER __Surface __Ground __Storm ☐ SOIL ☐ SEDIMENT ☐ OTHER	__ Glass, 1000 mL __ Plastic, 1000 mL __ Glass, 250 mL __ Plastic, 250 mL __ Plastic, 125 mL __ ISCO __ Glass, 60 mL __ Vial, 40 mL __ Vacutainer Other:	__ ICE __ H2SO4 __ HNO3 __ HCl __ H3PO4 __ RAW __ FILTERED __ GROUND	__ NH4 __ POC NO3 __ PN __ DIC OTHER __ DOC __ DP __ δ15N NH4 __ δ15N NO3 __ δ15N Sediment __ δ13C Sediment	LAB ID: COMMENTS:
Date: __/__/__ Time: ___:___ MILITARY	ID# __ __ __ __ __ __ __ __ __	☐ WATER __Surface __Ground __Storm ☐ SOIL ☐ SEDIMENT ☐ OTHER	__ Glass, 1000 mL __ Plastic, 1000 mL __ Glass, 250 mL __ Plastic, 250 mL __ Plastic, 125 mL __ ISCO __ Glass, 60 mL __ Vial, 40 mL __ Vacutainer Other:	__ ICE __ H2SO4 __ HNO3 __ HCl __ H3PO4 __ RAW __ FILTERED __ GROUND	__ NH4 __ POC __ NO3 __ PN __ DIC OTHER __ DOC __ DP __ δ15N NH4 __ δ15N NO3 __ δ15N Sediment __ δ13C Sediment	LAB ID: COMMENTS:
Date: __/__/__ Time: ___:___ MILITARY	ID# __ __ __ __ __ __ __ __ __	☐ WATER __Surface __Ground __Storm ☐ SOIL ☐ SEDIMENT ☐ OTHER	__ Glass, 1000 mL __ Plastic, 1000 mL __ Glass, 250 mL __ Plastic, 250 mL __ Plastic, 125 mL __ ISCO __ Glass, 60 mL __ Vial, 40 mL __ Vacutainer Other:	__ ICE __ H2SO4 __ HNO3 __ HCl __ H3PO4 __ RAW __ FILTERED __ GROUND	__ NH4 __ POC __ NO3 __ PN __ DIC OTHER __ DOC __ DP __ δ15N NH4 __ δ15N NO3 __ δ15N Sediment __ δ13C Sediment	LAB ID: COMMENTS:
Date: __/__/__ Time: ___:___ MILITARY	ID# __ __ __ __ __ __ __ __ __	☐ WATER __Surface __Ground __Storm ☐ SOIL ☐ SEDIMENT ☐ OTHER	__ Glass, 1000 mL __ Plastic, 1000 mL __ Glass, 250 mL __ Plastic, 250 mL __ Plastic, 125 mL __ ISCO __ Glass, 60 mL __ Vial, 40 mL __ Vacutainer Other:	__ ICE __ H2SO4 __ HNO3 __ HCl __ H3PO4 __ RAW __ FILTERED __ GROUND	__ NH4 __ POC NO3 __ PN __ DIC OTHER __ DOC __ DP __ δ15N NH4 __ δ15N NO3 __ δ15N Sediment __ δ13C Sediment	LAB ID: COMMENTS:

Sampler's Initials __________

Figure 8) Chain of Custody Form (Subsequent Pages)

Corrective Action/Equipment Failure Log

Date	Site ID	Equipment	Date and Time Maintenance/Failure Occurred

Nature of Maintenance/Failure (circle)				List Specific Part(s)
power	mechanical	electronic	other	

Describe Maintenance/Failure and Reasons for Maintenance/Failure	

Describe Impact of Maintenance/Failure on Sample Collection	

Describe Corrective Actions	

Equipment Resumed Operation	
Date	Time

Signature: _____

Figure 9) Corrective Actions/Failure Log

Data Exclusion Report

Date	Site ID	Storm Event No.	Date and Time Data Collected	Type of Data	Database Record No.
Reasons for Proposing Data Exclusion					

Impact of Excluding Data on other Data Collected	

Comments	

Final Decision: ☐ Data to be Excluded

☐ Data is Acceptable

Signature: _____

Quality Assurance Officer

Figure 10) Data Exclusion Report

Deviation From Method

Date	Method

Explain the Method Deviation	

Detailed reasons for deviations/potential limitations	

Signature: _____

Figure 11) Documentation of Method Deviation

Instrument Maintenance and Calibration Log

Instrument	Date/Time of Calibration or Maintenance	Reading Before Calibration (N/A for Maintenance)	Maintenance Performed (N/A for Calibration)	Notes

Figure 12) Maintenance and Calibration Log

NOAA Meteorological Data

Site _____

Date/Time	**Av. Temp** Celsius	**Precip** in	**%Sun** %	**Wind** ft/s	**Date Obtained**

Figure 13) Meteorological data template

Continuous Stream Data

Site _____

Date/Time	**Flow** cfs	**Stage** ft	**Precip** in	**Temp** Celsius	**Turbidity** NTU	**Date Obtained**

Figure 14) Continuous Stream Data template

Check-in Sheet (Please Date and Initial each step)

Site	Date	Sample Type	Sample ID #	Sent for Analysis/Analyzed

Figure 15) Check-in and progress sheet for laboratory analytical samples

TSS Analysis Data Sheet

Analyst: _____

Date Begun: _____

Sample ID	**Crucible #**	**Crucible Tare Weight** (grams)	**Sample Volume** (ml)	**Dried Crucible Weight** (grams)	**TSS Concentration** (mg/l)

Figure 16) TSS Analysis Datasheet

Sample Preparation Template for EA/IRMS Sediment Trap Samples

Site	Date	Sample ID	Empty Bottle Wt (g)	Bottle + Sample Wt (g)	Sample Wt (g)	SubSample Needed (g)	Sample Obtained (g)	Empty Bottle Wt (g)	Bottle + Sample Wt (g)	Fines Weight (g)	Notes

*Performed in the UK Hydraulics Laboratory. Prepartory steps include freeze drying, wet sieving, centrifuging, consolidating and weighing and grinding samples.

Figure 17) Sample Preparation Template for EA/IRMS Sediment Trap Samples

Checklist for IRMS Progress (Please initial and date each step)

Sample ID	Date	Consol & Weigh	Wet Sieve	Centri-fuge	Freeze	Freeze Dry	Consol & Weigh	Grind	Weigh

Figure 18) Checklist for laboratory procedure for analysis of $\delta^{15}N$, $\delta\ ^{13}C$, TOC,TN and C:N of sediment

Total Weights for EA/IRMS Sub-samples

	1	2	3	4	5	6	7	8	9	10	11	12
A												
B												
C												
D												
E												
F												
G												
V												

*Used in analysis of $\delta^{15}N$, $\delta^{13}C$, TOC,TN and C:N of sediment. Sample ID goes above the dotted line and sample weights go below.
Figure 19) Template for sediment sample weights before acid digestion

EA/IRMS Analysis Template Design

A	1 Blank	2 Cond. Int. std1	3 Cond. Int. std1	4 Cond. Int. std1	5 %Std 1	6 %Std 2	7 Int. Std1.1	8 Int. Std1.2	9	10	11	12
B	13	14 Int. Std1.3	15 Int. Std2.1	16	17	18	19	20 Int. Std1.4	21	22	23	24
C	25	26 Int. Std1.5	27	28	29	30	31	32 Int. Std1.6	33	34	35	36
D	37	38 Int. Std1.7	39 Int. Std2.2	40	41	42	43	44	45	46	47	48 Int. Std1.8
E	49 %Std 3											

*Template design includes the timing of the standards (two for isotopes and one for concentration) during the automated run.
Figure 20) Template Design for EA/IRMS procedure

Sample Preparation Template for $\delta^{15}N_{NH4}$

Sample ID	NH4 Conc.	Sample Volume	NaCl added	MgO added	DIDO added	Incubation Start Date	Incubation End Date	Notes

*Performed in the UK Hydraulics/ERTL Laboratory.

Figure 21) Template for preparation of streamwater samples for d15N analysis of ammonium

B.5.4) Data Handling and Management

B.5.4.1) Data Recording

Data will be entered electronically in excel spreadsheets. Data will be crosschecked with COC forms and with fieldbooks to ensure that transcription errors are minimized. Data will be entered into the database using the templates depicted in the preceding section. Database entries will be logged on the Database Entry Log sheet depicted in Figure 25.

B.5.4.2) Data Transformations and Data Reduction

B.5.4.2.1) Discharge Data

Storm runoff rates for each sample site will be obtained used the existing USGS gauging station at the watershed outlet. Discharge at each site will be determined by using a weighted area basis by applying an appropriate factor to the discharge from the USGS gauging stations. Discharges from the area weighted method will be cross checked against measured discharges in the tributaries.

B.5.4.2.2) Sediment, Carbon, Nitrogen and Phosphorus Fluxes

Constituent fluxes are determined using the discharge rate at the time the sediment samples were collected and multiplying the discharge rate by the sample constituent concentration (e.g. TSS, NH_4, NO_3, TP, DOC, DIC).

Any data conversions that occur will be recorded in the Data transformations log (Figure 26). ***At this time no data reduction procedures are planned***.

B.5.4.3) Data Transfer and Transmittal

All electronic data will be transmitted *via* email. All data will be emailed to co-managers. Backup copies of all data will be maintained at all times to insure data is not lost. The person transmitting the data should include a metadata file that includes the names, sizes, and descriptions of each of the files in the transmittal. Data recorded on paper will be transmitted by fax or scanned and converted to Adobe Acrobat format and transmitted as detailed above. An example of the electronic data transfer form used on this project is found in Figure 27. This form is used if electronic data is requested by project personnel.

B.5.4.4) Data Analysis

Microsoft EXCEL will be used to process and analyze data. The data will be used primarily for parameterizing and calibration/validation of a numerical model that is still under development but stems from work performed by Ford and Fox (2012), Russo and Fox (2012), and Fox et al. (2010).

B.5.4.5) Data Review

Microsoft EXCEL will also be utilized to review the data. Either R, or EXCEL will be used to perform statistical analysis of the data. Data review will be performed primarily by William Ford.

Database Entry Log

Date	Site ID	Data Entry Method			Type of Data Entered	Sample ID	Person Entering Data	Verified
		Electronic Import	Filename*	Manual				

*Filename needed if data were not collected manually.

Figure 22) Database Entry Log

Raw Data Transformation Log

Date	Site ID	Data Source*	Raw Data Filename		Transformed Data Filename		Person Performing Transformation

*Data Source includes YSI 600 OMS Multi Probe System

Figure 23) Raw Data Transformation Log

Data Request and Transfer Form

Data Requested:	(Please describe the requested and explain why it is being requested)

Requested by: _____ _____
(Signature)

Request Date: _____

Date Needed: _____

Data Format:
- □ Graph
- □ Table
- □ Spreadsheet
- □ Other (please specify format) _____

Figure 24) Data Transfer Request Form

B.5.5) Data Tracking and Control
B.5.5.1) Data Tracking
A Data Tracking Log (Figures 28 and 29) will be utilized to keep track of data through various stages. The project manager/database manager will be in charge of updating the data tracking logs.
B.5.5.1) Data Storage, Archiving, Retrieval
The data will be stored on a password protected computer. The Database Manager and the primary advisor are the only people authorized to access, correct, enter, change, or retrieve data within the database. Data will be available to all project personnel, provided they complete and submit a Data Request Form (Figure 27) to the Database Manager.
A hardcopy of all project logs, forms, records, and reports shall be archived by the database manager. Hardcopy documents shall be available to all project personnel upon request. Hardcopies of all logs, forms, records, and reports shall be made available to the Project Quality Assurance Officer on a quarterly basis.
After all data has been verified, validated and assessed for usability, it will be stored in a secured database (February 2014).
B.5.5.3) Data Security
All data will be stored in on the Database Manager's computer which is password protected. Data will be backed up and archived on a weekly basis on a password protected database. The Database Manager will be responsible for querying the database and exporting desired data in Microsoft EXCEL format to produce data reports.

Data Tracking Log

Consitutent:_____

Site ID	Date Samples Collected	Date Samples Shipped	Date Samples Received	Date Analysis Performed	Lab Data Sheets Received by QA/QC Manager

Figure 25) Data Tracking Log Template (to be filled out for each analyte)

Data Tracking Log: Electronic and Manually Recorded Data

Site ID/Data Type	Date Data Collected	Date Data Copied and Archived	Date Manual Data Entered into File	Date Data Transmitted to QA/QC Manager

Figure 26) Data Tracking Log (Electronic/Manually Collected Data)

Section C: Assessment/Oversight

C.1) Assessments and Response Actions

C.1.1) Planned Assessments

Internal assessment activities will consist of reviewing monthly data for completeness and representativeness. If the data fails to be complete and representative, a review of the data's history will be performed by William Ford to determine if any errors were committed in the logging, entry, transforming, and calculation processes. If logging, entry, transforming, or calculation errors come to light, the data will be flagged for exclusion from use in the statistical analysis. William Ford will also perform a Field Sampling, on-site analytical and off-site analytical TSA at the beginning of the sampling routine to ensure that all methods are conforming to the information displayed in this QAPP.

C.1.2) Assessment Findings and Corrective Action Responses

With regard to the internal audit process at the initiation of the project, any deficiencies will be documented using a corrective action response form (Figure 12), and stored in the project database. Thereafter corrective actions will be taken to ensure that the method corresponds with the criteria outlined in this QAPP. The parties involved (for example lab managers and the primary advisor) will be notified upon audit completion. The person in charge of sampling or the analytical procedures shall be the one in charged with receiving and addressing the corrective action report.

Data not meeting requirements for completeness or representativeness will be excluded from the data set, although included in the database and flagged for exclusion from statistical analyses. All data not meeting the Data Quality Objectives will be logged on the Data Exclusion Report sheet (Figure 13). The Data Exclusion Report will be archived by William Ford and will be available to all project personnel. After comment from project personnel, the William Ford will render the decision to include or exclude the data from further use. If the data has been excluded, the data will be flagged within the database as excluded from analyses.

C.2) QA Management Report

QA management reports will be generated quarterly by William Ford and distributed to all personnel involved with the project. As well, a final project report will include all QA management reports. In general these reports will address the following.

A summary of the project status and scheduled delays.
Conformance of project activities to QAPP requirements and procedures.
Deviations from the approved QAPP and approved amendments to the QAPP.
Data reports of all data available for publishing.
A complete copy of the Equipment Maintenance/Failure Log.
A complete copy of the Data Tracking Log.
A complete copy of the Database Correction Log.
A complete set of all Data Exclusion Reports.
A complete set of Chain-of-Custody Records.
All Data Quality Assessment Reports to date.
Data usability in terms of accuracy, precision, representativeness, completeness, comparibility, and sensitivity.
Any limitations on the generated data.
A summary of tasks yet to be completed.

C.3) Final Project Report

The final Project report will address the above concerns as well as additional QA concerns such as:

Narrative and timeline of project activities
Summary of PQO Development
Reconciliation of PQO Development
Summary of major problems encountered and their resolution
Data summary, including tables, charts, and graphs with appropriate sample identification or station location numbers, concentration units, and data quality flags.
Conclusions and reccomendations

Section D: Data Review

D.1) Overview

The data review process is outlined in the QAPP as a three step procedure. The following outlines these processes and the appropriate review steps and outputs.

Table 0-10) Requirements for Data Review (EPA-505-B-04-900A)

Process Term	Objective	Scope	Data Review Step	Output
Verification	Review to see if data required for the project are available.	– Sampling* – Analysis	I. Completeness check	Verification Report – May be checklist form – Package includes all documentation
Validation	– Assess and document the performance of the field sample collection process. – Assess and document the performance of the analytical process.	– Sampling* – Analysis	IIa. Check compliance with method, procedure, and contract requirements IIb. Compare with measurement performance criteria from the QAPP*	Validation Report – Includes qualified data – May be part of other report such as RI/FS
Usability Assessment*	Assess and document usability to meet project quality objectives.	- Sampling - Analysis	III. Assess usability of data by considering project quality objectives and the decision to be made*	Usability Report – May be part of other report such as RI/FS

*The scope of the term or the step involved is an expansion of current practice.

The following sections will detail the procedures associated with data review and will address how these procedures will be completed for the South Elkhorn project.

D.2) Data Review Steps

D.2.1) Step I: Verification

D.2.1.1) Responsible Personnel and Documentation

All data verification procedures will be handled by William Ford for sampling/handling and analytical procedures at the UK hydraulics lab and UKSIL. Jason Backus will assist with verification (as needed) at the KGS Lab and Erik Pollock will assist (as needed) with verification at the ASIL. All verification procedures need to be documented and included in quarterly reports.

D.2.1.2) Sample Collection

Sample collection procedures will be verified by checking that the field book data is consistent with the data loaded onto the electronic database. If inconsistencies are observed, appropriate changes will be made and the corrective action log will be filled out (Figure 12). If data from the field appears erroneous or in error, the QC manager will consult the sampler and mitigative actions will take place. Identification of the sampler will come from sampler signatures in the fieldbook. If no signature is present or if the sampler is unsure about the erroneous data/metadata in the field book the information will be flagged in both the field book and the database and a Data Exclusion Report will be filled out. If the error is recognized by the sampler and can be mitigated, a Corrective

Action Log will be filled out and appropriate database corrections will be made.

South Elkhorn Watershed Project

Database Correction Log

Date	Database Table	Table Field	Table Record No.	Wrong Value	Corrected Value	Person Making Correction	Comments

Figure 27) Database Correction Log

D.2.1.3) Sample Handling

Chain of custodies will be initiated by the sampler and will be signed over to the carrier. Upon receipt at the laboratory (KGS, ASIL, UKSIL, UK Hydraulics Lab) the responsible party will sign for the samples and the carrier will also initial that the samples were relinquished. A copy of the chain of custody form will be retained by William Ford and a binder will be kept with all chain of custody forms. For verification the forms will be uploaded to the database immediately after receipt of a copy from the respective labs. Likewise, information on the COC sheets will be cross checked with information present in the field books. For responsible parties for each lab see the preceding sections.

D.2.1.4) Analytical Procedures

Data generated by outside laboratories will be checked by the personnel in charge of laborartory before sending the spreadsheet to the project/database manager. Upon receipt of the data, the raw data and QC data will be checked to ensure that all constituents are present and QC samples are detailed. If the data is found to be in error or incomplete, the source of the error will be documented and necessary corrections made.

D.2.2) Step II: Validation

Validation procedures are conducted to identify data that don't meet established project quality objectives. Since error can occur at any point throughout the project, validation procedures need to be performed during each step. All validation activities must be documented and included in the quarterly reports.

D.2.2.1) Step IIa Validation Activities

This portion of the validation procedure ensures that methodological and procedural activities were consistent with what was outlined in the QAPP. The following table details the various portions of the project and discusses validation activities associated with the procedures.

Table 0-11) Compliance with methods and procedures (Modified from Table 10 of EPA-505-B-04-900A)

Project Component	**Validation Activity**
Data Deliverables and QAPP	Ensure that all required information on sampling and analysis from the verification step was provided
Analytes	Ensure that require lists of analytes were reported as specified in governing documents
Chain of custody	Examine traceability throughout project and examine COC records against method or procedural requirements.
Holding Times	Confirm/document if holding times were met. Ensure samples were analyzed within holding times. If not, ensure documentation of deviations.
Sample Handling	Ensure all appropriate procedures were followed and any deviations documented
Sampling Methods and Procedures	Establish that required sampling methods were used and that deviations were documented. Ensure performance criteria were met.
Field Transcription	Authenticate transcription accuracy of sampling data
Analytical Methods and Procedures	Establish that required analytical methods were used and that deviations were noted. Ensure QC samples met performance criteria and that deviations were documented.
Laboratory Transcription	Authenticate accuracy of the transcription of analytical data
Standards	Determine that standards are traceable and meet contract, method or procedural requirements
Communication	Establish that required communication procedures were followed by field or lab personnel
Audits	Review field and lab audit reports and accreditation and certification records the labs performance on specific methods
Step IIa Validation Report	Summarize deviations from methods or procedures. Include qualified data and explanation of all data qualifiers.

D.2.2.2) Step IIb Validation Activities

This portion of the validation procedure ensures that all data fulfill the requirements of the measurement performance criteria. The following table outlines procedures for this.

Table 0-12) Comparison with Measurement Performance Criteria (Modified from Table 11 of EPA-505-B-04-900A)

Project Component	**Validation Activity**
Data Deliverables and QAPP	Ensure that the data report from Step IIa was provided
Deviations	Determine the impacts of deviations. If deviations significantly impact the results determine the effectiveness of corrective actions
Sampling Plan	Determine if all components of sampling plan was executed as specified

Sampling Procedures	Determine whether all sampling procedures were conducted according to the specified methods (e.g. techniques, equipment, decontamination, volumes, and preservation techniques).
Field Duplicates	Compare results of field duplicates with established criteria
Project QLs	Determine that quantitation limits were achieved, as outlined in the QAPP and that the lab successfully analyzed a standard at the QL.
Confirmatory Analysis	Evaluate agreement of lab results if split samples are analyzed in different labs
Performance Criteria	Evaluate QC data against project-specific performance criteria in the QAPP
Step IIb Validation Report	Summarize outcome of comparison of data to MPC in the QAPP. Include qualified data and explanation of all data qualifiers.

D.2.3) Step III: Usability Assessment

Table 14 documents the usability assessment procedure for the South Elkhorn Project.

Table 0-13) Usability Assessment Procedure

Step 1	**Review the project's objectives and sampling design** *Review the key outputs defined during systematic planning (i.e.,PQOs or DQOs and MPCs) to make sure they are still applicable. Review the sampling design for consistency with stated objectives. This provides the context for interpreting the data in subsequent steps.*
Step 2	**Review the data verification and data validation outputs** *Review available QA reports, including the data verification and data validation reports. Perform basic calculations and summarize the data (using graphs, maps, tables, etc.). Look for patterns, trends, and anomalies (i.e., unexpected results). Review deviations from planned activities (e.g., number and locations of samples, holding time exceedances, damaged samples, non-compliant PT sample results, and SOP deviations) and determine their impacts on the data usability. Evaluate implications of unacceptable QC sample results.*
Step 3	**Verify the assumptions of the selected statistical method** *Verify whether underlying assumptions for selected statistical methods are valid. Common assumptions include the distributional form of the data, independence of the data, dispersion characteristics, homogeneity, etc. Depending on the robustness of the statistical method, minor deviations from assumptions usually are not critical to statistical analysis and data interpretation. If serious deviations from assumptions are discovered, then another statistical method may need to be selected.*
Step 4	**Implement the statistical method** *Implement the specified statistical procedures for analyzing the data and review underlying assumptions. For decision projects that involve hypothesis testing consider the consequences for selecting the incorrect alternative; for estimation projects, consider the tolerance for uncertainty in measurements.*

Step 5	**Document data usability and draw conclusions** *Determine if the data can be used as intended, considering implications of deviations and corrective actions. Discuss data quality indicators. Assess the performance of the sampling design and Identify limitations on data use. Update the conceptual site model and document conclusions. Prepare the data usability summary report which can be in the form of text and/or a table.*

D.2.3.1) Data Limitations and Action from Usability Assessment
Usability assessment will consider data quality indicators including precision, accuracy/bias, representativeness, comparibility, sensitivity and quantitation limits, and completeness.
D.2.3.2) Activities
The project team (primarily Ford and Fox) will perform the usability assessment once data validation and verification procedures have concluded on the project.
D.3) Streamlining Data Review
Since the dataset is not extremely dense, streamlining of data review is not necessary and all data will be verified and validated.

References

Alexander R.B., Smith, R.A., Schwarz G.E., Boyer, E.W., Nolan J.V., Brakebill, J.W. (2008) "Differences in Phosphorus and Nitrogen Delivery to The Gulf of Mexico from the Mississippi River Basin" *Environ. Sci. Technol.* 42, 822-830

Arango, C.P., and Tank, J.L. (2008). "Land use influences the spatiotemporal controls on nitrification and denitrification in headwater streams." *Journal of the North American Benthological Society*, 27, 90–107.

Conley, D.J.,Paerl, H.W., Howarth, R.W., Boesch, D.F., Seitzinger, S.P., Havens, K.E., Lancelot, C., and Likens, G.E. (2009). "Controlling Eutrophication: Nitrogen and Phosphorus." *Science*, 323, 1014-1015.

Diaz, R. J., and Rosenberg, R. (1995). "Marine benthic hypoxia: a review of its ecological effects and the behavioural responses of benthic macrofauna." *Oceanography and Marine Biology- an Annual Review*, 33, 245–303.

Findlay, S.E.G., Mulholland P.J., Hamilton, S.K., Tank, J.L., Bernot, M.J., Burgin A.J., Crenshaw, C.L., Dodds, W.K., Grimm, N.B., McDowell, W.H., Potter, J.D., Sobota, D.J. (2011) "Cross-stream comparison of substrate-specific denitrification potential." *Biogeochemistry* 104, 381-392.

Ford W.I., Fox, J.F. (2012) "Model of particulate organic carbon transport in an agriculturally impacted watershed" *Hydrological Processes* accepted.

Fox, J.F., Davis, C.M., and Martin, D.K. (2010). "Sediment source assessment in a lowland watershed using nitrogen stable isotopes." *Journal of the American Water Resources Association*, 46, 1192–1204.

Galloway, J.N. et al. (2008). "Transformation of the nitrogen cycle: recent trends, questions, and potential solutions." *Science*, 320, 889-892.

Kendall, C. (1998). "Tracing Nitrogen Sources and Cycling in Catchments." In: C. Kendall and J.J. McDonnell (Eds.), Isotope Tracers in Catchment Hydrology, Elsevier, Amsterdam, 519-576.

National Academy of Engineers (NAE) (2008). Grand Challenges of Engineering, Feb 16, 2008, Online at: http://www.engineeringchallenges.org/cms/8996/9221.aspx, last visited March 3, 2011.

Newcomer, T.A., Kaushal, S.S., Mayer, P.M., Shields, A.R., Canuel, E.A., Groffman, P.M., Gold, A.J. (2012) "Influence of natural and novel organic carbon sources on denitrification in forest, degraded urban, and restored streams." *Ecological Monographs* 82(4) 449-466.

Peterson, B.J., Wollheim, W.M., Mulholland, P.J., Webster, J.R., Meyer, J.L., Tank, J.L., Martõ, E., Bowden, W.B., Valett, H.M., Hershey, A.E., McDowell, W.H., Dodds, W.K., Hamilton, S.K., Gregory, S., and Morrall, D.D. (2001). "Control of Nitrogen Export from Watersheds by Headwater Streams." *Science*, 292, 86-90.

Rabalais, N.N., Turner, R.E., et al. (1996). "Nutrient changes in the Mississippi River and system responses on the adjacent continental shelf." *Estuaries*, 19, 386–407.

Russo, J.P. and Fox, J.F. (2012). "The role of the surface fine-grained laminae in a lowland watershed: a model approach." *Geomorphology*.

Seitzinger S. 2008. "Out of reach." *Nature*, 452:162-163.

Turner, R. E., and Rabalais, N. N. (1991). "Changes in Mississippi River water quality this century: implications for coastal food webs." *Bioscience*, 41, 140–147.

Turner, R. E., and Rabalais, N. N. (1994). "Coastal eutrophication near the Mississippi river delta." *Nature*, 368, 619–621.

Vitousek, P.M., Aber, J.B., Howarth, R.W., Likens, G.E., Matson, P.A., Schindler, D.W., Schlesinger, W.H., and Tilman, G.D. (1997). "Human alteration of the global nitrogen cycle: sources and consequences." *Ecological Applications*, 7, 737–750.

Zhou, X.; Helmers, M. J.; Asbjornsen, H.; Kolka, R.; Tomer, M. D. (2010) "Perennial filter strips reduce nitrate levels in soil and shallow groundwater after grassland-to-cropland conversion." *Journal of Environmental Quality*. 39, 2006-2015.

In the following Appendices, Standard Operating Procedures (SOPs) and reference material are provided for (1) standard water quality parameters (i.e. ammonium, nitrate, DIC, DOC, DP, and Sediment concentration) that have well established methods and collection procedures, (2) analytical field instrumentation and techniques (i.e. Fluid velocity, Stage, Turbidity, Temperature, DO, pH, and Conductivity) and (3) methods that involve some project specific alterations to accepted methods (i.e. $\delta^{15}N$ of nitrate, $\delta^{15}N$ of ammonium and $\delta^{15}N$ of Transported sediment, POC and PN). For the latter, SOPs developed for this project are provided to ensure QA.

A1) Ammonium

A1.1) Field SOP

See section A15.1

A1.2) Laboratory SOP-Ammonia as Nitrogen in Water--KGS 4500-NH_3-F

Ammonia as Nitrogen in Water

1. Discussion MDL = 0.02 as of 5/2002

Principle

An intensely blue compound, indophenol, is formed by the reaction of ammonia, hypochlorite, and phenol catalyzed by sodium nitroprusside.

Sensitivity

This method covers the range from 0.05 ppm to 1.00 ppm ammonia as nitrogen.

Interferences

Complexing magnesium and calcium with citrate eliminates interference produced by precipitation of these ions at high pH. There is no interference from other trivalent forms of nitrogen.

Sample Preservation

Samples may be preserved up to 28 days by adding concentrated sulfuric acid to adjust to pH 2 or less and refrigerating at 4°C.

2. Safety

Phenol is volatile, corrosive, and toxic. Use with proper ventilation and protective gear.

3. Apparatus

Varion 50 Spectroscopy system

Magnetic stirrer

Filtration apparatus:

Gelman 47 mm magnetic filter funnel.

Suction flasks, connected in series to a vacuum system.

Reservoir for the filtrate, 500 mL.

Trap which prevents liquid from entering the vacuum system, 1000 mL.

Glass fiber filters—Whatman 47 mm, 1 μm glass fiber filters.

4. Reagents

Purity of Reagents—Reagent grade chemicals shall be used in all tests. Unless otherwise indicated, all reagents shall conform to the specifications of the Committee on Analytical Reagents of the American Chemical Society. Other grades may be used, provided it is first ascertained that the reagent is sufficiently high in purity to permit its use without lessening the accuracy of the determinations.

Purity of Water—Unless otherwise indicated, references to water shall be understood to mean Type I reagent water conforming to the requirements in ASTM Specification D1193.

Sodium hydroxide solution, 1 N—Dissolve 40 g of NaOH in 500 mL of water. Dilute to 1 L.

Sulfuric acid solution, 1 N—Slowly add 28 mL of concentrated H_2SO_4 to 500 mL of water. Dilute to 1L.

Sodium hydroxide solution, 10 N—Dissolve 400 g of NaOH in 800 mL of water. Dilute to 1 L.

Sodium hypochlorite—5% solution that is available as commercial bleach. Purchase fresh bleach every two months.

Alkaline citrate—Dissolve 100 g of trisodium citrate and 5 g of sodium hydroxide in water. Dilute to 500 mL.

Phenol solution—Mix 11.1 mL phenol (≥89%) in ethanol (95%) to a final volume of 100 mL. Store out of light in a tin canister. This reagent **must be prepared weekly**.

CAUTION: Phenol is volatile and toxic. Use with proper ventilation and protective gear.

Oxidizing solution—Mix one part of the bleach with four parts of the alkaline citrate solution.
Prepare fresh daily.

Sodium nitroprusside solution—0.05% solution purchased from LabChem, Inc., or prepared by dissolving 0.5 g sodium nitroprusside in 1 liter of water. Store in a dark bottle for up to a month.

Stock ammonia as nitrogen solution—Purchased 1000 mg/L ammonia as nitrogen standard. (Fisher #13-641-924C).

Ammonia standard, 5 mg/L—Dilute 1 mL of the 1000 mg/L stock ammonia solution to 200 mL with water adjusted to a pH of 2 or less.

Blank—water adjusted to a pH of 2 or less. (This will have all reagents added in the same manner as the standards and samples.)

Ammonia QC Stock Solution—Using a commercially available quality control solution, dilute to a desired range and record manufacturers name, lot #, and date.

Quality control sample—Dilute ammonia QC stock solution so that QC value falls midway in analysis working range (0.05-1.00 ppm). Using 18 ppm QC stock solution, dilute 5 mL of ammonia stock to 250 mL, resulting in a concentration of 0.36 ppm.

5. Procedure

A. Standards Prep

Prepare standard concentrations, as described below, using the ammonia standard (5 mg/L) and diluting them to a volume of 50 mL with water of a pH $\leq$ 2. This is necessary if samples have been preserved with H_2SO_4..

Note: 50 drops of concentrated H_2SO_4 in 1 L of DI water yields the desired pH.

Volume of Ammonia standard, mL	Standard concentration, mg/L
0.5	0.05
1	0.10
3	0.30
5	0.50
8	0.80
10	1.00

Standards must be prepared **daily**.

The intense color development at concentrations greater than 0.8 ppm will be related in a curvilinear fashion. If it is necessary to work in ranges greater than 1.0ppm, it is important to remember this.

Do not accept any result outside the last point on the calibration curve. Sample must be diluted (to measures inside the 0.5-1.0ppm curve) and ran again on a new run

B. Sample Prep

Pour 50 mL portions of all standards, samples, and QC's into 100 mL plastic beakers.

Add 1 mL of the EDTA solution, if deemed necessary.

Adjust all standards, samples, blanks, and QC's in the pH range 9-11with H_2SO_4 and or NaOH. The pH can be determined using the using multi-color plastic pH test strip.

Note: The color reaction is pH dependent, so this is CRITICAL.

Filter the standards, samples, and QC's.

Volumetrically transfer 25 mL of each adjusted sample, standard, blank, and QC's into a 25 mL beaker.

Place stir bars in each beaker.

Add the following reagents to each:

a. 1 mL phenate solution

b. 1 mL sodium nitroprusside solution

c. 2.5 mL oxidizing solution

8. Cover with parafilm and place on stir plate. Develop for one hour at room temperature in subdued light. (Color is stable for 24 hrs.)

C. Sample Analysis

The spectrophotometer must be allowed to warm up for at least one hour before use. See Spectrophotometer SOP for a detailed listing of necessary computer commands.

For ammonia, the wavelength must be set to scan a range of **640nm.**.

Note: Phenol Waste from the this assay will react with the General Acidic Waste. KEEP THEM SEPARATE!!

Read and record absorbance on the spectrophotometer. This is usually done the morning following color development.

5. Pour leftover sample waste in phenate waste container.

For glassware clean up, refer to **"AMMONIA"** section of Glassware GLP.

Calculations

Results given are NH3-N (not NH3). Convert using NH3 = (NH3-N) / (0.8224**)**

6. Quality Control

A quality control sample should be run at the beginning and end of each sample delivery group (SDG) or at the frequency of one per every ten samples. The QC's value should fall between ± 10 % of its theoretical concentration.

A duplicate should be run for each SDG or at the frequency of one per every twenty samples, whichever is greater. The RPD (Relative Percent Difference) should be less than 10%. If this difference is exceeded, the duplicate must be reanalyzed

From each pair of duplicate analytes (X_1 and X_2) calculate their RPD value:

$$\% \, RPD = 2 \bullet \left(\frac{X_1 - X_2}{X_1 + X_2} \right) x \, 100$$

where: (X_1 - X_2) means the absolute difference between X_1 and X_2.

If a sample's value exceeds 1.00 ppm, the sample must be diluted. The samples must be diluted so that its concentration falls between 0.05 ppm and 1.00 ppm. The sample must diluted using volumetric flasks and pipettes.

7. Method Performance

The method detection limit (MDL) should be established by determining seven replicates that are 2 to 5 times the instrument detection limit. The MDL is defined as the minimum concentration that can be measured and reported with 99% confidence that the analyte concentration is greater than zero and is determined from analysis of a sample in a given matrix containing the analyte.

$$MDL = t_{(n-1,1-\alpha=99)}(S)$$

where:

t = the t statistic for n number of replicates used
n = number of replicates
S = standard deviation of replicates

8. References

Standard Methods for the Examination of Water and Wastewater, 20th edition (1998), Method 4500-NH_3-F, pg. 4-108

ASTM vol. 11.01 (1996), D 1193, " Specification for Reagent Water", pg. 116

A2) Nitrate

A2.1) Field SOP

See section A15.1

A2.2) Laboratory SOP- Ion Chromatography of Water --KGS 9056

Ion Chromatography of Water

1. Discussion

Principle

This method addresses the sequential determination of the following inorganic anions: *bromide, chloride, fluoride, nitrate, Kjeldahl nitrogen, total nitrogen* and *sulfate*. A small volume of water sample is injected into an ion chromatograph to flush and fill a constant volume sample loop. The sample is then injected into a stream of carbonate-bicarbonate eluent. The sample is pumped through three different ion exchange columns and into a conductivity detector. The first two columns, a precolumn (or guard column), and a separator column, are packed with low-capacity, strongly basic anion exchanger. Ions are separated into discrete bands based on their affinity for the exchange sites of the resin. The last column is a suppressor column that reduces the background conductivity of the eluent to a low or negligible level and converts the anions in the sample to their corresponding acids. The separated anions in their acid form are measured using an electrical conductivity cell. Anions are identified based on their retention times compared to known standards. Quantitation is accomplished by measuring the peak area and comparing it to a calibration curve generated from known standards.

Sensitivity

Ion Chromatography values for anions ranging from 0 to approximately 40 mg/L can be measured and greater concentrations of anions can be determined with the appropriate dilution of sample with deionized water to place the sample concentration within the working range of the calibration curve.

Interferences

Any species with retention time similar to that of the desired ion will interfere. Large quantities of ions eluting close to the ion of interest will also result in interference. Separation can be improved by adjusting the eluent concentration and /or flow rate. Sample dilution and/or the use of the method of Standard Additions can also be used. For example, high levels of organic acids may be present in industrial wastes, which may interfere with inorganic anion analysis. Two common species, formate and acetate, elute between fluoride and chloride. The water dip, or negative peak, that elutes near, and can interfere with, the fluoride peak can usually be eliminated by the addition of the equivalent of 1 mL of concentrated eluent (100X) to 100 mL of each standard and sample. Alternatively, 0.05 mL of 100X eluent can be added to 5 mL of each standard and sample.

Because bromide and nitrate elute very close together, they can potentially interfere with each other. It is advisable not to have Br-/NO3- ratios higher than 1:10 or 10:1 if both anions are to be quantified. If nitrate is observed to be an interference with bromide, use of an alternate detector (e.g., electrochemical detector) is recommended.

Method Interferences may be caused by contaminants in the reagent water, reagents, glassware, and other sample processing apparatus that lead to discrete artifacts or elevated baseline in ion chromatograms. Samples that contain particles larger than 0.45 micrometers and reagent solutions that contain particles larger than 0.20 micrometers require filtration to prevent damage to instrument columns and flow systems. If a packed bed suppressor column is used, it will be slowly consumed during analysis and, therefore, will need to

be regenerated. Use of either an anion fiber suppressor or an anion micro-membrane suppressor eliminates the time-consuming regeneration step by using a continuous flow of regenerant.

Because of the possibility of contamination, do not allow the nitrogen cylinder to run until it is empty. Once the regulator gauge reads 100 kPa, switch the cylinder out for a full one. The old cylinder should them be returned to room #19 for storage until the gas company can pick it up. Make sure that the status tag marks the cylinder as "EMPTY".

Sample Handling and Preservation
Samples should be collected in glass or plastic bottles that have been thoroughly cleaned and rinsed with reagent water. The volume collected should be sufficient to ensure a representative sample and allow for replicate analysis, if required. Most analytes have a 28 day holding time, with no preservative and cooled to 4°C. Nitrite, nitrate, and orthophosphate have a holding time of 48 hours. Combined nitrate/nitrite samples preserved with H_2SO_4 to a pH $\leq$2 can be held for 28 days; however, pH$\leq$2 and pH$\geq$12 can be harmful to the columns. It is recommended that the pH be adjusted to pH$\geq$2 and pH$\leq$12 just prior to analysis.

Note: Prior to analysis, the refrigerated samples should be allowed to equilibrate to room temperature for a stable analysis.

2. Apparatus
Dionex DX500
Dionex CD20 Conductivity Detector
Dionex GP50 Gradient Pump
Dionex Eluent Organizer
Dionex AS40 Automated Sampler
Dionex ASRS-Ultra Self-Regenerating Suppressor
Dionex Ionpac Guard Column (AG4A, AG9A, or AG14A)
Dionex Ionpac Analytical Column (AS4A, AS9A, or AS14A)
Dionex Chromeleon 6.8 Software Package
Dionex 5 mL Sample Polyvials and Filter Caps
2 L Regenerant Bottles
5 mL Adjustable Pipettor and Pipettor Tips
1 mL Adjustable Pipettor and Pipettor Tips
A Supply of Volumetric Flasks ranging in size from 25 mL to 2 L
A Supply of 45 micrometer pore size Cellulose Acetate Filtration Membranes
A Supply of 25x150 mm Test Tubes
Test Tube Racks for the above 25x150 mm Test Tubes
Gelman 47 mm Magnetic Vacuum Filter Funnel, 500 mL Vacuum Flask, and a Vacuum Supply

3. Reagents
Purity of Reagents—HPLC grade chemicals (where available) shall be used in all reagents for Ion Chromatography, due to the vulnerability of the resin in the columns to organic and trace metal contamination of active sites. The use of lesser purity chemicals will degrade the columns.

Purity of Water—Unless otherwise indicated, references to water shall be understood to mean Type I reagent grade water (Milli Q Water System) conforming to the requirements in ASTM Specification D1193.

Eluent Preparation for **SYSTEM2 NITRATE** *Methods, including Bromides (using AG4, AG4 and AS4 columns)*—All chemicals are predried at 105° C for 2 hrs then stored in the desiccator. Weigh out 0.191 g of sodium carbonate (Na_2CO_3) and 0.286 g of sodium bicarbonate ($NaHCO_3$) and dissolve in water. System 2 (the chromatography module that contains the AG4, AG4, and AS4 Dionex columns) to be sparged, using helium, of all dissolved gases before operation.

Eluent Preparation for **SYSTEM2 NITRATE** (F) *Method (using AG14 and AS14 columns)—W*eigh out 0.3696 g of sodium carbonate (Na_2CO_3) and 0.080 g of sodium bicarbonate (NaHCO3) and dissolve in water. Bring the volume to 1000 mL and place the eluent in the System 1 bottle marked for this eluent concentration. The eluent must be sparged using helium as in the above reagent for System 2.

Eluent Preparation for **SYSTEM2 TKN** (TKN) *Methods, including Total Nitrogen (using AG4A, AG4A, and AS4A columns)*—Weigh out 0.191 g of sodium carbonate (Na_2CO_3) and 0.143 g of sodium bicarbonate ($NaHCO_3$) and dissolve in water. Bring the volume up to 1000 ml and place in the System 2 bottle labeled "*IC-TKN 0.191/0.143*". Sparge the eluent as in the above reagent for System 2.

100X Sample Spiking Eluent—prepared by using the above carbonate/bicarbonate ratios, but increasing the concentration 100X. Weigh out 1.91 g of Na_2CO_3 and 2.86 g of $NaHCO_3$ into a 100 mL volumetric flask. 0.05 mL of this solution is added to 5 mL of all samples and standards to resolve the water dip associated with the fluoride peak.

Stock standard solutions, 1000 mg/L (1 mg/mL): Stock standard solutions may be purchased (SPEX) as certified solutions or prepared from ACS reagent grade materials (dried at 105° C for 30 minutes)

Calibration Standards—for the **SYSTEM2 NITRATE** (except Bromide) methods are prepared as follows:

Calibration Standard 1: Pipette 0.1 mL of 1000 mg/L $NaNO_3$ stock standard, 0.1 mL of 1000 mg/L NaF stock standard, 2 mL of 1000 mg/L NaCl stock standard, and 10 mL of 1000 mg/L K_2SO_4 stock standard into a 1000 mL volumetric flask partially filled with water, then fill to volume.
Calibration Standard 2: Pipette 0.5 mL of 1000 mg/L $NaNO_3$ stock standard, 0.5 mL of 1000 mg/L NaF stock standard, 5 ml of 1000 mg/L NaCl stock standard, and 20 mL of 1000 mg/L K_2SO_4 stock standard into a 1000 mL volumetric flask, partially filled with water, then fill to volume.
Calibration Standard 3: Pipette 2.5 mL of 1000 mg/mL $NaNO_3$ stock standard, 2.5 mL of 1000 mg/L NaF stock standard, 10 mL of 1000 mg/L NaCl stock standard, and 40 mL of 1000 mg/L K_2SO_4 stock standard into a 1000 mL volumetric flask partially filled with deionized water, then fill to volume.
Quality Control Sample: Pipette 1.0 mL of 1000 mg/L $NaNO_3$ stock solution, 1.0 mL of 1000 mg/L NaF stock solution, 8 mL of 1000 mg/L NaCl stock solution, and 30 mL of mg/L K_2SO_4 stock standard into a 1000 mL volumetric flask, partially filled with water, then fill to volume.

Calibration Standards—for the **SYSTEM2 NITRATE** (Fluoride) method are prepared as follows:
Calibration Standard 1: Pipette 0.01 mL of 1000 mg/L NaF stock standard into a 1000 mL volumetric flask partially filled with water, then fill to volume.
Calibration Standard 2: Pipette 0.05 mL of 1000 mg/L NaF stock standard into a 1000 mL volumetric flask partially filled with water, then fill to volume.
Calibration Standard 3: Pipette 0.1 mL of 1000 mg/mL NaF stock standard into a 1000 mL volumetric flask partially filled with water, then fill to volume.
Calibration Standard 4: Pipette 0.5 mL of 1000 µg/mL NaF stock standard into a 1000 mL volumetric flask partially filled with water, then fill to volume.
Calibration Standard 5: Pipette 1.0 mL of 1000 mg/L 1000 stock standard into a 1000 mL volumetric flask partially filled with water, then fill to volume.
Quality Control Standard: Pipette 0.1 mL of 1000 mg/L NaF from a separate source stock standard into a 1000 mL volumetric flask partially filled with water, then fill to volume.
Quality Control Standard: Pipette 0.4 mL of 1000 mg/L NaF from a separate source stock standard into a 1000 mL volumetric flask partially filled with water, then fill to volume.
Quality Control Standard: Pipette 1.0 mL of 1000 mg/L NaF from a separate source stock standard into a 1000 mL volumetric flask partially filled with water, then fill to volum

Calibration Standards—for the **SYSTEM2 NITRATE** (Bromide) method are prepared as follows:
1. *Calibration Standard 1*: Pipette 2 mL of 1000 mg/L NaBr stock standard into a 1000 mL volumetric flask partially filled with water, then fill to volume.
Calibration Standard 2: Pipette 5 mL of 1000 mg/L NaBr stock standard into a 1000 mL volumetric flask partially filled with water, then fill to volume.
Calibration Standard 3: Pipette 10 mL of 1000 mg/L NaBr stock standard into a 1000 mL volumetric flask partially filled with water, then fill to volume.
Quality Control Standard: Pipette 8 mL of 1000 mg/L NaBr stock standard into a 1000 mL volumetric flask partially filled with water, then fill to volume.

Outside Source Certified Quality Control Sample—ERA

4. Procedure
A. Instrument Preparation
Before turning on the Dionex Ion Chromatography System:
Fill the eluent reservoir(s) with fresh eluent.
Make certain the waste reservoir is empty of all waste.
Turn on the helium. The system pressure should be between 7 - 15psi. The system pressure can be regulated with the knob on the back of the Eluent Organizer.
Connecting a piece of tubing to the gas line going into the eluent bottle and putting the tubing into the eluent degasses the eluent reservoir(s). The gas knob on the Eluent Organizer that corresponds to the eluent bottle should be slowly opened until a constant bubbling stream can be seen in the eluent bottle.
The eluent should be degassed with helium, for a minimum of 30 minutes, before operation of the instrument.
After the eluent has been degassed, remove the tube from the eluent and tightly seal the eluent bottle. The eluent is now ready to introduce into the system.
Whether using the IP25 for Fluorides or the GP50 for everything else, turn off the browser, scroll to **REMOTE** on the screen, select **LOCAL** and **ENTER**.
Scroll to mL/min., change to 0 mL/min., and hit **ENTER**. If using the IP25 pump, skip to step #5.
Hit **MENU** and select **1**, then **ENTER**.
Insert syringe into the Priming Block, open the gas valve on the Eluent Organizer, turn the valve on the Priming Block counterclockwise, and turn on the pump that corresponds with the method to be ran by pushing the **OFF/ON** button.
If the syringe does not fill freely, assist by gently pulling back on the plunger of the syringe. Make certain that all of the air bubbles are removed from the eluent line to the pumps.
Press **OFF/ON** on the pump to turn it off.
Turn the valve on the Priming Block clockwise, remove the syringe and expel the air bubbles from the syringe.
Reinsert the syringe filled with eluent into the Priming Block.
Open the valve on the Pressure Transducer and the valve on the Priming Block with the eluent filled syringe still attached. This is accomplished by turning both counterclockwise.

Press **PRIME** on the pump and push the contents of the syringe into the Priming Block. After the eluent has been injected into the Priming Block, press **OFF/ON** to turn the prime pump off and to close the valves on the Pressure Transducer and Priming Block.
Remove the syringe from the Priming Block.
Scroll to the mL/min. on the screen for the pump. For the GP50, type 2 mL/min., and press **ENTER**. For the IP25, type 1.2 mL/min., and press **ENTER**.
Press **OFF/ON** to turn on the pump at the appropriate rate. The pressure should soon stabilize between both pumpheads after two minutes of pumping time.
If the pressure between pumpheads has a difference >20 psi, then shut down the pump and repeat steps 2-14 to remove air bubbles and prime the pumps.
Once the pump has a pumping pressure difference between pumpheads of <20 psi, then go to the computer and enter PeakNet.
On the computer**, turn on the Chromeleon 6.8 browser**, then choose either **System 1** (Fluoride) or **System 2** (all other anions including Bromide and TKN).
Go to **last run sequence, click to highlight and go to file, click save as.**. This will load the method of interest and a template for the current sequence run.
The sequence is edited to reflect the method and samples that are to be run.
SYSTEM2 NITRATE for Fluoride
SYSTEM2 NITRATE for Bromides
SYSTEM2 TKN for TKN and Total Nitrogen

Note: Data is reprocessed in the section of Chromelon 6.8 called *Sequence integration editor*. Only operators with a <u>minimum of three months</u> experience in Ion Chromatography should attempt to reprocess data for this analysis. Once data is optimized, then the nitrogen values from nitrate and nitrite analysis can be subtracted from this value for the TKN nitrogen value. If only Total Nitrogen is needed then use the optimized data value without the correction for nitrite and nitrate nitrogen.

SYSTEM 2 NITRATE for all other anions,
Observe the reading on the screen of the CD20 Conductivity Detector. A conductivity rate change of <0.03 μS over a 30 second time span is considered stable for analysis.
If using the GP50 pump, it will take about 15-30 minutes for the CD20 system to stabilize. If using the IP25, it will take between 30 minutes to 2 hours for stabilization.
Once the CD20 is stabilized, the Dionex DX500 Ion Chromatography
System is ready to start standardization.

NOTE: When using the GP50 Gradient Pump, all due care must be taken before one switches from local procedures to remote procedures. The bottle from which the eluent is being pumped (i.e., A, B, C, or D) must exactly match the bottle specified in the method. If there is a difference, then once the pump control is turned over to remote control, irreversible damage and destruction of suppressors, columns, piston seals, and check valves on the GP50 Gradient Pump will occur. <u>NEVER</u> switch from bottle C to A, B, or D without flushing the system lines with water to remove all traces of eluent from bottle C from the lines.

B. <u>Sample Preparation</u>

If the sample was not filtered in the field, it must be done so now. Transfer 50 mL of a well-mixed sample to the filtering apparatus. Apply the suction and collect the filtrate.
If the conductivity values for the sample are high, dilution will be necessary to properly run the sample within the calibration standard range. Dilutions are made in the Polyvials with the plastic Filter Caps. If the dilutions are > 20X, then volumetric glassware is required.
All dilutions are performed with reagent grade DI water. Be sure to mix the dilution well.
For Fluorides and Bromides, pipette 5.0 mL of the filtered samples into the Polyvials. For all other anions, including TKN and Total Nitrogen, first pipette 0.05 mL of 100X sample spiking eluent into the Polyvials, then pipette 4.95 mL of the filtered samples on top of the spiking eluent.
The Filter Caps are pressed into the Polyvials using the insertion tool.
Place the Polyvials into the Sample Cassette, which is placed into the Autosampler.
The white/black dot on the Sample Cassette should be located on right-hand side when loaded in the left-hand side of the Automated Sampler for System 2.

8. For every ten samples the following should be included:

a. 1 DI water blank
b. 1 Duplicate of any one sample
c. 1 Quality Control sample/calibration check

C. <u>Calibration and Sample Analysis</u>

Set up the instrument with proper operating parameters established in the operation condition procedure
The instrument must be allowed to become thermally stable before proceeding. This usually takes 1 hour from the point on initial degassing to the stabilization of the baseline conductivity.
To run samples on the Dionex Ion Chromatography System:
Make a run schedule on the Chromeleon 6.8 Software Section labeled **SEQUENCE**.
Double click the mouse on the **SYSTEM 1 SEQUENCES or SYSYTEM 2 SEQUENCES** to display the Scheduler Area. The name of the calibration standards must be entered under the sample name section as **Standard #1, Standard #2**, and **Standard #3**.

Note: Level must be changed to the corresponding standard level or the calibration will be in error. (Example: Standard #1 = Level #1; Standard #5 = Level #5)

Next, enter QC, blanks, QC, samples, duplicates, QC, and blanks, in that order.
Under sample type, click on either **Calibration Standard** or **Sample**, depending on what is being run.
Under the **Method** section, the method name must be entered. To do so, double click on the highlighted area under **Method**, scroll through the list of methods and double click on the method of interest.
Next under the **Data File** section, enter the name of the data file.
Finally, in the **Dil** area, type in the dilution factor if different from 1. Do this for all standards, blanks, quality controls, duplicates, and samples to be run under this schedule.
Save the schedule and obtain a printout of it.
Standardize the Dionex Ion Chromatography System by running the standards: **Standard #1**, **Standard #2**, and **Standard #3**.
Run the QC standards.
Run the prepblank and DI water blank.
Run the samples, duplicates, and blanks.
Run the QC standards at the end.

5. Calculations

Calculations are based upon the ratio of the peak area and concentration of standards to the peak area for the unknown. Peaks at the same or approximately the same retention times are compared. Once the method has been updated with the current calibration, this is calculated automatically by the software using linear regression. Remember that when dilutions are being run, the correct dilution factor must be entered.
Manual calculations are based upon the ratio of the peak and concentration of standards to the peak area for the unknown when the software will not automatically calculate the unknown concentration. Peaks at the same or approximately the same retention times are compared. The unknown concentration can be calculated from using this ratio. Remember that when dilutions are being run that the correct dilution factor must be entered before you will get the correct result.
When possible the unknown should be bracketed between two knowns and the calculation of the unknown made from both for comparison.

6. Quality Control

A quality control sample obtained from an outside source must first be used for the initial verification of the calibration standards. A fresh portion of this sample should be analyzed every week to monitor stability. If the results are not within +/- 10 % of the true value listed for the control sample, prepare a new calibration standard and recalibrate the instrument. If this does not correct the problem, prepare a new standard and repeat the calibration. A quality control sample should be run at the beginning and end of each sample delivery group (SDG) or at the frequency of one per every ten samples. The QC's value should fall between ± 10 % of its theoretical concentration.

A duplicate should be run for each SDG or at the frequency of one per every twenty samples, whichever is greater. The RPD (Relative Percent Difference) should be less than 10%. If this difference is exceeded, the duplicate must be reanalyzed.

From each pair of duplicate analytes (X_1 and X_2), calculate their RPD value:

$$\% \; RPD = 2 \bullet \left(\frac{X_1 - X_2}{X_1 + X_2} \right) x\, 100$$

where: (X_1 - X_2) means the absolute difference between X_1 and X_2.

7. Method Performance

The method detection limit (MDL) should be established by determining seven replicates that are 2 to 5 times the instrument detection limit. The MDL is defined as the minimum concentration that can be measured and reported with 99% confidence that the analyte concentration is greater than zero and is determined from analysis of a sample in a given matrix containing the analyte.

$$MDL = t_{(n-1,1-\alpha\,=99)}(S)$$

where: t = the t statistic for n number of replicates used (for n=7, t=3.143)
n = number of replicates
S = standard deviation of replicates

8. Reference

EPA SW 846-9056, Chapter 5, September 1994

U.S. EPA Method 300.0, March 1984

ASTM vol. 11.01 (1996), D 4327, "Standard Test Method for Anions in Water by Chemically Suppressed Ion Chromatography".

Discussion
2.Principle and iodine.
Reagents
Calibration Standards
Calibration Standard 1: Pipette 0.1 mL of 1000 mg/L I stock standard into a 1000 mL volumetric flask partially filled with water, then fill to volume.
Calibration Standard 2: Pipette 0.5 mL of 1000 mg/L I stock standard into a 1000 mL volumetric flask partially filled with water, then fill to volume.
Calibration Standard 3: Pipette 1.0 mL of 1000 mg/L I stock standard into a1000 mL volumetric flask partially filled with water, then fill to volume.
Calibration Standard 4: Pipette 5.0 mL of 1000 mg/L I stock standard into a1000 mL volumetric flask partially filled with water, then fill to volume.
Calibration Standard 5: Pipette 10.0 mL of 1000 mg/L I stock standard into a 1000 mL volumetric flask partially filled with water, then fill to volume.
Quality Control Sample: Pipette 5.0 mL of 1000 mg/L I stock standard into a1000 mL volumetric flask partially filled with water, then fill to volume.

A3) Dissolved Inorganic Carbon (DIC)
A3.1) Field SOP
See section A15.1.
A3.2) Laboratory SOP-Dissolved Inorganic Carbon-KGS DIC
1. Discussion
Principles
Dissolved Inorganic Carbon (DIC) is all inorganic carbon (e.g., carbon dioxide) dissolved in a given volume of water at a particular temperature and pressure.

Carbon dioxide gas evolved by dissolution in acid from carbonates In the sample is swept by a gas stream into a coulometer cell. The coulometer cell is filled with a partially aqueous medium containing ethanolamine and a colorimetric indicator. Carbon dioxide is quantitatively absorbed by the solution and reacts with the ethanolamine to form a strong, titratable acid which causes the indicator color to fade. The titration current automatically turns on and electrically generates base to return the solution to its original color (blue).

The coulometric determination of carbon dioxide has the unique distinction of performing with high degree of both precision and accuracy while maintaining relatively high sample throughput.

Working Range
<1 microgram up to 10,000 micrograms of Carbon for a single sample.

Interference
Coulometric system should remain a closed system. Outside air entering into the system after it has been purged will affect the results.

Sample Handle and Preparation
Sample should be taken to fill the bottle with no headspace, kept refrigerated at 4ºC and should not be opened until time of analysis. Sample should be analyzed ASAP from the time of collection

2. Safety
Safety glasses and gloves, and lab coat should be worn while performing this analysis due to the use of and possible exposure to strong acids and Silver Nitrate.

3. Apparatus
UIC Carbon Dioxide Coulometer CM5014
Becton Dickinson 5ml Syringes

4. Reagents
10% Phosphoric Acid – 50mls of O-Phosphoric Acid 85% in 450 mls of Mili-Q water

0.4M $AgNO_3$ Solution – 34g $AgNO_3$ in 500 mls of Milli-Q Water

Potassium Iodide (crystals) Fisher Brand – Bought from Fisher

UIC Carbon Anode Solution - Bought only from UIC

UIC Carbon Cathode Solution – Bought only from UIC

5. Procedure
A. Instrument Preparation

1. Check frit end is clean located in the back chamber in the $AgNO_3$ solution. ***If dirty then it must be cleaned, follow frit cleaning procedure Appendix A***
2. Check and fill titration bottle with 10% Phosphoric Solution
3. Remove or place a clean sample vial that will be used for acid blank reading.

B. Prepare Coulometer pH cup.

1. Wipe cup with kimwips to make sure there are **no fingerprints** or dust on cup. **(AVOID TOUCHING LARGE PART OF CUP)**
2. Large-cup – fill approximately 75mls with UIC Cathode Solution. Gently place the top on the cup, containing electrodes and air dispenser. Turn to have air dispenser toward the back of cup.
3. Arm of cup – Poor a layer of Potassium Iodide to approximately ¼ up the membrane between large cup and arm. Fill the arm with anode solution to equal level of solution in large cup. Gently place in silver electrode. **(DO NOT Touch Potassium Iodide)**
4. Place cup in the coulometer and attach the electrodes and the air fittings to their appropriately colored connections on the coulometer.

C. Starting the Coulometer

1. Turn on the water from the hood so that there is a constant drip running through coulometer and into the sink behind the instrument.
2. Turn on the gas 1.5 twists.
3. Turn on Titrator apparatus. Check flow meter it should be reading approximately 100.
4. Turn on power to coulometer. CELL BUTTON SHOULD STILL BE IN OFF POSITION.
5. Hit down arrow key ↓
6. Select Run Diagnostics
7. Select # 3 Set date and Time (set date and time used full year example 2008) and 00 for seconds
8. Select change Settings answer the questions as follows
    - Carbon
    - Weight
    - Milligrams
    - -0.7
    - 1.00
    - 6
    - 1.00 (minutes)
    - Coulometer end point
        - Manual
        - N
9. Select Print Settings
10. Select Exist Diagnostics
11. Select Run Cell Set-up

- Move cell around until you the cell to read as close to 3950 without going over once there press F2

13. Turn Cell button to on
14. Select Run Analysis
15. Wait approximately 30 minutes until the %T reading is at 29
16. When reading is at 29% press enter to start run

D. Running Samples

1. Blank will **ALWAYS** be first. Blank is the empty vial with stir rod place on during instrument set-up. Sample ID will be "BLANK" and it will not give you opportunity to put in weight. It will go right to place to, pipette in the acid (6 mls) from titrator bottle and hit enter QUICKLY. **Blank should always read less then 7.**
2. QC is the standard $CaCO_3$ Sample ID $CaCO_3$ Press enter. Enter weight in mg press enter. Put in acid from titrator bottle and then press enter quickly. *%C should be between 11.7-12.1*
3. If you are running solid sample weight out and follow the same procedure as the QC/ Standard.
4. If you are doing DIC –water samples then follow rest of this procedure
5. Place a clean vial on with stir rod.

Enter sample ID press enter. Enter weight or volume ml=mg. Use 3 to 5mls of sample pulled from sample bottle into a syringe. Titrate 3mls of acid into vial, inject sample into top of cylinder press enter and titrate another 3mls in quickly. Let coulometer run until a result is reached. This result is in %C.

6. Run each water sample in this way with duplicates at least every 10 samples preferably every 5. Use a new vial for each new sample and or aliquot. **Between each sample it will ask if you want to run another sample. Always select yes until you are finished.**
7. After running the last sample / QC select no to more samples and the coulometer will print final results page.

F. Breaking down Coulometer

1. Turn off Titrator / flow unit
2. Turn off the coulometer unit
3. Turn off gas and water to unit
4. Remove the cup from unit
5. Empty the cup contents in the blue hazardous drum.
6. Wash cup (do not use anything that would scratch glass) and rinse VERY WELL with Milli-Q water and place on tray to dry. Rinse all other parts off with Milli-Q and place on tray to dry.

6. Calculations

The value from the Coulometer is in Micrograms C.

Conversion to ppm C (DIC) in solution

$$\frac{\text{Coulometer reading – blank reading (of acid and vial) * 1 (density of water)}}{\text{Mls of sample injected into coulometer}}$$

Conversion to ppm CO_2 in solution

*ppm C (DIC) * 3.6658 = ppm CO_2 in solution*

7. Quality Control / Rate and Range

"This 100% efficient coulometric process gives results in basic theoretical units (coulombs) so calibration using standards is not required.

"The linear range and accuracy (better than 0.20% relative standard deviation for standard materials) of the coulometer generally exceeds that obtained by other detection methods."

"Working range of the CO_2 Coulometer is from less than one microgram C up to 10,000 micrograms of C for a single sample"

"Coulometer cell solution has an absorbance capacity of over 100mg for a single cell filling, typically allowing for a full day of sampling."

"Titrating at its max current (200ma) the CO_2 Coulometer can titrate approximately 1500 micrograms of carbon (5500ug of CO_2) per minute."

QC checks are measuring a standard of Calcium Carbonate.
Standard =12.0 %C
Acceptable Range = 11.7-12.1

Trouble Shooting- If qc's are not coming out
- Check to make sure there are not leaks in system (mainly at vial and screw-top lid.
- Check gas pressure and water pressure
- Another problem could be the weight. If samples are not weighed out properly, bad calibrated balance, sample results will not be accurate
- After checks run another qc sample if still not acceptable turn off instrument process will have to be started again from the beginning with new cell material

At *this point check the silver probe it may need replacing.*

8. Method Performance

MDL studies are not performed on this instrument based on the low range and the fact that it is not a calibrated instrument.

Repeatability of this instrument
Standard Deviation of at least 7 replicate readings of the QC ($CaCO_3$)
Task performed every 3 to 6 months.

9. References

UIC Carbon Dioxide Coulometer Application Note 1
UIC Carbon Dioxide Coulometer Application Note 3

Frit Cleaning Procedure

Remove the Frit and place in a small container of 9M HCL. Allow Frit to sit and with a bulb pull some of the HCL through the fit and empty into a HCL waste container. Should notice frit becoming lighter in color.

Rinse the frit WELL Pull clean Milli-Q water up through the fit and empty into waste container over and over. This process takes quite a few times.

Test the water from the fit on pH strips to make sure there is no residual acid present.

Empty the old AgNO3 solution into hazardous waste drum and fill approximately 1 inch of new AgNO3 solution.

Attach the frit apparatus back onto the coulometer.

Make sure you keep track of where the hoses belong when removing and reattaching the frit apparatus

A4) Dissolved Organic Carbon (DOC)
A4.1) Field SOP
See section A15.1

A4.2) Laboratory SOP-KGS Dissolved Organic Carbon (DOC) SOP--KGS 9060

Total Organic Carbon in Water (TOC)/
Dissolved Organic Carbon in Water (DOC)

MDL= 0.30 mg/L

1. Discussion

Principle

The organic carbon in water and wastewater is composed of a variety of organic compounds in various oxidation states. Biological or chemical processes can oxidize some of these carbon compounds further. The biochemical oxygen demand (BOD) and chemical oxygen demand (COD) tests may be used to characterize these factions; however, the presence of organic carbon that does not respond to either the BOD or COD tests make them unsuitable for the measurement of total organic carbon. While, total organic carbon (TOC) is a more convenient and direct expression of total organic content than either BOD or COD, it does not provide the same kind of information. If a repeatable empirical relationship is established between either BOD or COD, and TOC, then the TOC can be used to estimate the accompanying BOD or COD. However, this relationship must be established independently for each set of matrix conditions, such as various points in a treatment process. Unlike BOD and COD, TOC is independent of the oxidation state of the organic matter and does not measure other organically bound elements (i.e., nitrogen, hydrogen), or inorganics that can contribute to the oxygen demand measured by BOD and COD. TOC measurement does not replace BOD and COD testing.

Measurement of TOC is of vital importance to the operation of water treatment and waste treatment plants. Drinking water TOCs range from <100ug/L to > 25,00ug/L. Wastewater may contain very high levels of organic compounds TOC>100mg/L. The presence of these organic contaminants may serve as nutrient source for undesired biological growth and for drinking water they may react with disinfectants to produce potentially toxic and carcinogenic compounds.

To determine the quantity of organically bound carbon, the organic molecules must be broken down and converted to a since molecular form. TOC methods convert organic carbon to carbon dioxide (CO2). It is more appropriate to use the High temperature combustion with Samples that have high levels of TOCs and or have complex matrix.
DOC is the same process just analyzed on a filtered sample. The sample should be filtered in the field with a GF/F filter pore size in the range of 0.7-0.25um. Sample should also be preserved after filtering with H3PO4 as with the TOC sample.

Interferences

Removal of carbonate and bicarbonate by acidification and purging with purified gas results in the loss of volatile organic substances. The volatiles also can be lost during sample blending, particularly if the temperature is allowed to rise. Another loss can occur if carbon containing particulates are unable to enter the needle. Filtration, although sometimes necessary, when DOC is to be determined, can result in loss or gain of DOC.
The major limitation to high-temperature techniques is the magnitude and variability of the blank.
With any organic carbon measurement, contamination during sample handling and treatment is a likely source of interference. This is especially true of trace analysis. Take extreme care in sampling, handling, and analyzing samples below 1 mg TOC / L.

Sample Handling and Preparation

DOC samples shall be filtered in the field with a GF/F filter with a pore size range of 0.7-0.25 um then acidified the same as the TOC sample below**.**
Because of the possibility of oxidation or bacterial decomposition of some components of aqueous samples, the lapse of time between collection of samples and start of analysis should be kept to a minimum. All samples should be stored at 4°C with no headspace in the bottles, as this will reduce the chance of losing purgeable organics. If analysis cannot be performed within two hours of collection, the sample should be acidified to a pH of ≤ 2 with H_3PO_4. However, this acidification invalidates any inorganic carbon determination of the sample. TOC samples have a 28 day hold time.

2. Safety

Phosphoric acid (H_3PO_4) is used in this method. Utilize the proper safety equipment and procedures while performing this analysis.

3. Apparatus

Total organic carbon analyzer—Teledyne Tekmar TORCH
Tank of Ultra High Purity grade Compressed Air with regulator
Volumetric Glassware
Analytical Balance—capable of weighing to the nearest 0.0001 g

4. Reagents (Get Water directly from the Purification System)

Purity of Reagents—Reagent grade chemicals shall be used in all tests. Unless otherwise indicated, all reagents shall conform to the specifications of the Committee on Analytical Reagents of the American Chemical Society. Other grades may be used, provided it is first ascertained that the reagent is sufficiently high in purity to permit its use without lessening the accuracy of the determinations.

Purity of Water—Unless otherwise indicated, references to water shall be understood to mean Type 1 reagent grade water (Milli Q Water System) conforming to the requirements in ASTM Specification D1193.

Acid reagent-18 mL of 85% phosphoric acid (H_3PO_4)
94 ml of ultra pure water

TOC stock solution (1000 mg/L)—Dissolve 2.125 g of predried KHP in ultra pure water and dilute to a final volume of 1000 mL. Good for 1 month when stored between 2-8C

TOC standard solution (20 mg/L)—Dilute 5 mL of the TOC stock solution (1000 mg/L) to 250 mL with ultra pure water.

TOC standard solution (10 mg/L)— Dilute 2 mL of the TOC stock solution (1000 mg/L) to 200 mL with ultra pure water.

Quality Control Samples— Order from ERA Dilute to known concentration using instructions From ERA.

5. Procedure

A. Perform Instrument checks -(Preventative Maintenance Chart in drawer)

Daily-

Weekly-

Monthly-

Date all tasks that were performed and initial

B. Determine your calibration range and pour chosen stock standard into bottle in position B. Normally this is a 20 ppm Stock. Instrument will dilute this stock to chosen calibration points.

C. **Set up New Calibration**

New
Calibration
TOC
(Name Calibration ex. TOC today's date)
OK
Open
Method
TOC Drinking Water -0.75mls
Ok
Select (at the top right of screen)
Choose the name of calibration you just created
Ok
SAVE you must save or calibration will not work.

D. **Set up Schedule**

New
Schedule
Under sample Type choose
Clean – 2 reps
Clean – 2reps
Blank- click on Method area and choose TOC Drinking Water-0.75mls -3 reps
Blank- click on Method area and choose TOC Drinking Water- 0.75mls - 3reps
(*Instrument auto blank corrects*)
Cal Standard- choose "TOC 0.5-20.0 with the method that says TOC Drinking Water 0.75" Select **Position should be B or wherever you placed your 20ppm stock** 3 reps per calibration point
Clean - 3 reps
Sample -Position of vial, ex.# 1&2 will be a known value QC 5 ppm and 10 ppm made up from other source than the stock used to make the calibration.
Sample –Position #3, name it, then choose Method (same as blank and calibration set) –3reps.
After all samples are entered with appropriate positions, methods, and reps
Clean -3reps

** Using the last calibration ran.**- Can't be older than 2 months old.

Don't do a Cal Standard just run a known QC-for calibration check- after your blank, if it passes continue on with run if it fails stop run and recalibrate.

6. Calculations

Instrument auto blank corrects. This is why you only run a blank at the beginning of the run before the calibration and no more during the same run.

7. Quality Control

The quality control sample set should be run at the beginning and end of each sample group to be analyzed and at the frequency of one set per every ten samples. Each QC's value should fall between ± 10 % of its theoretical concentration.

The initial calibration verification QC sample should be run at the beginning of the day's analysis. The QC's value should fall between ± 10 % of its theoretical concentration.

A duplicate should be run at the end of each sample delivery group (SDG) or at the frequency of one per every ten samples, sufficient sample volume permitting. The RPD (Relative Percent Difference) should be less than 10%. If this difference is exceeded, the sample must be reanalyzed.

From each pair of duplicate analytes (X_1 and X_2), calculate their RPD value:

$$\% \, RPD = 2 \bullet \left(\frac{X_1 - X_2}{X_1 + X_2} \right) x\,100$$

where: (X_1 - X_2) means the absolute difference between X_1 and X_2.

8. Method Performance

The method detection limit (MDL) should be established by determining seven replicates that are 2 to 5 times the instrument detection limit. The MDL is defined as the minimum concentration that can be measured and reported with 99% confidence that the analyte concentration is greater than zero and is determined from analysis of a sample in a given matrix containing the analyte.

$$MDL = t_{(n-1,1-\alpha=99)}(S)$$

where:

t = the t statistic for n number of replicates used
n = number of replicates
S = standard deviation of replicates

9. References

EPA SW 846-9060A, September 1986.

U.S. EPA 415.1, December 1982.

Standard Methods for the Examination of Water and Wastewater, 20th edition (1998), Method 5310-B, pg. 5-20-21.

A5) Dissolved Phosphorus (DP)

A5.1) Field SOP

See section A15.1

A5.2) Analytical SOP- Total Phosphorus (TP) --KGS D515

Total Phosphorus in Water

1. Discussion MDL= 0.02 as of 5/2002

Principle

Separation into total dissolved and total recoverable forms of phosphorus depends on filtration of the water sample through a 0.45 μm membrane filter. Total recoverable phosphorus includes all phosphorus forms when the unfiltered, shaken sample is heated in the presence of sulfuric acid and ammonium peroxydisulfate. Total dissolved phosphorus includes all phosphorus forms when the filtered, shaken sample is heated in the presence of sulfuric acid and ammonium peroxydisulfate. Phosphorus is converted to orthophosphate by digesting the water sample with ammonium persulfate and diluted sulfuric acid. Ammonium molybdate and antimony potassium tartrate can then react in an acid medium with dilute solutions of orthophosphate to form an antimony-phosphate-molybdate complex. This complex is reduced to an intensely blue-colored complex by ascorbic acid. The color intensity is proportional to the phosphorus concentration.

Sensitivity

The range of determination for this method is 0.05 mg/L to 1.00 mg/L P.

Interferences

Ferric iron must exceed 50 mg/L, copper 10 mg/L, or silica 10 mg/L, before causing an interference. Higher silica concentrations cause positive interferences over the range of the test, as follows: results are high by 0.005 mg/L of phosphorus for 20 mg/L of SiO2, 0.015 mg/L of phosphorus for 50 mg/L, and 0.025 mg/L of phosphorus for 100 mg/L. Because arsenic and phosphorus are analyzed similarly, arsenic can cause an interference if its concentration is higher than that of phosphorus.

Sample Handling and Preparation

Samples should be preserved only by refrigeration at 4 °C. A raw sample should be used in the analysis. The holding time for this analysis is 28 days.

2. Safety

Safety glasses, gloves, and a lab coat should be worn while performing this analysis due to the use of, and possible exposure to, strong acids and bases.

3. Apparatus

Varion 50 Spectroscopy system

Filtration Apparatus

Coors 60242 Büchner funnels.
Suction flasks, connected in series to a vacuum system.
Reservoir for the filtrate, 500 mL.
Trap which prevents liquid from entering the vacuum system, 1000 mL

Paper filters—7.5 cm, 1 μm. (VWR Cat. # 28321-005)

Analytical balance, capable of weighing to the nearest 0.0001 g.

Drying oven.

Desiccator.

Thermix Stirring Hot Plate—Model 610T

HCl Acid washed glassware—Refer to the **"Total P"** section of the Glassware GLP for further details. Commercial detergents should never used. Glassware should be dedicated for Total P use only.
6 ½ oz. Disposable polystyrene specimen cups—Cups should be rinsed three times with DI water.
4. Reagents
Purity of Reagents—Reagent grade chemicals shall be used in all tests. Unless otherwise indicated, all reagents shall conform to the specifications of the Committee on Analytical Reagents of the American Chemical Society. Other grades may be used, provided it is first ascertained that the reagent is sufficiently high in purity to permit its use without lessening the accuracy of the determinations.

Purity of Water—Unless otherwise indicated, references to water shall be understood to mean Type I reagent grade water (Milli Q Water System) conforming to the requirements in ASTM Specification D1193.

Ammonium Peroxydisulfate—Place **20 g** of ammonium peroxydisulfate in a 50 mL volumetric flask. Dilute with water to volume. Add a magnetic stirrer to the flask and let the solution stir until all the crystals have dissolved (minimum of 20 minutes). Prepare daily.(*enough for 30 beakers total*)
Solution Mixture—Dissolve 0.13 g of antimony potassium tartrate and 5.6 g of ammonium molybdate in approximately 700 mL of water. **Cautiously** add 70 mL of concentrated sulfuric acid. Allow the solution to cool and dilute to 1 liter. The solution must be kept in a polyethylene bottle away from heat. This solution is stable for one year.

Combined Reagent—Dissolve 0.50 g solid ascorbic acid in 100 mL of solution mixture. Prepare daily.

Phenolphthalein indicator solution—Dissolve 0.5 g of phenolphthalein in a mixture of 50 mL isopropyl alcohol and 50 mL water.

Sulfuric acid (31 + 69)—Slowly add 310 mL of concentrated H_2SO_4 to approximately 600 mL of water. Allow solution to cool and dilute to 1 liter.

Sodium Hydroxide, 10 N—Dissolve 400 g of NaOH in approximately 800 mL of water. Allow solution to cool and dilute to 1 liter.

Sodium Hydroxide, 1 N—Dissolve 40 g of NaOH in approximately 800 mL of water. Allow solution to cool and dilute to 1 liter.

Phosphorus stock solution (50 mg/L)—Dissolve **0.2197 g** of predried (105 °C for one hour) KH_2PO_4 in water and dilute to 1 liter. Prepare **daily**.

Phosphorus standard solution (2.5 mg/L)—Dilute 50 mL of the stock solution to exactly 1 liter of water. Prepare **daily**.

Blank—reagent grade water.

Total phosphorus stock QC solution—Using a commercially available Quality Control solution, dilute to desired range and record manufactures name, lot #, and date.

Quality control sample—Dilute total P stock solution so that QC value falls midway in analysis working range (0.05-1.00 ppm). Using 6.11 ppm QC stock solution, dilute 25 mL of Total Phosphorous stock solution to 500 mL resulting in a concentration of 0.306 ppm.

Acid for glassware-Carefully add 250 mL of concentrated hydrochloric acid to approximately 600 ml of water. Dilute to 1 liter.
Procedure
Prepare the spectrophotometer by turning on the lamp and allowing it to warm up for at least one hour. See the Spectrophotometer GLP for a detailed listing of necessary computer commands.

B. Standards Prep
Prepare a series of phosphorus standards from the 2.5 mg/L phosphorus standard solution according to the following table. Dilute each to 50 mL with water.

Volume of phosphorus standard, mL	Standard concentration, ppm
0.05	
0.10	
4	0.20
0.35	
10	0.50
15	0.75
20	1.00

2. Prepare all standards **daily**.

C. Sample Prep
Pour 50 mL of each of the two blanks, standards, samples, duplicates, and Total P QC's into 100 mL glass beakers. Add 3 - 6 glass boiling beads to each beaker.
Mark beakers at top of liquid with a Sharpie.
Add 1 mL of ammonium peroxydisulfate solution and 1 mL of H_2SO_4 (31+69) to each marked beaker.

Place beakers on the large hot plates that are located in the hood.
Turn the Temp. knob on the hot plates to "HI."
Let each sample (blank, standard, duplicate, or QC) stay on the hot plate until its volume decreases to 10 mL. This process takes approximately 1 to 1 ½ hours. Do **not** allow the samples to completely evaporate.
Allow each sample to cool in the hood.
Add a drop of phenolphthalein indicator solution to each sample.
Add 1 mL of 10 N NaOH to each sample.
Continue adjusting the pH's by adding 1 N NaOH until each sample becomes faint pink in color. The pH is approximately 10 at this point.
Bring samples back to colorless by adding 1 N H_2SO_4 to each sample. The pH is approximately 4 at this point.
Bring each sample's volume back up to the mark with water.
13. Filter each of the samples using the acid washed ceramic funnels and 1 μm paper filters.
14. Pour 25 mL of each sample into its corresponding 4 ½ oz. plastic beaker.
15. Add 5 mL of combined reagent to the sample and mix thoroughly.
16. After a minimum of 10 minutes, but no longer than 30 minutes, measure the absorbance of the blue color at **880** nm with the spectrophotometer.

D. Sample Analysis

The computer, by comparing the concentration of each calibration standard against its absorbance, can plot a calibration curve. The correlation coefficient must be ≥ 0.994 to be acceptable. If above criteria is not met the standards may need to be remade and rerun.
Once the spectrophotometer is standardized properly, the samples may be analyzed.
Once the analysis is completed, print out a copy of the standard values, plotted curve, and the sample values. Copy the relevant data onto the Total Phosphorous Data Sheet.

E. Clean Up

Turn off the spectrophotometer lamp.
The waste must be placed in the acid waste container.
For glassware clean up, refer to the **"Total P"** section of the Glassware GLP.
6. Quality Control
A quality control sample should be run at the beginning and end of each sample
delivery group (SDG) or at the frequency of one per every ten samples. The QC's value should fall between ± 10 % of its theoretical concentration.

A duplicate analysis should be run for each SDG or at the frequency of one per every twenty samples, whichever is greater. The RPD (Relative Percent Difference) should be less than 10%. If this difference is exceeded, the duplicate must be reanalyzed.

From each pair of duplicate analytes (X_1 and X_2), calculate their RPD value:

$$\% \, RPD = 2 \bullet \left(\frac{X_1 - X_2}{X_1 + X_2} \right) x \, 100$$

where: (X_1 - X_2) means the absolute difference between X_1 and X_2.

7. Method Performance

The method detection limit (MDL) should be established by determining seven replicates that are 2 to 5 times the instrument detection limit. The MDL is defined as the minimum concentration that can be measured and reported with 99% confidence that the analyte concentration is greater than zero and is determined from analysis of a sample in a given matrix containing the analyte.

$$MDL = t_{(n-1,1-\alpha=99)}(S)$$

where:
t = the t statistic for n number of replicates used (for n=7, t=3.143)
n = number of replicates
S = standard deviation of replicates

8. References

ASTM vol. 11.01 (1996), D 515, "Standard Test Methods for Phosphorus in Water", pg. 24
ASTM vol. 11.01 (1996), D 1193, " Specification for Water", pg. 116
EPA 365.2 Phosphorous , All Forms (Colorimetric, Ascorbic Acid)

A6) Fluid Velocity

Operation, inspection, maintenance, storage and other analytical needs are covered in the manual for the Gurley Pygmy meter. The citation for the manual is:
GPI (2004) Gurley Precision Instruments Hydrological Equipment Operation and Maintenance Guide. Gurley Precision Instrument, Troy, NY, 12181-0088.

A7) Sediment Concentration

A7.1) Field SOP-

See section A15.2

A7.2) Laboratory SOP- Standard Methods for Total Suspend Solids EPA 160.2

METHOD #: 160.2 Approved for NPDES (Issued 1971)

TITLE: Residue, Non-Filterable (Gravimetric, Dried at 103-105°C)

ANALYTE: Residue ,Non-Filterable

INSTRUMENTATION: Drying Oven

STORET No. 00076

1.0 Scope and Application

1.1 This method is applicable to drinking, surface, and saline waters, domestic and industrial wastes.

1.2 The practical range of the determination is 4 mg/L to 20,000 mg/L.

2.0 Summary of Method

2.1 A well-mixed sample is filtered through a glass fiber filter and the residue retained on the filter is dried to constant weight at 103-105°C.

2.2 The filtrate from this method may be used for Residue, Filterable.

3.0 Definitions

3.1 Residue, non-filterable, is defined as those solids which are retained by a glass fiber filter and dried to constant weight at 103-105°C.

4.0 Sample Handling and Preservation

4.1 Non-representative particulates such as leaves, sticks, fish, and lumps of fecal matter should be excluded from the sample if it is determined that their inclusion is not desired in the final result.

4.2 Preservation of the sample is not practical; analysis should begin as soon aspossible. Refrigeration or icing to 4°C, to minimize microbiological decomposition of solids, is recommended.

5.0 Interferences

5.1 Filtration apparatus, filter material, pre-washing, post-washing, and drying temperature are specified because these variables have been shown to affect the results.

5.2 Samples high in Filterable Residue (dissolved solids), such as saline waters, brines and some wastes, may be subject to a positive interference. Care must be taken in selecting the filtering apparatus so that washing of the filter and any dissolved solids in the filter (7.5) minimizes this potential interference.

6.0 Apparatus

6.1 Glass fiber filter discs, without organic binder, such as Millipore AP-40, Reeves Angel 934-AH, Gelman type A/E, or equivalent.

NOTE: Because of the physical nature of glass fiber filters, the absolute pore size cannot be controlled or measured. Terms such as "pore size," collection efficiencies and effective retention are used to define this property in glass fiber filters. Values for these parameters vary for the filters listed above.

6.2 Filter support: filtering apparatus with reservoir and a coarse (40-60 microns) fritted disc as a filter support.

NOTE: many funnel designs are available in glass or porcelain. Some of the most common are Hirsch or Buchner funnels, membrane filter holders and Gooch crucibles. All are available with coarse fritted disc.

6.3 Suction flask.

6.4 Drying oven, 103-105°C.

6.5 Desiccator.

6.6 Analytical balance, capable of weighing to 0.1 mg.

7.0 Procedure

7.1 Preparation of glass fiber filter disc: Place the glass fiber filter on the membrane filter apparatus or insert into bottom of a suitable Gooch crucible with wrinkled surface up. While vacuum is applied, wash the disc with three successive 20 mL volumes of distilled water. Remove all traces of water by continuing to apply vacuum after water has passed through. Remove filter from membrane filter apparatus or both crucible and filter if Gooch crucible is used, and dry in an oven at 103-105°C for one hour. Remove to desiccator and store until needed. Repeat the drying cycle until a constant weight is obtained (weight loss is less than 0.5 mg). Weigh immediately before use. After weighing, handle the filter or crucible/filter with forceps or tongs only.

7.2 Selection of Sample Volume for a 4.7 cm diameter filter, filter 100 m L of sample. If weight of captured residue is less than 1.0 mg, the sample volume must be increased to provide 1.0 mg least 1.0 mg of residue. If other filter diameters are used, start with a sample volume equal to 7 m L/cm^2 of filter area and collect at least a weight of residue proportional to the 1.0 mg stated above.

NOTE: If during filtration of this initial volume the filtration rate drops rapidly or if filtration time exceeds 5 to 10 minutes, the following scheme is recommended: Use an unweighed glass fiber filter of choice affixed in the filter assembly. Add a known volume of sample to the filter funnel and record the time elapsed after selected volumes have passed through the filter. Twenty-five m L increments for timing are suggested. Continue to record the time and volume increments until filtration rate drops rapidly. Add additional sample if the filter funnel volume is inadequate to reach a reduced rate. Plot the observed time versus volume filtered. Select the proper filtration volume as that just short of the time a significant change in filtration rate occurred.

7.3 Assemble the filtering apparatus and begin suction. Wet the filter with a small volume of distilled water to seat it against the fritted support.

Shake the sample vigorously and quantitatively transfer the predetermined sample volume selected in 7.2 to the filter using a graduated cylinder. Remove all traces of water by continuing to apply vacuum after sample has passed through.

7.5 With suction on, wash the graduated cylinder, filter, non-filterable residue and filter funnel wall with three portions of distilled water allowing complete drainage between washing. Remove all traces of water by continuing to apply vacuum after water has passed through.

NOTE: Total volume of wash water used should equal approximately 2 m L per cm^2. For a 4.7 cm filter the total volume is 30 m L.

7.6 Carefully remove the filter from the filter support. Alternatively, remove crucible and filter from crucible adapter. Dry at least one hour at 103-105°C. Cool in a desiccator and weigh. Repeat the drying cycle until a constant weight is obtained (weight loss is less than 0.5 mg).

8.0 Calculations
8.1 Calculate non-filterable residue as follows:
A = weight of filter (or filter and crucible) + residue in mg
B = weight of filter (or filter and crucible) in mg
C = mL of sample filtered
9.0 Precision and Accuracy
9.1 Precision data are not available at this time.
9.2 Accuracy data on actual samples cannot be obtained.

Bibliography

1. NCASI Technical Bulletin No. 291, March 1977. National Council of the Paper Industry for Air and Stream Improvement, Inc., 260 Madison Ave., NY

A8) Stage
A8.1) Discrete Stage Measurements
Stage will be measured at quarter, half and three quarter stations in the stream cross-section and average stage will be reported for each site.
A8.2) Continuous Stage Measurements
Continuous measurements of stage are generated for the tributaries using Teledyne ISCO bubblers. Calibration, operation, inspection maintenance and other analytical needs are cover in the Teledyne manual for 730 Bubbler Module. The citation for the manual is:
Teledyne (2011) 730 Bubbler Module Installation and Operation Guide.. Teledyne ISCO, Inc., Lincoln, NE, 68501-2531, Revision L.
A9) Turbidity
Calibration, operation, inspection, maintenance, storage and other analytical needs are covered in the YSI manual for the 6136 Turbidity probe. The manual can be obtained from the YSI company at www.foundriest.com. The citation for the manual is:
YSI (2006) 6-Series Multiparameter Water Quality Sondes. YSI, Yellow Springs, OH, User Manual 069300 Revision D.
A10) Temperature
Calibration, operation, inspection, maintenance, storage and other analytical needs are covered in the YSI manual for the Temperature probe. The manual can be obtained from the YSI company at www.foundriest.com. The citation for the manual is:
YSI (2006) 6-Series Multiparameter Water Quality Sondes. YSI, Yellow Springs, OH, User Manual 069300 Revision D.

A11) $\delta^{15}N$ of Nitrate
A11.1) Field SOP
See section A15.1
A11.2) Analytical SOP

SOP for determining $\delta^{15}N$ of Nitrate
UK Dept. of Civil Engineering
2-1-13

1. Overview

The SOP for analyzing the stable nitrogen isotope signature of streamwater nitrate is derived from the methods published by the USGS Reston Stable Isotope Lab (Coplen, 2012). $\delta^{15}N$ will be analyzed in each sample to determine seasonal and hydrologic variability of streamwater inputs and the impacts of biological uptake on $\delta^{15}N$. Denitrification of streamwater nitrate is conducted using Pseudomonas (P.) chlororaphis or P. aureofaciens to convert nitrate (NO_3^-) to nitrous oxide (N_2O). These bacteria lack the ability to further reduce the compound to dinitrogen gas (N_2) making it ideal to study both the oxygen and nitrogen isotopes. The nitrate gas will be trapped in a small-volume trap and immersed in liquid nitrogen. The analyte was cleaned on a gas chromotograph and analyzed on a continuous flow IRMS.

2. Safety

The analysis will incorporate culturing of bacteria. Thus, safety gloves, lab coats, and protective eye wear should be used during the analysis.

3. Equipment, Reagents and Consumable Supplies

Lab Instrumentation

Centrifuge
Reciprocal Shaker
Analytical Balance
-80 Degrees Celsius freezer
Bunsen Burner
Autoclave
Sterile Hood
Finnigan Delta^{Plus} CF-IRMS
ISODAT 2.0

Reagents and Consumable Supplies

P. chlororaphis, P. aureofaciens
Tryptic Soy Agar
Tryptic Soy Broth
1-mL plastic vials
1000-mL Pyrex Flask
2000-mL Culture media flask with screw top
Petri dishes, 100mm
Crimp tops-aluminum with silicone septa

Decrimper
Crimper-crimping jaw and crimp mate unit
20-mL glass sample vials
250-mL Centrifuge tubes
500-mL Pyrex Plus coated media bottle
Glycerol
Antifoam B Emulsion
KNO_3
$(NH_4)_2SO_4$
Reagent Grade Alcohol
Autoclave bags
Needles: 25 G 5/8inch
Needles: 25 G 1.5 inch
1-mL glass syringe
22s gauge needle
Helium gas
Dry ice
Liquid Nitrogen

4. Sample Preparation

Bacteria Preparation

Samples are collected in the field using proper collection protocol and are immediately preserved by cooling the samples to 4 degrees Celsius. The samples are shipped to the appropriate lab (ASIL) immediately.

Plate media shall be made using a mix of 20 grams of tryptic soy agar, .505g KNO_3, .06607g $(NH_4)_2SO_4$ and 500-mL of deionized water. Ingredients are mixed and stirred on a hot plate using a magnetic stirrer. The flask will be autoclaved at 250 ^oF for 15 minutes. The media will be poured into 2 bags of sterile plates and dried under the hood for 15 minutes.

The plates are stored at 4 ^oC for 15 minutes. 1-L batches of culture media shall be made by mixing 40g of tryptic soy broth, 1.01 g KNO_3, 0.1321g $(NH_4)_2SO_4$ and 1000-mL of deionized water into a 2000-mL Pyrex flask, stirred as with the plate media. 412-416 mL of the media is poured into 500mL Pyrex media bottles and autoclaved. 500 mL of nitrate free media (20g soy broth, 500mL of deionized water) is then autoclaved and cooled similar to the plate and batch culture media.

250-mL centrifuge tubes and caps are autoclaved for sterilization purposes, and 32 sample vials are acid washed and placed in a muffle furnace at 500 ^OC for 4 hours.

A flamed loop will be used to streak bacteria onto two of the 500-mL media bottles. The bottles are placed on a shaker, allowing bacteria to grow for 4-6 days at ambient light and room temperatures.

The bacteria/media mixture in the 500-mL bottles are dispersed into four 250-mL centrifuge bottles and centrifuged at 2800 RPM for 15 minutes. The supernatant is poured off and 25-mL of nitrate free media is added to each bottle.

The bottles were consolidated into one bottle and centrifuged again pouring off the supernatant afterwards. The process was repeated 4 times, adding 100-mL of the nitrate free media after each cycle.

After the fourth time 110-mL of nitrate free media are added and the sample is homogenized and poured into a large, sterile glass-beaker.

Ten drops of anit-foam (sigma A6707-500ML) are added and mixed accordingly. Thereafter, 3-mL of samples is pipetted into 20 ml crimp top vials for IRMS analysis.

5. Analytical Procedures

Arkansas IRMS Analysis

Each of the vials was purged with helium gas for an hour to remove any air from the samples. The samples were diluted so that nitrate concentrations were around 20µM. One mL of the sample was added to a vial using a syringe. The process is repeated for each sample and standard, ensuring two duplicates of each. The 32 samples were placed on an automated sampler which extracted the sample by pumping helium into the sample through one needle and removing the He and N_2O mixture with an extraction needle. For each sample the mixture was sent through a water removal unit (Nafion dryer), a CO_2 removal unit ($Mg(ClO_4)_2$/Ascarite trap), a cryogenic trap, a GC column, a second water removal unit, and an open split.

A Finnigan Delta^{Plus} CF-IRMS was used to generate the $\delta^{15}N$ and $\delta^{18}O$ of the samples. This was accomplished by ionizing the gas/helium mixture with an electron emitting hot filament, accelerating the ions into the analyzer and separating the ion beams in the analyzer using a magnet. Thereafter the beams were collected in faraday cups and the intensity of the beams were measured. ISODAT 2.0 computer software was used to setup, calibrate the system and calculate the "δ" values.

6. QC and Calibration

Deionized water was utilized as a "Blank". Standards for the analysis were 20µM KNO_3, IAEA (International Atomic Energy Agency) N3 (19.975 µM N-KNO_3, $\delta^{15}N$=4.7‰ and $\delta^{18}O$=25.6‰), USGS 32 (19.7 µM KNO_3, $\delta^{15}N$=180 ‰ and $\delta^{18}O$=25‰), USGS 34 (20 µM KNO_3, $\delta^{15}N$=-1.8 ‰ and $\delta^{18}O$=-27.9‰), USGS 35 (20 µM KNO_3, $\delta^{15}N$=2.7‰ and $\delta^{18}O$=57.5‰). Duplicates and blanks were taken bimonthly from the field. For isotope analysis, splits are taken for ten percent of the samples.

7. Calculations

$$\delta = \left[\frac{R_{sample}}{R_{standard}} - 1\right] * 1000$$

where R denotes the isotopic ratio of a given constituent.

$$\sigma = \sqrt{\left[\frac{\sum(xbar - x)^2}{n-1}\right]}$$

where, *xbar* is the mean of the data and σ is the standard deviation of the data.

8. Data Quality Objectives

Based on Coplen et al. (2012), reference materials have been observed to have reproducibility of approximately + or – 0.25‰ given a range of values between -1.8-180‰ which encompasses the range found in nature. Blanks should not register a peak.

9. References

Coplen, T.B., Qi, Haiping, Révész, Kinga, Casciotti, Karen, and Hannon, J.E., 2012, Determination of the $\delta^{15}N$ and $\delta^{18}O$ of nitrate in water; RSIL lab code 2900, chap. 17 ***of*** Stable isotope-ratio methods, sec. C ***of*** Révész, Kinga, and Coplen, T.B. eds., Methods of the Reston Stable Isotope Laboratory (slightly revised from version 1.0 released in 2007): U.S. Geological Survey Techniques and Methods, book 10, 35 p., available only at http://pubs.usgs.gov/tm/2006/tm10c17/. (Supersedes version 1.0 released in 2007.)

A12) $\delta^{15}N$ of Ammonium

A12.1) Field SOP-

See section A15.1

A12.2) Analytical SOP- UK/ASIL

SOP for determining $\delta^{15}N$ of Ammonium
UK Dept. of Civil Engineering
2-1-13

1. Overview

The SOP for analyzing the stable nitrogen isotope signature of streamwater ammonium is derived from the methods published by the USGS Reston Stable Isotope Lab (RSIL, 2008). $\delta^{15}N$ of NH_4 will be analyzed to assess seasonal and hydrologic variability of the parameter in tributaries as well as the main stem of the watershed. MgO and NaCl will be added to the samples to lower the pH of the samples, volatilizing the inorganic NH_4^+ to a gas (NH_3). The gas then can diffuse through pre-made diffusion packets containing $KHSO_4$. Salts precipitate out inside the Teflon diffusion packet, trapping the nitrogen. The trap will then be dried and placed in tin capsules to be analyzed on a Costech Elemental Analyzer interfaced with a Finnigan Delta plus CF-IRMS.

2. Safety

Strong acids and bases will be used through the course of this analysis. Gloves, lab coats, and protective eyewear are required during procedures using these chemicals.

3. Equipment, Reagents and Consumable Supplies

Lab Instrumentation

Carlo Erba 2500 EA
ConFlo II open split
Finnigan Delta plus CF-IRMS
ISODAT 2.0 Software
Microbalance with .001 mg precision
Vacuum Oven
Muffle Furnace

Reagents and Consumable Supplies

$NAHSO_4$
MgO
NaCl
GF/C Filters
Hole punch
2.5 cm diameter polypropylene filters
Gloves
Forceps
micro spatulas
20 mL scintillation vials
HDPE bottles with tight fitting caps
Micro pipette with pipette tips
Desiccator with desiccant
Tin capsules
Concentrated H_2SO_4

4. Sample Preparation

Samples were collected in the field and filtered using 0.7 µm GF/F Whatman filters in the KGS laboratory. 100-mL of the filtered sample was placed in glass amber I-CHEM bottles which were preserved by adding 10-15 drops of concentrated sulfuric acid (H_2SO_4) to the sample and immediately placing the sample in a dark cooler. Samples were preserved by keeping them on ice, or refrigerated at 4^0C, and in the dark to reduce biological activity within the sample. The minimum quantity of ammonium used for a sample analysis was 0.2 mg/L as N.

Diffusion Packet

Construction of the diffusion packets were conducted on a clean workspace with gloves and standard laboratory safety equipment (safety glasses and lab coat) since hazardous materials were used during the procedure.

A thick layer of foil, two pairs of forceps, a ¼ inch diameter paper punch, and a "chuck tube" were cleaned with acetone before creation of the diffusion packets. 0.7 µm Whatman filters (cat. No 1825 025) were wrapped in tin foil and combusted for 3 hours in a 400^0C furnace and carefully cut using the paper punch. One piece of filter paper was used per diffusion packet.

An 8 cm piece of Teflon tape was cut and folded in half to serve as the outer layer of the diffusion packet. The ¼ inch filter was placed onto the Teflon tape and 20µL of 2.5 M $KHSO_4$ was added to the filter paper. The desired solution was produced by mixing K_2SO_4 (VWR-AAAA13975-0B) with an equivalent # of moles of H_2SO_4 and adding 17.03g of the resultant solution in 40 mL of DIDO water.

The Teflon tape was folded over and the opening of a "chuck tube" (slight greater than a ¼ inch diameter plastic tube) was used to seal the packet until the Teflon became transparent. The packet was placed and sealed in a Nalgene bottle to minimize exposure to the air.

Diffusion Procedure

Samples were prepared such that each sample had between 40-160 µgN-NH_4^+. Samples and 50 g/L of NaCl (VWR-EMD-SX0420-1)was mixed together in a 125-mL Nalgene polycarbonate container (Cole-Parmer-WU-06040-50) and NANOpure water was added to each container to ensure equal headspace distribution across all samples.
One diffusion packet and 3g/L of MgO was added to each sample bottle before sealing the sample. The sample was gently shaken to ensure mixing of MgO (VWR-200002-90:98%) in the sample solution. After seven days of incubation at 50 rpm and 30 ºC on a shaker table, the diffusion traps were removed, placed in a labeled aluminum foil packet and dried in a desiccator containing an open beaker of concentrated sulfuric acid (EDM SX1244-14) and silica desiccating agent (VWR-EM-DX0014-1).
A 5X9 mm tin capsule (Costech Analytical) was unfolded and the filter was placed on the surface of the capsule. Thereafter, the tin capsule was folded and compacted to a 5mm ball.

5. Analytical Procedures

EA/IRMS Analysis

The tin capsules are placed in a Carlo Erba Elemental analyzer(NC2500) equipped with a Costech "zero blank" autosampler.
Samples were preloaded into the elemental analyzer and data was input into the ISODAT 2.0 software for analysis.
Samples were dropped into an oxidation, combustion chamber in which "dynamic flash combustion" occurs at 1020 ºC. Oxidation of the samples was completed by passing the helium/gas mixture through a oxidative catalyst layer (Cr_2O_3).
The gas was then reduced to include only N_2, CO_2, and H_2O by flowing through a reducing agent (Cu) at 650 ºC.
Finally, water was removed by using an Magnesium perchlorate trap. The gas then flows through a GC column to separate the gasses, and the EA is interfaced with the IRMS through a ConFlo II open split.
Finnigan Delta plus CF-IRMS was used to generate the $\delta^{15}N$ of the samples. This was accomplished by ionizing the gas/helium mixture with an electron emitting hot filament, accelerating the ions into the analyzer and separating the ion beams in the analyzer using a magnet. Thereafter the beams were collected in faraday cups and the intensity of the beams was measured. ISODAT 2.0 computer software was used to setup, calibrate the system and calculate the "δ" values.

6. QC and Calibration

Samples were run in triplicate to verify precision of the instrument and repeatability of the diffusion procedure. Field blanks and field duplicates were collected bimonthly. Two pure ammonium sulfate reagants $(NH_4)_2SO_4$ were used as reference materials; USGS 25 with a $\delta^{15}N$=-30.41‰, and USGS26 with a $\delta^{15}N$=+53.7‰. The reference materials are used to calibrate each sample run. Standard deviations of the reference material samples were used to determine if performance criteria for the sample run were met.

7. Calculations

$$\delta = \left[\frac{R_{sample}}{R_{standard}} - 1\right] * 1000$$

where R denotes the isotopic ratio of a given constituent.

$$\sigma = \sqrt{\left[\frac{\sum(xbar - x)^2}{n-1}\right]}$$

where, *xbar* is the mean of the data and σ is the standard deviation of the data.

8. Data Quality Objectives

Based on Hannon et al. (2008), reference materials have been observed to have reproducibility of approximately + or – 0.4‰ given a range of values between 0-54‰. Blanks should not register a peak.

9. References

Hannon, Janet E., and Böhlke, John Karl, 2008, Determination of the $\delta(^{15}N/^{14}N)$ of ammonium (NH_4+) in water: RSIL lab code 2898, chap. C15 of Révész, Kinga, and Coplen, Tyler B., eds., Methods of the Reston Stable Isotope Laboratory: U.S. Geological Survey, Techniques and Methods, 10–C15, 30 p. Available at http://pubs.usgs.gov/tm/2007/tm10c15/

A13) $\delta^{15}N$ and $\delta^{13}C$ of Transported Sediment, POC and PN

A13.1) Field SOP

Refer to section A15.3

A13.2) Analytical SOP-UKSIL EA/IRMS

SOP for determining $\delta^{15}N$, $\delta^{13}C$, TOC and TN of Sediment Samples
UK Dept. of Civil Engineering
2-1-13

1. Overview

Measurement of elemental composition and stable isotopic abundance of carbon and nitrogen in fluvial sediments has important implications for carbon and nitrogen cycling in streams and rivers. The following SOP details the necessary procedures, QC sampling and calculations necessary to analytically estimate carbon and nitrogen elemental compositions and stable isotopic abundance utilizing a Finnigan Delta Plus isotope ratio mass spectrometer which is interfaced with a Costech elemental analyzer. Operating Procedures for analyzing elemental and stable isotope signatures (carbon and nitrogen) for sediments are covered in the EPA SIP/OP.01 (Griffis, 1999). The following will outline the procedures used to analyze the samples collected for this project.

2. Safety

Since a corrosive acid is to be used during the procedure, gloves, protective eye wear and an apron should be used during any procedures using strong or corrosive acids.

3. Equipment, Reagents and Consumable Supplies

Lab Instrumentation

Finnigan Delta Plus mass spectrometer

Costech Elemental Analyzer
Hewlett-Packard Model 689- high resolution gas chromatograph
ISODAT Software
Microbalance
DHAUS Scout pro Balance
Dupont Sorvall RC-5B Refrigerated Superspeed Centrifuge
OHAUS 2kg-5klb capacity Balance
OHAUS Scout Pro Electronic Balance
Thermo Modulyod Freeze Drier with Thermo Savant VLP 200 ValuPump
QL Model 30 GC Lab Oven
Rinn Crescent Wig-L-Bug Grinder
Pyrex Dessicator
Thermo Sorvall Legend RT+ Centrifuge

Reagents and Consumable Supplies

Deionized Ultra-Pure Water
Siphon line
Magnesium Chloride Hexahydrate
Drierite # 24001 Dessicating Agent
Metal Spatula
Grinder Vials with Steel Balls
Forceps
Number 200, 53µm U.S.A Standard Test Sieve
Accumax Pro Micropipette 10-100 µL with pipette tips
Fisher A307-1 Sulfurous Acid Certified ACS Grade 1L
750mL centrifuge bottles
250mL centrifuge bottles
125mL HDPE bottles
Small vials for ground samples
Costech #41067 Silver Capsules
Costech #080016 Sample Trays
Costech #011001 Chromium Oxide or equivalent
Costech #021022 Magnesium Perchlorate or Equivalent
Costech #011009 Tungesten Oxide on Aluminum or Equivalent
Costech #021025 Quartz turnings or equivalent
Costech #021020 Carbon Dioxide Absorbent or Equivalent
Costech #021026 Quartz Wool or Equivalent
Fisons #33821710 Cupric Oxide Wires or Equivalent
Costech #011005 Reduced Copper, Pure or Equivalent
Costech #061105 Opaque Quartz Reaction Tube or Equivalent
Finnigan #M0000-56911 Gasket or Equivalent
Finnigan #M00-1027920 Filament Assembly
Finnigan #M0000-69322 Gasket or Equivalent
Finnigan #00950-00911 Lubricant Cartridge for Turbo Molecular Drag Pump
Finnigan #00950-01116 Lubricant Cartridge for Turbo Molecular Drag Pump
Oxygen, Zero Grade, for Costech Elemental Analyzer
Helium, Ultra High Purity 99.999%, for Costech Elemental Analyzer
Nitrogen, Ultra High Purity, 99.999%, Delta Plus Reference Gas.
Carbon Dioxide, Coleman Grade, 99.99%, Delta Plus Reference Gas.

4. Sample Preparation

Settling/Decanting Field Samples

Bring sediment samples back to lab after collection in the field.
Leave samples undisturbed in buckets/appropriately-sized containers for 48 hours in refrigerator (Hydrolab basement Floor Raymond Bldg.) set to 4°C.
48 hours is a relative time that usually allows all of the sediment contained in the sample to settle to the bottom of the bucket/container. **If all sediment has not settled to the bottom of the bucket, allow more time for settling**.
Gently pour water off the top of settled sediment samples. If a large volume of water is present, may use small rubber tubing as siphon. This is up to the technician's preference.
Pour/siphon water from the bucket until either (a) the sediment nearly flows out of the bucket if pouring or (b) the sample has a manageable amount of water to allow for centrifugation.

Centrifuging (Bulk Sample)

Agitate decanted sample in bucket to encourage homogeneous mixture.
Pour sample into a clean (4 DI/DO rinses) 750 mL Nalgene pitcher until the pitcher is nearly full.
Place bucket, bottle (in bucket), and bottle cap for a sample on each side of balance.
Slowly fill one bottle with sample until nearly full (almost to neck).
Slowly fill opposing tube with sample until nearly balanced.
Using plastic pipette, delicately balance both bottles with DI/DO H_2O (see *"DI/DO H_2O"* procedure) until the two sides are the same weight.
Place cap on tube.
Align these two balanced bottles across from one another in centrifuge.

Repeat steps 1-7 with remaining two bottles so opposing tubes are well balanced.
Settings on centrifuge should be set as follows:
Rotational Velocity: 4.25 on knob or 4250 rpm
Time: 4-7 minutes
Temperature: room temp (20 degrees Celsius)
Rotor: SH-3000

Close top (will click).
Press start button (Play button located to the right of the temperature).
If vibration is severe upon spinning, samples are not well balanced. Press the stop button (square), inspect tube balance, add DI/DO H_2O, etc.
After centrifuge is **completely** stopped, centrifuge door light will come on open top by pressing door button.
Remove adapters/bottles two at a time, decant, and add additional sample from the Nalgene pitcher to each bottle, balancing opposing bottle as necessary.
Repeat previous steps until the sample is completely centrifuged into four bottle.
Consolidate entire sample into 1 labeled centrifuge tube (may need to use two centrifuge tubes if the sample contains a large amount of sediment).
After consolidation, bottle may have a large amount of supernatant above the sediment. If this occurs, place the single centrifuge bottle back into the cooler until another sample is centrifuged and contains a large amount of supernatant as well. These two separate samples can be balanced, centrifuged, and decanted to remove excess supernatant.
Place bottles in freezer (-40°C) after removing as much supernatant as possible.

Notes:
If, after spinning, sample has a large amount of fine sediment still in suspension (murky color), add ~10mL Magnesium Chloride Hexahydrate ($MgCl_2$-$6H_2O$) prepared at 0.5M (see *"Magnesium Chloride"* procedure).
Once the entire sample is poured into the Nalgene pitcher, spray off any sediment remaining on the inside of the bucket using DI/DO H_2O.
Once the entire sample is poured into the centrifuge tubes, spray off any sediment remaining on the inside of the Nalgene pitcher using DI/DO H_2O.

Freeze Drying
Check to make sure there is enough oil in the machine. (Look in the front at the tube).
Turn on the refrigeration unit by pressing the button that says "Fridge". (It is preferred to do this a little before the samples are put in so that the atmosphere will cool faster.)
This procedure differs depending on the size of the bottle. If the sample bottle fits in the glass jars, refer to section 1. If the sample bottle does not fit in the glass jars refer to section 2.
Section 1:
Be sure that the sample bottle is covered with cheesecloth and held with a rubber band.
Start the vacuum, by pressing the button on the front of the Freeze drier that says, "Pump". (don't turn on pump until fridge temperature <-41C)
Place a sample bottle into the glass jar and seal the jar with the rubber cap.
Push the cap firmly into the vacuum chamber and ensure that it is on tightly so that the glass jar does not fall off.
Turn the valve on the manifold from "Vent" to "Vac" to allow a vacuum to reach the sample.
Make sure the drain hose is removed and that all the pressure releases are closed.
Section 2:
Be sure that the sample bottle is covered with cheesecloth and held with a rubber band.
Remove the top glass piece from the vacuum chamber.
Place the sample bottles inside the chamber around the edge so that they are stable. (put samples with the most ice on top)
Put the top glass piece into its proper position. Be sure that there is a good seal.
Make sure the drain hose is removed and that all the pressure releases are closed.
Start the vacuum, by pressing the button on the front of the Freeze drier that says, "Pump". (don't turn on pump until fridge temperature < -41C)
Once the samples are dry:
Once samples are completely dry, turn off the vacuum by pressing the "Pump" button on the freeze drying unit.
Slightly turn a pressure release so that pressure is slowly restored to atmospheric pressure.
Remove glass piece or the jars to remove the samples.
Recap the samples.
a) If samples are going to be put on to the freeze dryer right away and the condenser does not have a lot of ice on it, leave the condenser on. Repeat the previous steps for more samples.
b) If not, turn the condenser off by pressing the same button that was used to turn it on. Be sure drain valve is open. Let the condenser drain until all of the ice is off the side wall.
Consolidation and Weighing
This is a dry procedure so all equipment used must be washed and acetone used to ensure dryness.
Weigh an empty Nalgene bottle and record the empty weight.
Using the spatula, break large soil particles into smaller particles so that they can be wet sieved easier.
Tip the centrifuge bottle into the Nalgene bottle (a funnel may be needed).
Using the spatula, scrape the side of the centrifuge tube so all soil particles fall to the bottom.
Tip the centrifuge bottle into the Nalgene bottle.
Using the spatula strongly tap the centrifuge bottle so that all of the soil gets knocked into the Nalgene bottle.
Repeat the three previous steps until all of the sediment is in the Nalgene bottle.

Weigh the Nalgene bottle with the sample and record the weight.
Label the Nalgene bottle with the appropriate name and number.

Wet Sieving
Use DIDO water to fill the Nalgene bottle and shake the bottle to break up particles.
Pour sediment solution through 3" diameter 53 micron sieve. Flush through sieve with DIDO water into sieve pan. (It helps to shake the sieve as you spray the sieve.)
Rinse bottom of 53 micron sieve with DIDO water into sieve pan. Repeat these two steps until water on top and bottom while washing remains clear.
Rinse fine solids retained on 53 micron sieve through plastic funnel leading to centrifuge tube (labeled w/sample #).
Pour contents of pan through funnel into separate centrifuge tube (labeled w/sample #).
Rinse funnel (4 DI/DO, 1 acetone) between each sample.
Each sample should now be split into two parts (>53µm, <53µm) and labeled accordingly.
Keep samples in labeled bucket in ERTL refrigerator (3rd Floor) until centrifugation.

Centrifuging (Wet Sieved Sample)
Agitate decanted sample in bucket to encourage homogeneous mixture.
Pour sample into a clean (4 DI/DO rinses) 250 mL Nalgene pitcher until the pitcher is nearly full.
Place bucket, tube (in bucket), and tube cap on each side of balance.
Slowly fill one tube with sample until nearly full (almost to neck) **Avoid any liquid on outside of tube or on insert (use pipette if necessary) if any fluid is on side of tube or insert dry before placing in centrifuge**.
Slowly fill opposing tube with sample until nearly balanced.
Using plastic pipette, delicately balance both tubes with DI/DO H_2O (see *"DI/DO H_2O"* procedure) until the two sides are the same weight.
Place cap on tube.
Align these two balanced tubes across from one another in centrifuge.
Repeat steps 1-7 with remaining two tubes so opposing tubes are well balanced.
Settings on centrifuge should be set as follows:
Rotational Velocity: 3200 * g
Time: 4 minutes 0.04 = 4 minutes 4.00 = 4 hours
Temperature: room temp (20 degrees Celsius)
Motor: 243 – Rotor
Acceleration (on left): 3
Brake (on right): 2
Close top gently will self set (will click).
Press start button (Play button located to the right of the temperature).
If vibration is severe upon spinning, samples are not well balanced. Press the stop button (square), inspect tube balance, add DI/DO H_2O, etc.
After centrifuge is **completely** stopped (0*g, centrifuge will beep and say "end"), open top by pressing appropriate button.
Remove adapters/tubes two at a time, decant, and add additional sample from the Nalgene pitcher to each tube, balancing opposing tubes as necessary.
Repeat previous steps until the sample is completely centrifuged into four tubes.
Consolidate entire sample into 1 labeled centrifuge tube (may need to use two centrifuge tubes if the sample contains a large amount of sediment).
After consolidation, tubes may have a large amount of supernatant above the sediment. If this occurs, place the single centrifuge tube back into the cooler until another sample is centrifuged and contains a large amount of supernatant as well. These two separate samples can be balanced, centrifuged, and decanted to remove excess supernatant.
Place tubes in freezer (-40°C) after removing as much supernatant as possible.

Consolidation and Weighing
Samples are again consolidated and weighed as in Step D
Grinding
Place the steel ball into the vial with.
Fill the stainless steel vial for the Wig-L-Bug grinder roughly halfway with sample using the funnel with the small opening. Be sure to scrape the funnel to ensure all the soil is in the vial. For soils, this volume is approximately equal to 1 gram of sample. For organics, this weight is much less. Place the cap on.
Secure the vial in the arms of the grinder. Make sure that the top of the vial is facing the rear of the grinder (towards the brass nut). Tighten the front screw using the provided allen wrench (two turns past hand tight is sufficient).
Run the Wig-L-Bug for 30 seconds.
Once the grinder has stopped, loosen the front screw and remove the vial.
Place the ground sample into the desired container.
Using a magnetic-tipped screwdriver, remove the steel ball from the vial.
If more ground sample is required, repeat steps 1-8.
Be sure to clean the equipment thoroughly between each sample. Consecutive runs of the same sample do not require cleaning the equipment. Follow the procedure below for each instrument:
Tap water rinse/wire brush scrub
4 DI/DO rinses
1 100% ethanol rinse or acetone
Dry with Kim-wipes
Weighing Subsamples and Acid Digestion

Clean tweezers/small spoon by wiping thoroughly with Kim-Wipes.
Calibrate scale (precision of 1μm) using 2g sample.
Hold Tare button until 'Busy' shows on screen.
Add 2g calibration weight using tweezers.
After 'Busy' is gone once again, gently remove calibration weight. If screen says 'H', start over.
Using tweezers, gently place molded silver caps in the plastic sample tray. Widen the tops of the caps by pressing on edges with tweezers/spoon.
Place the cap onto the scale. Tare the scale.
Using the spoon, add sample to the cap until desired amount is reached.
** If sample spilled onto weighing pan, remove cap, pick up pan w/tweezers and blow off **
Place cap w/sample back in plastic mass spec tray in the appropriate position.
** For each sample, record weight of sample tested + position in plastic tray **
Add 10,30,50 then 100μL of sulfurous acid to each sample (in silver cap). This will remove carbonates from sample and leave only organic carbons.
Place plastic tray w/caps in an oven at 60 degrees Celsius. Repeat 100μL once/hour until there is no reaction (gaseous bubbling) when adding acid.
Once the samples no longer react with the sulfurous acid, the samples can be prepared to run through the mass spectrometer. Perform the following steps for this preparation:
Remove the polyethylene block containing the samples from the oven.
Wipe the brass rod thoroughly with Kim-wipes.
Close the silver caps by squaring off the silver caps to form a small square pellet.

5. Analytical Procedures

Samples will be loaded into a Costech Elemental Analyzer in an automated sampler and combusted. All organic material contained in the sample is oxidized and ashes are left in the oxidation column. The helium stream in the EA carries the gas through a reduction column, a water trap and then through a Conflo IV interface to separate the gasses. The sample are ionized and

Costech Elemental Analyzer
The Costech EA is set up to run sediment samples under the following conditions
Oxygen Pressure = 100psi
Helium Pressure = 100psi
Helium Flow Rate = 90-92 cfs
Oxidation Furnace Temperature = 980 Degrees C
Reduction Furnace Temperature = 650 Degrees C
Actuator Compressed Air Pressure = 70 psi
Standy Conditions of the Costech EA are the following:
Oxygen Pressure= OFF
Helium Flow Rate=15-19cfs
Oxidation Furnace Temperature = 820 Degrees C
Reduction Furnace Temperature = 520 Degrees C
Since large sample masses are used for the present analysis, ashes must be removed, and the Quartz insert changed in the oxidation column after each sample run. The oxidation tube must be replaced approximately every 1000 analysis, the reduction tube every 500 analysis and the water trap every 300 analysis.
Samples are loaded into a 49 well automated sampler. Load samples using forceps, ensuring that each sample goes into the appropriate slot.
Make sure the EA is in work mode, check the flow rate.
After samples are loaded, close the lid of the automated sampler and hand tighten the screws that hold the lid down. Use clamps to help tighten the lid and finish hand tightening the screws. Make sure that the middle bolt is unscrewed and turn on the helium stream to remove any air from the autosampler. After 8 minutes simulataneously shut off the helium and close the screw such that are can't get into or out of the autosampler
Check the autosampler for helium leaks using the helium detector.
Open up the door that leads from the autosampler into the oxidation column
Check the autosampler again for helium leaks.
Conflo IV Interface
Reduces the speed of the helium stream
Introduces the CO_2 and N_2 reference gases that are used to ensure the IRMS instrument linearity and precision.
Isotopic signatures of reference gases are quantified relative to universal reference standards
Vienna Pee Dee Belemnite (VPDB)
Atrmospheric nitrogen
Dilutes the CO_2 sample
Since carbon concentrations for large samples create voltages outside of the IRMS sensitivity range samples need to be diluted. The Conflo IV will automatically dilute each sample by a specified percentage using the Helium Diluent. For this project an 80% dilution was found to place the samples in their optimum voltage range. Thereafter the ISODAT software will automatically correct for the dilution.
Pressure settings for the Conflo IV interface are as follows:
CO_2 Reference Gas = 1.5 bar
N_2 Reference Gas = 1.5 bar
Helium Diluent Gas = 2 bar
Finnigan Delta Plus IRMS

Refer to the Finnigan Delta Plus Operating manual (Finnigan MAT, 1997a) and the ISODAT software operating manual (Finnigan, 1996) for exhaustive information on the instrument operations
Samples are ionized and accelerated into a curved flight tube
A .75 Tesla electromagnet is located on the outside of the flight tube
Ions are focused into appropriate Faraday Cup detectors based on the ion beam momentum.
Three cups pick up masses 28, 29, and 30 for nitrogen and masses 44,45 and 46 for carbon dioxide.
The voltages measured from these beams are delivered to the ISODAT software and are converted to δ notation (see section 8).
Enter the appropriate information (e.g. sample identification number and weight of the sample) into the isodat software.
Run a sequence of nitrogen gas reference additions. If the standard deviation (see section 8) of the 11 reference additions is >0.1‰ rerun the sequence. Perform at least 4 sequences with 2-3 consecutive ones with standard deviations <0.1‰.
Air in the line could cause potential interferences as air contains ~70% nitrogen.
Perform a series of nitrogen linearity tests in which additions result in a reference peak between 0.5-10 volts. Check the linearity (denoted by the Diff/volt equation in section 8) and ensure that it is <0.1. If it's not working properly, perform an autocalibration (see the Finnigan operation manual).
Repeat the standard deviation and linearity tests for carbon using the carbon reference gas.
Once the instrument is tuned and functioning properly turn the remote setting on the elemental analyzer on.
Select all the samples in the desired sequence run, save the template and then click the run button.
Check the samples periodically to ensure that blanks aren't providing any peaks, samples are dropping properly into the EA and that the standards are giving appropriate results.

6. QC and Calibration

QC samples for the analysis include blanks (which are empty silver capsules that), two isotopic standards (DORM and CCHIX) and one concentration standard, acentanilide (ACE). Generating a field blank, or a blank that is taken through the preparation procedure isn't feasible. The DORM and ACE standards are used to calibrate each sample run. The following outlines the usage of the each of the QC standard types.

Blanks

One blank will be analyzed at the beginning of each sample run to ensure nothing is leaking into the system (e.g. background concentrations are low)

DORM

Dorm is the primary isotopic standard and it's carbon and nitrogen isotopic signature in nature is well defined ($\delta^{13}C$=-19.59‰,$\delta^{15}N$=12.46‰)
After each sample run the all samples are calibrated to the average Dorm value
Out of the 49 samples analyzed during a run the 7,8,14, 20,26,32,38 and 48th samples are DORMs.
The standard deviations of the standards are checked against performance criteria.

CCHIX

CCHIX is a secondary isotopic standard that also has well defined carbon and nitrogen isotopic compositions
If standard deviations of the DORMS do not meet performance criteria, the standard deviations of the secondary isotopic standards are checked.

ACE

ACE is an elemental standard with known concentrations of carbon and nitrogen (C=71.09% and N=10.36%)
The average value of ACEs are used to calibrate the concentrations for the run
Out of the 49 samples analyzed during a run the 5,6,49th samples are ACEs.

Split Samples

1 out of 10 samples will be analyzed in triplicate to generate a standard deviation of the sample. The standard deviation of the samples will be checked against the performance criteria.
If samples do not meet performance criteria, then the samples analyzed will be reanalyzed until the standard performance criteria are satisfied.

7. Calculations

$$\delta = \left[\frac{R_{sample}}{R_{standard}} - 1\right] * 1000$$

where R denotes the isotopic ratio of a given constituent.

$$\sigma = \sqrt{\left[\frac{\sum(xbar - x)^2}{n-1}\right]}$$

where, *xbar* is the mean of the data and σ is the standard deviation of the data.

$$\frac{Diff}{volt} = \frac{\delta_{Last} - \delta_{first}}{v_{Last} - v_{first}}$$

where, *v* is the voltage reading

8. Data Quality Objectives

The data quality objectives are best described using a table (seen below). These are based off EPA SIP/OP.01 (Griffis, 1999) data quality objectives and are consistent with that of the instrument to be used on this project. Sample runs analyzed for elemental and isotopic signatures need to meet the following specifications in order to be considered acceptable data.

Analysis	Range	Accuracy	Precision	Completeness
$\delta^{13}C$	1-10 Volts	±0.5‰	Stdev<0.5‰	N/A

$\delta^{15}N$	0.5-10 Volts	±0.5‰	Stdev<0.5‰	N/A
% Carbon	0-50%	90-110%	Stdev<10%	N/A
% Nitrogen	0-10%	90-110%	Stdev<10%	N/A

9. References

Griffis, W.L. 1999. Analysis of Environmental Samples Using Continuous Flow Gas Isotope Ratio Mass Spectrometry. EPA SIP/OP.01. Integrated Stable Isotope Research Facility.

A14) Field Parameters

Calibration, operation, inspection, maintenance, storage and other needed analytical needs are covered in the Hach manual for the pH, Conductivity, DO and Temperature probes. The manual can be obtained from the Hach company at www.hach.com. The citation for the manual is:

Hach Company. HACH HQ Series Portable Meters User Manual, September 2006, Edition 5. Catalog Number HG40d18. Hach Company, PO Box 389, Loveland, Colorado.

A15) Field Standard Operating Procedures

A15.1) Water Quality Parameters

Method

The direct method for streams (EPA #EH-01) will be utilized to sample NH_4^+, NO_3, DIC, DOC, DP, $\delta^{15}N_{NH4,NO3}$ at each site. Bulk samples will be collected for the suite of water quality parameters in pre-cleaned I-Chem, wide mouth, 1000 mL, HDPE, plastic bottles, which are EPA approved for water quality sample collection (KDOW, 2005). The total required volume of samples is 815 mL, hence the 1000 mL bottle will provide a sample subset for archiving. After the bottle is rinsed 3 times in the stream water, the sample is collected by placing the bottle under the water surface with the opening pointing upstream. The sampler will remain downstream of the container and the sample will be collected in a downstream to upstream motion without disturbing the substrate. Differing trains of thought are present on whether samples should be filtered in the field or in the lab. Field conditions are uncontrollable; hence there are numerous routes in which the sample can become contaminated. Therefore, for this study, samples will be collected (unfiltered) in the field and brought back to the lab immediately for filtration. Based on the sample collection guide from the USDA (Turk, 2003) samples that are most susceptible to degradation are ones that have high suspended solids (which are relatively low in this watershed during low-flow conditions based on previous TSS analysis at baseflow) or samples analyzed for trace constituents. Samples will be filtered using Whatman Glass Fiber 0.7µm, 47mm filters and then separated into their respective splits for analysis (see Analytical SOPs for sample preparation and preservation needs). During transport of water quality samples back to the lab, the samples are placed in zip lock bags to avoid contamination and then placed in a cooler to refrigerate the sample to 4^0C to assist in minimizing microbial activity. All split sample containers for water quality and sediment analysis will be new, pre-cleaned, disposable equipment and does not require decontamination. Standard decontamination procedures will be used for decontamination of the lab filtration apparatus (KDOW, 2005).

References

EPA, 2003, SOP # EH-01 Surface Water Collection, Adapted from ERT/REAC SOP 2013 Rev 1.0. East Helena Site, Montana.
Turk, J.T., 2001. Field Guide for Surface Water Sample Data Collection, USDA Forest Program, Washington, DC, 20250-9410.
KDOW, 2005. Kentucky Ambient/Watershed Water Quality Montioring Standard Operating Procedure Manual. Frankfort, Kentucky, 40601.

A15.2) Sediment Concentration Samples

A15.2.1) Depth Integrated Sediment Samples

Method

Sediment concentration will be collected using an isokinetic-depth integrated sampler to estimate sediment concentrations at fixed stations using accepted USGS methods for sample collection (USGS, 2003). Depth integrated suspended sediment samples will be collected in pint sized, plastic containers, of which about ¾ of the bottle shall be filled with sample. The samples will be stored in coolers at 4^0C until they can be refrigerated at 4^0C in the UK hydraulics lab. Holding times are up to 7 days as per EPA 160.2. Standard decontamination procedures for equipment cleaning and decontamination (KDOW, 2005) will be followed.

References

USGS, 2003. National Field Manual for the Collection of Water-Quality Data, Chapter A2. Selection of Equipment for Water Sampling. Reston, VA, 20192.
KDOW, 2005. Kentucky Ambient/Watershed Water Quality Montioring Standard Operating Procedure Manual. Frankfort, Kentucky, 40601.

A15.2.2) Fixed Point Automated Samples

Method

Sediment concentration will be collected using an automated pump sampler to collect dense concentration data during storm events. Methods for probe measurement, i.e., programming and operation, will follow manufacturer specifications (Teledyne, 2009). Automated samplers will collect 750 mL of sample in 1000 mL plastic bottles (see Teledyne ISCO manual). The samples will be stored in coolers at 4^0C until they can be refrigerated at 4^0C in the UK hydraulics lab. Holding times are up to 7 days as per EPA 160.2. Standard decontamination procedures for equipment cleaning and decontamination (KDOW, 2005) will be followed.

References

Teledyne, 2009. 6712 Portable Sampler Installation and Operation Guide. Revision Z. Lincoln, NE, 68501-2531.
KDOW, 2005. Kentucky Ambient/Watershed Water Quality Montioring Standard Operating Procedure Manual. Frankfort, Kentucky, 40601.

A15.3) Sediment Trap Samples

Method

Sediment trap samplers will be placed in the field for a specified time interval to generate a spatially and temporally integrated measure of $\delta^{15}N$ and $\delta^{13}C$ of Transported Sediment, POC and PN. Briefly, at the front of the trap (inlet) a 4mm diameter inlet tube allows acceleration of fluid into a 98mm diameter test section. The increase in area results in sedimentation, and subsequent trapping of fine sediments. The fluid exits the test section through another 4mm outlet tube. This method was originally published in Phillips et al. (2000). Samples are collected in a sediment trap as described in Phillips et al. (2000). Approximately 8L of a sediment/water mixture is poured into clean 5 gallon buckets. The samples are preserved by refrigerating at 4^0C to minimize microbial transformations. Samples are spun down and de-watered to a steady state as quickly as possible. Standard decontamination procedures for equipment cleaning and decontamination (KDOW, 2005) will be followed.

References

Phillips J, Russell M, Walling D. 2000. Time-integrated sampling of fluvial suspended sediment: a simple methodology for small catchments. *Hydrological Processes* 14: 2589–2602.

REFERENCES

Agudelo, S.C., Nelson, N.O., Barnes, P.L., Keane, T.D., Pierzynski, G.M. 2011. Phophorus adsorption and desorption potential of stream sediment and field soils in agricultural watersheds. J. Environ Quality. 40:144-152.

Akamatsu, F., Konayashi, S., Amano, K., Nakanishi, S., Oshima, Y., 2011. Longitudinal and seasonal changes in the origin and quality of transported particulate organic matter along a gravel-bed river. Hydrobiologia, 669, 183-197.

Aldrian, E., Chen, C.T.A., Adi, S., Prihartanto, Sudiana, N., Nugroho, S.P., 2008. Spatial and seasonal dynamics of riverine carbon fluxes of the Brantas catchment in East Java. J. Geophys. Res., 113, 1-13.

Alexander, R.B., Smith, R.A., Schwarz, G.E., Boyer, E.W., Nolan, J.V., Brakebill, J.W., 2008. Differences in phosphorus and nitrogen delivery to the Gulf of Mexico from the Mississippi River Basin. Evironmental Science and Technology, 42, 822-830.

Allan JD. 1995. *Stream Ecology: Structure and Function of Running Waters*. Chapman & Hall: New York.

Alvarez-Cobelas M, Angeler D, Sa´nchez-Carrillo S, Almendros G. 2010. A worldwide view of organic carbon export from catchments. *Biogeochemistry* 107:275-293 DOI: 10.1007.s10533-010-9553-z.

Alvarez S, Guerrero M. 2000. Enzymatic activities associated with decomposition of particulate organic matter in two shallow ponds. *Soil Biology and Biochemistry* 32:1941-1951.

Arango, C.P., Tank, J.L., 2008. Land use influences the spatiotemporal controls on nitrification and denitrification in headwater streams. J.N. Am. Benthol. Soc., 27(1), 90-107.

Arango, C.P., Tank, J.L., Schaller, J.L., Royer, T.V., Bernot, M.J., David, M.B., 2007. Benthic organic carbon influences denitrification in streams with high nitrate concentration. Freshw. Biol., 52, 1210-1222.

Bade, D.L., M.L. Pace, J.J. Cole, S.R. Carpenter, (2006), Can algal photosynthetic inorganic carbon isotope fractionation be predicted in lakes using existing models?, Aquat. Sci., 68, 142-153, doi:10.1007/s00027-006-0818-5.

Baker, D.W., Bledsoe, B.P., Price, J.M. 2012. Stream nitrate uptake and transient storage over a gradient of geomorphic complexity, north-central Colorado, USA. *Hydrological Processes*. 26: 3241-3252.

Battin, T.J., Kaplan, L.A., Newbold, J.D. and Hansen, C.M.E. 2003. Contributions of microbial biofilms to ecosystem processes in stream mesocosms, Nature 426, 439-442.

Battin, T.J., Kaplan, L.A., Findlay, S., Hopkinson, C.S., Marti, E., Packman, A.I., Newbold, J.A., Sabater, F., 2009. Biophysical controls on organic carbon fluxes in fluvial networks. Nat. Geosci., 1, 95-100.

Bellanger, B., Huon, S., Velasquez, F., Valles, V., Girardin, C., Mariotti, A. 2004. Monitoring soil organic carbon erosion with δ^{13}C and δ^{15}N on experimental field plots in the Venezuelan Andes. Catena, 58, 125-150.

Benkhaled, A., Higgins, H., Chebana, F., Necir, A., 2013. Frequency analysis of annual maximum suspended sediment concentrations in Abiod wadi, Biskra (Algeria). Hydrological Processes, doi: 10.1002/hyp.9880.

Bernhardt ES, Likens GE, Hall RO Jr, Buso DC, Fisher SG, Burton TM, Meyer JL, McDowell WH, Mayer MS, Bowden WB, Findlay SEG, MacNeale KH, Steltzer RS,

Lowe WH. 2005. Can't see the forest for the stream? In-stream processing and terrestrial nitrogen exports. BioScience 55:219–230.
Biggs, J.F. 2000. Eutrophication of streams and rivers: dissolved nutrient-chlorophyll relationships for benthic algae. J. N. Am. Benth. Soc., 19(1), 17-31.
Biggs B. 1996. Patterns in benthic algae of streams. In *Algal Ecology*, Stevenson RJ, Bothwell ML, Lowe RL. (eds). Academic Press: New York; 31-56.
Bingner, R., F.D. Theurer, Y. Yuan, (2011), AnnAGNPS technical processes, USDA-ARS, Version 5.2.
Birgand F.; Skaggs, R. W.; Chescheir, G. M.; Gilliam, J. W. Nitrogen removal in streams of agricultural catchments—a literature review. *Critical Reviews in Environmental Science and Technology.* 2007, 37, 381-487.
Bird, M.I, Robinson, R.A.J., Win Oo, N., Maung, A., Lu, X.X., Higgitt, D.L., Swe, A., Tun, T., Lhaing Win, S., Sandar Aye, K., Mi Mi Win, K., Hoey, T.B. 2008. A preliminary estimate of organic carbon transport by the Ayeyarwady (Irrawaddy) and Thanlwin (Salween) Rivers of Myanmar. Quartenary International, 186, 113-122.
Blair, N.E., Leithold, E.L., Brackley, H., Trustrum, N., Page, M., Childress, L., 2010. Terrestrial sources and export of particulate organic carbon in the Waipao sedimentary system: Problems, progress and processes. Mar. Geol., 270, 108-118.
Bonn, B.A. Rounds, S.A. 2010. Use of stable isotopes of carbon and nitrogen to identify sources of organic matter to bed sediments of the Tualatin River, Oregon. USGS Scientific Investigations Report, 2010-5154, 58p.
Brunet, F., Potot, C., Probst, A., Probst, J.-L. 2011. Stable carbon isotope evidence for nitrogenous fertilizer impact on carbonate weathering in a small agricultural watershed. Rapid Commun. Mass Spectrom., 25, 2682-2690, DOI:10.1002/rcm.5050.
Butman, D., P.A. Raymond, (2011), Significant efflux of carbon dioxide from streams and rivers in the United States, Nat. Geosci., doi:10.1038/ngeo1294.
Butturini A, Battin TJ, Sabater F. 1999. Nitrification in stream sediment biofilms: the role of ammonium concentration and DOC quality. *Water Research*, 34(2): 629-639.
Carey, A.E., Gardner, C.B., Goldsmith, S.T., Lyons, W.B., Hicks D.M., 2005. Organic carbon yields from small, mountainous rivers, New Zealand. Geophys. Res. Lett., 32, L15404.
Chang H. 1988. *Fluvial Processes in River Engineering.* Krieger Publishing Company: Malabar, Florida.
Chapra S, Pelletier G, Tao H. 2008. QUAL2K: A Modeling Framework for Simulating River and Stream Water Quality, Version 2.11: Documentation and User's Manual. Civil and Environmental Engineering Dept., Tufts University, Medford, MA.
Chen, F., Jia, G. 2009. Spatial and seasonal variations in δ^{13}C and δ^{15}N of particulate organic matter in a dam-controlled subtropical river. River Res. Applic., 25, 1169-1176.
Chien N. Wan Z. 1999. *Mechanics of sediment transport.* ASCE: Reston, Virginia; 446.
Christensen, J.H., B. Hewitson, A. Busuioc, A. Chen, X. Gao, I. Held, R. Jones, R.K. Kolli, W.-T. Kwon, R. Laprise, V. Magaña Rueda, L. Mearns, C.G. Menéndez, J. Räisänen, A. Rinke, A. Sarr and P. Whetton, 2007. Regional Climate Projections. In: *Climate Change 2007: The Physical Science Basis. Contribution of Working Group I to the Fourth Assessment Report of the Intergovernmental Panel on Climate Change,* Solomon, S., D. Qin, M. Manning, Z. Chen, M. Marquis, K.B. Averyt, M. Tignor and

H.L. Miller (eds.). Cambridge University Press, Cambridge, United Kingdom and New York, NY, USA.
Cole J, Prairie Y, Caraco N, McDowell W, Tranvik L, Striegl R, Duarte C, Kortelainen P, Downing J, Middelburg J, Melack J. 2007. Plumbing the global carbon cycle: Intergrating inland waters into the terrestrial carbon budget. *Ecosystems* 10:171-184.
Conley, D. J.; Paerl, H. W.; Howarth, R. W.; Boesch, D. F.; Seitzinger, S. P.; Havens, K. E.; Lancelot, C.; Likens, G. E. Controlling Eutrophication: Nitrogen and Phosphorus. *Science*. 2009, 323, 1014-1015.
Coplen, T.B., Qi, Haiping, Révész, Kinga, Casciotti, Karen, and Hannon, J.E., 2012, Determination of the $\boldsymbol{\delta}^{15}$N and $\boldsymbol{\delta}^{18}$O of nitrate in water; RSIL lab code 2900, chap. 17 ***of*** Stable isotope-ratio methods, sec. C ***of*** Révész, Kinga, and Coplen, T.B. eds., Methods of the Reston Stable Isotope Laboratory (slightly revised from version 1.0 released in 2007): U.S. Geological Survey Techniques and Methods, book 10, 35 p., available only at http://pubs.usgs.gov/tm/2006/tm10c17/. (Supersedes version 1.0 released in 2007.)
Cox E. 1990. Studies on the algae of a small softwater stream. I. Occurrence and distribution with particular reference to the diatoms. *Archiv für Hydrobiologie Supplement* 83:525-552.
Coynel, A., Etcheber, H., Abril, G., Maneux, E., Dumas, J., Hurtrez, JE., 2005. Contribution of small mountainous rivers to particulate organic carbon input in the Bay of Biscay. Biogeochemistry, 74, 151-171.
Cuffney, T.F., Wallace, J.B., 1988. Particulate organic matter export from three headwater streams: discrete versus continuous measurements. Can. J. Fish. Aquat. Sci., 45, 2010-2016.
Dalzell B, Filley T, Harbor J. 2005. Flood pulse influences on terrestrial organic matter export from an agricultural watershed. *J. Geophys. Res.* 110.
Dalzell B, Filley T, Harbor J. 2007. The role of hydrology in annual organic carbon loads and terrestrial organic matter export from a Midwestern agricultural watershed. *Geochimica et Cosmochimica Acta* 71:1448-1462.
Davis, J.M., Baxter, C.V., Minshall, G.W., Olson, N.F., Tang, C., Crosy, B.T. 2013. Climate-induced shift in hydrological regime alters basal resource dynamics in a wilderness river ecosystem. Freshwater Biology, 58, 306-319, DOI: 10.1111/fwb.12059.
Defarge C., Trichet J., Jaunet A-M., Robert M., Tribble J. and Sansone F.J. 1996. Texture of microbial sediments revealed by cryo-scanning electron microscopy: Journal of Sedimentary Research, v. 66, p. 935–947.
Dietrich W. 1982. Settling velocity of natural particles. *Water Resources Research* 18(6):1615-1626.
DiToro, D.M., (2001), Sediment Flux Modeling, John Wiley and Sons, Hoboken, New Jersey.
Doctor, D.H., C. Kendall, S.D. Sebestyen, J.B. Shanley, N. Ohte, E.W. Boyer, (2008), Carbon isotope fractionation of dissolved inorganic carbon (DIC) due to outgassing of carbon dioxide from a headwater stream, Hydrological Processes, 22, 2410-2423, doi: 10.1002/hyp.6833.

Dodds W, Smith V, Lohman K. 2002. Nitrogen and phosphorus relationships to benthic algal biomass in temperate streams. *Can. J. Fish. Aquat. Sci.* 59:865–74.
Dodds, W.K., (2007), Trophic state, eutrophication and nutrient criteria in streams, Trends in Ecology and Evolution, 22(12), 669-676, doi: 10.1016/j.tree.2007.07.010.
Donn, M.J., Menzies, N.W. 2005. Simulated rainwater effects on anion exchange capacity and nitrate retention in Ferrosols. *Australian Journal of Soil Research*. 43: 33-42.
Droppo I, Stone M. 1994. In-channel surficial fine grained sediment lamina. Part I: Physical Characteristics and formational processes. Hydrological Processes 8:101-111.
Droppo, I.G., and Amos, C.L. 2001. Structure, stability, and transformation of contaminated lacustrine surface fine-grained laminae. Journal of Sedimentary Research, Vol. 71, No. 5, pp 717-726.
Droppo I, Lau Y, Mitchell C. 2001. The effect of depositional history on contaminated bed sediment stability. *The Science of the Total Environment* 266:7-13
Dubois, K.D., D. Lee, J. Veizer, (2010), Isotopic constraints on alkalinity, dissolved organic carbon, and atmospheric carbon dioxide fluxes in the Mississippi River, Journal of Geophysical Research, 115, G02018, doi: 10.1029/2009JG001102.
Dunlap M, Marion W, Wilcox S. 2001. Solar radiation data manual for flat-plate and concentrating collectors, Report no. NREL/ TP-463–5607, Golden (CO): National Renewable Energy Laboratory.
Duvert, C., Gratiot, N., Nemery, J., Burgos, A., Navratil, O., 2011. Sub-daily variability of suspended sediment fluxes in small mountainous catchments- implications for community-based river monitoring. Hydrol. Earth Syst. Sci., 15, 703-713.
Eick, M.J., Brady, W.D., Lynch, C.K. 1999. Charge properties and nitrate adsorption of some acid southeastern soils. *J Environ. Qual*. 28: 138-144.
Emerson D, Vecchia A, Dahl A. 2005. Evaluation of drainage-area ratio method used to estimate streamflow for the Red River of the North Basin, North Dakota and Minnesota. In *U.S. Geological Survey Scientific Investigations Report* 2005–5017.
Enriquez, S., Duarte, C.M., Sand-Jensen, K. 1993. Patterns in decomposition rates among photosynthetic organisms: the importance of detritus C:N:P content. Oecologia, 94, 457-471.
Evans M, Warburton J, and Yang J. 2006. Eroding blanket peat catchments: Global and local implications of upland organic sediment budgets. *Geomorphology* 79: 45-57.
FAO-UNESCO, 2006. Soil Map of the World, digitized by ESRI. Soil climate map, USDA-NRCS, Soil Science Division, World Soil Resources, Washington D.C. Soil Pedon database, USDA-NRCS National Soil Survey Center, Lincoln, NE.
Fryirs, K., 2013. (Dis)Connectivity in catchment sediment cascades: a fresh look at the sediment delivery problem. Earth Surf. Process. Landforms, 38, 30-46.
Findlay, S.E.G., Mulholland, P.J., Hamilton, S.K., Tank, J.L., Bernot, M.J., Burgin, A.J., Crenshaw, C.L., Dodds, W.K., Grimm, N.B., McDowell, W.H., Potter J.D., Sobota, D.J., 2011. Cross-stream comparison of substrate-specific denitrification potential. Biogeochemistry, 104, 381-392.
Foo, K.Y., Hamed, B.H. 2010. Insights into the modeling of adsorption isotherm systems. *Chemical Engineering Journal*. 156: 2-10.

Ford, W.I., 2011. Particulate organic carbon fate and transport in a lowland temperate watershed, M.S. thesis, Dep. of Civil Engineering, University of Kentucky, Lexington, Kentucky.
Ford, W.I., Fox, J.F., 2014. Model of particulate organic carbon transport in an agriculturally impacted stream. Hydrol. Process., 28(5), DOI: 10.1002/hyp.9569
Ford, W.I., Fox, J.F., 2014. Statistical distribution of transported sediment carbon is a low-gradient stream. J. Hydrol., In Press
Fovet, O., G. Belaud, X. Litrico, S. Charpentier, C. Bertrand, A. Dauta, C. Hugodot, (2012), Modelling periphyton in irrigation canals, Ecological Modeling, 221, 1153-1161, doi: 10.1016/j.ecolmodel.2010.01.002.
Fox, J.F., Papanicolaou, A.N. 2007. The use of carbon and nitrogen isotopes to study watershed erosion processes. Journal of the American Water Resources, 43(4), 1047-1064
Fox, J.F., Papanicolaou, A.N., 2008. Application of the spatial distribution of nitrogen stable isotopes for sediment tracing at the watershed scale. J. Hydrol.,358, 46-55.
Fox J. 2009. Measurements of sediment transport processes in forested watersheds with surface coal mining disturbance using carbon and nitrogen isotopes. *Journal of the American Water Resources Association* 45(5): 1273-1289.
Fox J, Davis C, Martin D. 2010. Sediment source assessment in a lowland watershed using nitrogen stable isotopes. *Journal of American Water Resources Association* 46:1192-1204.
Fox, J., Ford, W., Strom, K., Villarini, G., Meehan, M., 2013. Benthic control upon the morphology of transported fine sediments in a low-gradient stream. Hydrological Processes, doi: 10.1002/hyp.9928.
Francoeur S, Biggs B, Smith R, Lowe R. 1999. Nutrient limitation of algal biomass accrual in streams: seasonal patterns and a comparison of methods. *J. N. Am. Benthol. Soc.* 18:242–260.
Freedman, D., Diaconis, P., 1981. On the histogram as a density estimator: L_2 theory. Z. Wahrscheinlichkeitstheorie verw. Gebiete, 57, 453-476.
French C, Rock L, Nolan K, Tobin J, Morrisey A. 2012. The potential for a suite of isotope and chemical markers to differentiate sources of nitrate contamination: A review. *Water Research* 46: 2023-2041.
Galloway, J. N.; Townsend, A. R.; Erisman J. W.; Bekunda, M.; Cai, Z.; Freney, J. R.; Martinelli, L. A.; Seitzinger, S. P.; Sutton, M. A. Transformation of the nitrogen cycle: recent trends, questions, and potential solutions. *Science.* 2008, 320, 889-892.
Galy, V., France-Lanord, C., Lartiges, B., 2008. Loading and fate of particulate organic carbon from the Himalaya to the Ganga-Brahmaputra delta. Geochim. Cosmochim. Acta, 72, 1767-1787.
Gao Q, Tao Z, Yao G, Ding J, Liu Z, Liu K. 2007. Elemental and isotopic signatures of particulate organic carbon in the Zengjiang River, southern China. *Hydrological Processes* 21:1318-1327.
Garcia-Aragon, J., Droppo, I.G., Krishnappan, B.G., Trapp, B. and Jaskot, C. 2011. Erosion characteristics and floc strength of Athabasca River cohesive sediments: towards managing sediment-related issues, J Soils Sediments 11:679–689.
Gerbersdorf SU, Jancke T, Westrich B, Paterson DM 2008. Microbial stabilization of riverine sediments by extracellular polymeric substances. Geobiology 6:57–69.

Gerbersdorf SU, Bittner R, Lubarsky H, Manz W, Paterson DM 2009. Microbial assemblages as ecosystem engineers. J Soils Sediments 9:640–652.
Godwin, C.M., Arthur, M.A., Carrick, H.J. 2009. Periphyton nutrient status in a temperate stream with mixed land-uses: implication for watershed nitrogen storage. *Hydrobiologia*. 623: 141-152.
Goldberg S, Criscenti LJ, Turner DR, Davis JA, Cantrell KJ. 2007. Adsorption-Desorption Processes in subsurface reactive transport modeling. *Vadose Zone Journal*, 6: 407-435.
Gomez B, Trustrum N, Hicks D, Rogers K, Page M, Tate K. 2003. Production, storage, and output of particulate organic carbon: Waipaoa River basin, New Zealand. *Water Resources Research* 39(6): ESG2-1-ESG2-8.
Gomez, B., Baisden, W.T., Rogers, K.M., 2010. Variable composition of particle-bound organic carbon in steepland river systems. J. Geophys. Res., 115, F04006.
Gosselain V, Hamilton P, Descy J. 2000. Estimating phytoplankton carbon from microscopic counts: an application for riverine systems. *Hydrobiologia* 438:75-90.
Graba, M., F.Y. Moulin, S. Bouletreau, F. Garabetian, A. Kettab, O. Eiff, J.M. Sanchez-Perez, S. Sauvage, (2010), Effect of near-bed turbulence on chronic detachment of epilithic biofilm: Experimental and modeling approaches, Water Resources Research, 46, W11531, doi: 10.1029/2009WR008679.
Graba, M., S. Sauvage, F.Y. Moulin, G. Urrea, S. Sabater, J.M. Sanchez-Perez, (2013), Interaction between local hydrodynamics and algal community in epilithic biofilm, Water Research, 47, 2153-2163, doi: 10.1016/j.watres.2013.01.011.
Graf W. 1984. *Hydraulics of Sediment Transport*. Water Resources Publications, LLC.
Griffiths, N.A., Tank, J.L., Royer, T.V., Warrner, T.J., Frauendorf, T.C., Rosi-Marshall, E.J., Whiles, M.R., 2012. Temporal variation in organic carbon spiraling in Midwestern agricultural streams. Biogeochemistry, 108, 149-169.
Gu, C., Hornberger, G.M., Mills, A.L., Herman, J.S., Flewelling, S.A. 2007. Nitrate reduction in streambed sediments: effects of flow and biogeochemical kinetics. *Water Resources Research*. 43: W12413.
Gu, B., Schelske, C.L., Waters, M.N. 2011. Patterns and controls of seasonal variability of carbon stable isotopes of particulate organic matter in lakes. Oecologia, 165, 1083-1094, DOI: 10.1007/s00442-010-1888-6.
Guo L, Macdonald R. 2006. Source and transport of terrigenous organic matter in the upper Yukon River: Evidence from isotope ($\delta^{13}C$, $\delta^{14}C$, and $\delta^{15}N$) composition of dissolved, colloidal, and particulate phases. *Global Biogeochem. Cycles* 20.
Hamdi, W., Gamaoun, F., Pelster, D.E., Seffen, M. 2013. Nitrate sorption in an agricultural soil profile. *Applied and Environmental Soil Science*, 1-7.
Hanson G, Simon A. 2001. Erodibility of cohesive streambeds in the loess area of the midwestern USA. *Hydrological Processes* 15(1):23–38.
Hantush, M.M. 2007. Modeling nitrogen-carbon cycling and oxygen consumption in bottom sediments. *Advances in Water Resources*. 30: 59-79.
Harvey, J.W., Bohlke, J.K., Voytek, M.A., Scott, D., Tobias, C.R. 2013. Hyporheic zone denitrification: Controls on effective reaction depth and contribution to whole-stream mass balance. *Water Resources Research*. 49: 6298-6316.

Hatten, J.A., Goni, M.A., Wheatcroft, R.A., 2012. Chemical characteristics of particulate organic matter from a small, mountainous river system in the Oregon Coast Range, USA. Biogeochemistry, 107, 43-66.

Helie J, Hillaire-Marcel C. 2006. Sources of particulate and dissolve organic carbon in the St Lawrence River: isotopic approach. *Hydrological Processes* 20:1945-1959.

Hill, J.C., Mcquaid, C.D. 2009. Variability in the fractionation of stable isotopes during degradation of two intertidal red algae. Estuarine, Coastal and Shelf Science, 82, 397-405.

Hilton, R.G., Galy, A., Hovius, N., 2008. Riverine particulate organic carbon from an active mountain belt: importance of landslides. Global Biogeochem. Cycles, 22, GB1017.

Hooper, D., Coughlan, J., Mullen, M., 2008. Structural Equation Modelling: Guidelines for Determining Model Fit. Electronic Journal of Business Research Methods, 6(1), 53-60.

Hope D, Billett M, Cresser M. 1994. A review of the export of carbon in river water: fluxes and processes. *Environ. Pollut.* 84:301–324.

Hope D, Billett M, Cresser M. 1997. Exports of organic carbon from two river systems in NE Scotland. *J. Hydrol*. 193: 61-82.

Huang, N.E., Shen, Z., Long, S.R., Wu, M.C., Shih, H.H., Zheng, Q., Yen, N., Tung, C.C., Liu, H.H. 1998. The empirical mode decomposition and the Hilbert spectrumfor nonlinear and non-stationary time series analysis. *Proceedings: Mathematical, Physical and Engineering Sciences*. 454(1971): 903-995.

Jacinthe, P.A., Lal, R., Owens, L.B., 2009. Application of stable isotope analysis to quantify retention of eroded carbon in grass filters at the North Appalachian experimental watersheds. Geoderma, 148, 405-412.

Jackson C, Vallaire S. 2007. Microbial activity and decomposition of fine particulate organic matter in a Louisiana cypress swamp. *J. N. Am. Benthol. Soc.* 26(4):743-753.

Johnson, L.T., (2008), The influence of land use on the role of dissolved organic carbon and nitrogen in stream nutrient processing, PhD Dissertation, Biological Sciences, University of Notre Dame.

Kendall, C., 1998. Tracing nitrogen sources and cycling in catchments. *In:* C. Kendall and J.J. McDonnell (Editors), Isotope Tracers in Catchment Hydrology, Elsevier, Amsterdam, pp. 519-576.

Kendall, C., Silva, S.R., Kelly, V.J. 2001. Carbon and nitrogen isotopic compositions of particulate organic matter in four large river systems across the United States. Hydrological Processes, 15, 1301-1346, DOI: 10.1002/hyp.216.

Kendall, C., Elliott, E.M., and Wankel, S.D., 2007. Tracing anthropogenic inputs of nitrogen to ecosystems, Chapter 12, In: R.H. Michener and K. Lajtha (Eds.), Stable Isotopes in Ecology and Environmental Science, 2nd edition, Blackwell Publishing, p. 375-449.

Kendall, C., M.B. Young, S.R. Silva, (2010), Applications of stable isotopes for regional to national-scale water quality and environmental monitoring programs. in Isoscapes: Understanding movement, pattern and processs on earth through isotope mapping, p. 89-111, Springer, New York.

Kies, L., Fast, T., Wolfstein, K., Hoberg, M. L., 1996. On the role of algae and their exopolymers in the formation of suspended particulate matter in the Elbe estuary

(Germany). Archives Hydrobiologica Special Issues on Advanced Limnology 47, 93-103.
Kim, J.-H., Zarzycka, B., Buscail, R., Peterse, F., Bonnin, J., Ludwig, W., Schouten, S., Shinninghe Damste, J.S., 2010. Contribution of river-borne soil organic carbon to the Gulf of Lions (NW Mediterranean). Limnol. Oceanogr., 55(2), 507-518.
Lane, C.S., Lyon, D.R., Ziegler, S.E. 2013. Cycling of two carbon substrates of contrasting lability by heterotrophic biofilms across a nutrient gradient of headwater streams. Aquat Sci, 75, 235-250, DOI: 10.1007/s00027-013-0269-0

Leithold, E.L., Blair, N.E., Perkey, D.W., 2006. Geomorphologic controls on the age of particulate organic carbon from small mountainous and upland rivers. Global Biogeochem. Cycles, 20, GB3022.
Lubowski, R.N., Vesterby, M., Bucholtz, S., Baez, A., Roberts M.J., 2006. Major uses of land in the United States, 2002. Economic Information Bulletin Number 13. Economic Research Service, United States Department of Agriculture, Washington.
Lyon, D.R., Ziegler, S.E. 2009. Carbon cycling within epilithic biofilm communities across a nutrient gradient of headwater streams. Limnol. Oceanogr., 54, 439-449.
Lyons, W.B, Nezat, C.A., Carey, A.E., Hicks, D.M., 2002. Organic carbon fluxes to the ocean from high-standing islands. Geology, 30, 443-446.
Machiwal, D., Jha, M.K. 2012. Hydrologic Time Series Analysis: Theory and Practice. Springer.
Maggi, F., W.J. Riley, (2010), Transient competitive complexation in biological kinetic isotope fractionation explains nonsteady isotopic effects: Theory and application to denitrification in soils, Journal of Geophysical Research, 114, G04012.
Marcarelli, A.M., Baxter, C.V., Mineau, M.M., Hall, R.O. 2011. Quantity and quality: unifying food web and ecosystem perspectives on the role of resource subsidies in freshwaters. Ecology, 92(6), 1215-1225.
Martin J, Ambrose R, Wool T. 2006. WASP7 Benthic Algae—Model Theory and User's Guide. U.S. Environmental Protection Agency, Athens, GA.
Martinez-Villegas, N., Flores-Velez, L.Ma., Dominguez, O. 2004. Sorption of lead in soil as a function of pH: a study case in Mexico. *Chemosphere*. 57:1537-1542.
Martinotti, W., Camusso, M., Guzzi, L., Patrolecco, L., Pettine, M. 1997. C,N and their stable isotopes in suspended and sedimented matter from the Po estuary (Italy). Water, Air, Soil Pollution, 99, 325-332.
Masiello C, Druffel E. 2001. Carbon isotope geochemistry of the Santa Clara River. *Global Biogeochem. Cycles* 15(2):407-416.
Matthei, C.D., Guggelberger, C., Huber, H. 2003. Local disturbance history affects patchiness of benthic river algae. Freshwater Biology, 48, 1514-1526.
McDonald, H.P., 1983. Soil Survey of Jessamine and Woodford Counties, Kentucky, Volumes 40-41. United States. Soil Conservation Service, Kentucky Agricultural Experiment Station, Kentucky. Dept. for Natural Resources and Environmental Protection. 94 pgs.
McGuire, K., J. McDonnell, (2008), Stable isotope tracers in watershed hydrology, Chapter 11, in Stable Isotopes in Ecology and Environmental Science, Second Edition, 334-374, John Wiley and Sons, Hoboken, New Jersey.

Meybeck, M., Laroche, L., Durr, H.H., Syvitski, J.P.M., 2003. Global variability of daily total suspended solids and their fluxes in rivers. Global and Planetary Change, 39, 65-93.

Milan, D. 2012. Geomorphic impact and system recovery following an extreme flood in an upland stream: Thinhope Burn, northern England, UK. Geomorphology, 138, 319-328.Mukundan, R., Radcliffe, D.E., Ritchie, J.C., Risse, L.M., McKinley, R.A. 2010. Sediment fingerprinting to determine the source of suspended sediment in a southern piedmont stream. J. Envrion. Qual., 39, 1328-1337, DOI: 10.2134/jeq2009.0405.

Millar R, Quick M. 1998. Stable width and depth of gravel-bed rivers with cohesive banks. *Journal of Hydraulic Engineering* 124(10):1005-1013.

Minshall G, Petersen R, Cummins K, Bott T, Sedell J, Cushing C, Vannote R. 1983. Interbiome comparison of stream ecosystem dynamics. *Ecological Monographs* 53(1):2-25.

Montoya, J.P. and J.J. McCarthy, 1995. Isotopic Fractionation During Nitrate Uptake by Phytoplankton Grown in Continuous Culture. Journal of Plankton Research 17(3):439-464.

Moriasi, D.N., J.G. Arnold, M.W. Van Liew, R.L. Bingner, R.D. Harmel, T.L. Veith, (2007), Model evaluation guidelines for systematic quantification of accuracy in watershed simulations, Transactions of the ASABE, 50(3), 885-900, doi: 10.13031/2013.23153.

Mulholland P, Helton A, Poole G, Hall R, Hamilton S, Peterson B, Tank J, Ashkenas L, Cooper L, Dahm C, Dodds W, Findlay S, Gregory S, Grimm N, Johnson S, McDowell W, Meyer J, Valett H, Webster J, Arango C, Beaulieu J, Bernot M, Burgin A, Crenshaw C, Johnson L, Niederlehner B, O'Brien J, Potter J, Sheibley R, Sobota D, Thomas S. Stream denitrification across biomes and its response to anthropogenic nitrate loading. *Nature* 452:202-206.

Munson, S.A., Carey, A.E., 2004. Organic matter sources and transport in an agriculturally dominated temperate watershed. Appl. Geochem., 19, 1111-1121.

Murdock, L., Ritchey, E. 2012. Lime and Nutrient Recommendations 2012-2013. Cooperative Extensive Service- UK College of Ag.

Naiman R, Bilby R. 1998. *River ecology and management: lessons from the Pacific coastal ecoregion.* Springer Verlag: New York.

Nash, D.B., 1994. Effective sediment-transporting discharge from magnitude-frequency analysis. J.Geol., 102.

Needoba, J.A., N.A. Waser, P.J. Harrison, and S.E. Calvert, 2003. Nitrogen Isotope Fractionation in 12 Species of Marine Phytoplankton During Growth on Nitrate. Marine Ecology Progress Series 255:81-91.

Neitsch, S.L., J.G. Arnold, J.R. Kiniry, J.R. Williams, (2011), Soil and Water Assessment Tool Theoretical Documentation Version 2009, Texas Water Resources Institute Technical Report No. 406, College Station, Texas.

Newcomer, T.A., Kaushal, S.S., Mayer, P.M., Shields A.R., Canuel, E.A., Groffman, P.M., Gold, A.J., 2012. Influence of novel organic carbon sources on denitrification in forest, degraded urban and restored streams. Ecol. Monogr., 82(4), 449-466.

Oeurng C, Sauvage S, Sanchez-Perez J. 2011. Assessment of hydrology, sediment and particulate organic carbon yield in a large agricultural catchment using the SWAT model. *Journal of Hydrology* 401:145-153.

Ohte, N., S. Silva, C. Kendal, C. Kratzer, R. Dahlgren, D. Doctor, (2007), Sources and transport of algae and nutrients in a Californian river in a semi-arid climate, Freshwater Biology, 2007, 12, 2476-2493, doi: 10.1111/j.1365-2427.2007.01849.x.
Olkin, I., Gleser, L.J., Derman, C., 1994. Probability Models and Applications, second ed. MacMillan, New York.
Onstad, G.D., Canfield, D.E., Quay, P.D., Hedges, J.L. 2000. Source of particulate organic matter in rivers from the continental USA: lignin phenol and stable carbon isotope compositions. Geochemica et Cosmochimica, 64(20), 3359-3546.
Owens, L.B., Shipitalo, M.J., 2011. Sediment-bound and dissolved carbon concentration and transport from a small pastured watershed. Agric. Ecosyst. Environ., 141, 162-166.
Palmer, S.M., Hope, D., Billett, M.F., Dawson, J.J.C., Bryant, C.L. 2001. Sources of organic and inorganic carbon in a headwater stream: evidence from carbon isotope studies. Biogeochemistry, 52, 321-338.
Panuccio, M.R., Muscolo, A., Nardi, S. 2001. Effect of humic substances on nitrogen uptake and assimilation in two species of pinus. *Journal of Plant Nutrition*. 24(4-5): 693-704.
Park, R.A., J.S. Clough, (2012), AQUATOX (Release 3.1) Modeling environmental fate and ecological effects in aquatic ecosystems, U.S. EPA, Washington, DC.
Parker, R.S., Troutman, B.M., 1989. Frequency Distribution of Suspended Sediment Loads. Water Resources Research, 25(7), 1567-1574.
Pawson R, Lord D, Evans M, Allott T. 2008. Fluvial organic carbon flux from an eroding peatland catchment, southern Pennines, UK. *Hydrol. Earth Syst. Sci.* 12:625-634.
Peterson, C. G. (1996) Response of benthic algal communities to natural physical disturbance. Pages 375-402, In (R. J. Stevenson, M. L. Bothwell, & R. L. Lowe, editors) Algal Ecology: Freshwater Benthic Ecosystems. Academic Press, San Diego.
Phillips J, Russell M, Walling D. 2000. Time-integrated sampling of fluvial suspended sediment: a simple methodology for small catchments. *Hydrological Processes* 14:2589-2602.
Phillips, D.L., Gregg, J.W. 2003. Source partitioning using stable isotopes: coping with too many sources. Oecologia, 136, 261-269, DOI: 10.1007/s00442-003-1218-3.
Raudkivi A. 1990. *Loose Boundary Hydraulics*. Pergamon Press.
Rato, R.T., Ortigueira, M.D., Batista, A.G. 2008. On the HHT, its problems, and some solutions. *Mechanical Systems and Signal Processing*. 22: 1374-1394.
Reidenbach MA, Limm M, Hondzo M, Stacey MT. 2010. Effects of bed roughness on boundary layer mixing and mass flux across the sediment water interface. *Water Resources Research*, 46: W07530.
Richardson J. 1992. Coarse particulate detritus dynamics in small montane streams of the southwestern British Columbia. *Can. J. Fish. Aquat. Sci.* 49: 337–346.
Riebesell, U., S. Burkhardt, A. Dauelsber, B. Kroon, (2000), Carbon isotope fractionation by a marine diatom: dependence on the growth-rate-limiting resource, Marine Ecology Progress Series, 193, 295-303.
Rier S, Kuehn K, Francoeur S. 2007. Algal regulation of extracellular enzyme activity in stream microbial communities associated with inert substrata and detritus. *J. N. Am. Benthol. Soc.* 26(3):439–449.

Riseng, C.M., Wiley, M.J., Stevenson, R.J. 2004. Hydrologic disturbance and nutrient effects on benthic community structure in Midwestern US streams: a covariance structure analysis. J. N. Am. Benthol. Soc., 23(2), 309-326.

Rode, M., U. Suhr, G. Wriedt, (2007), Multi-objective calibration of a river water quality model-Information content of calibration data, Ecological Modeling, 204, 129-142, doi: 10.1016/j.ecolmodel.2006.12.037.

Rowe, H.D., R.B. Dunbar, D.A. Mucciarone, G.O. Seltzer, P.A. Baker, S. Fritz, (2002), Insolation, moisture balance and climate change on the South American altiplano since the last glacial maximum, Climatic Change, 52, 175-199.

Russo, J. P., (2010), Investigation of surface fine grained laminae, streambed, and streambank processes using a watershed scale hydrologic and sediment transport model, M.S. thesis, Dep. Civil and Engineering, University of Kentucky, Lexington, Kentucky.

Russo J, Fox J. 2012. The role of the surface fine-grained laminae in low-gradient streams: A model approach. Geomorphology. DOI: 10.1016/j.geomorph.2012.05.012

Rutherford J, Scarsbrook M, Broekhuizen N. 2000. Grazer control of stream algae: modeling temperature and flood effects. *Journal of Environmental Engineering* 126:331–339.

Sakamaki, T., Richardson, J.S. 2011. Biogeochemical properties of fine particulate organic matter as an indicator of local and catchment impacts on forested streams. J. App. Eco., 48, 1462-1471, DOI: 10.1111/j.1365-2664.02038.x.

Saltelli, A., S. Tarantola, F. Campolongo, M. Ratto, (2004), Sensitivity Analysis in Practice. A Guide to Assessing Scientific Models, John Wiley and Sons, Hoboken, New Jersey.

Sarma V.V.S.S., Arya, J., Subbaiah, Ch.V., Naidu, S.A., Gawade, L., Kumar, P.P, Reddy, N.P.C. 2012. Stable isotopes of carbon and nitrogen in suspended matter and sediments from the Godavari estuary. J. Oceanogr., 68, 307-319, DOI: 10.1007/s10872-012-0100-5.

Schindler Wildhaber, Y., Liechti, R., Alewell, C. 2012. Organic matter dynamics and stable isotope signature as tracers of the sources of suspended sediment. Biogeosciences, 9, 1985-1996, DOI: 10.5194/bg-9-1985-2012.

Schlesinger W. 2000. Carbon sequestration in soils: some cautions amidst optimism. *Agriculture, Ecosystems and Environment* 82:121-127.

Schuster, P.F., Shanley, J.B., Marvin-Dipasquale, M., Reddy, M.M., Aiken, G.R., Roth, D.A., Taylor, H.E., Krabbenhoft, D.P., DeWild, J.F., 2008. Mercury and organic carbon dynamics during runoff episodes from a Northeastern USA watershed. Water Air Soil Pollut., 187, 89-108.

Sebestyen, S.D., Shanley, J.B., Boyer, E.W., Kendall, C., Doctor, D.H. 2014. Coupled hydrological and biogeochemical processes controlling variability of nitrogen species in streamflow during autumn in an upland forest. *Water Resources Research*. In Press.

Segura, C., Lazzati, D., Sankarasubramanian, A., 2013. The use of broken power-laws to describe the distributions of daily flow above the mean annual flow across the conterminous US. Journal of Hydrology, doi: http://dx.doi.org/10.1016/j.jhydrol.2013.09.016.

Seitzinger, S.P., J.A. Harrison, J.K. Bo¨hlke, A.F. Bouwman, R. Lowrance, B. Peterson, C. Tobias, and G. Van Drecht, 2006. Denitrification Across Landscapes and Waterscapes: A Synthesis. Ecological Applications 16:2064-2090.
Seitzinger, S. 2008. Out of reach. *Nature*, 45:162-163.
Sharma, P., Rai, S.C., 2004. Streamflow, sediment and carbon transport from a Himalayan watershed. *J. Hydrol.*, 289, 190-203.
Shih, J., R.B. Alexander, R.A. Smith, E.W. Boyer, G.E. Schwarz, S. Chung, (2010), An initial SPARROW model of land use and in-stream controls on total organic carbon in streams of the conterminous United States, U.S. Geological Survey Open-File Report, p. 22.
Short R, Canton S, Ward J. 1980. Detrital processing and associated macroinvertebrates in a Colorado mountain stream. *Ecology* 61(4):728-732.
Sigleo, A.C., Macko, S.A. 2002. Carbon and nitrogen isotopes in suspended particles and colloids, Chesapeake and San Francisco Estuaries, U.S.A. Estuarine, Coastal and Shelf Science, 54, 701-711.
Sinsabaugh R, Osgood M, Findlay S. 1994. Enzymatic models for estimating decomposition rates of particulate detritus. *J. N. Am. Benthol. Soc.* 13(2):160-169.
Six J, Jastrow J. 2002. Soil organic matter turnover. In *Encyclopedia of Soil Science*, Lal R. (eds). Boca Raton, FL; 936–942.
Smith D.J. and Underwood J.C. 1998 Exopolymer production by intertidal epipelic diatoms. Limnol Oceanogr 43(7):1578–1591.
Smith, B.N., Epstein, S. 1971. Two categories of $^{13}C/^{12}C$ ratios for higher plants. Plant Physiol., 47, 380-384.
Steiger, J.H., 2007. Understanding the limitations of global fit assessment in structural equation modeling. Pers. Individ. Dif., 42, 893-898.
Steinman, A.D., McIntire, C.D. 1990. Recovery of lotic periphyton communities after disturbance. Environmental Management, 14, 589-604.
Steinman, A.D., Mulholland, P.J., Palumbo, A.V., Flum, T.F., DeAngelis, D.L. 1991. Resistance of lotic ecosystems to a light elimination disturbance: a laboratory stream study. Oikos, 58, 80-90.
Stringfellow, W., J. Herr, G. Litton, M. Brunell, S. Borglin, J. Hanlon, C. Chen, J. Graham, R. Burks, R. Dahlgren, C. Kendall, R. Brown, N. Quin, (2009), Investigation of river eutrophication as part of a low dissolved oxygen total maximum daily load implementation, Water Science and Technology, 59.1, doi: 10.2166/wst.2009.739.
Tank J, Rosi-Marshall E, Griffiths N, Entrekin S, Stephen M. 2010. A review of allochthonous organic matter dynamics and metabolism in streams. *J. N. Am. Benthol. Soc.* 29:118–146.
Thorp, J.H., Delong, M.D., 2002. Dominance of autochthonous carbon in food webs of heterotrophic rivers. Oikos, 96(3), 543-550.
Thurman E. 1985. *Organic geochemistry of natural waters.* Nijhoff/Junk.
Tobias, C., J.K. Bohlke, (2011), Biological and geochemical controls on diel dissolved inorganic carbon cycling in a low-order agricultural stream: implications for reach scales and beyond, Chemical Geology, 283, 18-30, doi: 10.1016/j.chemgeo.2010.12.012.
Toy T, Foster G, Renard K. 2002. *Soil erosion: Processes, predictions, measurements, and control.* John Wiley & Sons: New York.

Trimmer, M., Grey, J., Heppell, C.M., Hildrew A.G., Lansdown, K., Stahl, H., Yvon-Durocher, G., 2012. River bed carbon and nitrogen cycling: State of play and some new directions. Sci. Total Environ., DOI: 10.1016/j.scitotenv.2011.10.074

Turlan, T., Birgand F., Marmonier, P. 2007. Comparative use of field and laboratory mesocosms for in-stream nitrate uptake measurement. *Ann. Limnol.-Int J. Lim.* 43(1): 41-51.

USDA. 2004. Soil Survey of Warren County, Kentucky.

U.S. Environmental Protection Agency (U.S. EPA). Data Quality Assessment: Statistical Methods for Practitioners. EPA/240/B-06/003. Washington, DC: Office of Environmental Information, 2006.

van Griensven, A., W. Bauwens, (2003), Multiobjective autocalibration for semidistributed water quality models, Water Resources Research, 39(12), 1348, doi: 10.1029/2003WR002284.

Verardo D, Froelich P, and McIntyre A. 1990. Determination of organic carbon and nitrogen in marine sediments using the Carlo Erba NA-1500 analyzer. *Deep Sea Res. Part A* 37: 157–165.

Vieira, A.A.H. Myklestad, S. 1986. Production of extracellular carbohydrate in cultures of Ankistrodesms densus. J. Plankton Res., 8, 985-994.

Wada E. 1980. Nitrogen isotope fractionation and its significance in biogeochemical processes occurring in marine environments. In: Marine Chemistry, E.O. Goldberg, Y. Horibe and K. Saruhashi (Editors). Uchida Rokahuko Publishing Company, Tokyo, pp. 375-398.

Waite, A.M., Olson, R.J., Dam, H.G., Passow, U. 1995. Sugar-containing compounds on the cell surfaces of marine diatoms measured using concanavalin A and flow cytometry. J. Phycol., 31, 925-933.

Wallin, M.B., T. Grabs, I. Buffam, H. Laudon, A. Agren, M.G. Oquist, K. Bishop, (2013), Evasion of CO_2 from streams- The dominant component of the carbon export through the aquatic conduit in a boreal landscape, Global Change Biology, 19(3), 785-797, doi: 10.1111/gcb.12083.

Walling D, Collins A, Jones P, Leeks G, Old G. 2006. Establishing fine-grained sediment budgets for the Pang and Lambourn LOCAR catchments. *Journal of Hydrology* 330:126-141.

Webster J, Benfield E, Ehrman T, Schaeffer M, Tank J, Hutchens J, D'Angelo D. 1999. What happens to allochthonous material that falls into streams? A synthesis of new and published information from Coweeta. *Freshwater Biology* 41:687-705.

Waterloo, M.J., Oliveira, S.M., Drucker, D.P., Nobre, A.D., Cuartas, L.A., Hodnett, M.G., Langedijk, I., JAns, W.W.P., Tomasella, J., Araujo, A.C., Pimentel, T.P., Estrada, J.C.M., 2006. Export of organic carbon in run-off from an Amazonian rainforest blackwater catchment. Hydrol. Process., 20, 2581-2597.

White P, Kalff J, Rasmussen J, Gasol J. 1991. The effect of temperature and algal biomass on bacterial production and specific growth rate in freshwater and marine habitats. *Microbial Ecology* 21:99-118.

Withers, P.J.A., Jarvie, H.P. 2008. Delivery and cycling of phosphorus in rivers: A review. *Science of the Total Environment*. 379-395.

Wool, T.A., R.B. Ambrose, J.L. Martin, E.A. Comer, (2006), Water Quality Analysis Simulation Program (WASP), Version 6, U.S. EPA, Washington, DC.

Wong, M.T.F., Wittwer, K. 2009. Positive charge discovered across Western Australian wheatbelt soils challenges key soil and nitrogen management assumptions. *Australian Journal of Soil Research*. 47:127-135.

Worall F, Reed M, Warburton J, Burt T. 2003. Carbon budget for a British upland peat catchment. *The Science of the Total Environment* 312: 133-146.

Wu, Z., Huang, N.E. 2004. A study of the characteristics of white noise using the empirical mode decomposition method.

Wu, Z., Huang, N.E., Peng, C. 2007. On the trend, detrending, and variability of nonlinear and nonstationary time series. *Proceedings of the National Academy of Sciences*. 104(38): 14889-14894.

Xue D, Botte J, Baets BD, Accoe F, Nestler A, Taylor P, Cleemput OV, Berglund M, Boechkx P. 2009. Present limitations and future prospects of stable isotope methods for nitrate source identification in surface- and groundwater. *Water Research* 43: 1159-1170.

Yalin M. 1990. *Mechanics of Sediment Transport*. Pergamon Press.

Yallop ML, Paterson DM, Wellsbury P 2000. Interrelationships between rates of microbial production, exopolymer production, microbial biomass and sediment stability in biofilms of intertidal sediments. Microb Ecol 39:116–127.

Yoshimura C, Gessner M, Tockner K, Furumai H. 2008. Chemical properties, microbial respiration, and decomposition of coarse and fine particulate organic matter. *J. N. Am. Benthol. Soc.* 27:664–673.

Zhang, X., Zhao, X., Liang, W., 2009. Profile distribution and storage of soil organic carbon and total nitrogen under conservation tillage in Northwest Liaoning, China. American-Eurasian Journal of Sustainable Agriculture, 3(4), 630-636.

Zahraeifard, V, Deng Z, Malone R. 2014. Modelling spatial variations in dissolved oxygen in fine-grained streams under uncertainty. *Hydrological Processes*, In Press.

Zarnetske, J.P., Haggerty, R., Wondzell, S.M., Baker, M.A. 2011. Dynamics of nitrate production and removal as a function of residence time in the hyporheic zone. *Journal of Geophysical Research*. 116: G01025.

Zarnetske, J.P., Haggerty, R., Wondzell, S.M., Bokil, V.A., Gonzalez-Pinzon, R. 2012. Coupled transport and reaction kinetics control the nitrate source-sink function of hyporheic zones. *Water Resources Research*. 48: W11508.

Vita

William I. Ford

Education	M. S. Civil Engineering, University of Kentucky, Lexington, KY, Dec, 2011. B. S. Civil Engineering, University of Kentucky, Lexington, KY, May, 2010. Stream and Watershed Science Certificate, University of Kentucky, May, 2013.
Professional Positions	Graduate Researcher, Univ. of Kentucky (May 2010-Present) Undergraduate Researcher, Univ. of Kentucky (October 2008- May 2010) Engineering Technician, MACTEC (May 2008-October 2008)
Scholastic and Professional Honors	Recipient of the Burt L Sims Graduate Fellowship (2013) Recipient of the *Kentucky Science and Engineering Foundation* (*KSEF*) graduate research fellowship (2012-2013) Recipient of the Tapp Family Environmental Graduate Fellowship (2012) Recipient of the NSF EPSCOR *Visual Observatory and Ecological Informatics System* (*VOEIS*) graduate research Fellowship (2010-2012) Recipient of the University of Kentucky Research Travel Grant (2011) Recipient of the NSF EPSCOR Research Experience for Undergraduates fellowship (2010) Outstanding University Scholar award recipient (2010) Recipient of the NSF Appalachian studies Research Experience for Undergraduates fellowship (2009)

Conference Proceedings

Ford, W.I., Fox, J.F. Watershed-scale stable isotope simulation of the fluvial organic carbon budget using ISOFLOC. Oral presentation at the Kentucky Water Resources Annual Symposium, March, 10, 2014, Lexington, KY.

Ford, W.I., Fox, J.F. Model of nitrogen source allocations and transformations using stable nitrogen isotopes. Oral presentation at the World Environmental & Water Resources Congress, ASCE, May 19-23, 2013, Cincinnati, Ohio.

Ford, W.I., Fox, J.F. Use of water quality model uncertainty analysis to develop sampling design criteria for in-stream carbon. Oral presentation at the World Environmental & Water Resources Congress, ASCE, May 19-23, 2013, Cincinnati, Ohio.

Ford, W.I., Fox, J.F. New metric for quality of carbon associated with fine sediments: a $\delta^{13}C$ modeling approach. Poster presentation at the World Environmental & Water Resources Congress, ASCE, May 19-23, 2013, Cincinnati, Ohio.

Fox, J.F., Martin, D.M., Ford, W.I., Stewart, R., Papanicolaou, T., Rowe, H.D., Huston, D. Sediment fingerprinting using carbon and nitrogen isotope tracers: Review of recent studies. Poster presentation at the World Environmental & Water Resources Congress, ASCE, May 19-23, 2013, Cincinnati, Ohio.

Ford, W.I., Fox, J.F. Watershed-scale model of carbon and nitrogen cycles in streams. Oral presentation at the Kentucky Water Resources Annual Symposium, March, 18, 2013, Lexington, KY.

Ford, W.I., Fox, J.F. Sediment bed dynamics resulting from hydraulic forcing and its impacts on physical and biogeochemical processes in a lowland fluvial system. Oral presentation at the World Environmental & Water Resources Congress, ASCE, May 20-24, 2012, Albuquerque, New Mexico.

Ford, W.I., Fox, J. F., Rowe, H.D. Ambient N-15 signature for

estimating seasonal nutrient transformations. Poster presentation at the American Geophysical Union Meeting, December 5-9, 2011, San Francisco, CA.

Ford, W.I., Fox, J. F. Organic carbon fate and transport in a lowland temperate watershed. Poster presentation at the American Geophysical Union Meeting, December 5-9, 2011, San Francisco, CA.

Ford, W.I., Fox, J.F. Geospatial modeling method to provide estimates of POC flux for regional-scale watersheds. Oral presentation at the World Environmental & Water Resources Congress, ASCE, May 22-26, 2011, Palm Springs, California.

Stewart, R.L., Ford, W.I., Fox, J.F., and Harnett, C. Development of new sensors for monitoring velocity and sediment discharge in a watershed. Poster presentation at the Kentucky Water Resources Annual Symposium, March, 21, 2011, Lexington, KY.

Ford, W.I., Fox, J.F. Integrated modeling approach to particulate organic carbon estimates on a regional scale basin. Poster presentation at the Kentucky Water Resources Annual Symposium, March, 21, 2011, Lexington, KY.

Ford, W.I., Fox, J.F. Estimates of particulate organic carbon flux in various levels of the watershed system. Poster presentation at the Kentucky Water Resources Annual Symposium, March, 22, 2010, Lexington, KY.

Publications

Ford, W.I., Fox, J.F. 2014. Model of particulate organic carbon transport in an agriculturally impacted stream. *Hydrological Processes*, 28(3): 662-675.

Fox, J. F., **Ford, W. I.,** Strom, K.B., Villarini, G., and Meehan, M. 2013. Benthic control upon the morphology of transported fine sediments in a low-gradient stream. *Hydrological Processes*, In press.

Ford, W.I., Fox, J.F. 2013. Statistical distribution of transported sediment carbon in a low-gradient stream. *Journal of Hydrology*, In Press.

Ford, W.I., Fox, J.F., Rowe, H. 2013. Impact of extreme hydrologic disturbances upon fine sediment carbon quality using stable isotopes. *Ecohydrology*, Accepted.

Ford, W.I., Fox, J.F. Watershed-scale stable isotope simulation of the fluvial organic carbon budget using ISOFLOC. *Water Resources Research*, In Review.

Ford, W.I., Fox, J.F., Rowe, H.D., Kolka, R.K. Testing assumptions surround the fluvial N cycle in low-gradient ag-disturbed streams. *ES&T*, Ready for submission.

Ford, W.I., Fox, J.F. Constraint of the fluvial nitrogen budget using a coupled process-based isotope model. *Advances in Water Resources*, In prep.